

Kinetics of Anorthite and Quartz Dissolution in Silicate Melts

by

Yi Yu

**A dissertation submitted in partial fulfillment
of the requirements for the degree of
Doctor of Philosophy
(Earth and Environment Sciences)
in the University of Michigan
2016**

Doctoral Committee:

**Professor Youxue Zhang, Chair
Professor H. Scott Fogler
Associate Professor Eric A. Hetland
Professor Rebecca A. Lange
Associate Professor Jie (Jackie) Li**

© Yi Yu 2016

To my mom, Zhishuang
and my grandpa, Yuguang

Acknowledgements

I would like to first thank my advisor, Dr. Youxue Zhang, for providing me with the great opportunity of learning and working as a scientific researcher at University of Michigan, and setting up the role model of integrity, high standard, patience, passion and hard-working. I would also like to thank my other committee members, Drs. Scott Fogler, Eric Hetland, Rebecca Lange, and Jie Li for their valuable critics, suggestions and inspirations to the progress in my research. Special thanks go to Dr. Eric Hetland for teaching me various computational techniques, to Dr. Rebecca Lange for the incisive view on the thermodynamics of minerals and melts, and to Dr. Jie Li for the informative dynamics class and the encouragement during my struggles. Finally, I would like to thank Dr. Scott Fogler, my cognate committee member, for bringing in ideas and suggestions from different and fresh perspectives.

I would like to thank all other people who have helped me grow and develop my academic expertise along the way as far. I thank Zhengjiu Xu for teaching me the experimental techniques, Dr. Yang Chen for the help with shaping my first research project, and Dr. Hejiu Hui for lively discussions on a lot of scientific matters. I thank Dr. Leslie Hayden and Dr. Gordon Moore for teaching me how to use different analytical equipments. I also want to thank my fellow colleagues, Peng Ni, Chenghuan Guo, Xiaofei Pu, Sean Hurt, Ke Yuan, and Jiachao Liu, with whom I bounced ideas back and forth.

I would not be able to come this far, without the support from my friends. I would like to express my genuine gratitude to the encouragement and advice from these people, to name but a few, Guodong Chen, Can Wang, Peng Ni, Shuang Song, Chenghuan Guo, Xiaofei Pu, Zuowei Wang, Xingyu Pan, Tianxiang Qi, and many more.

Lastly, I would like to thank Patricia, for adding the RGB onto my greyscale painting here and there.

Table of Contents

Dedication.....	ii
Acknowledgements.....	iii
List of Figures.....	vi
List of Tables.....	viii
List of Appendices.....	ix
Chapter	
I. Introduction.....	1
References.....	5
II. Kinetics of Anorthite Dissolution in Basaltic Melt.....	7
Abstract.....	7
2.1 Introduction.....	8
2.2 Experimental and analytical methods.....	10
2.3 Results.....	18
2.4 Discussion and application.....	32
2.5 Conclusion.....	50
References.....	52
III. Kinetics of quartz dissolution in silicate melts.....	60
Abstract.....	60
3.1. Introduction.....	61
3.2. Samples, experiments and analyses.....	63
3.3. Experimental results.....	68
3.4. Fitting the SiO ₂ concentration profiles of quartz dissolution experiments.....	77
3.5. Effect of H ₂ O on SiO ₂ diffusivity.....	88
3.6. Diffusive dissolution rates of quartz in rhyolitic and basaltic melts....	90
3.7. Quartz dissolution or growth rate in magma.....	95
3.8. Conclusions.....	99
References.....	101
IV. Conclusion.....	107
Appendices.....	112

List of Figures

2-1. Sketch of the experimental capsule design.....	13
2-2. Back-scattered electron image (a) and Al ₂ O ₃ concentration profiles (b) of an experimental sample (PDisBa-210).....	17
2-3. Types of anorthite-melt interface features at 1280, 1330, 1400 and 1500 °C	19
2-4. Concentration profiles of PDisBa-228 with fits of monotonic profiles.....	21
2-5. Elemental mapping of sample PDisBa-202	22
2-6. BSE image and high-spatial-resolution EDS analysis across the plagioclase-melt interface	23
2-7. Al ₂ O ₃ concentrations in interface melts vs. the experimental duration	26
2-8. Variation of anorthite dissolution distance with time.....	31
2-9. Interface Al ₂ O ₃ concentration model.....	37
2-10. Al ₂ O ₃ diffusivity	38
2-11. Comparison of Al ₂ O ₃ diffusivities.....	43
2-12. Density difference between anorthite (An# 94) and MORB at 1100-1500 °C and 1 bar.....	48
2-13. Convective dissolution model of anorthite crystal in MORB at 0.2 GPa.....	49
Fig 3-1. Back-scattered electron image (a) and SiO ₂ concentration profiles (b) of sample QzDisBa101	71

Fig 3-2. Oxide concentration profiles for sample QzDisRh104..... 72

Fig 3-3. Oxide concentration profiles for sample QzDisBa107..... 73

Fig 3-4. Normalized major concentration profiles for sample QzDisRh104..... 74

Fig 3-5. Normalized major concentration profiles for sample QzDisBa107 74

Fig 3-6. Temporal variation of SiO₂ concentrations of interface melts and melt growth
distance..... 75

Fig 3-7. Typical SiO₂ concentration profile and the corresponding fits..... 78

Fig 3-8. Boltzmann analyses and functional fitting results..... 82

Fig 3-9. Dependence of compositional dependence parameter *a* of SiO₂ diffusivity and
*D*₀ on temperature. 86

Fig 3-10. Effect of H₂O on SiO₂ diffusivity..... 90

Fig 3-11. Interface SiO₂ concentration model..... 92

Fig 3-12. Diffusive dissolution model of quartz dissolution in silicate melts 94

Fig 3-13. Calculated dissolution or growth rate of a quartz crystal in rhyolitic melts. 98

Fig 3-14. Calculated dissolution or growth rate of a quartz crystal in basaltic to andesitic
melts 99

List of Tables

2-1. Composition of anorthite crystal and basalt glass in experiments.....	11
2-2. Summary of experimental conditions	15
2-3. Fitted effective binary diffusivities of Al_2O_3 , TiO_2 , FeO_t , MgO and CaO	28
2-4. Interface melt composition of all the experiments.....	29
3-1. Compositions of quartz, cassiterite, and rhyolitic and basaltic glasses.....	64
3-2. Summary of experimental conditions	67
3-3. Interface-melt compositions of all experiments.....	76
3-4. Summary of fitting results for quartz dissolution experiments based on Eq. 3-4.....	83

List of Appendices

A. Composition profiles of anorthite dissolution in basaltic melt	113
B. Fittings to composition profiles of anorthite dissolution in basaltic melt	187
C. Literature data on Al ₂ O ₃ diffusivity during mineral dissolution experiments	211
D. Derivation of boltzmann analysis for diffusion during crystal dissolution	217
E. Composition profiles of quartz dissolution in rhyolitic and basaltic melts	219
F. Fittings to SiO ₂ concentration profiles of quartz dissolution in rhyolitic and basaltic melts	238

Chapter I

Introduction

For decades, scientists have been perplexed by the underlying mechanisms of various igneous processes, such as the crust formation of our Earth and its nearest neighbor - the Moon, magma crystallization and assimilation, xenolith and phenocryst digestion and etc. Although many theories and models have offered extensive explanations about these processes ([Watson, 1982](#); [Donaldson, 1985](#); [Zhang et al., 1989](#); [Morgan et al, 2006](#); [Chen and Zhang, 2008, 2009](#); [Yu et al, 2016](#)), there remains a lot more to be known. One of the important questions is how dissolution and growth of minerals contribute to the evolution of these igneous systems, i.e. the kinetic aspect of the igneous processes.

Different from an ‘equilibrium approach’, where the study emphasis is placed on the static equilibrium relation (i.e. phase relation) between the mineral assemblages and the coexisting magmatic melts, a kinetic approach stresses the dynamic nature of interaction between the minerals and their host magmatic melts. That is, a kinetic perspective connects different equilibrium ‘snapshots’ of the igneous systems via continuous evolving ‘footage’, introducing a temporal angle to see the processes in motion. Therefore it is necessary to take a kinetic perspective to examine mineral dissolution and growth.

[Zhang et al. \(1989\)](#) reviewed the theory of the mineral dissolution/growth processes, where these processes are accomplished by the coupling of two fundamental mechanisms: mineral-melt interface reaction and mass transport (including diffusion, convection or both). The controlling factor that determines the rate of mineral dissolution or growth is the slower of the two mechanisms. In a diffusive schema, the interface reaction is often demonstrated to be fast within the igneous temperature range, resulting in diffusion to be the rate-controlling mechanism of mineral dissolution. In such scenario, the mineral dissolution rate is inversely proportional to the square root of dissolution duration (i.e. a parabolic relation) after the interface melt composition reaches steady state. In a more vigorous convective schema, convection is often efficient in diminishing the chemical gradient outside a very thin layer of melt (i.e. the boundary layer) surrounding mineral crystals, resulting in diffusion to be dominant within the boundary layer. The quantification of such convective dissolution has been developed by [Kerr \(1995\)](#), and expanded by [Zhang and Xu \(2003\)](#) to a more vigorous fluid schema. Besides the theoretical progress, experimental studies have also contributed to our better understanding of mineral dissolution and growth kinetics. For example, [Zhang et al. \(1989\)](#) studied the diffusive dissolution of olivine, forsterite, diopside, quartz, spinel, and rutile in an andesitic melt. [Liang \(1999\)](#), [Shaw \(2004, 2006, 2012\)](#) and [Acosta-Vigil \(2006\)](#) studied quartz dissolution in simple three-to-five-component synthetic melts (such as $\text{CaO-Al}_2\text{O}_3\text{-SiO}_2$, $\text{CaO-MgO-Al}_2\text{O}_3\text{-SiO}_2$, $\text{K}_2\text{O-CaO-MgO-Al}_2\text{O}_3\text{-SiO}_2$, and haplogranitic melt). [Morgan et al. \(2006\)](#) studied anorthosite dissolution in basaltic melts of lunar basalt compositions. [Chen and Zhang \(2008, 2009\)](#) studied olivine and clinopyroxene dissolution in a basaltic melt. On one hand, the dissolution kinetics of

some minerals (such as olivine, and clinopyroxene) have been systematically quantified. On the other hand, the dissolution kinetics of many other minerals (such as anorthite, quartz and etc.) have only been sparsely explored in limited range of conditions, due to more complicated composition (like anorthite), much slower dissolution rate (like quartz), and potentially non-constant diffusion behavior of some diffusing components in the melt (Al_2O_3 , and SiO_2). Therefore it is necessary to systematically investigate the dissolution kinetics of those minerals that are both geologically abundant and significant, such as anorthite – a major constituent of the lunar crust, and quartz – a major constituent of Earth’s continental crust. With the above goals in mind, my dissertation studies aim to characterize the dissolution kinetics of anorthite and quartz in different silicate melts, with the first study focusing on kinetics of anorthite dissolution in basaltic melt, the second answering how fast quartz dissolves in dry rhyolitic melt, and the third further comparing and reconciling the differences in quartz dissolution in rhyolitic, basaltic, and andesitic melts.

Chapter II investigates the dissolution kinetics of anorthite in basaltic melt. Time-series diffusive dissolution experiments were at 1280-1500 °C and 0.5 Gpa on two different crystallographic surfaces, $(12\bar{1})$ and $(\bar{3}02)$. The experiments showed that the anisotropy in anorthite dissolution along different crystallographic directions is negligible, and the dissolution of anorthite in basaltic melt is primarily controlled by the diffusion of Al_2O_3 , which is also the equilibrium-determining component of anorthite. By incorporating previously published data on anorthite-melt equilibrium and effective binary diffusivities of Al_2O_3 (obtained by regarding all the other components together as ‘one component’ in a multiple-component system, and considering the whole system as

an simplified effective binary system), a simple and practical model was presented to approximate the anorthite-melt equilibrium using the Al_2O_3 concentration at the interface melt, and accounted for the variation in published Al_2O_3 diffusivities using a preliminary composition-dependent model. These results were then applied to model the convective dissolution of anorthite in the basaltic melt. Such model can be used to provide some preliminary insights into the formation of the lunar anorthosite crust.

In melts of different compositions, the dissolution behavior of a mineral can vary significantly, due to the change in mineral-melt equilibrium conditions in different silicate melt systems as well as the composition-dependent diffusivities. Quartz frequently appears in a wide range of silicate melts (from rhyolitic to andesitic to basaltic). It also plays important roles in many igneous processes, such as granite formation, magma mixing, and assimilation, and etc.). It is therefore useful to study quartz dissolution in silicate melts of different compositions and build a systematic model to account for the variation. In Chapter III, two closely related studies on quartz dissolution in rhyolitic melt and in basaltic melt were combined, and presented a diffusive quartz dissolution model in silicate melts ranging from rhyolitic to basaltic compositions. In these two studies, the Boltzmann analysis was developed for the diffusive mineral dissolution schema, and demonstrated that the composition-dependent SiO_2 diffusivity can be better explained using the cation mole fraction of Si+Al than using the weight percentage of SiO_2 across melts of rhyolitic and basaltic compositions. Via numerical fitting, the SiO_2 diffusivity was extracted in both rhyolitic and basaltic melts. Furthermore, with extra cassiterite dissolution experiments in different hydrous rhyolitic melts (from the same lab, Yang et al, submitted), the role of H_2O on SiO_2

diffusivity was shown to be simply dilution of Si+Al in the melt. Finally, the diffusive dissolution rate of quartz follows the expected parabolic relation, with the SiO₂ diffusivity to be roughly the geometric average of the maximum and minimum SiO₂ diffusivities across the concentration profiles during the quartz dissolution.

References

- Acosta-Vigil A., London D., Morgan G.B. and Dewers, T.A., 2006. Dissolution of quartz, albite, and orthoclase in H₂O-saturated haplogranitic melt at 800 C and 200 MPa: Diffusive transport properties of granitic melts at crustal anatexis conditions. *J. Petrol.* 47, 231-254.
- Chen Y. and Zhang Y., 2008. Olivine dissolution in basaltic melt. *Geochim. Cosmochim. Acta* 72, 4756-4777.
- Chen Y. and Zhang Y., 2009. Clinopyroxene dissolution in basaltic melt. *Geochim. Cosmochim. Acta* 73, 5730-5747.
- Donaldson C.H., 1985. The rates of dissolution of olivine, plagioclase, and quartz in a basalt melt. *Mineral. Mag.* 49, 683-693.
- Kerr R.C., 1995. Convective crystal dissolution. *Contrib. Mineral. Petrol.* 121, 237-246.
- Liang Y., 1999. Diffusive dissolution in ternary systems: Analysis with applications to quartz and quartzite dissolution in molten silicates. *Geochim. Cosmochim. Acta* 63, 3983-3995.

- Morgan Z., Liang Y. and Hess, P., 2006. An experimental study of anorthosite dissolution in lunar picritic magmas: Implications for crustal assimilation processes. *Geochim. Cosmochim. Acta* 70, 3477-3491.
- Shaw C.S.J., 2004. Mechanisms and rates of quartz dissolution in melts in the CMAS (CaO-MgO-Al₂O₃-SiO₂) system. *Contrib. Mineral. Petrol.* 148, 180-200.
- Shaw C.S.J., 2006. Effects of melt viscosity and silica activity on the rate and mechanism of quartz dissolution in melts of the CMAS and CAS systems. *Contrib. Mineral. Petrol.* 151, 665-680.
- Shaw C.S.J., 2012. The effects of potassium addition on the rate of quartz dissolution in the CMAS and CAS systems. *Contrib. Mineral. Petrol.* 164, 839-857.
- Watson, E.B., 1982. Basalt contamination by continental crust: some experiments and models. *Contrib. Mineral. Petrol.*, 80, 73-87.
- Yang, Y., Zhang, Y., Simon, A., and Ni, P., 2016. Cassiterite dissolution and Sn diffusion in silicate melts of variable water content. *Chem. Geol.*, submitted.
- Yu, Y., Zhang, Y., Chen, Y., and Xu, Z., 2016. Kinetics of anorthite dissolution in basaltic melt. *Geochim. Cosmochim. Acta*, 179, 257-274.
- Zhang Y., Walker D. and Lesher C.E., 1989. Diffusive crystal dissolution. *Contrib. Mineral. Petrol.* 102, 492-513.
- Zhang Y. and Xu Z., 2003. Kinetics of convective crystal dissolution and melting, with applications to methane hydrate dissolution and dissociation in seawater. *Earth Planet. Sci. Lett.* 213, 133-148.

Chapter II

Kinetics of Anorthite Dissolution in Basaltic Melt¹

Abstract

We report convection-free anorthite dissolution experiments in a basaltic melt at 1280-1500 °C and 0.5 GPa on two different crystallographic surfaces, $(12\bar{1})$ and $(\bar{3}02)$ to investigate dissolution kinetics. The anisotropy of the anorthite dissolution rate along these two surfaces is negligible. Time series experiments at ~1280 °C show that anorthite dissolution is mainly controlled by diffusion in the melt within experimental uncertainty. Analytical solutions were used to model the dissolution and diffusion processes, and to obtain the diffusivities and the saturation concentrations of the equilibrium-determining component (Al_2O_3) for anorthite dissolution into the basaltic melt. For the first time, we are able to show the physical and chemical characteristics of quench growth effect on the near-interface melt using high spatial resolution (0.3 μm) EDS analyses. For anorthite ($\text{An}\# \geq 90$) saturation in a melt with 39-53 wt% SiO_2 and ≤ 0.4 wt% H_2O , the concentration of Al_2O_3 in wt% depends on temperature as follows:

$$\ln C_{s, \text{Al}_2\text{O}_3} = 8.032(\pm 0.192) - \frac{7882(\pm 287)}{T},$$

where T is temperature in K, and errors are given at 1σ level. Al_2O_3 diffusivity in basaltic melt during plagioclase dissolution can be expressed as:

¹ This chapter has been published as Yu, Y., Zhang, Y., Chen, Y., and Xu, Z., 2016. Kinetics of anorthite dissolution in basaltic melt. *Geochim. Cosmochim. Acta*, 179, 257-274.

$$\ln D_{\text{Al}_2\text{O}_3}^{\text{EBD, plag diss}} = -13.69(\pm 1.57) - \frac{19313(\pm 2485)}{T},$$

where D is in m^2/s , and the activation energy is 161 ± 21 kJ/mol. These results are applied to model the convective dissolution of anorthite in basaltic melts. The model indicates that though anorthite crystals can survive for a longer time compared to olivine crystals of the same size in the same melt, the former would rise for a much smaller distance compared to the olivine sinking distance, due to the smaller density contrast between anorthite and melt.

2.1 Introduction

Mineral dissolution and crystallization are basic processes for understanding more complicated geological processes such as magma crystallization and assimilation, xenolith digestion and many other processes. Information such as diffusivity, interface melt composition, and mineral dissolution rate obtained from mineral dissolution/growth studies can be used to quantify processes such as crystal growth rate, and magma ocean evolution and differentiation.

Many authors have studied the mechanisms and rates of dissolution/growth of various minerals in a variety of silicate melts (e.g., Harrison and Watson, 1983; Donaldson, 1985; Zhang et al., 1989; Liang, 1999, 2000, 2003; Shaw, 2000, 2004, 2006, 2012; Acosta-Vigil et al., 2002, 2006; Morgan et al., 2006; Chen and Zhang, 2008, 2009). In general, convection-free mineral dissolution may be controlled either by interface reaction, by diffusion, or by both (e.g., Zhang, 2008, p. 50-54). If interface reaction plays a role, the interface melt composition would gradually evolve with time from the initial to

the final “steady-state” composition. If interface reaction is rapid, the interface melt composition would quickly reach the “steady-state” composition and be constant within error, and the dissolution would be controlled by diffusion. Such experiments can be used to extract diffusivity in the melt and the saturation melt composition. Convection can also influence the mineral dissolution rate. Zhang et al. (1989) investigated diffusive mineral dissolution in an andesitic melt and pointed out that some earlier experiments in the literature did not differentiate convective dissolution from diffusive dissolution, rendering the extracted diffusion data unreliable. Kerr (1995) quantified the convective dissolution of minerals in silicate melts for a Reynolds Number ($Re = \rho v L / \mu$, ρ is the density of the fluid; v is the relative velocity of the object to the fluid; L is the characteristic length of the object, and μ is the viscosity of the fluid) less than 1. Zhang and Xu (2003) expanded the application of the convective dissolution model to regimes with Re up to 10^5 . Within the framework of their approach, melt viscosity, and the diffusivity and interface melt concentration of the equilibrium-determining component are the three critical parameters needed to quantify convective dissolution (Levich, 1962; Clift et al., 1978; Kerr, 1995; Zhang and Xu, 2003; Chen and Zhang, 2008). Among these three parameters, saturation concentration and diffusivity can be obtained from diffusive mineral dissolution experiments. Therefore, recent studies on mineral dissolution have experimentally investigated diffusive dissolution and applied the results to quantify convective dissolution or growth in nature (Chen and Zhang, 2008, 2009; Zhang, 2013).

In this work, we investigate the kinetics of convection-free dissolution of Ca-rich plagioclase (An₉₄). One goal is to examine the role of interface reaction and diffusion for anorthite dissolution as compared to the dissolution studies on olivine, clinopyroxene and

some other minerals (Donaldson, 1985; Zhang et al., 1989; Liang, 1999; Acosta-Vigil et al., 2002, 2006; Baker et al., 2002; Shaw 2004, 2006, 2012; Morgan et al., 2006; Chen and Zhang, 2008, 2009). Another goal is to check for possible anisotropy of anorthite dissolution rate. The third goal is to extract the relevant diffusivities and saturation conditions for anorthite. The results will be applied to model the kinetics of anorthite dissolution in basaltic melts.

With these issues in mind, time-series experiments on convection-free anorthite dissolution in a basaltic melt are conducted at different temperatures to examine the role of interface reaction in controlling mineral dissolution. Important parameters, including the effective binary diffusivity of Al_2O_3 and the interface Al_2O_3 concentration, are obtained. To evaluate the possible anisotropy of anorthite dissolution rate, experiments along two different crystallographic directions of anorthite are conducted. Finally, modeling of anorthite dissolution in basaltic melt is discussed.

This work has been through peer review process and published on the journal *Geochimica et Cosmochimica Acta* (Yu et al, 2016).

2.2 Experimental and analytical methods

We followed the experimental procedure of Chen and Zhang (2008, 2009) to investigate anorthite dissolution in basaltic melt. Almost gem-quality anorthite crystals with molar compositions of $\text{Ca}/(\text{Ca}+\text{Na}+\text{K})=0.94$ and $\text{Na}/(\text{Ca}+\text{Na}+\text{K})=0.06$ (Waythomas et al., 2010), and a piece of MORB glass from Juan de Fuca Ridge (Dixon et al., 1986, 1988) were used to conduct anorthite dissolution experiments in a $\frac{1}{2}$ -inch piston-cylinder

apparatus. The compositions of the anorthite and tholeiitic basaltic glass are listed in [Table 2-1](#). We chose a plagioclase with high An# so that the solidus of the plagioclase is much higher than the liquidus of the basaltic melt for our dissolution experiments. Otherwise either the temperature interval is too small to constrain the Arrhenius relation, or there would be partial melting of the plagioclase crystal or partial crystallization of the basaltic melt, complicating the experiments. The basaltic glass (containing 0.25 to 0.40 wt% H₂O) used in this study is the same as that used by Chen and Zhang (2008, 2009); therefore, cross comparisons can be made with their olivine and clinopyroxene dissolution results.

Table 2-1. Composition of anorthite crystal and basalt glass in experiments.

Oxides	Anorthite		Basalt (JDF)	
	Composition (wt%)	StdDev (wt%)	Composition (wt%)	StdDev (wt%)
SiO ₂	44.77	0.15	51.49	0.48
TiO ₂	bdl	-	1.85	0.16
Al ₂ O ₃	35.07	0.24	13.40	0.22
FeO _t	0.50	0.03	12.23	0.23
MnO	nd	-	0.21	0.09
MgO	0.06	0.02	6.74	0.13
CaO	18.96	0.16	11.00	0.14
Na ₂ O	0.66	0.02	2.73	0.11
K ₂ O	0.01	0.01	0.18	0.03
H ₂ O			0.32	0.07
Total	100.03	-	99.84	

bdl means below detect limit, nd means not determined.

StdDev means one standard deviation.

FeO_t indicates that Fe was measured as Fe²⁺.

Two large anorthite crystals were cut and ground into round cylinders of 2.4-2.6 mm in diameter. The Miller indices of the base of one cylinder were $(12\bar{1})$, and the other $(\bar{3}02)$, as determined using single crystal X-Ray Diffraction (XRD). The angle between the normal directions of these two plane systems was calculated to be 50.5° . The cylinders were cut into wafers of ~ 0.5 mm in thickness. The MORB glass was prepared into discs in a similar way, with dimensions of ~ 2.0 mm in thickness and 1.80 mm in diameter. As shown in Fig. 2-1, the diameter of the glass was intentionally made smaller than that of the anorthite crystal so that the dissolution distance can be measured directly from the quenched experimental sample (Morgan et al., 2006; Chen and Zhang, 2008, 2009). For each experiment, one anorthite disc and one basaltic glass disc were packed into a cylindrical graphite capsule. The contact surfaces of the anorthite disc and the glass disc were polished to ensure the best surface contact. The experimental design (Fig. 2-1) followed that of Chen and Zhang (2008), except that the crystal disc was on top of the basaltic glass to ensure gravitational stability.

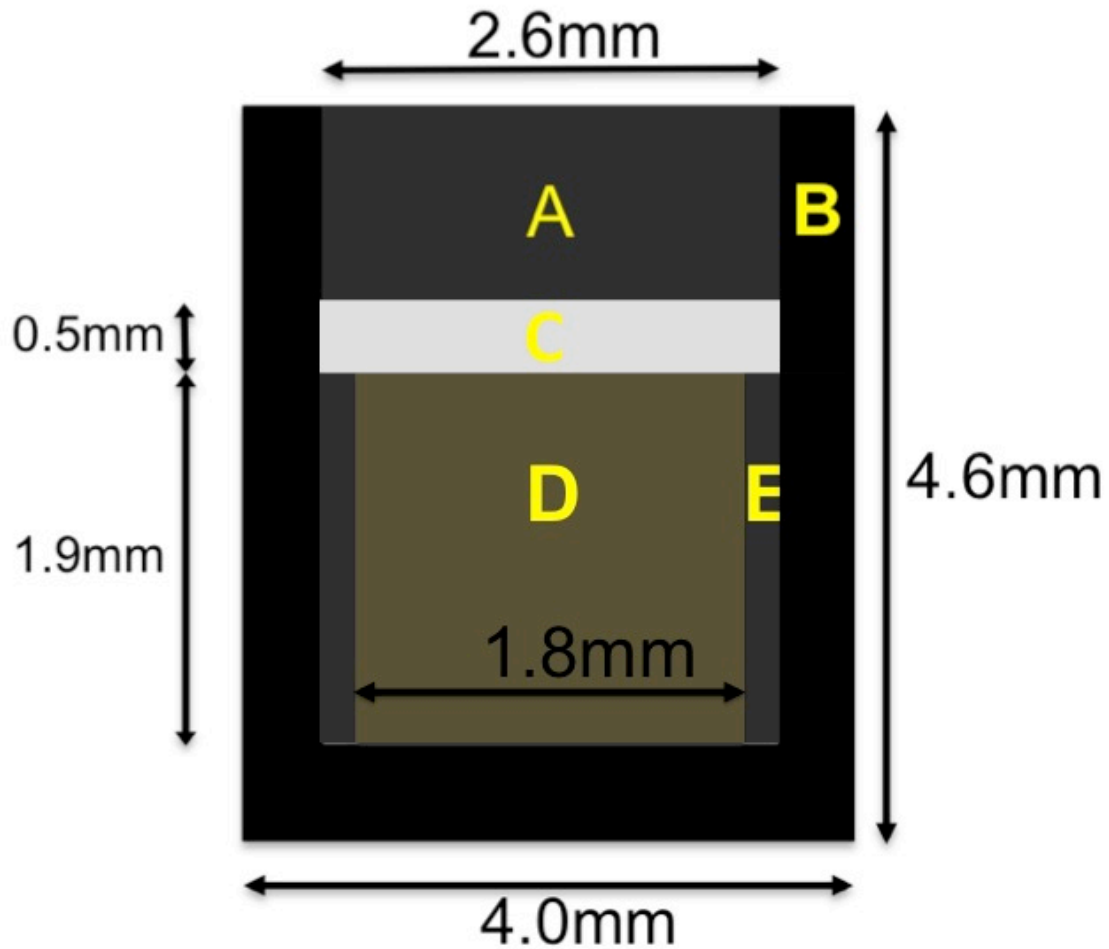


Figure. 2-1. Sketch of the experimental capsule design. A is the graphite cap, B is the graphite capsule, C is the anorthite wafer, D is the basalt glass wafer, and E is the graphite ring that surrounds the basalt.

Time-series experiments were conducted for dissolution on $(12\bar{1})$ surfaces (orientation 1) to examine the evolution of the interface melt composition with experimental duration at 0.5 GPa and three temperatures (1280°C, 1330°C, and 1400°C). For comparison, dissolution experiments (orientation 2) on another crystallographic surface, $(\bar{3}02)$, were also conducted at 1280 °C and 0.5 GPa to study possible anisotropy of the anorthite-melt interface reaction. A third set of time-series experiments (orientation 3, not determined) was carried out with extra care to examine whether the correlation

between the interface melt composition and the experimental duration was reproducible. The choice of crystallographic directions was determined after preparing anorthite samples along two distinct directions. The experimental temperatures (T1 in [Table 2-2](#)) were chosen to be above the liquidus of basalt and below the solidus of anorthite. The feasible temperature range is between $\sim 1243^{\circ}\text{C}$ (the liquidus of this basalt at 0.5 GPa based on the MELTS program; Ghiorso and Sack, 1995; Asimow and Ghiorso, 1998; Ghiorso et al., 2002) and $\sim 1527^{\circ}\text{C}$ (the solidus of plagioclase An94 at 0.5 GPa, interpolated from the phase diagram of plagioclase; Morse, 1980). Allowing uncertainties in the calculated and experimental temperatures, experiments were conducted at nominal temperatures of 1280, 1330, 1400 and 1500°C .

During an experiment, the sample assembly is first brought to the desired pressure and then heated to the planned temperature. The reported experimental temperature (T2 in [Table 2-2](#)) is the temperature at the plagioclase-melt interface using the calibration of Hui et al. (2008). The pressure was manually maintained during the whole experimental duration to within about 4 MPa. In total, 25 successful experiments were conducted ([Table 2-2](#)), although three experiments (214, 223, and 229) had other problems (discussed later).

Table 2-2. Summary of experimental conditions.

Exp No.	Crystallographic surface (<i>hkl</i>)	T1 (°C)	T2 (°C)	Duration (s)	L1 (μm)	L2 (μm)		
201	$(\bar{3}02)$	1280	1293	1826	--	37.6		
202			1284	6010	--	87.6		
203			1280	338	--	11.9		
205			1286	201	--	5.2		
207			1278	1223	22±4	18.9		
208			1278	6015	102±1	98.2		
209			1280	3615	--	43.9		
221			$(12\bar{1})$	1280	1284	1827	42±1	40.9
222					1279	329	--	8.6
223					1280	6005	--	141.8
227	1283	6009			66±4	71.1		
301	-	1280	1284	319	--	8.9		
302			1284	3615	--	52.9		
304			1281	149	--	9.4		
210	$(12\bar{1})$	1330	1333	1819	78±1	79.3		
211			1333	919	47±1	40.2		
212			1334	443	47±12	32.8		
213			1328	3615	103±4	104.5		
214			1327	2538	152±5	151.7		
215			1327	143	--	14.6		
216			1326	2540	103±1	95.7		
228		1400	1400	1408	143	--	37.1	
229				1404	621	--	-	
233				1405	620	--	87.4	
230	1500			1506	134	123±16	132.1	

Note:

T1 is the planned experimental temperature, and T2 is the corrected experimental temperature (Hui et al., 2008). All the experiments were done at 0.5 GPa.

L1 is the directly measured dissolution distance using the electron microscope. Sometimes L1 cannot be determined reliably because the plagioclase edge is missing from one side of the polished glass section, or because of many cracks. L2 is the dissolution distance calculated from Al₂O₃ concentration profiles using mass balance.

The crystallographic directions for experiments 301, 302 and 304 were not determined.

After quench, the sample assembly was taken out, mounted in epoxy, and then ground and polished to expose the anorthite and basaltic glass parallel to the center axis of the graphite capsule until the exposed area of the sample reached or was near the maximum. Epoxy was applied as needed during grinding/polishing to seal cracks in the sample. Well-polished samples were cleaned using ultrasonic cleaner and dried in a vacuum oven, and then prepared for measurement of composition profiles using a Cameca SX100 electron microprobe at the University of Michigan. The EPMA analysis conditions are: 15 kV and 10 nA focused beam (defocused beam was used for experiment 230 to obtain melt composition from glass containing quenched crystals), counting time of 30 s for Si, Mg, K, 40 s for Al, Fe, Ca, and Na; 20 s for Ti; and 10 s for Mn. Na was analyzed as one of the first elements on a spectrometer by counting for five 8-second periods, and the Na₂O concentration was calculated by extrapolating to zero time.

Two to three traverses ([Fig. 2-2a](#)) in the basaltic melt were analyzed for each experimental sample. When there were cracks, we used multiple traverses to estimate the actual gap across cracks as explained in Zhang et al. (1989) and Chen and Zhang (2008, 2009). A typical concentration profile is shown in [Fig. 2-2b](#). The electron microprobe data of all samples is available in the [Appendix A](#).

Selected samples were also examined using the new JEOL JSM 7800FLV SEM at the University of Michigan for high-spatial-resolution and semi-quantitative Energy-Dispersive X-ray Spectra (EDS) analyses (Salge, 2012) using an acceleration voltage of 7 kV, line scan spacing of 0.3 μm, and counting time of 30 s. An initial test run at 7 kV with a step size of 0.2 μm across a quartz-rhyolite interface showed that the spatial resolution of the EDS analyses is about 0.3 μm.

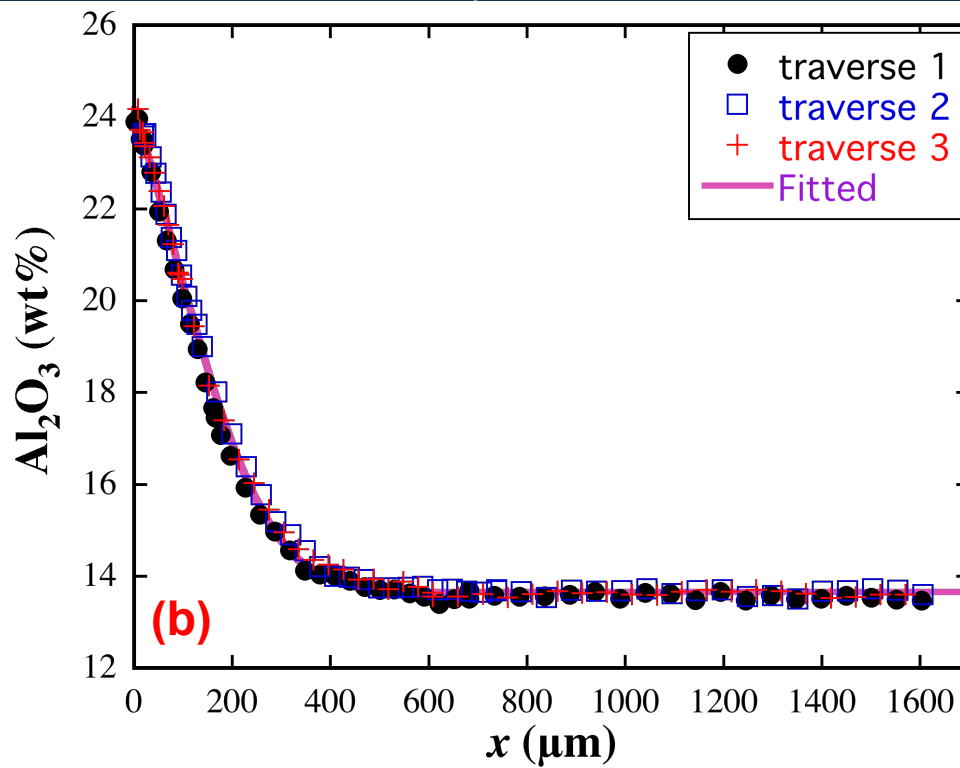
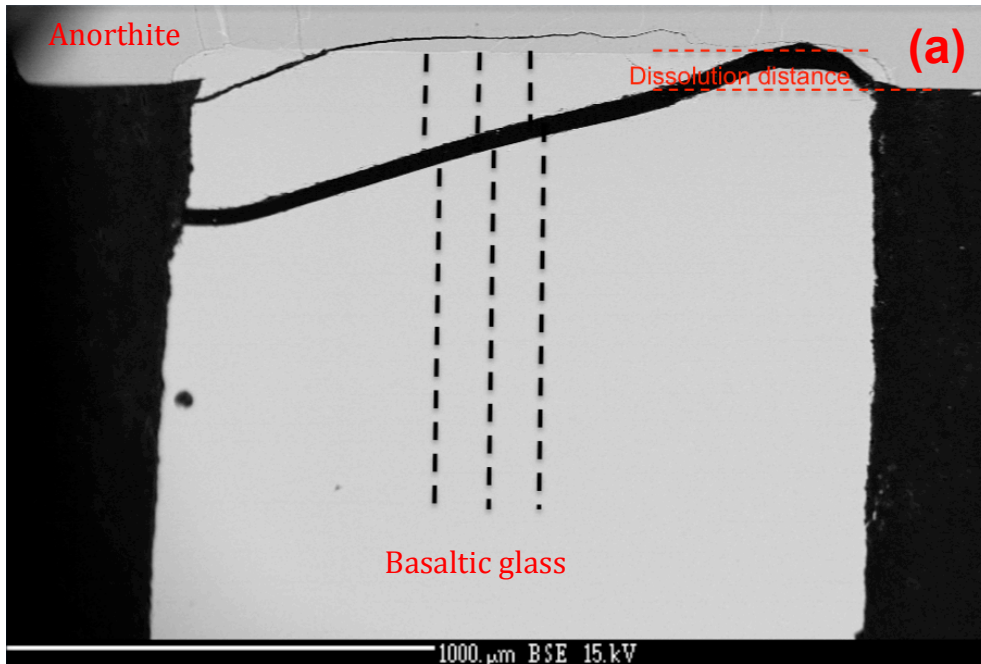


Figure 2-2. (a) Back-scattered electron image of the experiment sample PDisBa-210. The dissolution distance was obtained by directly measuring the distance between the anorthite-melt interface and the edge of the anorthite; (b) Al₂O₃ concentration profiles for the same sample. Three traverses were measured across the sample section (their locations are indicated in Fig. 2-2a). The fit by Eq. (2-1) is also plotted (solid purple curve).

2.3 Results

2.3.1. General

A list of run conditions of all successful anorthite dissolution experiments is shown in [Table 2-2](#). PIDisBa-201 to PIDisBa-209, PIDisBa-221 to PIDisBa-227, and AnDisBa-301 to AnDisBa304 are three sets of time-series experiments at 1280°C and 0.5GPa. PIDisBa-210 to PIDisBa-216 are time-series experiments at 1330°C. [Fig. 2-2a](#) shows a Back Scatter Electron (BSE) image of an experimental sample. Locations of the measured traverses were marked on it, and [Fig. 2-2b](#) displays the three measured Al₂O₃ profiles of the sample. The horizontal offset is slightly exaggerated to better show the analysis procedure.

Complications in some experiments are discussed below:

1. In experiments at and above 1400°C, the melt layer within 10-50 μm distance of the interface typically contains numerous oriented and needle-like crystals ([Fig. 2-3c and d](#)), extending off the anorthite-melt interface. The thickness of the layer increases with the experimental temperature. Experiments at lower temperatures typically show crystal-free interface regions, except for experiments PIDisBa-214 and PIDisBa-223 (discussed below). All the observed crystal needles are long (5~20 μm) but thin (~<1 μm). The electron microprobe cannot directly determine their composition. SEM-EDS analyses indicate that they have plagioclase compositions. These crystals are attributed to plagioclase growth during quench due to high degrees of plagioclase super-saturation when the temperature cooled from the experimental temperature. At 1280 and 1330°C, there is smooth cryptic overgrowth that can generate local artificial concentration profiles, which are not caused by the dissolution and diffusion at the experimental

temperature. More details of the latter type of quench overgrowth can be found in section 2.3.2.

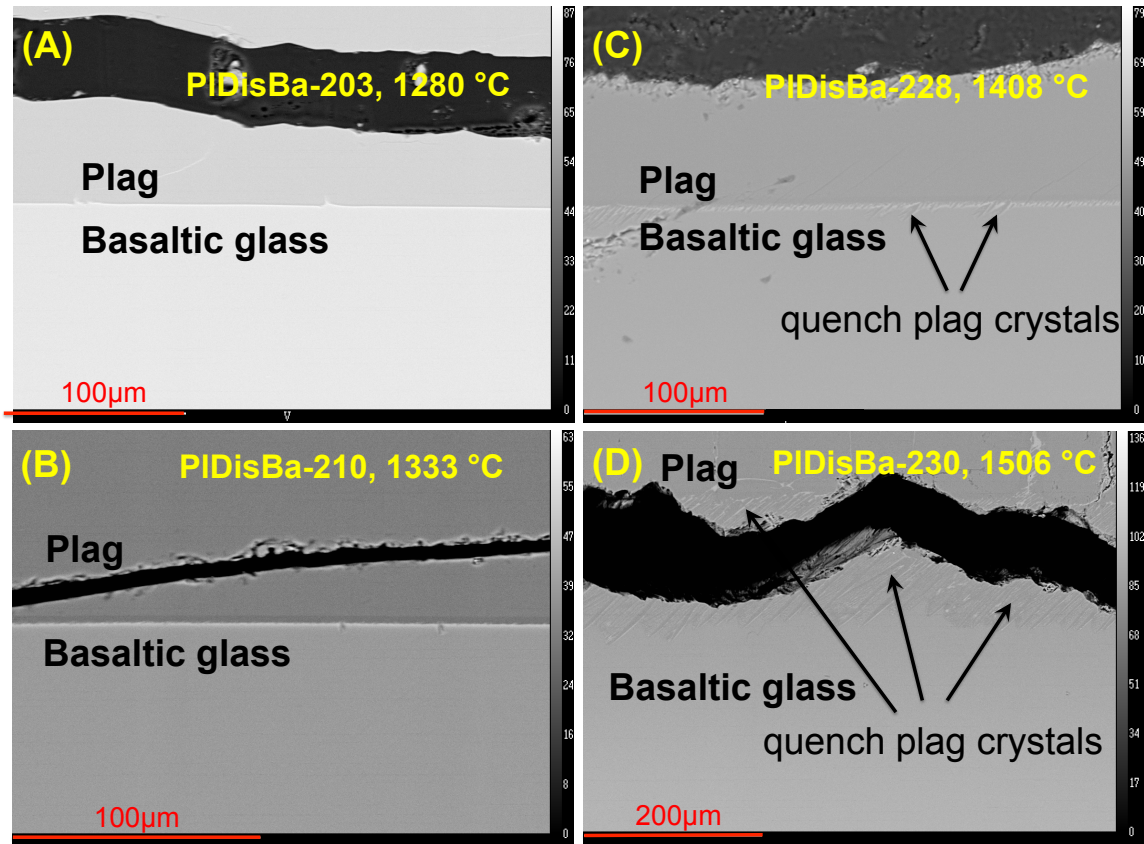


Figure 2-3. Types of anorthite-melt interface features at (A) 1280°C, (B) 1330°C, (C) 1400°C, and (D) 1500°C. At 1280 °C and 1330 °C, the interface is straight and sharp without visible quench crystals. At 1400 °C and 1500 °C, the interface region has numerous oriented dendritic plagioclase crystals.

2. For PIDisBa-214 (nominal temperature of 1330°C) and PIDisBa-223 (1280°C), a 10-20 μm thick layer of well-oriented needle-like crystals near the interface were observed. These are typical features of experiments conducted at higher temperatures. These two experiments also show other characteristics (higher output power during experiments, much higher interface concentration and effective binary diffusivity of Al_2O_3 compared to other experiments at the same temperature) that suggest that the

temperatures during these two experiments were significantly higher than the planned temperatures of 1330°C and 1280°C, respectively. The likely cause of the unexpectedly high experimental temperatures is the off-center placement of the crystal-melt interface when the capsules were prepared. The two experiments will not be used in the quantitative treatments below.

3. For P1DisBa-229 (1404°C), the anorthite-melt interface has been preserved, but a major part of the concentration profile was lost due to heavy cracking. Diffusivities cannot be reliably obtained, though the interface melt composition can be roughly estimated by averaging the points near the interface.

Concentration profiles of a selected experiment are shown in [Fig. 2-4](#), and important features are discussed below. The concentration profiles at the far field are generally flat, except for some cases where CaO concentrations of the far-field melt were altered due to the rapid diffusion of CaO. The altered far-field concentration of CaO violated the semi-infinite condition. In such cases, the effective binary diffusivity for CaO was not extracted.

Three methods are used to evaluate whether there was convection in the experiments. One is by comparing three concentration traverses in a single sample ([Fig. 2-2](#) and all other samples). The three traverses are typically in excellent agreement ([Figs. 2-2 and 2-4](#)), consistent with no convection. The second is to make elemental maps of some sections ([Fig. 2-5](#)) that would reveal “fingers” or convection cell patterns if there were convection (Morgan et al., 2006). Such features are absent in all the mapped sections. Thirdly, time series experiments have been conducted with experiment duration varying by a factor of 20 (P1DisBa-201 to P1DisBa-209, 200 to 6000 s), and the extracted

Al₂O₃ diffusion coefficients from these experiments agree within a factor of 2.5, which is a normal range of experimental errors for non-convective mineral dissolution experiments. These lines of evidence together demonstrate that the experiments were not affected by convection.

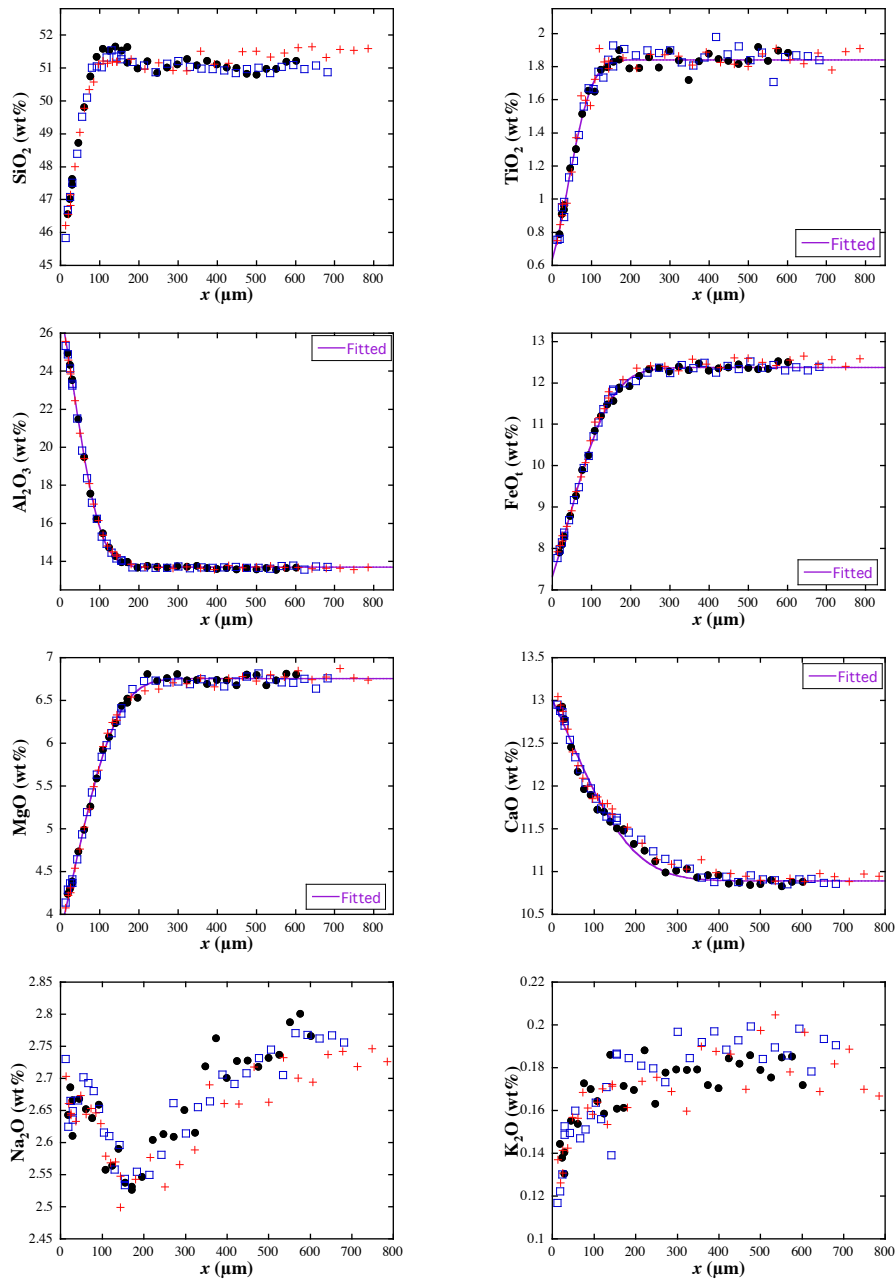


Figure 2-4. Concentration profiles of major oxide components in PIDisBa-228 (1408 °C, 143 s) with fits of monotonic profiles using Eq. (2-1).

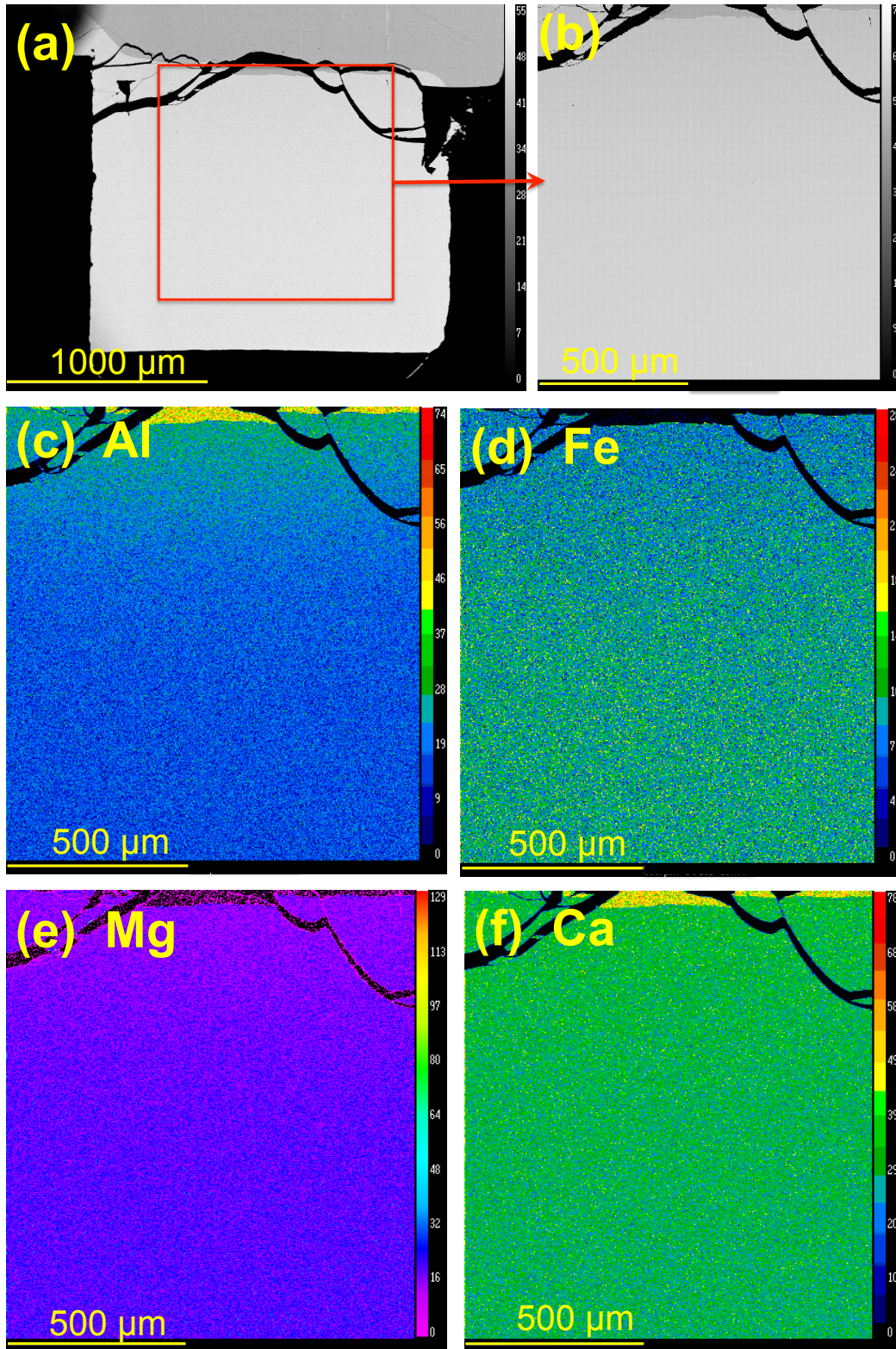


Figure 2-5. Elemental mapping of sample PIDisBa-202. Al, Mg, Fe, and Ca are mapped using WDS. (a) is back-scattered electron image of the whole sample showing the region (b) for elemental mapping. (c), (d), (e) and (f) are elemental maps of Al, Fe, Mg, and Ca.

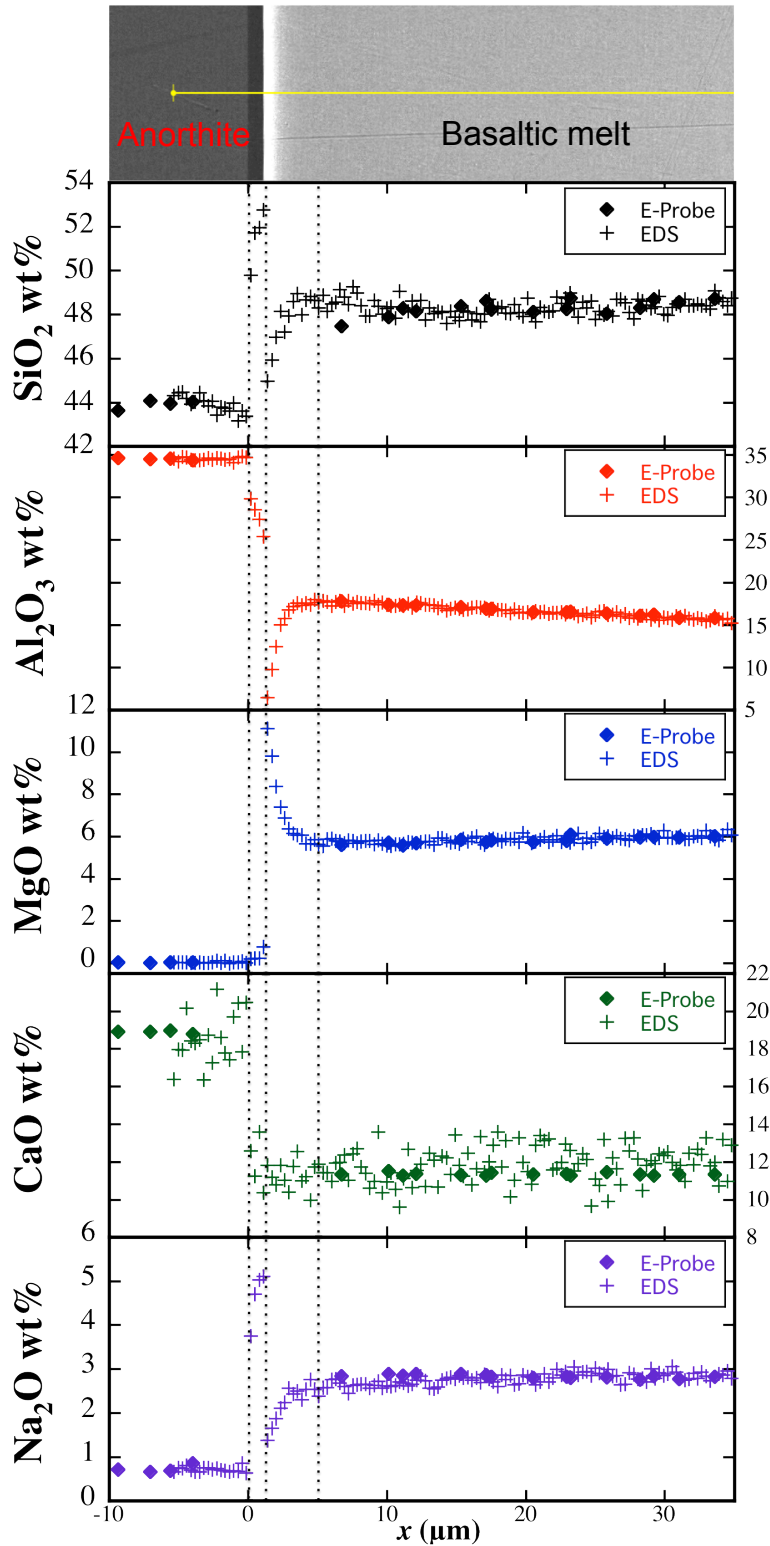


Figure 2-6. BSE image and high-spatial-resolution EDS analysis across the plagioclase-melt interface. EDS analysis is calibrated using the EPMA analysis on the same sample. From the anorthite into the basaltic melt (from left to right), four units can be recognized: the original anorthite (gray), the overgrown plagioclase An₆₇₋₇₄ (narrow darker region), the plagioclase-constituent-depleted melt due to quench growth (narrow bright region), and basaltic melt with the normal diffusion profile.

2.3.2. Crystal overgrowth at the interface during quench

Zhang et al. (1989) observed that even though the general trend of MgO concentration profile in the melt during olivine dissolution is to increase towards the olivine-melt interface, very near the interface (within about 10 μm), the trend reverses and MgO concentration decreases toward the interface (Fig. 6 in Zhang et al., 1989). This was explained to be a consequence of cryptic overgrowth of olivine as the interface melt becomes supersaturated with olivine during quench. Other authors have also observed the same phenomenon (Chen and Zhang, 2008, 2009), and we also observed this phenomenon for the Al_2O_3 concentration profile during anorthite dissolution. However, the quench overgrowth layer of the crystal is thin (1 μm or less), and the spatial resolution of EPMA at 15 kV is about 2 μm . Hence, the quench overgrowth layer has never been resolved before. We analyzed the quench overgrowth layer using an SEM (JEOL 7800 FLV) equipped with a silicon drift detector (SDD) that is able to perform high-spatial-resolution semi-quantitative EDS analyses at low voltages (Salge, 2012). EDS traverses with 0.3 μm step sizes were made across the anorthite-basalt interface. Fig. 2-6 shows a BSE image across the interface between the anorthite crystal and the basaltic glass, with an EDS traverse (the yellow horizontal line) marked. EDS data are calibrated using EPMA analyses in spots near the EDS traverse, and the resulting concentration profiles are shown in Fig. 6 below the BSE image. The compositional data clearly reveal the layer of overgrown plagioclase with high SiO_2 , high Na_2O , and nearly zero MgO, roughly matching a plagioclase formula of An_{67-74} . The newly grown plagioclase has lower Ca and higher Na concentrations compared to the original anorthite. In the BSE image, this newly grown plagioclase can be seen as the dark grey band between the original anorthite

(less dark) and the basaltic glass (light grey). The quench overgrowth produced a narrow (1 μm thick) bright band next to the dark band, and caused SiO_2 and Al_2O_3 depletion in a melt layer of about 3 μm , and Na_2O depletion and MgO enrichment in a melt layer of about 5 μm in this example. The composition of this melt layer near the interface is hence not part of the normal concentration profile for crystal dissolution. The width of the layer increases as the experimental temperature increases. The bent concentration trend near the interface (known as the quench effect) is excluded from profile fitting (Zhang et al., 1989; Chen and Zhang, 2008, 2009).

2.3.3. Interface Al_2O_3 concentration

The interface Al_2O_3 concentration in each experiment (Table 2-4) is obtained by extrapolating the non-quench-affected Al_2O_3 profile to the interface ($x = 0$). Some authors have argued that convection-free plagioclase dissolution may be partially controlled by interface reaction (Acosta-Vigil, 2002, 2006; Shaw, 2004, 2006, 2012), which would manifest itself as gradual evolution of the interface Al_2O_3 from the initial concentration in the melt to the saturation concentration for the case of anorthite dissolution. To test this, we determined the interface Al_2O_3 concentrations in experiments of different durations. Initial data appeared to indicate a trend of systematic variation of interface Al_2O_3 concentration with the experimental duration, especially at 1280°C, but data scatter made it difficult to determine whether the trend is real. A third set of experiments was therefore carried out at 1280°C (exp. 301, 302, and 304 in Tables 2-2 and 2-4; “1280°C, v3” in Fig. 2-7) and showed that there is no systematic trend (Fig. 2-7); e.g., the Al_2O_3 interface concentration of the shortest duration (2 min.) experiment is almost the same as that for

the 60-minute experiment (19.1 vs. 19.7 wt%). That is, we are not confident that our experiments can resolve the possible evolution of the interface melt composition with time and we will treat the interface melt composition at a given temperature to be constant within error. In addition, anorthite growth rates in its own melt are high according to Kirkpatrick et al. (1976), about 100 $\mu\text{m/s}$ at $\sim 1350^\circ\text{C}$, indicating rapid interface reaction rate and therefore diffusion control of non-convective dissolution. Hence, below we assume that the interface reaction is rapid and plagioclase dissolution is controlled by diffusion.

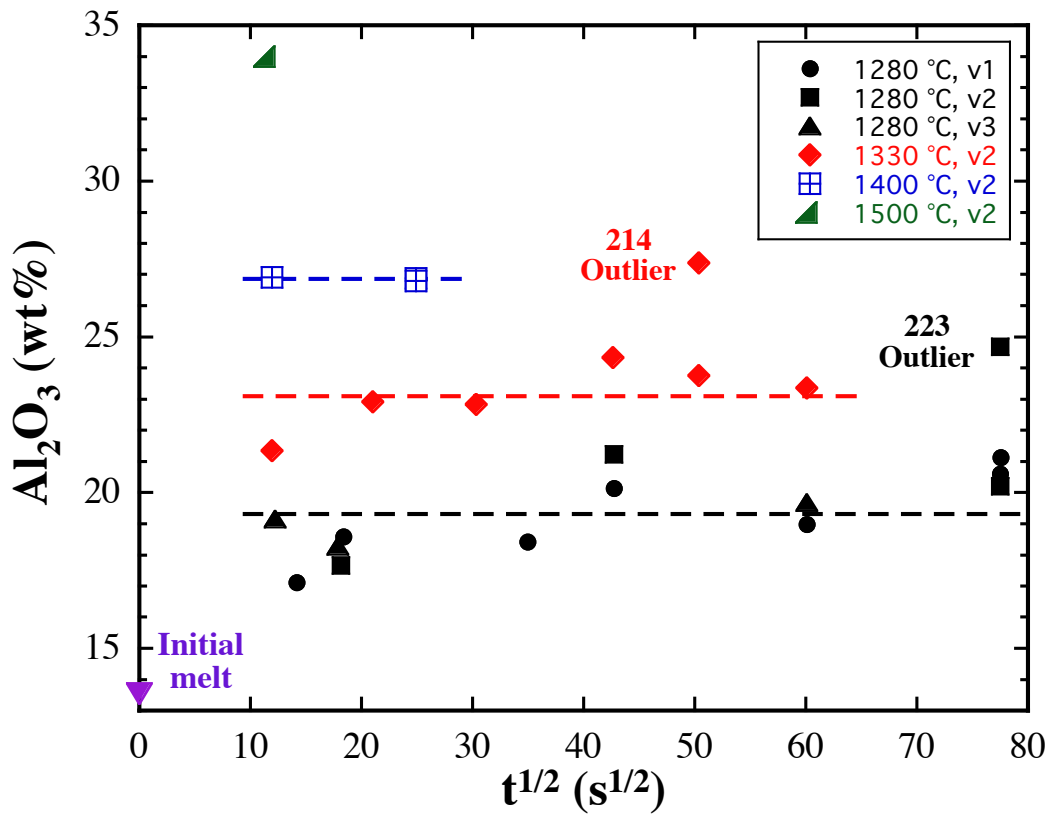


Figure 2-7. Al_2O_3 concentrations in interface melts versus the experimental duration. Orientation 1 (v1) represents crystallographic surface $(\bar{3}02)$; orientation 2 (v2) represents $(12\bar{1})$; orientation 3 (v3) is not determined. Average interface concentrations of Al_2O_3 at each experimental temperature are shown as the dashed lines. Experiments 223 and 214 are considered as outliers, and not included in the quantitative results.

2.3.4. Concentration profiles and fits

Fig. 2-4 displays concentration profiles of major components in the basaltic glass in selected experiments. Concentrations of SiO₂, TiO₂, MgO and FeO in the melt decrease toward the anorthite-melt interface, whereas Al₂O₃ and CaO concentrations increase toward the interface. These are expected because the dissolving anorthite crystal contains lower SiO₂, TiO₂, MgO, and FeO concentrations, and higher Al₂O₃ and CaO concentrations than the basaltic melt. SiO₂ shows weak uphill diffusion with a small maximum. Despite the relatively large data scatter, Na₂O shows obvious uphill diffusion with a minimum in the middle of the profile (e.g., Fig. 2-4), and sometimes even both a minimum and a maximum, demonstrating complicated multicomponent diffusion effects. MnO and K₂O concentration profiles are scattered due to their low concentration. Compositional profiles and digital data of all the experiments are provided in [Appendix A and B](#).

Monotonic concentration profiles C vs. x are fitted by the following equation (Zhang et al., 1989):

$$C = C_{\infty} + (C_0 - C_{\infty}) \frac{\operatorname{erfc}\left(\frac{x}{\sqrt{4Dt}} - \alpha\right)}{\operatorname{erfc}(-\alpha)}, \quad (2-1)$$

where x is the distance in the melt from the crystal-melt interface, t is the experimental duration, C , C_{∞} , and C_0 are the concentrations of the oxide at x , in the initial (far-field) melt ($x = \infty$), and the interface melt ($x = 0$), α is related to the melt growth distance L ($L = 2\alpha\sqrt{Dt}$), and C_0 and α satisfy:

$$\exp(\alpha^2)\operatorname{erfc}(-\alpha)\sqrt{\pi}\alpha = \frac{C_0 - C_\infty}{C_c - C_0}. \quad (2-2)$$

All the fit D values are listed in [Table 2-3](#), and the fits are shown in [Fig. 2-4](#) and in the [Appendix B](#).

Table 2-3. Fitted effective binary diffusivities of Al₂O₃, TiO₂, FeO_t, MgO and CaO.

Exp No.	Diffusivity (10 ⁻¹² m ² /s)				
	Al ₂ O ₃	TiO ₂	FeO _t	MgO	CaO
201	4.7(1)	4.0(6)	8.3(5)	8.2(6)	-
202	6.5(2)	6.0(6)	12.7(4)	15.8(3)	-
203	4.5(1)	3.7(5)	11.1(6)	9.8(4)	44.2(4.5)
205	3.0(1)	2.7(6)	6.6(6)	5.3(6)	-
207	3.6(1)	3.5(4)	5.9(2)	6.4(4)	-
208	7.2(1)	6.6(4)	15.8(1)	15.6(4)	-
209	5.1(1)	4.3(4)	10.5(4)	10.8(5)	-
221	4.1(1)	3.8(4)	8.3(4)	9.6(5)	-
222	4.0(1)	3.2(7)	7.5(6)	7.4(6)	-
301	2.9(1)	2.2(4)	5.9(4)	5.6(5)	-
302	5.5(2)	3.8(6)	9.8(7)	11.0(8)	-
304	5.1(2)	5.6(1.4)	9.8(8)	7.4(7)	-
227	5.5(1)	5.2(5)	11.7(4)	11.4(4)	-
210	6.8(1)	6.5(4)	16.6(3)	17.3(4)	-
211	5.0(1)	4.1(3)	10.5(3)	10.6(3)	29.2(2.1)
212	6.4(1)	4.9(4)	15.7(4)	15.4(5)	40.6(2.5)
213	7.5(1)	6.7(4)	19.3(5)	18.4(5)	-
215	6.5(1)	5.8(7)	16.6(7)	15.0(7)	27.1(22.8)
216	8.0(1)	7.4(3)	20.7(4)	20.2(5)	-
228	10.1(1)	8.5(4)	27.5(6)	25.6(5)	56.4(3.1)
233	13.3(1)	11.6(4)	36.6(6)	35.0(8)	83.9(5.9)
230	22.3(3)	17.6(4)	57.9(1.5)	56.1(1.3)	100.1(4.2)

Note:

The value in parentheses indicates 1σ error on the last digit of the diffusivity. EBDs of CaO are not provided when the semi-infinite boundary condition is not satisfied.

Table 2-4. Interface melt composition of all the experiments.

Sample#	SiO ₂ ^a	TiO ₂	Al ₂ O ₃	FeO	MnO ^a	MgO	CaO ^a	Na ₂ O ^a	K ₂ O ^a
201	47.5	1.17(2)	20.14(5)	9.51(3)	0.18	5.18(3)	11.9	2.7	0.17
202	47.3	1.16(1)	20.61(2)	9.52(1)	0.20	5.07(1)	12.0	2.7	0.16
203	48.7	1.36(2)	18.59(3)	10.17(3)	0.20	5.56(1)	11.6	2.8	0.16
205	49.2	1.46(2)	17.12(4)	10.44(3)	0.23	5.83(3)	11.3	2.9	0.17
207	48.8	1.36(2)	18.42(3)	10.14(2)	0.20	5.60(2)	11.6	2.8	0.17
208	47.2	1.11(1)	21.12(2)	9.19(1)	0.17	4.99(1)	12.2	2.7	0.16
209	47.8	1.31(1)	18.98(3)	10.01(2)	0.18	5.49(1)	11.6	2.8	0.17
221	48.2	1.10(2)	21.22(3)	9.44(3)	0.20	5.15(2)	12.0	2.8	0.17
222	48.9	1.44(3)	17.66(3)	10.43(3)	0.20	5.83(2)	11.4	2.8	0.17
227	48.1	1.24(1)	20.20(2)	9.80(2)	0.19	5.35(1)	11.7	2.8	0.16
301	47.8	1.36(2)	18.27(5)	10.88(3)	0.20	5.61(2)	11.3	2.9	0.18
302	47.0	1.21(2)	19.68(3)	9.83(4)	0.21	5.30(2)	11.6	2.9	0.17
304	49.0	1.29(2)	19.14(6)	9.78(5)	0.19	5.51(3)	11.3	2.9	0.18
210	45.8	0.84(1)	24.33(3)	8.37(2)	0.15	4.50(2)	12.5	2.6	0.14
211	46.7	0.98(2)	22.83(2)	8.92(2)	0.16	4.79(2)	12.1	2.8	0.16
212	46.7	0.92(2)	22.91(3)	8.52(2)	0.18	4.60(2)	12.3	2.7	0.14
213	47.4	0.90(1)	23.36(3)	8.49(2)	0.16	4.57(1)	12.3	2.5	0.15
215	48.5	1.09(3)	21.35(4)	8.91(3)	0.15	4.99(2)	12.0	2.8	0.16
216	46.8	0.89(1)	23.76(4)	8.39(2)	0.15	4.44(1)	12.6	2.6	0.13
228	45.7	0.62(2)	26.92(4)	7.39(3)	0.11	3.87(2)	13.0	2.6	0.12
229 ^b	45.2	0.6	26.8	6.5	0.1	3.4	13.5	2.7	0.12
233	45.9	0.61(1)	26.87(4)	7.27(3)	0.14	3.85(2)	13.1	2.6	0.12
230 ^c	44.5	0.02	34	2.66	0.05	1.26	16.6	2.0	0.04

Note:

Interface melt compositions are extrapolated by fitting the diffusion profiles using the analytical solution to the diffusion equation (eqs. 2-2a&b), 1 σ fitting errors are given in the parentheses, meaning the uncertainty on the last digit.

a. SiO₂, Na₂O, K₂O and MnO do not have obvious “normal” diffusion profiles. Therefore, the interface concentrations of these components are estimated by finding the mean of the points near the interface, and the error is not provided for these three components.

b. Sample PIDisBa-229 is heavily cracked near the interface, losing a majority of the diffusion profile. Therefore estimation of the interface composition is obtained by averaging the points near the interface.

c. Quench crystals near the interface of PIDisBa-230 disrupt the diffusion profiles near the interface. Therefore, the interface composition is roughly obtained by averaging the near-interface data points.

2.3.5. Dissolution distance

The dissolution distances of anorthite for each sample are determined by two methods. One is based on the direct measurement of how much the melt moved into the anorthite wafer using BSE images (L1 in [Table 2-2](#)). However, L1 is not always measurable. Sometimes, the experimental charge is too cracked and L1 cannot be estimated reliably. In other samples, melt encroachment into the anorthite crystal can only be seen from one side, with anorthite on the other side either missing or cracked. In these cases, L1 estimation is not reliable and not reported. In the second method, dissolution distance is calculated from the measured Al_2O_3 concentration profiles based on mass balance using eq. 16 in Zhang et al. (1989) assuming constant density in the glass and $\rho_{\text{anorthite}}/\rho_{\text{glass}} = 1$ (L2 in [Table 2-2](#)). The dissolution distance given by these two methods are generally consistent with each other. The directly measured dissolution distance L1 is a good independent (though redundant) determination of the dissolution distance. The independent verification by the two methods strengthens our data and discussion. Both L1 (when available) and L2 were used in figures.

The dissolution distance is plotted against the square root of the experimental duration in [Fig. 2-8](#). The dissolution distance at each temperature is roughly proportional to $t^{1/2}$ considering data scatter, consistent with the diffusion controlled dissolution. At $\sim 1400^\circ\text{C}$, the fit equation is $L = (3.43 \pm 0.11)t^{1/2}$ (blue short-dashed line) with t in s, L in μm and errors at 1σ level hereafter. At $\sim 1330^\circ\text{C}$, $L = (1.79 \pm 0.06)t^{1/2}$ (red solid line). At $\sim 1280^\circ\text{C}$, $L = (0.99 \pm 0.05)t^{1/2}$ (black long-dashed line).

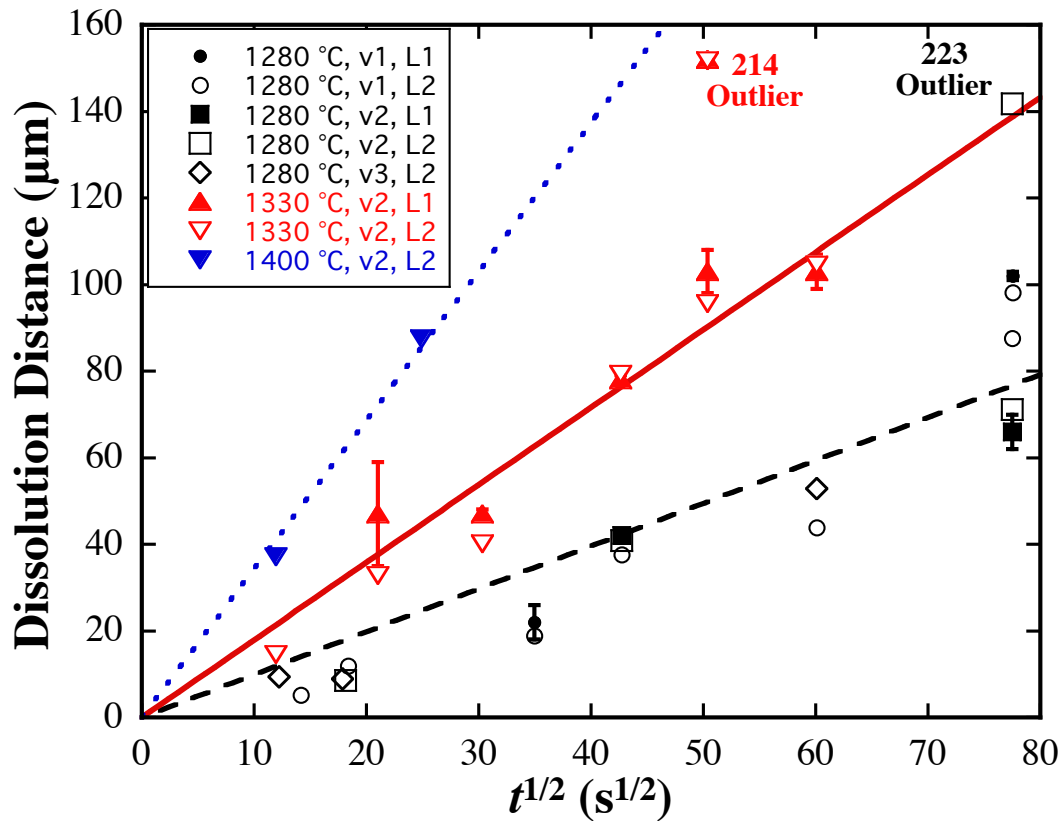


Figure 2-8. Variation of anorthite dissolution distance with time. L1 represents the directly measured dissolution distance under BSE image, 1s error of L1 (solid symbols) is also drawn on the plot, and error is not shown when it is smaller than the symbol size; L2 is the calculated dissolution distance based on mass conservation using Al_2O_3 concentration profiles. v1 represents the crystallographic direction $[\bar{3}02]$; while v2 represents the direction $[12\bar{1}]$. v3 is not determined. The straight-line (linear proportionality) fits assume pure-diffusion control.

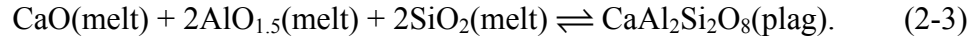
2.4 Discussion and application

2.4.1. Al₂O₃ concentration at anorthite saturation

Concentrations of oxides in the interface melt can be estimated from the concentration profiles by extrapolation. When the MELTS program (Ghiorso and Sack, 1995; Asimow and Ghiorso, 1998) is used to calculate the liquidus temperature and phase using the interface melt composition, the calculated liquidus phase is plagioclase (the calculated composition of the liquidus plagioclase is An₇₄₋₈₃ at 1280 °C, ~An₈₂₋₈₇ at 1330 °C, ~An₉₀ at 1400 °C, and ~An₉₅ at 1500 °C) and the calculated liquidus temperatures are within 33°C of our experimental temperature at 1280-1330°C (excluding the two outliers described above), but are lower by 51°C to 93°C at 1400°C to 1500°C. When the thermobarometers of Putirka (2005) are used to estimate the temperature or pressure, the calculated temperatures are higher than the experimental temperature by 15°C to 58°C, and the calculated pressures are off by 5 kb to 28 kb. When the model of Namur et al. (2012) is applied to estimate the temperature at which the interface melt is in equilibrium with plagioclase An₉₄, the calculated equilibrium temperatures are 1267-1317°C for experiments at 1280°C, and 1190-1197°C for experiments at 1400°C. At experimental temperatures of 1400°C and 1500°C, the large differences between the calculated and experimental temperatures by the different models are likely due to the paucity of experimental data at such high temperatures when these models were calibrated.

Plagioclase-melt equilibrium is controlled by multiple components (Al₂O₃, CaO, SiO₂, and Na₂O in the melt; e.g., Drake, 1976; Panjasawatwong et al., 1995; Putirka,

2005; Namur et al., 2012) whose activities depend on factors such as H₂O concentration (Lange et al., 2009). The anorthite-melt equilibrium can be expressed as:



The equilibrium constant can be written as:

$$K = \frac{a_{\text{CaAl}_2\text{Si}_2\text{O}_8}^{\text{plag}}}{a_{\text{CaO}} a_{\text{AlO}_{1.5}}^2 a_{\text{SiO}_2}^2}, \quad (2-4)$$

where a is the chemical activity in the plagioclase (indicated by superscript “plag”) and the melt (not indicated). However, models based on eqs. 2-3 and 2-4 cannot be applied easily to model crystal growth and dissolution unless the multicomponent activity model and diffusivity matrix are available (e.g., Liang, 1999; Alexander, 2011). Therefore, there is a need to develop simpler models for Ca-rich plagioclase saturation.

To simplify the problem, we will consider only “dry” systems (with less than 0.4 wt% H₂O in the melt) and for plagioclase with $X_{\text{An}} > 0.90$, which would be applicable to the formation of anorthosite crust on Moon. During plagioclase dissolution, the Al₂O₃ concentration gradient (or the difference between Al₂O₃ concentration in the interface melt and that in the far-field melt) clearly is the largest compared to the gradients of other components. For example, in experiment PIDisBa-228 (1408 °C, 142.7 s), the CaO concentration varies from 10.9 wt% in the far field to 13.0 wt% at the interface (a relative variation of about 19%), and the SiO₂ concentration varies from 51.2 wt% to 45.7 wt% (about –11% relative variation), whereas the Al₂O₃ concentration varies from 13.6 wt% to 26.9 wt% (a relative variation of about 97%). In addition, the CaO concentration in the melt increases toward the interface and the SiO₂ concentration decreases toward the interface, leading to only small variations of $C_{\text{CaO}}C_{\text{SiO}_2}^2$ (where C is concentration) across

the whole diffusion profile. The calculated activity product of $a_{\text{CaO}}a_{\text{SiO}_2}^2$ using MELTS (Ghiorso and Stack, 1995) also does not vary much across the whole diffusion profile either. That is, the Al_2O_3 concentration largely controls the saturation of anorthite in our experiments. In Figs. 2-9a and c, we plot all available literature plagioclase-melt equilibrium data in “dry” melts (including terrestrial basalts and komatiite, lunar basalts, a chondritic melt, and eucrites) with $X_{\text{An}} > 0.90$ and compare the dependence of $-\ln K$ (either activity- or concentration-based) and $\ln(\text{Al}_2\text{O}_3)$ on $1000/T$, where the activities of SiO_2 , Al_2O_3 and CaO are calculated using MELTS (Ghiorso and Stack, 1995), and $-\ln K$ (rather than $\ln K$) is used so as to enable a more straightforward comparison. Fig. 2-9 shows that:

(1) The equilibrium melt compositions from phase equilibrium experiments and interface melt saturation compositions from anorthite dissolution experiments are similar. For example, at 0.5 GPa, our anorthite dissolution data are consistent with the equilibrium data of Panjasawatwong et al. (1995). That is, there is no need to distinguish between phase equilibrium data and anorthite dissolution data.

(2) Experimental data on lunar basalts (Grove and Raudsepp, 1978; Grove and Beaty, 1980; Finnila et al., 1994) are broadly consistent with data on terrestrial basalts. Hence, it is not necessary to develop special models for lunar basalts with low SiO_2 and alkali contents, high FeO contents, and highly variable TiO_2 contents.

(3) The available experimental data do not show systematic variations of either $\ln K$ or $\ln(\text{Al}_2\text{O}_3)$ with pressure. For example, the 10^{-4} GPa data (black symbols) and the 0.5 GPa data (red symbols) fall on the same trend within error, the 0.6 GPa data (purple symbols) are above the trend, the 0.8 GPa point (green symbols) is below the trend, and the 1 GPa

point (blue symbols) is on the trend. Lange et al. (2009) showed that the fusion volume of anorthite is small (the corresponding contribution to ΔG is at most 0.7 kJ/mol; while that for albite is larger, 3 to 4 kJ/mol at 0.5 GPa; In addition, the enthalpy of fusion of pure anorthite is about 133.0 kJ/mol at 1557 °C) and varies weakly with pressure, with a contribution to $\ln K$ of no more than 0.09 when pressure is less than 1 GPa. Therefore, it is difficult to accurately obtain the pressure dependence using the above dataset due to the experimental uncertainties within and between studies.

(4) The data scatter in $\ln K$ vs. $1/T$ is not noticeably smaller than in $\ln(\text{Al}_2\text{O}_3)$ vs. $1/T$ (in fact, the r^2 value for the $\ln(\text{Al}_2\text{O}_3)$ vs. $1/T$ fit is slightly better than that for the $\ln K$ vs. $1/T$ fit). That is, using K to characterize the anorthite saturation condition is not noticeably more accurate.

(5) The data of Morgan et al. (2006) are slightly off the trend in the three plots.

In conclusion, the multicomponent treatment using K as shown in [Figs. 2-9a and b](#) does not have much advantage over simply using Al_2O_3 concentration at least for the subset of data we are considering. We also tried to relate $\ln(\text{Al}_2\text{O}_3/X_{\text{An}})$ vs. $1/T$ to characterize anorthite saturation. It turns out that the simple approach of $\ln(\text{Al}_2\text{O}_3)$ vs. $1/T$ ([Fig. 2-9c](#)) provides a more consistent linear correlation, and hence it is adopted. We realize that our approach to use Al_2O_3 rather than K to characterize the saturation is an approximation. Nevertheless, the simple saturation model for anorthite is useful in modeling anorthite growth and dissolution kinetics, similar to the use of MgO to model olivine saturation (e.g., Niu et al., 2002; Chen and Zhang, 2008).

From Fig. 2-9c, excluding the data of Morgan et al. (2006), the Al_2O_3 concentration data in the melt at plagioclase-melt equilibrium can be fitted as a function of temperature by the following equation:

$$\ln C_{s,\text{Al}_2\text{O}_3} = 8.032(\pm 0.192) - \frac{7882(\pm 287)}{T}, \quad (2-5)$$

where the errors provided in the parentheses are at 1σ level, and $r^2 = 0.948$. The above equation can reproduce the experimental $\ln C_{s,\text{Al}_2\text{O}_3}$ to within 0.16 $\ln C$ units with 1σ prediction error of 0.07 $\ln C$ units, and the experimental temperatures to within 44°C with 1σ prediction error of 20°C , except for the data of Morgan et al. (2006), for which the errors are 0.18-0.26 in $\ln C$, and $65\text{-}99^\circ\text{C}$ in temperature. That is, for plagioclase saturation in “anhydrous” melts when $X_{\text{An}} \geq 0.90$ and when SiO_2 in the silicate melt is between 39 wt% to 53 wt%, the simple equation above (eq. 2-5) is about as good as the more sophisticated models of MELTS (Ghiorso and Sack, 1995; Asimow and Ghiorso, 1998) and Putirka (2005).

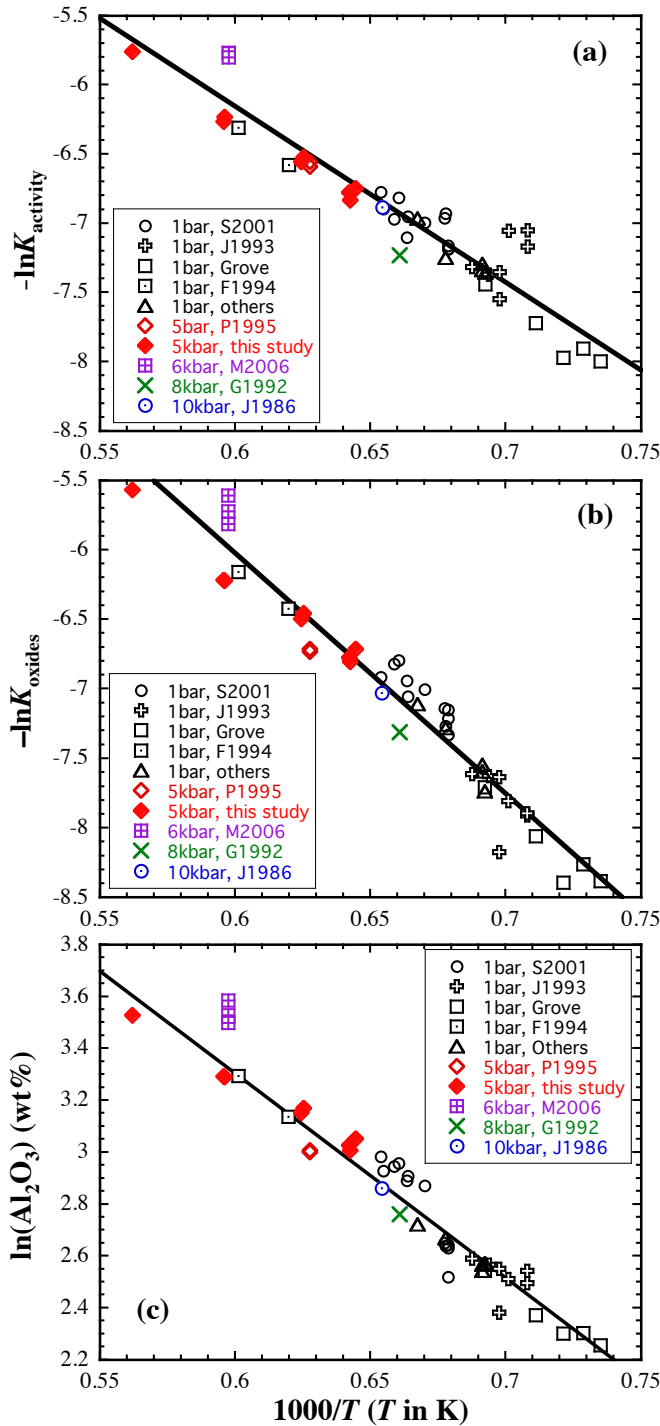


Figure 2-9. Experimental plagioclase saturation data from phase equilibrium and plagioclase dissolution experiments in “dry” melts for $X_{\text{An}} \geq 0.90$. (a) $-\ln K$ vs. $1000/T$, where K is defined by eq. (2-4) with calculated activities using MELTS. (b) $-\ln K_{\text{oxides}}$ vs. $1000/T$, where K_{oxides} is calculated based on the concentrations of SiO_2 , Al_2O_3 and CaO . (c) $\ln(\text{Al}_2\text{O}_3)$ vs. $1000/T$, where Al_2O_3 is saturation concentration in wt%. The line is a fit to all data except for Morgan et al. (2006). The data appear to indicate weak nonlinearity, which is ignored. References: S2001 = Sugawara (2001) phase equilibrium experiments on basalt to dacite; J1993 = Jurewicz et al. (1993) on chondritic high-FeO basalts; Grove = Grove and

Raudsepp (1978) on Apollo 15 basalts, Grove and Beatty (1980) on Apollo 11 basalts; F1994 = Finnila et al. (1994) on plagioclase dissolution in lunar basalt; others = two points from Kinzler and Grove (1985) on komatiite, one point from Yang et al. (1996) on MORB, one point from Stolper (1977) on eucrite and one point from Longhi and Pan (1988); P1995 = Panjasawatwong et al. (1995) on basalts; M2006 = 0.6-GPa data of Morgan et al. (2006) on plagioclase dissolution in lunar basalts; G1992 = 0.8-GPa point from Grove et al. (1992) on MORB; J1986 = 1-GPa point from Johnston (1986) on island arc basalts.

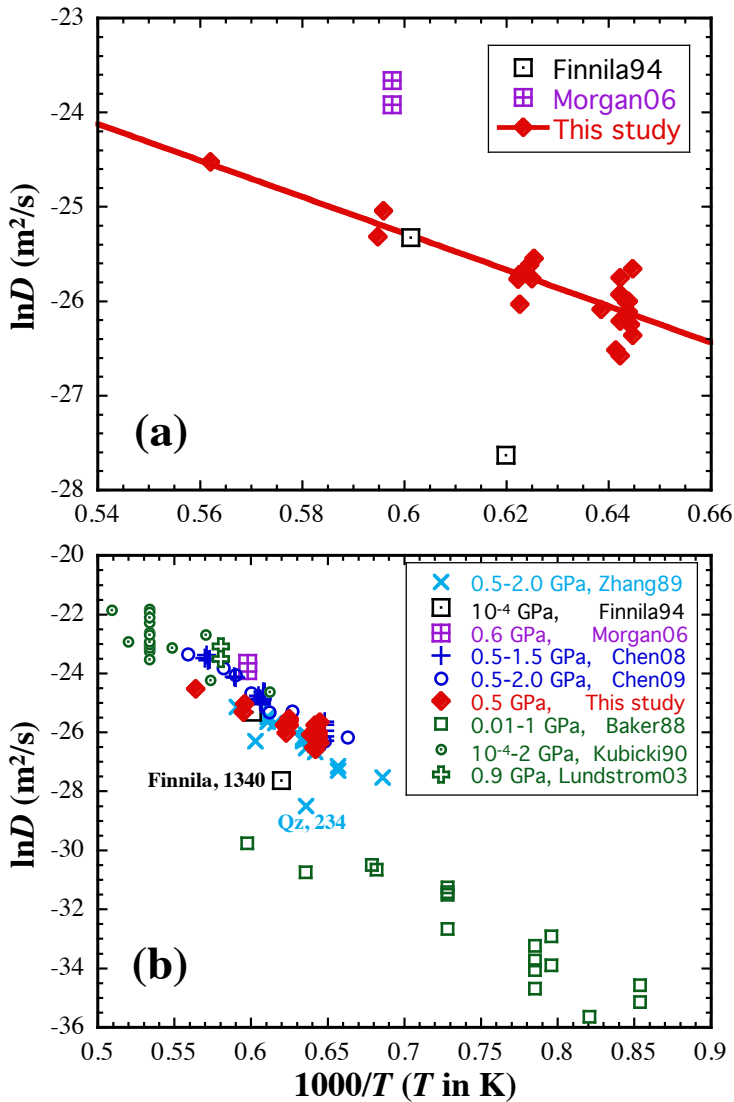


Figure 2-10. (a) A comparison of effective binary diffusivity (EBD) of Al_2O_3 from anorthite dissolution experiments. (b) EBD of Al_2O_3 from dissolution experiments of various minerals. References: Zhang89 = Zhang et al. (1989) various minerals dissolution into andesite melt at 0.5 to 2 GPa Finnila94 = Finnila et al. (1994), anorthite dissolution in lunar basalt at 10^{-4} GPa; Morgan06 = Morgan et al. (2006), anorthite dissolution in lunar basalt at 0.6 GPa; Chen08 and Chen 09 = Chen and Zhang (2008, 2009), olivine and diopside dissolution in terrestrial basalt at from 0.5 to 2 GPa; Baker88 = Baker and Watson (1988), Cl- and F-bearing silicate melt diffusion couples; Kubicki90 = Kubicki et al, 1990, diffusion couples of diopside to $\text{Di}_{40}\text{An}_{60}$ composition; Lundstrom03 = Lundstrom, 2003.

2.4.2. Effective binary diffusivity of Al₂O₃

The effective binary diffusivity (EBD) of Al₂O₃ is another essential parameter in modeling anorthite dissolution and growth rates and is also of general interest, and it is well constrained from our experiments, by fitting the concentration profiles with the analytical solution (eq. 2-1). The fits are shown in Fig. 2-4 and Appendix B. The fitting results are listed in Table 2-3 and Appendix C. The Al₂O₃ diffusion data in our study can be fitted by the following Arrhenius relation (Fig. 2-10a):

$$\ln D_{\text{Al}_2\text{O}_3}^{\text{EBD, plag diss}} = -13.69(\pm 1.57) - \frac{19313(\pm 2485)}{T}, \quad r^2 = 0.75 \quad (2-6)$$

where T is in K and uncertainties are given at 1σ level. The above equation can reproduce experimental $\ln D$ values to within 0.49 $\ln D$ units, with 1σ uncertainty of 0.24 $\ln D$ units. Note that the above equation can only be applied to the case of anorthite dissolution in a basaltic melt due to limitations of EBDs.

Al₂O₃ diffusivity in lunar basalts (Finnila et al., 1994; Morgan et al., 2006) and terrestrial basalts during anorthite dissolution experiments (this study) are compared in Fig. 10a. Note that the Al₂O₃ diffusivities determined by Finnila et al. (1994) are only order-of-magnitude estimates according to the authors. The data in Fig. 2-10a show that limited Al₂O₃ diffusion data in lunar melts are scattered, though the calculated viscosity (calculated at 1300 °C) of the basaltic melt (~1.0 Pa·s) used by Finnila et al. (1994) is similar to those of the very low Ti and low Ti basaltic melts (~1.2 Pa·s and ~1.3 Pa·s) used by Morgan et al. (2006). The scatter is likely due to the fact that the diffusivities reported by Finnila et al. (1994) are only order-of-magnitude estimates.

To better understand the factors controlling the EBDs of Al₂O₃, diffusion data during dissolution experiments of various minerals (olivine, diopside, quartz, anorthite,

and spinel) and diffusion couple experiments in natural melts (lunar basalt, terrestrial basalt, and andesite) are compared in [Fig. 2-10b](#). The mineral dissolution data include those for corundum dissolution into $\text{CaSiO}_3\text{-Al}_2\text{O}_3$ melt (Cooper and Kingery, 1964) at 0.0001 GPa, dissolution of olivine, diopside, spinel, and quartz into an andesitic melt at 0.5-2 GPa (Zhang et al., 1989), anorthite dissolution into a lunar basalt at 0.0001 GPa (Finnila et al., 1994) and 0.6 GPa (Morgan et al., 2006), olivine and diopside dissolution into a basaltic melt (Chen and Zhang, 2008, 2009), and this study. The diffusion couple data include those in the diopside-anorthite system (Kubicki et al., 1990), the dacite-rhyolite system (Baker et al., 1988), and the tholeiite-basanite system (Lunstrom, 2003). The data are displayed in [Fig. 2-10b](#) and show that:

(1) Experimental pressure does not significantly affect the EBDs of Al_2O_3 , at least within the 0.5 to 2.0 GPa pressure range, consistent with the conclusion of weak pressure dependence by Chen and Zhang (2008, 2009).

(2) EBDs of Al_2O_3 during diffusive mineral dissolution experiments depend on the initial (far-field) melt composition or viscosity. For example, [Fig. 2-10b](#) shows that the Al_2O_3 diffusivities during mineral dissolution in andesitic melt obtained by Zhang et al. (1989) are less than those in basaltic melt (Chen and Zhang, 2008, 2009; this study), as expected. When the diffusivity model of Mungall (2002) is applied to calculate EBDs of Al_2O_3 (Mungall's model for Al diffusivity is largely related to melt viscosity) from mineral dissolution experiments ([Fig. 2-11a](#)), it works well for the data in this study and in Chen and Zhang (2008, 2009), but not so well for the data in Zhang et al. (1989) and Morgan et al. (2006).

(3) EBDs of Al_2O_3 during mineral dissolution experiments also vary with the interface melt composition. For instance, Al_2O_3 diffusivities in basaltic melts during olivine dissolution and during diopside dissolution are similar (Chen and Zhang, 2008, 2009), but they are different from those during plagioclase dissolution (Fig. 2-10b). In particular, the activation energy for Al_2O_3 diffusion during plagioclase dissolution is lower than that during olivine and diopside dissolution. Another example is quartz dissolution in andesitic melt (Zhang et al., 1989) in which the Al_2O_3 diffusivity is much smaller (Fig. 2-10b, labeled as “Qz, 234”) due to the very silicic composition of the interface melt. Preliminary modeling using a few simple compositional parameters cannot reconcile this datum with other data, but more complicated relations are not well constrained by the data.

After some trials, we approximate the compositional effect of $D_{\text{Al}_2\text{O}_3}$ in mineral dissolution experiments using a linear relation between $\ln D$ and $X_{\text{Si+Al}}$ of the far-field (initial) melt as well as that of the mineral. Because our goal is to understand the variation of $D_{\text{Al}_2\text{O}_3}$ in the melt during mineral dissolution experiments, and because the diffusion couple data cannot be treated the same way due to the presence of two far-field compositions, the diffusion couple data are not included in the treatment. For olivine, diopside and anorthite dissolution in basaltic melt JDF, we obtain

$$\ln D_{\text{Al}_2\text{O}_3}^{\text{EBD in basalt}} = -15.630(\pm 1.451)X_{\text{Si+Al}}^{\text{mineral}} - \frac{39863(\pm 158) - 23366(\pm 2255)X_{\text{Si+Al}}^{\text{mineral}}}{T} \quad (2-7)$$

where $X_{\text{Si+Al}}^{\text{mineral}}$ is cation mole fraction of Si+Al in the mineral, errors are given at 1σ level, and $r^2 = 0.938$. The above equation can reproduce the data in Chen and Zhang

(2008, 2009) and this study within 0.50 $\ln D$ units with 1σ reproducibility of 0.23 $\ln D$ units.

For the more extensive data on mineral dissolution in andesitic to basaltic melts (including lunar melts), excluding one quartz dissolution data point from Zhang et al. (1989) and the order-of-magnitude data from Finnila et al. (1994), the Al_2O_3 diffusivity data of Zhang et al. (1989), Morgan et al. (2006), Chen and Zhang (2008, 2009) and this study can be fitted as a function of experimental temperature, $X_{\text{Si+Al}}$ in the far-field melts and in the minerals as follows:

$$\ln D_{\text{Al}_2\text{O}_3}^{\text{EBD}} = -15.332(\pm 1.537)X_{\text{Si+Al}}^{\text{mineral}} - \frac{31983(\pm 898) + 12991(\pm 1303)X_{\text{Si+Al}}^{\text{melt},\infty} - 23157(\pm 2414)X_{\text{Si+Al}}^{\text{mineral}}}{T}, \quad (2-8)$$

where $X_{\text{Si+Al}}^{\text{melt},\infty}$ is the cation mole fraction of Si+Al in the far-field melt (H is included in the calculation), and $r^2 = 0.928$. The above equation can reproduce the data to within 0.72 $\ln D_{\text{Al}_2\text{O}_3}$ units with a 1σ uncertainty of 0.264 $\ln D$ units. The fit quality of this equation is shown in Fig. 2-11b. Cross-validation analyses (2-folds and 10-folds) of this model (eq. 2-8) and other models with fewer parameters were carried out, and the results show that eq. (2-8) gives the smallest mean square error (MSE) and hence does not over-fit the data. The effect of very high SiO_2 concentration in the melt on diffusivity (such as that during quartz dissolution) is not resolved in this study.

Comparing the fit of $D_{\text{Al}_2\text{O}_3}$ using eq. (2-8) as shown in Fig. 2-11b and the prediction using the model of Mungall (2002) as shown in Fig. 2-11a, it can be seen that our specific model predicts $D_{\text{Al}_2\text{O}_3}$ significantly better than the general model of Mungall (2002). Note that the model of Mungall (2002) is for tracer diffusivity and not for effective binary diffusivity. In addition, Mungall (2002) modeled the diffusivity of

Al₂O₃, SiO₂ and other high field strength elements to be the same and controlled primarily by viscosity. Hence, in a way, eq. (2-8) is similar to the diffusivity of Mungall (2002) in that $X_{\text{Si+Al}}$ in the melt is a main control of melt viscosity. On the other hand, melt viscosity cannot be the single control for the effective binary diffusivity of Al₂O₃, SiO₂ and other high field strength elements, because effective binary diffusivity of Al₂O₃ is about 50% larger than that of SiO₂ (e.g., Zhang et al., 1989), contrary to the assumption of identical diffusivities by Mungall (2002).

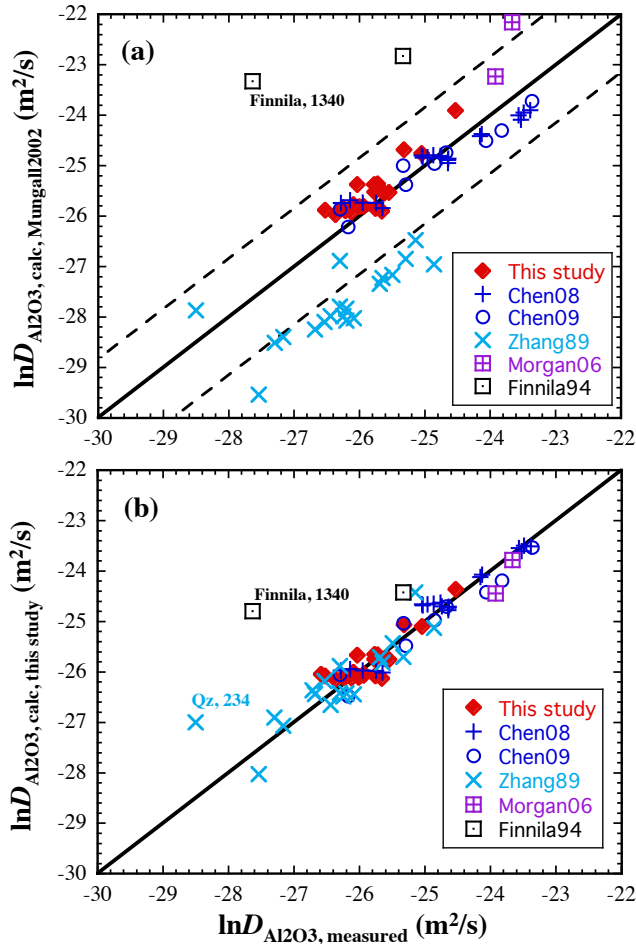


Figure 2-11. (a) Comparison of the calculated Al₂O₃ diffusivity using Mungall's model (2002) and the fitted EBD of Al₂O₃ of literature data. The solid line is the 1:1 line. The dashed lines are 0.5 $\log_{10} D$ units off the 1:1 line. (b) Comparison of the calculated EBD of Al₂O₃ using Eq. (2-8) and the fitted EBD of Al₂O₃ of literature data. The solid line is the 1:1 line.

2.4.3. Effective binary diffusivities of TiO₂, FeO_t, MgO, and CaO

The EBDs of TiO₂, FeO_t, and MgO are also obtained using the analytical solution (listed in [Table 2-3](#)); while fitting for CaO is only carried out when the semi-infinite boundary condition holds ([Table 2-3](#)). The EBDs of SiO₂ are not fitted, due to weak uphill diffusion of this component, a manifestation of multicomponent diffusion.

The diffusivity of TiO₂ is about 16% smaller than that of Al₂O₃ in the same anorthite dissolution experiment. The EBDs of FeO_t and MgO are similar and about 2.5 times that of Al₂O₃. Compared with the EBD data from olivine and clinopyroxene dissolution experiments (Chen and Zhang, 2008, 2009), the EBDs of TiO₂, FeO_t and MgO from this study are significantly smaller and give much smaller activation energies for diffusivity, indicating compositional as well as compositional-gradient dependences for EBDs of TiO₂, FeO_t and MgO. TiO₂ and FeO_t often show uphill diffusion in various dissolution situations (Zhang et al., 1989; Chen and Zhang, 2008, 2009), indicating multicomponent effects.

Though we have attempted to fit the EBDs of CaO using eqs. 2-1 and 2-2, there is sometimes systematic misfit ([Fig. 2-4](#)). CaO often displays multicomponent diffusion effects, manifested by the uphill diffusion in the CaO concentration profiles of in previous dissolution studies on olivine, forsterite, spinel, and rutile (Zhang et al., 1989; Chen and Zhang, 2008). Although no uphill diffusion pattern is apparent in our CaO concentration profiles, the multicomponent diffusion effect may still result in complicated diffusion behavior of CaO. In other words, the cross-component terms of the diffusivity matrix are as significant as the diagonal term for CaO, resulting in the complicated diffusion feature in CaO concentration profiles. It is likely that using

multicomponent approach can solve the issue. However, the set of experiments in this study cannot constrain the diffusivity matrix in an 8-component basaltic system (Trial and Spera, 1994).

2.4.4. Convective dissolution of anorthite in basaltic melt

The theory of convective crystal dissolution has been developed by Kerr (1995) and Zhang and Xu (2003), further verified by Zhang (2005) and Zhang and Xu (2008), and reviewed in Zhang (2008, 2013) and Liang (2010). To model convective dissolution or growth of anorthite in a basaltic melt requires knowledge of the densities of the melt and anorthite, the solubility and diffusivity of Al_2O_3 in the melt, the viscosity of the melt, the initial crystal size, the temperature and the pressure. The procedure for this modeling has been explained in Chen and Zhang (2008, 2009) in detail. The following calculation uses the basalt composition in [Table 2-1](#) with 0.3 wt% H_2O (Chen and Zhang, 2008). We have verified that ≤ 0.3 wt% H_2O does not affect significantly the anorthite-melt equilibrium temperature and viscosity at $\geq 1280^\circ\text{C}$, using the MELTS program and the viscosity model of Shaw (1972).

We calculated the melt density based on the model of Lange and Carmichael (1987) and Ochs and Lange (1999), the anorthite density ($\text{An}\# > 90$) based on the equation of state model of Angel (2004), and the melt viscosity based on the model of Hui and Zhang (2007). The dependence of anorthite density on temperature was obtained using the thermal expansion coefficient data from Tribaudino et al. (2010). The upper limit of pressure for applying the anorthite density model is 3 GPa. No viscosity model is available for basaltic melt at 1 GPa, but pressure does not significantly affect viscosity in

this pressure range (e.g., Hui et al., 2008). Hence, the viscosity model at 1 bar pressure conditions is used for pressures of ≤ 1 GPa pressure range. Based on the above models, anorthite dissolution in basaltic melt was modeled over a temperature range from 1100°C to 1500°C, a pressure range of 10^{-4} GPa to 1 GPa, and an anorthite composition range from An90 to An100.

The modeling results show that the Reynolds number (Re) ranges from 4×10^{-11} to ~ 1 for anorthite crystals of 1-8 mm effective radius. The steady-state falling/rising velocity of anorthite crystals in the melt is determined using Stokes' law, because Re is smaller than 1. The steady-state falling/rising velocity of anorthite is $\leq 2 \times 10^{-4}$ m/s for a 1-mm-radius single crystal, and ≤ 0.01 m/s for a 8-mm-radius crystal. Compared to the olivine dissolution estimates of Chen and Zhang (2008), the largest steady-state rising velocity in our anorthite convective dissolution model is about 1 order of magnitude smaller than the corresponding values of olivine, due to the smaller density difference between anorthite and the basaltic melt than that between olivine and the basaltic melt. [Fig. 2-12](#) shows the difference in density between anorthite (An#94) and MORB under different temperature and pressure conditions. In MORB, the typical density difference is less than 0.05 g/cc for anorthite, while that for olivine is about 0.5 g/cc. According to the Stokes' Law or eq. 7a-c in Chen and Zhang (2008), the steady rising/sinking velocity of a crystal is proportional to the crystal-melt density difference, while the boundary layer thickness increases as the crystal-melt density difference decreases. A thicker boundary layer slows the convective dissolution rate (Eq. 20 of Zhang et al, 1989). According to our modeling results, anorthite crystals of the same size can survive about 1 order of magnitude longer than olivine at the same temperature and pressure, while the maximum

rising distance is about an order of magnitude smaller than olivine's sinking distance (Fig. 2-13). When the temperature rises, the dissolution rate increases, and both the survival time and distance of the same-size anorthite crystal shorten. Unlike for olivine dissolution, the density difference between anorthite and basalt (with 0.3 wt% H₂O) becomes zero when temperature reaches ~1220°C at 0.2 GPa (but the density crossover depends on the H₂O content; e.g., a completely dry basaltic melt would have a density crossover at ~1455°C at 0.2 GPa). At zero density difference, the dissolution would be controlled by pure diffusion. When temperature further increases to above ~1220°C, the density of MORB drops below that of anorthite, resulting in anorthite sinking in the basaltic melt.

We hoped to model convective growth and flotation of anorthite crystals in the late stages of lunar magma ocean, which presumably led to the formation of the anorthosite crust of the moon. However, because the pressure effect of anorthite-melt equilibrium is small (Lange et al, 2009), and its relative magnitude compared to the geotherm of the late stage of lunar magma ocean is not resolved, this application must wait for future progress in understanding plagioclase-melt equilibrium in more detail. On the other hand, the weak pressure dependence is an advantage in predicting anorthite equilibrium temperature, and in predicting convective plagioclase crystallization/dissolution rate and rising/falling velocity in a magma chamber (Fig. 2-13) where the pressure variation is small. Moreover, the small pressure effect suggests that a small degree of undercooling would lead to plagioclase oversaturation in a large range of depths, resulting in the formation, growth and flotation of plagioclase, and possibly rapid formation of anorthosite crust.

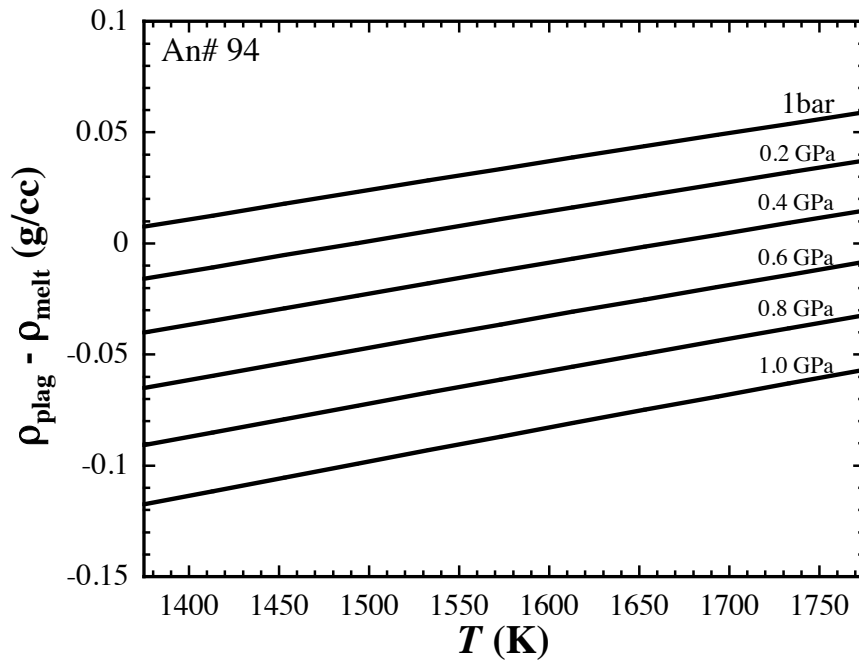


Figure 2-12. Density difference between anorthite (An#94) and MORB at 1100 – 1500°C and 10^{-4} – 1GPa.

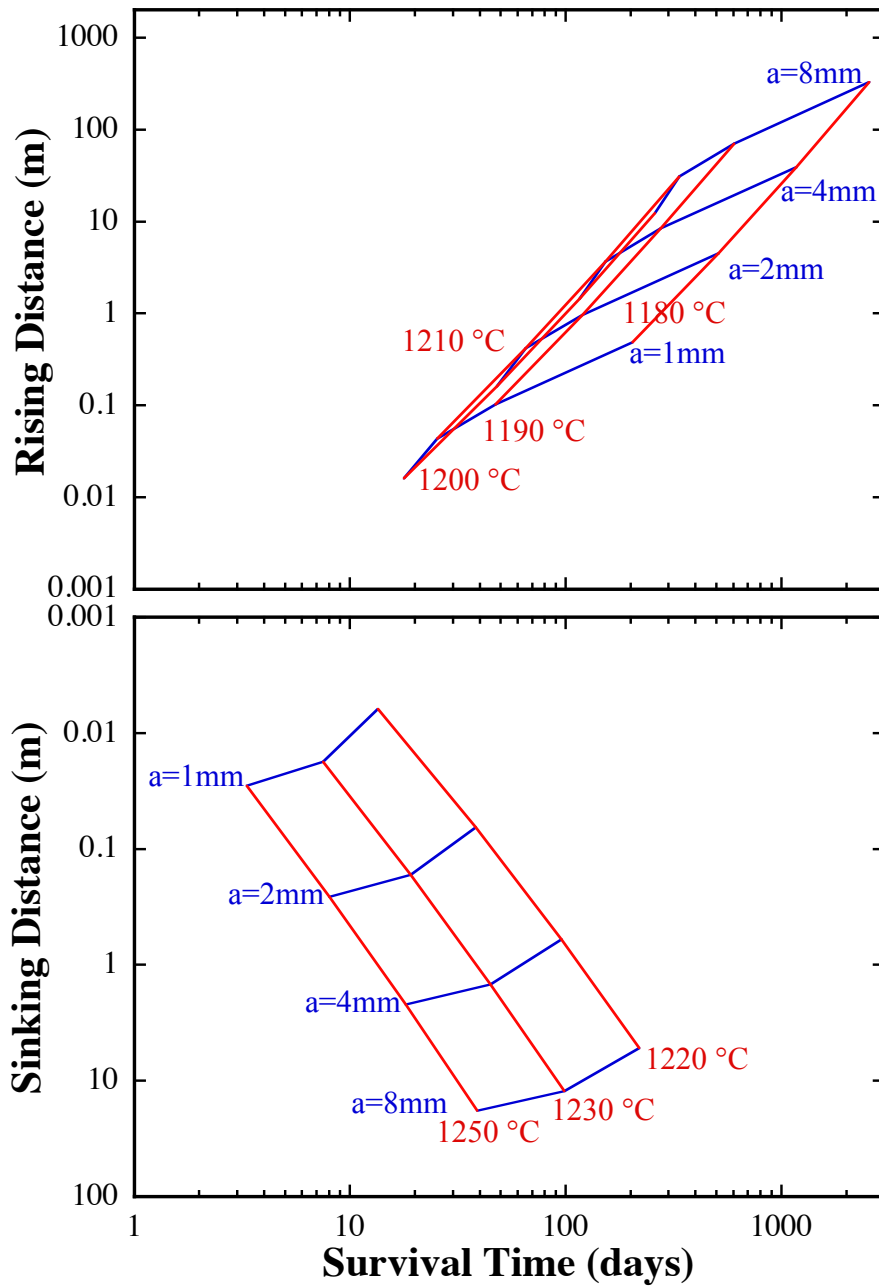


Figure 2-13. Falling/rising distance and survival time of a convectively dissolving anorthite crystal as a function of temperature and initial radius of the anorthite crystal (An#94) in MORB at 0.2 GPa.

2.5 Conclusion

1. Our time-series experiments (covering 1280~1400 °C, at 0.5 GPa) on olivine dissolution in a basaltic melt were unable to confidently resolve the variation of the interface Al_2O_3 concentration. Experiments for dissolution from two different crystallographic surfaces ($12\bar{1}$) and ($\bar{3}02$) of anorthite do not show anisotropic dissolution.

2. The overgrowth of the dissolution crystal during quench has been resolved well by high-spatial resolution EDS analyses.

3. The effective binary diffusivity of Al_2O_3 , FeO , MgO and TiO_2 , and the interface concentration of Al_2O_3 were obtained from experiments. The effective binary diffusivity of Al_2O_3 depends on the melt composition, which is approximately characterized by the cation mole fraction of (Si+Al) in the melt. The effective binary diffusivity of TiO_2 is just slightly smaller than that of Al_2O_3 , whereas those of FeO and MgO are about 2.5 times Al_2O_3 diffusivity.

4. The interface melt Al_2O_3 concentration data at anorthite near-saturation obtained in this work are consistent with literature data on anorthite-melt equilibrium. The pressure effect on anorthite-melt equilibrium temperature cannot be resolved from available data.

5. Our new data coupled with literature data allow quantitative modeling of the dissolution rate of a rising or sinking plagioclase in magma. Compared to the convective dissolution of olivine at a similar degree of undersaturation, plagioclase can survive for a longer time but would rise/sink for a shorter distance in a magma.

Acknowledgements

We thank Pavel Izbekov and Owen Neill for providing the anorthite crystals, Keith Putirka for providing his collection of literature data regarding plagioclase-melt equilibrium, and Jeff Kampf for helping with the single crystal XRD analysis of anorthite crystals. Constructive formal reviews by Cliff Shaw, Conel Alexander, Mike Toplis, Yan Liang, and an anonymous reviewer are highly appreciated. Y. Yu thanks Gordon Moore and Leslie Hayden for training and help on electron microprobe analyses. This research is supported by NSF grants EAR-1019440 and EAR-1524473 and NASA grant NNX15AH37G. Electron microprobe work is carried out on a Cameca SX100 instrument at Electron Microbeam Analysis Laboratory of the University of Michigan, which was supported by NSF grant EAR-9911352.

References

- Acosta-Vigil A., London D. and Dewers T.A., Morgan, G.B. (2002) Dissolution of corundum and andalusite in H₂O-saturated haplogranitic melts at 800 C and 200 MPa: constraints on diffusivities and the generation of peraluminous melts. *J. Petrol.* 43, 1885-1908.
- Acosta-Vigil A., London D., Morgan G.B. and Dewers, T.A. (2006) Dissolution of quartz, albite, and orthoclase in H₂O-saturated haplogranitic melt at 800 C and 200 MPa: Diffusive transport properties of granitic melts at crustal anatexis conditions. *J. Petrol.* 47, 231-254.
- Alexander, C. M. D. (2011). Modeling diffusive dissolution in silicate melts. *Geochim. Cosmochim. Acta* 75, 588-607.
- Angel R.J. (2004) Equations of state of Plagioclase Feldspars. *Contrib. Mineral. Petrol.* 146, 506-512.
- Asimow P.D. and Ghiorso M.S. (1998) Algorithmic modifications extending MELTS to calculate subsolidus phase relations. *Am. Mineral.* 83, 1127-1132.
- Baker D.R., Conte A., Freda C. and Ottolini, L. (2002) The effect of halogens on Zr diffusion and zircon dissolution in hydrous metaluminous granitic melts. *Contrib. Mineral. Petrol.* 142, 666-678.
- Baker, D.R., and Watson, E.B. (1988) Diffusion of major and trace elements in compositionally complex Cl- and F-bearing silicate melts. *J. Non-Cryst. Solids.* 102(1), 62-70.
- Chen Y. and Zhang Y. (2008) Olivine dissolution in basaltic melt. *Geochim. Cosmochim. Acta* 72, 4756-4777.

- Chen Y. and Zhang Y. (2009) Clinopyroxene dissolution in basaltic melt. *Geochim. Cosmochim. Acta* 73, 5730-5747.
- Clift R., Grace J. and Weber, M. (1978) *Bubbles, Drops and Particles*. Academic Press. New York.
- Cooper JR A.R. and Kingery, W.D. (1964) Dissolution in ceramic systems: I, molecular diffusion, natural convection, and forced convection studies of sapphire dissolution in calcium aluminum silicate. *J. Am. Ceram. Soc.* 47, 37-43
- Cooper JR A.R. (1968) The use and limitations of the concept of an effective binary diffusion coefficient for multicomponent diffusion. *Mass Transport in Oxides*, 296, 79-84
- Dixon J.E., Clague D.A. and Eissen J.A. (1986) Gabbroic xenoliths and host ferrobasalt from the southern Juan de Fuca Ridge. *J. Geophys. Res.* 91, 3795-3820.
- Dixon J.E., Stolper E. and Delaney J.R. (1988) Infrared spectroscopic measurements of CO₂ and H₂O in Juan de Fuca Ridge basaltic glasses. *Earth Planet. Sci. Lett.* 90, 87-104.
- Donaldson C.H. (1985) The rates of dissolution of olivine, plagioclase, and quartz in a basalt melt. *Mineral. Mag.* 49, 683-693.
- Drake M.J. (1976) Plagioclase-melt equilibria. *Geochim. Cosmochim. Acta* 40, 457-465.
- Finnila A., Hess P. and Rutherford M. (1994) Assimilation by lunar mare basalts: Melting of crustal material and dissolution of anorthite. *J. Geophys. Res.* 99, 14677-14690.
- Ghiorso M.S. and Sack R.O. (1995) Chemical mass transfer in magmatic processes IV. A revised and internally consistent thermodynamic model for the interpolation and

extrapolation of liquid-solid equilibria in magmatic systems at elevated temperatures and pressures. *Contrib. Mineral. Petrol.* 119, 197-212.

Ghiorso M.S., Hirschmann M.M., Reiners P.W. and Kress V.C. (2002) The pMELTS: A revision of MELTS for improved calculation of phase relations and major element partitioning related to partial melting of the mantle to 3 GPa. *Geochem. Geophys. Geosyst.* 3, 1-35.

Grove T. and Beaty D. (1980) Classification, experimental petrology and possible volcanic histories of the Apollo 11 high-K basalts, *P. Lunar Planet. Sci. C.*, 149-177.

Grove T.L., Kinzler R.J. and Bryan, W.B. (1992) Fractionation of mid-ocean ridge basalt (MORB). *Geoph. Monog. Series* 71, 281-310.

Grove T.L. and Raudsepp M. (1978) Effects of kinetics on the crystallization of quartz normative basalt 15597-an experimental study, *P. Lunar Planet. Sci. C.*, 585-599.

Harrison T.M. and Watson, E.B. (1983) Kinetics of zircon dissolution and zirconium diffusion in granitic melts of variable water content. *Contrib. Mineral. Petrol.* 84, 66-72.

Hui H. and Zhang Y. (2007) Toward a general viscosity equation for natural anhydrous and hydrous silicate melts. *Geochim. Cosmochim. Acta* 71, 403-416.

Hui H., Zhang Y., Xu Z. and Behrens H. (2008) Pressure dependence of the speciation of dissolved water in rhyolitic melts. *Geochim. Cosmochim. Acta* 72, 3229-3240.

James G., Witten D., Hastie T. and Tibshirani R. (2013) *An Introduction to Statistical Learning.* Springer, New York.

Johnston A.D. (1986) Anhydrous PT phase relations of near-primary high-alumina basalt from the South Sandwich Islands. *Contrib. Mineral. Petrol.* 92, 368-382.

- Jurewicz A., Mittlefehldt D. and Jones J. (1993) Experimental partial melting of the Allende (CV) and Murchison (CM) chondrites and the origin of asteroidal basalts. *Geochim. Cosmochim. Acta* 57, 2123-2139.
- Kerr R.C. (1995) Convective crystal dissolution. *Contrib. Mineral. Petrol.* 121, 237-246.
- Kinzler R.J. and Grove T.L. (1985) Crystallization and differentiation of Archean komatiite lavas from Northeast Ontario; phase equilibrium and kinetic studies. *Am. Mineral.* 70, 40-51.
- Kirkpatrick, R.J., Robinson, G.R., Hays, J.F., 1976. Kinetics of crystal growth from silicate melts: anorthite and diopside. *J. Geophys. Res.* 81, 5715-5720.
- Kubicki, J.D., Muncill, G.E., & Lasaga, A.C. (1990) Chemical diffusion in melts on the CaMgSi₂O₆-CaAl₂Si₂O₈ join under high pressures. *Geochim. Cosmochim. Acta* 54, 2709-2715.
- Lange R.A. and Carmichael I.S. (1987) Densities of Na₂O-K₂O-MgO-MgO-FeO-Fe₂O₃-Al₂O₃-TiO₃-SiO₃ liquids: New measurements and derived partial molar properties. *Geochim. Cosmochim. Acta* 51, 2931-2946.
- Lange R.A., Frey H.M. and Hector J. (2009) A thermodynamic model for the plagioclase-liquid hygrometer/thermometer. *Am. Mineral.* 94, 494-506.
- Levich V.G. (1962) *Physicochemical Hydrodynamics*. Prentice-Hall, Englewood Cliffs, NJ.
- Liang Y. (1999) Diffusive dissolution in ternary systems: Analysis with applications to quartz and quartzite dissolution in molten silicates. *Geochim. Cosmochim. Acta* 63, 3983-3995.

- Liang Y. (2000) Dissolution in molten silicates: effects of solid solution. *Geochim. Cosmochim. Acta* 64, 1617-1627.
- Liang Y. (2003) Kinetics of crystal-melt reaction in partially molten silicates: 1. Grain scale processes. *Geochem. Geophys., Geosyst.* 4, 1045
- Liang Y. (2010) Multicomponent diffusion in molten silicates: theory, experiments, and geological applications. *Rev. Mineral. Geochem.* 72, 409-446.
- Lindsley D.H. (1968) Melting relations of plagioclase at high pressures. *Origin of anorthosite and related rocks (YW Isachsen, ed.)*, Mem 18, 39-46.
- Longhi J. and Pan V. (1988) A reconnaissance study of phase boundaries in low-alkali basaltic liquids. *J. Petrol.* 29, 115-147.
- Lundstrom, C.C. (2003) An experimental investigation of the diffusive infiltration of alkalis into partially molten peridotite: implications for mantle melting processes. *Geochem. Geophys. Geosyst.* 4, 8614.
- Morgan Z., Liang Y. and Hess, P. (2006) An experimental study of anorthosite dissolution in lunar picritic magmas: Implications for crustal assimilation processes. *Geochim. Cosmochim. Acta* 70, 3477-3491.
- Morse S. (1980) Basalts and Phase Diagrams: An Introduction to the Quantitative Use of Phase Diagrams in Igneous Petrology. *Springer*.
- Mungall, J. E. (2002). Empirical models relating viscosity and tracer diffusion in magmatic silicate melts. *Geochim. Cosmochim. Acta.* 66, 125-143.
- Namur O., Charlier B., Toplis M.J. and Vander Auwera J. (2012) Prediction of plagioclase-melt equilibria in anhydrous silicate melts at 1-atm. *Contrib. Mineral. Petrol.* 163, 133-150.

- Niu Y., Gilmore T., Mackie S., Greig A. and Bach W. (2002) Mineral chemistry, whole-rock compositions and petrogenesis of Leg 176 gabbros: data and discussion. *Proc. ODP, Sci. Results* 176, 1-60
- Ochs F.A. and Lange, R.A. (1999) The density of hydrous magmatic liquids. *Science* 283, 1314-1317.
- Panjasawatwong Y., Danyushevsky L.V., Crawford A.J. and Harris K.L. (1995) An experimental study of the effects of melt composition on plagioclase-melt equilibria at 5 and 10 kbar: implications for the origin of magmatic high-An plagioclase. *Contrib. Mineral. Petrol.* 118, 420-432.
- Putirka K.D. (2005) Igneous thermometers and barometers based on plagioclase + liquid equilibria: Tests of some existing models and new calibrations. *Am. Mineral.* 90, 336-346.
- Salge, T., 2012. EDS analysis with silicon drift detectors at high spatial resolution. *G.I.T. Imaging and Microscopy*, 19-21.
- Shaw C.S.J. (2000) The effect of experiment geometry on the mechanism and rate of dissolution of quartz in basanite at 0.5 GPa and 1350 C. *Contrib, Mineral. Petrol.* 139, 509-525.
- Shaw C.S.J. (2004) Mechanisms and rates of quartz dissolution in melts in the CMAS (CaO-MgO-Al₂O₃-SiO₂) system. *Contrib. Mineral. Petrol.* 148, 180-200.
- Shaw C.S.J. (2006) Effects of melt viscosity and silica activity on the rate and mechanism of quartz dissolution in melts of the CMAS and CAS systems. *Contrib. Mineral. Petrol.* 151, 665-680.

- Shaw C.S.J. (2012) The effects of potassium addition on the rate of quartz dissolution in the CMAS and CAS systems. *Contrib. Mineral. Petrol.* 164, 839-857.
- Shaw H. (1972) Viscosities of magmatic silicate liquids; an empirical method of prediction. *Am. J. Sci.* 272, 870-893.
- Stolper E. (1977) Experimental petrology of eucritic meteorites. *Geochim. Cosmochim. Acta* 41, 587-611.
- Sugawara T. (2000) Empirical relationships between temperature, pressure and MgO content in olivine and pyroxene saturated liquid. *J. Geophys. Res.* 105, 8457-8472.
- Sugawara T. (2001) Ferric iron partitioning between plagioclase and silicate liquid: thermodynamics and petrological applications. *Contrib. Mineral Petrol.* 141, 659-686.
- Trial A. F. and Spera F. J. (1994) Measuring the multicomponent diffusion matrix: experiemntal design and data analysis for silicate melts. *Geochim. Cosmochim. Acta* 58, 3769-3783
- Tribaudino M., Angel R.J., Camara F., Nestola F., Pasqual D. and Margiolaki I. (2010) Thermal expansion of plagioclase feldspars. *Contrib. Mineral. Petrol.* 160, 899-908.
- Waythomas C.F., Scott W.E., Prejean S.G., Schneider D.J., Izbekov P. and Nye C.J. (2010) The 7-8 August 2008 eruption of Kasatochi Volcano, central Aleutian Islands, Alaska. *J. Geophys. Res.: Solid Earth* 115.
- Yang H.J., Kinzler R.J. and Grove T. (1996) Experiments and models of anhydrous, basaltic olivine-plagioclase-augite saturated melts from 0.001 to 10 kbar. *Contrib. Mineral. Petrol.* 124, 1-18.

- Zhang Y. (2005) Fate of rising CO₂ droplets in seawater. *Environ. Sci. Technol.* 39, 7719-7724.
- Zhang Y. (2008) *Geochemical kinetics*. Princeton University Press, Princeton, NJ.
- Zhang Y. (2013) Kinetics and dynamics of mass-transfer-controlled mineral and bubble dissolution or growth: a review. *Eur. J. Mineral.* 25, 255-266.
- Zhang Y. and Xu Z. (2003) Kinetics of convective crystal dissolution and melting, with applications to methane hydrate dissolution and dissociation in seawater. *Earth Planet. Sci. Lett.* 213, 133-148.
- Zhang Y. and Xu Z. (2008) “Fizzics” of bubble growth in beer and champagne. *Elements* 4, 47-49.
- Zhang Y., Walker D. and Lesher C.E. (1989) Diffusive crystal dissolution. *Contrib. Mineral. Petrol.* 102, 492-513.

Chapter III

Kinetics of quartz dissolution in silicate melts²

Abstract

As the most abundant component in silicate melts, SiO₂ diffusion plays major roles in controlling the kinetics and dynamics of various igneous processes, such as quartz growth or dissolution, magma mixing, etc. The diffusivity of SiO₂ is small and highly dependent on melt compositions (Watson, 1982; Lesher and Walker, 1986; Koyaguchi, 1989), but has not been well characterized in various melts. We conducted quartz dissolution experiments in rhyolitic (0.1wt% H₂O, 73 wt% SiO₂) and basaltic (~0.3 wt% H₂O, and 50 wt% SiO₂) melts at 1300-1600 °C. All experiments were conducted at 0.5 GPa using piston cylinder apparatus. Combined with other data from our lab and literature, we show that $\ln D_{\text{SiO}_2}$ decreases linearly with X , where X is the cation mole fraction of Si+Al in melts, instead of just the SiO₂ concentration across different silicate melt systems (rhyolitic to andesitic to basaltic), and the effect of H₂O is also captured by X when H₂O is included in the cation mole fraction calculation. By fitting concentration profiles of quartz dissolution experiments at different temperatures using $D_{\text{SiO}_2} = D_0 e^{a(1-X)}$, the results show that the parameter a is roughly composition-independent across all experiments and is linear to $1/T$:

² The work in this chapter has been submitted to the journal *Geochimica et Cosmochimica Acta*, and is currently in review process.

$$a = -0.552 (\pm 1.322) + 38650(\pm 2188)/T, \quad r^2 = 0.948.$$

The parameter D_0 (in m^2/s) can be expressed as:

$$\ln D_0 = -13.308(\pm 2.105) - 35253(\pm 3482)/T, \quad r^2 = 0.858.$$

Hence, for quartz dissolution in rhyolitic, andesitic and basaltic melts,

$$D_{\text{SiO}_2}^{\text{quartz dissolution}} = 1.661 \times 10^{-6} \exp\left(0.552(X-1) - \frac{35253 + 38650(X-1)}{T}\right),$$

where $X > 0.6$ in the melts used in our experiments. Based on these results, a diffusive dissolution model of quartz in rhyolitic and basaltic melts is further presented.

3.1. Introduction

Quartz is a major mineral in silicic igneous rocks. A good understanding of the kinetic interaction between quartz and silicate melts can help shed light on modeling of quartz growth and dissolution in melts. There have been many studies on different aspects of quartz dissolution in various silicate melts. For example, [Watson \(1982\)](#) studied the quartz dissolution in basaltic melt with an emphasis on a convective dissolution schema. [Zhang et al. \(1989\)](#) conducted one quartz dissolution experiment in an andesitic melt. [Liang \(1999\)](#) investigated the diffusivity matrix during the quartz dissolution in a ternary CAS ($\text{CaO-Al}_2\text{O}_3\text{-SiO}_2$) melt system. [Shaw \(2000, 2004, 2006, 2012\)](#) and [Acosta-Vigil \(2006\)](#) focused on the interface reaction between quartz and natural and various synthetic melts. Though all these works have provided insightful

understanding regarding different aspects of quartz dissolution kinetics, there are still missing pieces on quartz dissolution kinetics, such as how to quantify quartz dissolution rate, and SiO₂ diffusivities in different silicate melts. Therefore it is necessary to systematically investigate the kinetics of quartz dissolution in different silicate melts at various conditions.

Mineral dissolution may be controlled by either mineral-melt interface reaction or mass transport of the mineral-constituent components in the melts (Zhang et al. 1989). In the scenario of the diffusive mineral dissolution, the interface reaction is rapid so that mineral dissolution is diffusion-controlled. A good understanding of the diffusion of mineral-constituent components in the melt would therefore provide insights regarding the mineral dissolution kinetics. As the only constituent of quartz, SiO₂ is also the most dominant component in silicate melts. SiO₂ diffusion in silicate melts plays a major role not only in quartz dissolution/ growth but also in a wide spectrum of igneous processes, including magma assimilation, double diffusive convection, magmatic volatile transport of SiO₂, etc. Extensive studies on SiO₂ diffusion have been carried out (see review by [Zhang et al., 2010](#)), and include both SiO₂ self-diffusion and SiO₂ effective binary diffusion (EBD, [Cooper, 1968](#)). Self-diffusivities were obtained primarily from Si isotopic tracer diffusion experiments in various synthetic and natural silicate melt systems ([Leshner et al., 1996](#); [Liang et al., 1996](#); [Reid et al., 2001](#); [Tinker and Leshner, 2001](#); [Tinker et al., 2003](#)). Effective binary diffusivity coefficients (EBDCs) include results from diffusion-couple experiments ([Watson, 1982](#); [Koyaguchi, 1989](#); [Kubicki et al., 1990](#); [Baker, 1988, 1990, 1991, 1993](#); [Baker and Bossanyi, 1994](#); [van der Laan et al., 1994](#); [Lundstrom, 2003](#)), mineral dissolution experiments ([Zhang et al., 1989](#); [Chen and](#)

Zhang, 2008, 2009; Yu et al., 2016; Yang et al., submitted), and Soret diffusion experiments (Lesher and Walker, 1986). In diffusion-couple studies, EBDCs of SiO₂ are often expressed to depend exponentially on the SiO₂ concentration in the melt based on Boltzman-Matano analysis (Watson, 1982; Koyaguchi, 1989) for each experiment. Though such dependence on the concentrations has been observed, it has not been quantified systematically (Fig. 22 in Zhang et al., 2010). In contrast to the diffusion-couple studies, EBDCs of SiO₂ in mineral dissolution studies were often treated as constant, though there is sometimes noticeable difference between the data and the constant-diffusivity fit (e.g. the quartz dissolution experiment of Zhang et al., 1989; Shaw, 2012), which is likely due to the compositional dependence of SiO₂ diffusivity.

To quantify the kinetics of quartz dissolution in silicate melts and SiO₂ diffusion during the dissolution process, we have conducted two series of quartz dissolution experiments in rhyolitic and basaltic melts respectively. Combined with cassiterite dissolution experiments in various hydrous rhyolitic melt (Yang et al., submitted), we focus on characterizing the compositional dependence of SiO₂ diffusivities during quartz dissolution in rhyolitic, andesitic and basaltic melts. Using these results, we further developed a diffusive dissolution model of quartz in rhyolitic and basaltic melts.

3.2. Samples, experiments and analyses

Gem-quality quartz crystals, natural and synthetic rhyolitic and basaltic glasses were used in the dissolution experiments conducted in a ½ inch piston-cylinder apparatus. The quartz crystals are essentially pure SiO₂ (Table 3-1). The rhyolitic glasses include

NCO, CIT, KS, and H6a with water concentrations of 0.1, 0.1, 0.9, and 5.9 wt%, respectively. NCO, CIT and KS are natural rhyolites (Newman et al., 1986), and H6a is a synthetic rhyolitic glass prepared in the study of Hui et al. (2008). The basaltic glass is a MORB glass sample from the Juan de Fuca Ridge (Dixon et al., 1986, 1988), the same as that used by Chen and Zhang (2008) and Yu et al. (2016). The water content in the basaltic glass is 0.25-0.40 wt%, based on the analyses by Chen and Zhang (2008). The compositions of the starting melts are listed in Table 3-1.

Table 3-1. Compositions of quartz, cassiterite, and rhyolitic and basaltic glasses.

Oxides	Minerals		Rhyolitic Glass				Basaltic Glass
	Quartz	Cassiterite	NCO	CIT	KS	H6a	JDF
SiO ₂	99.78)	-	72.89	76.3	76.46	74.67	49.9
SnO ₂	nd	99.86	nd	-	-	-	nd
TiO ₂	0.01	-	0.22	0.05	0.06	0.26	1.83
Al ₂ O ₃	0.12	-	14.23	12.98	12.43	13.44	13.53
FeO _t	0.11	0.2	1.93	0.91	1.02	1.72	12.93
MnO	0.01	-	0.06	nd	nd	nd	0.22
MgO	-	-	0.18	0.02	0.03	0.27	6.81
CaO	0.02	-	0.86	0.41	0.49	1.22	10.81
Na ₂ O	-	-	4.73	4.06	4.25	3.92	2.65
K ₂ O	0.01	-	4.24	5.28	5.01	4.49	0.17
H ₂ O	-	-	0.1	0.1	0.9	5.9	0.32
Dry total	100.06	99.88	99.35	100.01	99.75	99.99	98.85

nd means not determined

KS and H6a compositions are given on an anhydrous basis,

Water content in JDF is given by averaging the range 0.25-0.4 wt% H₂O given by Chen and Zhang (2008)

Starting quartz crystals were prepared into small round disks with the surface perpendicular to its c axis. The disks are of ~1 mm in thickness, and ~2.4-2.6 mm in

diameter. Rhyolitic and basaltic glasses were ground into cylinders about ~2 mm in length and ~2.4-2.6 mm in diameter. With one side well polished, one piece of crystal disk and one piece of glass cylinder were stacked together on the polished side, and then packed into a graphite capsule. To ensure the gravitational stability in the melt, the quartz disk was on top of the glass cylinder. The capsule design is similar to that used in the plagioclase dissolution experiments by [Yu et al. \(2016\)](#).

According to the SiO₂ phase diagram ([Fig. 6 in Hudon et al., 2002](#)), β -quartz is stable between ~750 and ~1650 °C at 0.5 GPa. The quartz dissolution experiments were carried out in β -quartz stability field at 1300-1600 °C and 0.5 GPa. At all experimental temperature and pressure conditions, the corresponding glass samples were molten. Experimental durations were accordingly chosen to be long enough to obtain measurable concentration profiles, but still short enough to comply with the semi-infinite boundary condition. Time-series experiments were implemented to rule out convection in the molten glass and to check the reproducibility of our experiments. A summary of all the experimental conditions is listed in [Table 3-2](#). During each experimental run, the temperature and pressure conditions were maintained automatically using a programmed temperature controller and a pressure controller. The variation in experimental temperature is 1 °C, and that in pressure is within 4 MPa. The experimental procedure has been detailed in [Yu et al. \(2016\)](#). Reported temperatures and pressures in [Table 3-2](#) have been corrected using the temperature gradient calibration of [Hui et al. \(2008\)](#) and pressure calibration of [Ni and Zhang. \(2008\)](#).

After quench of each experiment, the sample assembly was mounted in epoxy and then ground and polished along the central axis of symmetry, until the exposed area of

the sample reached near maximum. The well-polished sample was further cleaned using ultrasonic cleaner, dried in a vacuum oven, and carbon-coated before Electron Probe Microanalyzer (EPMA) analysis using a Cameca SX100 electron microprobe at the University of Michigan. The analysis condition was 15 kV and 5 nA focused beam. Counting times are 60 s for Si, 40 s for Al, 30 s for Fe, Ca, and K, 20 s for Mg and Ti, and 10 s for Mn. Na was counted as one of the first elements on a spectrometer for six 5-second periods, and then extrapolated to zero time. Three to four concentration traverses in the glass were measured for each dissolution experiment sample, starting from the mineral-glass interface to the far-field melt. The effect of quench cracks in the glass on distances of measured points to interface was corrected by cross-matching different traverses across the cracks. The method has also been used and detailed in [Yu et al. \(2016\)](#). The electron microprobe data of all experimental samples is provided in the [Appendix F](#).

Cassiterite dissolution experiments and data are from and described in [Yang et al. \(submitted\)](#). Cassiterite dissolution experiments were carried out in rhyolitic melt containing 0.1-5.9 wt% H₂O and at 750-1100 °C and 0.5 GPa. The goal of the experiments is to investigate tin diffusion and cassiterite dissolution kinetics. However, some experiments display resolvable and significant SiO₂ concentration profiles, which provide some constraints on SiO₂ diffusion and are used in this study. [Table 3-2](#) also includes a summary of these experiments.

Table 3-2. Summary of experimental conditions.

Type	Exp#	Melt used	T (°C)	Duration (s)	L_{melt} (μm)	L_{mineral} (μm)
Quartz dissolution in rhyolitic melt	QzDisRh103	NCO	1303	172811	12.5	11.6
	QzDisRh111		1304	87060	14.8	13.7
	QzDisRh112		1305	43219	9.0	8.3
	QzDisRh115		1293	346258	24.1	22.3
	QzDisRh201		1294	21583	6.4	5.9
	QzDisRh203		1292	86397	12.9	11.9
	QzDisRh105		1408	86433	36.5	33.8
	QzDisRh113		1414	44970	20.9	19.3
	QzDisRh114		1403	21627	21.2	19.6
	QzDisRh102		1505	14386	17.2	15.9
	QzDisRh104		1501	86432	50.3	46.5
	QzDisRh106		1600	14435	43.8	40.5
	Quartz dissolution in basaltic melt		QzDisBa101	JDF	1293	3667
QzDisBa102		1306	918		17.6	19.2
QzDisBa103		1304	257		8.6	9.4
QzDisBa110		1394	1232		39.1	42.6
QzDisBa111		1400	318		17.4	19.0
QzDisBa104		1508	928		43.3	47.2
QzDisBa107		1576	322		34.9	38.1
Cassiterite dissolution in rhyolitic melt	CassDis8	H6a	950	239	1.5	0.5
	CassDis9		750	634	--	--
	CassDis6		850	299	--	--
	CassDis12		850	1519	--	--
	CassDis10	KS	900	18026	0.4	0.1
	CassDis3		1000	18092	2.4	0.8
	CassDis1		1100	1856	1.6	0.5
	CassDis11	CIT	1000	18000	2.2	0.7
CassDis13	1100		3633	--	--	

All experiments were conducted at 0.5 GPa pressure condition.

Experimental temperature T is the corrected temperature using the procedure developed by Hui et al., 2008.

Melt growth distance L_{melt} is calculated from SiO_2 concentration profiles using mass balance for quartz dissolution and cassiterite dissolution experiments; mineral dissolution distance (L_{mineral}) is further

calculated by using $L_{\text{mineral}} = L_{\text{melt}} \frac{\rho_{\text{melt}}}{\rho_{\text{mineral}}}$, β -quartz density of 2.54 g/cc; NCO, KS and CIT densities

of 2.35 g/cc; H6a density of 2.28 g/cc; JDF basalt density of 2.77 g/cc; cassiterite density of 6.99 g/cc.

3.3. Experimental results

A list of run conditions of all experiments is summarized in [Table 3-2](#). There are 12 experiments on the quartz dissolution in Newberry rhyolitic melt (NCO), 7 experiments on the quartz dissolution in JDF basaltic melt, and 9 experiments on the cassiterite dissolution in various dry and hydrous rhyolitic melts (CIT, KS and H6a). We will include only 5 (CassDis1, 3, 8, 10, and 11) of the 9 cassiterite dissolution experiments in this work because in the other 4 experiments (CassDis6, 9, 12 and 13) there are no discernible SiO₂ concentration profiles to constrain SiO₂ diffusivities. [Figure 3-1](#) shows the Back Scatter Electron (BSE) image of a typical sample, with measured EPMA traverses marked on them. By comparing all measured traverses within the same experiment, the corresponding concentration profiles are shown to be consistent within errors, supporting no convection during the experiments. Agreements between time-series experiments further support no convection. In quartz dissolution experiments, SiO₂ concentration decreases from the interface melts toward the far-field melts. [Figures 3-2](#) and [3-3](#) show examples of oxide concentration profiles during quartz dissolution in rhyolitic and basaltic melts, respectively. As quartz dissolves into rhyolitic melt, the SiO₂ concentration increases toward the quartz-melt interface, and the concentrations of other components (e.g. TiO₂, Al₂O₃, FeO_t, MgO, CaO, Na₂O, and K₂O) are expected to be diluted and to decrease toward the interface. For quartz dissolution into rhyolitic melts, the profiles of these other components exhibit the “expected” pattern. During quartz dissolution in basaltic melt, the profiles of SiO₂, TiO₂, Al₂O₃, FeO_t, MgO, and CaO also show the “expected” behavior. However, Na₂O and K₂O profiles demonstrate complex uphill diffusion patterns in the basaltic melt, with Na₂O profile showing a maximum and

K₂O profile diffusing against its concentration gradient without a visible maximum. For those components with normal diffusion pattern, the concentration profiles cannot be fit well by assuming constant diffusivity (Fig. 3-2 and 3-3). In Fig. 3-4 and 3-5, normalized major oxide concentration profiles of two quartz dissolution experiments in a rhyolitic melt and a basaltic melt are compared respectively. The lengths of the concentration profiles do not match previously observed differences in the tracer diffusivities (Zhang et al., 2010): e.g., in Fig. 3-4, K₂O profile is the shortest and Na₂O profile is about the same length as the SiO₂ profile, even though Na and K tracer diffusivities are much higher than SiO₂ diffusivity. These features demonstrate that the effective binary diffusion of other components is largely controlled by the SiO₂ diffusion profile (Watson, 1982). In cassiterite dissolution experiments, SiO₂ concentration decreases toward the cassiterite-melt interface as the dissolution of cassiterite dilutes all other components in the melt except SnO₂.

Figure 3-6 shows temporal variations of interface melt concentrations of SiO₂ and melt growth distances at different temperature conditions for quartz dissolution. The interface SiO₂ concentrations were obtained by fitting the SiO₂ concentration profiles and extrapolating the profile to the interface position. The fitting procedure will be discussed in section 4. Since the amount of quartz dissolved is small or indiscernible, direct measurements of the dissolution distance using microscope or BSE were difficult to carry out and unreliable. Consequently, the melt growth distance was first calculated based on mass balance at the interface. That is, at the interface boundary, the cumulative (integral) increase of SiO₂ across the melt equals to the amount of SiO₂ dissolved from the quartz crystal (Zhang et al., 1989). With density correction ($L_{\text{mineral}} = L_{\text{melt}} \frac{\rho_{\text{melt}}}{\rho_{\text{mineral}}}$), the quartz

dissolution distance was indirectly calculated from the melt growth distance. Because microprobe distances are measured at room temperature and pressure, glass density rather than melt density is used. Because the dissolving mineral during the experiments is β -quartz (not α -quartz), the estimated density of β -quartz, about 2.54 g/cc at room temperature and pressure conditions (Bourova and Richet, 1998; Hudon et al, 2002) is used. That is, the reported crystal dissolution distance is for β -quartz dissolution. For cassiterite, it is about 6.99 g/cc (Yang et al, submitted). Densities of rhyolitic glasses were calculated using the density equation $(2.350/(1 + 0.31X_{\text{H}_2\text{O}}))$ by Zhang (1999), where $X_{\text{H}_2\text{O}}$ is the mole fraction of H_2O on a single-oxygen basis in the rhyolitic glass. For NCO, CIT, and KS rhyolitic glasses, the density is about 2.35 g/cc; and for H6a rhyolitic glass, it is about 2.28 g/cc. Density of basaltic glass is about 2.77 g/cc at ambient temperature and pressure conditions (Tilley, 1922). For the quartz dissolution in rhyolite experiments, the SiO_2 concentrations at the interface melts remain roughly the same within errors at a given experimental temperature (1300, 1400, and 1500 °C) regardless of experimental durations. For quartz dissolution in basalt experiments, the interface melt concentration of SiO_2 is roughly constant at 1300 °C; while there is relatively large variation for the two experiments at 1400 °C. The likely cause of the large difference is the difficulty in extrapolating SiO_2 concentrations at the interface melts, where the concentration gradients are the steepest, and interface melts were not well preserved during quench of the experiments. There are good linear relations ($L = b\sqrt{t}$) between the melt growth distance (L) and the square root of experimental durations (\sqrt{t}). Therefore, we assume that quartz dissolution in both rhyolitic and basalt melts is primarily controlled by diffusion of SiO_2 , implying rapid interface reaction. Similarly, two

cassiterite dissolution experiments at 850 °C (Table 3-3) showed consistent interface-melt concentrations of SnO₂ (1.53 wt% for 5-min experiment CassDis6), and 1.61 wt% for 25-min experiment CassDis12). Therefore, we also assume that the dissolution of cassiterite is diffusion-controlled. A summary of interface-melt compositions of all the experiments can be found in Table 3-3.

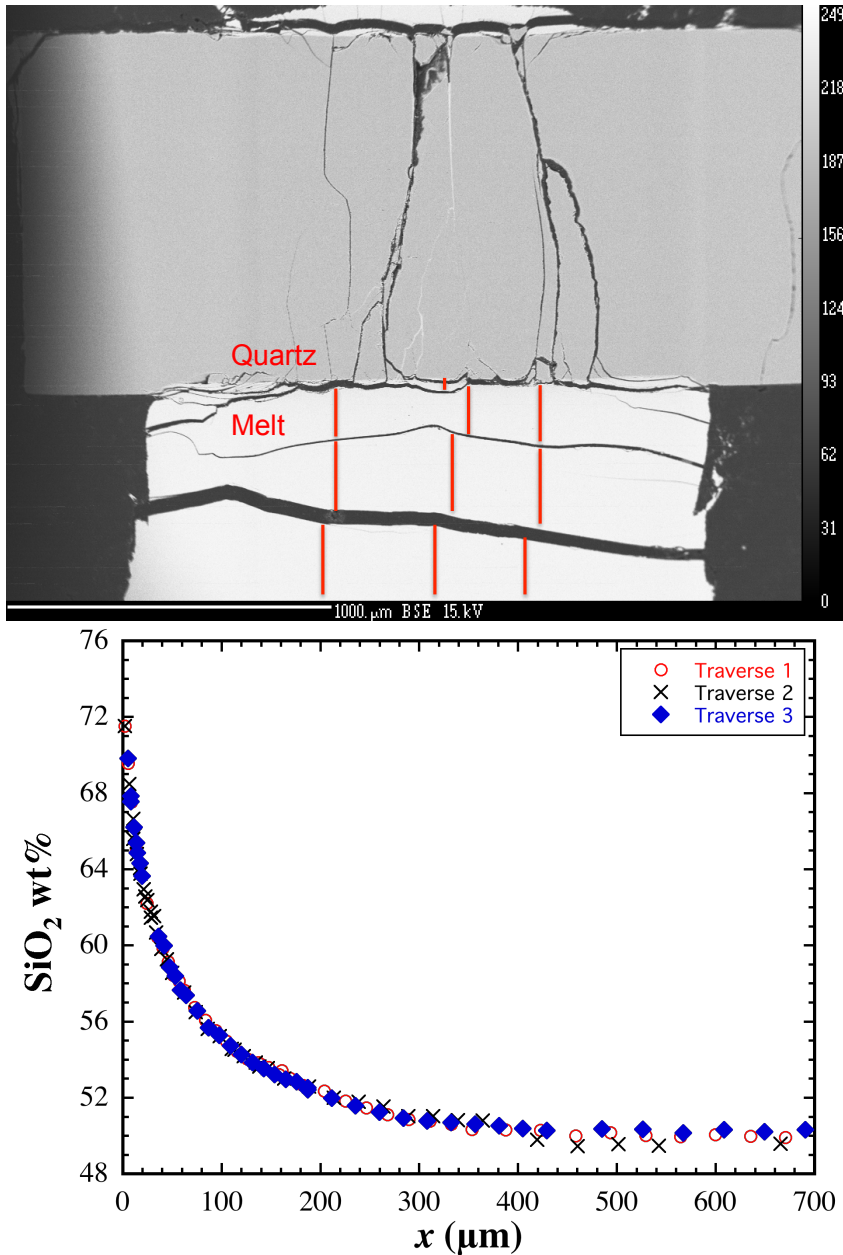


Figure 3-1. Top, back-scattered electron image of the experiment sample QzDisBa101, with 3 measured traverses (red lines) marked on it. Bottom, SiO₂ concentration profiles for the same sample.

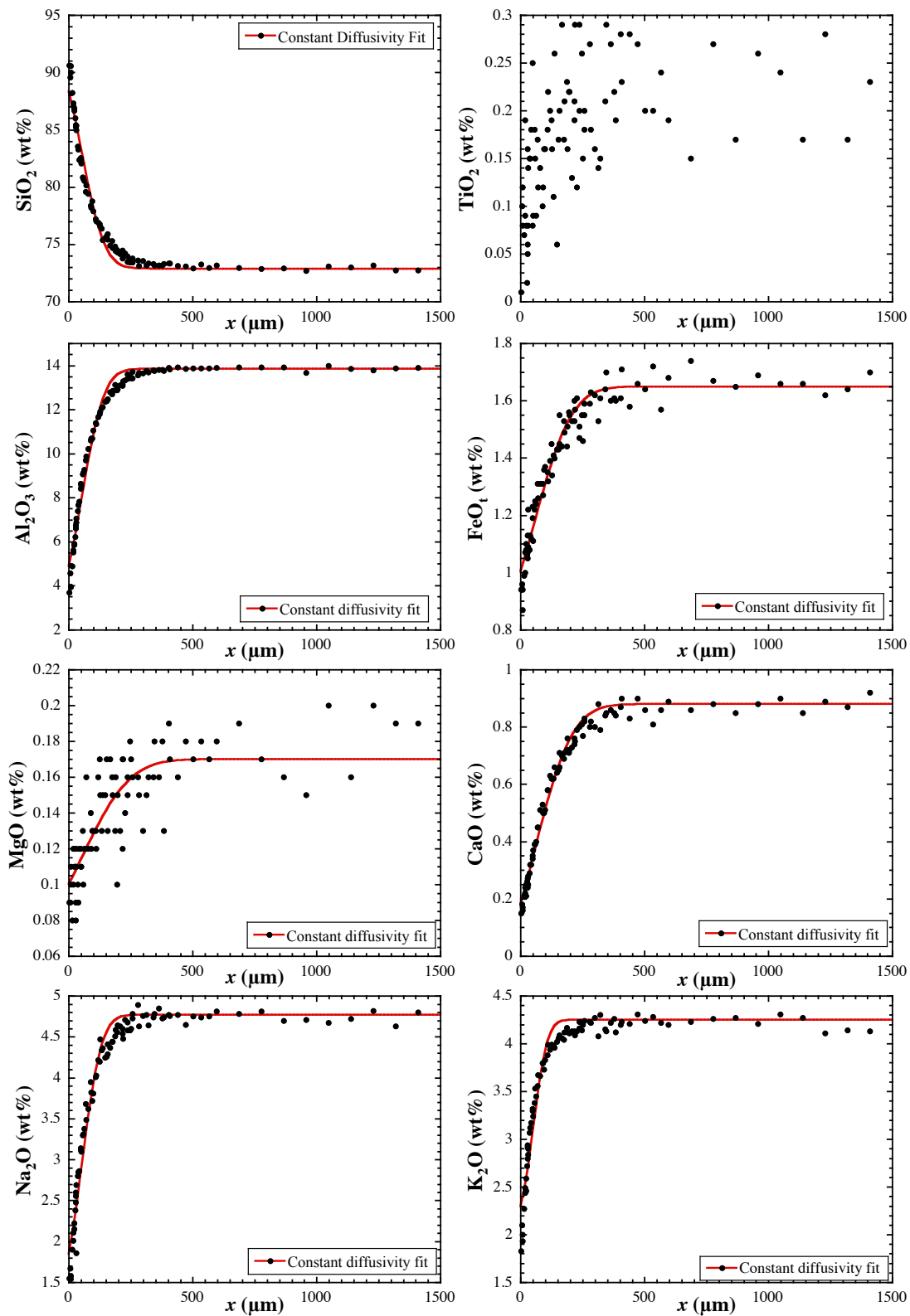


Figure 3-2. Oxide concentration profiles for a quartz dissolution experiment in rhyolitic melt (QzDisRh104, 1501 °C, 0.5 GPa, 86432 s).

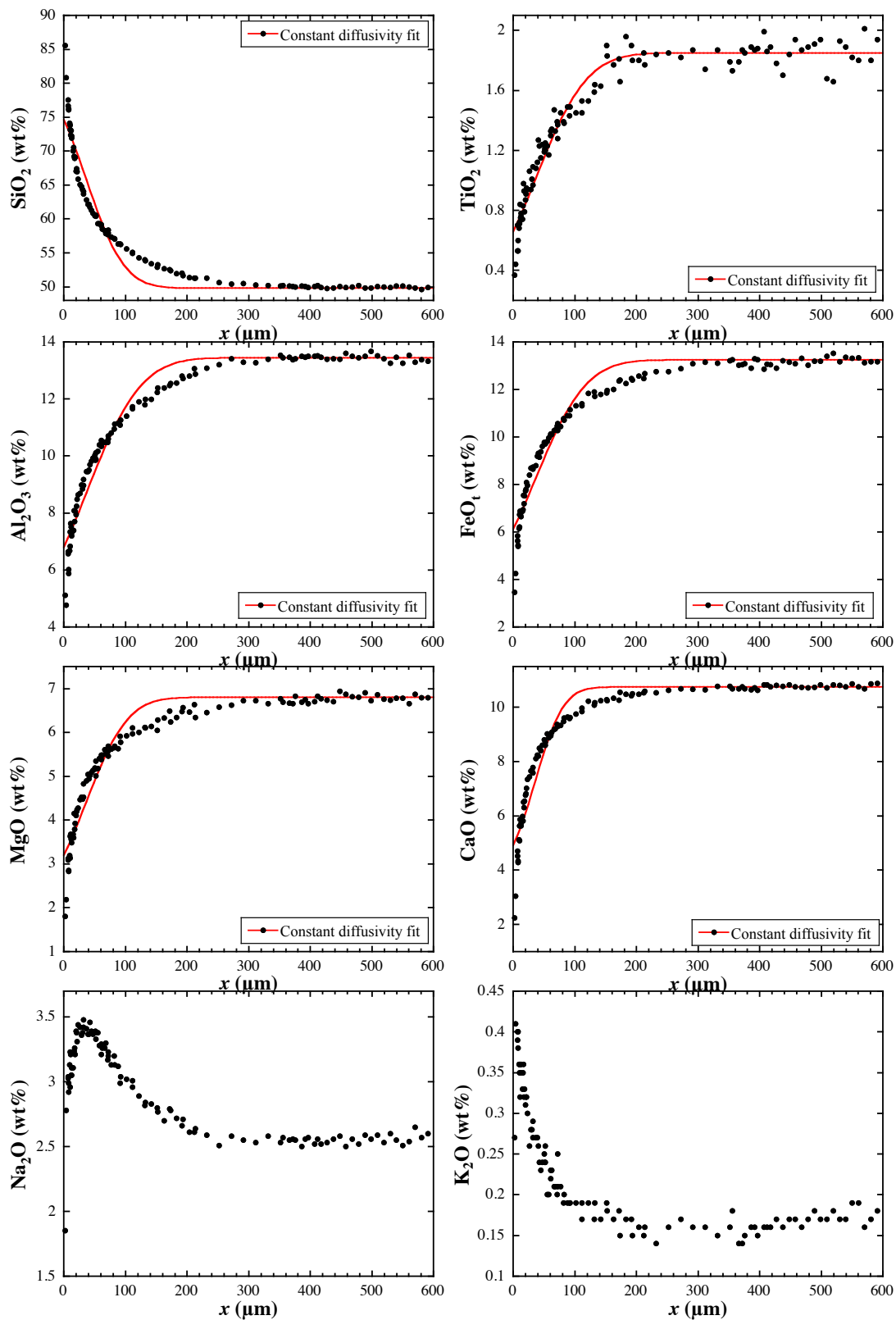


Figure 3-3. Oxide concentration profiles for a quartz dissolution experiment in basaltic melt (QzDisBa107, 1576 °C, 0.5 GPa, 322 s).

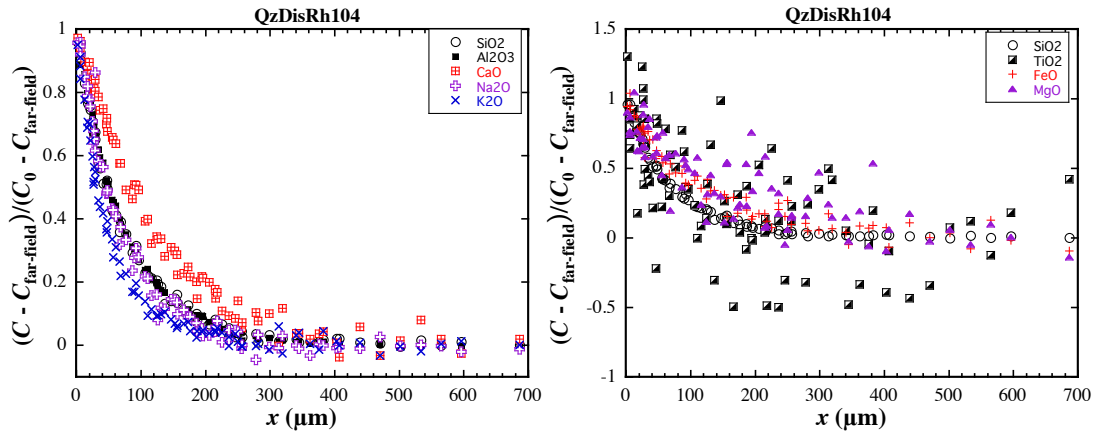


Figure 3-4. Normalized major concentration profiles for a quartz dissolution experiment in a rhyolitic melt (QzDisRh104, 1501 °C, 0.5 GPa, 86432 s).

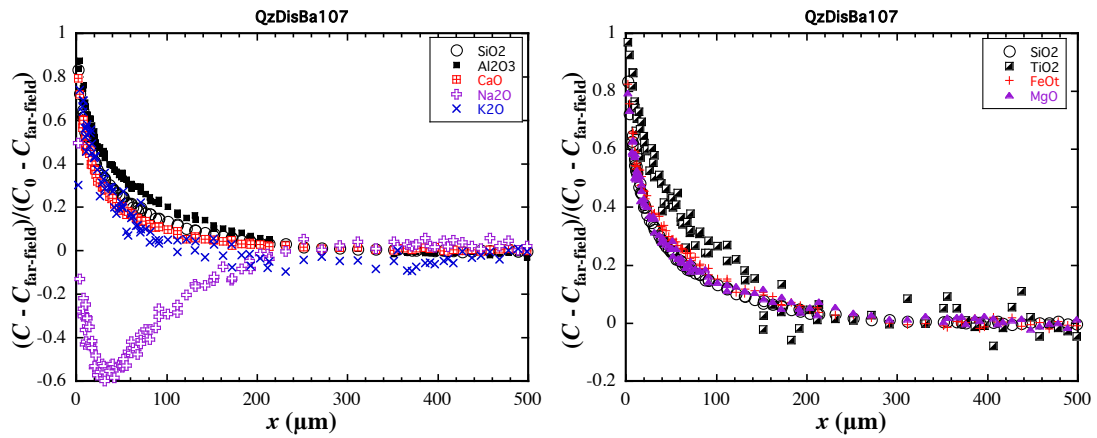


Figure 3-5. Normalized major concentration profiles for a quartz dissolution experiment in a basaltic melt (QzDisBa107, 1576 °C, 0.5 GPa, 322 s).

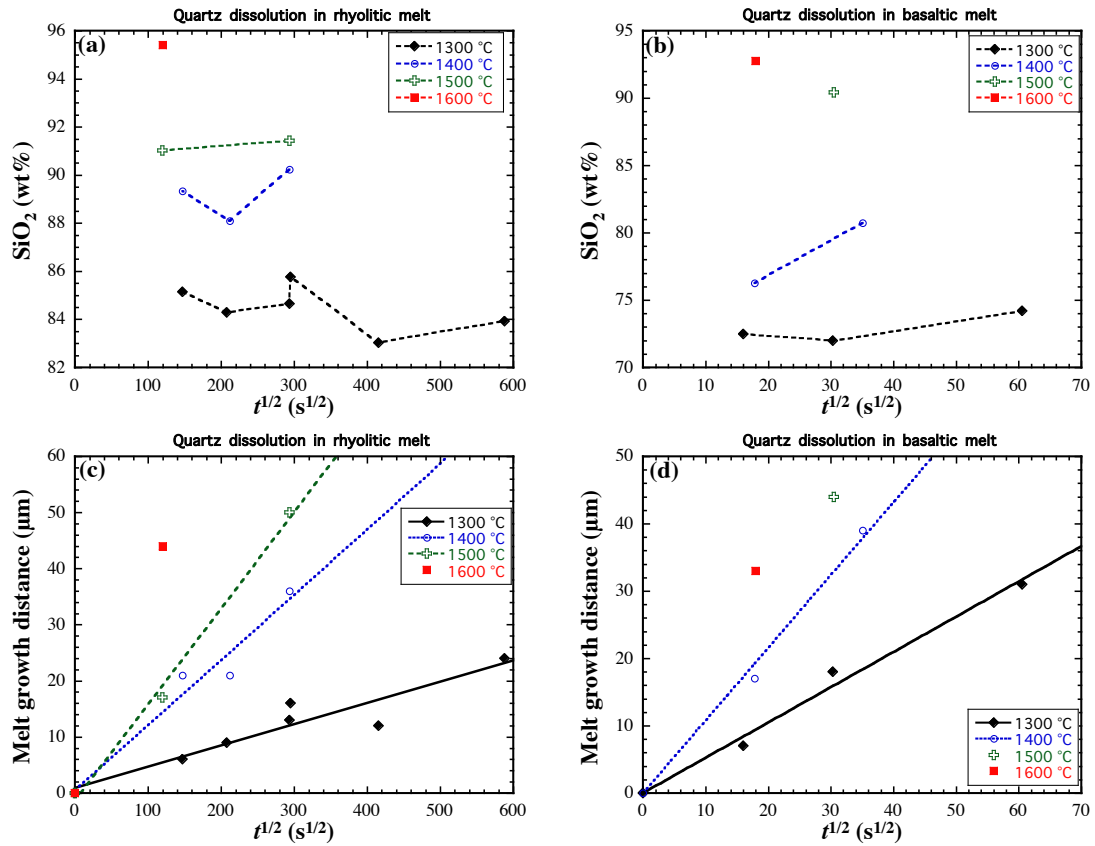


Figure 3-6. (a) (b), SiO₂ concentrations of the interface-melts versus the experimental duration for quartz dissolution experiments in rhyolite and basalt respectively. (c) (d), Variation of melt growth distance with time for the two sets of quartz dissolution experiments. Melt growth distances were calculated using mass balance.

Table 3-3. Interface-melt compositions of all experiments.

Sample#	^a SiO ₂	^b SnO ₂	TiO ₂	Al ₂ O ₃	FeO _t	MnO	MgO	CaO	Na ₂ O	K ₂ O	Total
QzDisRh103	82.96	-	0.13	8.8	1.3	0.03	0.07	0.28	3.5	3.1	100.17
QzDisRh111	85.61	-	0.10	6.4	1.1	0.04	0.09	0.21	3.0	2.9	99.45
QzDisRh112	84.22	-	0.12	7.8	1.2	0.05	0.09	0.28	2.6	2.9	99.26
QzDisRh115	83.86	-	0.13	7.8	1.3	0.02	0.10	0.30	3.1	3.0	99.61
QzDisRh201	84.92	-	0.10	7.5	1.5	0.05	0.11	0.30	2.2	3.2	99.88
QzDisRh203	84.58	-	0.13	7.3	1.3	0.04	0.12	0.26	2.3	3.0	99.03
QzDisRh105	90.14	-	0.10	3.9	0.9	0.02	0.07	0.14	1.3	1.8	98.37
QzDisRh113	88.02	-	0.14	5.8	1.2	0.05	0.09	0.20	2.3	2.4	100.20
QzDisRh114	89.26	-	0.05	4.6	1.1	0.05	0.08	0.18	1.5	2.0	98.82
QzDisRh102	90.92	-	0.15	4.8	1.1	0.04	0.07	0.14	1.8	2.3	101.32
QzDisRh104	91.40	-	0.06	3.4	0.9	-	0.08	0.13	1.4	1.7	99.07
QzDisRh106	95.38	-	0.06	0.9	0.8	0	0.06	0.08	0.8	0.8	98.88
QzDisBa101	73.54	-	0.82	8.1	6.1	0.09	3.10	5.00	3.6	0.5	100.81
QzDisBa102	71.52	-	0.78	8.1	6.3	0.09	3.15	4.90	4.0	0.5	99.29
QzDisBa103	71.87	-	0.73	8.5	6.6	0.10	3.30	5.50	3.7	0.4	100.70
QzDisBa110	80.29	-	0.55	5.9	4.0	0.03	2.20	3.20	2.9	0.5	99.52
QzDisBa111	75.99	-	0.72	7.1	5.6	0.06	2.80	4.20	3.1	0.5	100.02
QzDisBa104	90.02	-	0.26	5.1	2.2	0	0.50	0.00	0.9	0.5	99.48
QzDisBa107	92.66	-	0.32	3.5	1.4	0	0.50	0.00	1.1	0.5	99.98
CassDis8	66.39	5.00	0.25	12.2	2.0	-	0.28	1.57	3.4	3.8	94.89
CassDis10	70.71	5.37	0.06	11.1	1.3	-	0.03	1.30	3.7	4.2	97.77
CassDis3	68.62	9.56	0.06	11.2	1.3	-	0.03	1.00	3.3	4.0	99.07
CassDis1	64.15	12.83	0.06	10.8	1.4	-	0.03	1.10	3.3	3.8	97.47
CassDis11	66.00	12.49	0.05	10.3	1.3	-	0.02	1.20	3.5	3.5	98.36

^a Interface-melt concentrations were estimated by eyeballing the concentration profiles to the interface, except for SiO₂, whose values were extracted from fitting SiO₂ concentration profiles using eq. 4. FeO_t stands for total iron oxide.

Cassiterite dissolution experiments with no discernible or low-quality SiO₂ concentration profiles are not reported in this table.

^b SnO₂ concentrations at the interface-melt were only determined for cassiterite dissolution experiment.

3.4. Fitting the SiO₂ concentration profiles of quartz dissolution experiments

For diffusion-controlled mineral dissolution, if the effective binary diffusivity of a given component is constant across the whole concentration profile, the concentration profile can be fit by the following equation (Zhang et al., 1989):

$$C = C_{\infty} + (C_0 - C_{\infty}) \frac{\operatorname{erfc}\left(\frac{x}{\sqrt{4Dt}} - \alpha\right)}{\operatorname{erfc}(-\alpha)}, \quad (3-1)$$

$$\exp(\alpha^2) \operatorname{erfc}(-\alpha) \sqrt{\pi} \alpha = \frac{C_0 - C_{\infty}}{C_c - C_0}, \quad (3-2)$$

where C_{∞} , C_0 , and C are the concentrations of the diffusing component at the far-field melt, interface melt and the melt at distance x away from the mineral-melt interface; D is the EBDC of the diffusing component, and t is the experimental duration.

However, a comparison (Figure 3-7) between the SiO₂ concentration data and the constant-diffusivity fit by Eq. 3-1 and 3-2 (blue dashed curve) shows obvious misfit, indicating that there is significant variation in the SiO₂ EBDC across the concentration profile. Furthermore, the misfit is systematic, with data forming steeper trend at higher SiO₂ and shallower trend at lower SiO₂ compared to the constant-diffusivity curve, indicating decreasing D with increasing SiO₂ (Watson, 1982; Lesher and Walker, 1986; Koyaguchi, 1989). Therefore it is necessary to determine how the EBDC of SiO₂ varies along a profile. We will use both the Boltzmann analysis and the fit of concentration profiles using a functional dependence of $D(C)$ to determine the variation of SiO₂ EBDCs along a profile. Then we will compare the composition-dependent diffusivity in different experiments to evaluate the best parameter to characterize the compositional dependence.

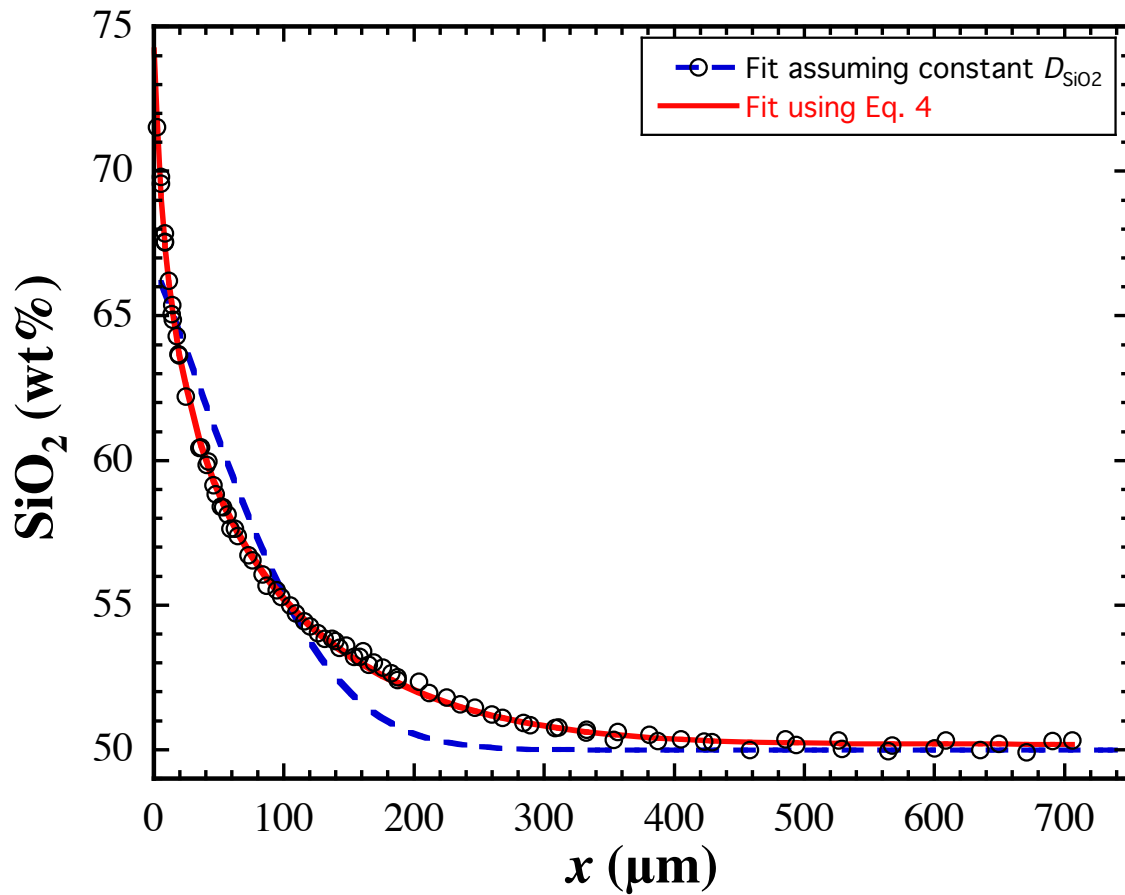


Figure 3-7. Typical SiO₂ concentration profile (black open circles, sample QzDisBa101) and fitting results using constant diffusivity (blue dash line, Eqs. 3-1 and 3-2) and composition-dependent diffusivity (red solid line, Eq. 3-4).

3.4.1. Boltzmann analysis of concentration profiles of quartz dissolution experiments

In diffusion-couple experiments, Boltzmann-Matano analysis (Matano, 1933) has usually been used to investigate the trend between EBDCs of SiO₂ and melt compositions without assuming any relation between the two (e.g., Watson, 1982; Koyaguchi, 1989). The quality of such approach not only largely depends on the original data precision of the concentration profiles, but also depends on how the derivative is calculated (Zhang and Stolper, 1991; Zhang, 2008). Watson (1982) and Koyaguchi (1989) implemented this approach and showed that the logarithm of EBDC of SiO₂ linearly depends on the SiO₂ weight percentage. However, Boltzmann-Matano method cannot be directly applied to analyze the concentration profiles of mineral dissolution experiments. Therefore, we use the Boltzmann analysis to treat diffusive mineral dissolution and derive the following equation to show the relation between EBDC and the melt composition during diffusive mineral dissolution (the derivation can be found in Appendix D):

$$D = \frac{\frac{C_{\infty} - C_x}{C_c - C_{\infty}} \int_{C_0}^{C_{\infty}} x dC + \int_{C_x}^{C_{\infty}} x dC}{2t \left. \frac{\partial C}{\partial x} \right|_x}, \quad t > 0, \quad (3-3)$$

where C_{∞} , C_0 , and C_x are the concentrations of the major diffusing (or equilibrium-determining) component (SiO₂ here) in the far-field melt, interface melt, and the melt at distance x away from the mineral-melt interface; C_c is the concentration of the component in the crystal, D is the EBDC of the diffusing component, and t is the experimental duration. Note here that the interface position is known and fixed, rather than the adjustable Matano interface.

To implement the above approach, a MATLAB program (The Mathwork, Inc.) was written, in which a profile is first smoothed using a moving average filter with a span of 10-25 points (less points (e.g. 10) are used near the interface as the concentration gradient is steeper, while more points (e.g. 25) are used near the far-field as the concentration gradient is shallower). Note that the number of points spanned by the moving average filter can not be too small (less than 5 points), as it will cause the processed profile to be zigzag and introduce large variation (or even values of an opposite sign) in the calculation of the denominator of Eq. 3-3. Neither can the number of points be too large (more than 50 points), as it will result in over-averaging the profile with substantial mismatch between the processed profile and the original data, in spite of smoothly changing slopes along the processed profile. The integral and slope in Eq. 3-3 are calculated using the smoothed profile. Then the D value at a given position (or given concentration) is calculated using Eq. 3-3. At and near the far-field, the concentration slope in the denominator of Eq. 3-3 cannot be evaluated accurately. Near the interface, the concentration profile is steep but less constrained. Hence, the calculated D values at both ends of the concentration profile are inaccurate and show large fluctuation. To examine the compositional dependence of D , we first plot $\ln D$ vs. SiO_2 concentration as in previous studies. Only the smooth part of the trend in the large middle part of the concentration range (e.g., for exp. QzDisBa110, $C_\infty = 50.0$ wt%, $C_0 = 80.7$ wt%, but only D values from 52 to 74 wt% SiO_2) are chosen (Fig. 3-8) in quartz dissolution experiments in both rhyolitic melt and basaltic melt, and cassiterite dissolution experiments in various hydrous rhyolitic melt. In addition, one experiment of quartz dissolution into andesitic melt at 1300 °C from Zhang et al, 1989 is also included in the above analysis (shown as

the black crosses in Fig. 3-8). The SiO₂ diffusivity trend of quartz dissolution in the andesitic melt is slightly higher than that in the basaltic melt. The likely cause of this difference is due to some difference in the experimental temperature among different experiments. We first note that $\ln D$ is roughly linear to SiO₂ concentration in a given composition and temperature. When comparing the trends (Fig. 3-8) across different experimental sets (such as quartz dissolution in rhyolite, andesite and basalt) at the same temperature, it can be seen that there is a significant offset among the trends in the two or three melt systems (i.e. different intercepts) when using SiO₂ wt% as the compositional parameter, indicating that other compositional parameters also play a role in the diffusion of SiO₂. Hence, we also examined $\ln D$ vs. $X_{\text{Si+Al}}$ plot (Fig. 3-8), where $X_{\text{Si+Al}}$ is the total cation mole fraction of Si and Al. Our results show that $\ln D$ vs. $X_{\text{Si+Al}}$ show a better aligned trend at a given temperature (e.g. 1400 °C and 1600 °C in Fig. 3-8) across different melt systems within experimental error. These observations imply that $X_{\text{Si+Al}}$ (simplified as X hereafter) is a better parameter to characterize the compositional effect on SiO₂ EBDC than using SiO₂ wt% alone.

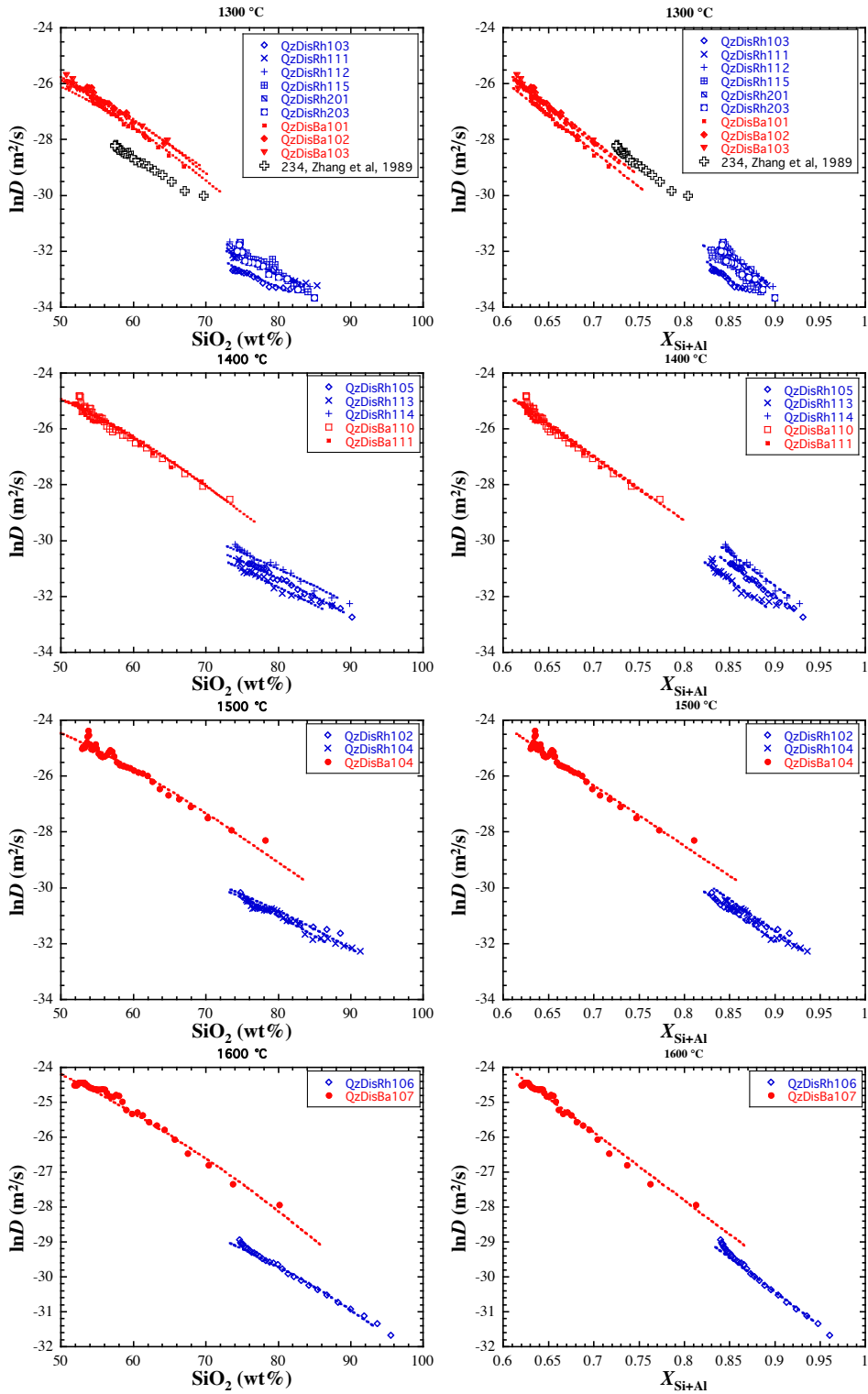


Figure 3-8. Boltzmann analyses (scatter symbols) and functional fitting results (dash line) of SiO_2 diffusivity dependence on melt compositions using SiO_2 (left column) and X (right column) as the compositional parameter respectively. The analyzed samples are quartz dissolution experiments in rhyolitic (Newberry) and basaltic (JDF) melts at 1300, 1400, 1500, and 1600 °C. One quartz dissolution experiment in andesitic melt at 1300 °C is from Zhang et al, 1989

Table 3-4. Summary of fitting results for quartz dissolution experiments based on Eq. 3-4.

ExpNum	a	B ($\mu\text{m/s}^{1/2}$)	C_0 (wt%)	$\ln D_0$ (m^2/s)	$\ln D_{\text{farfield}}$ (m^2/s)	$\ln D_{\text{interface}}$ (m^2/s)	$\ln D$ (m^2/s)						
							$X=0.65$	$X=0.70$	$X=0.75$	$X=0.80$	$X=0.85$	$X=0.90$	$X=0.95$
QzDisRh103	23.92(19)	0.0155(3)	82.96(19)	-36.60(23)	-32.42(21)	-33.60	-28.23	-29.43	-30.62	-31.82	-33.01	-34.21	-35.41
QzDisRh111	23.92(19)	0.0235(4)	85.61(20)	-36.04(23)	-31.92(21)	-33.50	-27.67	-28.87	-30.07	-31.26	-32.46	-33.65	-34.85
QzDisRh112	23.92(19)	0.0216(3)	84.22(11)	-35.69(23)	-31.95(21)	-33.25	-27.32	-28.52	-29.71	-30.91	-32.10	-33.30	-34.50
QzDisRh115	23.92(19)	0.0211(3)	83.86(10)	-36.12(23)	-31.81(21)	-33.34	-27.75	-28.94	-30.14	-31.34	-32.53	-33.73	-34.92
QzDisRh201	23.92(19)	0.0221(4)	84.92(32)	-35.76(23)	-32.03(21)	-33.45	-27.39	-28.59	-29.78	-30.98	-32.17	-33.37	-34.57
QzDisRh203	23.92(19)	0.0209(2)	84.58(10)	-35.96(23)	-31.98(21)	-33.53	-27.59	-28.79	-29.98	-31.18	-32.37	-33.57	-34.77
QzDisRh105	22.75(15)	0.0595(5)	90.14(9)	-34.28(19)	-30.56(17)	-32.71	-26.31	-27.45	-28.59	-29.73	-30.86	-32.00	-33.14
QzDisRh113	22.75(15)	0.0464(8)	88.02(19)	-34.85(19)	-30.82(17)	-32.70	-26.89	-28.03	-29.17	-30.30	-31.44	-32.58	-33.72
QzDisRh114	22.75(15)	0.0695(7)	89.26(14)	-33.88(19)	-30.22(17)	-32.17	-25.92	-27.06	-28.19	-29.33	-30.47	-31.61	-32.74
QzDisRh102	21.55(12)	0.0717(9)	90.92(31)	-34.02(15)	-30.18(14)	-32.59	-26.48	-27.56	-28.63	-29.71	-30.79	-31.87	-32.94
QzDisRh104	21.55(12)	0.0809(8)	91.40(11)	-33.70(16)	-30.10(14)	-32.34	-26.16	-27.23	-28.31	-29.39	-30.47	-31.54	-32.62
QzDisRh106	19.53(14)	0.1723(13)	95.83(17)	-32.38(17)	-29.13(16)	-31.64	-25.54	-26.52	-27.50	-28.47	-29.45	-30.43	-31.40
QzDisBa101	23.92(19)	0.2376(28)	73.54(23)	-35.52(21)	-26.28(16)	-30.12	-27.15	-28.35	-29.54	-30.74	-31.94	-33.13	-34.33
QzDisBa102	23.92(19)	0.2794(23)	71.52(23)	-35.11(21)	-25.87(16)	-29.45	-26.74	-27.94	-29.13	-30.33	-31.53	-32.72	-33.92
QzDisBa103	23.92(19)	0.2729(25)	71.87(25)	-35.21(21)	-25.98(16)	-29.36	-26.84	-28.03	-29.23	-30.42	-31.62	-32.81	-34.01
QzDisBa110	22.75(15)	0.4992(51)	80.29(27)	-33.73(17)	-24.96(13)	-30.01	-25.77	-26.91	-28.05	-29.18	-30.32	-31.46	-32.60
QzDisBa111	22.75(15)	0.4729(47)	75.99(22)	-33.79(17)	-24.99(13)	-29.15	-25.83	-26.96	-28.10	-29.24	-30.38	-31.51	-32.65
QzDisBa104	21.55(12)	0.7018(54)	90.02(42)	-32.72(14)	-24.45(11)	-30.92	-25.18	-26.25	-27.33	-28.41	-29.49	-30.56	-31.64
QzDisBa107	19.53(14)	0.9570(82)	92.66(48)	-31.72(16)	-24.17(13)	-30.31	-24.89	-25.86	-26.84	-27.82	-28.79	-29.77	-30.75

$D_{\text{interface}}$ is the calculated SiO_2 diffusivity at the interface melt of each experiment using Eq. 3-4, and corresponding values of parameter a , C_0 and D_0 from Table 3-4.

SiO_2 diffusivities at specific melt compositions ($X = 0.65, 0.7, 0.75, 0.8, 0.85, 0.9, 0.95$) are calculated based on Eq. 3-4.

The values in the parentheses indicate 1σ errors on the last two or three digits of the fitting results

3.4.2. Fitting SiO₂ profiles of quartz dissolution experiments by using exponential dependence of SiO₂ diffusivity

Though it shows the rough compositional dependence of SiO₂ diffusivities, the Boltzmann analysis cannot constrain the uncertainties on the SiO₂ diffusivities well, and is often sensitive to the smoothness of the concentration profiles. In addition, there is some arbitrariness in deciding which part of the $D(C)$ relation to take as the reliable part. To further verify the relation between SiO₂ diffusivity and composition, and to constrain the diffusivities with estimation of uncertainties, we fit the SiO₂ concentration profiles using a relation, in which D depends on SiO₂ concentration exponentially based on insights from the preceding section and from the literature (Watson, 1982; Lesher et al., 1986; Koyaguchi, 1989; Zhang et al., 2010). The following diffusivity relation is adopted:

$$D = D_0 e^{-a(C-C_0)} = D_{\text{farfield}} e^{-a(C-C_{\text{farfield}})} = D_p e^{-aC}, \quad (3-4)$$

where D , D_0 , D_{farfield} are the SiO₂ diffusivity in the melt of composition C , composition C_0 , and the far-field melt (C_{farfield}); a is the compositional-dependence coefficient of diffusivity. When using X as the compositional parameter, $X_0 = 1$ (SiO₂+Al₂O₃ melt) is adopted below.

Combining the parabolic melt growth rate ($V_{\text{melt}} = B / \sqrt{t}$, where B is an unknown constant to be fitted) and the compositional dependent diffusivity (Eq. 3-4), the diffusion-dissolution equation with semi-infinite boundary condition (Eqs. (D-1) and (D-2) in Appendix D) can be numerically solved. A non-linear least squares method (A written script based on Levenberg-Marquardt algorithm to minimize the sum square of errors of all the measured points along a concentration profile, by searching the parameter space

consisting of D_0 , a , B , and C_0) was applied to extract the EBDCs of SiO_2 in the extrapolated fully polymerized melt (D_0) and in the far-field melt (D_{farfield}), and the compositional dependence coefficient of SiO_2 diffusivity (a). Since the slopes in the plot of $\ln D$ versus C (either SiO_2 or X) are almost the same at the same experimental temperature between rhyolitic system and basaltic system (shown in Fig. 3-8), we fit all the concentration profiles (regardless of melt compositions and experimental durations) at the same experimental temperature together by minimizing the total misfit. That is, we simultaneously fit a batch of concentration profiles from quartz dissolution studies in both rhyolitic melts and basaltic melts at the same experimental temperature ($\sim 1300^\circ\text{C}$, $\sim 1400^\circ\text{C}$, $\sim 1500^\circ\text{C}$, or $\sim 1600^\circ\text{C}$) to obtain the value of a at this T . The benefit of doing so is to best constrain the parameters of D_0 and a , which are correlated. All fitting results are summarized in Table 3-4. SiO_2 diffusivities at some intermediate melt compositions ($X_{\text{Si+Al}} = 0.65, 0.7, 0.75, 0.8, 0.85, 0.9, \text{ and } 0.95$) are also provided in the table. In addition, SiO_2 diffusivities accompanied with the melt composition profiles are also provided in the Appendix F. A comparison between the fit concentration profile and the measured concentration profile for all the experiments is exemplified in Fig. 3-7 as the red solid line. Other fits are shown in the Appendix E. The D versus C relations obtained from the fits are shown in Fig. 3-8 as lines (red dash lines for quartz dissolution in basalt, and blue dash lines for quartz dissolution in rhyolite), which are in good agreement with the numerical results using the Boltzmann analysis.

As observed in section 4.1, the composition-dependent D_{SiO_2} in different melt systems (rhyolitic and basaltic) can be reconciled (roughly forming a single trend) within experimental error when expressed as a function of X , but not when expressed as a

function of SiO_2 concentration. It does make sense since Al is similar to Si in that Al is also a network former, which to a large extent controls the silicate melt structure. In plagioclase dissolution experiments, Yu et al. (2016) reached a similar conclusion that Si and Al together control the diffusivities of Al_2O_3 . Zhang and Xu (2016) also showed that Zr diffusivity depends on Si+Al rather than on SiO_2 alone.

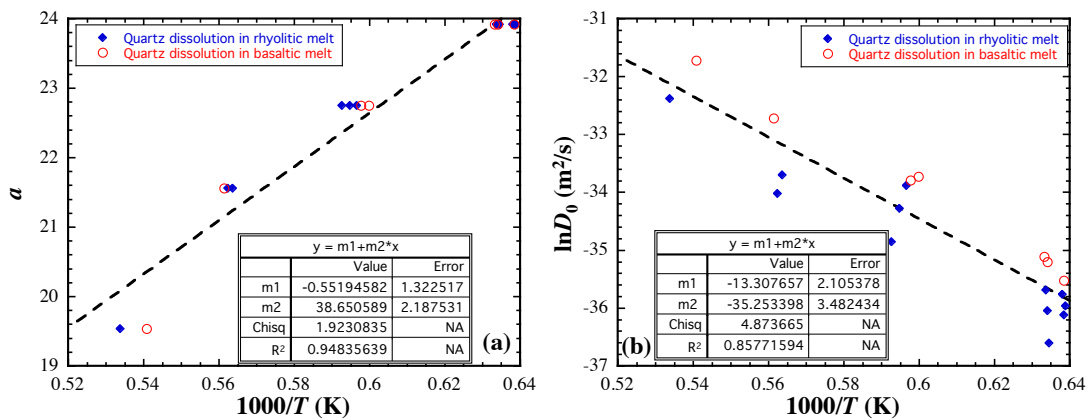


Figure 3-9. (a) Dependence of the compositional dependence parameter a of SiO_2 diffusivity on temperature based on quartz dissolution experiments in rhyolitic and basaltic melts; (b) Dependence of D_0 on temperature.

3.4.3. Compositional dependence coefficient (a) and SiO_2 diffusivity (D_0) in fully polymerized silicate melt

It is not uncommon to see the composition-dependent diffusivities of the diffusing components. For instance, H_2O diffusion studies in various silicate melts have demonstrated strong compositional dependence of H_2O diffusivities (Zhang et al., 1991; Zhang and Stoper, 1991).

In this study, the time-series experimental design and the wide range of experimental temperatures enable us to isolate the compositional dependence of SiO_2

diffusivities, and to assess how it relates to the temperature. Following the fitting procedure in section 4.2, we have reported all the fitting results in [Table 3-4](#) and plotted the compositional dependence coefficient (a) and the SiO₂ diffusivity (D_0) in extrapolated fully polymerized silicate melt in [Fig. 3-9](#). From the figure we observe that:

- (1) As shown in the Boltzmann analysis [Fig. 3-8](#), the parameter a is roughly independent of silicate melt compositions. That is, at the same temperature, the dependence of SiO₂ diffusivity can be roughly expressed by a single line in $\ln D$ versus X for basaltic, andesitic and rhyolitic melts. The coefficient (a) for the compositional dependence of SiO₂ diffusivities has a linear dependence on $1/T$ within the errors over a temperature span of 1300-1600°C. This relation is similar to the case of H₂O diffusion ([Zhang and Behrens, 2000](#); [Ni and Zhang, 2008](#)). Based on [Fig. 3-9a](#), we fitted a linear relation between a and $1/T$ as below:

$$a = -0.552(\pm 1.322) + \frac{38650(\pm 2188)}{T}, \quad (3-5)$$

where r^2 of the above fitting is 0.948.

- (2) SiO₂ diffusivity in fully polymerized silicate melt (D_0) follows typical Arrhenius relation ([Fig. 3-9b](#)). A linear fit between $\ln D_0$ and $1/T$ gives:

$$\ln D_0 = -13.308(\pm 2.105) - \frac{35253(\pm 3482)}{T}, \quad (3-6)$$

where r^2 is 0.858, 1 σ error in $\ln D_0$ is 0.52 $\ln D$ unit, and the maximum error is 0.93 $\ln D$ unit. Although the general equation is adequate to describe D_0 in both rhyolitic and basaltic melts, there is a small offset between rhyolitic and basaltic data in [Fig. 3-9b](#). If data in each melt are fit, we obtain:

$$\ln D_0 = -14.799(\pm 2.078) - \frac{33286(\pm 3427)}{T}, \text{ in rhyolitic melt, } r^2 = 0.904; \quad (3-6a)$$

$$\ln D_0 = -11.868(\pm 0.977) - \frac{36792(\pm 1623)}{T}, \text{ in basaltic melt, } r^2 = 0.990. \quad (3-6b)$$

Because the general Eq. (3-6) has acceptable accuracy, it is used in our discussion below.

Combining Eq. (3-5) and Eq. (3-6), the composition-dependent EBDCs of SiO₂ during quartz dissolution in rhyolitic and basaltic melts can be expressed as:

$$D_{\text{SiO}_2}^{\text{quartz dissolution}} = 1.661 \times 10^{-6} \exp\left(0.552(X-1) - \frac{35253 + 38650(X-1)}{T}\right). \quad (3-7)$$

As the above model is developed using data from quartz dissolution experiments in rhyolitic and basaltic melts, Eqs. 3-5, 3-6 and 3-7 are best used for interpolation, i.e. $X > 0.6$, $T = 1300\text{-}1600$ °C.

3.5. Effect of H₂O on SiO₂ diffusivity

Volatiles, especially H₂O, have long been demonstrated to have significant and complex effects on diffusivities of other components (Koyaguchi, 1989; Baker, 1991; Baker and Bossanyi, 1994; Zhang et al, 2010). Empirically speaking, the addition of H₂O in the silicate melt usually accelerates the diffusion of other components. Such phenomena have often been attributed to the depolymerization of the melt structure by H₂O. Quantitative attempts to model these effects have often treated H₂O concentration as a separate parameter using various relations (such as linear, logarithmic, and square

root) between D and H₂O content (Zhang et al, 2010). Though the empirical relations are useful, it is desirable to seek simpler relations.

In this study, we have included cassiterite dissolution experiments in various hydrous rhyolitic melts, containing 0.1, 0.9 and 5.9 wt% H₂O respectively. Two of the experiments (CassDis3 and CassDis11) were conducted at the same experimental temperature (1000 °C) in KS (0.9 wt% H₂O) and CIT (0.1 wt% H₂O) rhyolitic glasses and are shown to have relatively large variation ($\Delta \ln D > 1$) in SiO₂ diffusivity across the profile in Fig. 3-10; while the changes in SiO₂ diffusivities in the other three cassiterite dissolution experiments (CassDis1, CassDis8 and CassDis10) are small and not obviously discernible. In the Boltzmann analysis, when X is calculated based on dry glass composition, the $\ln D$ versus X trends of these two experiments clearly offset. But when including H the same way as other cations (such as Fe, Ca, Na) in the calculation of X , the $\ln D$ versus X plots of the two experiments fall into the same trend within errors (Fig. 3-10). This observation indicates that the effect of H₂O on Si diffusivities is the simple dilution of the mole fraction of network forming cations (Si and Al). Zhang and Xu (2016) showed that Zr diffusivity is also consistent with this observation. Therefore, there is no need to separately treat the effect of H₂O on Si and Zr diffusivities differently.

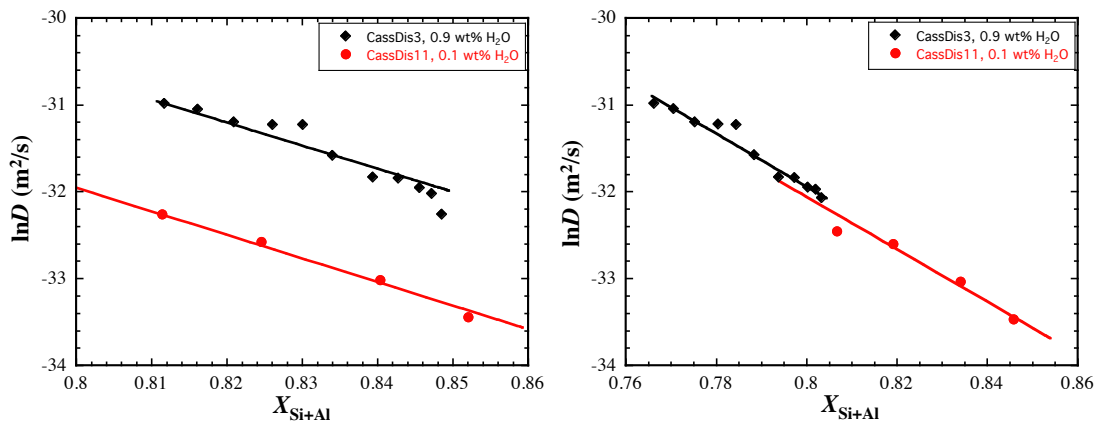


Figure 3-10. Boltzmann analyses (scatter symbols) and functional fitting results (solid line) of two cassiterite dissolution experiments in CIT and KS rhyolitic melts at 1000 °C. Left panel shows the data comparison without considering H₂O when calculating X ; right panel shows the comparison by considering H as cation when calculating X .

3.6. Diffusive dissolution rates of quartz in rhyolitic and basaltic melts

For diffusive crystal dissolution when the diffusivity is constant across the concentration profile, the melt growth distance can be expressed by the parabolic relation $L = 2\alpha\sqrt{Dt}$ (Zhang et al., 1989), where t is the experimental duration, D is the diffusivity of the equilibrium-controlling component in the melt, and α is determined by the concentrations of the equilibrium-controlling component of the interface melt (C_0), far-field melt (C_∞) and the mineral (C_c) as defined in Eq. 3-2. In the case of quartz dissolution, the diffusivity of SiO₂ (the equilibrium-determining component) is not constant. This section addresses how the melt growth distance or mineral dissolution distance can be estimated for the case of compositionally dependent diffusivity.

Figs. 3-6b and 3-6d show that quartz dissolution distance is proportional to \sqrt{t} , consistent with the results of the Boltzmann analysis in Appendix D. Hence, in modeling the melt growth distance during quartz dissolution in silicate melts, we will use the same

expression ($L = 2\alpha\sqrt{Dt}$), but interpreting D in the above expression to be the average \bar{D}_{SiO_2} . We hence need to find how \bar{D}_{SiO_2} is related to the D_{SiO_2} values in the interface melt and in the far-field melt. With this approach, the interface SiO_2 concentration (for the estimation of α .) and the average D_{SiO_2} are the two critical parameters to constrain the diffusive dissolution/growth rates of quartz crystals in silicate melts.

3.6.1. Interface SiO_2 concentration

As shown in Fig. 3-6a,c the interface SiO_2 concentrations during quartz dissolution in basaltic and rhyolitic melts are roughly constant regardless of the experimental duration. As argued by Zhang et al. (1989), the interface melts can be regarded as in near-equilibrium with the in-contact quartz crystals. Chen and Zhang (2008), and Yu et al. (2016) have also showed that the interface melts are in near-equilibrium with the dissolving olivine or anorthite crystals during the corresponding dissolution experiments, respectively. As the only constituent component of quartz, it is therefore critical to quantify the SiO_2 activities (denoted as C_{activity}) at the interface melts in order to quantify the quartz-melt equilibrium condition. However, SiO_2 activity coefficient depends on the starting melt compositions. In melts like the interface melts in our experiments with very high silica concentration (~72-92 wt% for quartz dissolution in basaltic melt; ~85-96 wt% for quartz dissolution in rhyolitic melt), neither are there enough data to constrain the effect of melt composition on SiO_2 activity coefficient, nor does the classic activity model of Ghiorso and Sack (1995) work in such compositional range (Fig. 3-11a). For example, the calculated SiO_2 activity of the interface melt does not depend on temperature monotonically (Fig. 3-11a), and the calculated liquidus

temperatures of the interface melts using MELTs program (Ghiorso and Sack, 1995) are 142 °C to 297 °C higher than the actual experimental temperature for rhyolitic melts, and are about 93 °C lower for basaltic melts, though quartz is predicted to be the liquidus phase. Hence, a simplified and practical way to approximate the quartz-melt equilibrium for the purpose of quantifying quartz dissolution kinetics is to relate the SiO₂ oxide concentration with the experimental temperature separately for different melt systems (Fig. 3-11b). Because the interface SiO₂ concentration (C_0) is essentially an equilibrium constant, we express $\ln C_0 = A + \Delta H/(RT)$. In addition, the melting temperature of β -quartz at 0.5 GPa is about 1690°C (Jackson, 1976; Hudon et al., 2002), meaning $C_0 = 100\%$ at the temperature. We construct the quartz-melt equilibrium relation for the rhyolitic and basaltic systems respectively forcing them to go through $C_0 = 100\%$ at 1963.15 K:

$$\text{In rhyolite: } \ln C_0 = 5.299(\pm 0.020) - 1362(\pm 39)/T, \quad r^2 = 0.900, \quad (3-8a)$$

$$\text{In basalt: } \ln C_0 = 5.926(\pm 0.052) - 2594(\pm 102)/T, \quad r^2 = 0.938. \quad (3-8b)$$

where C_0 is SiO₂ concentration in wt% in the interface melt. The fits are shown in Fig. 3-11b.

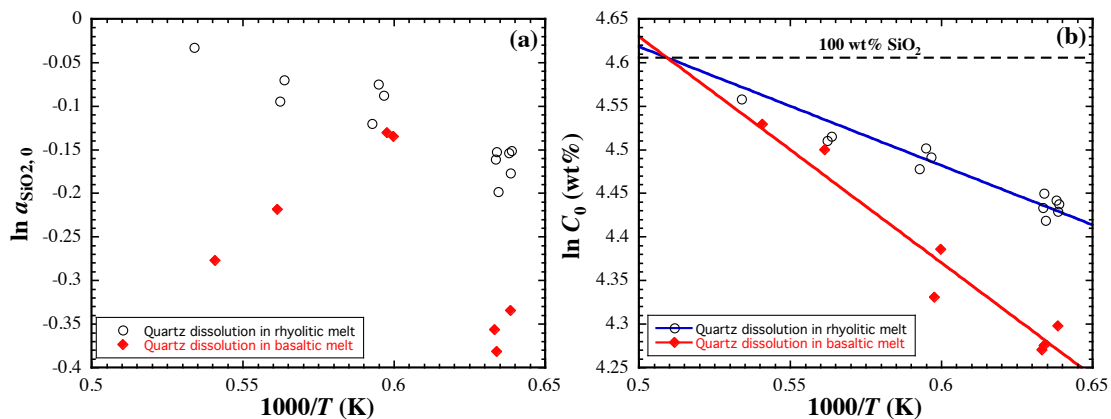


Figure 3-11. (a) Calculated activity of SiO₂ at the interface melt using the activity model of Ghiorso and Sack (1995) v.s. $1000/T$; (b) interface SiO₂ concentration v.s. $1000/T$ with linear regression lines and 100 wt% SiO₂ horizontal line marked.

3.6.2 Average SiO₂ diffusivity during quartz dissolution

As explained earlier, we model diffusive quartz dissolution rate as

$$V_{\text{quartz}} = \frac{\rho_{\text{melt}}}{\rho_{\text{quartz}}} V_{\text{melt}} = \frac{\rho_{\text{melt}}}{\rho_{\text{quartz}}} \frac{B}{\sqrt{t}} = \frac{\rho_{\text{melt}}}{\rho_{\text{quartz}}} \alpha \sqrt{\frac{D}{t}}, \text{ where } \rho \text{ is the density, } D \text{ is } \bar{D}_{\text{SiO}_2}, \text{ and } B$$

is given in Table 3-4. Therefore, B can be related to \bar{D}_{SiO_2} as:

$$\ln \frac{B}{\alpha} = \frac{1}{2} \ln \bar{D}_{\text{SiO}_2}, \quad (3-9)$$

where α for each experiment is calculated from Eq. 3-2 with C_0 from Table 3-4. Since \bar{D}_{SiO_2} is an effective average diffusivity across the entire SiO₂ concentration profiles, it is reasonable to express it as a combination of the SiO₂ diffusivities at the interface melt and the far-field melt:

$$\ln \bar{D}_{\text{SiO}_2} = k \ln D_{\text{SiO}_2, \text{ interface}} + (1-k) \ln D_{\text{SiO}_2, \text{ farfield}}, \quad (3-10)$$

Combining Eqs. 3-9 and 3-10, we can get:

$$\ln \frac{B}{\alpha} = \frac{1}{2} (k \ln D_{\text{SiO}_2, \text{ interface}} + (1-k) \ln D_{\text{SiO}_2, \text{ farfield}}), \quad (3-11)$$

By fitting Eq. 3-11 using the SiO₂ diffusivity data from Table 3-4, we obtain $k = 0.5538 (\pm 0.0101)$, $r^2 = 0.994$. An independent test using the quartz dissolution experiment in andesitic melt from Zhang et al. (1989) confirms the above approach (marked as blue crosses in Fig. 3-12). A comparison of the fit is shown in Fig. 3-12. Hence, the effective average SiO₂ diffusivity during quartz dissolution experiments can be expressed as:

$$\bar{D}_{\text{SiO}_2} = (D_{\text{SiO}_2, \text{ interface}})^{0.5538} (D_{\text{SiO}_2, \text{ farfield}})^{0.4462}, \quad (3-12)$$

Combining $V_{\text{quartz}} = \frac{\rho_{\text{melt}}}{\rho_{\text{quartz}}} \alpha \sqrt{\frac{\bar{D}_{\text{SiO}_2}}{t}}$ and Eq. 3-12, one can calculate the diffusive

dissolution rate of quartz in either the rhyolitic melt or the basaltic melt as:

$$V_{\text{quartz}} = \frac{\rho_{\text{melt}}}{\rho_{\text{quartz}}} \alpha \sqrt{\frac{(D_{\text{SiO}_2, \text{interface}})^{0.5538} (D_{\text{SiO}_2, \text{farfield}})^{0.4462}}{t}}, \quad (3-13)$$

where α is defined in Eq. 3-2, and $t > 0$. When C_0 is larger than C_∞ , α is positive and quartz dissolves into the melt. When C_0 is smaller than C_∞ , α takes a negative sign and quartz will grow.

For modeling the convective dissolution or growth of a rising or sinking quartz crystal, similar approached as in [Chen and Zhang \(2008, 2009\)](#) and [Yu et al. \(2016\)](#) can be used, but average \bar{D}_{SiO_2} calculated from Eq. 3-12 needs to be used.

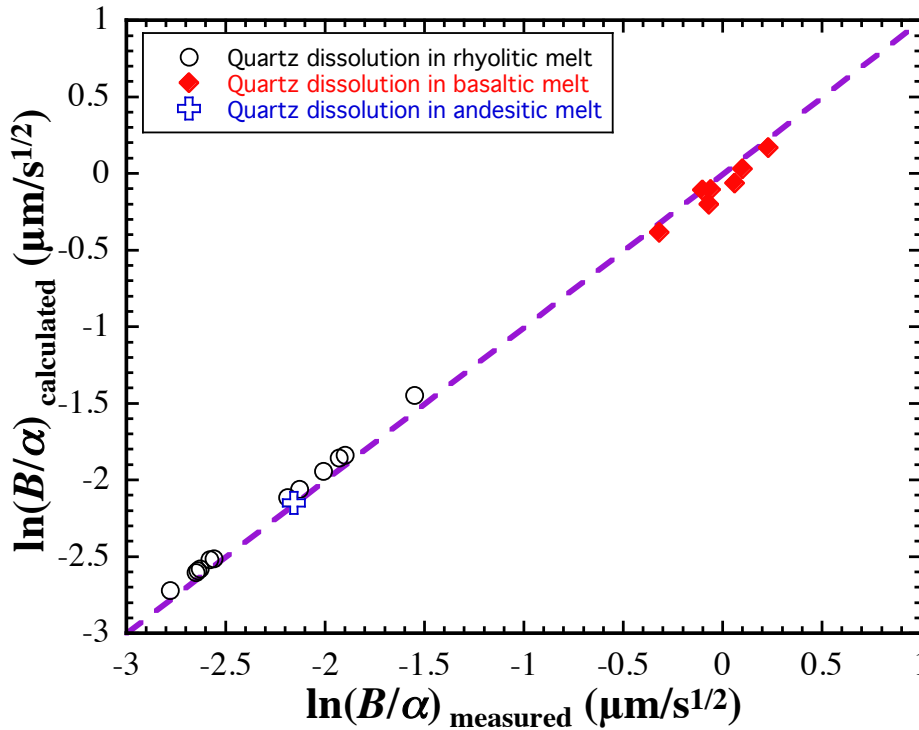


Figure 3-12. Comparison between the fitted $\ln(B/a)$ value (Table 3-4) and the calculated $\ln(B/a)$ value using Eq. 3-11. 1:1 ratio line is marked on the plot. The quartz dissolution experiment in andesitic melt (blue cross) is from [Zhang et al \(1989\)](#).

3.7. Quartz dissolution or growth rate in magma

Depending on the melt composition and the environment temperature and pressure conditions, a quartz crystal may undergo dissolution and growth in a natural magma chamber, such as quartz phenocrysts commonly found in rhyolites and quartz xenocryst found in basaltic andesites (Blatter and Carmichael, 1998). It is of special interest to quantify the dissolution or growth rate of quartz in the magmatic system and use it as a tool to constrain the evolution history of the host magmatic melt.

The convective dissolution or growth rate of a quartz crystal can be estimated as (Kerr, 1995; Zhang and Xu, 2003; Zhang, 2008):

$$\left| \frac{da}{dt} \right| = \frac{\rho_{\text{melt}}}{\rho_{\text{quartz}}} \frac{C_0 - C_\infty}{C_c - C_0} \frac{D_{\text{SiO}_2}}{\delta} \quad (3-14)$$

where a is the effective radius of a quartz crystal, t is the time, ρ is the density, C_∞ , C_0 , and C_c are the SiO_2 concentrations of the host magma, the quartz-melt interface melt and the quartz crystal, δ is the effective compositional boundary layer thickness, D_{SiO_2} is the average diffusivity of SiO_2 within the boundary layer surrounding the quartz crystal.

The empirical estimation of δ largely depends on the flow pattern in the magma, which is characterized primarily by the Peclet number and Reynolds number $\text{Re} = 2a u \rho_{\text{melt}} / \eta$, where u is the relatively velocity of the quartz crystal to the magma, η is the viscosity of the magma. Within the realm of $\text{Re} < 1$, the steady-state free falling velocity of the quartz crystal in the magma can be calculated from the Stoke's law:

$$u = 2ga^2\Delta\rho / (9\eta) \quad (3-15)$$

where g is Earth's gravitational acceleration ($\sim 9.8 \text{ m/s}^2$), $\Delta\rho$ is the density difference between quartz and the magma.

Within the same range of Re , the effective compositional boundary layer thickness can be estimated as (Kerr, 1995):

$$\delta = 2a / [1 + (1 + Pe)^{1/3}] \quad (3-16)$$

where Pe is introduced as Peclet number, defined as the mass transfer rate ratio between convection and diffusion:

$$Pe = 2au / D_{\text{SiO}_2} \quad (3-17)$$

3.7.1 Quartz dissolution or growth in rhyolitic melts

As the density difference between quartz and the rhyolitic melt is small ($\sim 0.1\text{-}0.2 \text{ g/cc}$) and the relatively dry rhyolitic melt is rather viscous, the steady-state free falling velocity of a quartz crystal in the magma is also small, resulting in a small Reynolds number ($\sim 10^{-15}$ for a 2mm-radius quartz crystal falling in the magma). Therefore the above equations (3-15, 3-16 and 3-17) are confirmed to apply for quartz dissolution or growth in the rhyolitic magma. Note that the accuracy of the calculated dissolution or growth rate using the above approach has been experimentally shown to be within about 15% when the necessary parameters are well known.

Combining eqs. 3-15, 3-16 and 3-17, and the previous models regarding the average SiO_2 diffusivity (Eq. 3-12), the interface SiO_2 concentration during quartz dissolution in a rhyolitic melt (Eq. 3-8a), the melt viscosity and density (Hui and Zhang, 2007; Ochs and Lange, 1999), we can model the dissolution or growth of a free-falling quartz crystal in the rhyolitic magma. By varying the SiO_2 concentration (70, 72, 74, 76,

78, 80 wt% SiO₂) of the magma, and the magma temperature (800-1250 °C), the dissolution or growth rates of a quartz crystal of 150 µm in radius were calculated. In Fig. 3-13, different dissolution or growth rates of the quartz crystal in magma of various SiO₂ concentrations and temperatures are shown. At temperature above the quartz-magma equilibrium temperature, the dissolution rate increase monotonically as the temperature escalates; while during the growth temperature domain, the quartz growth rate first increases and then decreases, as the magma temperature gradually drops. For example, in a dry rhyolitic magma with 74 wt% SiO₂, the maximum quartz growth rate is about 11 µm/yr when the magma temperature is about 1030 °C. If the magma cools very slowly or maintains constant temperature during the growth process of a quartz crystal, it would take about 80 years for a quartz crystal to grow from a 150 µm nucleus into a 1 mm phenocryst – a typical size of a quartz phenocryst in rhyolites.

3.7.2 Quartz dissolution in basaltic melts

Quartz xenocrysts have been sometimes found in melts of andesitic to basaltic compositions. For instance, 0.5-3.5% quartz xenocrysts (e.g. ~250 µm across) were observed in all the sampled lavas from Mexican Volcanic Belt (MVB) by Blatter and Carmichael (1998). On one hand, quartz xenocrysts can provide clues for the magma mixing origin of the andesitic melt; on the other hand, the presence of quartz xenocrysts can be used to put some time constraints on the evolution history for the mixing process, such as how long it would take for the basaltic melt to digest the quartz phenocryst of certain sizes.

The Reynolds number for a 2mm-radius steadily free-rising quartz crystal in a

basaltic melt was calculated to be about 10^{-5} . Quartz dissolution or growth was modeled in melts of basalt to basaltic andesite compositions with SiO_2 ranging from 50 wt% to 60 wt%, at temperature ranging from 900 °C to 1300 °C. In Fig. 3-14, the dissolution rates of quartz crystal at different melt compositions and temperatures are shown. Quartz dissolution rates generally increases as temperature. Below the equilibrium temperature, quartz grows. For example, in an andesite melt with 58 wt% SiO_2 , the dissolution rate of quartz crystal is about 65 $\mu\text{m}/\text{day}$ at 1200 °C and 0.5 GPa. It would take about 30 days for a 2mm-radius quartz crystal to completely dissolve in the host melt. Because the survival time of quartz xenocryst is short, it is most likely that the magma picked up the xenocrysts from the conduit during an eruption. That is, the quartz xenocrysts did not fall into and reside in the magma chamber.

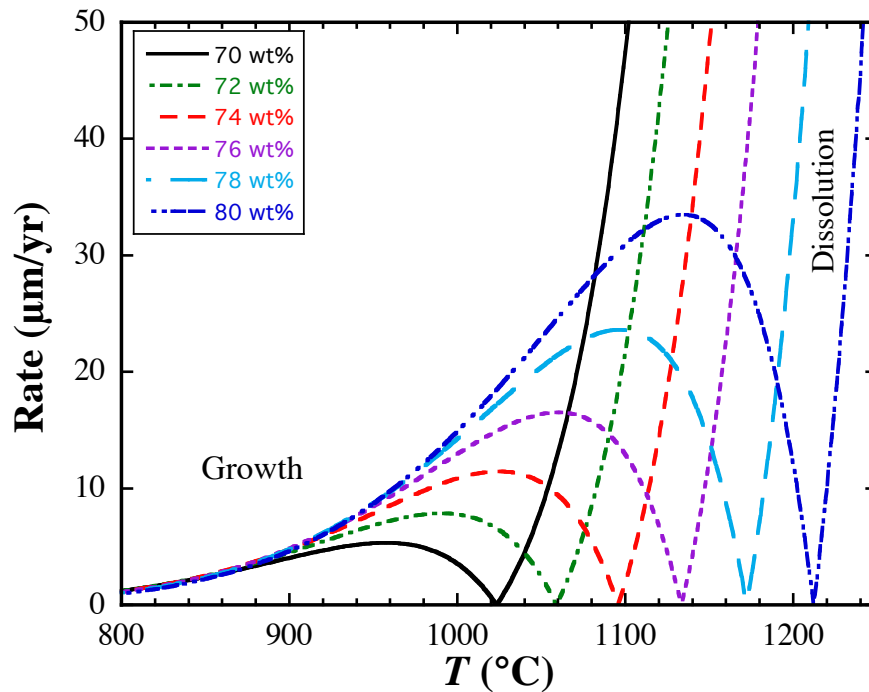


Figure 3-13. Calculated dissolution or growth rate of a quartz crystal of 150 μm in radius as a function of magma composition (SiO_2 concentration) and temperature in rhyolitic melts. The pressure condition is 0.5 GPa. The minimum of each curve (rate = 0) indicates the equilibrium between quartz and the corresponding magma. At temperature above the equilibrium temperature, quartz dissolves; below the equilibrium temperature, quartz grows.

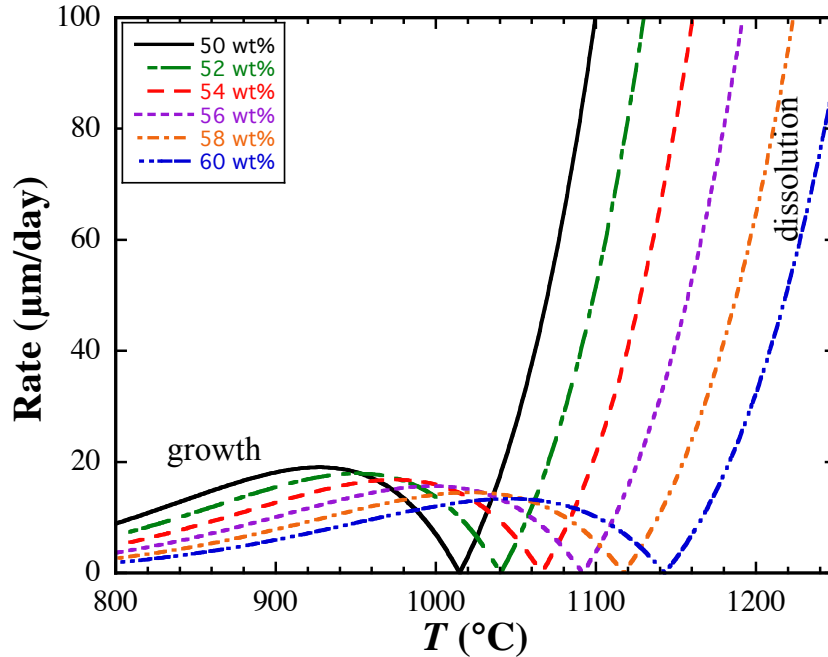


Figure 3-14. Calculated dissolution or growth rate of a quartz crystal of 2 mm in radius as a function of magma composition (SiO_2 concentration) and temperature in basaltic to andesitic melts. The pressure condition is 0.5 GPa. The minimum of each curve (rate = 0) indicates the equilibrium between quartz and the corresponding magma. At temperature above the equilibrium temperature, quartz dissolves; below the equilibrium temperature, quartz grows.

3.8. Conclusions

1. During quartz dissolution, the SiO_2 concentration profile cannot be described by a constant diffusivity. The compositional dependence of, including the effect of H_2O on, SiO_2 diffusivity can be roughly described as an exponential dependence on the cation mole fraction of Si + Al. The part that cannot be accounted for by this parameter cannot be well-modeled with the available data.

2. The compositional dependence of $\ln D_{\text{SiO}_2}$ (parameter a in Eq. 3-5) becomes weaker as temperature increases (Eq. 3-5). SiO_2 diffusivities during quartz dissolution in

rhyolitic and basaltic melts can be roughly accounted for using a simple model (Eq. 3-7) within 1 σ error of 0.52 $\ln D$ unit.

3. The diffusive dissolution rate of quartz in these silicate melts can still be described using $V_{\text{quartz}} = \frac{\rho_{\text{melt}}}{\rho_{\text{quartz}}} \alpha \sqrt{\frac{D}{t}}$, but with D interpreted as the average SiO₂ diffusivity across the concentration profile (Eq. 3-12). The convective dissolution or growth rate of quartz in magmas has been illustrated in Fig. 3-13 and 3-14. Such modeling shows that it would take about 80 years for a quartz crystal to grow from 150 μm in radius to 1 mm in radius at its maximum growth rate in a rhyolitic magma with 74 wt% SiO₂ at 1030 °C and it would take about 28 days for a quartz xenocryst of 2 mm in radius to completely dissolve into a basaltic andeistic melt with 58 wt% SiO₂ at 1200 °C.

4. We have developed the method of using Boltzmann analysis to treat concentration-dependent diffusivity from diffusion profiles during diffusive crystal dissolution.

Acknowledgement

This research is supported by NSF grants EAR-1019440 and EAR-1524473. Electron microprobe work is carried out on a Cameca SX100 instrument at Electron Microbeam Analysis Laboratory of the University of Michigan, which is supported by NSF grant EAR-9911352.

References

- Acosta-Vigil A., London D., Morgan G.B. and Dewers, T.A., 2006 Dissolution of quartz, albite, and orthoclase in H₂O-saturated haplogranitic melt at 800 C and 200 MPa: Diffusive transport properties of granitic melts at crustal anatexis conditions. *J. Petrol.* 47, 231-254.
- Baker, D.R., and Watson, E.B., 1988. Diffusion of major and trace elements in compositionally complex Cl- and F-bearing silicate melts. *J. Non-Cryst. Solids*, 102, 62-70.
- Baker, D.R., 1990. Chemical interdiffusion of dacite and rhyolite: anhydrous measurements at 1 atm and 10 kbar, application of transition state theory, and diffusion in zoned magma chambers. *Contrib. Mineral. Petrol.*, 104, 407-423.
- Baker, D.R., 1991. Interdiffusion of hydrous dacitic and rhyolitic melts and the efficacy of rhyolite contamination of dacitic enclaves. *Contrib. Mineral. Petrol.*, 106, 462-473.
- Baker, D.R., 1993. The effect of F and Cl on the interdiffusion of peralkaline intermediate and silicic melts. *Am. Mineral.*, 78, 316-324.
- Baker, D.R., and Bossányi, H., 1994. The combined effect of F and H₂O on interdiffusion between peralkaline dacitic and rhyolitic melts. *Contrib. Mineral. Petrol.*, 117, 203-214.

- Bourova, E. and Richet, P., 1998. Quartz and Cristobalite: high temperature cell parameters and volumes of fusion. *Geophys. Res. Lett.*, 25, 2333-2336.
- Chen, Y., and Zhang, Y., 2008. Olivine dissolution in basaltic melt. *Geochim. Cosmochim. Acta* 72, 4756-4777.
- Chen, Y., and Zhang, Y., 2009. Clinopyroxene dissolution in basaltic melt. *Geochim. Cosmochim. Acta* 73, 5730-5747.
- Cooper, A.R., 1968. The use and limitations of the concept of an effective binary diffusion coefficient for multicomponent diffusion. *Mass Transport in Oxides*, 296, 79-84. Nat. Bur. Stand. Spec. Publ.
- Dixon, J.E., Clague, D.A., and Eissen, J.A., 1986. Gabbroic xenoliths and host ferrobasalt from the southern Juan de Fuca Ridge. *J. Geophys. Res.* 91, 3795-3820.
- Dixon, J.E., Stolper, E., and Delaney, J.R., 1988. Infrared spectroscopic measurements of CO₂ and H₂O in Juan de Fuca Ridge basaltic glasses. *Earth Planet. Sci. Lett.* 90, 87-104.
- Hudon, P., Jung, I.H., and Baker, D.R., 2002. Melting of β -quartz up to 2.0 GPa and thermodynamic optimization of the silica liquidus up to 6.0 GPa. *Phys. Earth Planet. Inter.*, 130, 159-174.
- Hui, H., Zhang, Y., Xu, Z., and Behrens, H., 2008. Pressure dependence of the speciation of dissolved water in rhyolitic melts. *Geochim. Cosmochim. Acta* 72, 3229-3240.
- Jackson, I., 1976. Melting of the silica isotypes SiO₂, BeF₂ and GeO₂ at elevated pressures. *Phys. Earth Planet. Inter.*, 13, 218-231.
- Kerr R.C., 1995. Convective crystal dissolution. *Contrib. Mineral. Petrol.* 121, 237-246.

- Koyaguchi, T., 1989. Chemical gradient at diffusive interfaces in magma chambers. *Contrib. Mineral. Petrol.*, 103, 143-152.
- Kubicki, J.D., Muncill, G.E., and Lasaga, A.C., 1990. Chemical diffusion in melts on the $\text{CaMgSi}_2\text{O}_6$ - $\text{CaAl}_2\text{Si}_2\text{O}_8$ join under high pressures. *Geochim. Cosmochim. Acta*, 54, 2709-2715.
- Leshner, C.E., and Walker, D., 1986. Solution properties of silicate liquids from thermal diffusion experiments. *Geochim. Cosmochim. Acta*, 50, 1397-1411.
- Leshner, C.E., Hervig, R.L., and Tinker, D., 1996. Self diffusion of network formers (silicon and oxygen) in naturally occurring basaltic liquid. *Geochim. Cosmochim. Acta*, 60, 405-413.
- Liang, Y., Richter, F.M., Davis, A.M., and Watson, E.B., 1996. Diffusion in silicate melts: I. Self diffusion in $\text{CaO-Al}_2\text{O}_3\text{-SiO}_2$ at 1500° C and 1 GPa. *Geochim. Cosmochim. Acta*, 60, 4353-4367.
- Liang, Y., 1999. Diffusive dissolution in ternary systems: analysis with applications to quartz and quartzite dissolution in molten silicates. *Geochim. Cosmochim. Acta*, 63, 3983-3995.
- Lundstrom, C.C., 2003. An experimental investigation of the diffusive infiltration of alkalis into partially molten peridotite: implications for mantle melting processes. *Geochem. Geophys. Geosyst.* 4, 8614.
- Matano, C., 1933. On the relation between the diffusion-coefficients and concentrations of solid metals (the nickel-copper system). *Jpn. J. Phys.*, 8, 109-113.
- Newman, S., Stolper, E.M., and Epstein, S., 1986. Measurement of water in rhyolitic glasses: Calibration of an infrared spectroscopic technique, *Am. Mineral.*, 71, 1527-

1541.

Ni, H. and Zhang, Y., 2008. H₂O diffusion models in rhyolitic melt with new high pressure data. *Chem. Geol.* 250, 68-78.

Ochs F.A. and Lange, R.A., 1999. The density of hydrous magmatic liquids. *Science* 283, 1314-1317.

Reid, J.E., Poe, B.T., Rubie, D.C., Zotov, N., and Wiedenbeck, M., 2001. The self-diffusion of silicon and oxygen in diopside (CaMgSi₂O₆) liquid up to 15 GPa. *Chem. Geol.*, 174, 77-86.

Shaw C.S.J., 2000. The effect of experiment geometry on the mechanism and rate of dissolution of quartz in basanite at 0.5 GPa and 1350 C. *Contrib. Mineral. Petrol.* 139, 509-525.

Shaw C.S.J., 2004. Mechanisms and rates of quartz dissolution in melts in the CMAS (CaO-MgO-Al₂O₃-SiO₂) system. *Contrib. Mineral. Petrol.* 148, 180-200.

Shaw C.S.J., 2006. Effects of melt viscosity and silica activity on the rate and mechanism of quartz dissolution in melts of the CMAS and CAS systems. *Contrib. Mineral. Petrol.* 151, 665-680.

Shaw, C.S., 2012. The effects of potassium addition on the rate of quartz dissolution in the CMAS and CAS systems. *Contrib. Mineral. Petrol.*, 164, 839-857.

Tilley C. E., 1922. Density, refractivity, and composition relations of some natural glasses. *Miner. Mag.*, 19, 275-294.

Tinker, D., and Lesher, C.E., 2001. Self diffusion of Si and O in dacitic liquid at high pressures. *Am. Mineral.*, 86, 1-13.

- Tinker, D., Lesher, C.E., and Hutcheon, I.D., 2003. Self-diffusion of Si and O in diopside-anorthite melt at high pressures. *Geochim. Cosmochim. Acta*, 67, 133-142.
- van der Laan, S., Zhang, Y., Kennedy, A.K., and Wyllie, P.J., 1994. Comparison of element and isotope diffusion of K and Ca in multicomponent silicate melts. *Earth Planet. Sci. Lett.*, 123, 155-166.
- Watson, E.B., 1982. Basalt contamination by continental crust: some experiments and models. *Contrib. Mineral. Petrol.*, 80, 73-87.
- Yang, Y., Zhang, Y., Simon, A., and Ni, P., 2016. Cassiterite dissolution and Sn diffusion in silicate melts of variable water content. *Chem. Geol.*, submitted.
- Yu, Y., Zhang, Y., Chen, Y., and Xu, Z., 2016. Kinetics of anorthite dissolution in basaltic melt. *Geochim. Cosmochim. Acta*, 179, 257-274.
- Zhang, Y., Walker, D., and Lesher, C.E., 1989. Diffusive crystal dissolution. *Contrib. Mineral. Petrol.*, 102, 492-513.
- Zhang, Y., Stolper, E.M., Wasserburg, G.J., 1991. Diffusion of water in rhyolitic glasses. *Geochim. Cosmochim. Acta*, 55, 441-456.
- Zhang, Y., Stolper, E.M., 1991. Water diffusion in a basaltic melt. *Nature*, 351, 306-309.
- Zhang, Y., 1999. H₂O in rhyolitic glasses and melts: measurement, speciation, solubility, and diffusion. *Rev. Geophys.*, 37, 493-516.
- Zhang, Y. and Behrens, H., 2000. H₂O diffusion in rhyolitic melts and glasses. *Chem. Geol.*, 169, 243-262.
- Zhang Y. and Xu Z., 2003. Kinetics of convective crystal dissolution and melting, with applications to methane hydrate dissolution and dissociation in seawater. *Earth Planet. Sci. Lett.* 213, 133-148.

- Zhang Y. (2008) *Geochemical kinetics*. Princeton University Press, Princeton, NJ.
- Zhang, Y., Ni, H., and Chen, Y., 2010. Diffusion data in silicate melts. *Rev. Mineral. Geochem.* 72, 311-408.
- Zhang, Y., Xu, Z., 2016. Zircon saturation and Zr diffusion in rhyolitic melts, and zircon growth geospeedometer. *Am. Mineral.*, in press,
http://www.minsocam.org/msa/ammin/AM_Preprints/5462ZhangPreprint.pdf.

Chapter IV

Conclusion

The central goal of my dissertation is to provide tools to model the dynamic nature of actual geological systems, such as lunar crust formation, and Earth's granitic continental crust evolution. By conducting series of experimental studies on anorthite and quartz dissolution, this work has provided useful insights in the quantification of the dissolution and growth process and in the diffusive properties of the corresponding silicate melts.

In Chapter II, three fundamental aspects of anorthite dissolution have been concluded: 1. Al_2O_3 concentration of anorthite-melt interface melt can be used as a simple and practical indicator of anorthite-melt equilibrium condition; 2. Anorthite dissolution is primarily controlled by diffusion in a non-convective magmatic environment, that is, the diffusive dissolution rate of anorthite in basaltic melt follows a parabolic relation; 3. Diffusivities of Al_2O_3 depend on melt composition.

Mineral-melt equilibrium can be as complex as one wants to fine-tune into the 'polynomials' of interactions among different chemical components. However, simple-compositional minerals at saturation with melts can have relatively straightforward equilibrium-determining components, such as MgO for olivine (Chen and Zhang, 2008), MgO and CaO for diopside (Chen and Zhang, 2009), Al_2O_3 for anorthite, and SiO_2 for

quartz. A composition-complex system can be viewed as a collection of equilibrium pairs between different minerals and their host melts. Such coarse determination is by no means a precise characterization of the equilibrium condition, but it serves well the practical purpose of quantifying the rate of the kinetic processes. With proper determination of equilibrium condition, kinetic potential of mineral dissolution (undersaturation) and growth (oversaturation) can be reasonably evaluated. This serves as the first side of a coin.

On the flip side, mass transport of the equilibrium-determining component controls if the kinetic potential can be achieved or at what degree the kinetic potential can be realized in the case of mineral dissolution or growth. Therefore, it is of special importance to quantify the diffusion behavior of the equilibrium-determining component – Al_2O_3 in the case of anorthite dissolution. Based on the above results, Chapter II gave rise to a convective dissolution model of anorthite in the basaltic melt, showing that anorthite could survive for a longer time but would rise/sink for a shorter distance in a magma reservoir due to the smaller density contrast between anorthite and the basaltic melt, compared to the convective olivine dissolution in the basaltic melt (Chen and Zhang, 2008). An interesting consequence is the seemingly disagreement between the short rising/surviving distance (a few kilometers) from the above modeling and the need of anorthite crystals floating through a magmatic ocean of tens of kilometer thick in order to form lunar anorthosite crust. The possible resolution may rely on the relatively magnitude between the pressure dependence of anorthite-melt equilibrium temperature and the geotherm of the late stage lunar magma ocean. If the former were smaller than the latter, anorthite crystals would start to crystallize at a certain depth of the lunar

magma ocean, and continue to grow until they reach near surface of Moon. In contrast, if the former were larger than the latter, there would be a layer of dissolving domain, through which anorthite crystals have to survive after their initial growth at depth in order to reach near surface of Moon. Future experimental studies are needed to quantitatively compare the relative magnitudes of the pressure dependence of anorthite-melt equilibrium temperature and the geotherm of the late stage lunar magma ocean, and eventually paint the picture of the formation of lunar anorthosite crust.

Started with a similar approach as Chapter II, Chapter III initially aimed to separately investigate the kinetics of quartz dissolution in two different silicate melts (rhyolitic and basaltic) but ended up combining the two studies and coming up with a unifying diffusive dissolution model across rhyolitic, andesitic and basaltic melts.

Similarly controlled by diffusion, an emphasis of quartz dissolution was placed on extracting the composition-dependent diffusivities of SiO_2 from experiments, as the analytical model, which assumes constant SiO_2 diffusivity, failed to fit the SiO_2 concentration profile well. Two approaches were therefore developed to process SiO_2 concentration profiles. The first approach - Boltzmann analysis, is similar to the Boltzmann-Montana method used in diffusion-couple experiments, but is extended to also apply in the schema of diffusive mineral dissolution. Based on the Boltzmann analysis, the natural logarithm of SiO_2 diffusivity is shown to be linearly dependent on $X_{\text{Si+Al}}$ - the cation mole fraction of Si+Al in silicate melts, that is, more polymerized melt will see SiO_2 to diffuse slower. What is more, SiO_2 diffusivities across different melt compositions (rhyolitic and basaltic) are shown to roughly follow the same trend at same

temperatures. The second approach - functional fitting, takes an explicit functional relation, learned from the Boltzmann analysis, between SiO₂ diffusivities and melt compositions, and provides better statistical constraints on the fitted values and errors. These results better showed that the composition-dependence of SiO₂ diffusivities has strong temperature dependence. That is, at higher temperature, the compositional dependence of SiO₂ diffusivities is weaker; as microscopic particles of the silicate melts have more kinetic energy to overcome the constraints of the melt structure.

The above quartz studies made an attempt to use a unifying model to account for the SiO₂ diffusivities across silicate melt of different compositions during quartz dissolution. With the proper choice of the compositional parameter ($X_{\text{Si+Al}}$), variation in melt compositions and H₂O contents can be simply addressed. Yet, this is just the beginning. Such compositional dependence is not unique to SiO₂, as shown by Al₂O₃ diffusivities from the anorthite dissolution study. By comparing the diffusivity data across a wide range of melt compositions, it is possible to resolve the composition dependence of other components in the melt and probe deeper into understanding the silicate melt structure. Hence, some work remains to be done along this direction.

Based on the above results, the application of estimating the dissolution or growth rate of quartz crystals in anhydrous magma was applied. Specifically, it could take a minimum of about 80 years for a quartz crystal in magma with 74 wt% SiO₂ at 1030 °C to grow from a 150 μm nucleus to a 1 mm phenocryst – a typical size of quartz phenocryst observed in rhyolitic extrusion. In terms of quartz xenocryst digestion, it could take about 30 days for a quartz xenocryst of 2 mm in radius to dissolve in a basaltic andesite with 58 wt% SiO₂ at 1200 °C. Some important stretches of this modeling are to

quantify the dissolution or growth rate in hydrous rhyolitic melts and in basaltic melts. Though SiO₂ diffusivity model in various silicate melts during quartz dissolution has been established, the effects of H₂O and melt composition on quartz-melt equilibrium have not been quantified. Further work is needed to make up for the comprehensive quartz dissolution or growth model in hydrous rhyolitic melts and basaltic melts.

Granitic magma can form millimeter-scale fine-grained granite that paves the floors of buildings; but it can also grow into colossal pegmatite, a rock with crystals several meters in diameter. Comparably, large scale igneous processes such as the evolution of Moon's crusts is not only much more extensive but also much more complicated. Regardless of the scale, one of the key issues at center is what dynamic elements of the system contribute to different outcomes. My dissertation takes a kinetic perspective and quantifies the dissolution processes of anorthite and quartz in different silicate melts. These basic model units can be further used to provide more insights and constraints on many other processes of interest.

Appendices

Appendix A

Composition Profiles of Anorthite Dissolution in Basaltic Melt

Exp 201

x / μm	Oxides (wt%)										
	SiO2	SiO2*	TiO2	Al2O3	FeO	MnO	MgO	CaO	Na2O	K2O	Total
9.0	47.48	48.69	1.23	19.65	9.58	0.17	5.25	11.84	2.73	0.16	98.09
15.0	47.77	48.61	1.21	19.75	9.64	0.19	5.18	11.88	2.67	0.16	98.46
21.0	47.92	48.56	1.24	19.51	9.85	0.16	5.30	11.83	2.67	0.17	98.66
27.0	47.78	48.87	1.19	19.29	9.77	0.20	5.38	11.75	2.68	0.17	98.21
27.0	47.94	48.74	1.35	19.32	9.79	0.19	5.34	11.80	2.63	0.16	98.50
42.8	48.33	49.10	1.32	18.71	9.91	0.18	5.46	11.77	2.67	0.18	98.53
58.6	48.53	49.41	1.42	18.14	10.11	0.23	5.48	11.72	2.63	0.16	98.41
74.5	48.94	49.75	1.39	17.70	10.22	0.20	5.60	11.59	2.69	0.17	98.49
90.3	49.13	50.02	1.52	17.29	10.23	0.16	5.64	11.60	2.68	0.16	98.41
121.9	49.69	50.34	1.47	16.47	10.57	0.17	5.91	11.50	2.69	0.17	98.65
137.7	50.13	50.76	1.56	15.96	10.77	0.12	5.93	11.42	2.61	0.17	98.68
153.5	50.07	50.99	1.56	15.64	10.82	0.17	5.93	11.37	2.65	0.17	98.38
169.4	50.32	50.87	1.74	15.29	10.95	0.20	6.04	11.35	2.68	0.17	98.74
185.2	50.57	51.09	1.67	15.01	11.09	0.21	6.00	11.42	2.63	0.18	98.78
201.0	50.98	51.29	1.71	14.63	11.07	0.24	6.19	11.30	2.68	0.18	99.00
191.5	50.31	50.79	1.76	14.81	11.27	0.20	6.36	11.31	2.63	0.18	98.82
212.2	50.37	51.27	1.76	14.37	11.31	0.16	6.26	11.38	2.60	0.18	98.39
232.8	50.61	51.43	1.75	14.13	11.39	0.16	6.37	11.30	2.59	0.18	98.48
253.0	50.65	51.18	1.89	13.87	11.59	0.17	6.59	11.26	2.58	0.17	98.77
292.5	50.60	51.68	1.79	13.56	11.56	0.25	6.52	11.19	2.58	0.17	98.22
332.0	50.73	51.61	1.78	13.56	11.58	0.20	6.65	11.18	2.56	0.18	98.42
371.5	50.71	51.33	1.80	13.46	11.93	0.22	6.61	11.22	2.57	0.17	98.67
410.9	50.48	51.81	1.77	13.33	11.69	0.23	6.61	11.10	2.57	0.19	97.97
450.4	50.49	51.57	1.96	13.29	11.90	0.18	6.56	11.11	2.54	0.18	98.22
489.9	50.64	51.60	1.64	13.40	11.86	0.25	6.76	11.07	2.53	0.19	98.35
529.4	50.61	51.40	1.87	13.28	12.10	0.20	6.65	11.04	2.58	0.17	98.51
568.9	50.68	51.34	1.90	13.38	11.88	0.22	6.78	11.02	2.60	0.18	98.64
608.4	50.54	51.35	1.86	13.39	11.95	0.19	6.72	11.01	2.64	0.18	98.50
647.9	50.68	51.78	1.75	13.25	11.88	0.23	6.57	11.10	2.56	0.18	98.20
8.3	47.58	48.33	1.24	19.85	9.53	0.23	5.39	11.85	2.71	0.17	98.55
14.0	47.83	48.47	1.27	19.82	9.63	0.13	5.33	11.83	2.69	0.15	98.66
19.8	48.08	48.63	1.22	19.46	9.70	0.19	5.37	11.86	2.68	0.18	98.75
25.5	48.15	48.80	1.21	19.31	9.82	0.14	5.34	11.82	2.71	0.16	98.65
25.5	48.25	48.88	1.29	19.34	9.88	0.17	5.23	11.74	2.62	0.16	98.67
46.5	48.94	49.39	1.23	18.46	10.01	0.18	5.49	11.66	2.71	0.17	98.85
67.7	49.26	49.83	1.38	17.77	10.04	0.23	5.69	11.51	2.67	0.17	98.72
88.8	49.75	50.23	1.49	16.89	10.45	0.21	5.68	11.51	2.68	0.16	98.82

110.0	49.97	50.61	1.55	16.46	10.47	0.14	5.77	11.48	2.66	0.16	98.67
131.1	50.27	50.72	1.61	15.84	10.74	0.21	5.88	11.42	2.71	0.17	98.85
152.3	50.84	50.73	1.69	15.44	11.01	0.21	6.00	11.38	2.68	0.17	99.41
173.4	51.23	51.27	1.80	14.80	10.97	0.26	6.14	11.21	2.65	0.19	99.26
178.7	50.50	51.29	1.72	14.69	11.13	0.24	6.19	11.31	2.56	0.17	98.51
213.7	50.87	51.28	1.73	14.25	11.42	0.20	6.32	11.31	2.62	0.17	98.89
248.7	50.91	51.77	1.75	13.60	11.56	0.17	6.46	11.17	2.64	0.18	98.45
238.8	50.69	51.42	1.79	13.81	11.57	0.22	6.57	11.20	2.56	0.17	98.57
279.0	50.58	51.37	1.90	13.66	11.63	0.21	6.52	11.27	2.58	0.16	98.50
319.2	50.65	51.27	1.84	13.63	11.81	0.24	6.57	11.19	2.57	0.18	98.69
359.5	50.43	51.45	1.87	13.43	11.80	0.19	6.60	11.21	2.58	0.18	98.28
399.7	50.54	51.74	1.75	13.33	11.86	0.18	6.66	11.03	2.56	0.18	98.11
439.9	50.47	51.43	1.87	13.33	11.88	0.22	6.67	11.11	2.61	0.18	98.34
480.1	50.27	51.51	1.83	13.28	11.92	0.21	6.66	11.11	2.60	0.18	98.06
520.4	50.68	51.47	1.83	13.43	11.98	0.21	6.59	10.99	2.62	0.18	98.51
560.5	50.53	51.51	1.91	13.41	11.75	0.20	6.73	11.03	2.58	0.17	98.33
600.7	50.53	51.33	1.94	13.34	11.89	0.23	6.74	11.04	2.61	0.19	98.50

SiO₂* = SiO₂ + (99.3-Total)

Exp 202

x / μm	Oxides (wt%)										
	SiO2	SiO2*	TiO2	Al2O3	FeO	MnO	MgO	CaO	Na2O	K2O	Total
13.1	47.50	48.24	1.15	20.43	9.55	0.12	5.10	11.98	2.58	0.14	98.56
18.2	47.42	48.20	1.24	20.20	9.60	0.16	5.10	12.08	2.57	0.15	98.52
23.3	47.50	48.12	1.32	20.23	9.67	0.14	5.12	11.95	2.59	0.17	98.69
28.4	47.48	48.03	1.22	20.27	9.70	0.21	5.12	11.97	2.62	0.16	98.75
33.6	47.36	48.44	1.11	19.91	9.71	0.20	5.23	11.94	2.60	0.16	98.22
38.7	47.66	48.32	1.19	20.07	9.62	0.20	5.20	11.90	2.64	0.15	98.64
43.8	47.60	48.27	1.23	19.97	9.76	0.15	5.20	11.95	2.59	0.17	98.63
48.9	47.70	48.32	1.23	20.01	9.65	0.13	5.20	11.99	2.62	0.14	98.68
48.9	47.85	48.34	1.40	19.85	9.76	0.15	5.21	11.89	2.56	0.15	98.82
59.5	47.56	48.81	1.13	19.54	9.85	0.13	5.20	11.86	2.65	0.15	98.05
70.1	47.73	48.96	1.21	19.37	9.69	0.15	5.20	11.93	2.64	0.14	98.07
80.7	47.91	48.59	1.29	19.34	10.02	0.14	5.27	11.82	2.66	0.16	98.62
91.4	48.05	48.45	1.43	19.21	10.00	0.20	5.30	11.86	2.71	0.14	98.90
101.9	48.28	48.87	1.42	18.99	9.95	0.10	5.31	11.85	2.65	0.16	98.71
112.5	48.30	48.74	1.28	19.07	10.07	0.15	5.37	11.77	2.66	0.18	98.86
123.1	48.54	48.74	1.40	18.88	10.05	0.23	5.38	11.77	2.69	0.16	99.10
133.7	48.44	49.25	1.37	18.37	10.18	0.19	5.37	11.79	2.61	0.17	98.49
144.3	48.68	49.28	1.44	18.38	9.98	0.16	5.39	11.82	2.65	0.19	98.70
154.9	48.67	49.44	1.41	18.20	10.03	0.17	5.41	11.79	2.69	0.16	98.53
165.6	48.60	49.76	1.36	17.77	10.19	0.17	5.52	11.72	2.64	0.17	98.14
176.2	48.62	49.90	1.27	17.71	10.25	0.18	5.53	11.65	2.65	0.16	98.02
186.8	49.19	49.70	1.45	17.67	10.21	0.20	5.51	11.70	2.71	0.16	98.79
186.8	48.93	49.92	1.31	17.50	10.28	0.14	5.56	11.78	2.64	0.16	98.31
206.9	48.98	49.96	1.40	17.40	10.40	0.18	5.56	11.58	2.64	0.18	98.32
227.0	49.24	50.07	1.56	16.96	10.33	0.19	5.64	11.70	2.69	0.16	98.47
247.1	49.47	50.22	1.51	16.70	10.46	0.11	5.73	11.73	2.65	0.19	98.55
267.2	49.61	50.29	1.63	16.31	10.66	0.23	5.77	11.63	2.59	0.17	98.62
287.3	49.83	50.50	1.48	16.30	10.74	0.18	5.78	11.47	2.67	0.17	98.62
307.4	50.11	51.02	1.57	15.81	10.68	0.21	5.81	11.44	2.58	0.17	98.39
327.5	50.24	50.99	1.46	15.72	10.82	0.14	5.82	11.53	2.66	0.16	98.56
347.6	50.03	50.81	1.64	15.53	10.92	0.17	5.95	11.48	2.63	0.16	98.52
367.6	50.04	50.73	1.73	15.32	11.00	0.20	6.05	11.43	2.67	0.15	98.61
387.7	50.03	51.12	1.67	14.97	11.05	0.24	6.01	11.48	2.60	0.16	98.22
407.8	50.25	51.05	1.79	14.91	11.11	0.23	6.05	11.40	2.61	0.17	98.50
427.9	50.33	51.04	1.70	14.85	11.11	0.30	6.11	11.39	2.64	0.15	98.59
448.0	50.25	51.41	1.72	14.41	11.25	0.27	6.12	11.40	2.55	0.17	98.14
468.1	50.48	51.40	1.72	14.48	11.27	0.16	6.17	11.32	2.61	0.17	98.38
488.2	50.36	51.66	1.76	14.17	11.27	0.18	6.20	11.31	2.59	0.16	98.00
508.3	50.69	51.38	1.73	14.24	11.28	0.21	6.24	11.40	2.62	0.19	98.61
528.4	50.44	51.57	1.78	13.97	11.40	0.19	6.32	11.37	2.52	0.17	98.17

548.5	50.54	51.21	1.84	14.11	11.44	0.25	6.37	11.33	2.60	0.15	98.63
568.6	50.60	51.46	1.85	13.73	11.54	0.30	6.39	11.31	2.56	0.17	98.44
588.7	50.57	51.52	1.78	13.82	11.58	0.19	6.48	11.27	2.50	0.17	98.36
588.7	50.62	51.40	1.89	14.03	11.46	0.15	6.40	11.33	2.47	0.17	98.52
629.1	50.35	51.71	1.68	13.72	11.57	0.19	6.42	11.30	2.53	0.18	97.94
669.4	50.76	51.33	1.89	13.68	11.78	0.25	6.48	11.19	2.53	0.17	98.73
709.8	50.67	51.72	1.69	13.56	11.77	0.18	6.52	11.13	2.57	0.17	98.26
750.2	51.02	51.50	1.81	13.54	11.74	0.24	6.56	11.19	2.55	0.17	98.82
790.7	50.94	51.37	1.79	13.51	11.85	0.26	6.59	11.20	2.55	0.18	98.87
831.1	50.86	51.63	1.79	13.30	11.87	0.15	6.59	11.21	2.61	0.16	98.53
871.5	50.43	51.35	1.77	13.40	11.94	0.23	6.62	11.16	2.64	0.19	98.38
911.8	50.96	51.36	1.94	13.39	11.77	0.22	6.69	11.14	2.62	0.18	98.90
952.2	50.79	51.40	1.84	13.28	11.98	0.22	6.68	11.14	2.59	0.17	98.70
992.6	50.60	51.76	1.65	13.38	11.84	0.18	6.72	11.04	2.57	0.17	98.14
1033.0	50.65	51.30	1.99	13.37	11.91	0.20	6.72	11.08	2.56	0.17	98.64
1073.4	50.65	51.35	1.92	13.40	11.99	0.25	6.64	11.05	2.52	0.19	98.60
1113.8	50.99	51.40	1.79	13.29	11.96	0.21	6.73	11.14	2.61	0.16	98.89
1154.3	50.80	51.39	1.82	13.41	11.89	0.20	6.75	11.08	2.59	0.17	98.71
1194.6	50.69	51.82	1.77	13.24	11.78	0.16	6.74	11.06	2.56	0.17	98.17
1235.0	50.70	51.42	1.83	13.31	11.89	0.16	6.81	11.09	2.60	0.20	98.59
1275.4	50.75	51.37	1.79	13.42	12.02	0.17	6.75	11.02	2.59	0.17	98.68
9.4	47.35	47.82	1.30	20.54	9.52	0.22	5.13	11.95	2.66	0.16	98.84
14.6	47.23	48.21	1.18	20.33	9.55	0.14	5.10	11.93	2.70	0.16	98.32
19.7	47.37	48.37	1.19	20.03	9.60	0.21	5.16	11.95	2.64	0.15	98.30
24.9	47.59	48.18	1.20	20.21	9.65	0.20	5.14	11.95	2.63	0.14	98.71
30.0	47.66	48.12	1.23	20.16	9.77	0.16	5.18	11.87	2.65	0.17	98.84
35.2	47.48	48.58	1.14	19.89	9.65	0.18	5.17	11.93	2.62	0.15	98.20
40.3	47.66	48.35	1.18	19.94	9.75	0.18	5.15	11.95	2.65	0.15	98.62
45.5	47.74	48.91	1.23	19.56	9.56	0.20	5.17	11.91	2.62	0.14	98.13
50.6	47.67	48.72	1.04	19.64	9.87	0.18	5.18	11.89	2.63	0.15	98.25
55.8	47.45	48.73	1.38	19.48	9.66	0.14	5.20	11.91	2.65	0.16	98.02
60.9	48.04	48.43	1.20	19.60	9.99	0.20	5.24	11.82	2.66	0.16	98.91
66.1	47.74	48.78	1.16	19.44	9.79	0.17	5.25	11.93	2.64	0.16	98.27
66.1	48.07	48.44	1.36	19.66	9.79	0.13	5.26	11.88	2.63	0.14	98.93
76.5	48.09	48.85	1.20	19.26	9.86	0.14	5.29	11.86	2.68	0.17	98.55
87.0	47.92	49.04	1.31	18.98	9.96	0.15	5.31	11.78	2.63	0.16	98.18
97.4	48.13	49.06	1.31	18.86	9.98	0.17	5.35	11.72	2.70	0.16	98.37
107.8	48.10	49.21	1.35	18.75	9.95	0.11	5.35	11.76	2.67	0.16	98.19
128.7	48.43	49.44	1.44	18.30	10.01	0.18	5.41	11.69	2.69	0.15	98.29
139.1	48.61	49.62	1.23	18.13	10.11	0.20	5.46	11.71	2.67	0.16	98.30
149.5	48.77	49.48	1.39	18.17	10.15	0.23	5.44	11.61	2.66	0.17	98.59
160.0	48.74	49.59	1.47	17.81	10.20	0.13	5.50	11.74	2.70	0.15	98.45
170.4	48.74	49.56	1.57	17.76	10.25	0.15	5.47	11.74	2.66	0.15	98.49

180.8	48.62	50.11	1.43	17.39	10.25	0.13	5.55	11.62	2.68	0.14	97.82
191.2	48.93	49.88	1.40	17.32	10.38	0.18	5.59	11.72	2.68	0.15	98.35
201.7	49.11	50.07	1.52	17.11	10.32	0.24	5.58	11.65	2.64	0.16	98.34
212.1	49.51	49.93	1.47	17.13	10.46	0.15	5.65	11.68	2.67	0.16	98.88
212.1	49.38	49.89	1.40	17.20	10.54	0.19	5.64	11.70	2.57	0.17	98.79
232.7	49.46	50.27	1.57	16.68	10.53	0.20	5.67	11.59	2.65	0.15	98.49
253.4	49.32	50.21	1.64	16.56	10.48	0.19	5.78	11.60	2.70	0.16	98.41
273.9	49.42	50.46	1.50	16.25	10.78	0.21	5.75	11.54	2.63	0.17	98.27
294.6	49.68	50.67	1.44	16.09	10.74	0.20	5.83	11.52	2.64	0.16	98.31
315.2	49.95	50.63	1.55	15.77	10.98	0.19	5.88	11.52	2.60	0.18	98.61
335.9	49.74	50.68	1.56	15.72	10.99	0.11	5.95	11.48	2.62	0.19	98.37
356.5	50.07	51.14	1.63	15.28	10.96	0.14	5.88	11.47	2.63	0.17	98.22
377.2	50.00	51.15	1.54	15.02	11.16	0.18	6.10	11.42	2.56	0.19	98.16
397.8	50.36	51.15	1.66	14.91	11.14	0.21	6.06	11.41	2.57	0.18	98.51
418.5	50.32	50.74	1.72	14.82	11.41	0.22	6.09	11.50	2.65	0.16	98.88
439.1	50.27	51.24	1.83	14.61	11.15	0.20	6.13	11.42	2.56	0.15	98.32
459.8	50.15	51.22	1.90	14.45	11.22	0.14	6.17	11.40	2.63	0.17	98.23
480.4	50.32	51.08	1.69	14.47	11.44	0.23	6.16	11.44	2.62	0.18	98.53
501.1	50.53	51.40	1.82	14.03	11.40	0.21	6.27	11.35	2.63	0.18	98.43
521.7	50.18	51.67	1.73	14.00	11.43	0.15	6.26	11.29	2.61	0.16	97.81
542.2	50.60	51.69	1.68	13.91	11.47	0.17	6.34	11.29	2.58	0.17	98.20
562.9	50.75	51.37	1.81	13.83	11.67	0.20	6.29	11.33	2.61	0.18	98.68
562.9	50.54	51.53	1.82	14.02	11.47	0.17	6.37	11.25	2.50	0.16	98.31
604.0	50.78	51.37	1.78	13.84	11.64	0.26	6.43	11.25	2.55	0.17	98.71
645.1	51.01	51.17	1.84	13.71	11.88	0.19	6.47	11.30	2.56	0.17	99.14
686.2	50.71	51.41	1.85	13.69	11.69	0.17	6.51	11.27	2.53	0.17	98.60
727.4	50.67	51.45	1.73	13.56	11.82	0.28	6.53	11.26	2.53	0.16	98.52
768.5	51.03	51.40	1.81	13.46	11.90	0.18	6.58	11.27	2.54	0.16	98.93
809.5	50.69	51.39	1.78	13.51	11.96	0.20	6.59	11.17	2.53	0.16	98.60
850.6	50.55	51.39	1.81	13.43	11.94	0.24	6.60	11.16	2.57	0.16	98.46
891.7	50.58	51.14	1.92	13.46	11.92	0.19	6.65	11.26	2.59	0.17	98.75
932.9	50.75	51.28	1.75	13.43	11.94	0.23	6.70	11.21	2.59	0.17	98.77
974.0	50.51	51.41	1.87	13.38	11.87	0.23	6.66	11.15	2.58	0.16	98.40
1015.1	50.87	51.12	1.89	13.49	12.01	0.21	6.72	11.17	2.52	0.17	99.04
1056.2	50.86	51.49	1.75	13.31	11.96	0.23	6.68	11.10	2.60	0.18	98.67
1097.2	50.57	51.57	1.76	13.36	11.92	0.21	6.71	11.04	2.55	0.18	98.30
1138.3	50.72	51.41	1.76	13.37	11.96	0.19	6.77	11.10	2.58	0.16	98.60
1179.5	50.70	51.29	1.71	13.48	12.03	0.20	6.76	11.07	2.57	0.19	98.71
1220.6	50.66	51.46	1.79	13.35	11.95	0.15	6.77	11.01	2.64	0.18	98.50
1261.7	50.74	51.43	1.82	13.33	11.99	0.17	6.78	11.03	2.60	0.17	98.61
10.6	47.46	47.99	1.19	20.63	9.48	0.15	5.09	11.91	2.71	0.15	98.77
15.3	47.50	48.04	1.11	20.49	9.52	0.21	5.15	11.96	2.68	0.14	98.76
20.0	47.56	48.08	1.12	20.46	9.61	0.17	5.08	11.99	2.65	0.15	98.78

24.7	47.45	47.68	1.32	20.55	9.59	0.21	5.13	12.01	2.64	0.17	99.07
29.5	47.65	47.93	1.22	20.45	9.61	0.22	5.16	11.93	2.63	0.16	99.01
34.2	47.51	48.06	1.23	20.24	9.68	0.26	5.14	11.91	2.62	0.16	98.75
38.9	47.58	48.07	1.34	20.10	9.72	0.21	5.21	11.88	2.64	0.14	98.81
43.6	47.84	48.34	1.13	20.02	9.71	0.15	5.18	11.97	2.64	0.17	98.81
48.4	47.91	48.25	1.20	20.05	9.75	0.17	5.19	11.89	2.66	0.14	98.96
53.1	47.96	48.53	1.24	19.65	9.77	0.20	5.18	11.88	2.69	0.16	98.73
53.1	47.76	48.31	1.27	20.01	9.83	0.19	5.18	11.81	2.55	0.16	98.75
62.6	47.80	48.58	1.32	19.65	9.71	0.14	5.23	11.85	2.66	0.15	98.52
72.2	47.95	48.65	1.18	19.40	9.87	0.15	5.30	11.89	2.69	0.17	98.60
81.7	48.25	48.58	1.23	19.43	9.96	0.18	5.34	11.79	2.64	0.15	98.97
91.3	48.23	48.93	1.37	18.99	9.87	0.18	5.29	11.85	2.66	0.15	98.60
100.8	48.10	48.94	1.27	19.01	9.91	0.14	5.34	11.85	2.68	0.16	98.46
110.4	48.16	49.34	1.22	18.65	9.88	0.19	5.34	11.86	2.65	0.16	98.12
119.9	48.35	49.12	1.39	18.68	9.93	0.15	5.38	11.80	2.68	0.16	98.53
129.5	48.49	49.13	1.33	18.50	10.21	0.22	5.40	11.71	2.61	0.18	98.66
139.0	48.44	49.16	1.51	18.44	10.07	0.21	5.43	11.67	2.65	0.17	98.58
148.6	48.54	49.27	1.28	18.25	10.16	0.21	5.48	11.77	2.72	0.15	98.57
158.1	48.94	49.55	1.36	17.96	10.17	0.21	5.50	11.71	2.69	0.15	98.69
158.1	48.83	49.22	1.43	18.23	10.25	0.18	5.50	11.74	2.59	0.16	98.91
178.6	48.86	49.64	1.35	17.57	10.42	0.18	5.57	11.73	2.68	0.17	98.51
199.2	48.99	49.73	1.58	17.41	10.38	0.23	5.61	11.55	2.67	0.16	98.57
219.8	49.56	49.77	1.61	17.11	10.39	0.27	5.67	11.60	2.72	0.17	99.08
240.4	49.57	50.00	1.58	16.85	10.54	0.21	5.69	11.61	2.67	0.15	98.87
261.0	49.49	50.21	1.50	16.61	10.65	0.16	5.80	11.52	2.68	0.18	98.59
281.6	49.57	50.21	1.72	16.33	10.65	0.22	5.78	11.57	2.65	0.17	98.66
302.2	49.79	50.85	1.56	15.83	10.76	0.17	5.84	11.49	2.65	0.16	98.25
322.8	50.00	50.79	1.60	15.72	10.89	0.14	5.91	11.47	2.59	0.18	98.50
343.4	50.03	50.84	1.61	15.51	10.91	0.17	6.03	11.38	2.66	0.18	98.49
364.0	50.33	50.85	1.59	15.36	10.98	0.16	5.99	11.47	2.71	0.17	98.78
384.6	50.58	50.76	1.68	15.16	11.12	0.22	6.06	11.51	2.65	0.16	99.13
405.2	50.19	50.86	1.68	14.94	11.30	0.19	6.12	11.45	2.60	0.17	98.63
425.8	50.43	50.97	1.67	14.77	11.38	0.21	6.16	11.34	2.62	0.18	98.76
446.3	50.35	51.20	1.76	14.58	11.23	0.20	6.17	11.35	2.64	0.17	98.45
466.9	50.53	51.04	1.89	14.39	11.45	0.19	6.24	11.34	2.60	0.16	98.78
487.5	50.73	51.56	1.69	14.28	11.30	0.21	6.23	11.32	2.54	0.16	98.47
508.1	50.41	51.21	1.74	14.24	11.48	0.19	6.30	11.33	2.64	0.17	98.50
528.7	50.94	51.24	1.86	14.14	11.48	0.18	6.32	11.32	2.59	0.17	99.00
549.3	50.61	51.46	1.67	14.03	11.48	0.22	6.37	11.33	2.57	0.17	98.44
569.9	50.48	51.39	1.85	14.03	11.36	0.19	6.34	11.37	2.61	0.17	98.39
569.9	50.84	51.61	1.68	13.99	11.49	0.20	6.36	11.28	2.53	0.17	98.54
610.1	50.72	51.15	1.87	13.90	11.64	0.24	6.41	11.29	2.63	0.17	98.87
650.3	50.79	51.47	1.82	13.79	11.53	0.23	6.48	11.29	2.52	0.17	98.62

690.6	50.78	51.43	1.75	13.71	11.76	0.20	6.45	11.25	2.58	0.18	98.65
730.7	50.46	51.42	1.84	13.43	11.78	0.22	6.62	11.27	2.57	0.16	98.34
770.9	50.70	51.19	1.81	13.66	11.88	0.19	6.60	11.20	2.59	0.18	98.81
811.1	50.66	51.57	1.68	13.50	11.73	0.20	6.57	11.30	2.56	0.18	98.38
851.3	51.11	51.64	1.80	13.42	11.77	0.17	6.60	11.22	2.50	0.19	98.77
891.6	50.74	51.43	1.85	13.45	11.88	0.19	6.65	11.17	2.49	0.18	98.61
931.8	50.81	51.34	1.74	13.50	11.89	0.22	6.68	11.17	2.58	0.17	98.77
972.0	50.48	51.51	1.76	13.28	11.93	0.18	6.66	11.21	2.60	0.17	98.26
1012.1	50.91	51.40	1.72	13.46	11.91	0.22	6.74	11.12	2.56	0.17	98.82
1052.4	51.00	51.29	1.86	13.31	11.97	0.25	6.76	11.11	2.58	0.17	99.01
1092.6	50.67	51.34	1.89	13.34	12.03	0.24	6.72	11.03	2.54	0.18	98.63
1132.8	50.84	51.26	1.81	13.36	12.10	0.17	6.79	11.04	2.58	0.19	98.88
1173.0	50.92	51.15	1.88	13.32	12.09	0.25	6.70	11.10	2.61	0.19	99.07
1213.2	50.86	51.25	1.92	13.29	12.06	0.17	6.80	11.02	2.60	0.19	98.91
1253.4	50.85	51.28	1.76	13.40	11.95	0.20	6.77	11.11	2.62	0.20	98.87
1293.6	50.52	51.48	1.84	13.34	11.86	0.24	6.82	11.00	2.55	0.17	98.34

Exp 203

x / μm	Oxides (wt%)										
	SiO2	SiO2*	TiO2	Al2O3	FeO	MnO	MgO	CaO	Na2O	K2O	Total
5.4	48.85	49.10	1.38	18.26	10.22	0.19	5.61	11.56	2.81	0.18	99.05
9.9	48.75	49.30	1.47	18.00	10.16	0.22	5.63	11.58	2.79	0.16	98.75
9.9	49.24	49.26	1.38	18.18	10.21	0.21	5.66	11.55	2.69	0.16	99.28
20.8	49.51	49.56	1.44	17.29	10.60	0.20	5.78	11.50	2.76	0.17	99.25
31.8	49.86	49.82	1.61	16.78	10.60	0.17	5.89	11.44	2.82	0.17	99.34
42.8	50.32	50.46	1.63	15.90	10.87	0.14	5.97	11.40	2.74	0.18	99.16
53.8	50.37	50.56	1.66	15.35	11.16	0.18	6.07	11.38	2.76	0.18	99.12
64.8	50.50	50.77	1.82	14.92	11.14	0.23	6.13	11.35	2.77	0.18	99.03
75.8	50.55	51.07	1.70	14.52	11.31	0.17	6.29	11.35	2.73	0.18	98.78
86.7	50.66	50.98	1.78	14.28	11.42	0.22	6.33	11.35	2.76	0.18	98.98
86.7	51.16	51.03	1.78	14.33	11.45	0.15	6.38	11.38	2.63	0.17	99.43
106.2	51.00	51.06	1.87	13.79	11.62	0.24	6.57	11.31	2.66	0.18	99.24
125.8	50.90	51.16	1.87	13.65	11.79	0.22	6.51	11.25	2.67	0.18	99.04
145.4	51.03	50.86	1.85	13.53	12.08	0.21	6.62	11.30	2.69	0.17	99.47
164.8	50.98	51.24	2.01	13.36	11.78	0.29	6.59	11.16	2.69	0.17	99.04
184.4	51.20	51.09	1.81	13.45	12.11	0.24	6.65	11.19	2.60	0.18	99.41
203.9	51.00	50.94	1.73	13.46	12.16	0.23	6.69	11.26	2.64	0.19	99.35
223.5	51.15	51.06	1.84	13.47	12.11	0.18	6.64	11.17	2.65	0.18	99.39
242.9	51.42	50.90	1.95	13.52	12.11	0.19	6.71	11.09	2.66	0.17	99.82
262.5	51.29	51.06	1.76	13.32	12.13	0.20	6.78	11.19	2.69	0.18	99.53
262.5	51.48	51.04	1.84	13.50	12.26	0.17	6.73	11.12	2.48	0.18	99.75
293.1	51.11	51.12	1.92	13.33	12.03	0.19	6.71	11.08	2.73	0.19	99.29
323.5	51.11	50.81	1.93	13.45	12.16	0.29	6.70	11.05	2.71	0.19	99.60
354.1	51.42	51.16	1.82	13.32	12.09	0.25	6.68	11.06	2.73	0.18	99.56
384.7	51.40	51.01	1.82	13.34	12.21	0.23	6.72	11.02	2.75	0.18	99.69
415.2	51.31	51.15	1.80	13.36	12.16	0.22	6.68	11.04	2.69	0.19	99.46
445.7	51.39	50.89	1.83	13.47	12.28	0.21	6.68	11.08	2.67	0.19	99.80
476.2	51.32	50.83	1.83	13.45	12.26	0.21	6.73	11.09	2.71	0.18	99.79
506.8	51.53	50.74	1.86	13.43	12.37	0.23	6.77	10.95	2.75	0.19	100.09
537.3	51.52	51.04	1.93	13.35	12.19	0.21	6.74	10.94	2.72	0.20	99.78
567.8	51.56	50.75	1.89	13.42	12.38	0.18	6.70	11.02	2.76	0.19	100.10
598.4	51.41	51.04	1.78	13.42	12.20	0.25	6.73	10.94	2.75	0.19	99.67
628.9	51.42	50.81	1.76	13.37	12.31	0.25	6.78	11.06	2.76	0.19	99.90
659.4	51.39	51.09	1.83	13.38	12.15	0.22	6.78	10.95	2.72	0.18	99.59
689.9	51.75	50.94	1.83	13.40	12.21	0.21	6.81	10.99	2.75	0.18	100.11
3.0	48.76	48.91	1.41	18.31	10.34	0.19	5.61	11.56	2.77	0.19	99.14
8.0	48.99	48.98	1.43	17.97	10.43	0.16	5.65	11.69	2.82	0.16	99.31
13.0	49.17	49.23	1.45	17.72	10.40	0.21	5.68	11.65	2.82	0.16	99.24
13.0	49.38	49.31	1.46	17.73	10.35	0.19	5.70	11.70	2.71	0.16	99.38
23.4	49.77	49.82	1.42	16.96	10.62	0.21	5.77	11.54	2.79	0.16	99.25

33.7	49.85	49.96	1.65	16.38	10.76	0.19	5.90	11.59	2.70	0.16	99.19
44.1	50.19	50.11	1.65	15.76	11.04	0.23	6.04	11.50	2.79	0.17	99.38
54.5	50.50	50.71	1.65	15.21	11.15	0.14	6.12	11.47	2.67	0.18	99.09
64.9	50.76	50.64	1.65	14.92	11.36	0.17	6.17	11.45	2.76	0.18	99.41
75.2	50.85	50.50	1.84	14.58	11.54	0.22	6.31	11.38	2.76	0.17	99.65
85.5	50.82	51.07	1.77	14.11	11.61	0.13	6.37	11.32	2.72	0.19	99.06
95.9	51.00	51.06	1.82	13.94	11.64	0.23	6.43	11.33	2.68	0.18	99.24
95.9	51.31	50.95	1.75	14.10	11.58	0.20	6.49	11.44	2.61	0.17	99.65
116.4	51.09	51.20	1.77	13.68	11.83	0.23	6.46	11.29	2.65	0.18	99.19
136.9	50.93	50.90	1.85	13.69	12.01	0.24	6.51	11.24	2.69	0.17	99.33
157.3	50.95	50.92	1.90	13.43	11.99	0.28	6.65	11.28	2.69	0.17	99.33
177.8	50.90	51.15	1.89	13.34	12.04	0.24	6.63	11.17	2.66	0.18	99.05
198.3	51.06	51.12	1.81	13.37	12.12	0.22	6.59	11.16	2.73	0.18	99.24
218.8	51.18	50.91	1.79	13.38	12.31	0.23	6.70	11.09	2.72	0.17	99.57
239.2	50.93	51.35	1.80	13.34	12.09	0.15	6.65	11.11	2.63	0.18	98.88
259.7	51.02	50.86	1.75	13.47	12.24	0.24	6.74	11.04	2.77	0.18	99.46
280.2	50.97	50.81	1.93	13.40	12.24	0.21	6.67	11.16	2.69	0.18	99.46
300.7	50.82	50.70	1.87	13.52	12.29	0.24	6.70	11.05	2.76	0.18	99.42
321.1	50.71	51.07	1.83	13.33	12.28	0.20	6.68	11.06	2.68	0.18	98.94
341.6	50.83	51.02	1.87	13.28	12.26	0.21	6.77	11.05	2.64	0.20	99.11
341.6	51.20	51.01	1.75	13.54	12.21	0.25	6.79	11.08	2.49	0.18	99.49
373.5	50.89	50.94	1.83	13.45	12.29	0.22	6.68	11.00	2.71	0.19	99.25
405.3	51.01	51.24	1.73	13.35	12.26	0.26	6.69	10.90	2.69	0.18	99.07
437.2	50.87	51.10	1.82	13.41	12.29	0.14	6.67	11.00	2.70	0.19	99.07
469.0	51.03	51.19	1.81	13.45	12.17	0.18	6.66	10.90	2.76	0.18	99.14
500.9	51.16	51.16	1.88	13.33	12.17	0.21	6.66	10.98	2.71	0.19	99.30
532.7	51.22	50.89	1.89	13.50	12.21	0.26	6.68	11.00	2.70	0.18	99.64
564.6	51.52	51.09	1.82	13.45	12.15	0.21	6.74	10.93	2.72	0.19	99.73
596.5	51.28	50.85	1.87	13.39	12.30	0.21	6.74	10.98	2.76	0.18	99.73
628.3	51.53	51.11	1.80	13.39	12.23	0.22	6.70	10.98	2.68	0.19	99.72
660.2	51.52	51.14	1.85	13.35	12.17	0.16	6.73	11.01	2.71	0.18	99.68
4.6	48.73	48.91	1.34	18.41	10.27	0.18	5.60	11.52	2.87	0.20	99.12
9.2	48.70	48.81	1.50	17.99	10.30	0.19	5.68	11.73	2.94	0.17	99.18
13.9	48.97	49.23	1.40	17.86	10.40	0.21	5.66	11.64	2.73	0.17	99.04
13.9	49.19	49.58	1.42	17.81	10.18	0.24	5.63	11.62	2.66	0.17	98.92
24.6	49.40	49.84	1.54	16.97	10.49	0.19	5.82	11.50	2.77	0.17	98.86
35.3	49.68	50.11	1.50	16.33	10.81	0.20	5.88	11.57	2.72	0.19	98.87
46.0	50.18	50.36	1.61	15.71	10.98	0.21	6.02	11.45	2.80	0.18	99.12
56.7	50.43	50.58	1.70	15.24	11.09	0.18	6.07	11.50	2.76	0.17	99.15
67.4	50.49	50.92	1.67	14.74	11.23	0.20	6.18	11.44	2.73	0.18	98.87
78.1	50.79	50.89	1.82	14.57	11.32	0.17	6.29	11.36	2.71	0.17	99.20
88.8	50.81	51.09	1.79	14.09	11.43	0.21	6.41	11.37	2.74	0.17	99.03
88.8	51.04	50.85	1.80	14.26	11.57	0.21	6.42	11.43	2.59	0.16	99.49

110.5	50.96	51.20	1.87	13.84	11.62	0.20	6.42	11.30	2.67	0.19	99.06
132.0	50.99	50.93	1.87	13.66	11.91	0.18	6.56	11.32	2.69	0.17	99.36
153.7	51.05	50.74	1.87	13.66	12.07	0.25	6.60	11.27	2.68	0.17	99.61
175.4	50.96	51.21	1.80	13.54	12.00	0.19	6.63	11.14	2.62	0.17	99.05
197.0	51.01	51.20	1.73	13.34	12.10	0.25	6.67	11.19	2.65	0.17	99.11
218.6	51.12	51.37	1.82	13.29	12.10	0.18	6.64	11.10	2.64	0.16	99.05
240.3	51.06	50.89	1.92	13.45	12.22	0.23	6.70	11.08	2.65	0.17	99.47
261.9	51.00	50.83	1.91	13.46	12.22	0.19	6.76	11.04	2.72	0.17	99.48
283.5	51.26	51.21	1.78	13.40	12.13	0.19	6.67	11.08	2.66	0.18	99.36
305.2	51.24	51.11	1.85	13.38	12.02	0.23	6.73	11.10	2.69	0.17	99.43
326.8	51.21	50.74	1.81	13.43	12.31	0.30	6.76	11.05	2.71	0.18	99.77
348.5	51.27	50.71	1.84	13.50	12.38	0.20	6.73	11.00	2.77	0.18	99.86
370.1	51.25	51.02	1.68	13.36	12.33	0.24	6.76	10.98	2.76	0.18	99.53
391.7	51.20	51.03	1.89	13.31	12.22	0.22	6.70	11.00	2.76	0.17	99.47
413.4	51.51	51.25	1.84	13.37	12.13	0.19	6.70	10.98	2.67	0.19	99.57
413.4	51.50	51.14	1.81	13.47	12.16	0.25	6.75	11.00	2.54	0.18	99.66
444.5	51.42	50.88	1.90	13.42	12.24	0.20	6.74	11.02	2.71	0.19	99.84
475.8	51.41	50.83	1.90	13.41	12.26	0.16	6.75	11.03	2.76	0.20	99.87
507.0	51.44	50.97	1.84	13.41	12.21	0.21	6.74	11.07	2.68	0.17	99.78
538.2	51.55	50.88	1.85	13.38	12.27	0.16	6.81	11.03	2.75	0.17	99.96
569.4	51.63	50.86	1.86	13.50	12.21	0.20	6.72	11.00	2.76	0.18	100.07
600.6	51.69	51.07	1.80	13.36	12.18	0.25	6.71	11.03	2.73	0.18	99.92
631.8	51.65	50.79	1.94	13.42	12.27	0.22	6.81	10.96	2.71	0.18	100.16
663.0	51.79	51.12	1.82	13.34	12.21	0.20	6.78	10.96	2.68	0.19	99.98

Exp 205

x / μm	Oxides (wt%)										
	SiO2	SiO2*	TiO2	Al2O3	FeO	MnO	MgO	CaO	Na2O	K2O	Total
4.7	48.94	50.16	1.48	16.74	10.54	0.26	5.92	11.19	2.82	0.20	98.08
9.7	49.08	50.58	1.51	16.44	10.57	0.20	5.85	11.24	2.76	0.17	97.80
10.0	48.88	50.67	1.53	16.36	10.60	0.22	5.81	11.19	2.73	0.18	97.51
15.0	49.88	50.41	1.63	16.04	10.76	0.23	6.00	11.37	2.70	0.16	98.77
20.0	49.78	51.00	1.64	15.54	10.76	0.27	5.95	11.30	2.66	0.18	98.09
25.0	50.09	50.95	1.67	15.32	10.98	0.21	6.04	11.26	2.66	0.20	98.44
30.0	50.15	51.04	1.63	15.13	10.99	0.22	6.19	11.18	2.73	0.19	98.41
35.0	50.58	51.25	1.78	14.65	11.29	0.22	6.10	11.21	2.62	0.19	98.64
11.1	49.23	50.39	1.59	16.28	10.65	0.26	6.02	11.24	2.69	0.18	98.14
16.2	49.51	50.77	1.63	15.77	10.71	0.26	6.04	11.19	2.75	0.18	98.03
21.4	49.76	50.80	1.63	15.53	10.90	0.24	6.04	11.24	2.76	0.16	98.26
26.5	49.98	50.99	1.82	15.12	10.93	0.25	6.10	11.27	2.65	0.18	98.30
31.7	50.18	51.01	1.66	14.97	11.13	0.20	6.34	11.10	2.71	0.19	98.47
36.8	50.29	51.24	1.76	14.59	11.22	0.21	6.28	11.20	2.62	0.17	98.35
42.0	50.54	51.09	1.74	14.52	11.29	0.31	6.30	11.15	2.73	0.18	98.75
47.1	50.61	51.52	1.72	14.14	11.37	0.20	6.27	11.11	2.75	0.20	98.39
47.1	50.82	50.94	1.80	14.31	11.59	0.22	6.42	11.23	2.59	0.20	99.18
57.7	50.74	51.36	1.85	13.89	11.43	0.20	6.47	11.20	2.72	0.20	98.68
68.4	50.64	51.52	1.88	13.67	11.56	0.18	6.64	11.06	2.60	0.19	98.42
79.0	50.62	51.59	1.90	13.51	11.71	0.25	6.57	11.03	2.56	0.17	98.32
89.6	50.37	51.68	1.76	13.42	11.61	0.27	6.60	11.10	2.69	0.17	97.99
100.2	50.57	51.43	1.92	13.46	11.84	0.26	6.61	11.01	2.61	0.18	98.44
110.9	50.80	51.60	1.76	13.46	11.73	0.21	6.65	11.06	2.66	0.18	98.50
121.4	50.59	51.42	1.92	13.32	11.88	0.20	6.68	11.03	2.67	0.17	98.48
132.0	50.54	51.83	1.88	13.26	11.89	0.21	6.49	10.93	2.64	0.18	98.02
132.0	50.70	51.49	1.83	13.39	11.97	0.25	6.61	11.02	2.56	0.18	98.51
147.6	50.72	51.40	1.91	13.42	11.92	0.26	6.57	10.94	2.69	0.19	98.62
163.1	51.06	51.38	1.91	13.32	12.03	0.26	6.72	10.86	2.65	0.18	98.98
178.7	50.83	51.44	1.84	13.27	12.05	0.20	6.72	10.93	2.66	0.18	98.68
194.2	51.13	51.00	1.89	13.36	12.16	0.24	6.77	11.04	2.67	0.18	99.43
209.8	51.22	51.66	1.74	13.36	11.93	0.22	6.63	10.95	2.63	0.18	98.86
225.3	51.19	51.37	1.83	13.32	12.03	0.25	6.64	10.98	2.71	0.18	99.12
240.9	51.05	51.26	1.76	13.43	12.14	0.20	6.72	10.86	2.74	0.20	99.09
256.4	51.17	51.24	1.86	13.47	12.07	0.30	6.68	10.84	2.67	0.18	99.23
272.0	50.83	51.59	1.85	13.22	12.05	0.25	6.54	10.94	2.66	0.19	98.54
3.3	49.59	49.94	1.48	16.79	10.60	0.16	6.01	11.28	2.84	0.20	98.95
8.8	49.93	50.73	1.47	16.27	10.47	0.24	5.89	11.31	2.72	0.18	98.49
14.3	50.23	50.48	1.55	16.11	10.71	0.22	5.95	11.30	2.83	0.17	99.05
19.8	50.61	50.92	1.65	15.66	10.63	0.19	6.03	11.27	2.77	0.18	99.00
21.2	49.69	50.67	1.73	15.84	10.82	0.21	6.22	11.06	2.58	0.17	98.32

26.0	50.38	51.08	1.66	15.11	10.99	0.24	6.28	11.15	2.63	0.16	98.60
30.8	50.45	51.29	1.62	14.80	11.24	0.23	6.22	11.08	2.65	0.17	98.46
35.6	50.60	51.35	1.69	14.53	11.06	0.25	6.34	11.16	2.73	0.19	98.56
40.4	50.88	51.24	1.75	14.26	11.39	0.24	6.42	11.16	2.67	0.17	98.95
45.2	50.79	51.45	1.76	14.11	11.44	0.22	6.35	11.11	2.67	0.18	98.64
45.2	51.01	51.32	1.73	14.37	11.44	0.18	6.45	11.13	2.50	0.18	99.00
56.4	51.07	51.37	1.83	13.83	11.52	0.26	6.51	11.07	2.71	0.20	98.99
67.5	51.14	51.63	1.74	13.63	11.65	0.26	6.55	11.00	2.68	0.17	98.81
78.7	51.13	51.69	1.83	13.57	11.65	0.27	6.47	11.04	2.62	0.16	98.75
89.9	51.06	51.63	1.81	13.54	11.60	0.28	6.62	11.00	2.63	0.19	98.74
101.0	50.89	51.65	1.79	13.49	11.77	0.17	6.61	11.08	2.55	0.18	98.54
112.2	51.07	51.46	1.88	13.44	11.93	0.21	6.57	11.02	2.62	0.17	98.91
112.2	51.29	51.22	1.96	13.57	11.91	0.23	6.59	11.02	2.62	0.19	99.38
132.3	50.94	51.42	1.78	13.51	11.89	0.29	6.62	11.00	2.62	0.18	98.83
152.5	51.00	51.51	1.90	13.38	11.88	0.26	6.58	10.94	2.66	0.19	98.79
172.6	50.80	51.35	1.87	13.48	11.95	0.27	6.73	10.90	2.58	0.19	98.75
192.7	50.71	51.26	1.80	13.45	12.03	0.26	6.68	10.89	2.74	0.18	98.75
212.8	50.57	51.62	1.77	13.35	11.82	0.23	6.69	10.89	2.75	0.18	98.25
233.0	50.31	51.61	1.80	13.35	11.93	0.28	6.63	10.89	2.62	0.18	98.00
253.1	50.24	51.55	2.00	13.35	11.88	0.19	6.68	10.82	2.64	0.20	97.99
5.3	49.99	49.95	1.51	16.86	10.59	0.19	5.93	11.27	2.81	0.19	99.34
11.3	50.38	50.05	1.59	16.46	10.61	0.27	5.98	11.28	2.88	0.17	99.62
15.5	50.04	50.50	1.59	15.98	10.79	0.24	6.14	11.12	2.77	0.17	98.84
20.5	50.25	50.56	1.64	15.60	11.00	0.24	6.18	11.24	2.64	0.19	98.99
25.5	50.46	50.72	1.66	15.33	11.05	0.25	6.19	11.13	2.78	0.18	99.04
30.5	50.52	51.05	1.73	14.89	11.13	0.20	6.22	11.24	2.65	0.18	98.77
30.5	50.79	51.02	1.70	15.11	11.09	0.21	6.24	11.20	2.58	0.16	99.07
40.6	50.94	51.34	1.70	14.52	11.30	0.26	6.23	11.13	2.65	0.18	98.91
50.7	51.09	51.27	1.81	14.16	11.38	0.25	6.41	11.14	2.73	0.17	99.12
60.8	51.10	51.54	1.92	13.80	11.42	0.23	6.49	11.11	2.62	0.17	98.86
71.0	51.32	51.50	1.85	13.68	11.65	0.22	6.47	11.06	2.70	0.18	99.12
81.1	51.11	51.73	1.86	13.48	11.65	0.26	6.52	11.00	2.63	0.18	98.68
91.3	51.38	51.36	1.90	13.55	11.69	0.23	6.61	11.11	2.68	0.18	99.32
101.4	51.39	51.39	1.84	13.39	11.89	0.16	6.66	11.01	2.79	0.18	99.30
101.4	51.55	51.51	1.89	13.49	11.70	0.22	6.68	11.03	2.63	0.17	99.34
121.7	51.50	51.65	1.92	13.44	11.75	0.21	6.54	11.00	2.60	0.18	99.15
142.0	51.39	51.50	1.85	13.48	11.83	0.25	6.72	10.89	2.60	0.19	99.19
162.3	51.37	51.37	1.78	13.47	11.92	0.23	6.73	10.92	2.69	0.18	99.30
182.5	51.22	51.50	1.80	13.48	11.89	0.21	6.78	10.84	2.61	0.20	99.01
202.8	51.46	51.55	1.78	13.47	11.85	0.26	6.67	10.91	2.64	0.18	99.22
223.1	51.46	51.65	1.81	13.43	11.82	0.28	6.62	10.85	2.66	0.16	99.11
243.3	51.37	51.52	1.87	13.36	11.84	0.20	6.75	10.81	2.78	0.18	99.15

Exp 207

x / μm	Oxides (wt%)										
	SiO ₂	SiO ₂ *	TiO ₂	Al ₂ O ₃	FeO	MnO	MgO	CaO	Na ₂ O	K ₂ O	Total
5.0	48.66	49.12	1.35	18.32	10.10	0.20	5.71	11.50	2.82	0.19	98.83
9.7	48.88	49.06	1.42	18.19	10.22	0.21	5.72	11.57	2.75	0.16	99.12
14.5	49.04	49.06	1.45	17.96	10.26	0.19	5.75	11.70	2.76	0.17	99.28
19.2	49.05	49.25	1.47	17.82	10.49	0.17	5.67	11.55	2.71	0.17	99.10
19.2	49.42	49.49	1.36	17.77	10.28	0.19	5.73	11.62	2.71	0.17	99.23
30.0	49.34	49.60	1.46	17.23	10.54	0.22	5.77	11.53	2.79	0.17	99.04
40.7	49.97	49.59	1.53	16.90	10.63	0.15	5.96	11.59	2.78	0.17	99.68
51.5	50.10	50.03	1.46	16.51	10.62	0.22	6.00	11.55	2.74	0.16	99.37
62.2	50.25	50.22	1.60	16.11	10.92	0.20	5.88	11.47	2.74	0.17	99.34
73.0	50.22	50.40	1.54	15.84	10.90	0.19	6.07	11.43	2.73	0.18	99.12
83.7	50.54	50.47	1.68	15.43	11.08	0.18	6.08	11.42	2.78	0.18	99.37
94.5	50.68	50.54	1.66	15.23	11.14	0.20	6.20	11.43	2.73	0.18	99.44
105.2	50.82	50.83	1.76	14.76	11.23	0.24	6.19	11.40	2.72	0.16	99.29
105.2	50.90	50.84	1.62	14.96	11.22	0.22	6.24	11.35	2.65	0.19	99.36
126.2	50.98	50.91	1.75	14.49	11.37	0.21	6.36	11.37	2.66	0.18	99.37
147.2	50.91	51.06	1.74	14.20	11.45	0.24	6.43	11.30	2.70	0.17	99.14
168.2	50.99	50.97	1.74	13.83	11.71	0.25	6.60	11.33	2.70	0.17	99.32
189.2	51.11	50.90	1.90	13.77	11.86	0.21	6.56	11.28	2.64	0.18	99.51
210.2	51.24	50.95	1.86	13.49	11.96	0.19	6.68	11.31	2.68	0.18	99.59
231.2	51.12	51.12	1.87	13.38	12.07	0.22	6.56	11.20	2.70	0.17	99.30
252.2	51.27	51.13	1.82	13.38	12.07	0.19	6.66	11.24	2.65	0.18	99.45
273.2	51.29	51.07	1.82	13.50	12.10	0.18	6.65	11.19	2.60	0.18	99.51
294.2	51.41	51.33	1.86	13.18	12.11	0.18	6.70	11.16	2.62	0.17	99.38
315.2	51.41	51.04	1.91	13.31	12.03	0.20	6.79	11.22	2.64	0.17	99.66
315.2	51.56	51.05	1.79	13.40	12.13	0.20	6.74	11.27	2.55	0.17	99.81
345.8	51.34	51.12	1.89	13.33	12.06	0.25	6.70	11.16	2.62	0.17	99.52
376.4	51.35	51.38	1.76	13.32	12.06	0.21	6.67	11.05	2.66	0.18	99.27
407.0	51.33	50.98	1.92	13.34	12.08	0.20	6.74	11.21	2.65	0.18	99.65
437.7	51.51	51.17	1.92	13.23	12.15	0.16	6.74	11.07	2.68	0.17	99.65
468.3	51.46	51.18	1.91	13.29	12.11	0.22	6.72	11.02	2.69	0.17	99.58
498.9	51.41	51.31	1.85	13.32	12.15	0.21	6.66	10.94	2.67	0.18	99.40
529.5	51.62	51.38	1.81	13.23	12.10	0.22	6.74	10.94	2.70	0.17	99.54
560.1	51.42	51.08	1.95	13.31	12.14	0.17	6.80	10.95	2.72	0.17	99.63
590.7	51.56	51.50	1.91	13.21	11.94	0.19	6.71	10.97	2.69	0.18	99.36
621.4	51.68	51.43	1.80	13.25	11.94	0.24	6.80	10.92	2.73	0.19	99.56
652.0	51.71	51.46	1.82	13.37	12.03	0.16	6.74	10.84	2.69	0.19	99.55
682.6	51.55	51.43	1.90	13.25	11.95	0.22	6.77	10.88	2.73	0.17	99.41
767.4	50.91	51.40	1.85	13.31	11.98	0.16	6.68	11.01	2.71	0.20	98.81

802.9	50.98	51.22	1.88	13.36	11.93	0.25	6.77	10.99	2.73	0.18	99.06
5.6	48.68	49.15	1.35	18.25	10.21	0.19	5.64	11.48	2.85	0.18	98.83
10.4	48.85	49.21	1.42	18.04	10.29	0.16	5.61	11.60	2.79	0.17	98.94
15.2	49.13	49.11	1.42	18.06	10.20	0.19	5.77	11.59	2.81	0.16	99.32
20.0	49.26	49.43	1.40	17.71	10.34	0.18	5.67	11.62	2.79	0.16	99.13
24.8	49.54	49.49	1.41	17.45	10.42	0.24	5.62	11.67	2.83	0.17	99.35
24.8	48.80	49.53	1.47	17.42	10.52	0.17	5.90	11.46	2.67	0.16	98.56
35.4	49.38	49.73	1.52	16.96	10.64	0.20	5.79	11.48	2.83	0.16	98.95
46.0	49.78	49.96	1.66	16.50	10.70	0.16	5.96	11.43	2.75	0.18	99.13
56.6	49.99	50.13	1.46	16.19	10.75	0.26	6.10	11.48	2.75	0.17	99.16
67.2	50.11	50.08	1.65	15.98	11.00	0.19	6.06	11.40	2.76	0.17	99.33
77.8	50.35	50.57	1.66	15.49	11.00	0.18	6.11	11.39	2.73	0.18	99.08
88.4	50.33	50.46	1.56	15.30	11.28	0.25	6.18	11.37	2.73	0.17	99.17
99.0	50.63	50.86	1.82	14.81	11.15	0.18	6.24	11.35	2.73	0.17	99.07
109.6	50.66	50.66	1.76	14.80	11.24	0.26	6.36	11.32	2.74	0.16	99.31
120.2	50.75	50.61	1.72	14.71	11.41	0.23	6.38	11.33	2.74	0.17	99.44
130.8	50.97	50.96	1.83	14.37	11.46	0.20	6.32	11.28	2.71	0.19	99.32
130.8	51.08	50.63	1.82	14.57	11.55	0.20	6.37	11.37	2.61	0.17	99.75
149.9	50.81	51.17	1.84	14.09	11.51	0.13	6.44	11.27	2.68	0.17	98.94
169.0	51.16	51.08	1.84	13.92	11.70	0.16	6.48	11.28	2.69	0.17	99.38
188.1	51.26	51.12	1.75	13.81	11.73	0.22	6.51	11.25	2.72	0.19	99.44
207.2	51.12	51.03	1.92	13.65	11.88	0.19	6.49	11.29	2.68	0.18	99.39
226.3	51.18	50.99	1.82	13.60	11.82	0.23	6.69	11.27	2.69	0.19	99.48
245.4	51.13	50.84	1.81	13.67	12.08	0.15	6.69	11.22	2.70	0.16	99.59
264.5	51.35	51.08	1.86	13.37	11.96	0.15	6.75	11.25	2.69	0.18	99.57
283.6	51.29	51.28	1.77	13.34	12.02	0.19	6.62	11.23	2.68	0.17	99.31
302.7	51.25	50.82	1.87	13.40	12.12	0.27	6.73	11.26	2.66	0.18	99.72
321.8	51.38	51.22	1.72	13.42	12.03	0.19	6.73	11.17	2.65	0.18	99.46
321.8	51.44	51.21	1.84	13.40	12.00	0.22	6.79	11.16	2.52	0.16	99.53
353.1	51.20	51.12	1.83	13.34	12.15	0.22	6.73	11.05	2.69	0.17	99.38
384.4	51.16	51.01	1.87	13.36	12.10	0.28	6.73	11.09	2.67	0.18	99.45
415.7	51.31	51.33	1.84	13.30	12.00	0.23	6.69	11.07	2.67	0.17	99.29
447.0	51.36	51.29	1.81	13.35	12.03	0.22	6.74	11.01	2.69	0.16	99.37
478.3	51.51	51.05	1.89	13.41	12.10	0.24	6.78	11.00	2.67	0.17	99.76
509.6	51.56	51.10	1.74	13.50	12.09	0.23	6.83	10.96	2.69	0.16	99.75
541.0	51.47	51.25	1.79	13.39	11.94	0.30	6.74	11.01	2.70	0.18	99.52
572.3	51.61	51.26	1.77	13.30	12.14	0.25	6.74	10.92	2.74	0.19	99.66
603.6	51.70	51.27	1.84	13.35	12.13	0.20	6.66	10.95	2.73	0.17	99.73
634.9	51.65	51.17	1.84	13.38	12.01	0.24	6.72	11.02	2.74	0.18	99.78
666.2	51.65	51.28	1.85	13.42	11.96	0.21	6.70	10.99	2.72	0.17	99.67
697.5	51.95	51.40	1.86	13.27	11.83	0.24	6.89	10.89	2.73	0.18	99.84

764.4	51.02	50.83	1.78	13.64	12.13	0.21	6.84	11.02	2.68	0.17	99.49
799.4	51.13	51.20	1.78	13.38	11.92	0.23	6.88	10.99	2.73	0.19	99.24
6.9	48.84	48.88	1.40	18.42	10.22	0.17	5.59	11.58	2.87	0.17	99.27
12.4	49.02	49.25	1.38	18.03	10.20	0.19	5.65	11.63	2.82	0.15	99.08
17.9	49.52	49.27	1.45	17.83	10.23	0.22	5.64	11.64	2.86	0.16	99.55
23.4	50.40	49.80	1.46	17.15	10.32	0.16	5.54	11.70	3.00	0.18	99.91
18.0	48.66	49.32	1.42	17.86	10.39	0.12	5.78	11.55	2.71	0.16	98.65
28.9	49.41	49.46	1.50	17.36	10.60	0.17	5.82	11.45	2.76	0.18	99.26
39.8	49.75	49.95	1.55	16.76	10.56	0.17	5.91	11.47	2.74	0.18	99.10
50.7	49.85	49.76	1.56	16.64	10.84	0.17	5.94	11.44	2.77	0.18	99.39
61.6	49.98	50.01	1.60	16.12	10.86	0.22	6.05	11.48	2.79	0.17	99.27
72.5	50.16	50.40	1.56	15.86	10.94	0.21	5.96	11.42	2.77	0.18	99.06
83.4	50.84	50.47	1.59	15.53	11.02	0.17	6.20	11.44	2.72	0.17	99.68
94.3	50.69	50.53	1.70	15.19	11.16	0.21	6.23	11.36	2.73	0.17	99.45
105.2	50.95	50.76	1.67	14.85	11.24	0.16	6.29	11.38	2.76	0.19	99.49
116.1	51.03	50.77	1.63	14.75	11.46	0.16	6.30	11.34	2.71	0.17	99.56
127.0	50.90	50.91	1.74	14.56	11.36	0.21	6.45	11.26	2.64	0.17	99.30
127.0	50.91	50.79	1.73	14.66	11.46	0.20	6.35	11.37	2.58	0.17	99.42
147.2	50.80	51.19	1.65	14.15	11.54	0.23	6.39	11.29	2.69	0.18	98.92
167.4	50.91	51.11	1.78	13.90	11.59	0.19	6.54	11.35	2.66	0.18	99.10
187.6	51.17	51.18	1.79	13.83	11.74	0.19	6.44	11.29	2.66	0.17	99.29
207.8	51.16	51.06	1.83	13.67	11.81	0.20	6.56	11.23	2.75	0.18	99.40
228.0	51.38	50.81	1.94	13.59	11.99	0.23	6.60	11.25	2.70	0.19	99.87
248.2	51.32	51.01	1.84	13.51	12.00	0.16	6.72	11.20	2.66	0.19	99.60
268.4	51.28	51.13	1.78	13.50	11.95	0.24	6.70	11.17	2.66	0.17	99.45
288.6	51.17	51.04	1.87	13.45	11.95	0.27	6.69	11.17	2.69	0.17	99.44
308.8	51.36	50.89	1.90	13.40	12.12	0.25	6.71	11.20	2.65	0.18	99.77
329.0	51.17	51.01	1.95	13.42	11.98	0.20	6.74	11.16	2.67	0.17	99.46
329.0	51.47	50.75	1.88	13.69	11.97	0.20	6.87	11.21	2.56	0.16	100.02
361.5	51.27	50.90	1.94	13.45	12.03	0.23	6.74	11.16	2.67	0.18	99.67
394.0	51.22	51.18	1.73	13.48	12.10	0.16	6.67	11.09	2.69	0.19	99.34
426.5	51.39	51.00	1.80	13.36	12.16	0.24	6.73	11.11	2.72	0.19	99.70
459.0	51.19	51.21	1.84	13.40	12.14	0.20	6.66	11.01	2.67	0.18	99.28
491.5	51.33	51.07	1.85	13.45	12.03	0.20	6.81	11.01	2.70	0.18	99.56
524.0	51.31	51.20	1.87	13.48	12.06	0.16	6.69	10.96	2.71	0.17	99.42
556.5	51.35	51.11	1.90	13.37	12.07	0.23	6.61	11.09	2.74	0.17	99.54
589.0	51.35	50.91	1.81	13.43	12.11	0.29	6.84	11.04	2.69	0.18	99.74
621.5	51.48	50.88	1.92	13.38	12.14	0.25	6.88	10.97	2.70	0.18	99.90
654.0	51.43	51.05	1.83	13.37	12.18	0.20	6.70	11.06	2.72	0.19	99.68
686.5	51.45	51.03	1.78	13.44	12.10	0.21	6.82	11.01	2.72	0.18	99.72
719.0	51.47	51.14	1.84	13.34	12.11	0.23	6.73	11.01	2.74	0.18	99.63

Exp 208

x / μm	Oxides (wt%)										
	SiO ₂	SiO ₂ *	TiO ₂	Al ₂ O ₃	FeO	MnO	MgO	CaO	Na ₂ O	K ₂ O	Total
8.1	47.06	47.82	1.05	21.02	9.16	0.16	4.97	12.25	2.72	0.16	98.55
12.9	47.45	47.83	1.05	21.03	9.22	0.16	4.99	12.22	2.63	0.16	98.92
17.7	47.24	47.75	1.17	21.06	9.11	0.16	5.03	12.26	2.63	0.14	98.78
22.5	47.41	47.83	1.12	20.81	9.29	0.19	5.06	12.27	2.59	0.15	98.89
22.5	47.42	47.76	1.08	20.98	9.28	0.19	5.00	12.28	2.56	0.17	98.96
42.0	47.73	47.84	1.19	20.58	9.39	0.11	5.19	12.26	2.59	0.15	99.20
61.4	47.84	48.48	1.23	19.96	9.45	0.18	5.12	12.13	2.60	0.16	98.65
80.9	48.07	48.34	1.25	19.84	9.54	0.12	5.24	12.16	2.66	0.16	99.03
100.3	48.17	48.89	1.24	19.28	9.64	0.18	5.24	12.07	2.62	0.14	98.58
119.8	48.43	49.10	1.26	18.95	9.70	0.16	5.24	12.11	2.62	0.16	98.63
139.2	48.49	49.12	1.37	18.76	9.68	0.20	5.36	12.04	2.60	0.17	98.67
158.7	48.65	49.30	1.45	18.33	9.86	0.17	5.37	12.01	2.65	0.17	98.65
178.1	48.88	49.42	1.39	18.21	9.99	0.12	5.43	11.93	2.64	0.17	98.76
197.6	49.08	49.50	1.38	17.87	10.08	0.23	5.56	11.85	2.67	0.17	98.89
217.0	49.28	49.92	1.43	17.49	10.12	0.19	5.55	11.76	2.67	0.17	98.67
236.5	49.58	49.91	1.52	17.29	10.17	0.18	5.60	11.77	2.68	0.16	98.97
236.5	49.61	49.63	1.49	17.41	10.38	0.15	5.61	11.91	2.53	0.19	99.28
256.6	49.65	49.79	1.55	16.98	10.35	0.23	5.76	11.81	2.66	0.17	99.16
276.6	49.82	50.08	1.57	16.80	10.34	0.18	5.72	11.83	2.61	0.17	99.04
296.7	49.80	50.36	1.58	16.46	10.49	0.19	5.72	11.76	2.57	0.17	98.74
316.7	49.89	50.80	1.56	16.20	10.38	0.20	5.69	11.72	2.58	0.17	98.39
336.8	50.11	50.45	1.64	16.10	10.53	0.21	5.82	11.73	2.64	0.18	98.95
356.8	50.23	50.46	1.59	15.78	10.73	0.22	5.99	11.74	2.63	0.17	99.07
376.9	50.35	50.80	1.58	15.50	10.82	0.19	5.97	11.68	2.59	0.16	98.84
396.9	50.36	50.93	1.66	15.33	10.83	0.25	5.94	11.54	2.65	0.18	98.73
417.0	50.25	50.81	1.71	15.21	10.98	0.20	5.93	11.62	2.67	0.18	98.74
437.0	50.46	50.86	1.69	14.96	11.06	0.14	6.18	11.65	2.59	0.17	98.90
457.1	50.64	50.98	1.73	14.77	10.97	0.21	6.23	11.63	2.61	0.17	98.96
477.1	50.68	50.88	1.77	14.60	11.21	0.26	6.27	11.53	2.61	0.18	99.10
497.2	50.68	50.98	1.69	14.54	11.28	0.24	6.23	11.55	2.64	0.16	99.01
517.2	50.48	51.35	1.84	14.24	11.08	0.23	6.24	11.55	2.60	0.17	98.43
537.3	50.54	50.95	1.81	14.36	11.37	0.21	6.30	11.55	2.59	0.16	98.90
557.3	50.76	51.34	1.77	14.23	11.17	0.18	6.37	11.49	2.59	0.17	98.72
577.4	50.72	51.26	1.74	14.08	11.52	0.19	6.32	11.50	2.52	0.16	98.76
597.4	50.49	51.22	1.74	14.04	11.35	0.24	6.41	11.56	2.56	0.18	98.57
617.5	50.76	51.28	1.84	13.93	11.48	0.18	6.31	11.56	2.57	0.16	98.79
637.5	50.66	51.03	1.85	13.94	11.60	0.19	6.45	11.51	2.57	0.17	98.93
637.5	50.88	51.16	1.91	13.93	11.58	0.21	6.38	11.50	2.47	0.17	99.02
677.6	50.89	51.31	1.81	13.72	11.55	0.24	6.46	11.47	2.58	0.16	98.88
717.7	50.99	51.19	1.89	13.60	11.72	0.23	6.49	11.46	2.56	0.17	99.10

757.8	50.90	51.23	1.79	13.71	11.67	0.22	6.60	11.37	2.52	0.19	98.96
797.9	50.84	51.42	1.86	13.46	11.64	0.21	6.59	11.37	2.59	0.17	98.71
838.0	50.95	51.07	1.96	13.47	11.86	0.22	6.58	11.38	2.56	0.20	99.18
878.0	50.72	51.34	1.85	13.43	11.86	0.22	6.58	11.30	2.55	0.17	98.68
918.1	50.84	51.35	1.83	13.44	11.85	0.20	6.61	11.30	2.54	0.18	98.79
958.2	50.99	51.26	1.80	13.42	11.90	0.14	6.73	11.31	2.54	0.18	99.03
998.3	50.83	51.24	1.94	13.41	11.83	0.18	6.71	11.30	2.51	0.19	98.88
1038.4	50.96	51.39	1.82	13.44	11.79	0.21	6.62	11.30	2.56	0.17	98.87
1078.5	50.79	51.30	1.82	13.27	11.89	0.23	6.79	11.27	2.55	0.16	98.79
1118.6	50.92	51.39	1.89	13.40	11.84	0.21	6.68	11.19	2.53	0.18	98.84
1158.7	50.81	51.41	1.85	13.28	12.05	0.21	6.64	11.15	2.55	0.17	98.71
1198.8	50.66	51.08	1.89	13.39	12.08	0.22	6.63	11.29	2.55	0.18	98.88
1238.9	50.76	51.63	1.89	13.26	11.79	0.17	6.71	11.18	2.50	0.17	98.43
1279.0	50.94	51.37	1.84	13.37	12.00	0.26	6.67	11.10	2.52	0.17	98.87
1319.0	50.76	51.22	1.92	13.24	12.09	0.22	6.74	11.14	2.56	0.18	98.84
1359.1	50.82	51.23	1.86	13.31	12.13	0.20	6.69	11.16	2.54	0.17	98.89
1399.2	50.81	51.05	1.93	13.42	12.12	0.17	6.75	11.13	2.55	0.17	99.05
1439.3	50.72	51.22	1.82	13.31	11.97	0.26	6.75	11.21	2.57	0.19	98.79
1479.4	50.62	51.03	1.95	13.25	12.08	0.20	6.87	11.19	2.56	0.17	98.88
1519.5	50.70	51.02	1.97	13.27	12.08	0.25	6.82	11.14	2.59	0.17	98.98
11.0	47.26	47.53	1.16	21.27	9.21	0.15	4.98	12.20	2.67	0.14	99.03
12.4	47.08	47.67	1.14	21.15	9.18	0.14	5.11	12.16	2.60	0.15	98.71
23.1	47.21	47.82	1.14	20.87	9.28	0.16	5.05	12.17	2.66	0.16	98.69
33.7	47.45	47.98	1.17	20.65	9.27	0.15	5.10	12.23	2.62	0.14	98.77
44.4	47.55	48.23	1.15	20.40	9.36	0.16	5.11	12.12	2.62	0.15	98.63
55.1	47.72	47.90	1.29	20.31	9.50	0.19	5.19	12.11	2.66	0.15	99.11
65.7	47.66	48.27	1.23	20.16	9.54	0.18	5.13	12.03	2.61	0.16	98.69
76.4	47.91	48.26	1.24	20.01	9.54	0.20	5.14	12.11	2.64	0.15	98.95
87.1	47.97	48.59	1.25	19.73	9.51	0.15	5.23	12.04	2.65	0.14	98.68
97.6	48.24	48.66	1.26	19.54	9.55	0.12	5.32	12.04	2.66	0.15	98.88
108.3	48.27	48.74	1.33	19.31	9.59	0.17	5.34	12.00	2.65	0.17	98.82
119.0	48.43	48.86	1.29	19.17	9.72	0.17	5.27	12.02	2.66	0.14	98.87
129.6	48.45	48.82	1.38	19.09	9.69	0.14	5.34	12.03	2.63	0.17	98.93
151.0	48.69	48.88	1.39	18.77	9.93	0.16	5.38	11.98	2.65	0.17	99.11
161.6	48.79	49.31	1.31	18.42	9.88	0.12	5.43	11.96	2.71	0.16	98.78
183.0	49.04	49.53	1.36	18.16	9.95	0.15	5.47	11.85	2.67	0.16	98.81
193.6	49.18	49.56	1.39	17.91	10.06	0.17	5.46	11.91	2.65	0.18	98.93
204.3	49.30	49.69	1.44	17.69	10.06	0.15	5.60	11.88	2.62	0.16	98.91
215.0	49.36	49.65	1.47	17.72	10.18	0.20	5.48	11.81	2.63	0.16	99.01
225.6	49.36	49.84	1.47	17.39	10.23	0.19	5.56	11.82	2.64	0.17	98.82
236.3	49.56	50.00	1.47	17.26	10.16	0.21	5.51	11.87	2.65	0.18	98.86
236.3	49.73	49.72	1.49	17.40	10.22	0.24	5.67	11.78	2.61	0.17	99.31
257.8	49.68	49.99	1.59	17.01	10.27	0.20	5.61	11.83	2.63	0.18	99.00

279.2	49.77	50.28	1.48	16.71	10.39	0.18	5.72	11.73	2.65	0.17	98.80
300.7	49.87	50.45	1.47	16.45	10.55	0.16	5.63	11.77	2.65	0.17	98.72
322.1	50.17	50.48	1.61	16.08	10.52	0.22	5.94	11.65	2.64	0.16	98.98
343.6	50.33	50.34	1.64	15.98	10.78	0.21	5.89	11.67	2.63	0.17	99.29
365.1	50.42	50.48	1.71	15.65	10.76	0.21	6.01	11.70	2.61	0.17	99.23
386.5	50.47	50.77	1.77	15.39	10.81	0.14	6.06	11.57	2.63	0.18	99.01
408.0	50.35	50.89	1.70	15.24	10.89	0.20	5.93	11.63	2.63	0.18	98.76
429.5	50.35	51.07	1.74	14.94	10.97	0.21	6.03	11.58	2.59	0.17	98.58
450.9	50.38	51.16	1.75	14.79	11.04	0.22	6.02	11.57	2.59	0.16	98.52
472.4	50.58	51.39	1.73	14.63	11.06	0.16	6.07	11.51	2.57	0.18	98.49
493.8	50.56	50.94	1.76	14.54	11.28	0.27	6.17	11.55	2.61	0.17	98.92
515.3	50.52	51.03	1.77	14.49	11.21	0.18	6.32	11.55	2.58	0.17	98.79
515.3	51.05	51.35	1.70	14.41	11.16	0.23	6.31	11.49	2.49	0.16	99.00
556.1	50.79	51.14	1.78	14.22	11.40	0.18	6.34	11.48	2.59	0.16	98.95
596.8	50.90	51.21	1.95	13.96	11.40	0.17	6.35	11.49	2.59	0.16	98.99
637.5	50.89	51.50	1.77	13.92	11.44	0.23	6.29	11.46	2.53	0.16	98.69
678.3	50.96	51.20	1.82	13.79	11.71	0.19	6.44	11.43	2.54	0.18	99.06
719.1	50.94	51.34	1.81	13.66	11.79	0.18	6.44	11.36	2.56	0.16	98.91
759.9	51.23	51.24	2.00	13.55	11.61	0.21	6.56	11.41	2.55	0.18	99.29
800.6	51.14	51.40	1.80	13.50	11.71	0.20	6.56	11.38	2.59	0.16	99.04
841.4	50.99	51.45	1.83	13.43	11.80	0.23	6.57	11.27	2.53	0.19	98.83
882.2	50.82	51.45	1.99	13.41	11.67	0.22	6.57	11.27	2.55	0.18	98.67
923.0	50.86	51.49	1.85	13.39	11.83	0.18	6.65	11.22	2.52	0.17	98.67
963.8	50.94	51.41	1.91	13.29	11.87	0.17	6.59	11.33	2.56	0.17	98.83
1004.5	50.92	51.59	1.80	13.35	11.89	0.18	6.61	11.18	2.54	0.17	98.62
1045.3	50.94	51.48	1.82	13.34	11.81	0.19	6.62	11.30	2.57	0.18	98.76
1086.1	51.06	51.10	1.86	13.41	12.04	0.17	6.72	11.23	2.60	0.18	99.25
1126.8	50.85	51.32	1.79	13.51	11.92	0.23	6.70	11.12	2.53	0.18	98.84
1167.5	51.05	51.19	1.93	13.21	12.00	0.24	6.72	11.26	2.57	0.20	99.16
1208.3	51.01	51.38	1.90	13.30	11.98	0.24	6.64	11.13	2.56	0.17	98.93
1249.1	50.94	51.35	1.69	13.34	12.00	0.19	6.77	11.21	2.57	0.19	98.89
1289.9	50.83	51.16	1.85	13.41	11.98	0.21	6.75	11.23	2.53	0.19	98.97
1330.7	50.96	51.30	1.87	13.29	12.06	0.22	6.65	11.16	2.58	0.17	98.95
1371.4	50.89	51.32	1.85	13.22	12.08	0.19	6.70	11.21	2.55	0.18	98.87
1412.2	50.96	51.12	1.87	13.36	12.04	0.24	6.72	11.16	2.61	0.18	99.14
1453.0	50.93	51.23	1.90	13.26	12.12	0.19	6.73	11.14	2.56	0.17	99.01
1493.8	50.94	51.03	1.87	13.33	12.28	0.21	6.76	11.10	2.56	0.17	99.21
1534.5	50.95	51.16	1.97	13.21	12.07	0.20	6.72	11.21	2.57	0.19	99.08
1575.3	51.05	51.29	1.81	13.32	12.09	0.18	6.72	11.14	2.59	0.18	99.06
1616.0	51.06	51.00	1.85	13.24	12.17	0.27	6.85	11.14	2.59	0.19	99.36
5.5	47.03	47.71	1.07	21.13	9.19	0.21	4.98	12.18	2.69	0.15	98.62
9.5	46.95	47.81	1.10	21.10	9.19	0.17	4.93	12.22	2.62	0.16	98.44
10.0	47.19	47.64	1.14	21.09	9.31	0.15	5.05	12.16	2.61	0.15	98.85

20.8	47.61	47.65	1.13	20.83	9.46	0.19	5.06	12.22	2.62	0.15	99.27
31.7	47.53	48.08	1.10	20.58	9.34	0.18	5.11	12.18	2.58	0.14	98.75
42.5	47.66	48.19	1.18	20.30	9.40	0.16	5.19	12.09	2.63	0.15	98.77
53.4	47.94	48.41	1.18	20.14	9.39	0.13	5.21	12.09	2.61	0.15	98.83
64.2	48.04	48.31	1.17	20.01	9.53	0.11	5.23	12.14	2.63	0.15	99.03
75.1	48.19	48.55	1.20	19.74	9.58	0.18	5.24	12.04	2.63	0.15	98.94
85.9	48.22	48.69	1.31	19.56	9.56	0.13	5.18	12.06	2.66	0.14	98.83
96.7	48.44	48.55	1.25	19.52	9.61	0.21	5.31	12.05	2.65	0.16	99.19
107.6	48.48	48.71	1.36	19.19	9.70	0.16	5.34	12.07	2.62	0.16	99.07
118.4	48.57	48.88	1.28	19.14	9.63	0.20	5.32	12.04	2.64	0.18	98.99
129.3	48.83	48.78	1.28	18.98	9.91	0.16	5.36	12.00	2.66	0.18	99.35
140.1	48.77	49.16	1.31	18.74	9.81	0.19	5.31	11.96	2.64	0.18	98.90
150.9	48.76	49.23	1.40	18.61	9.81	0.19	5.37	11.90	2.63	0.15	98.83
161.8	48.93	49.59	1.36	18.20	9.85	0.15	5.35	11.94	2.71	0.16	98.64
172.6	49.06	49.38	1.46	18.09	9.98	0.18	5.47	11.91	2.67	0.16	98.97
183.5	49.16	49.45	1.36	18.01	10.13	0.20	5.44	11.85	2.69	0.17	99.01
194.3	49.12	49.42	1.45	17.91	10.11	0.18	5.58	11.84	2.65	0.17	99.00
205.2	49.25	49.72	1.34	17.62	10.25	0.16	5.51	11.89	2.64	0.16	98.83
216.0	49.50	49.75	1.48	17.47	10.28	0.16	5.48	11.81	2.71	0.16	99.05
216.0	49.61	49.61	1.48	17.61	10.25	0.15	5.55	11.92	2.57	0.17	99.30
235.9	49.71	49.72	1.57	17.25	10.25	0.17	5.62	11.89	2.66	0.17	99.29
255.8	49.90	50.30	1.53	16.85	10.22	0.18	5.68	11.73	2.65	0.17	98.91
275.6	50.10	49.91	1.61	16.77	10.55	0.22	5.75	11.66	2.66	0.17	99.49
295.5	49.92	50.40	1.51	16.36	10.47	0.25	5.73	11.75	2.64	0.18	98.82
315.4	50.14	50.66	1.55	16.10	10.49	0.21	5.80	11.69	2.63	0.17	98.78
335.3	50.35	50.63	1.62	15.84	10.67	0.17	5.92	11.66	2.62	0.17	99.02
355.2	50.59	50.74	1.60	15.60	10.71	0.24	6.02	11.57	2.65	0.17	99.15
375.1	50.62	50.80	1.63	15.55	10.88	0.17	5.91	11.58	2.61	0.17	99.11
394.9	50.50	50.99	1.72	15.27	10.74	0.10	6.03	11.67	2.62	0.16	98.81
414.8	50.65	51.05	1.64	15.11	10.89	0.21	6.05	11.58	2.59	0.17	98.90
434.7	50.84	50.88	1.80	14.87	11.04	0.22	6.19	11.55	2.58	0.17	99.26
454.6	50.70	51.06	1.70	14.71	11.10	0.17	6.16	11.62	2.61	0.17	98.94
474.4	50.81	51.21	1.77	14.63	11.17	0.21	6.10	11.48	2.55	0.17	98.90
494.3	51.12	51.05	1.76	14.55	11.18	0.26	6.18	11.58	2.56	0.18	99.37
514.1	51.03	51.26	1.85	14.40	11.19	0.12	6.23	11.52	2.56	0.17	99.07
534.0	51.16	51.15	1.77	14.19	11.35	0.18	6.36	11.48	2.62	0.19	99.30
553.9	51.03	51.08	1.82	14.15	11.39	0.25	6.35	11.49	2.61	0.18	99.25
553.9	51.15	51.34	1.86	14.22	11.28	0.15	6.35	11.45	2.46	0.18	99.10
594.6	50.97	51.31	1.83	13.84	11.56	0.20	6.35	11.45	2.59	0.18	98.96
635.3	51.19	51.54	1.80	13.62	11.39	0.23	6.49	11.52	2.55	0.18	98.96
676.0	50.98	51.24	1.86	13.76	11.67	0.24	6.44	11.37	2.58	0.15	99.04
716.7	51.20	51.40	1.78	13.70	11.55	0.23	6.55	11.37	2.54	0.17	99.10
757.4	51.17	51.67	1.72	13.44	11.75	0.22	6.47	11.38	2.48	0.17	98.80

798.1	51.17	51.19	1.96	13.54	11.75	0.18	6.65	11.33	2.54	0.16	99.27
838.7	51.05	51.03	1.93	13.46	11.90	0.25	6.66	11.36	2.53	0.18	99.31
879.4	51.08	51.39	1.79	13.47	11.77	0.17	6.66	11.34	2.56	0.17	98.99
920.1	51.00	51.53	1.91	13.35	11.69	0.19	6.64	11.26	2.56	0.18	98.77
960.7	51.04	51.06	1.95	13.45	11.93	0.21	6.65	11.33	2.57	0.16	99.28
1001.4	50.95	51.08	1.90	13.45	11.85	0.23	6.78	11.29	2.54	0.19	99.17
1042.1	50.84	51.33	1.83	13.42	11.96	0.21	6.64	11.19	2.55	0.18	98.81
1082.8	50.91	51.21	1.95	13.29	12.03	0.22	6.72	11.12	2.56	0.19	99.00
1123.5	51.05	51.57	1.73	13.33	11.94	0.19	6.63	11.18	2.55	0.18	98.78
1164.2	50.92	51.35	1.73	13.42	11.95	0.24	6.62	11.27	2.52	0.19	98.87
1204.9	50.86	51.11	1.94	13.42	12.03	0.19	6.76	11.13	2.53	0.19	99.04
1245.6	50.76	51.31	1.92	13.27	12.09	0.20	6.61	11.16	2.56	0.18	98.76
1286.3	50.92	51.27	1.86	13.41	12.04	0.22	6.68	11.10	2.54	0.18	98.95
1327.0	50.88	51.31	1.88	13.32	12.10	0.21	6.67	11.08	2.55	0.18	98.87
1367.6	50.81	50.96	1.92	13.40	12.13	0.25	6.78	11.06	2.61	0.19	99.15
1408.3	51.00	51.31	1.91	13.38	11.95	0.22	6.66	11.12	2.58	0.18	98.99
1449.0	50.94	51.15	1.84	13.29	12.15	0.20	6.79	11.14	2.56	0.18	99.09
1489.6	50.98	51.21	1.87	13.31	12.05	0.25	6.74	11.15	2.56	0.16	99.07
1530.3	51.05	50.94	1.83	13.42	12.22	0.25	6.78	11.19	2.50	0.17	99.40
1571.0	50.87	51.14	1.86	13.34	12.08	0.21	6.72	11.17	2.60	0.18	99.02
1611.7	51.08	50.99	1.76	13.39	12.13	0.24	6.80	11.23	2.59	0.18	99.38

Exp 209

x / μm	Oxides (wt%)										
	SiO2	SiO2*	TiO2	Al2O3	FeO	MnO	MgO	CaO	Na2O	K2O	Total
8.3	47.74	48.58	1.36	19.03	10.12	0.17	5.47	11.70	2.71	0.16	98.46
13.8	47.87	49.06	1.33	18.71	10.01	0.16	5.51	11.62	2.72	0.17	98.11
19.3	48.11	49.00	1.32	18.68	10.13	0.17	5.52	11.65	2.68	0.15	98.41
19.3	48.48	48.84	1.34	18.74	10.10	0.19	5.66	11.69	2.58	0.16	98.94
35.2	48.48	49.15	1.40	18.40	10.13	0.19	5.59	11.57	2.70	0.16	98.63
51.1	48.75	49.51	1.40	17.98	10.08	0.14	5.67	11.62	2.72	0.17	98.54
67.0	48.99	49.10	1.49	17.78	10.45	0.26	5.67	11.65	2.75	0.15	99.19
82.9	49.06	49.92	1.47	17.29	10.41	0.18	5.68	11.48	2.71	0.16	98.45
98.7	49.05	49.76	1.52	16.96	10.61	0.21	5.87	11.48	2.72	0.17	98.59
114.6	49.83	49.59	1.53	16.87	10.75	0.23	5.88	11.57	2.72	0.15	99.53
130.5	49.81	50.03	1.60	16.40	10.74	0.19	5.91	11.53	2.73	0.16	99.08
146.4	49.90	50.32	1.51	16.18	10.83	0.25	5.89	11.48	2.66	0.16	98.88
162.3	50.11	50.35	1.55	16.04	10.84	0.25	6.03	11.38	2.68	0.19	99.06
178.2	50.60	50.33	1.59	15.88	10.98	0.20	6.09	11.39	2.66	0.17	99.57
194.1	50.42	50.71	1.71	15.49	10.96	0.20	6.08	11.27	2.70	0.18	99.01
210.0	50.44	50.85	1.65	15.19	11.05	0.22	6.15	11.36	2.66	0.17	98.89
225.9	50.54	50.75	1.58	15.08	11.25	0.24	6.24	11.30	2.68	0.18	99.09
241.7	50.46	50.77	1.73	15.00	11.19	0.21	6.23	11.32	2.66	0.18	98.99
257.6	50.60	50.71	1.80	14.93	11.28	0.20	6.20	11.31	2.70	0.18	99.19
273.5	50.42	50.90	1.79	14.57	11.34	0.22	6.33	11.33	2.65	0.17	98.82
289.4	50.52	50.78	1.82	14.48	11.48	0.15	6.48	11.27	2.67	0.16	99.04
305.3	50.88	51.06	1.79	14.42	11.37	0.21	6.33	11.32	2.65	0.16	99.12
309.9	50.79	51.14	1.75	14.43	11.42	0.19	6.32	11.27	2.62	0.16	98.95
339.2	50.74	51.28	1.75	14.18	11.43	0.25	6.40	11.22	2.64	0.16	98.76
368.3	50.83	50.99	1.78	14.14	11.70	0.21	6.46	11.21	2.65	0.17	99.14
397.6	50.78	51.39	1.83	13.84	11.56	0.21	6.54	11.13	2.63	0.16	98.69
426.9	50.67	51.31	1.84	13.70	11.75	0.27	6.48	11.17	2.60	0.17	98.66
456.2	50.88	51.34	1.77	13.73	11.77	0.21	6.54	11.16	2.62	0.16	98.84
485.4	50.84	51.42	1.83	13.54	11.85	0.21	6.57	11.15	2.57	0.16	98.72
514.7	50.68	51.48	1.85	13.47	11.77	0.20	6.61	11.12	2.63	0.17	98.49
544.0	50.78	51.24	1.99	13.50	11.86	0.22	6.57	11.18	2.57	0.17	98.84
573.3	50.54	51.70	1.83	13.18	11.84	0.21	6.60	11.14	2.63	0.17	98.14
602.5	50.85	51.58	1.76	13.43	11.81	0.14	6.67	11.11	2.62	0.18	98.57
631.8	50.29	51.63	1.79	13.27	11.92	0.16	6.56	11.13	2.66	0.18	97.96
661.7	50.71	51.21	1.81	13.59	11.88	0.20	6.73	11.12	2.59	0.17	98.80
706.1	50.76	51.18	1.83	13.42	12.09	0.21	6.63	11.11	2.64	0.17	98.88
750.5	50.87	51.18	1.85	13.49	12.04	0.19	6.74	11.01	2.60	0.19	98.99
795.0	50.43	51.62	1.78	13.45	11.94	0.19	6.57	10.97	2.60	0.18	98.11
839.4	50.47	50.97	1.90	13.46	12.11	0.20	6.76	11.09	2.64	0.17	98.79
883.8	50.60	51.39	1.78	13.54	11.98	0.16	6.70	10.94	2.63	0.18	98.51

928.2	50.31	51.05	1.87	13.43	12.04	0.21	6.82	11.03	2.67	0.17	98.56
972.6	50.32	51.68	1.72	13.26	11.97	0.25	6.72	10.92	2.60	0.18	97.94
1017.1	50.55	51.06	1.91	13.31	12.16	0.26	6.80	10.97	2.64	0.20	98.79
1061.5	50.35	51.23	1.74	13.27	12.19	0.23	6.76	11.05	2.66	0.18	98.42
1105.9	50.38	51.28	1.84	13.26	12.14	0.21	6.73	11.02	2.63	0.19	98.41
1150.3	49.96	51.38	1.78	13.35	12.16	0.17	6.68	10.97	2.63	0.19	97.88
1194.8	50.13	51.32	1.78	13.27	12.10	0.24	6.83	10.93	2.64	0.18	98.11
1239.2	49.93	51.38	1.85	13.32	12.11	0.20	6.67	10.91	2.68	0.18	97.85
1283.6	50.06	51.01	1.92	13.31	12.16	0.29	6.86	10.91	2.65	0.18	98.34
1328.0	50.03	51.13	1.91	13.31	12.17	0.29	6.73	10.93	2.67	0.17	98.20
1372.4	50.12	51.43	1.80	13.29	12.05	0.18	6.81	10.90	2.66	0.19	97.99
1416.9	49.84	51.65	1.81	13.22	11.89	0.22	6.69	10.98	2.66	0.18	97.50
1461.3	50.18	51.61	1.69	13.16	12.02	0.22	6.79	10.99	2.64	0.18	97.86
1505.6	49.93	51.54	1.82	13.27	11.94	0.17	6.69	11.02	2.67	0.18	97.70
7.6	47.94	48.53	1.25	18.82	10.35	0.19	5.77	11.43	2.78	0.19	98.71
12.2	48.05	48.87	1.34	18.86	9.98	0.21	5.46	11.69	2.74	0.15	98.48
16.8	48.24	48.70	1.30	18.98	9.97	0.15	5.57	11.74	2.74	0.16	98.85
21.4	48.06	48.95	1.28	18.62	10.17	0.19	5.50	11.71	2.73	0.16	98.41
26.0	48.38	48.80	1.45	18.62	10.10	0.19	5.59	11.67	2.71	0.16	98.88
26.0	48.44	48.93	1.35	18.68	10.20	0.19	5.52	11.67	2.59	0.17	98.81
41.4	48.25	49.43	1.29	18.21	10.05	0.15	5.61	11.68	2.70	0.17	98.11
56.8	48.49	49.68	1.40	17.75	10.28	0.17	5.61	11.55	2.70	0.15	98.11
72.2	48.72	49.66	1.48	17.37	10.48	0.16	5.65	11.60	2.72	0.18	98.35
87.6	49.01	49.74	1.42	17.21	10.55	0.18	5.69	11.62	2.72	0.17	98.57
102.9	49.01	49.95	1.53	16.93	10.55	0.14	5.79	11.55	2.69	0.17	98.36
118.3	49.30	50.19	1.57	16.53	10.61	0.19	5.80	11.52	2.72	0.17	98.42
133.7	49.42	50.55	1.60	16.24	10.65	0.12	5.86	11.42	2.68	0.18	98.18
149.1	49.52	50.45	1.62	16.09	10.73	0.17	5.94	11.43	2.70	0.17	98.37
164.5	49.58	50.40	1.65	15.86	10.91	0.22	5.92	11.48	2.70	0.16	98.48
179.9	49.76	50.90	1.60	15.48	10.85	0.22	6.00	11.42	2.66	0.19	98.17
195.2	49.77	50.95	1.55	15.33	11.02	0.14	6.01	11.38	2.73	0.19	98.12
210.6	49.93	51.03	1.57	15.17	10.95	0.17	6.16	11.39	2.69	0.18	98.20
226.0	49.88	51.00	1.70	14.99	11.13	0.16	6.16	11.32	2.67	0.17	98.18
241.3	49.79	50.98	1.68	14.82	11.19	0.19	6.20	11.38	2.69	0.17	98.11
256.7	50.17	50.92	1.80	14.64	11.24	0.19	6.27	11.40	2.69	0.17	98.55
272.1	50.08	51.09	1.75	14.48	11.32	0.16	6.30	11.31	2.71	0.17	98.29
287.5	50.20	51.14	1.82	14.41	11.32	0.21	6.27	11.31	2.65	0.17	98.36
302.9	50.38	50.89	1.79	14.35	11.48	0.18	6.38	11.39	2.68	0.16	98.79
320.1	50.34	51.40	1.74	14.03	11.44	0.24	6.31	11.31	2.66	0.17	98.24
337.6	49.81	51.11	1.78	14.16	11.39	0.24	6.53	11.26	2.65	0.18	98.00
367.1	49.85	51.14	1.84	13.97	11.57	0.22	6.43	11.28	2.66	0.19	98.01
396.5	49.99	51.27	1.84	13.74	11.66	0.21	6.48	11.28	2.66	0.18	98.03
426.0	49.85	51.37	1.94	13.70	11.70	0.18	6.45	11.18	2.61	0.17	97.79

455.4	49.77	51.14	1.90	13.64	11.71	0.24	6.50	11.38	2.60	0.18	97.93
484.9	49.80	51.08	1.78	13.65	11.82	0.25	6.67	11.26	2.62	0.17	98.03
514.3	49.66	51.53	1.78	13.55	11.71	0.26	6.57	11.13	2.61	0.18	97.43
543.8	49.94	51.54	1.78	13.50	11.89	0.22	6.51	11.06	2.65	0.16	97.70
573.2	49.83	51.39	1.77	13.44	11.93	0.20	6.64	11.15	2.59	0.18	97.73
602.7	50.15	51.06	1.88	13.47	11.96	0.22	6.74	11.16	2.62	0.19	98.38
632.1	50.02	51.21	1.88	13.52	11.92	0.22	6.71	11.11	2.57	0.15	98.11
661.6	50.11	51.56	1.80	13.24	11.90	0.21	6.60	11.19	2.64	0.16	97.85
703.4	50.33	51.22	1.88	13.49	11.93	0.20	6.77	11.03	2.62	0.16	98.42
744.6	50.07	51.35	1.90	13.32	11.96	0.23	6.68	11.05	2.65	0.16	98.03
785.9	49.91	51.41	1.86	13.25	11.96	0.20	6.82	11.01	2.62	0.17	97.80
827.1	50.03	51.32	1.83	13.38	12.00	0.18	6.76	11.04	2.62	0.18	98.01
868.4	49.75	51.27	1.89	13.35	11.94	0.22	6.75	11.07	2.61	0.20	97.78
909.6	50.07	51.18	1.85	13.30	12.13	0.24	6.64	11.07	2.70	0.18	98.18
950.9	49.86	51.52	1.88	13.24	12.02	0.25	6.67	10.90	2.64	0.18	97.64
992.1	50.00	51.32	1.82	13.21	12.10	0.28	6.74	11.01	2.63	0.20	97.98
1033.4	49.86	51.01	1.90	13.35	12.13	0.25	6.84	11.02	2.64	0.16	98.15
1074.6	49.52	51.21	1.84	13.37	12.11	0.21	6.73	10.98	2.67	0.18	97.61
1115.9	49.75	51.19	1.79	13.29	12.30	0.21	6.73	10.99	2.65	0.16	97.86
1157.1	49.82	51.40	1.81	13.33	12.03	0.22	6.68	10.99	2.66	0.19	97.73
1198.4	49.68	51.09	1.97	13.35	12.14	0.23	6.81	10.92	2.63	0.17	97.89
1239.6	49.57	51.25	1.81	13.28	12.05	0.25	6.82	11.03	2.64	0.17	97.62
1280.9	49.64	51.35	1.85	13.32	12.04	0.20	6.70	10.99	2.68	0.19	97.59
1322.1	49.46	51.59	1.84	13.23	12.02	0.17	6.70	10.95	2.62	0.17	97.17
1363.4	49.67	51.14	1.85	13.39	12.15	0.21	6.83	10.86	2.69	0.18	97.83
1404.6	49.65	51.41	1.87	13.22	12.14	0.17	6.75	10.91	2.65	0.17	97.54
1445.9	49.77	51.30	1.86	13.32	12.12	0.22	6.71	10.92	2.68	0.17	97.77
1487.1	49.77	51.35	1.88	13.26	12.08	0.24	6.69	10.95	2.66	0.19	97.72
11.1	47.86	48.85	1.32	18.83	9.89	0.18	5.56	11.73	2.75	0.18	98.31
16.1	47.79	48.70	1.34	18.91	10.08	0.18	5.48	11.73	2.72	0.16	98.39
21.1	48.09	48.82	1.38	18.75	10.14	0.14	5.55	11.64	2.71	0.16	98.57
21.1	48.12	49.04	1.40	18.66	9.95	0.18	5.54	11.69	2.69	0.15	98.38
36.7	48.46	49.16	1.43	18.32	10.10	0.17	5.60	11.65	2.73	0.15	98.60
52.3	48.88	49.67	1.35	17.79	10.22	0.20	5.63	11.56	2.73	0.15	98.51
67.9	49.04	49.55	1.54	17.48	10.39	0.19	5.69	11.57	2.73	0.17	98.79
83.5	49.27	50.01	1.52	16.97	10.52	0.17	5.77	11.49	2.68	0.18	98.57
99.2	49.62	50.22	1.51	16.59	10.54	0.21	5.82	11.53	2.72	0.17	98.70
114.8	49.56	50.45	1.53	16.36	10.69	0.18	5.79	11.42	2.70	0.18	98.41
130.4	49.84	50.18	1.57	16.22	10.73	0.27	5.94	11.47	2.73	0.19	98.95
146.0	49.71	50.42	1.62	15.96	10.85	0.25	5.93	11.35	2.76	0.17	98.59
161.6	50.14	50.74	1.64	15.68	10.81	0.22	5.96	11.42	2.67	0.16	98.70
177.2	49.95	50.66	1.69	15.48	10.97	0.21	6.00	11.41	2.71	0.17	98.59
192.8	50.14	50.90	1.67	15.34	10.92	0.14	6.09	11.34	2.72	0.17	98.54

208.4	50.23	50.76	1.59	15.27	11.12	0.21	6.14	11.33	2.69	0.18	98.76
224.0	50.19	50.82	1.68	14.95	11.19	0.18	6.22	11.37	2.71	0.17	98.67
239.7	50.28	51.02	1.69	14.93	11.11	0.21	6.22	11.26	2.68	0.18	98.56
255.3	50.04	50.93	1.65	14.70	11.35	0.20	6.29	11.32	2.68	0.18	98.41
270.9	50.27	51.14	1.72	14.56	11.36	0.14	6.26	11.28	2.67	0.16	98.42
286.5	50.33	50.95	1.79	14.45	11.30	0.22	6.42	11.31	2.70	0.16	98.68
302.1	50.36	51.37	1.70	14.33	11.34	0.21	6.26	11.27	2.64	0.17	98.29
269.0	50.25	50.89	1.79	14.60	11.42	0.26	6.29	11.26	2.62	0.17	98.65
290.0	50.37	51.13	1.80	14.33	11.47	0.21	6.32	11.20	2.66	0.17	98.54
301.0	50.56	51.12	1.80	14.31	11.51	0.16	6.34	11.25	2.62	0.19	98.74
319.4	49.94	50.98	1.79	14.33	11.51	0.16	6.45	11.29	2.60	0.18	98.26
348.7	50.28	50.98	1.79	14.07	11.71	0.27	6.41	11.19	2.69	0.19	98.60
378.1	50.29	51.30	1.87	13.89	11.59	0.18	6.51	11.17	2.63	0.16	98.30
407.4	50.22	51.10	1.93	13.90	11.59	0.24	6.57	11.19	2.61	0.17	98.42
436.7	50.13	51.09	1.83	13.79	11.80	0.25	6.57	11.18	2.62	0.16	98.35
466.1	50.35	51.05	1.79	13.71	11.87	0.18	6.67	11.22	2.62	0.18	98.60
495.4	50.12	51.08	1.84	13.63	11.89	0.16	6.66	11.22	2.66	0.17	98.35
524.7	50.26	50.84	1.94	13.70	12.06	0.22	6.54	11.21	2.61	0.18	98.72
554.1	50.31	51.31	1.87	13.57	11.89	0.19	6.64	11.04	2.59	0.19	98.30
583.4	50.08	50.96	1.83	13.56	11.98	0.27	6.76	11.15	2.62	0.17	98.42
612.7	50.12	51.37	1.76	13.60	11.85	0.23	6.62	11.10	2.59	0.18	98.05
642.1	50.40	51.42	1.83	13.35	11.97	0.21	6.70	11.01	2.65	0.17	98.28
671.4	50.51	51.77	1.73	13.30	11.82	0.28	6.55	11.03	2.65	0.17	98.03
691.8	50.19	51.11	1.81	13.61	11.87	0.22	6.79	11.10	2.61	0.17	98.38
731.3	49.92	51.25	1.86	13.49	11.94	0.23	6.66	11.09	2.61	0.17	97.97
770.8	50.28	51.25	1.82	13.58	11.97	0.28	6.64	10.99	2.60	0.17	98.33
810.3	50.22	51.15	1.79	13.48	12.03	0.25	6.81	10.96	2.64	0.18	98.37
849.8	50.19	51.02	1.85	13.53	12.09	0.19	6.82	11.03	2.59	0.18	98.47
889.3	50.16	51.12	1.82	13.49	11.99	0.25	6.83	11.00	2.61	0.19	98.34
928.8	50.09	51.46	1.83	13.29	12.02	0.19	6.69	10.95	2.67	0.19	97.93
968.3	50.16	51.01	1.82	13.55	12.12	0.20	6.81	10.97	2.65	0.17	98.45
1007.8	50.24	51.34	1.89	13.39	11.97	0.17	6.76	10.96	2.63	0.19	98.20
1047.2	50.31	51.01	1.84	13.45	12.14	0.29	6.79	10.96	2.63	0.20	98.60
1086.7	49.98	51.27	1.89	13.40	11.99	0.28	6.76	10.90	2.63	0.18	98.01
1126.2	50.16	51.12	1.71	13.43	11.99	0.31	6.85	11.04	2.68	0.19	98.35
1165.7	50.22	51.11	1.78	13.56	12.06	0.25	6.80	10.93	2.63	0.18	98.41
1205.2	50.25	51.38	1.83	13.38	12.08	0.20	6.68	10.92	2.64	0.19	98.16
1244.7	50.28	51.20	1.81	13.49	12.07	0.21	6.74	10.92	2.67	0.18	98.39
1284.2	50.41	51.19	1.75	13.44	12.19	0.20	6.71	10.97	2.70	0.17	98.52
1323.7	50.24	51.29	1.83	13.42	11.94	0.18	6.77	11.04	2.65	0.19	98.26
1363.2	50.55	51.38	1.70	13.39	12.05	0.23	6.75	10.91	2.71	0.18	98.46
1402.7	50.33	51.06	1.83	13.54	12.17	0.20	6.78	10.83	2.70	0.19	98.57
1442.2	50.53	51.26	1.82	13.48	12.02	0.19	6.82	10.89	2.62	0.20	98.56

1481.7	50.50	51.08	1.88	13.40	12.10	0.21	6.87	10.90	2.67	0.19	98.72
--------	-------	-------	------	-------	-------	------	------	-------	------	------	-------

Exp 221

x / μm	Oxides (wt%)										
	SiO2	SiO2*	TiO2	Al2O3	FeO	MnO	MgO	CaO	Na2O	K2O	Total
14.1	48.23	47.44	1.06	20.83	9.60	0.18	5.20	12.04	0.16	2.79	100.08
21.1	48.44	47.67	1.18	20.48	9.60	0.19	5.25	12.07	0.15	2.73	100.07
28.0	48.73	47.46	1.26	20.22	9.86	0.22	5.34	12.02	0.16	2.76	100.58
28.0	48.63	47.76	1.15	20.21	9.87	0.23	5.36	11.98	0.15	2.59	100.18
43.8	48.96	48.15	1.32	19.68	9.78	0.23	5.32	11.93	0.16	2.72	100.11
59.4	49.47	48.66	1.37	19.05	9.90	0.13	5.44	11.86	0.18	2.72	100.10
75.1	49.45	49.16	1.25	18.41	10.11	0.16	5.53	11.85	0.16	2.68	99.59
90.7	50.16	49.24	1.45	17.94	10.19	0.19	5.59	11.76	0.17	2.77	100.22
87.4	50.19	48.98	1.39	18.00	10.28	0.17	5.71	11.77	0.17	2.85	100.51
102.9	50.14	49.27	1.52	17.54	10.39	0.19	5.70	11.78	0.17	2.75	100.17
118.4	50.86	49.68	1.53	16.82	10.54	0.25	5.81	11.71	0.15	2.80	100.48
133.9	50.73	49.89	1.59	16.41	10.86	0.14	5.88	11.66	0.15	2.71	100.14
149.4	51.22	50.11	1.63	15.97	11.03	0.17	5.90	11.61	0.18	2.70	100.41
165.0	51.14	50.30	1.61	15.64	11.06	0.13	5.96	11.66	0.16	2.78	100.14
180.4	51.27	50.38	1.69	15.35	11.21	0.24	6.11	11.55	0.16	2.61	100.19
195.9	51.56	50.56	1.71	15.06	11.27	0.16	6.21	11.48	0.18	2.67	100.31
229.5	51.61	50.82	1.83	14.29	11.54	0.18	6.25	11.55	0.18	2.66	100.09
230.4	50.96	50.81	1.70	14.48	11.46	0.25	6.46	11.31	0.18	2.64	99.45
241.4	52.02	51.25	1.73	14.04	11.49	0.20	6.28	11.52	0.17	2.62	100.07
251.3	51.70	50.78	1.87	14.03	11.76	0.20	6.45	11.43	0.16	2.62	100.23
296.2	51.89	50.51	1.85	13.89	12.04	0.19	6.66	11.49	0.18	2.49	100.68
341.2	51.67	50.62	1.85	13.63	12.10	0.26	6.64	11.42	0.16	2.62	100.35
386.0	51.72	50.95	1.88	13.54	11.89	0.21	6.63	11.34	0.18	2.68	100.07
430.9	51.72	51.07	1.72	13.66	11.87	0.20	6.63	11.42	0.16	2.57	99.95
475.9	51.72	50.66	1.91	13.62	12.10	0.18	6.72	11.32	0.19	2.60	100.35
520.8	51.87	50.63	1.81	13.62	12.07	0.24	6.80	11.23	0.18	2.71	100.54
565.7	51.42	50.77	1.82	13.64	12.11	0.21	6.74	11.18	0.17	2.67	99.95
610.6	51.71	50.86	1.76	13.56	12.21	0.21	6.66	11.18	0.19	2.67	100.14
655.6	51.96	50.62	1.88	13.61	12.20	0.19	6.75	11.15	0.18	2.72	100.64
700.4	51.97	50.70	1.90	13.57	12.27	0.22	6.78	11.16	0.15	2.54	100.57
745.3	51.89	50.65	1.91	13.54	12.19	0.21	6.77	11.13	0.18	2.72	100.54
790.3	52.00	50.73	1.91	13.63	12.13	0.24	6.75	11.08	0.18	2.65	100.57
835.2	51.76	50.79	1.86	13.71	12.10	0.20	6.81	11.02	0.19	2.62	100.26
880.1	51.88	51.09	1.72	13.55	12.14	0.18	6.78	11.00	0.17	2.68	100.08
925.1	52.13	50.48	1.97	13.61	12.20	0.18	6.89	11.04	0.17	2.77	100.95
970.0	51.85	50.82	1.86	13.62	12.13	0.23	6.80	10.99	0.18	2.68	100.33
1014.8	51.78	50.47	1.90	13.69	12.24	0.23	6.84	11.02	0.19	2.72	100.61
1059.7	51.68	50.79	1.81	13.75	12.05	0.23	6.73	11.02	0.18	2.75	100.19
1104.7	51.63	50.90	1.84	13.55	12.03	0.18	6.89	11.01	0.18	2.72	100.02
1149.6	51.63	50.80	1.79	13.74	12.06	0.22	6.84	10.96	0.19	2.68	100.13
1194.5	51.83	50.64	1.91	13.59	12.21	0.25	6.79	11.05	0.17	2.70	100.49
1239.5	51.87	50.90	1.79	13.61	12.09	0.28	6.77	10.98	0.19	2.70	100.27
1284.3	52.03	51.07	1.89	13.51	12.02	0.19	6.67	11.07	0.20	2.68	100.26
9.5	48.58	47.29	1.19	20.80	9.67	0.15	5.27	11.98	0.18	2.78	100.58
14.5	48.30	47.33	1.13	20.68	9.79	0.15	5.29	12.03	0.16	2.73	100.27
19.5	48.65	47.71	1.18	20.35	9.61	0.18	5.33	12.00	0.17	2.77	100.24
24.4	48.63	47.77	1.23	20.26	9.67	0.19	5.27	11.97	0.18	2.76	100.17
24.4	48.69	47.62	1.29	20.21	9.81	0.16	5.32	12.04	0.15	2.70	100.37
37.7	49.13	47.81	1.26	19.78	9.89	0.20	5.43	11.98	0.16	2.79	100.62
51.0	49.32	48.37	1.30	19.11	10.02	0.17	5.54	11.83	0.18	2.78	100.25

64.2	49.82	49.21	1.23	18.41	10.03	0.18	5.50	11.80	0.18	2.75	99.92
92.6	49.98	49.32	1.41	17.77	10.27	0.23	5.69	11.71	0.16	2.74	99.96
107.5	50.54	49.51	1.38	17.17	10.65	0.17	5.74	11.73	0.17	2.78	100.33
122.2	50.76	49.98	1.55	16.58	10.72	0.20	5.82	11.63	0.18	2.65	100.09
137.0	51.10	50.09	1.57	16.23	10.81	0.08	5.96	11.66	0.16	2.73	100.31
151.7	51.32	50.20	1.70	15.67	10.94	0.21	6.09	11.63	0.17	2.70	100.42
166.6	51.50	50.21	1.71	15.27	11.28	0.21	6.16	11.60	0.18	2.68	100.59
181.3	51.10	50.54	1.70	15.06	11.31	0.21	6.15	11.50	0.17	2.65	99.86
196.1	51.60	50.76	1.74	14.75	11.31	0.13	6.30	11.47	0.17	2.68	100.15
258.3	51.47	50.66	1.84	14.10	11.74	0.22	6.62	11.32	0.14	2.65	100.11
304.1	51.52	50.67	1.88	13.77	12.02	0.21	6.69	11.31	0.17	2.59	100.15
349.8	51.89	50.74	1.78	13.69	12.09	0.23	6.70	11.35	0.19	2.54	100.44
395.6	51.47	51.00	1.82	13.59	11.93	0.22	6.64	11.30	0.18	2.63	99.77
441.2	51.81	51.07	1.73	13.56	11.99	0.21	6.75	11.17	0.16	2.66	100.04
487.0	51.75	50.92	1.81	13.71	11.99	0.16	6.73	11.24	0.17	2.56	100.12
532.8	51.64	51.25	1.77	13.53	12.03	0.20	6.67	11.19	0.18	2.48	99.69
578.5	51.27	51.02	1.88	13.62	11.98	0.21	6.73	11.14	0.17	2.54	99.55
624.3	51.73	50.90	1.84	13.66	12.08	0.15	6.78	11.10	0.16	2.63	100.13
669.9	51.53	50.90	1.78	13.66	12.14	0.18	6.72	11.12	0.19	2.60	99.93
715.7	51.45	50.90	1.87	13.57	11.98	0.21	6.83	11.14	0.18	2.61	99.85
761.4	51.95	50.79	1.87	13.66	12.16	0.23	6.68	11.07	0.16	2.68	100.46
807.2	51.57	50.86	1.74	13.62	12.14	0.26	6.81	11.07	0.16	2.64	100.01
853.0	51.51	51.04	1.82	13.54	12.13	0.23	6.73	10.99	0.18	2.64	99.77
898.6	51.51	50.78	1.76	13.66	12.21	0.20	6.80	11.00	0.20	2.68	100.03
944.4	51.79	50.56	1.82	13.68	12.25	0.15	6.94	10.97	0.18	2.74	100.53
990.1	51.48	50.90	1.74	13.58	12.18	0.22	6.79	10.99	0.17	2.72	99.88
1035.9	51.43	50.93	1.79	13.55	12.26	0.21	6.71	11.00	0.19	2.66	99.79
1081.7	51.81	50.76	1.82	13.67	12.17	0.25	6.74	10.99	0.18	2.72	100.35
1127.4	51.48	51.07	1.70	13.60	12.18	0.23	6.81	10.94	0.17	2.61	99.72
1173.1	51.57	50.63	1.85	13.66	12.32	0.22	6.79	11.00	0.19	2.64	100.24
1218.8	51.78	50.92	1.77	13.59	12.23	0.18	6.84	10.96	0.17	2.65	100.16
1264.6	51.38	50.98	1.81	13.54	12.11	0.20	6.81	10.95	0.18	2.73	99.70
1310.3	51.48	50.72	1.93	13.62	12.06	0.21	6.87	10.94	0.20	2.74	100.05
1356.1	51.43	50.98	1.76	13.63	12.05	0.26	6.80	10.98	0.17	2.67	99.76

Exp 222

x / μm	Oxides (wt%)										
	SiO2	SiO2*	TiO2	Al2O3	FeO	MnO	MgO	CaO	Na2O	K2O	Total
7.8	49.21	49.71	1.44	17.19	10.57	0.20	5.95	11.32	2.75	0.17	98.80
14.0	49.35	49.79	1.65	16.82	10.61	0.20	5.98	11.30	2.77	0.18	98.87
20.3	49.55	49.68	1.66	16.61	10.85	0.21	5.98	11.38	2.77	0.17	99.17
26.5	49.87	50.26	1.56	16.13	10.88	0.18	6.07	11.31	2.74	0.18	98.91
26.5	49.95	50.10	1.42	16.30	10.94	0.21	6.14	11.32	2.70	0.17	99.15
36.8	49.75	50.40	1.74	15.56	11.06	0.17	6.27	11.21	2.72	0.19	98.65
47.0	50.34	50.72	1.76	15.12	11.23	0.12	6.22	11.25	2.71	0.17	98.92
42.5	50.44	50.44	1.75	15.30	11.26	0.24	6.22	11.25	2.68	0.16	99.30
58.4	50.58	50.46	1.79	14.73	11.53	0.18	6.49	11.26	2.67	0.20	99.42
74.2	51.51	50.59	1.77	14.36	11.86	0.19	6.50	11.20	2.68	0.16	100.22
90.1	50.96	51.09	1.83	13.85	11.80	0.17	6.51	11.26	2.64	0.17	99.17
105.9	50.30	50.86	1.87	13.67	11.91	0.25	6.74	11.17	2.67	0.16	98.75
121.8	50.83	51.23	1.79	13.55	11.92	0.15	6.71	11.13	2.61	0.21	98.90
137.6	50.89	50.99	1.85	13.55	12.02	0.26	6.77	11.04	2.64	0.18	99.20
153.5	50.99	51.19	1.89	13.49	12.00	0.17	6.73	11.05	2.63	0.17	99.10
153.5	50.93	50.86	1.80	13.71	12.08	0.21	6.75	11.11	2.60	0.17	99.36
185.7	50.61	50.71	1.88	13.62	12.16	0.19	6.88	11.02	2.67	0.17	99.20
217.9	50.67	50.94	1.86	13.63	12.19	0.20	6.73	10.91	2.65	0.18	99.03
250.0	50.93	51.04	1.77	13.43	12.22	0.20	6.79	10.99	2.68	0.18	99.19
282.2	50.67	50.96	1.88	13.49	12.18	0.20	6.81	10.92	2.67	0.19	99.01
314.4	50.77	51.00	1.84	13.42	12.20	0.21	6.82	10.96	2.66	0.19	99.06
346.6	50.70	51.03	1.85	13.42	12.20	0.19	6.80	10.93	2.68	0.19	98.97
378.7	50.82	50.86	1.82	13.47	12.22	0.17	6.94	10.95	2.68	0.18	99.26
410.9	50.53	50.75	1.88	13.62	12.17	0.27	6.82	10.90	2.70	0.19	99.07
443.1	51.13	50.91	1.75	13.52	12.27	0.19	6.86	10.92	2.69	0.19	99.52
475.3	50.98	50.98	1.89	13.58	12.02	0.20	6.82	10.94	2.69	0.17	99.30
507.4	50.46	50.92	1.81	13.54	12.21	0.26	6.77	10.91	2.70	0.18	98.84
539.6	50.36	50.87	1.78	13.52	12.22	0.22	6.85	10.91	2.74	0.20	98.80
571.8	50.72	50.88	1.87	13.50	12.22	0.17	6.82	10.93	2.73	0.18	99.14
603.9	50.50	50.87	1.76	13.56	12.16	0.23	6.87	10.92	2.75	0.18	98.93
636.0	50.84	51.00	1.80	13.48	12.15	0.17	6.86	10.94	2.72	0.19	99.15
668.2	50.45	51.08	1.83	13.47	12.08	0.20	6.85	10.88	2.74	0.18	98.67
700.4	50.36	51.04	1.87	13.41	12.19	0.18	6.77	10.92	2.74	0.18	98.63
5.8	49.22	49.56	1.49	17.23	10.61	0.20	5.96	11.29	2.79	0.18	98.96
11.0	49.57	49.81	1.48	16.99	10.46	0.20	5.92	11.51	2.76	0.17	99.06
16.3	49.71	49.83	1.58	16.77	10.77	0.19	5.89	11.35	2.76	0.17	99.18
21.5	49.84	49.82	1.64	16.42	10.90	0.13	6.12	11.32	2.76	0.19	99.32
21.5	49.52	49.79	1.54	16.53	10.87	0.22	6.08	11.39	2.70	0.18	99.03
36.5	50.04	50.36	1.67	15.62	10.95	0.19	6.31	11.29	2.73	0.18	98.98
51.5	50.52	50.68	1.64	14.92	11.39	0.14	6.37	11.27	2.72	0.18	99.14

66.5	50.98	50.70	1.83	14.56	11.54	0.16	6.48	11.21	2.65	0.18	99.59
81.5	50.63	50.97	1.79	14.07	11.57	0.20	6.62	11.21	2.70	0.17	98.96
96.5	50.96	50.95	1.83	13.94	11.83	0.18	6.58	11.18	2.66	0.17	99.31
111.5	50.66	51.21	1.82	13.65	11.68	0.25	6.74	11.11	2.68	0.16	98.75
126.5	50.54	50.86	1.86	13.64	12.00	0.22	6.67	11.16	2.71	0.17	98.98
141.5	50.56	50.74	1.95	13.52	12.16	0.23	6.86	10.99	2.67	0.19	99.12
156.5	50.47	51.24	1.77	13.51	11.87	0.24	6.74	11.13	2.64	0.17	98.53
129.5	50.57	51.06	1.83	13.57	11.91	0.25	6.72	11.08	2.67	0.20	98.82
144.0	50.53	51.08	1.83	13.48	12.12	0.15	6.72	11.08	2.67	0.16	98.75
158.4	50.91	51.13	1.77	13.56	11.98	0.16	6.80	11.08	2.66	0.18	99.07
172.9	50.54	50.92	1.93	13.42	12.12	0.24	6.81	11.00	2.68	0.19	98.91
187.3	50.61	50.97	1.96	13.53	11.98	0.23	6.77	11.05	2.63	0.18	98.94
201.8	50.59	50.69	1.90	13.55	12.21	0.19	6.97	10.95	2.67	0.18	99.20
216.2	50.27	50.88	1.86	13.51	12.29	0.20	6.73	11.00	2.67	0.18	98.69
230.7	50.86	50.92	1.91	13.59	12.21	0.18	6.68	10.99	2.64	0.19	99.25
245.1	50.64	50.64	1.82	13.53	12.37	0.20	6.81	11.13	2.61	0.19	99.30
245.1	50.84	50.71	1.92	13.55	12.35	0.20	6.70	11.07	2.62	0.18	99.43
274.3	51.07	50.64	1.89	13.71	12.07	0.22	6.97	10.86	2.76	0.19	99.73
303.4	50.71	50.99	1.84	13.57	12.09	0.18	6.83	10.96	2.67	0.17	99.02
332.6	50.62	50.92	1.86	13.55	12.12	0.21	6.77	11.00	2.71	0.17	99.00
361.7	50.43	51.16	1.91	13.42	12.03	0.20	6.81	10.91	2.70	0.17	98.57
390.9	50.64	51.27	1.72	13.46	12.11	0.17	6.75	10.94	2.69	0.20	98.67
420.0	50.71	51.06	1.83	13.54	12.19	0.22	6.74	10.85	2.70	0.18	98.95
449.2	50.69	51.05	1.78	13.41	12.14	0.22	6.88	10.94	2.71	0.17	98.93
478.3	50.96	50.94	1.80	13.58	12.08	0.23	6.94	10.84	2.69	0.18	99.32
507.5	50.98	51.12	1.75	13.56	12.07	0.24	6.82	10.85	2.71	0.18	99.16
536.6	50.45	50.97	1.86	13.61	12.16	0.21	6.77	10.85	2.69	0.19	98.78
565.8	50.64	51.05	1.85	13.56	12.17	0.15	6.74	10.91	2.69	0.17	98.90
594.9	50.63	50.68	1.82	13.66	12.34	0.23	6.78	10.92	2.72	0.17	99.25
624.0	50.81	51.30	1.90	13.49	11.97	0.26	6.72	10.80	2.68	0.19	98.81
6.3	48.90	49.75	1.51	17.31	10.44	0.14	5.93	11.30	2.75	0.18	98.45
12.0	49.41	49.81	1.43	17.07	10.53	0.21	5.90	11.37	2.81	0.17	98.90
17.8	49.19	50.01	1.51	16.68	10.67	0.20	5.91	11.40	2.75	0.17	98.48
23.5	49.43	50.09	1.56	16.41	10.86	0.14	6.11	11.26	2.71	0.17	98.65
23.5	49.55	50.05	1.53	16.51	10.87	0.19	6.04	11.30	2.66	0.17	98.81
38.8	49.98	50.43	1.53	15.59	11.14	0.18	6.18	11.32	2.73	0.18	98.85
54.0	50.46	50.93	1.68	14.87	11.33	0.19	6.25	11.20	2.68	0.16	98.83
69.3	50.42	50.86	1.77	14.37	11.54	0.22	6.47	11.20	2.69	0.17	98.86
84.5	50.63	50.79	1.80	14.14	11.86	0.17	6.51	11.15	2.69	0.18	99.13
99.8	50.59	50.98	1.78	13.88	11.85	0.18	6.62	11.17	2.65	0.18	98.91
115.0	50.95	51.17	1.75	13.74	11.84	0.23	6.63	11.14	2.62	0.18	99.08
130.3	50.73	50.65	1.96	13.71	12.03	0.21	6.82	11.09	2.67	0.17	99.38
145.5	50.68	51.25	1.89	13.49	11.86	0.22	6.64	11.11	2.67	0.17	98.73

160.8	50.66	51.06	1.88	13.63	11.90	0.22	6.72	11.04	2.66	0.18	98.90
176.0	50.77	50.93	1.93	13.47	12.02	0.19	6.86	11.06	2.68	0.17	99.14
191.3	50.81	51.04	1.84	13.55	12.10	0.18	6.73	11.01	2.68	0.17	99.07
206.5	51.03	50.61	1.85	13.59	12.27	0.26	6.73	11.13	2.69	0.16	99.72
182.9	50.58	50.96	1.83	13.60	12.08	0.19	6.77	10.99	2.71	0.17	98.92
197.5	50.59	50.96	1.89	13.47	12.14	0.28	6.75	10.97	2.66	0.18	98.93
212.2	50.28	51.25	1.83	13.42	12.01	0.18	6.81	10.97	2.65	0.18	98.33
226.8	50.43	51.05	1.77	13.55	12.04	0.21	6.81	10.98	2.70	0.19	98.67
241.4	50.41	50.90	1.77	13.59	12.17	0.25	6.86	10.94	2.66	0.17	98.81
256.1	50.42	50.97	1.75	13.49	12.22	0.20	6.79	10.98	2.71	0.18	98.75
270.7	50.56	50.85	1.83	13.61	12.17	0.24	6.72	11.03	2.67	0.18	99.01
285.4	50.25	50.98	1.92	13.61	12.11	0.17	6.73	10.91	2.68	0.19	98.57
300.0	50.51	51.19	1.83	13.42	12.13	0.19	6.84	10.84	2.67	0.18	98.62
314.6	50.24	50.98	1.87	13.58	12.17	0.19	6.74	10.89	2.68	0.19	98.56
329.3	50.26	51.17	1.77	13.46	12.06	0.20	6.80	10.97	2.68	0.19	98.40
343.9	50.46	50.86	1.87	13.50	12.21	0.18	6.84	10.94	2.71	0.19	98.91
343.9	50.39	50.78	1.83	13.53	12.31	0.28	6.84	10.91	2.64	0.18	98.91
373.6	50.62	50.87	1.92	13.56	12.15	0.18	6.80	10.94	2.71	0.18	99.06
403.3	50.34	51.08	1.76	13.40	12.31	0.20	6.85	10.88	2.65	0.17	98.56
433.0	50.55	50.69	1.94	13.63	12.14	0.25	6.92	10.84	2.70	0.19	99.16
462.7	50.27	51.17	1.79	13.48	12.10	0.19	6.80	10.86	2.72	0.18	98.40
492.4	50.37	51.03	1.84	13.42	12.15	0.25	6.82	10.89	2.72	0.19	98.65
522.1	50.68	50.85	1.84	13.64	12.15	0.22	6.81	10.89	2.73	0.18	99.13
551.8	50.29	51.44	1.76	13.31	12.16	0.15	6.82	10.82	2.67	0.18	98.15
581.5	50.09	50.99	1.90	13.49	12.15	0.18	6.86	10.79	2.74	0.19	98.40
611.2	50.21	51.01	1.81	13.56	12.12	0.17	6.87	10.87	2.71	0.18	98.49

Exp 227

x / μm	Oxides (wt%)										
	SiO ₂	SiO ₂ *	TiO ₂	Al ₂ O ₃	FeO	MnO	MgO	CaO	Na ₂ O	K ₂ O	Total
12.7	47.91	47.66	1.30	20.06	9.93	0.22	5.44	11.71	2.81	0.16	99.55
19.7	48.17	47.96	1.28	19.93	9.88	0.13	5.45	11.75	2.74	0.16	99.51
26.7	48.00	47.99	1.28	19.81	9.92	0.19	5.43	11.77	2.76	0.15	99.31
33.7	48.25	48.18	1.28	19.57	9.94	0.23	5.43	11.81	2.72	0.15	99.37
33.7	48.29	48.14	1.23	19.71	9.94	0.13	5.40	11.86	2.71	0.17	99.45
49.0	48.47	48.53	1.33	19.20	10.02	0.15	5.44	11.73	2.72	0.18	99.23
64.3	48.67	48.27	1.34	19.26	10.18	0.15	5.54	11.69	2.72	0.16	99.70
79.6	48.87	48.41	1.35	19.05	10.15	0.21	5.56	11.70	2.72	0.16	99.76
94.9	49.00	49.01	1.34	18.49	10.11	0.18	5.58	11.66	2.76	0.16	99.29
110.2	49.07	49.00	1.44	18.28	10.14	0.16	5.66	11.73	2.71	0.18	99.36
125.5	49.32	48.94	1.48	18.08	10.33	0.22	5.75	11.63	2.71	0.17	99.69
140.8	49.45	49.34	1.48	17.78	10.41	0.15	5.69	11.53	2.75	0.17	99.40
156.1	49.48	49.47	1.45	17.54	10.38	0.21	5.70	11.62	2.74	0.19	99.31
171.3	49.80	49.60	1.52	17.31	10.49	0.17	5.80	11.52	2.71	0.18	99.49
186.6	49.88	49.78	1.58	17.06	10.56	0.14	5.74	11.52	2.74	0.18	99.41
201.9	50.05	49.58	1.66	16.87	10.65	0.18	5.94	11.54	2.68	0.18	99.77
217.2	50.19	49.90	1.55	16.60	10.74	0.16	5.88	11.57	2.75	0.16	99.59
232.5	50.38	50.18	1.61	16.29	10.76	0.19	5.89	11.47	2.74	0.16	99.51
247.8	50.35	50.02	1.67	16.30	10.74	0.16	6.08	11.43	2.73	0.19	99.64
263.1	50.38	50.20	1.61	16.07	10.85	0.21	6.02	11.46	2.70	0.18	99.49
278.4	50.63	50.42	1.53	15.83	11.02	0.14	6.03	11.43	2.73	0.17	99.51
293.7	50.59	50.25	1.66	15.70	11.06	0.15	6.11	11.51	2.68	0.18	99.64
293.7	50.79	50.21	1.72	15.64	11.01	0.22	6.15	11.56	2.63	0.16	99.88
333.2	50.74	50.55	1.67	15.27	11.32	0.12	6.21	11.31	2.69	0.16	99.49
372.7	50.73	50.71	1.72	14.90	11.24	0.17	6.29	11.41	2.69	0.17	99.31
412.3	50.85	50.53	1.83	14.79	11.38	0.17	6.37	11.40	2.66	0.17	99.62
451.8	50.97	50.87	1.81	14.19	11.59	0.18	6.42	11.39	2.67	0.17	99.40
491.3	50.96	50.79	1.83	14.19	11.66	0.19	6.43	11.38	2.68	0.16	99.48
530.8	50.85	50.95	1.90	13.97	11.64	0.18	6.47	11.38	2.63	0.17	99.21
570.3	50.98	50.87	1.79	13.92	11.74	0.19	6.65	11.29	2.66	0.19	99.40
609.8	50.96	50.73	1.86	13.97	11.90	0.23	6.50	11.29	2.63	0.18	99.53
649.4	50.87	50.89	1.73	13.86	11.89	0.21	6.57	11.34	2.64	0.18	99.28
688.9	51.00	50.77	1.87	13.80	12.02	0.20	6.65	11.20	2.62	0.17	99.52
728.4	51.04	51.08	1.69	13.67	12.01	0.25	6.57	11.23	2.64	0.17	99.26
767.9	50.82	50.87	1.86	13.73	11.95	0.21	6.73	11.16	2.59	0.18	99.25
807.4	50.90	50.94	1.83	13.58	11.96	0.24	6.74	11.17	2.67	0.17	99.26
846.8	50.81	51.24	1.83	13.49	11.93	0.19	6.60	11.27	2.58	0.18	98.87

886.4	50.72	51.11	1.78	13.50	12.00	0.21	6.73	11.14	2.64	0.17	98.91
925.9	50.85	51.07	1.74	13.60	12.06	0.18	6.72	11.12	2.62	0.19	99.08
965.4	50.72	50.99	1.87	13.44	11.97	0.27	6.77	11.17	2.65	0.17	99.03
1004.9	50.76	50.87	1.82	13.51	12.09	0.24	6.81	11.14	2.65	0.17	99.20
1044.4	50.56	51.17	1.85	13.56	12.08	0.24	6.57	11.05	2.62	0.16	98.70
1083.9	50.56	50.83	1.86	13.59	12.10	0.18	6.83	11.08	2.64	0.18	99.03
1123.5	50.82	50.81	1.88	13.54	12.23	0.21	6.75	11.03	2.64	0.20	99.31
1163.0	50.78	50.97	1.75	13.54	12.15	0.21	6.81	11.07	2.63	0.17	99.11
1202.5	50.60	50.76	1.86	13.50	12.15	0.26	6.86	11.07	2.66	0.18	99.14
1242.0	50.52	51.02	1.67	13.49	12.24	0.21	6.80	11.07	2.63	0.18	98.80
1281.5	50.66	50.64	1.82	13.48	12.23	0.26	6.90	11.15	2.65	0.17	99.31
1321.0	50.65	50.68	1.89	13.59	12.21	0.21	6.84	11.04	2.66	0.18	99.27
1360.6	50.58	51.03	1.75	13.46	12.14	0.19	6.81	11.07	2.68	0.17	98.84
1400.1	50.66	50.56	1.86	13.59	12.31	0.27	6.80	11.05	2.68	0.19	99.41
1439.6	50.30	50.63	1.89	13.62	12.21	0.26	6.74	11.12	2.64	0.19	98.97
11.0	47.87	47.83	1.19	20.14	9.94	0.15	5.39	11.75	2.76	0.16	99.35
17.0	48.01	47.97	1.29	19.98	9.89	0.13	5.34	11.76	2.79	0.15	99.33
23.0	48.34	47.96	1.35	19.85	9.90	0.16	5.34	11.87	2.71	0.16	99.68
23.0	48.65	47.76	1.34	19.95	9.95	0.17	5.53	11.74	2.72	0.15	100.18
37.5	48.88	47.89	1.28	19.78	9.99	0.17	5.50	11.76	2.77	0.16	100.29
52.1	48.72	48.42	1.33	19.19	10.12	0.15	5.51	11.71	2.71	0.16	99.60
66.6	48.76	48.77	1.36	18.97	10.08	0.16	5.41	11.65	2.75	0.15	99.29
81.2	48.88	48.49	1.43	18.80	10.27	0.17	5.56	11.69	2.73	0.16	99.69
95.7	49.37	48.75	1.30	18.64	10.32	0.20	5.55	11.63	2.75	0.16	99.92
110.2	49.55	48.74	1.42	18.36	10.32	0.17	5.75	11.64	2.76	0.15	100.11
124.8	49.52	49.14	1.47	18.01	10.20	0.16	5.70	11.66	2.78	0.19	99.69
139.3	49.75	49.01	1.48	17.90	10.51	0.19	5.70	11.64	2.71	0.17	100.04
153.8	49.87	49.46	1.48	17.62	10.38	0.15	5.79	11.55	2.71	0.16	99.71
168.4	49.58	49.54	1.52	17.49	10.43	0.16	5.73	11.53	2.74	0.17	99.35
182.9	50.14	49.50	1.51	17.21	10.61	0.21	5.84	11.49	2.75	0.17	99.94
197.5	50.41	49.60	1.49	16.99	10.69	0.14	5.92	11.59	2.70	0.17	100.11
212.0	50.62	49.82	1.62	16.69	10.70	0.17	5.86	11.49	2.78	0.17	100.10
212.0	50.46	49.84	1.47	16.72	10.76	0.20	5.90	11.54	2.69	0.18	99.92
251.8	50.65	50.14	1.64	16.18	10.87	0.14	5.95	11.47	2.72	0.18	99.80
291.6	50.67	50.34	1.58	15.70	11.09	0.20	6.07	11.42	2.73	0.17	99.62
331.4	50.82	50.54	1.64	15.34	11.15	0.16	6.21	11.40	2.69	0.17	99.57
371.2	50.88	50.67	1.67	14.91	11.35	0.20	6.29	11.35	2.69	0.18	99.52
411.0	50.82	50.76	1.79	14.51	11.50	0.20	6.31	11.38	2.67	0.18	99.36
450.8	51.20	50.43	1.77	14.64	11.64	0.19	6.36	11.38	2.73	0.17	100.07
490.6	50.94	50.48	1.77	14.30	11.79	0.20	6.53	11.33	2.72	0.17	99.76
530.4	51.03	50.69	1.83	14.06	11.75	0.18	6.53	11.38	2.70	0.18	99.64

570.1	51.29	50.77	1.88	13.88	11.92	0.18	6.55	11.30	2.67	0.16	99.82
609.9	50.93	50.80	1.88	13.86	11.92	0.21	6.55	11.27	2.65	0.17	99.42
649.7	50.76	50.79	1.89	13.76	12.00	0.19	6.61	11.22	2.67	0.18	99.27
689.5	50.90	50.82	1.95	13.79	11.79	0.24	6.68	11.23	2.63	0.17	99.38
729.3	50.86	50.91	1.77	13.59	12.06	0.21	6.76	11.18	2.65	0.17	99.26
769.1	50.62	50.73	1.85	13.71	12.01	0.22	6.78	11.22	2.63	0.17	99.19
808.9	50.76	50.95	1.86	13.60	11.99	0.21	6.72	11.18	2.60	0.19	99.11
848.7	50.67	50.96	1.75	13.65	11.99	0.17	6.70	11.22	2.69	0.18	99.01
888.4	50.85	50.80	1.74	13.70	12.10	0.25	6.70	11.20	2.63	0.18	99.36
928.2	50.77	50.88	1.86	13.56	12.10	0.20	6.70	11.13	2.70	0.17	99.19
968.0	50.76	50.76	1.91	13.64	12.21	0.17	6.67	11.12	2.64	0.18	99.30
1007.8	50.54	50.76	1.90	13.53	12.14	0.25	6.77	11.17	2.63	0.17	99.08
1047.6	50.73	50.90	1.80	13.62	12.18	0.20	6.75	11.07	2.62	0.16	99.14
1087.4	50.60	50.91	1.75	13.63	12.20	0.22	6.69	11.06	2.65	0.19	98.99
1127.2	50.65	50.71	1.88	13.45	12.27	0.23	6.79	11.13	2.67	0.18	99.25
1167.0	50.60	50.61	1.95	13.58	12.25	0.24	6.80	11.06	2.63	0.18	99.29
1206.8	50.29	50.47	1.96	13.61	12.42	0.24	6.75	11.04	2.62	0.19	99.13
1246.5	50.47	50.70	1.91	13.54	12.22	0.17	6.82	11.04	2.67	0.21	99.06
1286.3	50.65	50.91	1.79	13.50	12.20	0.22	6.79	11.04	2.67	0.19	99.04
1326.1	50.34	50.79	1.89	13.59	12.17	0.23	6.77	11.05	2.64	0.18	98.85
1365.9	50.64	50.78	1.81	13.58	12.19	0.18	6.86	11.05	2.67	0.17	99.16
1405.7	50.74	51.10	1.69	13.53	12.23	0.22	6.78	11.00	2.58	0.18	98.94
1445.5	50.56	50.78	1.87	13.51	12.17	0.19	6.89	11.05	2.67	0.18	99.09
1485.3	50.83	50.55	1.98	13.51	12.38	0.14	6.88	11.07	2.62	0.19	99.58
1525.1	50.81	50.99	1.91	13.36	12.15	0.26	6.77	11.00	2.67	0.19	99.11
1564.9	50.36	51.10	1.80	13.65	12.01	0.19	6.68	11.02	2.67	0.18	98.55
15.0	48.53	47.77	1.24	20.21	9.93	0.18	5.35	11.70	2.76	0.16	100.06
20.2	48.62	47.96	1.29	19.96	9.90	0.18	5.36	11.73	2.75	0.17	99.96
25.4	48.63	48.02	1.16	19.89	9.86	0.16	5.49	11.80	2.76	0.16	99.90
25.4	48.32	48.03	1.20	19.82	9.93	0.19	5.45	11.79	2.74	0.15	99.59
40.6	48.64	48.25	1.34	19.56	9.89	0.15	5.50	11.72	2.75	0.16	99.69
55.8	48.99	48.12	1.49	19.23	10.08	0.20	5.55	11.68	2.79	0.17	100.17
71.0	49.24	48.31	1.41	18.97	10.16	0.24	5.64	11.67	2.74	0.16	100.24
86.2	49.10	48.88	1.33	18.59	10.13	0.19	5.56	11.71	2.73	0.17	99.52
101.5	49.02	48.77	1.41	18.53	10.21	0.17	5.65	11.62	2.76	0.18	99.55
116.7	49.34	49.41	1.34	18.03	10.28	0.15	5.61	11.59	2.74	0.16	99.22
131.9	49.68	49.30	1.44	17.87	10.25	0.15	5.72	11.66	2.73	0.17	99.68
147.1	49.55	49.30	1.44	17.78	10.40	0.15	5.74	11.55	2.76	0.18	99.55
162.3	49.70	49.60	1.41	17.45	10.49	0.17	5.64	11.60	2.77	0.17	99.40
177.5	49.62	49.50	1.56	17.02	10.73	0.16	5.86	11.54	2.75	0.18	99.42
192.7	50.17	49.66	1.50	16.97	10.70	0.14	5.89	11.51	2.77	0.17	99.81

207.9	50.35	49.87	1.62	16.79	10.69	0.19	5.81	11.46	2.72	0.16	99.79
223.1	49.79	49.83	1.60	16.56	10.85	0.18	5.92	11.44	2.76	0.17	99.26
238.3	50.30	50.06	1.53	16.29	10.85	0.16	6.03	11.44	2.74	0.19	99.54
253.6	50.67	50.21	1.68	16.01	10.90	0.18	6.01	11.45	2.69	0.17	99.76
268.8	50.65	50.00	1.68	15.96	11.00	0.23	6.10	11.42	2.75	0.17	99.95
284.0	50.62	50.20	1.62	15.78	11.06	0.24	6.10	11.40	2.75	0.16	99.72
299.2	50.68	50.18	1.65	15.63	11.22	0.21	6.11	11.41	2.71	0.18	99.80
314.4	50.44	50.64	1.65	15.36	11.05	0.16	6.14	11.40	2.71	0.18	99.10
314.4	50.61	50.21	1.70	15.48	11.19	0.21	6.23	11.42	2.68	0.17	99.71
353.7	50.68	50.76	1.57	15.06	11.19	0.23	6.30	11.29	2.73	0.17	99.21
392.9	50.76	50.66	1.76	14.84	11.28	0.22	6.32	11.34	2.70	0.17	99.40
432.2	50.69	50.69	1.70	14.51	11.69	0.16	6.40	11.32	2.66	0.18	99.30
471.4	50.87	50.61	1.83	14.30	11.71	0.20	6.48	11.33	2.68	0.17	99.56
510.7	50.53	50.60	1.87	14.16	11.69	0.23	6.63	11.29	2.63	0.19	99.23
549.9	50.80	50.67	1.73	14.08	11.82	0.22	6.60	11.34	2.67	0.17	99.43
589.2	50.78	50.92	1.84	13.89	11.84	0.21	6.54	11.24	2.64	0.17	99.16
628.4	50.86	50.82	1.88	13.77	11.95	0.22	6.61	11.25	2.63	0.18	99.34
667.7	50.71	50.87	1.94	13.77	11.89	0.16	6.72	11.15	2.64	0.17	99.13
706.9	50.73	50.86	1.90	13.68	12.10	0.18	6.55	11.22	2.64	0.17	99.17
746.2	50.61	50.74	1.77	13.75	12.06	0.23	6.71	11.30	2.58	0.16	99.17
785.4	50.96	50.88	1.89	13.58	12.08	0.28	6.69	11.14	2.60	0.17	99.37
824.7	50.67	50.60	1.86	13.78	12.15	0.19	6.69	11.21	2.64	0.18	99.37
863.9	50.83	50.61	1.84	13.62	12.27	0.23	6.72	11.18	2.64	0.18	99.52
903.2	50.69	50.95	1.79	13.63	12.12	0.19	6.66	11.15	2.65	0.17	99.04
942.4	50.76	50.69	1.91	13.59	12.10	0.22	6.74	11.18	2.68	0.19	99.37
981.7	50.50	50.71	1.83	13.62	12.20	0.16	6.79	11.15	2.67	0.19	99.09
1020.9	50.52	50.91	1.80	13.68	12.09	0.18	6.69	11.14	2.66	0.17	98.91
1060.2	50.63	50.73	1.77	13.71	12.16	0.23	6.71	11.12	2.68	0.18	99.20
1099.4	50.45	50.93	1.87	13.61	11.97	0.26	6.83	11.04	2.64	0.16	98.83
1138.7	50.55	51.06	1.73	13.49	12.33	0.22	6.63	10.99	2.68	0.18	98.79
1177.9	50.57	50.74	1.83	13.55	12.22	0.23	6.85	11.07	2.65	0.18	99.14
1217.2	50.71	50.98	1.95	13.48	12.16	0.18	6.67	11.08	2.65	0.16	99.03
1256.4	50.52	50.71	1.84	13.49	12.36	0.22	6.78	11.04	2.68	0.18	99.10
1295.7	50.74	50.92	1.77	13.64	12.06	0.17	6.79	11.07	2.70	0.19	99.12
1334.9	50.59	50.90	1.88	13.48	12.21	0.23	6.79	10.98	2.65	0.17	98.99
1374.2	50.74	50.79	1.85	13.50	12.24	0.20	6.82	11.04	2.69	0.17	99.25
1413.4	50.72	50.75	1.86	13.53	12.19	0.21	6.75	11.12	2.70	0.19	99.27
1452.7	50.90	50.86	1.80	13.61	12.14	0.19	6.80	11.02	2.69	0.18	99.34
1491.9	50.71	50.72	1.79	13.56	12.26	0.23	6.83	11.03	2.70	0.17	99.29
1531.1	50.75	50.77	1.89	13.50	12.18	0.26	6.77	11.05	2.69	0.19	99.27
1570.3	50.89	50.74	1.93	13.47	12.14	0.21	6.88	11.03	2.72	0.18	99.45

Exp 210

x / μm	Oxides (wt%)										
	SiO ₂	SiO ₂ *	TiO ₂	Al ₂ O ₃	FeO	MnO	MgO	CaO	Na ₂ O	K ₂ O	Total
14.2	45.76	45.76	0.88	23.96	8.47	0.22	4.58	12.61	2.69	0.13	99.30
19.7	45.62	46.36	0.93	23.53	8.48	0.14	4.53	12.63	2.57	0.13	98.56
25.2	46.05	46.31	0.92	23.38	8.61	0.13	4.57	12.63	2.62	0.13	99.04
25.2	46.27	46.31	0.88	23.50	8.65	0.12	4.53	12.64	2.54	0.14	99.26
41.0	46.59	46.69	0.97	22.81	8.69	0.17	4.65	12.60	2.58	0.14	99.20
56.8	46.93	47.51	1.08	21.94	8.82	0.13	4.71	12.42	2.55	0.14	98.72
72.6	47.49	47.76	1.13	21.31	9.01	0.17	4.84	12.34	2.59	0.15	99.03
88.4	47.78	48.01	1.24	20.69	9.20	0.18	4.94	12.26	2.63	0.16	99.06
104.2	48.34	48.21	1.22	20.06	9.56	0.16	5.08	12.18	2.68	0.15	99.43
120.0	48.75	48.67	1.27	19.49	9.55	0.19	5.12	12.18	2.67	0.16	99.38
135.8	49.01	49.08	1.34	18.95	9.62	0.16	5.23	12.10	2.66	0.17	99.23
151.6	49.43	49.67	1.36	18.23	9.79	0.18	5.29	11.94	2.67	0.17	99.06
167.3	49.67	49.75	1.52	17.66	9.95	0.20	5.46	11.92	2.68	0.16	99.21
183.1	50.16	50.11	1.45	17.08	10.22	0.17	5.56	11.90	2.66	0.16	99.35
178.2	49.52	50.09	1.45	17.46	10.00	0.11	5.57	11.84	2.64	0.16	98.73
208.6	50.37	50.29	1.56	16.62	10.37	0.15	5.63	11.88	2.64	0.16	99.38
239.0	50.41	50.64	1.65	15.93	10.58	0.21	5.72	11.79	2.60	0.17	99.06
269.4	50.83	51.03	1.64	15.34	10.73	0.21	5.89	11.70	2.61	0.16	99.10
299.7	51.06	50.95	1.72	14.98	11.01	0.18	6.12	11.61	2.57	0.17	99.41
330.2	50.85	50.94	1.82	14.57	11.18	0.22	6.27	11.58	2.57	0.16	99.21
360.6	50.86	51.20	1.80	14.12	11.42	0.17	6.25	11.59	2.56	0.18	98.97
391.0	50.92	50.98	1.86	14.05	11.65	0.23	6.41	11.42	2.55	0.16	99.24
421.4	50.91	51.02	1.77	14.01	11.63	0.23	6.50	11.48	2.50	0.16	99.19
451.8	50.81	51.06	1.81	13.90	11.69	0.19	6.51	11.45	2.53	0.16	99.05
482.1	50.87	50.82	1.96	13.77	11.85	0.25	6.50	11.40	2.58	0.17	99.35
512.5	50.80	51.10	1.81	13.70	11.85	0.20	6.51	11.43	2.52	0.18	99.00
542.9	50.92	51.02	1.87	13.72	11.80	0.20	6.59	11.39	2.56	0.16	99.20
573.4	50.74	50.96	1.77	13.63	11.97	0.25	6.70	11.27	2.58	0.17	99.08
603.8	50.61	51.13	1.82	13.56	11.92	0.21	6.67	11.30	2.51	0.16	98.78
634.2	50.56	51.14	1.78	13.40	12.14	0.20	6.62	11.32	2.53	0.18	98.73
664.5	50.76	51.12	1.78	13.50	12.04	0.19	6.71	11.29	2.49	0.17	98.94
694.9	50.91	50.87	1.92	13.52	12.12	0.23	6.72	11.22	2.53	0.17	99.34
694.9	50.84	51.09	1.79	13.70	11.99	0.23	6.60	11.31	2.42	0.16	99.05
746.1	50.70	51.13	1.73	13.57	12.10	0.23	6.64	11.17	2.55	0.18	98.87
797.2	50.72	51.25	1.73	13.56	12.03	0.17	6.67	11.14	2.57	0.18	98.78
848.3	50.80	51.09	1.76	13.57	12.06	0.20	6.71	11.15	2.60	0.16	99.01
899.5	50.74	50.91	1.79	13.60	12.14	0.17	6.85	11.07	2.60	0.17	99.13
950.6	50.58	50.98	1.73	13.66	12.13	0.21	6.78	11.00	2.62	0.18	98.90

1001.8	50.66	51.23	1.79	13.51	12.08	0.20	6.66	11.04	2.62	0.18	98.73
1052.9	50.88	50.84	1.92	13.65	12.08	0.21	6.79	11.00	2.62	0.18	99.34
1104.0	50.47	50.96	1.77	13.62	12.20	0.19	6.79	10.96	2.62	0.18	98.81
1155.2	50.49	50.92	1.92	13.48	12.15	0.23	6.74	11.02	2.66	0.19	98.87
1206.4	50.67	50.88	1.85	13.66	12.17	0.16	6.74	11.00	2.66	0.17	99.10
1257.4	50.54	51.29	1.87	13.48	11.97	0.22	6.68	10.92	2.68	0.18	98.55
1308.6	50.75	51.08	1.80	13.59	12.11	0.23	6.67	10.96	2.70	0.17	98.97
1359.8	50.67	51.22	1.68	13.51	12.11	0.21	6.83	10.92	2.63	0.19	98.75
1410.8	50.47	51.31	1.87	13.52	12.03	0.23	6.63	10.89	2.64	0.17	98.46
1462.0	50.69	51.03	1.84	13.57	12.04	0.25	6.85	10.87	2.66	0.18	98.96
1513.2	50.78	51.02	1.87	13.54	12.11	0.21	6.84	10.83	2.70	0.18	99.06
1564.3	50.89	50.98	1.85	13.50	12.14	0.22	6.78	10.95	2.71	0.19	99.21
1615.4	50.85	51.22	1.86	13.48	12.00	0.21	6.84	10.88	2.64	0.19	98.93
16.2	46.10	45.36	0.99	23.63	9.13	0.15	4.65	12.36	2.89	0.15	100.04
21.0	46.30	45.96	0.95	23.64	8.62	0.12	4.62	12.58	2.66	0.13	99.64
25.8	46.52	45.91	0.94	23.64	8.65	0.18	4.55	12.66	2.64	0.12	99.90
25.8	46.81	46.17	0.86	23.58	8.65	0.15	4.62	12.58	2.53	0.15	99.93
36.2	46.79	46.24	0.92	23.13	8.73	0.20	4.74	12.54	2.68	0.13	99.85
46.5	47.21	46.64	0.97	22.77	8.81	0.20	4.67	12.49	2.62	0.13	99.88
56.9	47.50	46.77	1.06	22.37	8.86	0.17	4.80	12.48	2.64	0.15	100.03
67.3	47.77	47.15	1.05	21.88	9.01	0.21	4.89	12.30	2.65	0.15	99.92
77.7	47.98	47.75	1.05	21.37	8.96	0.19	4.83	12.32	2.68	0.15	99.53
88.1	48.55	47.63	1.11	21.09	9.18	0.18	4.91	12.37	2.66	0.16	100.22
98.5	48.60	48.13	1.10	20.56	9.31	0.19	4.98	12.22	2.65	0.17	99.77
108.9	48.73	48.44	1.26	20.09	9.29	0.17	5.08	12.14	2.68	0.16	99.59
119.3	48.95	48.61	1.19	19.79	9.41	0.19	5.18	12.11	2.68	0.16	99.64
129.7	49.54	48.78	1.31	19.49	9.49	0.15	5.15	12.12	2.67	0.15	100.06
139.8	48.47	48.96	1.31	19.01	9.70	0.22	5.28	12.01	2.66	0.16	98.81
169.8	49.67	49.78	1.38	18.01	9.95	0.15	5.36	11.89	2.63	0.16	99.19
199.7	50.20	50.09	1.38	17.10	10.30	0.23	5.53	11.82	2.69	0.17	99.41
229.7	50.45	50.55	1.50	16.38	10.44	0.15	5.78	11.69	2.62	0.18	99.20
259.6	50.71	50.68	1.56	15.78	10.73	0.16	5.86	11.71	2.64	0.19	99.33
289.5	50.79	50.88	1.71	15.19	10.91	0.17	5.98	11.69	2.60	0.18	99.21
319.4	51.01	50.82	1.78	14.90	11.15	0.14	6.19	11.60	2.55	0.16	99.49
349.4	50.96	51.07	1.83	14.55	11.11	0.23	6.25	11.52	2.56	0.17	99.18
379.3	50.98	51.21	1.81	14.21	11.39	0.20	6.31	11.45	2.54	0.17	99.07
409.3	50.93	51.25	1.82	14.00	11.51	0.15	6.34	11.51	2.55	0.16	98.98
439.2	50.98	51.06	1.83	13.98	11.74	0.14	6.40	11.47	2.50	0.18	99.22
469.1	51.05	51.04	1.76	13.93	11.73	0.23	6.46	11.46	2.54	0.15	99.31
499.0	51.22	51.09	1.83	13.75	11.79	0.19	6.48	11.44	2.57	0.16	99.43
529.0	51.12	51.09	1.72	13.75	11.86	0.17	6.55	11.44	2.57	0.16	99.33

558.9	51.15	51.18	1.73	13.76	11.96	0.20	6.56	11.25	2.50	0.16	99.27
588.9	51.23	50.81	1.90	13.78	12.05	0.21	6.58	11.22	2.58	0.17	99.73
618.8	50.87	50.82	1.93	13.70	11.98	0.24	6.71	11.19	2.56	0.17	99.35
648.7	50.90	51.01	1.84	13.71	11.93	0.18	6.66	11.23	2.57	0.17	99.19
678.6	50.96	51.13	1.79	13.68	11.97	0.18	6.64	11.21	2.55	0.16	99.13
708.6	51.00	51.10	1.87	13.65	11.93	0.20	6.72	11.15	2.52	0.16	99.20
738.5	50.80	51.01	1.76	13.69	12.00	0.22	6.76	11.16	2.55	0.17	99.09
738.5	50.90	50.97	1.83	13.70	12.06	0.18	6.70	11.17	2.50	0.17	99.23
789.6	50.98	50.85	1.81	13.66	12.07	0.22	6.84	11.10	2.56	0.19	99.43
840.6	50.73	51.03	1.84	13.53	12.13	0.21	6.73	11.08	2.58	0.16	99.00
891.8	50.80	50.97	1.84	13.70	11.91	0.23	6.81	11.07	2.60	0.18	99.13
942.9	50.80	50.97	1.82	13.67	12.04	0.20	6.83	10.98	2.60	0.18	99.13
994.0	50.63	50.87	1.89	13.69	12.05	0.26	6.76	10.99	2.63	0.17	99.07
1045.0	50.43	51.11	1.82	13.73	12.03	0.18	6.66	10.99	2.60	0.18	98.62
1096.1	50.56	50.98	1.80	13.63	12.20	0.22	6.70	10.93	2.66	0.18	98.87
1147.2	50.73	51.00	1.86	13.68	12.07	0.26	6.67	10.92	2.65	0.19	99.03
1198.4	50.52	51.07	1.77	13.71	11.98	0.19	6.79	10.94	2.67	0.18	98.75
1249.4	50.70	50.98	2.00	13.56	12.05	0.25	6.69	10.91	2.68	0.18	99.02
1300.5	50.63	51.05	1.85	13.58	12.09	0.26	6.73	10.92	2.64	0.18	98.88
1351.6	50.55	51.18	1.76	13.50	12.06	0.16	6.83	10.97	2.63	0.21	98.66
1402.6	50.39	51.04	1.86	13.67	11.99	0.15	6.80	10.94	2.66	0.18	98.66
1453.7	50.55	50.95	1.94	13.68	12.08	0.22	6.69	10.88	2.67	0.18	98.90
1504.9	50.86	50.92	1.84	13.73	12.09	0.22	6.71	10.92	2.68	0.19	99.24
1556.0	50.59	50.88	1.89	13.70	11.99	0.18	6.83	10.96	2.70	0.18	99.02
1607.0	50.52	50.98	1.84	13.60	12.14	0.25	6.74	10.90	2.66	0.19	98.85
7.0	45.51	45.54	0.91	23.85	8.78	0.16	4.71	12.17	3.01	0.17	99.27
11.8	45.89	45.74	0.79	24.17	8.48	0.16	4.54	12.49	2.79	0.14	99.45
16.5	45.97	46.32	0.86	23.72	8.41	0.11	4.53	12.53	2.69	0.13	98.95
21.3	46.15	46.10	0.84	23.67	8.57	0.08	4.57	12.65	2.66	0.15	99.35
26.1	46.06	46.27	0.93	23.36	8.64	0.13	4.63	12.58	2.62	0.15	99.09
26.1	46.34	46.28	0.92	23.44	8.61	0.17	4.64	12.53	2.58	0.13	99.35
35.7	46.56	46.45	0.96	23.12	8.62	0.18	4.69	12.50	2.62	0.16	99.41
45.4	46.63	46.62	0.99	22.78	8.84	0.17	4.64	12.48	2.64	0.14	99.31
55.0	46.85	46.85	1.02	22.39	8.93	0.15	4.73	12.45	2.62	0.17	99.30
64.6	47.24	47.08	1.08	22.06	8.96	0.18	4.82	12.35	2.61	0.15	99.46
74.2	47.46	47.48	1.04	21.65	8.98	0.19	4.86	12.31	2.63	0.16	99.28
83.9	47.69	47.69	1.16	21.24	9.09	0.16	4.93	12.24	2.65	0.15	99.31
93.5	47.98	48.47	1.14	20.61	9.10	0.17	4.83	12.15	2.67	0.16	98.81
103.1	48.41	48.29	1.21	20.47	9.12	0.18	5.01	12.16	2.71	0.15	99.41
98.0	48.55	48.03	1.22	20.57	9.30	0.20	5.00	12.15	2.66	0.16	99.82
128.4	49.28	48.70	1.28	19.44	9.64	0.18	5.16	12.05	2.67	0.17	99.88

158.8	49.70	49.92	1.27	18.15	9.76	0.20	5.26	11.91	2.66	0.16	99.08
189.1	50.18	49.99	1.33	17.39	10.24	0.18	5.51	11.85	2.67	0.14	99.50
219.5	50.37	50.52	1.55	16.55	10.24	0.16	5.73	11.71	2.67	0.17	99.15
250.0	50.55	50.30	1.78	16.03	10.57	0.21	5.88	11.73	2.62	0.18	99.55
280.4	50.75	50.68	1.65	15.45	10.90	0.20	6.01	11.61	2.62	0.18	99.36
310.8	50.98	51.00	1.70	14.95	11.02	0.11	6.18	11.58	2.59	0.17	99.28
341.2	51.14	50.81	1.74	14.59	11.28	0.21	6.28	11.66	2.55	0.18	99.64
371.5	51.12	50.85	1.88	14.36	11.48	0.16	6.29	11.55	2.58	0.15	99.57
401.9	51.15	50.92	1.71	14.25	11.58	0.21	6.36	11.52	2.59	0.15	99.53
432.3	51.15	50.86	1.84	14.15	11.71	0.21	6.43	11.43	2.52	0.15	99.59
462.7	51.27	50.94	1.86	13.92	11.73	0.20	6.52	11.40	2.57	0.16	99.63
493.2	51.12	50.87	1.80	13.94	11.74	0.20	6.63	11.44	2.51	0.17	99.55
523.6	50.96	50.96	1.80	13.71	11.96	0.22	6.59	11.36	2.56	0.15	99.31
553.9	50.85	50.83	1.78	13.88	11.91	0.21	6.72	11.26	2.54	0.16	99.32
584.3	51.04	50.91	1.81	13.77	12.00	0.19	6.59	11.33	2.54	0.16	99.43
614.7	51.04	50.99	1.87	13.56	12.02	0.21	6.66	11.26	2.55	0.17	99.34
614.7	50.67	51.12	1.78	13.64	12.00	0.18	6.62	11.29	2.51	0.16	98.85
665.3	50.76	51.22	1.88	13.56	11.87	0.20	6.57	11.25	2.57	0.18	98.84
716.0	50.73	50.99	1.83	13.61	12.06	0.25	6.73	11.14	2.51	0.17	99.04
766.5	50.90	50.94	1.93	13.54	12.05	0.21	6.74	11.12	2.60	0.18	99.26
817.1	50.69	51.13	1.83	13.61	12.02	0.25	6.70	10.98	2.58	0.19	98.86
867.8	50.55	51.04	1.74	13.68	12.03	0.27	6.72	11.12	2.54	0.17	98.81
918.4	50.73	51.00	1.78	13.63	12.03	0.22	6.79	11.09	2.58	0.19	99.03
968.9	50.51	51.29	1.78	13.65	11.98	0.17	6.70	10.93	2.62	0.19	98.51
1019.6	50.56	50.89	1.84	13.61	12.06	0.25	6.84	11.01	2.63	0.18	98.96
1070.2	50.52	51.26	1.80	13.59	11.95	0.18	6.71	11.01	2.61	0.19	98.56
1120.7	50.73	50.93	1.82	13.67	12.10	0.16	6.78	10.99	2.67	0.19	99.10
1171.3	50.62	51.03	1.77	13.71	12.04	0.22	6.73	10.94	2.67	0.18	98.88
1222.0	50.65	51.22	1.83	13.66	12.00	0.20	6.66	10.89	2.65	0.17	98.73
1272.6	50.65	50.71	1.78	13.71	12.22	0.20	6.77	11.04	2.68	0.19	99.24
1323.1	50.76	51.02	1.78	13.67	12.10	0.19	6.77	10.94	2.67	0.17	99.04
1373.8	50.45	51.05	1.80	13.63	12.10	0.22	6.73	10.93	2.66	0.18	98.69
1424.4	50.65	51.18	1.80	13.52	12.07	0.21	6.79	10.88	2.66	0.18	98.77
1475.0	50.72	51.17	1.89	13.55	11.97	0.21	6.76	10.85	2.72	0.18	98.86
1525.6	50.76	50.97	1.87	13.59	12.15	0.23	6.82	10.80	2.68	0.18	99.10
1576.2	50.75	50.98	1.82	13.60	12.25	0.22	6.78	10.83	2.65	0.18	99.07

Exp 211

x / μm	Oxides (wt%)										
	SiO ₂	SiO ₂ *	TiO ₂	Al ₂ O ₃	FeO	MnO	MgO	CaO	Na ₂ O	K ₂ O	Total
5.6	46.95	46.65	0.98	22.23	9.41	0.15	5.05	11.75	2.91	0.18	99.60
10.8	47.32	46.75	1.12	22.19	9.11	0.16	4.87	12.17	2.78	0.15	99.87
16.1	47.33	46.93	1.21	22.05	9.18	0.14	4.86	12.03	2.74	0.16	99.70
21.3	47.37	47.24	1.13	21.63	9.27	0.22	4.93	12.06	2.68	0.15	99.43
21.3	47.47	46.72	1.15	21.87	9.40	0.13	5.08	12.14	2.66	0.15	100.05
31.8	47.76	47.63	1.15	20.96	9.33	0.19	5.16	12.08	2.66	0.15	99.44
42.2	47.97	47.85	1.29	20.46	9.54	0.19	5.20	11.92	2.68	0.17	99.42
52.7	48.44	48.51	1.25	19.81	9.54	0.16	5.27	11.86	2.73	0.16	99.23
63.1	48.69	48.53	1.34	19.28	9.88	0.19	5.32	11.88	2.72	0.17	99.46
73.6	49.12	49.21	1.34	18.60	9.98	0.16	5.36	11.78	2.70	0.17	99.21
84.1	49.24	49.19	1.53	18.13	10.17	0.21	5.53	11.68	2.70	0.17	99.35
94.4	49.80	49.70	1.45	17.69	10.21	0.11	5.61	11.68	2.69	0.17	99.40
104.9	50.16	49.80	1.60	17.06	10.51	0.15	5.66	11.64	2.73	0.15	99.66
115.4	50.33	50.04	1.62	16.53	10.63	0.19	5.83	11.58	2.71	0.18	99.59
125.8	50.54	50.33	1.71	16.27	10.63	0.18	5.88	11.48	2.65	0.17	99.51
136.3	50.67	50.59	1.61	15.60	10.98	0.19	5.95	11.52	2.68	0.17	99.38
146.7	50.88	50.68	1.63	15.38	11.15	0.16	6.09	11.38	2.66	0.17	99.50
157.2	50.94	50.77	1.78	15.01	11.12	0.18	6.18	11.45	2.64	0.17	99.47
157.2	50.93	50.66	1.75	15.02	11.19	0.19	6.28	11.50	2.53	0.17	99.57
186.3	51.16	51.00	1.73	14.40	11.54	0.17	6.27	11.42	2.60	0.18	99.46
215.5	51.17	51.17	1.71	13.89	11.83	0.19	6.45	11.31	2.59	0.16	99.30
244.6	50.81	50.76	1.85	13.75	11.95	0.18	6.64	11.42	2.58	0.16	99.34
273.7	50.88	50.91	1.77	13.63	12.09	0.24	6.65	11.25	2.57	0.18	99.26
302.8	50.97	50.84	1.77	13.73	12.10	0.16	6.73	11.24	2.57	0.16	99.43
332.0	50.91	50.72	1.91	13.70	12.14	0.22	6.67	11.17	2.58	0.18	99.48
361.1	50.85	51.01	1.75	13.60	12.19	0.21	6.67	11.06	2.63	0.18	99.14
390.1	51.17	50.88	1.87	13.66	12.16	0.21	6.81	10.99	2.57	0.17	99.59
419.2	50.91	50.83	1.82	13.75	12.10	0.29	6.63	11.06	2.63	0.18	99.38
448.4	50.93	51.00	1.81	13.65	12.17	0.20	6.60	11.08	2.60	0.19	99.23
477.5	50.93	50.87	1.88	13.55	12.18	0.17	6.76	11.07	2.64	0.19	99.37
506.6	50.85	50.76	1.79	13.61	12.31	0.26	6.75	10.97	2.65	0.19	99.39
535.7	50.92	50.93	1.90	13.59	12.17	0.25	6.69	10.98	2.62	0.18	99.29
564.9	51.20	50.72	1.87	13.68	12.30	0.19	6.79	10.93	2.62	0.20	99.79
594.0	51.11	50.93	1.85	13.60	12.21	0.24	6.70	10.98	2.62	0.18	99.49
623.1	51.17	50.72	1.87	13.66	12.24	0.26	6.76	10.93	2.65	0.19	99.75
623.1	50.73	50.71	1.74	13.80	12.21	0.19	6.85	11.03	2.58	0.18	99.32
685.8	50.96	50.81	1.80	13.63	12.32	0.25	6.82	10.85	2.64	0.18	99.45
748.6	50.87	50.85	1.82	13.58	12.25	0.22	6.81	10.90	2.69	0.19	99.32

811.4	50.72	50.84	1.78	13.73	12.16	0.22	6.77	10.92	2.70	0.17	99.18
874.2	51.01	50.78	1.76	13.63	12.21	0.23	6.96	10.86	2.68	0.19	99.52
937.0	50.82	50.71	1.82	13.72	12.29	0.17	6.82	10.92	2.67	0.18	99.41
999.7	50.89	50.71	1.80	13.61	12.28	0.24	6.87	10.87	2.75	0.18	99.48
1062.5	50.93	50.90	1.80	13.66	12.22	0.19	6.76	10.88	2.71	0.18	99.33
1125.3	50.84	50.95	1.69	13.72	12.17	0.21	6.78	10.82	2.78	0.19	99.19
1188.1	50.87	50.76	1.91	13.71	12.19	0.20	6.75	10.83	2.75	0.21	99.42
1250.8	51.04	51.05	1.73	13.69	12.17	0.20	6.71	10.83	2.73	0.19	99.28
1313.6	50.94	50.94	1.90	13.62	12.12	0.23	6.79	10.79	2.73	0.19	99.30
1376.4	51.14	50.93	1.74	13.75	12.09	0.17	6.78	10.91	2.74	0.18	99.51
1439.2	51.16	51.02	1.84	13.68	12.08	0.16	6.73	10.88	2.72	0.17	99.43
1502.0	51.18	51.02	1.89	13.67	11.93	0.20	6.75	10.91	2.73	0.20	99.47
1564.7	51.50	51.04	1.77	13.70	12.03	0.23	6.64	10.91	2.79	0.18	99.76
6.9	46.75	46.55	0.99	22.35	9.40	0.17	4.95	11.85	2.86	0.17	99.50
12.4	47.07	46.90	1.03	22.07	9.25	0.16	4.96	12.06	2.72	0.15	99.48
17.9	47.13	47.10	1.18	21.76	9.15	0.12	4.98	12.13	2.71	0.16	99.33
23.4	47.70	47.21	1.10	21.51	9.32	0.15	5.02	12.10	2.75	0.14	99.79
23.4	47.62	47.46	1.08	21.48	9.23	0.14	5.02	12.14	2.61	0.14	99.46
33.6	48.07	47.60	1.22	21.03	9.40	0.15	4.98	12.05	2.73	0.16	99.77
43.7	48.37	47.97	1.15	20.30	9.57	0.18	5.14	12.07	2.75	0.17	99.71
53.9	48.86	48.44	1.28	19.67	9.63	0.13	5.24	12.03	2.72	0.14	99.72
63.9	49.08	48.67	1.36	19.26	9.83	0.17	5.33	11.85	2.67	0.17	99.71
74.1	49.53	48.92	1.39	18.71	9.95	0.21	5.43	11.82	2.73	0.15	99.91
84.2	49.78	49.28	1.48	17.99	10.11	0.19	5.59	11.81	2.68	0.17	99.79
94.4	50.25	49.56	1.54	17.56	10.35	0.15	5.66	11.65	2.67	0.17	99.99
104.5	50.35	49.77	1.47	17.11	10.53	0.16	5.80	11.60	2.69	0.17	99.88
114.7	50.72	50.16	1.54	16.50	10.62	0.15	5.82	11.64	2.71	0.16	99.86
124.8	50.82	50.27	1.56	16.25	10.66	0.21	5.86	11.63	2.69	0.17	99.84
135.0	51.23	50.48	1.59	15.76	10.89	0.18	6.03	11.53	2.68	0.17	100.06
145.1	51.06	50.64	1.70	15.42	11.12	0.17	5.98	11.45	2.64	0.17	99.72
155.3	51.37	50.76	1.71	15.23	11.14	0.17	6.10	11.40	2.63	0.17	99.91
155.3	51.46	50.66	1.78	15.15	11.16	0.20	6.14	11.49	2.55	0.17	100.09
185.1	51.39	50.72	1.83	14.47	11.48	0.22	6.35	11.41	2.62	0.19	99.97
214.9	51.56	50.77	1.91	14.11	11.65	0.19	6.57	11.32	2.60	0.18	100.09
244.7	51.41	50.63	1.93	13.93	11.88	0.31	6.48	11.39	2.58	0.17	100.08
274.5	51.33	50.95	1.84	13.64	11.91	0.20	6.71	11.31	2.57	0.17	99.68
304.3	51.41	50.74	1.90	13.67	12.09	0.23	6.69	11.18	2.63	0.19	99.97
334.1	51.13	50.82	1.85	13.60	12.20	0.15	6.72	11.17	2.62	0.17	99.61
363.8	51.37	50.88	1.87	13.65	12.10	0.24	6.67	11.13	2.60	0.17	99.78
393.6	51.17	51.16	1.87	13.56	12.04	0.18	6.64	11.06	2.60	0.18	99.31
423.4	51.31	50.33	1.87	13.86	12.29	0.20	6.77	11.13	2.67	0.18	100.28

453.2	51.14	50.51	1.89	13.71	12.27	0.25	6.70	11.16	2.64	0.17	99.94
483.0	51.41	50.86	1.79	13.70	12.19	0.18	6.72	11.04	2.64	0.17	99.86
512.8	51.54	50.73	1.82	13.65	12.34	0.21	6.78	10.95	2.63	0.18	100.11
542.6	51.50	50.77	1.84	13.65	12.16	0.17	6.91	11.02	2.62	0.16	100.03
572.4	51.62	50.78	1.80	13.67	12.23	0.21	6.79	10.99	2.64	0.18	100.15
602.2	51.18	50.95	1.82	13.66	12.17	0.18	6.71	10.97	2.66	0.19	99.53
602.2	51.47	50.67	1.90	13.76	12.28	0.21	6.73	11.06	2.52	0.17	100.10
664.0	51.24	50.87	1.90	13.76	12.09	0.16	6.76	10.91	2.67	0.19	99.67
725.9	51.26	50.89	1.79	13.67	12.21	0.20	6.82	10.90	2.66	0.17	99.67
787.7	51.25	50.90	1.83	13.67	12.17	0.18	6.79	10.92	2.65	0.19	99.64
849.6	51.15	51.04	1.68	13.65	12.21	0.24	6.64	10.94	2.72	0.18	99.41
911.4	50.87	51.05	1.74	13.56	12.31	0.22	6.70	10.80	2.72	0.19	99.12
973.3	51.18	50.98	1.79	13.65	12.28	0.20	6.69	10.86	2.68	0.18	99.50
1035.1	51.19	50.92	1.80	13.76	12.15	0.23	6.65	10.86	2.73	0.20	99.57
1097.0	50.87	51.13	1.77	13.68	12.23	0.20	6.69	10.76	2.67	0.17	99.04
1158.9	51.04	50.78	1.78	13.76	12.19	0.24	6.81	10.85	2.72	0.16	99.55
1220.7	50.80	51.06	1.72	13.61	12.18	0.21	6.77	10.85	2.72	0.18	99.05
1282.5	50.99	50.97	1.79	13.65	12.10	0.21	6.85	10.82	2.73	0.18	99.31
1344.4	50.51	50.93	1.82	13.66	12.16	0.21	6.72	10.92	2.70	0.19	98.87
1406.3	50.92	50.79	1.78	13.70	12.15	0.24	6.84	10.89	2.75	0.17	99.43
1468.2	51.01	51.02	1.84	13.72	11.99	0.20	6.75	10.87	2.71	0.19	99.28
1529.9	50.78	50.74	1.88	13.69	12.19	0.25	6.70	10.88	2.79	0.19	99.35
1591.8	50.92	51.15	1.75	13.65	11.95	0.18	6.80	10.89	2.74	0.20	99.07
9.9	46.62	46.85	1.00	22.22	9.12	0.20	4.90	11.98	2.86	0.17	99.07
15.1	46.76	46.90	1.05	22.08	9.08	0.17	4.91	12.18	2.77	0.16	99.15
20.4	46.97	47.31	1.09	21.63	9.15	0.12	4.97	12.15	2.71	0.16	98.96
25.6	46.98	47.12	1.09	21.48	9.34	0.19	5.01	12.23	2.68	0.15	99.16
25.6	47.42	47.04	1.11	21.56	9.24	0.17	5.08	12.26	2.68	0.15	99.68
36.1	47.76	47.91	1.06	20.84	9.32	0.19	5.06	12.09	2.69	0.15	99.15
46.5	48.14	47.88	1.23	20.34	9.60	0.16	5.17	11.98	2.77	0.17	99.56
57.0	48.59	48.46	1.23	19.66	9.66	0.14	5.29	11.97	2.70	0.17	99.43
67.5	48.96	48.78	1.34	19.13	9.84	0.18	5.30	11.84	2.72	0.17	99.48
77.9	49.24	49.28	1.41	18.46	9.90	0.12	5.39	11.83	2.74	0.17	99.26
88.4	49.45	49.51	1.43	17.95	10.15	0.18	5.52	11.67	2.72	0.17	99.24
98.9	49.67	49.78	1.39	17.48	10.30	0.19	5.61	11.68	2.70	0.17	99.19
109.3	50.04	49.93	1.43	17.03	10.40	0.19	5.77	11.66	2.73	0.16	99.41
119.8	50.06	50.19	1.61	16.52	10.60	0.16	5.73	11.61	2.69	0.19	99.18
130.3	50.15	49.89	1.74	16.09	10.84	0.20	6.00	11.65	2.71	0.17	99.56
140.6	50.45	50.37	1.71	15.71	10.91	0.22	5.99	11.54	2.68	0.17	99.37
151.1	50.45	50.35	1.71	15.43	11.10	0.18	6.13	11.54	2.70	0.16	99.41
161.6	50.37	50.58	1.74	15.21	11.23	0.19	6.09	11.48	2.61	0.18	99.09

172.0	50.66	50.93	1.70	14.87	11.15	0.18	6.17	11.49	2.65	0.17	99.04
182.5	50.54	50.90	1.79	14.75	11.35	0.19	6.15	11.40	2.61	0.17	98.94
182.5	51.24	50.84	1.75	14.69	11.38	0.18	6.28	11.46	2.56	0.16	99.70
211.8	51.15	51.00	1.84	14.18	11.51	0.12	6.40	11.46	2.62	0.16	99.44
241.1	50.97	51.02	1.66	14.01	11.73	0.22	6.46	11.41	2.61	0.17	99.25
270.4	50.92	50.44	1.84	13.97	12.08	0.24	6.64	11.34	2.58	0.17	99.78
299.6	50.84	51.03	1.74	13.58	12.11	0.20	6.63	11.27	2.58	0.16	99.11
328.9	50.98	51.05	1.72	13.66	12.04	0.20	6.63	11.20	2.62	0.18	99.24
358.2	50.99	50.40	1.86	13.72	12.38	0.20	6.77	11.24	2.56	0.18	99.89
387.5	50.83	50.87	1.81	13.68	12.08	0.26	6.64	11.15	2.63	0.17	99.27
416.8	51.19	50.62	1.80	13.65	12.37	0.22	6.71	11.13	2.62	0.17	99.87
446.0	51.04	50.74	1.73	13.76	12.25	0.20	6.78	11.10	2.57	0.17	99.59
475.3	51.08	50.60	1.86	13.77	12.21	0.27	6.64	11.16	2.61	0.18	99.78
504.5	51.27	50.75	1.77	13.78	12.20	0.23	6.69	11.07	2.63	0.19	99.82
533.8	51.16	50.76	1.82	13.67	12.27	0.23	6.70	11.06	2.63	0.17	99.71
563.1	51.37	51.07	1.78	13.57	12.14	0.23	6.70	10.99	2.63	0.18	99.60
592.4	51.30	51.01	1.79	13.59	12.20	0.23	6.71	10.93	2.66	0.19	99.59
592.4	51.18	50.95	1.86	13.65	12.11	0.23	6.76	10.96	2.60	0.18	99.53
654.2	51.21	51.00	1.74	13.71	12.12	0.24	6.77	10.87	2.66	0.18	99.51
715.8	51.26	50.78	1.76	13.74	12.17	0.23	6.81	10.98	2.66	0.19	99.79
777.6	51.02	50.81	1.75	13.68	12.24	0.24	6.86	10.84	2.70	0.18	99.52
839.3	51.25	50.97	1.76	13.57	12.06	0.26	6.85	10.94	2.72	0.18	99.58
901.1	51.13	50.92	1.77	13.66	12.21	0.23	6.70	10.92	2.71	0.18	99.51
962.8	51.12	50.71	1.87	13.71	12.20	0.17	6.83	10.92	2.71	0.17	99.71
1024.5	51.01	50.47	1.81	13.78	12.38	0.21	6.82	10.92	2.73	0.17	99.84
1086.2	51.12	50.83	1.83	13.73	12.28	0.17	6.75	10.83	2.69	0.19	99.59
1148.0	50.87	50.97	1.79	13.65	12.13	0.16	6.84	10.88	2.69	0.18	99.20
1209.7	51.00	50.99	1.71	13.67	12.16	0.23	6.79	10.88	2.71	0.17	99.31
1271.4	50.90	50.93	1.85	13.63	12.18	0.24	6.76	10.82	2.72	0.17	99.28
1333.1	50.87	51.00	1.82	13.60	12.20	0.22	6.75	10.77	2.76	0.18	99.17
1394.9	50.92	50.72	1.83	13.80	12.14	0.21	6.79	10.87	2.74	0.20	99.50
1456.6	51.09	50.84	1.82	13.59	12.09	0.24	6.88	10.92	2.74	0.18	99.55
1518.4	51.10	50.81	1.83	13.71	12.09	0.21	6.88	10.86	2.74	0.17	99.59
1580.0	51.11	50.71	1.80	13.70	12.20	0.23	6.78	10.93	2.76	0.18	99.70

Exp 212

x / μm	Oxides (wt%)										
	SiO ₂	SiO ₂ *	TiO ₂	Al ₂ O ₃	FeO	MnO	MgO	CaO	Na ₂ O	K ₂ O	Total
7.5	46.59	47.15	0.92	22.45	8.83	0.19	4.78	12.03	2.79	0.16	98.75
13.0	47.46	47.23	1.10	21.98	8.84	0.16	4.79	12.34	2.69	0.16	99.53
18.5	47.17	47.40	1.02	21.85	8.91	0.16	4.87	12.31	2.64	0.14	99.08
24.0	47.95	47.69	1.13	21.19	9.19	0.17	4.95	12.15	2.68	0.15	99.55
24.0	47.86	47.84	1.13	21.24	9.10	0.20	4.82	12.15	2.64	0.17	99.32
34.8	48.30	48.49	1.12	20.28	9.28	0.12	4.97	12.20	2.67	0.16	99.11
45.4	48.93	48.81	1.32	19.49	9.57	0.18	5.14	11.93	2.70	0.17	99.42
56.2	49.26	49.33	1.43	18.68	9.75	0.16	5.13	11.98	2.69	0.16	99.24
81.4	50.18	50.36	1.46	16.95	10.28	0.14	5.48	11.77	2.69	0.16	99.12
102.4	50.11	50.65	1.68	15.81	10.71	0.20	5.75	11.67	2.66	0.17	98.77
123.4	50.73	50.84	1.74	15.14	11.05	0.24	5.97	11.51	2.64	0.17	99.19
144.3	50.56	51.13	1.73	14.53	11.26	0.18	6.12	11.56	2.63	0.17	98.73
165.3	50.58	51.16	1.94	14.06	11.47	0.17	6.25	11.49	2.57	0.18	98.72
186.3	50.64	50.90	1.70	13.92	11.86	0.20	6.46	11.45	2.61	0.18	99.04
207.3	50.31	51.30	1.91	13.68	11.69	0.18	6.53	11.31	2.53	0.17	98.31
228.3	50.53	51.12	1.88	13.53	11.89	0.19	6.58	11.36	2.58	0.17	98.71
249.3	50.20	51.30	1.78	13.54	11.93	0.17	6.49	11.34	2.58	0.18	98.20
270.3	49.97	51.13	1.86	13.50	12.01	0.22	6.58	11.30	2.55	0.17	98.14
291.3	50.28	51.03	1.95	13.55	12.08	0.19	6.48	11.25	2.57	0.19	98.55
293.8	50.95	51.05	1.95	13.46	12.08	0.22	6.69	11.12	2.56	0.18	99.20
335.1	50.63	51.12	1.79	13.52	12.05	0.24	6.64	11.16	2.60	0.18	98.81
376.3	50.87	51.44	1.73	13.40	12.13	0.17	6.70	10.98	2.58	0.17	98.73
417.6	50.60	50.98	1.87	13.40	12.35	0.23	6.63	11.04	2.59	0.20	98.92
458.8	50.85	51.08	1.87	13.39	12.29	0.16	6.67	11.04	2.61	0.19	99.07
500.0	50.78	51.18	1.85	13.37	12.23	0.26	6.64	10.93	2.66	0.18	98.90
541.3	50.83	51.29	1.80	13.28	12.20	0.20	6.71	10.94	2.70	0.18	98.84
582.5	50.69	51.25	1.79	13.32	12.26	0.20	6.68	10.94	2.67	0.19	98.74
623.8	50.82	51.13	1.89	13.34	12.26	0.17	6.77	10.91	2.65	0.17	98.99
665.1	50.77	50.96	1.81	13.44	12.23	0.26	6.81	10.90	2.70	0.19	99.11
706.3	50.74	51.04	1.86	13.47	12.26	0.28	6.65	10.86	2.69	0.19	98.99
747.6	50.78	51.07	1.83	13.43	12.40	0.18	6.62	10.93	2.63	0.20	99.01
788.9	50.70	51.28	1.85	13.31	12.24	0.18	6.77	10.82	2.65	0.20	98.72
830.0	50.65	51.18	1.86	13.30	12.35	0.19	6.73	10.85	2.66	0.18	98.77
871.3	50.91	51.24	1.82	13.36	12.34	0.20	6.66	10.88	2.63	0.17	98.97
912.5	50.86	51.10	1.83	13.37	12.25	0.24	6.68	10.94	2.70	0.19	99.05
953.8	50.66	51.20	1.88	13.38	12.21	0.21	6.66	10.89	2.69	0.18	98.76
995.1	50.74	51.41	1.83	13.24	12.26	0.19	6.61	10.90	2.68	0.18	98.64
1036.3	50.65	51.25	1.87	13.30	12.20	0.21	6.71	10.87	2.69	0.20	98.70

1077.6	50.65	51.24	1.70	13.40	12.28	0.27	6.68	10.88	2.69	0.18	98.72
7.5	46.18	47.06	0.97	22.35	8.82	0.18	4.74	12.25	2.79	0.14	98.42
12.5	46.87	47.55	0.97	21.90	8.74	0.21	4.71	12.36	2.71	0.14	98.62
17.5	46.39	47.39	1.01	21.88	8.93	0.17	4.72	12.37	2.69	0.15	98.31
22.5	46.81	47.48	1.12	21.52	9.02	0.20	4.90	12.27	2.65	0.14	98.63
22.5	47.54	47.97	1.06	21.14	9.04	0.13	4.93	12.24	2.63	0.16	98.87
31.9	48.02	47.95	1.17	20.61	9.27	0.14	5.04	12.25	2.71	0.16	99.36
41.2	48.29	48.81	1.21	19.82	9.40	0.17	5.03	12.07	2.63	0.16	98.78
50.6	48.99	49.13	1.29	19.10	9.57	0.22	5.13	12.01	2.68	0.17	99.16
60.0	49.33	49.52	1.38	18.33	9.80	0.13	5.26	12.04	2.67	0.17	99.11
69.4	50.12	49.80	1.48	17.74	9.97	0.14	5.44	11.83	2.74	0.16	99.62
69.4	49.45	49.84	1.47	17.72	10.04	0.16	5.32	11.91	2.67	0.17	98.90
90.7	49.99	50.43	1.68	16.49	10.39	0.18	5.56	11.77	2.63	0.17	98.86
112.0	50.22	50.83	1.64	15.56	10.65	0.25	5.92	11.66	2.62	0.16	98.68
133.3	50.42	51.17	1.66	14.88	11.06	0.19	6.07	11.54	2.56	0.17	98.55
154.5	50.59	51.12	1.86	14.29	11.31	0.20	6.17	11.56	2.59	0.18	98.77
175.8	50.74	51.34	1.90	13.78	11.56	0.19	6.28	11.50	2.57	0.16	98.70
197.1	50.52	51.07	1.88	13.75	11.76	0.20	6.48	11.46	2.53	0.17	98.75
214.7	50.65	51.07	1.89	13.65	11.90	0.21	6.51	11.35	2.53	0.18	98.87
254.9	50.71	51.30	1.75	13.41	12.13	0.15	6.52	11.33	2.54	0.18	98.72
295.2	51.02	51.09	1.87	13.43	12.30	0.21	6.49	11.16	2.58	0.17	99.23
335.4	51.06	51.38	1.72	13.43	12.16	0.17	6.64	11.06	2.57	0.17	98.98
375.6	50.45	50.97	2.00	13.47	12.12	0.24	6.71	11.02	2.61	0.17	98.79
415.9	51.11	51.04	1.94	13.38	12.25	0.24	6.61	11.06	2.62	0.17	99.37
456.1	50.86	51.21	1.88	13.47	12.11	0.19	6.62	11.06	2.59	0.19	98.95
496.3	50.93	51.12	1.84	13.48	12.20	0.21	6.71	10.98	2.58	0.18	99.11
536.4	50.82	50.90	1.89	13.43	12.26	0.26	6.71	11.05	2.61	0.18	99.23
576.7	50.94	51.19	1.77	13.39	12.23	0.21	6.76	10.95	2.60	0.19	99.04
616.9	50.84	51.08	1.80	13.44	12.36	0.23	6.70	10.93	2.59	0.18	99.07
657.1	51.36	51.17	1.90	13.37	12.23	0.18	6.72	10.90	2.67	0.17	99.49
697.4	51.21	50.86	1.87	13.52	12.38	0.21	6.74	10.91	2.63	0.18	99.65
737.6	51.32	51.12	1.89	13.39	12.26	0.22	6.65	10.96	2.63	0.18	99.50
777.8	51.08	50.96	1.82	13.51	12.38	0.18	6.74	10.89	2.63	0.19	99.41
818.1	51.15	51.37	1.82	13.26	12.22	0.18	6.68	10.93	2.66	0.18	99.08
858.3	51.32	51.00	1.83	13.47	12.38	0.20	6.70	10.90	2.65	0.18	99.62
898.4	51.33	51.14	1.86	13.31	12.33	0.23	6.67	10.93	2.65	0.17	99.49
938.7	51.32	51.21	1.80	13.38	12.29	0.19	6.65	10.99	2.63	0.17	99.42
978.9	51.10	51.07	1.83	13.46	12.28	0.27	6.70	10.94	2.59	0.17	99.33
1019.1	50.97	51.19	1.80	13.41	12.23	0.16	6.75	10.91	2.66	0.19	99.07
1059.3	50.97	51.01	1.87	13.44	12.25	0.24	6.72	10.95	2.64	0.18	99.26
1099.6	51.16	51.36	1.83	13.36	12.21	0.17	6.61	10.91	2.68	0.17	99.10

1139.8	50.92	51.13	1.80	13.32	12.29	0.20	6.73	10.99	2.66	0.18	99.09
1180.0	51.07	51.01	1.90	13.49	12.29	0.19	6.73	10.84	2.66	0.19	99.36
1220.3	51.37	51.13	1.83	13.41	12.26	0.20	6.72	10.89	2.67	0.18	99.54
1260.5	51.18	51.28	1.87	13.31	12.18	0.24	6.67	10.89	2.68	0.18	99.20
7.5	47.40	47.05	0.98	22.35	8.69	0.11	4.75	12.44	2.77	0.15	99.65
12.5	47.72	47.43	0.99	22.14	8.72	0.17	4.70	12.33	2.69	0.13	99.59
17.5	47.84	47.60	1.07	21.70	8.83	0.16	4.77	12.33	2.69	0.15	99.54
22.4	48.04	47.78	1.06	21.36	8.96	0.20	4.78	12.32	2.69	0.16	99.56
27.4	48.40	48.13	1.14	20.89	9.01	0.14	4.87	12.31	2.66	0.15	99.57
27.4	48.33	47.87	1.18	21.04	9.09	0.19	4.93	12.22	2.62	0.16	99.76
37.3	48.51	48.63	1.20	20.15	9.26	0.13	4.97	12.11	2.68	0.16	99.18
47.2	49.11	48.60	1.37	19.64	9.56	0.15	5.18	11.96	2.67	0.16	99.81
57.1	49.51	49.23	1.29	18.74	9.80	0.20	5.23	11.95	2.69	0.18	99.58
67.0	49.97	49.84	1.38	18.00	9.82	0.18	5.27	11.97	2.65	0.18	99.43
76.9	50.37	50.12	1.44	17.49	10.06	0.17	5.35	11.86	2.64	0.17	99.55
86.8	50.68	50.32	1.53	16.74	10.26	0.23	5.57	11.79	2.71	0.16	99.66
96.7	50.79	50.56	1.68	16.21	10.37	0.17	5.83	11.66	2.65	0.16	99.53
106.6	50.90	50.84	1.62	15.84	10.65	0.16	5.77	11.59	2.64	0.18	99.36
116.5	51.13	50.99	1.67	15.43	10.84	0.20	5.84	11.59	2.58	0.18	99.44
134.8	51.04	51.35	1.81	14.93	10.88	0.14	5.96	11.51	2.55	0.18	98.99
157.9	51.21	51.23	1.83	14.34	11.35	0.16	6.20	11.48	2.56	0.15	99.28
181.1	51.25	51.12	1.90	13.99	11.53	0.20	6.36	11.53	2.51	0.16	99.44
204.3	51.34	51.23	1.90	13.68	11.72	0.23	6.43	11.40	2.53	0.17	99.41
227.5	51.08	51.04	1.84	13.63	12.06	0.17	6.56	11.31	2.50	0.19	99.34
250.8	51.23	51.38	1.87	13.38	12.04	0.18	6.51	11.28	2.51	0.17	99.16
274.0	51.22	51.10	1.82	13.43	12.17	0.19	6.67	11.19	2.54	0.17	99.42
297.2	51.09	51.08	1.93	13.51	11.99	0.24	6.67	11.20	2.54	0.17	99.32
320.4	50.86	51.03	1.90	13.41	12.11	0.22	6.75	11.15	2.57	0.18	99.13
343.6	50.95	51.32	1.80	13.33	12.14	0.20	6.66	11.14	2.56	0.17	98.94
366.8	51.23	50.99	1.82	13.48	12.15	0.22	6.71	11.19	2.56	0.18	99.54
390.0	51.01	51.04	1.85	13.47	12.22	0.22	6.66	11.08	2.58	0.18	99.27
413.2	51.14	51.16	1.75	13.56	12.06	0.26	6.71	11.03	2.59	0.18	99.28
436.4	50.82	51.30	1.78	13.33	12.20	0.19	6.74	11.04	2.53	0.19	98.82
459.6	50.54	51.10	1.92	13.42	12.22	0.19	6.64	11.03	2.59	0.20	98.74
482.9	50.87	50.96	1.90	13.52	12.26	0.25	6.74	10.92	2.58	0.18	99.21
506.1	51.03	51.25	1.79	13.44	12.25	0.20	6.67	10.94	2.56	0.19	99.07
529.2	51.14	51.17	1.84	13.48	12.20	0.15	6.70	10.96	2.63	0.18	99.27
552.4	50.95	50.94	1.79	13.51	12.29	0.22	6.77	10.97	2.64	0.17	99.31
575.6	50.83	51.16	1.95	13.30	12.22	0.25	6.64	11.00	2.62	0.18	98.97
575.6	51.22	51.01	1.80	13.52	12.23	0.27	6.65	11.07	2.57	0.18	99.51
615.1	51.11	51.05	1.91	13.43	12.31	0.20	6.66	10.94	2.60	0.19	99.36

654.7	51.23	51.23	1.81	13.44	12.29	0.16	6.62	10.94	2.62	0.19	99.31
694.2	51.04	50.95	1.87	13.43	12.25	0.26	6.70	11.03	2.64	0.18	99.39
733.7	51.14	50.95	1.77	13.46	12.33	0.25	6.83	10.92	2.63	0.17	99.49
773.2	51.14	50.82	1.90	13.50	12.28	0.25	6.81	10.97	2.60	0.17	99.63
812.8	50.82	50.97	1.80	13.48	12.25	0.22	6.74	11.00	2.67	0.18	99.15
852.3	51.18	50.99	1.94	13.45	12.28	0.22	6.72	10.89	2.63	0.19	99.49
891.8	51.09	51.39	1.75	13.36	12.22	0.18	6.67	10.92	2.64	0.19	99.00
931.3	50.75	51.36	1.84	13.38	12.23	0.17	6.62	10.91	2.61	0.18	98.70
970.8	50.99	51.20	1.81	13.48	12.20	0.17	6.66	10.94	2.66	0.19	99.09
1010.3	51.33	51.19	1.89	13.36	12.19	0.21	6.75	10.86	2.66	0.19	99.45
1049.9	51.24	51.38	1.86	13.32	12.15	0.22	6.62	10.94	2.63	0.19	99.16
1089.4	51.40	51.19	1.85	13.44	12.18	0.20	6.59	11.03	2.64	0.19	99.51
1128.9	51.37	51.10	1.76	13.51	12.24	0.19	6.68	10.94	2.68	0.19	99.57
1168.4	51.12	51.10	1.85	13.35	12.30	0.21	6.76	10.92	2.63	0.19	99.32
1208.0	51.31	51.00	1.91	13.47	12.08	0.28	6.71	10.94	2.70	0.20	99.61
1247.5	51.26	50.95	1.90	13.35	12.34	0.23	6.76	10.91	2.67	0.18	99.62

Exp 213

x / μm	Oxides (wt%)										
	SiO ₂	SiO ₂ *	TiO ₂	Al ₂ O ₃	FeO	MnO	MgO	CaO	Na ₂ O	K ₂ O	Total
11.1	47.07	46.74	0.89	23.21	8.60	0.18	4.58	12.17	2.77	0.16	99.63
16.7	47.55	46.80	0.92	22.98	8.64	0.15	4.65	12.39	2.64	0.15	100.05
22.3	47.23	46.76	1.02	22.91	8.60	0.19	4.66	12.38	2.63	0.14	99.76
27.8	47.55	47.03	0.90	22.73	8.66	0.16	4.65	12.36	2.66	0.15	99.82
33.3	47.76	47.23	0.97	22.49	8.68	0.12	4.66	12.39	2.61	0.15	99.83
38.9	47.99	47.15	1.00	22.65	8.62	0.15	4.70	12.20	2.69	0.14	100.14
54.5	48.07	47.30	1.02	21.97	9.02	0.14	4.88	12.25	2.56	0.15	100.07
69.4	48.34	47.71	1.09	21.49	9.04	0.14	4.88	12.24	2.57	0.15	99.93
84.1	48.82	47.94	1.19	21.05	9.03	0.15	4.99	12.16	2.63	0.15	100.18
99.0	48.99	48.22	1.20	20.69	9.19	0.15	5.01	12.09	2.62	0.15	100.07
113.8	49.25	48.25	1.22	20.30	9.28	0.19	5.11	12.12	2.67	0.15	100.29
128.7	49.45	48.83	1.28	19.93	9.27	0.13	5.11	11.96	2.63	0.16	99.92
143.4	49.49	49.13	1.20	19.41	9.47	0.13	5.20	11.96	2.65	0.15	99.67
158.3	49.90	49.40	1.32	18.94	9.58	0.17	5.12	11.94	2.67	0.16	99.80
173.2	50.16	49.21	1.34	18.81	9.65	0.14	5.33	11.97	2.68	0.17	100.25
187.9	50.14	49.55	1.46	18.59	9.61	0.11	5.33	11.81	2.68	0.15	99.89
202.8	50.43	49.99	1.31	18.01	9.71	0.19	5.37	11.89	2.68	0.15	99.75
217.6	50.73	50.17	1.42	17.66	9.93	0.16	5.39	11.77	2.63	0.16	99.86
232.5	50.74	49.98	1.46	17.52	10.09	0.16	5.50	11.75	2.68	0.18	100.07
247.2	51.19	50.26	1.48	17.14	10.16	0.20	5.55	11.66	2.65	0.19	100.23
262.1	51.14	50.53	1.56	16.73	10.18	0.16	5.67	11.66	2.63	0.17	99.91
262.1	51.18	50.93	1.53	16.71	10.13	0.17	5.59	11.51	2.55	0.18	99.54
293.0	51.54	50.78	1.54	16.34	10.35	0.16	5.70	11.64	2.63	0.16	100.06
324.0	51.78	50.85	1.74	15.91	10.45	0.20	5.87	11.46	2.64	0.18	100.23
354.9	51.79	51.16	1.68	15.35	10.55	0.22	6.07	11.50	2.59	0.18	99.93
385.9	51.90	51.44	1.69	15.11	10.76	0.20	6.00	11.37	2.56	0.18	99.76
416.8	52.08	51.36	1.72	14.74	10.98	0.15	6.14	11.47	2.57	0.17	100.01
447.7	51.99	51.37	1.82	14.43	11.18	0.20	6.24	11.33	2.56	0.17	99.92
478.7	52.01	51.51	1.81	14.31	11.13	0.13	6.39	11.33	2.52	0.17	99.81
509.6	51.84	51.98	1.78	14.02	11.06	0.23	6.30	11.24	2.53	0.16	99.16
540.6	52.21	51.42	1.82	14.06	11.37	0.24	6.42	11.25	2.54	0.17	100.09
571.5	52.21	51.69	1.75	13.88	11.42	0.15	6.37	11.34	2.54	0.16	99.82
602.4	52.16	51.92	1.75	13.74	11.41	0.16	6.44	11.19	2.53	0.17	99.53
633.4	52.24	51.64	1.83	13.78	11.55	0.15	6.45	11.21	2.51	0.18	99.89
664.3	52.19	51.37	1.94	13.61	11.81	0.21	6.46	11.18	2.54	0.17	100.12
664.3	52.38	51.70	1.92	13.75	11.52	0.16	6.41	11.26	2.43	0.15	99.98
715.2	52.20	51.69	1.74	13.46	11.74	0.23	6.58	11.13	2.56	0.16	99.80
766.1	52.22	51.94	1.87	13.45	11.56	0.13	6.56	11.11	2.50	0.18	99.59

817.0	52.28	51.58	1.74	13.52	11.96	0.21	6.52	11.09	2.52	0.16	100.00
867.9	51.93	51.55	1.81	13.46	11.93	0.20	6.63	10.98	2.57	0.17	99.68
918.8	52.04	51.37	1.84	13.44	11.99	0.19	6.74	11.02	2.54	0.17	99.97
969.7	51.96	51.77	1.75	13.42	11.76	0.22	6.71	10.96	2.53	0.17	99.49
1020.6	51.78	51.55	1.89	13.32	12.01	0.18	6.67	10.96	2.58	0.16	99.53
1071.5	51.85	51.76	1.88	13.44	11.82	0.17	6.56	10.99	2.50	0.18	99.39
1122.4	51.81	51.30	1.91	13.44	12.08	0.28	6.61	10.98	2.53	0.17	99.81
1173.3	51.69	51.83	1.77	13.27	11.86	0.15	6.77	10.91	2.56	0.19	99.16
1224.2	51.77	51.53	1.73	13.43	11.89	0.23	6.77	10.97	2.57	0.19	99.54
1275.1	51.78	51.62	1.82	13.40	11.89	0.22	6.67	10.90	2.60	0.18	99.46
1326.0	51.79	51.41	1.85	13.40	12.09	0.13	6.76	10.91	2.57	0.18	99.68
1376.9	51.52	51.66	1.69	13.36	12.08	0.21	6.67	10.87	2.59	0.17	99.16
1427.8	51.90	51.45	1.77	13.36	12.10	0.19	6.73	10.89	2.62	0.19	99.75
1478.8	51.87	51.56	1.76	13.30	12.02	0.21	6.74	10.93	2.61	0.18	99.60
1529.7	51.66	51.82	1.80	13.23	11.94	0.24	6.68	10.80	2.61	0.18	99.14
1580.6	51.51	51.67	1.84	13.24	12.04	0.20	6.71	10.87	2.56	0.17	99.13
10.9	47.52	46.86	0.96	23.24	8.42	0.17	4.61	12.20	2.72	0.13	99.96
16.4	47.54	47.12	0.90	22.89	8.49	0.17	4.65	12.20	2.72	0.14	99.71
21.9	47.73	47.38	0.92	22.62	8.59	0.17	4.58	12.26	2.64	0.14	99.66
58.2	48.02	47.04	0.99	22.53	8.77	0.22	4.86	12.13	2.60	0.15	100.28
73.7	48.16	48.04	1.06	21.58	8.84	0.18	4.82	12.03	2.61	0.14	99.42
89.3	48.67	48.04	1.09	21.35	9.00	0.15	4.82	12.09	2.60	0.16	99.93
104.9	48.80	48.51	1.05	20.88	8.95	0.17	4.88	12.05	2.64	0.16	99.60
120.5	49.11	48.65	1.17	20.51	9.10	0.20	4.97	11.90	2.65	0.15	99.76
136.0	49.26	48.91	1.21	20.03	9.26	0.16	5.01	11.88	2.67	0.18	99.65
151.6	49.55	48.99	1.27	19.72	9.35	0.18	5.12	11.86	2.65	0.16	99.86
167.2	50.04	49.35	1.28	19.40	9.34	0.19	5.10	11.82	2.67	0.16	100.00
182.7	49.93	49.33	1.30	19.01	9.57	0.24	5.15	11.86	2.68	0.16	99.91
198.3	50.34	49.69	1.35	18.67	9.61	0.15	5.26	11.78	2.63	0.17	99.95
213.9	50.38	50.00	1.34	18.28	9.65	0.21	5.30	11.70	2.66	0.15	99.68
229.4	50.71	50.17	1.42	17.84	9.80	0.15	5.39	11.65	2.72	0.16	99.84
245.0	50.74	50.26	1.47	17.55	9.91	0.16	5.50	11.64	2.64	0.17	99.79
260.6	50.98	50.23	1.53	17.34	10.01	0.17	5.52	11.64	2.69	0.17	100.05
276.2	51.29	50.55	1.56	16.98	10.15	0.13	5.57	11.54	2.66	0.17	100.04
291.7	51.36	50.87	1.49	16.70	10.05	0.20	5.58	11.60	2.65	0.16	99.79
291.7	51.15	50.67	1.47	16.83	10.18	0.22	5.64	11.52	2.60	0.16	99.78
321.5	51.55	51.25	1.56	16.18	10.20	0.19	5.60	11.46	2.69	0.16	99.60
351.2	51.96	51.10	1.50	15.73	10.68	0.18	5.82	11.50	2.61	0.17	100.17
381.0	51.88	51.46	1.70	15.29	10.57	0.24	5.83	11.40	2.63	0.17	99.72
410.7	52.04	51.50	1.74	14.92	10.79	0.16	6.02	11.39	2.61	0.17	99.84
440.4	51.94	51.61	1.65	14.58	11.05	0.20	6.13	11.31	2.60	0.17	99.63

470.2	52.24	51.57	1.79	14.47	11.11	0.22	6.00	11.35	2.60	0.17	99.96
499.9	52.21	51.67	1.76	14.29	11.20	0.17	6.19	11.29	2.56	0.18	99.84
529.7	52.17	51.61	1.77	14.11	11.24	0.18	6.32	11.30	2.59	0.17	99.85
559.4	52.21	51.63	1.80	14.06	11.29	0.25	6.32	11.23	2.54	0.17	99.88
589.2	52.01	51.74	1.89	13.88	11.29	0.22	6.35	11.22	2.53	0.19	99.58
618.9	52.27	51.72	1.77	13.75	11.45	0.21	6.45	11.26	2.51	0.18	99.85
648.6	52.16	51.86	1.77	13.64	11.52	0.21	6.43	11.19	2.51	0.17	99.60
678.4	52.20	51.61	2.00	13.64	11.55	0.20	6.50	11.08	2.56	0.16	99.89
708.1	52.01	51.81	1.83	13.54	11.59	0.15	6.49	11.21	2.52	0.17	99.50
737.9	52.19	51.70	1.81	13.58	11.66	0.19	6.50	11.16	2.54	0.18	99.80
737.9	52.26	51.47	1.74	13.67	11.80	0.21	6.58	11.20	2.46	0.17	100.09
788.8	52.24	51.53	1.89	13.47	11.67	0.22	6.59	11.16	2.58	0.18	100.01
839.7	52.19	51.67	1.85	13.42	11.71	0.24	6.55	11.16	2.52	0.18	99.82
890.6	52.13	51.34	1.95	13.50	11.89	0.16	6.64	11.16	2.49	0.18	100.09
941.5	52.11	51.56	1.83	13.47	11.81	0.19	6.66	11.06	2.56	0.18	99.86
992.4	52.11	51.45	1.87	13.48	11.89	0.18	6.71	10.99	2.57	0.16	99.96
1043.3	52.22	51.43	1.85	13.42	11.94	0.19	6.78	10.98	2.53	0.18	100.09
1094.2	51.98	51.27	1.79	13.44	11.94	0.23	6.77	11.08	2.60	0.19	100.02
1145.1	52.00	51.45	1.77	13.35	11.96	0.22	6.77	11.03	2.57	0.18	99.86
1196.0	52.11	51.71	1.77	13.33	11.86	0.18	6.78	10.89	2.62	0.16	99.70
1246.9	52.03	51.55	1.83	13.34	11.98	0.21	6.69	10.96	2.58	0.17	99.77
1297.8	51.85	51.36	1.85	13.33	12.04	0.23	6.73	10.96	2.60	0.19	99.79
1348.7	51.96	51.55	1.92	13.28	11.95	0.23	6.74	10.90	2.55	0.18	99.71
1399.6	52.07	51.66	1.86	13.31	11.98	0.16	6.66	10.92	2.56	0.18	99.71
1450.5	52.06	51.40	1.70	13.40	12.08	0.18	6.81	10.95	2.60	0.18	99.96
1501.4	51.91	51.47	1.83	13.26	12.06	0.25	6.79	10.86	2.61	0.17	99.74
1552.3	52.00	51.26	1.86	13.45	12.15	0.22	6.67	10.97	2.55	0.17	100.04
1603.2	52.10	51.47	1.85	13.37	12.01	0.24	6.74	10.80	2.62	0.18	99.93
1654.1	52.05	51.24	1.74	13.42	12.22	0.25	6.78	10.81	2.65	0.19	100.11
10.7	47.58	47.00	0.95	23.05	8.49	0.15	4.55	12.24	2.73	0.14	99.88
16.3	47.57	46.88	0.91	23.04	8.50	0.17	4.61	12.36	2.68	0.15	100.00
21.9	47.54	47.04	0.91	22.83	8.58	0.14	4.65	12.36	2.64	0.16	99.80
27.5	47.83	46.96	1.03	22.62	8.71	0.20	4.68	12.31	2.66	0.14	100.18
33.0	47.75	47.30	0.94	22.57	8.68	0.13	4.65	12.27	2.60	0.14	99.74
38.6	47.94	47.20	1.00	22.41	8.80	0.20	4.69	12.21	2.64	0.15	100.04
54.5	48.17	47.70	1.06	21.98	8.77	0.13	4.87	12.10	2.55	0.14	99.77
69.7	48.31	48.14	1.04	21.38	8.85	0.14	4.89	12.13	2.60	0.14	99.47
84.7	48.76	48.67	1.09	20.95	8.85	0.17	4.79	11.99	2.64	0.15	99.40
99.9	48.97	48.47	1.13	20.69	9.14	0.17	4.94	11.95	2.67	0.14	99.80
115.0	49.28	48.65	1.10	20.34	9.27	0.17	4.95	11.96	2.70	0.16	99.94
130.2	49.46	48.76	1.34	19.91	9.25	0.13	5.17	11.93	2.66	0.16	100.01

145.2	49.66	49.05	1.22	19.60	9.45	0.14	5.14	11.88	2.67	0.16	99.91
160.4	50.15	49.43	1.29	19.23	9.48	0.12	5.11	11.74	2.71	0.18	100.02
175.5	50.18	49.51	1.26	18.95	9.51	0.20	5.29	11.72	2.69	0.17	99.96
190.6	50.38	49.74	1.35	18.61	9.57	0.14	5.29	11.77	2.64	0.18	99.94
205.7	50.49	49.95	1.37	18.18	9.77	0.18	5.35	11.70	2.65	0.15	99.84
220.9	50.76	50.17	1.41	17.93	9.85	0.20	5.30	11.62	2.68	0.14	99.89
235.9	50.77	50.62	1.31	17.38	9.88	0.22	5.46	11.63	2.63	0.16	99.45
251.1	50.91	50.27	1.51	17.24	10.06	0.22	5.57	11.61	2.66	0.16	99.94
251.1	51.10	50.65	1.44	17.35	9.93	0.19	5.44	11.59	2.53	0.18	99.75
280.8	51.22	50.71	1.58	16.75	10.13	0.17	5.58	11.58	2.64	0.17	99.82
310.3	51.59	50.76	1.51	16.33	10.37	0.19	5.75	11.56	2.68	0.15	100.13
339.9	51.81	51.10	1.60	15.93	10.46	0.18	5.73	11.48	2.65	0.17	100.01
369.6	51.84	51.48	1.59	15.38	10.56	0.19	5.90	11.42	2.63	0.16	99.66
399.1	51.98	51.53	1.59	14.97	10.76	0.15	5.99	11.52	2.62	0.17	99.75
428.8	52.03	51.68	1.61	14.87	10.71	0.18	6.10	11.37	2.61	0.17	99.65
458.4	52.12	51.71	1.83	14.49	10.93	0.16	6.07	11.39	2.55	0.17	99.71
488.0	52.22	51.89	1.78	14.26	11.06	0.21	6.12	11.22	2.59	0.17	99.63
517.6	51.96	51.64	1.80	14.07	11.28	0.17	6.31	11.28	2.58	0.18	99.62
547.2	52.24	51.61	1.74	13.99	11.42	0.15	6.34	11.32	2.55	0.18	99.93
576.8	52.22	52.01	1.86	13.77	11.30	0.14	6.32	11.20	2.53	0.17	99.50
606.4	52.22	51.71	1.72	13.87	11.51	0.18	6.35	11.24	2.56	0.16	99.81
636.1	52.02	51.85	1.82	13.69	11.47	0.25	6.34	11.16	2.55	0.17	99.48
665.6	52.27	51.86	1.76	13.56	11.57	0.20	6.53	11.12	2.52	0.17	99.71
695.3	52.05	52.04	1.76	13.49	11.48	0.23	6.46	11.15	2.49	0.18	99.31
724.9	52.21	51.74	1.86	13.51	11.65	0.28	6.43	11.10	2.56	0.16	99.77
754.4	52.19	51.49	1.90	13.56	11.56	0.27	6.66	11.13	2.56	0.17	100.00
784.1	52.30	51.50	1.89	13.54	11.66	0.24	6.62	11.15	2.53	0.17	100.10
784.1	52.44	51.63	1.70	13.56	11.68	0.27	6.72	11.14	2.43	0.17	100.11
833.2	52.16	51.71	1.81	13.48	11.74	0.19	6.60	11.10	2.49	0.17	99.75
882.2	52.19	51.96	1.71	13.39	11.68	0.22	6.59	11.05	2.54	0.16	99.53
931.3	52.05	51.80	1.81	13.28	11.76	0.19	6.66	11.08	2.55	0.17	99.54
980.4	52.10	51.56	1.87	13.44	11.87	0.17	6.62	11.00	2.59	0.18	99.84
1029.4	52.03	51.79	1.74	13.38	11.90	0.19	6.58	11.02	2.54	0.17	99.54
1078.5	51.96	51.45	1.86	13.46	11.88	0.21	6.70	10.98	2.57	0.19	99.82
1127.6	51.95	51.58	1.81	13.43	11.86	0.26	6.71	10.92	2.56	0.18	99.66
1176.6	51.87	51.77	1.77	13.34	11.85	0.23	6.64	10.95	2.58	0.18	99.40
1225.7	52.10	51.55	1.80	13.38	11.93	0.18	6.77	10.92	2.61	0.16	99.85
1274.8	51.83	51.41	1.82	13.38	12.00	0.19	6.77	10.93	2.62	0.18	99.72
1323.8	51.54	51.59	1.82	13.44	11.93	0.18	6.69	10.88	2.60	0.18	99.25
1372.9	52.11	51.47	1.79	13.46	12.06	0.15	6.70	10.90	2.59	0.17	99.94
1422.1	51.80	51.66	1.73	13.35	11.98	0.20	6.69	10.90	2.61	0.19	99.44

1471.1	51.79	51.22	1.82	13.39	12.17	0.20	6.87	10.88	2.56	0.18	99.87
1520.2	51.96	51.57	1.86	13.33	11.93	0.22	6.75	10.88	2.58	0.19	99.69
1569.3	52.05	51.58	1.80	13.32	11.97	0.19	6.76	10.89	2.62	0.17	99.77
1618.3	52.05	51.46	1.78	13.32	12.15	0.21	6.79	10.80	2.60	0.19	99.89
1667.4	51.98	51.61	1.74	13.37	12.06	0.19	6.68	10.91	2.55	0.19	99.66

Exp 215

x / μm	Oxides (wt%)										
	SiO ₂	SiO ₂ *	TiO ₂	Al ₂ O ₃	FeO	MnO	MgO	CaO	Na ₂ O	K ₂ O	Total
7.6	48.83	48.02	1.20	20.57	9.36	0.13	5.18	11.93	2.75	0.16	100.11
13.3	49.08	48.61	1.33	19.76	9.35	0.18	5.22	11.96	2.73	0.17	99.76
19.1	50.20	48.83	1.23	19.19	9.65	0.19	5.33	11.96	2.77	0.15	100.67
24.8	50.45	49.55	1.33	18.45	9.75	0.14	5.41	11.78	2.75	0.16	100.20
42.4	50.86	50.07	1.50	16.83	10.39	0.11	5.79	11.77	2.67	0.17	100.08
57.9	51.80	51.02	1.65	15.41	10.76	0.17	5.94	11.49	2.69	0.17	100.08
73.5	51.93	51.24	1.79	14.65	11.08	0.23	6.10	11.38	2.66	0.18	99.99
89.0	52.26	51.21	1.84	14.15	11.32	0.28	6.33	11.36	2.65	0.17	100.35
104.5	52.21	51.49	1.78	13.71	11.53	0.19	6.49	11.33	2.61	0.17	100.03
120.0	52.08	51.28	1.96	13.69	11.66	0.21	6.44	11.30	2.59	0.17	100.10
135.6	52.03	51.39	1.74	13.67	11.74	0.19	6.56	11.25	2.60	0.16	99.94
151.1	52.04	51.47	1.82	13.57	11.68	0.21	6.60	11.19	2.60	0.17	99.87
166.6	52.21	51.10	1.93	13.62	11.89	0.22	6.66	11.12	2.61	0.15	100.41
182.1	51.99	51.27	1.89	13.52	11.95	0.17	6.62	11.05	2.66	0.17	100.02
197.7	52.28	51.02	1.83	13.62	12.01	0.24	6.70	11.03	2.67	0.18	100.56
213.2	52.42	51.28	1.76	13.55	11.93	0.19	6.71	11.04	2.66	0.16	100.44
213.2	52.35	51.24	1.86	13.64	11.85	0.23	6.71	11.03	2.55	0.19	100.40
248.0	52.21	51.37	1.92	13.46	11.93	0.11	6.73	10.98	2.61	0.18	100.15
282.9	52.48	51.28	1.83	13.60	11.85	0.26	6.76	10.85	2.70	0.18	100.50
317.8	52.29	51.25	1.89	13.58	11.96	0.20	6.70	10.83	2.71	0.18	100.33
352.6	52.21	51.24	1.82	13.50	12.02	0.21	6.74	10.87	2.71	0.17	100.27
387.5	52.26	51.23	1.72	13.55	12.05	0.23	6.78	10.85	2.72	0.18	100.32
422.3	51.79	51.25	1.79	13.67	11.96	0.22	6.71	10.84	2.67	0.18	99.84
457.3	52.08	51.03	1.90	13.61	12.01	0.23	6.75	10.87	2.70	0.19	100.35
492.1	51.92	51.27	1.84	13.49	11.93	0.24	6.75	10.89	2.73	0.17	99.94
526.9	52.24	51.17	1.81	13.48	12.02	0.21	6.76	10.88	2.78	0.18	100.37
561.8	52.12	51.15	1.80	13.52	12.04	0.22	6.77	10.86	2.76	0.18	100.27
596.7	52.29	51.14	1.86	13.58	12.08	0.18	6.71	10.86	2.72	0.18	100.45
631.6	52.32	51.16	1.74	13.56	12.06	0.24	6.75	10.87	2.73	0.18	100.46
666.4	52.20	51.18	1.93	13.54	12.03	0.17	6.65	10.88	2.75	0.17	100.32
6.9	48.81	47.97	1.19	20.69	9.23	0.15	5.25	11.85	2.82	0.16	100.14
12.0	49.37	48.25	1.34	20.22	9.23	0.17	5.23	11.92	2.79	0.16	100.42
17.2	49.85	48.76	1.24	19.47	9.51	0.19	5.22	11.93	2.81	0.16	100.39
22.4	50.13	49.22	1.36	18.94	9.64	0.14	5.29	11.78	2.76	0.16	100.21
27.6	50.56	49.91	1.37	17.98	9.66	0.20	5.55	11.74	2.74	0.16	99.95
27.6	50.81	49.68	1.36	18.41	9.70	0.17	5.47	11.71	2.62	0.19	100.43
42.4	51.32	50.55	1.47	16.74	10.20	0.21	5.70	11.56	2.70	0.17	100.07
57.1	51.79	50.98	1.71	15.56	10.56	0.19	6.01	11.44	2.67	0.18	100.11

71.8	51.66	51.16	1.73	14.87	10.91	0.15	6.22	11.43	2.66	0.16	99.80
86.5	51.93	51.15	1.87	14.27	11.29	0.18	6.39	11.30	2.66	0.18	100.08
101.3	52.12	51.09	1.95	13.92	11.46	0.22	6.60	11.29	2.61	0.15	100.33
116.0	52.08	51.39	1.79	13.74	11.55	0.21	6.54	11.26	2.64	0.16	99.98
130.8	51.93	51.09	1.92	13.69	11.84	0.20	6.59	11.19	2.63	0.16	100.14
145.4	51.98	51.12	1.84	13.61	11.88	0.19	6.72	11.17	2.61	0.16	100.15
160.2	52.19	51.42	1.74	13.53	11.82	0.23	6.72	11.07	2.61	0.16	100.07
174.9	51.84	51.44	1.75	13.47	11.85	0.23	6.65	11.11	2.64	0.17	99.70
189.7	52.05	51.11	1.94	13.51	11.88	0.24	6.75	11.05	2.65	0.17	100.23
204.3	51.96	51.35	1.90	13.44	11.87	0.18	6.73	11.02	2.64	0.18	99.91
204.3	52.25	51.25	1.74	13.60	12.05	0.18	6.75	11.04	2.50	0.18	100.29
238.7	51.99	51.17	1.80	13.37	12.06	0.23	6.78	11.06	2.65	0.18	100.12
273.0	52.04	51.14	1.90	13.55	12.02	0.21	6.71	10.95	2.65	0.17	100.21
307.5	52.09	51.23	1.80	13.55	12.00	0.21	6.70	10.94	2.69	0.19	100.17
341.8	51.86	51.20	1.82	13.48	12.12	0.21	6.78	10.86	2.68	0.17	99.96
376.1	51.82	51.09	1.89	13.49	12.08	0.23	6.73	10.89	2.72	0.18	100.02
410.5	51.81	50.89	1.84	13.60	12.11	0.22	6.83	10.90	2.73	0.18	100.22
444.8	51.97	51.12	1.81	13.62	11.98	0.23	6.76	10.88	2.73	0.17	100.15
479.2	51.77	51.31	1.89	13.42	12.05	0.27	6.61	10.85	2.74	0.17	99.76
513.6	51.90	50.91	1.94	13.55	12.06	0.21	6.81	10.90	2.72	0.19	100.30
548.0	51.97	51.11	1.85	13.56	12.07	0.19	6.75	10.88	2.73	0.17	100.17
582.3	51.72	51.24	1.76	13.62	11.89	0.24	6.77	10.86	2.72	0.19	99.78
616.7	51.63	51.03	1.79	13.64	12.08	0.25	6.70	10.89	2.72	0.19	99.90
7.5	49.09	48.51	1.15	20.38	9.09	0.13	5.23	11.81	2.84	0.17	99.88
13.1	49.56	48.97	1.13	20.00	9.08	0.15	5.20	11.80	2.82	0.16	99.89
18.7	49.99	49.42	1.22	19.23	9.26	0.14	5.26	11.77	2.84	0.16	99.86
24.3	50.28	49.85	1.46	18.43	9.36	0.20	5.35	11.74	2.75	0.17	99.73
29.9	50.60	49.99	1.43	17.78	9.75	0.24	5.48	11.64	2.83	0.15	99.90
29.9	50.66	50.08	1.45	17.94	9.69	0.15	5.42	11.72	2.70	0.17	99.89
44.7	51.01	50.84	1.60	16.27	10.19	0.18	5.78	11.51	2.77	0.16	99.46
59.3	51.47	51.25	1.69	15.41	10.55	0.15	5.93	11.46	2.71	0.16	99.52
74.1	51.72	51.65	1.78	14.43	10.90	0.20	6.16	11.31	2.70	0.18	99.36
88.8	51.76	51.52	1.77	14.16	11.14	0.23	6.34	11.32	2.64	0.17	99.54
103.6	51.53	51.26	1.85	13.82	11.50	0.22	6.50	11.31	2.64	0.19	99.57
118.2	51.72	51.18	1.92	13.64	11.70	0.21	6.57	11.28	2.62	0.17	99.83
133.0	51.52	51.24	1.89	13.63	11.75	0.20	6.68	11.14	2.60	0.16	99.58
147.7	51.42	51.36	1.88	13.47	11.79	0.22	6.64	11.14	2.62	0.17	99.36
162.5	51.54	51.04	1.89	13.54	12.01	0.24	6.68	11.11	2.60	0.19	99.79
177.1	51.57	50.81	1.93	13.61	12.02	0.24	6.75	11.07	2.69	0.18	100.06
191.9	51.42	51.19	1.93	13.46	12.04	0.20	6.66	11.03	2.62	0.17	99.53
206.6	52.08	58.94	1.85	13.64	12.20	0.26	6.71	2.86	2.67	0.18	92.44

206.6	51.78	50.85	1.90	13.61	12.20	0.25	6.69	10.99	2.62	0.18	100.23
241.3	51.69	51.30	1.88	13.45	12.05	0.15	6.66	10.92	2.68	0.19	99.69
276.0	51.53	51.35	1.82	13.57	11.97	0.18	6.65	10.91	2.67	0.18	99.47
310.7	51.59	50.92	1.92	13.65	12.13	0.25	6.65	10.90	2.69	0.17	99.96
345.4	51.74	51.36	1.81	13.58	11.98	0.23	6.60	10.87	2.68	0.19	99.68
380.1	51.53	51.38	1.84	13.43	12.04	0.22	6.62	10.85	2.74	0.19	99.45
414.7	51.39	51.21	1.87	13.53	12.05	0.24	6.69	10.82	2.70	0.18	99.48
449.5	51.62	50.99	1.81	13.64	12.13	0.28	6.69	10.83	2.74	0.18	99.92
484.1	51.64	51.25	1.82	13.47	12.02	0.29	6.67	10.83	2.76	0.19	99.69
518.9	51.56	51.21	1.83	13.49	12.00	0.24	6.73	10.89	2.75	0.18	99.65
553.5	51.54	51.20	1.97	13.51	11.96	0.18	6.71	10.90	2.70	0.18	99.65
588.3	51.52	51.20	1.90	13.49	11.94	0.26	6.74	10.84	2.75	0.18	99.62
622.9	51.90	51.23	1.79	13.50	12.08	0.20	6.70	10.90	2.74	0.16	99.97

Exp 216

x / μm	Oxides (wt%)										
	SiO ₂	SiO ₂ *	TiO ₂	Al ₂ O ₃	FeO	MnO	MgO	CaO	Na ₂ O	K ₂ O	Total
5.2	46.13	46.09	0.99	23.82	8.52	0.14	4.40	12.60	2.61	0.14	99.34
10.4	46.66	46.48	0.90	23.34	8.50	0.16	4.48	12.73	2.57	0.14	99.49
15.6	46.62	46.56	0.96	23.19	8.45	0.11	4.54	12.80	2.56	0.12	99.36
20.8	46.83	46.76	0.90	23.17	8.49	0.12	4.50	12.72	2.51	0.13	99.37
20.8	46.83	46.51	0.94	23.22	8.59	0.14	4.63	12.73	2.41	0.13	99.62
36.7	46.94	47.53	0.96	22.32	8.58	0.16	4.59	12.52	2.52	0.13	98.71
52.5	47.65	47.21	1.01	22.09	8.83	0.12	4.70	12.65	2.55	0.14	99.74
68.4	48.21	47.51	1.15	21.62	8.88	0.17	4.71	12.55	2.55	0.16	99.99
84.3	48.28	47.96	1.19	21.03	9.00	0.20	4.83	12.37	2.58	0.15	99.63
100.1	48.77	48.17	1.19	20.56	9.12	0.18	4.88	12.49	2.58	0.13	99.90
116.0	48.90	48.32	1.21	20.20	9.28	0.21	4.94	12.35	2.63	0.15	99.88
131.9	49.17	48.89	1.25	19.60	9.37	0.15	5.05	12.20	2.63	0.16	99.58
147.7	49.57	49.13	1.27	19.12	9.46	0.20	5.14	12.20	2.62	0.17	99.74
163.5	49.58	49.62	1.36	18.52	9.51	0.14	5.12	12.24	2.63	0.17	99.26
179.4	49.99	49.31	1.38	18.42	9.75	0.19	5.38	12.12	2.60	0.17	99.98
195.2	50.16	50.06	1.35	17.84	9.88	0.11	5.20	12.06	2.62	0.17	99.39
211.1	50.39	50.11	1.40	17.51	9.90	0.12	5.39	12.11	2.61	0.16	99.58
227.0	50.67	50.29	1.46	17.13	9.97	0.19	5.47	12.03	2.62	0.15	99.68
242.8	51.06	50.64	1.48	16.75	10.18	0.19	5.42	11.85	2.65	0.14	99.73
258.7	50.92	50.51	1.55	16.56	10.30	0.17	5.64	11.85	2.55	0.17	99.71
258.7	51.26	50.71	1.52	16.45	10.20	0.16	5.68	11.91	2.50	0.17	99.85
293.3	51.43	51.04	1.63	15.70	10.46	0.21	5.61	11.94	2.56	0.17	99.69
328.0	51.49	50.98	1.64	15.44	10.80	0.14	5.81	11.75	2.58	0.17	99.82
362.6	51.60	51.14	1.81	14.78	10.87	0.19	6.10	11.71	2.55	0.15	99.75
397.2	51.81	51.20	1.85	14.38	11.08	0.22	6.07	11.81	2.51	0.18	99.91
431.7	51.89	51.42	1.76	14.20	11.11	0.16	6.25	11.71	2.54	0.14	99.77
466.4	52.12	51.32	1.80	14.13	11.31	0.27	6.25	11.60	2.47	0.15	100.11
501.0	51.96	51.66	1.79	13.79	11.39	0.20	6.18	11.59	2.53	0.17	99.60
535.6	52.11	51.19	1.78	13.88	11.58	0.17	6.43	11.59	2.50	0.18	100.22
570.2	51.86	51.40	1.82	13.66	11.70	0.20	6.33	11.57	2.46	0.15	99.76
604.9	51.68	51.31	1.76	13.63	11.89	0.11	6.41	11.53	2.48	0.18	99.67
639.5	51.77	51.07	1.92	13.60	11.82	0.21	6.48	11.52	2.53	0.16	100.00
674.1	51.72	51.14	1.81	13.56	11.88	0.21	6.58	11.49	2.48	0.16	99.88
708.6	51.67	51.52	1.80	13.38	11.83	0.20	6.56	11.37	2.47	0.17	99.45
743.3	51.75	51.30	1.69	13.37	11.84	0.27	6.75	11.40	2.53	0.17	99.75
777.9	51.87	51.18	1.87	13.48	11.92	0.22	6.58	11.37	2.50	0.18	100.00
812.5	51.54	51.23	1.91	13.49	11.93	0.18	6.57	11.32	2.52	0.16	99.61
812.5	52.04	51.01	1.88	13.72	11.89	0.16	6.74	11.33	2.41	0.16	100.32

864.3	51.85	51.11	1.82	13.49	12.05	0.23	6.73	11.22	2.48	0.16	100.04
916.1	51.96	51.45	1.85	13.40	11.91	0.20	6.53	11.27	2.51	0.18	99.81
967.8	51.63	51.07	1.93	13.51	12.05	0.20	6.65	11.15	2.55	0.17	99.85
1019.6	51.63	51.26	1.84	13.38	12.08	0.19	6.65	11.15	2.58	0.17	99.67
1071.4	51.63	51.35	1.79	13.41	12.08	0.22	6.63	11.08	2.58	0.16	99.58
1123.2	51.54	51.25	1.88	13.47	12.01	0.21	6.63	11.08	2.59	0.18	99.59
1175.0	51.42	51.14	1.86	13.34	12.16	0.23	6.75	11.05	2.58	0.18	99.58
1226.7	51.35	51.16	1.83	13.37	12.12	0.24	6.73	11.09	2.58	0.17	99.49
1278.5	51.46	51.44	1.87	13.33	11.88	0.18	6.73	11.05	2.63	0.18	99.32
1330.3	51.17	51.21	1.81	13.49	12.16	0.19	6.61	11.07	2.58	0.18	99.26
1382.1	51.32	51.29	1.87	13.41	12.09	0.19	6.70	10.97	2.61	0.18	99.33
1433.9	51.49	51.22	1.86	13.38	12.13	0.16	6.70	11.03	2.63	0.19	99.57
1485.6	51.52	51.19	1.88	13.41	12.18	0.14	6.76	10.93	2.62	0.18	99.63
1537.4	51.70	51.31	1.75	13.37	12.23	0.24	6.67	10.97	2.59	0.17	99.69
1589.2	51.26	51.09	1.90	13.33	12.37	0.21	6.68	10.98	2.58	0.16	99.47
11.5	46.69	46.15	0.88	23.66	8.55	0.09	4.49	12.73	2.62	0.13	99.84
17.0	46.88	46.30	0.87	23.43	8.61	0.21	4.41	12.78	2.56	0.13	99.87
22.5	47.06	46.69	0.88	23.32	8.50	0.11	4.54	12.65	2.48	0.13	99.67
22.5	47.05	46.17	0.96	23.55	8.61	0.13	4.53	12.72	2.50	0.15	100.18
37.7	47.54	46.56	0.96	22.96	8.73	0.13	4.60	12.68	2.55	0.14	100.28
52.9	47.71	47.08	1.04	22.25	8.74	0.16	4.69	12.62	2.58	0.14	99.92
68.1	48.21	47.47	1.08	21.75	8.85	0.15	4.78	12.50	2.55	0.15	100.04
83.3	48.35	47.92	1.07	21.13	9.07	0.15	4.81	12.45	2.57	0.14	99.73
98.5	48.77	47.99	1.19	20.94	9.05	0.15	4.81	12.42	2.62	0.14	100.08
113.7	49.02	48.40	1.16	20.30	9.23	0.17	4.96	12.34	2.59	0.15	99.93
128.9	49.24	48.63	1.31	19.94	9.20	0.19	4.97	12.33	2.59	0.15	99.91
144.1	49.77	49.10	1.33	19.50	9.27	0.17	5.01	12.17	2.61	0.15	99.97
159.3	49.60	48.99	1.35	19.12	9.51	0.19	5.10	12.25	2.64	0.16	99.92
174.5	49.76	49.28	1.34	18.76	9.62	0.19	5.26	12.11	2.61	0.13	99.78
189.7	50.21	49.69	1.43	18.12	9.77	0.16	5.26	12.12	2.61	0.16	99.82
204.8	50.24	49.65	1.48	17.98	9.79	0.24	5.38	12.00	2.63	0.16	99.89
220.0	50.70	49.96	1.49	17.53	9.96	0.18	5.39	12.02	2.63	0.16	100.05
235.2	50.57	50.41	1.48	17.07	9.93	0.19	5.48	11.95	2.64	0.16	99.46
250.4	50.67	50.27	1.51	16.88	10.19	0.17	5.53	11.98	2.61	0.16	99.70
250.4	51.02	50.39	1.49	16.98	10.19	0.19	5.54	11.91	2.45	0.16	99.93
284.5	50.99	50.54	1.64	16.18	10.39	0.19	5.69	11.87	2.64	0.15	99.75
318.6	51.36	50.73	1.64	15.64	10.69	0.18	5.85	11.81	2.59	0.17	99.93
352.7	51.51	51.05	1.77	15.07	10.77	0.20	5.96	11.77	2.57	0.16	99.76
386.8	51.70	51.08	1.73	14.85	11.11	0.13	5.95	11.76	2.52	0.17	99.93
421.0	51.48	51.16	1.78	14.55	11.17	0.16	6.13	11.68	2.51	0.16	99.62
455.1	51.40	51.42	1.77	14.20	11.16	0.22	6.20	11.67	2.52	0.14	99.28

489.1	51.31	51.20	1.78	14.15	11.42	0.18	6.31	11.62	2.46	0.16	99.40
523.2	51.99	51.44	1.73	13.89	11.41	0.26	6.32	11.60	2.50	0.15	99.86
557.3	51.51	51.58	1.77	13.69	11.50	0.24	6.26	11.60	2.50	0.17	99.23
591.4	51.81	51.28	1.85	13.55	11.74	0.19	6.56	11.44	2.52	0.18	99.83
625.5	51.84	51.25	1.85	13.69	11.69	0.19	6.53	11.48	2.47	0.16	99.89
659.6	51.88	51.27	1.83	13.56	11.86	0.16	6.51	11.49	2.44	0.17	99.91
693.7	51.95	51.27	1.87	13.45	11.81	0.17	6.60	11.48	2.51	0.15	99.98
727.9	51.89	51.31	1.84	13.54	11.75	0.18	6.61	11.44	2.47	0.16	99.88
761.9	51.87	51.11	1.76	13.48	11.87	0.24	6.72	11.40	2.55	0.17	100.06
796.0	51.88	51.31	1.88	13.48	11.86	0.24	6.53	11.33	2.50	0.16	99.87
830.1	51.75	50.94	1.94	13.34	12.10	0.22	6.67	11.39	2.53	0.18	100.11
864.2	51.49	51.40	1.77	13.48	11.90	0.14	6.61	11.30	2.53	0.16	99.39
864.2	52.58	51.31	1.78	13.52	11.89	0.22	6.66	11.36	2.37	0.18	100.57
913.7	52.29	51.46	1.84	13.52	11.79	0.20	6.54	11.22	2.55	0.18	100.13
963.2	52.35	51.44	1.84	13.34	12.00	0.19	6.60	11.18	2.54	0.17	100.22
1012.6	52.10	51.20	1.92	13.49	11.84	0.29	6.60	11.23	2.53	0.19	100.20
1062.1	51.95	51.29	1.83	13.26	11.84	0.27	6.86	11.19	2.57	0.19	99.96
1111.6	52.11	51.27	1.76	13.39	12.18	0.20	6.65	11.09	2.58	0.18	100.14
1161.1	52.17	51.33	1.77	13.42	12.08	0.23	6.69	11.01	2.58	0.18	100.14
1210.6	52.07	51.46	1.85	13.36	12.01	0.22	6.62	11.03	2.58	0.17	99.91
1260.1	52.00	51.15	1.88	13.46	12.04	0.23	6.74	11.02	2.61	0.17	100.15
1309.5	51.92	51.30	1.90	13.35	12.11	0.25	6.68	10.98	2.56	0.17	99.92
1359.0	52.08	51.06	1.84	13.48	12.20	0.20	6.71	11.03	2.61	0.17	100.32
1408.5	52.12	51.26	1.89	13.38	12.09	0.25	6.66	10.99	2.61	0.17	100.15
1458.0	52.05	51.20	1.92	13.33	12.19	0.19	6.73	10.94	2.64	0.17	100.16
1507.5	51.92	51.22	1.82	13.51	12.09	0.18	6.77	10.95	2.58	0.18	99.99
1556.9	51.82	51.36	1.81	13.38	12.03	0.23	6.70	11.00	2.62	0.17	99.76
6.8	46.91	46.00	0.87	23.67	8.64	0.18	4.59	12.43	2.77	0.16	100.21
11.8	47.18	46.29	0.93	23.50	8.45	0.18	4.50	12.70	2.61	0.13	100.19
16.8	47.18	46.01	0.94	23.80	8.45	0.15	4.52	12.75	2.55	0.14	100.47
21.8	47.13	46.65	0.90	23.26	8.45	0.21	4.48	12.65	2.57	0.14	99.78
21.8	47.30	46.40	0.95	23.49	8.45	0.13	4.58	12.71	2.48	0.11	100.20
37.6	47.37	46.60	0.92	22.92	8.66	0.18	4.56	12.75	2.58	0.13	100.07
53.4	47.56	46.98	0.93	22.43	8.73	0.19	4.73	12.61	2.56	0.14	99.88
69.3	47.88	47.39	1.07	21.92	8.90	0.10	4.70	12.55	2.56	0.13	99.80
85.0	48.25	47.60	1.17	21.30	8.99	0.15	4.83	12.48	2.63	0.15	99.94
100.8	48.60	47.70	1.20	20.86	9.22	0.15	4.89	12.50	2.63	0.15	100.20
116.6	49.03	48.08	1.20	20.58	9.17	0.16	4.99	12.42	2.56	0.13	100.25
132.5	49.11	48.56	1.26	19.89	9.30	0.15	5.01	12.34	2.65	0.15	99.86
148.3	49.28	49.02	1.30	19.40	9.29	0.20	5.07	12.29	2.57	0.16	99.56
164.1	49.64	49.29	1.26	19.02	9.43	0.16	5.21	12.20	2.58	0.15	99.65

179.9	50.12	49.42	1.37	18.70	9.63	0.16	5.14	12.11	2.61	0.16	100.01
195.8	50.11	49.56	1.47	18.28	9.69	0.19	5.24	12.12	2.62	0.15	99.85
211.6	50.26	50.03	1.41	17.77	9.86	0.24	5.23	11.99	2.61	0.16	99.53
227.4	50.26	49.84	1.52	17.60	10.00	0.20	5.39	11.95	2.64	0.15	99.72
243.2	50.64	50.29	1.44	17.12	10.08	0.20	5.46	11.96	2.61	0.14	99.65
259.1	50.58	50.16	1.56	16.87	10.22	0.20	5.56	11.97	2.62	0.16	99.73
274.9	50.68	50.35	1.52	16.59	10.37	0.21	5.62	11.88	2.59	0.18	99.64
290.7	50.97	50.77	1.55	16.00	10.55	0.18	5.65	11.85	2.61	0.15	99.50
290.7	51.27	50.50	1.60	16.28	10.50	0.16	5.69	11.95	2.46	0.16	100.07
326.5	51.36	50.57	1.67	15.63	10.75	0.19	5.92	11.83	2.57	0.18	100.09
362.2	51.61	51.20	1.70	15.10	10.70	0.16	6.00	11.74	2.52	0.17	99.71
398.0	51.65	51.10	1.81	14.76	11.04	0.20	5.98	11.73	2.54	0.15	99.85
433.9	51.67	51.04	1.87	14.49	11.15	0.23	6.09	11.73	2.54	0.16	99.94
469.7	51.86	51.21	1.79	14.22	11.37	0.18	6.28	11.61	2.50	0.15	99.94
505.5	52.17	51.30	1.82	13.94	11.36	0.21	6.42	11.59	2.52	0.14	100.17
541.3	51.83	51.50	1.84	13.80	11.42	0.20	6.36	11.55	2.48	0.16	99.63
577.1	51.87	51.42	1.91	13.61	11.67	0.21	6.34	11.50	2.49	0.16	99.74
612.8	51.74	51.13	1.82	13.77	11.80	0.16	6.56	11.43	2.49	0.15	99.91
648.6	51.96	51.26	1.87	13.56	11.76	0.23	6.54	11.40	2.51	0.17	99.99
684.4	52.03	51.21	1.77	13.56	11.89	0.22	6.52	11.43	2.54	0.16	100.11
720.3	52.04	51.41	1.78	13.53	11.84	0.13	6.54	11.37	2.53	0.17	99.93
756.1	52.12	51.48	1.76	13.41	11.91	0.23	6.56	11.29	2.51	0.15	99.94
791.9	52.13	51.47	1.76	13.36	11.81	0.20	6.65	11.33	2.53	0.18	99.96
827.7	52.15	51.47	1.85	13.39	11.74	0.22	6.63	11.35	2.49	0.17	99.99
863.5	51.86	51.34	1.81	13.47	12.03	0.15	6.56	11.23	2.53	0.18	99.82
863.5	52.32	51.40	1.85	13.60	11.82	0.19	6.57	11.27	2.42	0.17	100.22
912.7	52.25	51.22	1.91	13.50	11.92	0.19	6.63	11.26	2.50	0.17	100.33
962.0	52.27	51.24	1.90	13.38	12.03	0.15	6.62	11.24	2.58	0.18	100.33
1011.3	52.23	51.26	1.84	13.36	12.06	0.27	6.58	11.21	2.55	0.17	100.27
1060.5	52.04	51.15	1.94	13.43	11.94	0.25	6.71	11.17	2.53	0.18	100.19
1109.8	51.96	51.08	1.89	13.39	12.09	0.21	6.77	11.17	2.55	0.15	100.18
1159.0	51.95	51.24	1.78	13.47	12.00	0.25	6.70	11.11	2.57	0.18	100.00
1208.3	51.89	51.25	1.85	13.45	12.05	0.23	6.62	11.11	2.58	0.17	99.95
1257.6	52.01	51.25	1.88	13.39	11.99	0.22	6.72	11.06	2.61	0.20	100.06
1306.9	52.09	51.24	1.98	13.37	12.10	0.20	6.70	10.97	2.58	0.16	100.14
1356.2	52.23	51.10	1.92	13.43	12.13	0.23	6.68	11.00	2.62	0.19	100.44
1405.4	52.01	51.48	1.80	13.43	12.08	0.21	6.61	10.94	2.58	0.18	99.83
1454.6	52.02	51.11	1.76	13.48	12.23	0.24	6.70	10.97	2.62	0.18	100.20
1503.9	52.06	51.24	1.89	13.42	12.06	0.18	6.72	10.96	2.63	0.19	100.12
1553.2	52.08	51.34	1.74	13.39	12.15	0.17	6.79	10.96	2.58	0.18	100.03

Exp 228

x / μm	Oxides (wt%)										
	SiO2	SiO2*	TiO2	Al2O3	FeO	MnO	MgO	CaO	Na2O	K2O	Total
12.5	46.09	44.66	0.76	25.78	7.92	0.17	4.14	12.95	2.81	0.12	100.73
17.9	46.56	45.59	0.79	24.96	7.91	0.13	4.24	12.91	2.64	0.14	100.27
23.3	47.01	45.78	0.91	24.35	8.09	0.13	4.30	12.93	2.69	0.14	100.53
28.7	47.63	46.45	0.96	23.54	8.29	0.10	4.37	12.78	2.67	0.14	100.48
28.7	47.46	46.49	0.94	23.57	8.27	0.13	4.39	12.78	2.61	0.13	100.27
44.5	48.73	47.66	1.19	21.49	8.79	0.16	4.73	12.46	2.67	0.16	100.37
60.3	49.81	49.13	1.30	19.47	9.27	0.16	4.99	12.17	2.65	0.15	99.99
76.0	50.74	50.13	1.52	17.57	9.90	0.15	5.26	11.97	2.64	0.17	99.91
91.8	51.34	50.70	1.66	16.24	10.25	0.14	5.59	11.90	2.66	0.17	99.94
107.6	51.58	50.76	1.65	15.47	10.84	0.20	5.92	11.73	2.56	0.16	100.12
123.4	51.52	50.84	1.78	14.73	11.20	0.26	6.07	11.70	2.56	0.16	99.99
139.1	51.65	50.98	1.80	14.27	11.47	0.18	6.24	11.59	2.59	0.19	99.97
154.9	51.53	51.09	1.83	13.95	11.57	0.23	6.44	11.50	2.54	0.16	99.74
170.7	51.63	50.64	1.90	13.98	11.88	0.20	6.52	11.48	2.53	0.16	100.30
170.7	51.17	50.77	1.84	13.95	11.85	0.22	6.47	11.49	2.53	0.17	99.70
196.1	50.98	51.19	1.79	13.68	11.92	0.16	6.53	11.32	2.55	0.17	99.09
221.4	51.20	50.53	1.79	13.77	12.17	0.19	6.81	11.24	2.60	0.19	99.97
246.8	50.85	50.53	1.86	13.72	12.33	0.24	6.73	11.12	2.61	0.16	99.62
272.1	51.02	50.73	1.80	13.66	12.36	0.21	6.76	10.99	2.61	0.18	99.59
297.5	51.11	50.51	1.89	13.74	12.27	0.23	6.81	11.01	2.65	0.18	99.90
322.8	51.27	50.60	1.84	13.73	12.39	0.19	6.74	11.03	2.62	0.18	99.97
348.2	51.08	50.73	1.72	13.76	12.30	0.22	6.74	10.93	2.72	0.18	99.65
373.5	51.22	50.56	1.83	13.65	12.47	0.20	6.69	10.96	2.76	0.17	99.95
398.9	51.11	50.74	1.88	13.61	12.30	0.20	6.74	10.96	2.70	0.17	99.67
424.2	51.01	50.73	1.85	13.64	12.35	0.23	6.73	10.86	2.73	0.18	99.58
449.6	51.00	50.80	1.83	13.59	12.38	0.24	6.68	10.87	2.73	0.18	99.50
474.9	50.83	50.67	1.82	13.64	12.45	0.17	6.80	10.84	2.72	0.19	99.45
500.3	50.80	50.77	1.84	13.57	12.36	0.20	6.80	10.85	2.73	0.18	99.33
525.6	50.98	50.74	1.92	13.64	12.33	0.19	6.68	10.90	2.74	0.18	99.54
551.0	50.97	50.81	1.84	13.55	12.34	0.23	6.73	10.83	2.79	0.18	99.45
576.3	51.19	50.29	1.90	13.64	12.53	0.27	6.81	10.88	2.80	0.19	100.21
601.7	51.22	50.42	1.88	13.66	12.50	0.21	6.80	10.88	2.77	0.17	100.10
6.8	45.22	44.51	0.67	25.95	8.00	0.13	4.32	12.38	3.20	0.16	100.01
12.6	45.83	45.42	0.75	25.33	7.77	0.10	4.13	12.95	2.73	0.12	99.70
18.4	46.69	45.62	0.76	24.87	7.96	0.17	4.29	12.88	2.62	0.12	100.37
24.2	47.07	45.98	0.95	24.12	8.14	0.09	4.36	12.86	2.66	0.13	100.39
30.0	47.51	46.59	0.98	23.33	8.38	0.16	4.37	12.71	2.64	0.15	100.22
30.0	47.51	46.78	0.89	23.24	8.30	0.14	4.41	12.75	2.65	0.15	100.04
42.5	48.39	47.82	1.13	21.51	8.68	0.17	4.64	12.54	2.67	0.15	99.87
55.0	49.52	48.88	1.23	19.81	9.16	0.10	4.93	12.33	2.70	0.16	99.94

67.5	50.09	49.71	1.39	18.37	9.47	0.12	5.19	12.20	2.69	0.15	99.67
80.0	51.00	50.25	1.56	17.08	9.95	0.17	5.42	12.04	2.68	0.15	100.05
92.5	51.04	50.58	1.67	16.22	10.23	0.19	5.63	11.97	2.65	0.16	99.76
105.0	51.01	50.99	1.66	15.29	10.71	0.19	5.84	11.85	2.62	0.16	99.32
117.5	51.32	50.88	1.77	14.91	11.03	0.23	5.98	11.74	2.61	0.16	99.74
130.0	51.52	51.08	1.73	14.45	11.36	0.19	6.12	11.64	2.56	0.17	99.75
142.5	51.34	50.94	1.84	14.13	11.59	0.16	6.26	11.63	2.60	0.14	99.70
155.0	51.37	50.74	1.80	14.03	11.83	0.20	6.34	11.63	2.54	0.19	99.94
155.0	51.26	50.60	1.93	14.05	11.80	0.20	6.41	11.59	2.53	0.19	99.96
184.3	51.18	50.68	1.91	13.68	11.98	0.23	6.63	11.45	2.55	0.18	99.79
213.6	51.07	50.64	1.87	13.66	12.04	0.26	6.72	11.37	2.55	0.18	99.73
242.8	50.86	50.52	1.90	13.64	12.24	0.28	6.73	11.23	2.58	0.18	99.65
272.1	51.12	50.49	1.88	13.65	12.36	0.24	6.71	11.15	2.66	0.17	99.93
301.4	51.21	50.57	1.90	13.73	12.24	0.25	6.72	11.09	2.61	0.20	99.94
330.7	51.02	50.68	1.82	13.62	12.43	0.19	6.69	11.03	2.65	0.18	99.64
359.9	50.97	50.73	1.81	13.67	12.35	0.21	6.75	10.93	2.66	0.19	99.53
389.2	50.96	50.61	1.85	13.64	12.48	0.22	6.72	10.88	2.71	0.20	99.65
418.5	50.92	50.69	1.98	13.67	12.24	0.25	6.66	10.94	2.69	0.19	99.53
447.8	50.84	50.59	1.87	13.69	12.41	0.25	6.72	10.87	2.71	0.19	99.55
477.1	50.95	50.57	1.92	13.65	12.33	0.16	6.78	10.95	2.73	0.20	99.68
506.3	51.00	50.47	1.84	13.64	12.51	0.19	6.81	10.90	2.74	0.18	99.83
535.6	50.83	50.71	1.88	13.61	12.37	0.20	6.75	10.89	2.71	0.19	99.42
564.9	51.02	50.73	1.71	13.74	12.43	0.19	6.71	10.85	2.77	0.19	99.60
594.2	51.08	50.55	1.86	13.77	12.30	0.24	6.71	10.91	2.77	0.20	99.83
623.4	50.96	50.67	1.87	13.55	12.37	0.23	6.75	10.91	2.76	0.18	99.59
652.7	51.06	50.72	1.86	13.72	12.30	0.23	6.64	10.87	2.77	0.19	99.65
682.0	50.87	50.64	1.84	13.70	12.39	0.18	6.76	10.85	2.76	0.19	99.54
7.6	45.68	44.76	0.74	26.05	7.71	0.11	4.09	12.73	2.99	0.12	100.22
13.6	46.20	45.04	0.75	25.55	7.92	0.09	4.07	13.04	2.70	0.14	100.47
19.6	46.54	45.77	0.84	24.58	8.07	0.09	4.22	12.94	2.66	0.13	100.07
25.6	47.14	46.23	0.90	23.85	8.30	0.13	4.25	12.87	2.65	0.13	100.21
25.6	46.82	46.18	0.97	23.95	8.18	0.17	4.31	12.76	2.64	0.14	99.94
37.5	48.00	47.19	0.97	22.43	8.53	0.20	4.54	12.66	2.63	0.14	100.11
49.4	49.03	48.31	1.16	20.74	8.91	0.20	4.76	12.40	2.67	0.16	100.02
61.3	49.77	48.95	1.37	19.39	9.37	0.17	5.01	12.23	2.64	0.16	100.12
73.2	50.34	49.55	1.62	18.07	9.72	0.19	5.23	12.09	2.65	0.17	100.09
85.1	50.57	50.19	1.60	16.99	10.07	0.16	5.49	11.99	2.65	0.16	99.67
97.0	51.11	50.49	1.56	16.13	10.60	0.20	5.68	11.85	2.63	0.16	99.92
108.9	51.20	50.39	1.72	15.37	11.05	0.19	5.96	11.87	2.58	0.16	100.11
120.8	51.13	50.67	1.91	14.79	11.16	0.12	6.12	11.79	2.57	0.17	99.76
132.7	51.17	50.68	1.83	14.49	11.37	0.18	6.24	11.79	2.57	0.15	99.80
144.6	51.18	50.43	1.83	14.32	11.78	0.23	6.33	11.66	2.55	0.17	100.05
144.6	51.19	50.71	1.79	14.26	11.63	0.25	6.27	11.73	2.50	0.17	99.78

180.2	51.26	50.55	1.85	13.84	12.07	0.23	6.54	11.51	2.54	0.16	100.01
215.8	50.95	50.60	1.79	13.69	12.35	0.19	6.61	11.33	2.58	0.17	99.65
251.4	51.14	50.68	1.87	13.67	12.40	0.21	6.63	11.14	2.53	0.18	99.77
287.0	50.91	50.74	1.87	13.63	12.39	0.15	6.70	11.08	2.57	0.17	99.47
322.7	50.91	50.79	1.86	13.69	12.29	0.20	6.70	11.03	2.59	0.16	99.42
358.3	51.50	50.28	1.81	13.63	12.57	0.24	6.76	11.14	2.69	0.19	100.52
393.9	51.11	50.74	1.89	13.55	12.45	0.19	6.66	10.98	2.66	0.19	99.67
429.5	51.14	50.51	1.82	13.76	12.36	0.27	6.75	10.97	2.66	0.19	99.93
465.1	51.49	50.38	1.81	13.65	12.60	0.25	6.77	10.94	2.72	0.17	100.41
500.7	51.50	50.54	1.80	13.69	12.59	0.20	6.72	10.90	2.66	0.20	100.26
536.3	51.33	50.28	1.87	13.74	12.49	0.30	6.80	10.89	2.73	0.20	100.36
571.9	51.44	50.49	1.91	13.67	12.42	0.25	6.77	10.92	2.70	0.18	100.26
607.5	51.62	50.43	1.84	13.66	12.54	0.21	6.84	10.88	2.69	0.20	100.49
643.2	51.64	50.41	1.82	13.61	12.64	0.21	6.74	10.98	2.74	0.17	100.53
678.8	51.31	50.48	1.88	13.62	12.44	0.24	6.77	10.94	2.74	0.18	100.13
714.4	51.56	50.49	1.78	13.63	12.56	0.19	6.87	10.88	2.72	0.19	100.37
750.0	51.52	50.58	1.89	13.56	12.39	0.24	6.76	10.97	2.75	0.17	100.24
785.6	51.58	50.36	1.91	13.66	12.58	0.22	6.73	10.94	2.73	0.17	100.52

Exp 233

x / μm	Oxides (wt%)										
	SiO2	SiO2*	TiO2	Al2O3	FeO	MnO	MgO	CaO	Na2O	K2O	Total
8.7	45.41	44.44	0.67	26.60	7.46	0.14	3.98	13.00	2.88	0.13	100.28
15.9	45.67	45.38	0.64	25.90	7.44	0.12	3.93	13.20	2.58	0.11	99.59
23.2	45.87	45.13	0.72	25.72	7.69	0.14	3.97	13.23	2.56	0.13	100.04
30.4	46.25	45.19	0.70	25.47	7.75	0.13	4.19	13.22	2.52	0.13	100.36
30.4	46.32	45.35	0.81	25.39	7.72	0.18	4.10	13.15	2.47	0.13	100.26
45.8	46.85	45.88	0.87	24.50	8.05	0.11	4.19	13.04	2.52	0.13	100.27
61.2	47.50	46.54	0.84	23.73	8.04	0.15	4.36	12.96	2.53	0.13	100.25
76.6	47.95	47.32	0.98	22.62	8.24	0.15	4.49	12.83	2.53	0.14	99.93
91.9	48.72	47.55	1.08	21.98	8.49	0.18	4.67	12.64	2.57	0.14	100.47
107.3	49.30	48.02	1.13	21.10	8.76	0.17	4.81	12.56	2.59	0.16	100.59
122.7	49.71	48.90	1.21	20.17	8.84	0.12	4.81	12.50	2.60	0.16	100.12
138.1	50.13	49.01	1.29	19.48	9.16	0.14	5.07	12.34	2.66	0.15	100.42
153.5	50.70	49.29	1.49	18.71	9.38	0.16	5.18	12.29	2.65	0.16	100.71
168.9	51.10	49.89	1.39	18.00	9.69	0.17	5.23	12.18	2.60	0.15	100.51
184.2	51.30	50.38	1.48	17.40	9.72	0.13	5.31	12.15	2.55	0.17	100.22
199.6	51.46	50.33	1.61	16.92	10.08	0.17	5.40	12.07	2.56	0.16	100.42
215.0	51.67	50.75	1.59	16.36	10.23	0.16	5.54	11.93	2.57	0.17	100.22
230.4	51.56	50.54	1.71	16.04	10.46	0.18	5.75	11.94	2.53	0.15	100.32
230.4	51.81	50.85	1.60	16.02	10.36	0.18	5.74	11.99	2.40	0.16	100.26
254.9	52.01	50.83	1.69	15.48	10.53	0.24	5.96	11.86	2.55	0.15	100.47
279.5	51.97	50.70	1.66	15.12	10.97	0.18	6.09	11.87	2.53	0.16	100.56
304.0	51.95	51.02	1.71	14.65	11.15	0.17	6.14	11.81	2.50	0.16	100.23
328.5	51.97	50.90	1.78	14.47	11.29	0.15	6.27	11.82	2.45	0.17	100.38
353.1	51.84	50.88	1.88	14.16	11.33	0.19	6.39	11.76	2.52	0.17	100.26
377.6	52.08	50.97	1.81	14.01	11.66	0.20	6.40	11.61	2.47	0.17	100.41
402.1	52.06	50.76	1.85	14.01	11.76	0.21	6.47	11.62	2.47	0.15	100.59
426.7	52.04	50.96	1.78	13.77	11.83	0.19	6.51	11.62	2.48	0.16	100.38
451.2	51.96	50.95	1.84	13.78	11.74	0.19	6.54	11.60	2.49	0.17	100.31
475.7	51.98	51.05	1.81	13.63	11.86	0.21	6.60	11.50	2.48	0.16	100.23
500.3	52.10	51.01	1.86	13.62	11.91	0.22	6.61	11.41	2.50	0.17	100.40
524.8	52.08	50.89	1.78	13.66	11.97	0.22	6.68	11.44	2.49	0.16	100.49
549.3	52.09	50.84	1.88	13.64	12.09	0.17	6.63	11.37	2.52	0.17	100.55
573.9	51.94	50.80	1.88	13.58	12.08	0.19	6.69	11.40	2.50	0.18	100.45
598.4	51.90	50.97	1.81	13.64	12.02	0.22	6.64	11.32	2.51	0.17	100.22
598.4	51.68	50.91	1.92	13.54	12.06	0.21	6.67	11.35	2.47	0.17	100.07
640.9	51.70	51.03	1.83	13.52	12.05	0.21	6.66	11.32	2.52	0.17	99.97
683.2	51.62	50.92	1.83	13.52	12.14	0.21	6.75	11.23	2.53	0.18	100.01
725.7	51.53	50.94	1.82	13.47	12.22	0.27	6.64	11.22	2.54	0.18	99.89
768.1	51.75	51.12	1.85	13.40	12.20	0.19	6.69	11.14	2.54	0.16	99.93
810.6	51.45	50.80	1.90	13.52	12.22	0.22	6.84	11.04	2.59	0.17	99.94

853.0	51.58	50.99	1.77	13.48	12.28	0.24	6.68	11.11	2.59	0.16	99.89
895.5	51.73	50.86	1.83	13.58	12.23	0.20	6.84	11.00	2.57	0.20	100.17
937.9	51.52	50.62	1.92	13.52	12.35	0.27	6.79	11.08	2.58	0.17	100.20
980.4	51.68	50.74	1.82	13.55	12.32	0.20	6.92	10.96	2.59	0.19	100.24
1022.8	51.67	50.91	1.89	13.56	12.20	0.23	6.83	10.93	2.58	0.18	100.06
1065.3	51.56	50.85	1.80	13.60	12.24	0.17	6.85	11.01	2.60	0.18	100.01
1107.7	51.51	50.88	1.85	13.54	12.20	0.22	6.80	11.04	2.60	0.17	99.93
1150.2	51.50	51.00	1.88	13.53	12.10	0.18	6.88	10.94	2.63	0.17	99.80
1192.6	51.65	50.75	1.90	13.58	12.25	0.19	6.89	10.95	2.62	0.18	100.20
1235.1	51.87	50.92	1.88	13.45	12.29	0.18	6.91	10.86	2.62	0.19	100.25
1277.5	51.38	50.49	1.84	13.66	12.35	0.31	6.89	10.97	2.62	0.17	100.19
1320.0	51.96	50.68	1.84	13.65	12.31	0.17	6.92	10.91	2.64	0.18	100.59
1362.4	51.79	50.43	1.89	13.67	12.39	0.21	6.88	10.98	2.65	0.19	100.66
1404.9	51.38	50.71	1.81	13.53	12.30	0.22	6.82	11.10	2.63	0.18	99.98
1447.3	51.46	50.82	1.89	13.47	12.19	0.26	6.83	11.02	2.64	0.18	99.94
7.4	46.41	45.72	0.51	27.48	6.28	0.06	3.38	13.47	2.29	0.12	99.99
13.8	46.10	44.44	0.69	27.01	7.15	0.15	3.66	13.81	2.30	0.10	100.96
20.2	45.88	44.86	0.71	26.06	7.71	0.11	4.02	13.15	2.56	0.12	100.32
26.6	46.16	45.00	0.73	25.87	7.70	0.15	4.09	13.12	2.51	0.13	100.46
33.0	46.32	45.45	0.77	25.24	7.81	0.14	4.14	13.10	2.52	0.12	100.16
33.0	46.67	45.60	0.70	25.45	7.59	0.12	4.21	13.10	2.43	0.12	100.37
48.3	47.28	45.88	0.82	24.46	8.07	0.13	4.35	12.93	2.52	0.13	100.70
63.6	47.64	46.38	0.91	23.64	8.29	0.18	4.40	12.81	2.54	0.14	100.56
78.8	48.32	46.93	0.93	22.73	8.46	0.16	4.55	12.80	2.59	0.15	100.69
94.1	48.69	47.70	1.11	21.66	8.59	0.12	4.71	12.68	2.60	0.13	100.28
109.4	49.50	48.45	1.16	20.93	8.65	0.14	4.77	12.52	2.53	0.15	100.35
124.7	49.90	48.76	1.19	20.10	9.04	0.13	4.91	12.38	2.62	0.16	100.45
139.9	49.74	49.05	1.31	19.44	9.17	0.15	5.02	12.38	2.61	0.17	99.99
155.2	50.49	49.65	1.32	18.64	9.45	0.16	5.09	12.22	2.60	0.17	100.13
170.5	50.99	50.04	1.42	17.98	9.56	0.20	5.29	12.04	2.63	0.15	100.25
185.8	50.87	50.12	1.53	17.38	9.89	0.21	5.31	12.11	2.58	0.17	100.06
201.1	51.27	50.39	1.61	16.81	10.15	0.15	5.49	11.94	2.60	0.16	100.17
216.3	51.45	50.65	1.54	16.41	10.32	0.14	5.61	11.93	2.53	0.17	100.10
231.6	51.64	50.76	1.59	15.92	10.45	0.23	5.74	11.88	2.55	0.19	100.18
246.9	51.79	50.69	1.62	15.64	10.65	0.25	5.81	11.92	2.56	0.16	100.40
262.2	51.75	50.69	1.64	15.31	10.91	0.21	5.98	11.88	2.53	0.16	100.36
277.4	51.87	50.91	1.74	15.01	10.88	0.19	6.04	11.84	2.52	0.16	100.26
292.7	51.82	50.76	1.73	14.74	11.14	0.26	6.13	11.84	2.54	0.16	100.36
308.0	51.71	51.00	1.73	14.57	11.17	0.17	6.20	11.78	2.52	0.17	100.01
308.0	51.80	51.28	1.71	14.54	11.15	0.16	6.24	11.72	2.32	0.18	99.83
339.2	51.92	50.92	1.78	14.44	11.40	0.18	6.28	11.68	2.47	0.16	100.31
370.4	51.74	50.93	1.79	14.08	11.50	0.23	6.41	11.71	2.49	0.15	100.12
401.5	51.85	50.84	1.90	13.91	11.69	0.23	6.41	11.65	2.50	0.19	100.31

432.6	51.68	50.79	1.88	13.84	11.73	0.22	6.56	11.62	2.49	0.17	100.20
463.8	51.95	50.90	1.86	13.75	11.86	0.19	6.55	11.54	2.49	0.16	100.34
495.0	51.84	51.02	1.79	13.62	11.97	0.20	6.63	11.43	2.48	0.15	100.11
526.2	51.72	51.04	1.78	13.66	11.99	0.18	6.52	11.48	2.49	0.17	99.98
557.4	51.73	50.82	1.85	13.66	12.09	0.17	6.70	11.38	2.47	0.17	100.21
588.5	51.54	50.98	1.80	13.50	12.14	0.20	6.70	11.32	2.48	0.17	99.86
619.7	51.46	51.03	1.81	13.36	12.20	0.21	6.77	11.30	2.45	0.17	99.73
650.9	51.63	51.16	1.87	13.47	11.97	0.17	6.74	11.22	2.51	0.19	99.77
650.9	51.82	51.20	1.81	13.65	12.10	0.19	6.63	11.13	2.42	0.17	99.92
693.1	51.66	50.78	1.90	13.60	12.25	0.19	6.67	11.20	2.54	0.16	100.19
735.3	51.83	50.62	1.91	13.61	12.20	0.24	6.87	11.15	2.55	0.16	100.51
777.5	51.46	50.90	1.92	13.68	12.18	0.19	6.65	11.09	2.53	0.17	99.87
819.7	51.62	50.97	1.85	13.60	12.10	0.19	6.79	11.11	2.55	0.15	99.95
861.9	51.42	50.86	1.77	13.51	12.30	0.18	6.84	11.08	2.57	0.17	99.86
904.1	51.24	50.71	1.88	13.67	12.20	0.24	6.79	11.04	2.61	0.17	99.83
946.3	51.39	50.81	1.91	13.53	12.24	0.24	6.72	11.10	2.57	0.17	99.88
988.5	51.68	50.99	1.89	13.58	12.18	0.20	6.77	10.94	2.57	0.17	99.98
1030.7	51.74	50.66	1.88	13.61	12.32	0.19	6.83	11.04	2.60	0.17	100.38
1072.9	51.56	50.89	1.75	13.54	12.26	0.21	6.87	10.99	2.62	0.17	99.97
1115.1	52.00	50.68	1.85	13.63	12.41	0.19	6.84	10.91	2.61	0.18	100.62
1157.3	51.62	50.94	1.91	13.54	12.15	0.22	6.83	10.96	2.57	0.17	99.98
1199.5	51.65	50.93	1.87	13.50	12.23	0.16	6.90	10.94	2.60	0.17	100.02
1241.7	51.39	50.72	1.82	13.66	12.36	0.24	6.75	10.97	2.60	0.17	99.97
1283.8	51.76	50.72	1.81	13.61	12.31	0.18	6.86	10.95	2.66	0.19	100.35
1326.0	51.76	51.17	1.81	13.45	12.26	0.26	6.71	10.90	2.58	0.16	99.89
1368.2	51.93	50.49	1.86	13.80	12.35	0.19	6.86	10.96	2.64	0.15	100.74
1410.4	51.83	50.73	1.89	13.43	12.30	0.23	6.95	10.96	2.64	0.18	100.41
1452.6	52.05	50.84	1.87	13.59	12.22	0.27	6.78	10.93	2.62	0.19	100.51
1494.8	52.07	50.65	1.95	13.55	12.21	0.26	6.89	10.95	2.66	0.19	100.72
7.1	45.48	44.38	0.64	26.47	7.19	0.11	3.83	11.96	4.58	0.15	100.39
13.6	45.96	44.88	0.62	26.19	7.61	0.15	3.99	13.14	2.60	0.11	100.37
20.1	45.85	44.78	0.67	26.19	7.64	0.16	4.00	13.17	2.57	0.13	100.37
26.6	46.33	45.12	0.72	25.74	7.73	0.16	4.06	13.13	2.52	0.13	100.51
26.6	46.42	45.32	0.72	25.63	7.68	0.15	4.10	13.11	2.49	0.11	100.41
42.2	46.96	45.72	0.77	24.83	7.99	0.16	4.24	12.94	2.51	0.14	100.54
57.9	47.58	46.38	0.84	23.99	8.17	0.14	4.30	12.81	2.54	0.12	100.50
73.5	48.21	47.01	0.98	22.85	8.35	0.19	4.56	12.69	2.54	0.14	100.50
89.1	48.60	47.44	1.03	22.04	8.60	0.16	4.61	12.70	2.57	0.15	100.46
104.8	49.19	47.87	1.12	21.17	8.80	0.15	4.85	12.53	2.64	0.17	100.62
120.4	49.82	48.44	1.18	20.38	8.97	0.18	4.93	12.46	2.61	0.15	100.68
136.1	49.82	48.78	1.35	19.53	9.32	0.20	4.96	12.40	2.60	0.15	100.34
151.7	50.61	49.48	1.35	18.76	9.37	0.14	5.18	12.23	2.63	0.15	100.43
167.3	51.17	49.79	1.50	18.10	9.63	0.16	5.18	12.12	2.64	0.17	100.68

183.0	51.44	50.08	1.49	17.55	9.68	0.21	5.44	12.08	2.59	0.17	100.66
198.6	51.63	50.32	1.58	16.99	9.99	0.16	5.47	12.04	2.59	0.16	100.60
198.6	51.24	50.26	1.47	17.16	10.06	0.16	5.47	12.03	2.52	0.17	100.28
224.2	51.72	50.44	1.63	16.30	10.39	0.20	5.71	11.89	2.59	0.15	100.59
249.7	51.89	50.64	1.77	15.68	10.59	0.17	5.80	11.96	2.54	0.16	100.55
275.3	52.02	50.76	1.79	15.17	10.88	0.18	5.96	11.88	2.53	0.15	100.56
300.9	51.65	50.96	1.70	14.78	11.06	0.17	6.03	11.87	2.56	0.16	99.99
326.5	51.86	50.66	1.78	14.61	11.32	0.28	6.17	11.78	2.53	0.17	100.50
351.9	52.05	50.75	1.87	14.38	11.42	0.19	6.34	11.69	2.50	0.15	100.60
377.5	51.83	51.02	1.83	14.10	11.58	0.20	6.25	11.65	2.52	0.16	100.11
403.1	52.00	51.10	1.88	13.99	11.53	0.16	6.38	11.64	2.45	0.16	100.20
428.6	51.83	50.96	1.82	13.86	11.67	0.25	6.48	11.56	2.53	0.17	100.17
454.2	51.81	50.91	1.90	13.84	11.84	0.22	6.45	11.46	2.49	0.17	100.19
479.8	51.70	51.12	1.95	13.79	11.77	0.15	6.47	11.41	2.47	0.16	99.87
505.4	51.84	50.87	1.84	13.65	11.89	0.24	6.69	11.47	2.46	0.18	100.27
530.9	51.58	50.79	1.87	13.65	11.91	0.20	6.82	11.40	2.46	0.18	100.09
556.5	51.66	50.53	1.85	13.82	12.06	0.26	6.69	11.39	2.55	0.16	100.44
556.5	51.12	51.04	1.81	13.70	11.99	0.15	6.58	11.41	2.46	0.17	99.38
597.0	51.43	50.96	1.90	13.57	11.96	0.22	6.77	11.26	2.49	0.18	99.77
637.5	51.45	51.15	1.77	13.56	12.14	0.21	6.61	11.17	2.52	0.17	99.60
677.9	51.56	50.77	1.82	13.62	12.19	0.23	6.80	11.17	2.52	0.18	100.09
718.4	51.14	50.81	1.91	13.60	12.18	0.14	6.77	11.19	2.52	0.17	99.62
758.9	51.41	50.80	1.90	13.63	12.23	0.25	6.74	11.07	2.50	0.18	99.91
799.4	50.83	50.83	1.84	13.62	12.24	0.19	6.76	11.07	2.58	0.18	99.30
839.8	51.31	50.82	1.81	13.48	12.31	0.24	6.76	11.13	2.56	0.18	99.79
880.3	51.21	50.95	1.97	13.49	12.29	0.20	6.70	10.97	2.55	0.18	99.56
920.8	50.40	50.51	1.92	13.64	12.32	0.26	6.83	11.08	2.56	0.18	99.19
961.3	51.00	51.00	1.77	13.49	12.35	0.22	6.78	10.90	2.60	0.19	99.29
1001.8	51.10	51.20	1.72	13.55	12.20	0.20	6.67	10.98	2.59	0.17	99.19
1042.2	50.84	50.81	1.79	13.59	12.36	0.20	6.68	11.06	2.63	0.17	99.32
1082.7	51.02	50.98	1.77	13.64	12.33	0.19	6.71	10.91	2.61	0.17	99.34
1123.2	50.67	51.07	1.84	13.63	12.15	0.22	6.60	10.97	2.62	0.19	98.90
1163.7	50.85	51.04	1.78	13.46	12.32	0.26	6.71	10.95	2.60	0.17	99.11
1204.1	50.75	50.86	1.79	13.57	12.39	0.22	6.72	11.00	2.57	0.17	99.18
1244.5	50.86	50.84	1.93	13.51	12.31	0.18	6.75	10.97	2.62	0.19	99.32
1285.0	50.54	50.80	1.80	13.54	12.37	0.24	6.75	11.01	2.62	0.16	99.05
1325.5	50.86	50.77	1.89	13.54	12.25	0.22	6.83	11.00	2.62	0.17	99.39
1366.0	50.83	50.63	1.87	13.48	12.32	0.29	6.92	10.98	2.61	0.19	99.50
1406.4	50.74	50.96	1.87	13.51	12.29	0.16	6.73	10.98	2.64	0.17	99.08
1446.9	50.98	50.90	1.75	13.63	12.25	0.23	6.74	11.00	2.60	0.20	99.38
1487.4	50.91	50.89	1.89	13.54	12.21	0.23	6.81	10.92	2.64	0.18	99.33

Exp 230

x / μm	Oxides (wt%)										
	SiO2	SiO2*	TiO2	Al2O3	FeO	MnO	MgO	CaO	Na2O	K2O	Total
59.2	44.43	43.88	0.24	30.86	4.40	0.08	2.28	15.47	2.01	0.08	99.85
85.5	45.13	44.40	0.43	29.12	5.29	0.12	2.88	14.91	2.08	0.08	100.03
111.9	46.67	45.82	0.71	26.59	6.14	0.10	3.34	14.34	2.15	0.11	100.15
138.2	48.30	48.04	0.97	23.20	6.97	0.12	3.81	13.78	2.28	0.13	99.56
164.6	50.10	49.55	1.33	20.12	7.97	0.15	4.43	13.27	2.34	0.14	99.85
190.9	51.08	50.72	1.49	17.47	9.06	0.21	4.97	12.85	2.37	0.15	99.66
217.3	51.49	51.28	1.74	15.57	9.90	0.17	5.58	12.57	2.33	0.16	99.51
243.6	51.36	51.31	1.86	14.54	10.64	0.18	5.99	12.33	2.31	0.16	99.35
270.0	51.31	51.10	1.88	13.97	11.24	0.17	6.31	12.18	2.29	0.16	99.51
296.3	51.15	51.02	1.89	13.71	11.58	0.20	6.51	11.92	2.31	0.15	99.43
322.6	51.18	51.04	1.82	13.65	11.89	0.15	6.65	11.58	2.36	0.17	99.44
349.0	51.16	50.70	1.93	13.54	12.03	0.23	6.73	11.55	2.42	0.18	99.76
375.3	51.35	50.86	1.88	13.55	12.08	0.20	6.76	11.32	2.45	0.19	99.79
401.7	51.21	50.90	1.89	13.66	12.14	0.14	6.72	11.21	2.49	0.17	99.61
428.0	50.73	50.62	1.99	13.59	12.23	0.24	6.78	11.09	2.57	0.19	99.42
454.4	51.07	50.81	1.91	13.59	12.16	0.17	6.87	11.04	2.58	0.18	99.57
480.7	50.85	50.69	1.81	13.47	12.33	0.27	6.89	11.01	2.64	0.19	99.46
507.1	50.72	50.69	1.91	13.58	12.34	0.26	6.79	10.92	2.63	0.18	99.33
533.4	50.67	51.20	1.86	13.47	12.22	0.20	6.73	10.82	2.62	0.19	98.78
559.8	50.89	51.00	1.93	13.55	12.22	0.22	6.76	10.80	2.65	0.18	99.19
586.1	50.67	50.85	1.95	13.48	12.30	0.19	6.75	10.92	2.69	0.18	99.13
612.4	50.65	51.06	1.87	13.32	12.28	0.21	6.78	10.90	2.68	0.20	98.89
638.8	50.80	50.92	1.89	13.48	12.29	0.19	6.83	10.80	2.73	0.17	99.18
665.1	50.97	50.87	1.80	13.54	12.25	0.17	6.84	10.97	2.70	0.18	99.40
691.5	50.53	50.95	1.79	13.42	12.24	0.26	6.86	10.92	2.67	0.19	98.89
717.8	50.89	51.22	1.83	13.42	11.79	0.31	6.84	11.00	2.72	0.18	98.97
770.5	51.22	51.07	1.93	13.60	11.47	0.22	7.02	11.05	2.75	0.18	99.44
796.9	50.89	50.90	1.80	13.57	12.20	0.21	6.83	10.89	2.73	0.17	99.29
823.2	51.01	50.90	1.85	13.54	12.26	0.16	6.85	10.83	2.72	0.19	99.41
33.2	43.76	43.37	0.23	31.67	4.20	0.10	1.90	15.78	2.00	0.06	99.70
48.3	43.73	42.92	0.28	30.56	5.59	0.07	2.83	15.35	1.62	0.08	100.11
63.3	44.03	43.98	0.30	30.34	4.68	0.08	2.48	15.35	2.03	0.07	99.35
78.4	44.49	44.12	0.40	29.43	5.17	0.09	2.82	15.10	2.08	0.08	99.67
93.4	45.03	44.71	0.53	28.34	5.64	0.10	2.96	14.81	2.14	0.09	99.62
108.5	46.00	45.49	0.69	26.96	5.98	0.13	3.31	14.47	2.16	0.10	99.80
123.5	46.88	46.68	0.85	25.05	6.50	0.09	3.54	14.22	2.25	0.12	99.50
138.6	47.97	47.62	0.93	23.44	7.02	0.15	3.84	13.84	2.33	0.13	99.65
153.6	49.05	48.77	1.08	21.68	7.54	0.10	4.16	13.50	2.34	0.12	99.58
168.7	49.91	49.60	1.31	19.90	8.12	0.15	4.43	13.23	2.40	0.15	99.61
183.7	50.45	50.26	1.37	18.62	8.60	0.14	4.79	13.01	2.37	0.15	99.49

198.8	50.95	50.91	1.57	17.17	9.08	0.17	5.08	12.81	2.36	0.15	99.35
213.8	51.07	51.13	1.68	16.29	9.57	0.14	5.33	12.62	2.39	0.15	99.24
228.9	51.17	51.18	1.76	15.46	10.05	0.17	5.67	12.54	2.31	0.16	99.29
243.9	51.05	51.29	1.72	14.92	10.46	0.12	5.81	12.47	2.34	0.16	99.05
259.0	51.06	51.40	1.75	14.44	10.78	0.19	6.03	12.26	2.30	0.13	98.96
274.0	50.76	51.24	1.82	14.18	11.03	0.23	6.17	12.19	2.29	0.15	98.81
289.1	50.87	51.11	1.86	13.95	11.30	0.20	6.38	12.02	2.33	0.16	99.06
289.1	50.90	51.03	1.89	14.00	11.36	0.18	6.29	12.12	2.29	0.14	99.17
341.4	50.63	51.00	1.90	13.54	11.77	0.21	6.62	11.69	2.40	0.18	98.93
393.8	50.86	50.88	1.71	13.66	12.16	0.20	6.70	11.40	2.42	0.17	99.28
446.1	50.76	50.84	1.92	13.61	12.17	0.16	6.78	11.15	2.50	0.17	99.22
498.4	50.64	51.01	1.87	13.50	12.15	0.20	6.80	11.04	2.55	0.17	98.94
550.8	50.73	50.78	1.80	13.58	12.23	0.22	6.85	11.05	2.59	0.19	99.24
603.1	50.70	51.24	1.78	13.43	12.17	0.13	6.79	10.94	2.65	0.19	98.76
655.4	50.73	50.75	1.97	13.59	12.14	0.24	6.89	10.85	2.69	0.17	99.28
707.8	50.84	50.89	1.89	13.46	12.18	0.19	6.86	10.99	2.66	0.18	99.25
760.1	50.74	50.91	1.82	13.46	12.31	0.20	6.82	10.91	2.69	0.19	99.12
54.4	44.26	43.32	0.20	31.39	4.28	0.09	2.27	15.66	2.02	0.08	100.23
70.1	44.54	43.47	0.28	30.66	4.80	0.08	2.54	15.39	2.01	0.07	100.37
85.7	44.99	44.08	0.41	29.38	5.29	0.11	2.79	15.06	2.10	0.08	100.21
101.3	45.68	44.80	0.57	28.01	5.69	0.15	3.08	14.75	2.16	0.09	100.18
117.0	46.52	45.83	0.71	26.47	6.04	0.11	3.29	14.55	2.20	0.11	99.99
132.6	47.57	46.97	0.85	24.91	6.57	0.07	3.57	14.00	2.26	0.11	99.90
148.3	48.47	47.95	1.01	23.10	7.01	0.11	3.91	13.75	2.33	0.13	99.82
164.0	49.56	48.99	1.16	21.38	7.59	0.11	4.14	13.48	2.34	0.12	99.87
179.6	50.39	49.98	1.32	19.60	8.15	0.09	4.37	13.28	2.37	0.14	99.71
195.3	50.83	50.59	1.47	18.35	8.56	0.16	4.69	12.94	2.39	0.16	99.54
211.0	51.14	50.69	1.64	17.21	9.06	0.14	5.12	12.88	2.39	0.17	99.75
226.6	51.45	51.00	1.68	16.24	9.69	0.18	5.36	12.65	2.33	0.16	99.74
242.3	51.37	51.09	1.71	15.42	10.21	0.19	5.62	12.56	2.34	0.16	99.59
258.0	51.36	51.09	1.88	14.91	10.51	0.17	5.84	12.42	2.32	0.15	99.57
273.6	51.44	51.06	1.89	14.65	10.78	0.16	5.91	12.37	2.33	0.16	99.68
289.3	51.33	51.06	1.89	14.17	11.07	0.20	6.19	12.26	2.30	0.16	99.57
305.0	51.37	51.16	1.86	14.01	11.25	0.15	6.30	12.13	2.28	0.16	99.51
320.6	51.15	50.74	1.96	13.90	11.58	0.22	6.44	12.02	2.29	0.16	99.71
336.3	51.11	51.11	1.88	13.70	11.56	0.16	6.47	11.91	2.34	0.17	99.30
336.3	51.14	50.77	1.80	13.88	11.72	0.20	6.46	12.05	2.28	0.16	99.68
376.9	51.00	50.82	1.90	13.73	11.85	0.23	6.56	11.70	2.34	0.18	99.49
417.6	50.99	50.69	1.93	13.63	11.92	0.21	6.78	11.52	2.44	0.18	99.60
458.2	51.04	50.57	1.78	13.75	12.19	0.21	6.79	11.33	2.49	0.19	99.77
498.8	51.15	50.58	1.79	13.60	12.38	0.20	6.85	11.24	2.50	0.18	99.87
539.5	51.14	50.86	1.81	13.60	12.19	0.24	6.84	11.07	2.51	0.18	99.58
580.1	51.07	50.96	1.82	13.46	12.21	0.21	6.80	11.02	2.61	0.19	99.41

620.8	51.14	50.82	1.88	13.53	12.22	0.23	6.93	10.94	2.57	0.17	99.62
661.4	51.21	50.68	1.88	13.58	12.25	0.20	6.93	10.95	2.64	0.20	99.83
702.0	51.24	50.69	1.92	13.55	12.28	0.20	6.83	10.99	2.66	0.18	99.85
742.7	51.11	50.71	1.88	13.57	12.30	0.23	6.92	10.85	2.66	0.17	99.70
783.3	51.12	50.68	1.87	13.44	12.39	0.18	6.93	10.92	2.70	0.18	99.74
5.2	43.61	43.63	0.05	32.92	3.15	0.03	1.12	16.59	1.75	0.07	99.28
15.6	43.79	43.59	0.04	32.77	3.14	0.04	1.31	16.39	1.97	0.05	99.50
26.1	44.02	44.20	0.03	32.83	2.54	0.00	1.05	16.82	1.77	0.05	99.12
36.5	44.30	43.98	0.12	32.52	2.92	0.08	1.31	16.72	1.63	0.03	99.62
47.0	44.54	44.03	0.16	32.14	3.16	0.04	1.41	16.60	1.70	0.06	99.81
57.4	43.89	44.09	0.28	30.45	4.47	0.08	2.03	15.47	2.34	0.09	99.10
67.9	44.53	44.76	0.31	29.66	4.68	0.12	2.30	15.32	2.06	0.09	99.07
78.3	44.98	45.22	0.43	28.77	5.01	0.06	2.51	15.13	2.09	0.09	99.06
88.8	45.54	45.66	0.49	27.82	5.32	0.11	2.70	14.95	2.15	0.09	99.18

Exp 301

x / μm	Oxides (wt%)										
	SiO2	SiO2*	TiO2	Al2O3	FeO	MnO	MgO	CaO	Na2O	K2O	Total
3.6	48.29	48.83	1.34	18.09	11.03	0.22	5.69	11.17	2.75	0.18	98.76
4.2	47.81	48.36	1.45	18.10	11.14	0.21	5.73	11.25	2.86	0.19	98.75
5.6	47.91	48.35	1.39	17.96	11.36	0.23	5.74	11.27	2.81	0.20	98.86
6.6	48.23	48.49	1.45	17.93	11.14	0.20	5.70	11.32	2.91	0.16	99.04
9.2	48.32	48.90	1.44	17.66	10.98	0.21	5.69	11.36	2.86	0.19	98.72
9.4	48.63	49.20	1.44	17.67	10.96	0.12	5.70	11.27	2.76	0.17	98.73
11.6	48.37	48.66	1.48	17.60	11.21	0.19	5.82	11.33	2.86	0.16	99.01
14.2	48.34	48.96	1.53	17.42	11.14	0.18	5.76	11.32	2.80	0.18	98.68
14.8	48.29	48.90	1.47	17.36	11.24	0.22	5.76	11.37	2.80	0.18	98.69
15.2	48.81	49.31	1.48	17.25	11.13	0.16	5.90	11.21	2.69	0.17	98.79
15.6	48.85	49.30	1.44	17.26	11.11	0.20	5.76	11.28	2.78	0.18	98.85
21.0	49.00	49.68	1.51	16.79	11.14	0.21	5.82	11.27	2.69	0.19	98.62
24.0	48.61	49.49	1.50	16.70	11.36	0.15	5.81	11.38	2.73	0.19	98.42
26.8	49.33	49.97	1.62	16.34	11.29	0.17	5.96	11.20	2.57	0.19	98.66
30.1	49.50	49.62	1.55	16.19	11.55	0.19	6.06	11.22	2.73	0.18	99.17
31.2	48.98	49.60	1.61	16.03	11.63	0.21	5.95	11.31	2.77	0.19	98.68
32.6	49.30	50.48	1.53	15.92	11.35	0.19	5.89	11.16	2.60	0.18	98.12
33.1	48.88	49.76	1.60	15.99	11.62	0.16	5.97	11.21	2.82	0.17	98.41
38.4	49.78	50.24	1.58	15.58	11.55	0.20	6.12	11.16	2.70	0.18	98.84
40.3	49.59	49.93	1.60	15.51	11.87	0.23	6.08	11.17	2.73	0.17	98.96
44.2	49.87	50.14	1.74	15.28	11.82	0.14	6.16	11.17	2.64	0.20	99.03
46.8	49.77	50.25	1.66	15.20	11.82	0.21	6.12	11.14	2.71	0.19	98.83
50.0	49.76	50.39	1.80	15.03	11.74	0.22	6.19	11.08	2.70	0.17	98.67
50.4	49.84	50.10	1.71	14.97	12.00	0.21	6.22	11.19	2.73	0.18	99.04
55.8	49.97	50.58	1.70	14.72	11.94	0.16	6.19	11.13	2.69	0.18	98.69
60.6	49.86	50.26	1.76	14.55	12.22	0.25	6.29	11.10	2.70	0.17	98.91
61.6	50.10	50.46	1.81	14.52	12.11	0.18	6.32	11.09	2.62	0.18	98.93
62.5	49.93	50.49	1.75	14.39	12.16	0.19	6.30	11.12	2.73	0.19	98.74
67.4	49.99	50.41	1.81	14.40	12.23	0.21	6.34	11.05	2.67	0.18	98.88
70.7	49.82	50.30	1.86	14.22	12.31	0.22	6.39	11.13	2.68	0.18	98.82
73.2	50.04	50.54	1.72	14.10	12.31	0.21	6.41	11.12	2.70	0.19	98.80
78.1	50.20	50.48	1.77	13.99	12.38	0.22	6.49	11.07	2.71	0.18	99.02
79.0	50.06	50.48	1.78	14.10	12.37	0.17	6.39	11.11	2.72	0.18	98.88
80.9	50.11	50.57	1.75	14.02	12.40	0.18	6.39	11.14	2.68	0.16	98.84
84.8	49.97	50.69	1.71	13.86	12.40	0.20	6.49	11.13	2.65	0.17	98.57
90.5	49.90	50.24	1.86	13.86	12.65	0.22	6.52	11.04	2.73	0.17	98.95
91.0	49.95	50.42	1.86	13.81	12.55	0.17	6.48	11.13	2.70	0.18	98.83
93.7	50.01	50.63	1.80	13.79	12.55	0.13	6.54	11.03	2.66	0.17	98.67
96.3	50.23	50.65	1.92	13.69	12.46	0.19	6.55	10.99	2.65	0.18	98.88
101.2	50.03	50.37	1.79	13.70	12.73	0.20	6.55	11.07	2.69	0.19	98.96

102.1	50.14	50.64	1.83	13.63	12.50	0.21	6.56	11.05	2.71	0.18	98.80
107.9	49.81	50.70	1.78	13.75	12.52	0.21	6.52	11.00	2.67	0.17	98.41
109.3	50.19	50.60	1.77	13.72	12.47	0.28	6.64	10.97	2.67	0.18	98.90
111.3	50.13	50.50	1.84	13.68	12.63	0.23	6.54	10.99	2.70	0.18	98.93
121.5	49.89	50.43	1.77	13.74	12.67	0.20	6.63	10.98	2.71	0.17	98.76
124.9	50.08	50.53	1.76	13.70	12.73	0.20	6.58	10.91	2.71	0.18	98.85
131.6	49.87	50.84	1.78	13.50	12.57	0.18	6.60	11.01	2.66	0.17	98.33
140.5	49.80	50.42	1.89	13.57	12.79	0.26	6.61	10.93	2.68	0.17	98.69
141.8	49.99	50.49	1.73	13.58	12.78	0.24	6.63	11.01	2.68	0.17	98.80
151.9	50.03	50.59	1.90	13.52	12.68	0.22	6.64	10.96	2.62	0.17	98.73
156.2	50.39	50.68	1.72	13.61	12.76	0.18	6.56	10.93	2.69	0.18	99.01
162.1	49.94	50.60	1.85	13.50	12.66	0.20	6.60	11.01	2.71	0.18	98.64
171.8	50.14	50.44	1.81	13.61	12.79	0.22	6.57	10.93	2.75	0.19	99.00
172.2	50.01	50.67	1.77	13.58	12.65	0.17	6.59	10.99	2.71	0.18	98.65
182.4	50.01	50.14	1.80	13.53	12.87	0.22	6.74	11.03	2.79	0.18	99.16
187.4	49.67	50.53	1.87	13.59	12.79	0.21	6.48	10.90	2.74	0.19	98.44
192.5	49.92	50.30	1.83	13.59	12.83	0.27	6.59	11.02	2.68	0.19	98.92
202.7	49.78	50.39	1.84	13.54	12.84	0.23	6.64	10.98	2.68	0.17	98.68
212.8	49.53	50.46	1.79	13.59	12.80	0.23	6.60	10.92	2.73	0.18	98.37
223.0	49.43	50.45	1.84	13.63	12.78	0.21	6.53	10.91	2.76	0.19	98.28
284.7	50.34	50.41	1.82	13.66	12.81	0.19	6.77	10.76	2.69	0.19	99.23
301.0	50.05	50.59	1.89	13.64	12.69	0.17	6.72	10.75	2.68	0.18	98.75
317.4	49.93	50.75	1.82	13.60	12.69	0.19	6.64	10.77	2.68	0.17	98.48
333.7	50.03	50.59	1.79	13.54	12.73	0.24	6.70	10.79	2.73	0.18	98.73
350.0	49.97	50.68	1.64	13.63	12.77	0.25	6.63	10.82	2.69	0.18	98.59
366.4	50.06	50.35	1.80	13.62	12.82	0.17	6.72	10.84	2.80	0.18	99.01
382.7	50.12	50.54	1.80	13.58	12.83	0.20	6.69	10.79	2.68	0.19	98.88
399.0	50.14	50.46	1.74	13.65	12.81	0.23	6.66	10.82	2.76	0.17	98.97
415.4	50.09	50.62	1.81	13.72	12.66	0.19	6.60	10.77	2.74	0.19	98.77
431.7	50.20	50.34	1.77	13.72	12.85	0.17	6.73	10.76	2.77	0.20	99.16

Exp 302

x / μm	Oxides (wt%)										
	SiO ₂	SiO ₂ *	TiO ₂	Al ₂ O ₃	FeO	MnO	MgO	CaO	Na ₂ O	K ₂ O	Total
8.6	47.05	47.29	1.20	20.20	10.48	0.21	5.30	11.54	2.90	0.17	99.05
13.6	47.07	47.49	1.32	19.97	10.40	0.17	5.27	11.63	2.89	0.15	98.88
18.6	47.23	47.61	1.27	19.81	10.48	0.15	5.35	11.66	2.80	0.17	98.92
23.6	47.23	47.77	1.21	19.71	10.44	0.21	5.36	11.65	2.80	0.16	98.76
27.0	47.36	47.72	1.31	19.65	10.48	0.18	5.39	11.65	2.77	0.15	98.94
28.6	47.28	47.50	1.27	19.69	10.63	0.24	5.39	11.59	2.84	0.16	99.09
50.4	47.86	48.28	1.22	18.96	10.77	0.17	5.43	11.59	2.72	0.16	98.87
51.1	47.73	47.95	1.32	18.93	10.83	0.21	5.52	11.62	2.74	0.17	99.08
75.4	48.10	48.53	1.37	18.28	10.83	0.21	5.59	11.54	2.78	0.17	98.86
80.0	48.41	48.43	1.39	18.37	10.99	0.20	5.48	11.53	2.75	0.17	99.28
99.6	48.49	49.06	1.42	17.56	11.05	0.17	5.67	11.46	2.73	0.18	98.73
100.8	48.41	48.90	1.44	17.72	10.93	0.20	5.73	11.48	2.72	0.19	98.80
123.9	48.82	48.78	1.62	17.27	11.27	0.20	5.68	11.52	2.78	0.17	99.35
148.1	49.02	49.29	1.60	16.75	11.32	0.20	5.82	11.43	2.73	0.16	99.03
151.0	49.03	49.59	1.57	16.69	11.15	0.24	5.77	11.39	2.73	0.17	98.73
160.1	49.14	49.40	1.55	16.91	11.29	0.20	5.79	11.33	2.67	0.16	99.04
172.3	49.44	49.58	1.59	16.29	11.61	0.15	5.81	11.37	2.72	0.18	99.15
196.5	49.30	49.78	1.56	15.83	11.75	0.19	5.95	11.37	2.72	0.16	98.82
201.4	49.40	49.68	1.61	16.03	11.51	0.20	6.02	11.37	2.70	0.19	99.02
220.8	49.54	49.85	1.68	15.48	11.78	0.18	6.09	11.40	2.69	0.16	98.99
240.3	49.66	50.08	1.72	15.67	11.68	0.18	5.92	11.24	2.65	0.16	98.88
245.0	49.50	50.02	1.58	15.36	11.87	0.18	6.15	11.31	2.66	0.18	98.78
251.7	49.75	49.86	1.73	15.38	11.82	0.26	6.13	11.28	2.69	0.15	99.18
269.2	49.70	49.91	1.73	15.00	12.04	0.21	6.19	11.27	2.76	0.19	99.09
293.4	49.77	50.08	1.79	14.81	12.01	0.23	6.24	11.28	2.70	0.17	98.99
302.1	49.97	50.28	1.73	14.78	12.08	0.20	6.19	11.24	2.62	0.18	98.98
317.7	50.04	50.19	1.71	14.67	12.09	0.20	6.35	11.23	2.69	0.17	99.15
320.4	49.89	50.50	1.68	14.92	11.89	0.22	6.26	11.04	2.62	0.17	98.69
341.9	49.73	50.26	1.71	14.40	12.28	0.19	6.30	11.33	2.66	0.18	98.77
352.5	49.98	50.30	1.83	14.52	12.15	0.23	6.32	11.12	2.67	0.17	98.98
366.2	49.88	50.19	1.83	14.37	12.30	0.17	6.36	11.21	2.71	0.18	99.00
378.3	49.99	50.17	1.82	14.26	12.37	0.24	6.36	11.25	2.64	0.19	99.12
400.6	50.14	50.40	1.71	14.45	12.13	0.28	6.43	11.13	2.59	0.18	99.04
402.7	49.96	50.19	1.76	14.37	12.31	0.19	6.40	11.25	2.65	0.19	99.07
403.3	49.81	50.07	1.86	14.14	12.45	0.24	6.50	11.23	2.65	0.17	99.03
428.3	49.96	50.37	1.79	14.07	12.47	0.21	6.40	11.19	2.63	0.17	98.89
453.1	50.10	50.28	1.65	14.22	12.51	0.20	6.45	11.15	2.67	0.18	99.12
453.2	50.13	50.28	1.75	14.05	12.47	0.24	6.47	11.17	2.71	0.16	99.16
478.2	49.94	50.39	1.81	13.99	12.49	0.23	6.44	11.15	2.61	0.18	98.85
480.7	50.00	50.64	1.72	14.12	12.23	0.19	6.48	11.08	2.66	0.18	98.65

503.2	49.91	50.38	1.81	13.98	12.48	0.17	6.56	11.14	2.60	0.17	98.83
503.4	50.01	50.23	1.80	14.12	12.42	0.16	6.53	11.18	2.67	0.17	99.08
528.2	50.02	50.50	1.78	13.89	12.51	0.24	6.58	11.01	2.63	0.17	98.81
553.2	49.99	50.73	1.71	13.79	12.57	0.24	6.44	11.01	2.62	0.18	98.56
553.8	50.06	50.51	1.82	13.91	12.45	0.24	6.43	11.10	2.66	0.17	98.84
560.9	50.27	50.48	1.76	13.97	12.43	0.27	6.59	10.98	2.65	0.17	99.08
578.1	49.90	50.50	1.73	13.85	12.58	0.25	6.43	11.09	2.69	0.18	98.70
604.1	50.08	50.57	1.77	13.85	12.41	0.19	6.56	11.10	2.66	0.17	98.81
641.0	50.04	50.62	1.83	13.87	12.43	0.18	6.53	11.05	2.62	0.17	98.71
654.5	50.05	50.51	1.77	13.85	12.46	0.21	6.60	11.07	2.65	0.19	98.84
704.7	50.02	50.53	1.73	13.75	12.57	0.19	6.62	11.06	2.68	0.18	98.79
721.1	50.12	50.48	1.85	13.74	12.69	0.20	6.57	10.95	2.65	0.17	98.94
755.1	50.11	50.39	1.92	13.67	12.69	0.19	6.70	10.91	2.66	0.18	99.02
801.3	50.04	50.54	1.81	13.64	12.70	0.17	6.65	10.91	2.69	0.18	98.80
805.5	49.88	50.30	1.84	13.65	12.78	0.24	6.70	10.97	2.64	0.18	98.88
855.8	50.01	50.36	1.80	13.71	12.72	0.23	6.60	11.02	2.67	0.18	98.95
881.4	50.09	50.45	1.86	13.69	12.72	0.18	6.70	10.85	2.68	0.16	98.94
906.2	50.07	50.43	1.92	13.73	12.64	0.18	6.64	10.96	2.63	0.18	98.94
956.4	49.97	50.39	1.80	13.62	12.71	0.25	6.64	10.96	2.74	0.19	98.87
961.5	49.99	50.50	1.79	13.74	12.63	0.20	6.77	10.80	2.66	0.19	98.79
1006.8	50.07	50.57	1.80	13.66	12.71	0.19	6.64	10.90	2.65	0.18	98.80
1041.7	50.17	50.42	1.72	13.62	12.79	0.21	6.76	10.92	2.67	0.18	99.04
1057.1	49.80	50.52	1.83	13.74	12.70	0.20	6.57	10.83	2.72	0.19	98.59
1121.8	50.11	50.32	1.82	13.81	12.68	0.20	6.78	10.86	2.63	0.19	99.09
1202.0	50.05	50.24	1.84	13.71	12.82	0.22	6.76	10.78	2.75	0.18	99.11
1282.1	49.90	50.37	1.81	13.67	12.84	0.21	6.72	10.79	2.70	0.19	98.84
1362.3	50.03	50.29	1.88	13.65	12.94	0.20	6.65	10.78	2.73	0.19	99.04
1442.4	49.90	50.12	1.84	13.68	12.84	0.26	6.79	10.82	2.77	0.18	99.08
1522.5	49.53	50.59	1.82	13.58	12.85	0.26	6.54	10.71	2.76	0.19	98.24

Exp 304

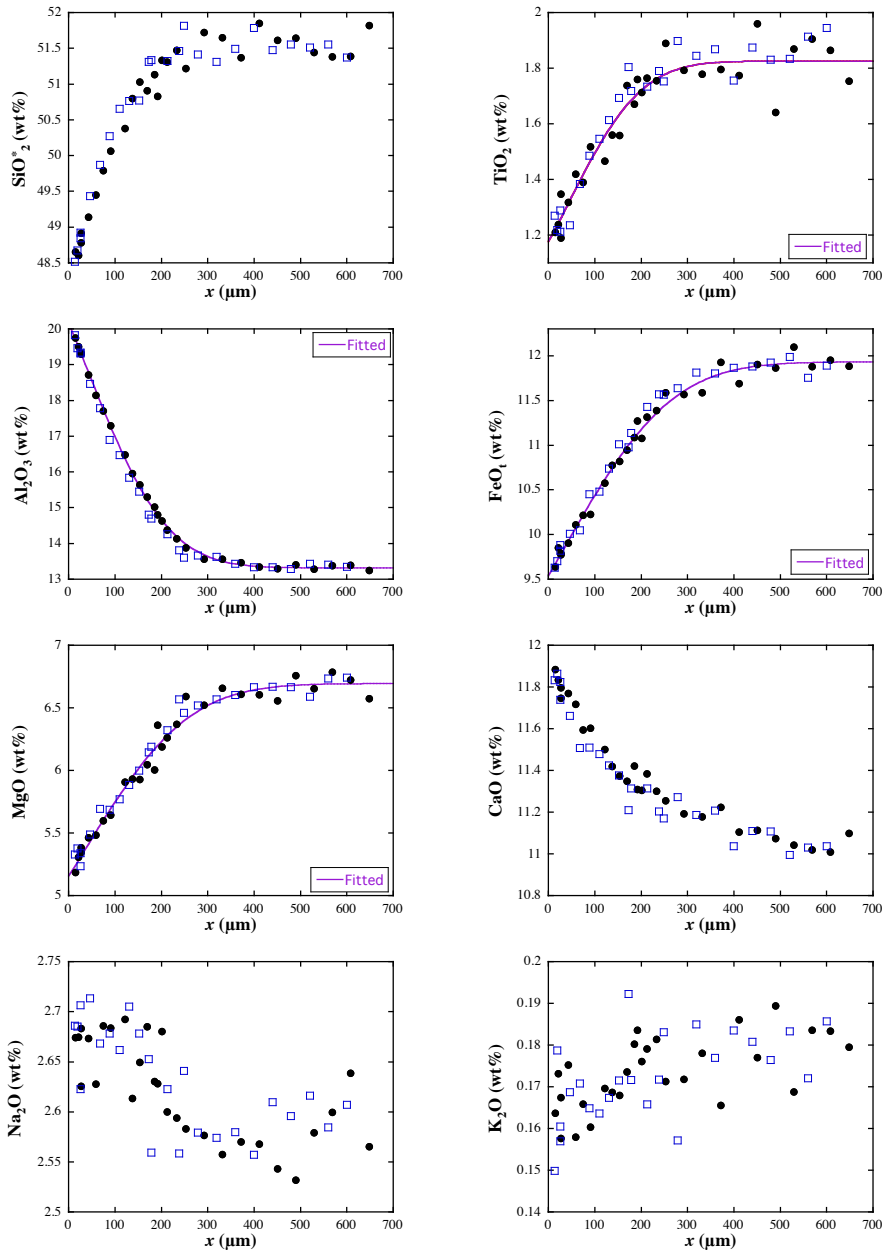
x / μm	Oxides (wt%)										
	SiO2	SiO2*	TiO2	Al2O3	FeO	MnO	MgO	CaO	Na2O	K2O	Total
5.0	49.14	49.10	1.31	18.72	10.07	0.18	5.69	11.22	2.81	0.20	99.34
5.2	49.48	49.27	1.32	18.72	9.91	0.17	5.59	11.26	2.87	0.18	99.51
10.2	49.53	49.05	1.30	18.18	10.36	0.19	5.81	11.45	2.78	0.17	99.78
10.5	49.70	49.49	1.39	18.20	10.03	0.20	5.63	11.29	2.90	0.16	99.51
10.5	49.94	49.55	1.42	18.19	10.08	0.16	5.62	11.30	2.82	0.17	99.70
15.8	50.07	49.90	1.39	17.73	10.15	0.16	5.66	11.28	2.84	0.18	99.47
16.1	49.93	49.81	1.46	17.61	10.18	0.24	5.83	11.26	2.74	0.16	99.41
20.3	50.05	50.04	1.44	16.95	10.60	0.22	5.86	11.28	2.75	0.17	99.30
21.1	50.43	50.01	1.49	17.04	10.28	0.25	5.92	11.33	2.82	0.16	99.72
21.7	50.19	50.10	1.43	17.07	10.48	0.25	5.84	11.17	2.78	0.18	99.39
26.4	50.74	50.48	1.52	16.50	10.50	0.14	5.90	11.24	2.83	0.18	99.56
27.2	50.51	49.96	1.51	16.59	10.92	0.20	5.98	11.17	2.79	0.17	99.85
30.5	50.62	50.53	1.60	15.95	10.83	0.19	6.09	11.20	2.74	0.17	99.40
31.7	50.86	50.43	1.67	16.09	10.73	0.16	6.00	11.21	2.84	0.18	99.73
32.8	50.79	50.70	1.45	16.02	10.80	0.21	6.07	11.18	2.70	0.17	99.38
37.0	50.91	50.61	1.62	15.60	11.01	0.20	6.08	11.14	2.87	0.18	99.60
38.3	50.70	50.78	1.61	15.66	10.89	0.25	6.16	11.03	2.75	0.19	99.21
40.6	51.03	50.51	1.77	15.33	11.19	0.17	6.14	11.27	2.73	0.19	99.82
42.3	51.04	50.77	1.51	15.26	11.19	0.16	6.25	11.18	2.81	0.17	99.56
43.9	50.96	50.63	1.63	15.32	11.23	0.20	6.25	11.13	2.72	0.18	99.63
47.6	50.90	51.04	1.60	15.00	11.20	0.22	6.20	11.13	2.75	0.16	99.16
49.5	51.09	50.86	1.59	15.13	11.37	0.19	6.16	11.09	2.73	0.16	99.53
50.8	50.89	51.00	1.73	14.63	11.54	0.21	6.23	11.17	2.63	0.16	99.19
52.9	51.05	50.91	1.68	14.74	11.51	0.17	6.31	11.07	2.75	0.17	99.44
55.0	51.11	50.98	1.75	14.77	11.33	0.16	6.43	11.04	2.69	0.16	99.43
60.6	51.17	50.86	1.68	14.64	11.58	0.18	6.43	11.05	2.69	0.19	99.61
61.0	51.08	51.08	1.79	14.23	11.55	0.21	6.48	11.15	2.64	0.17	99.30
66.2	50.93	51.22	1.74	14.22	11.65	0.22	6.36	11.03	2.68	0.17	99.00
71.1	50.96	51.03	1.82	13.97	11.90	0.19	6.48	11.14	2.62	0.16	99.24
71.7	51.03	51.05	1.69	14.21	11.81	0.18	6.48	11.02	2.68	0.19	99.28
77.3	50.78	51.32	1.75	13.89	11.78	0.16	6.54	11.05	2.62	0.19	98.76
81.3	50.85	51.31	1.57	13.74	12.03	0.20	6.62	11.02	2.63	0.17	98.83
82.8	51.08	50.87	1.83	13.98	11.96	0.21	6.57	11.07	2.64	0.17	99.51
88.4	50.93	51.21	1.73	13.80	11.95	0.20	6.65	10.91	2.66	0.18	99.02
91.4	50.93	51.36	1.79	13.47	12.04	0.17	6.62	11.03	2.66	0.17	98.87
101.6	50.86	51.18	1.83	13.54	12.17	0.27	6.59	10.91	2.67	0.15	98.99
111.7	50.82	51.46	1.73	13.46	12.07	0.21	6.61	11.02	2.58	0.17	98.67
121.9	50.90	51.37	1.77	13.38	12.16	0.13	6.73	10.95	2.64	0.16	98.83
132.1	50.47	50.91	1.82	13.47	12.32	0.22	6.72	11.04	2.64	0.17	98.87
142.2	50.76	50.93	1.87	13.35	12.40	0.30	6.66	10.96	2.65	0.18	99.14

152.4	50.92	51.20	1.87	13.38	12.32	0.18	6.63	10.92	2.63	0.18	99.01
162.5	50.71	51.10	1.78	13.44	12.39	0.21	6.65	10.90	2.66	0.17	98.91
172.7	50.50	50.95	1.90	13.41	12.40	0.27	6.68	10.88	2.65	0.17	98.85
182.8	50.90	51.21	1.83	13.48	12.28	0.18	6.68	10.85	2.61	0.19	98.98
193.0	50.90	51.00	1.79	13.43	12.51	0.21	6.63	10.88	2.67	0.18	99.20

Appendix B

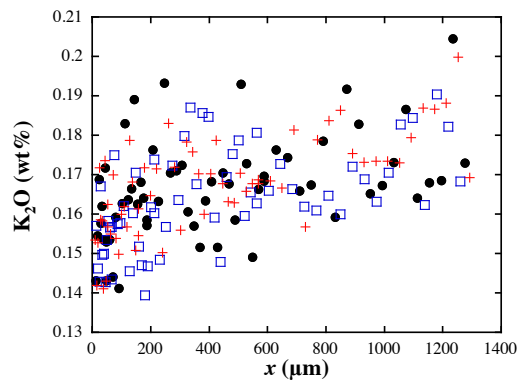
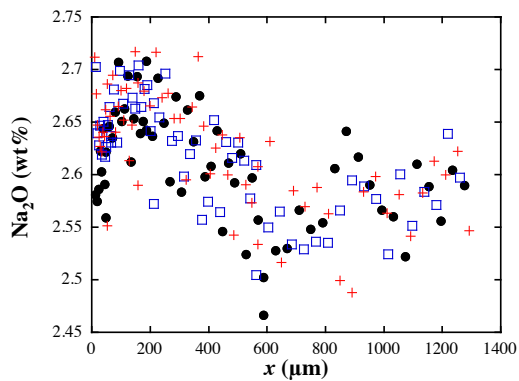
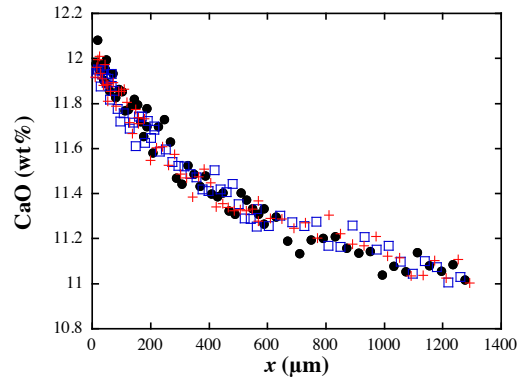
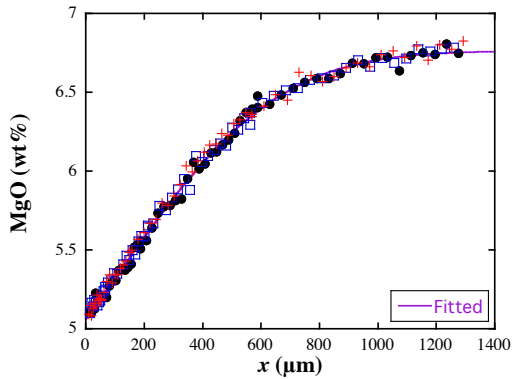
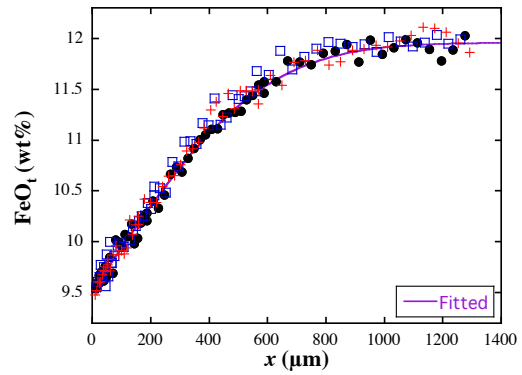
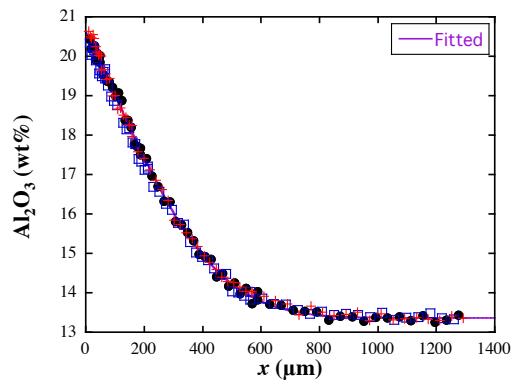
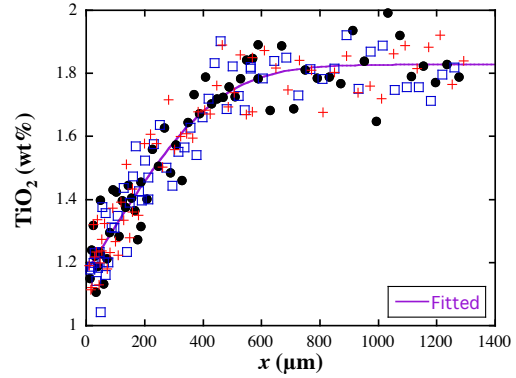
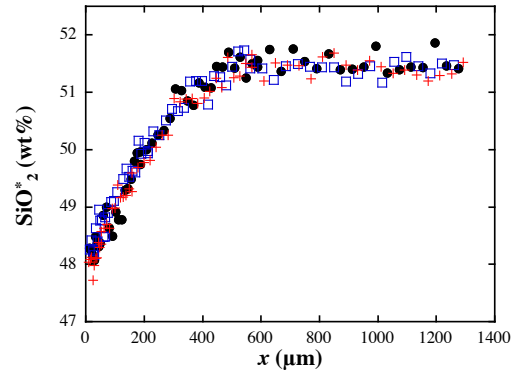
Fittings to Composition Profiles of Anorthite Dissolution in Basaltic Melt

Exp 201 (1293 °C, 0.5 GPa, 1826s)

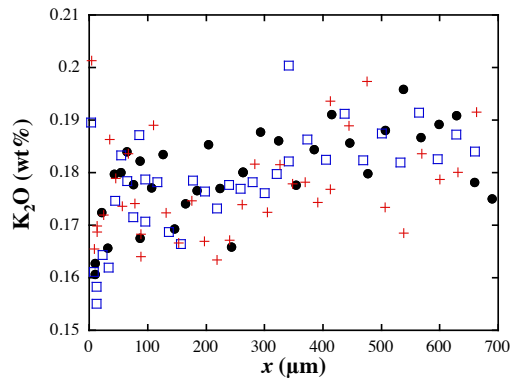
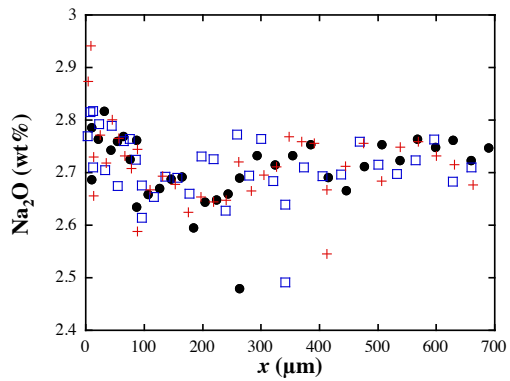
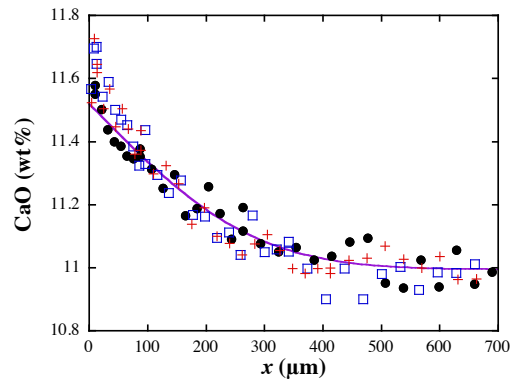
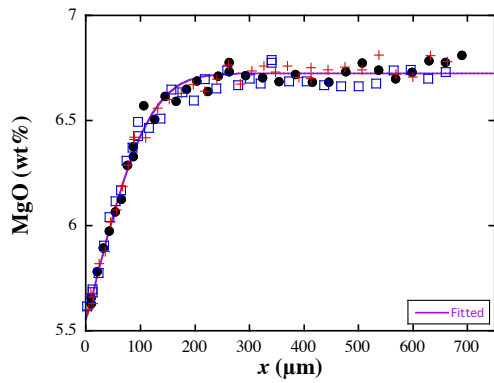
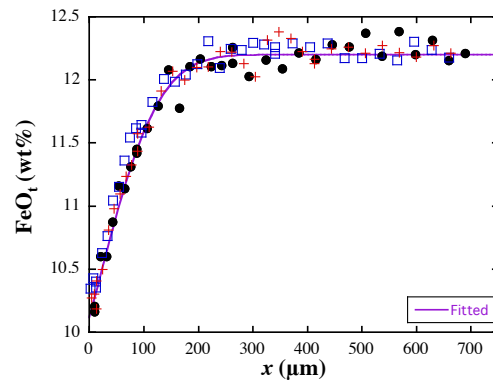
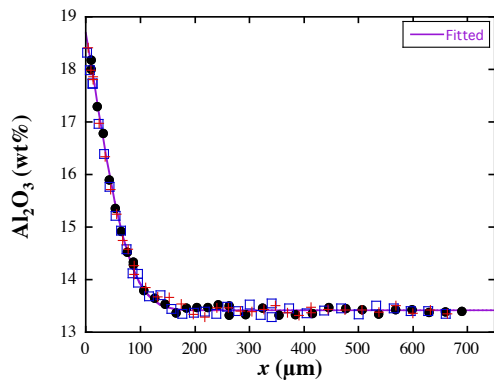
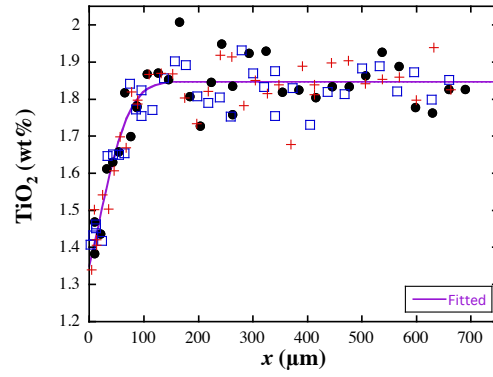
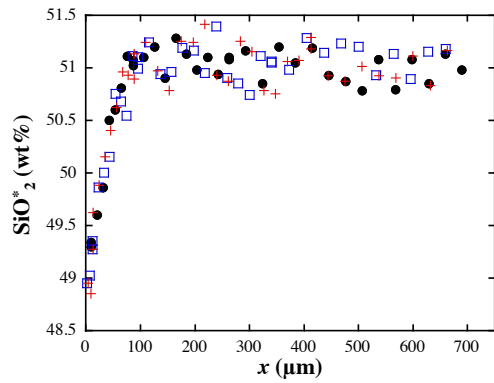


Note: $\text{SiO}_2^* = \text{SiO}_2 + 99.3 - \text{Total}$

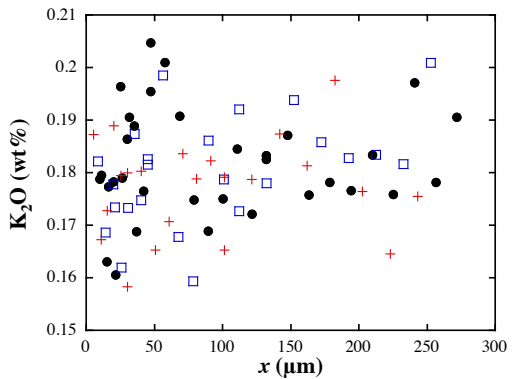
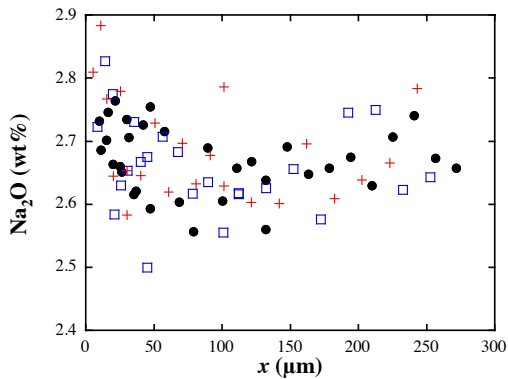
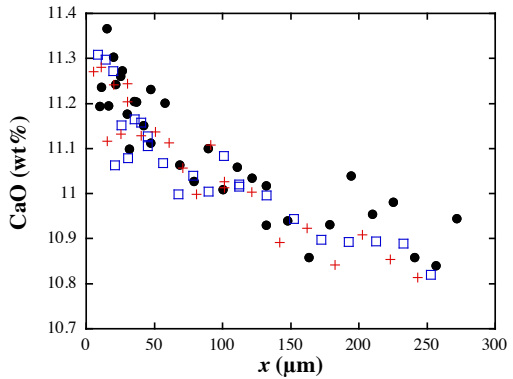
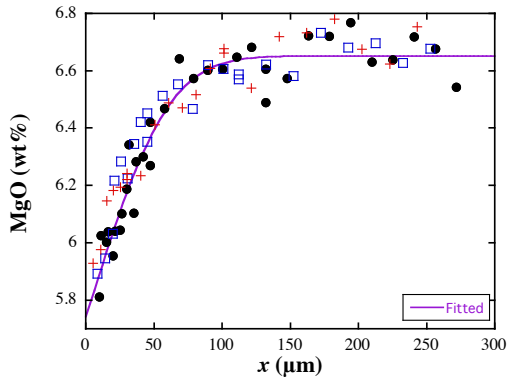
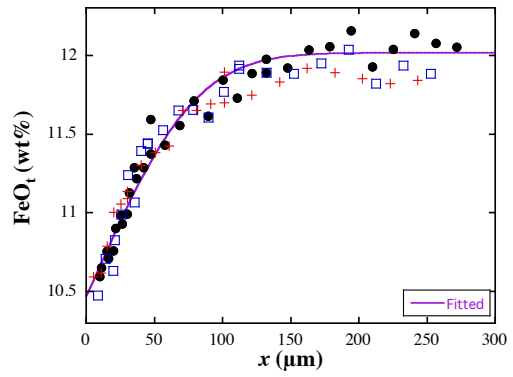
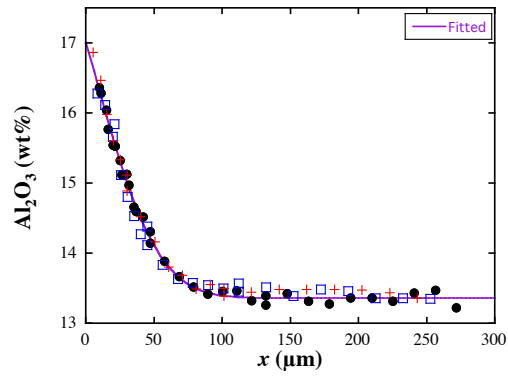
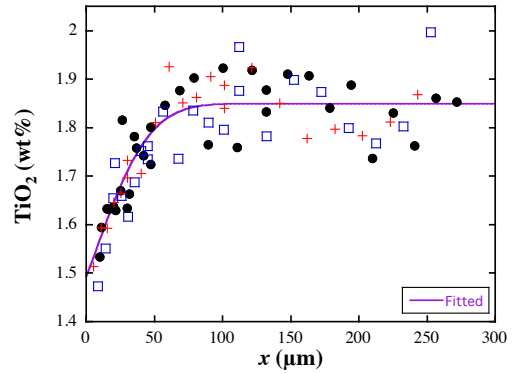
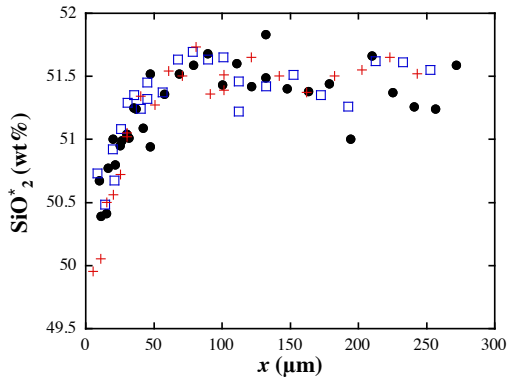
Exp 202 (1284 °C, 0.5 GPa, 6010s)



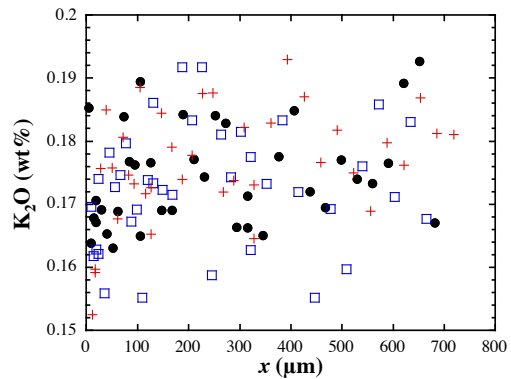
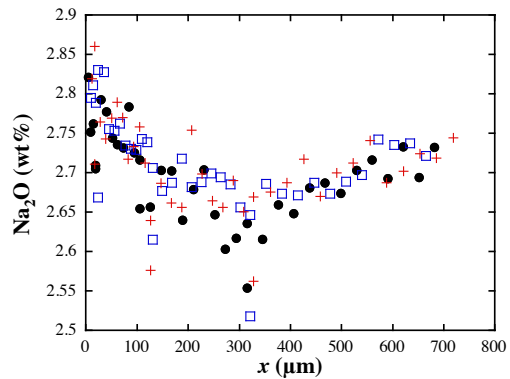
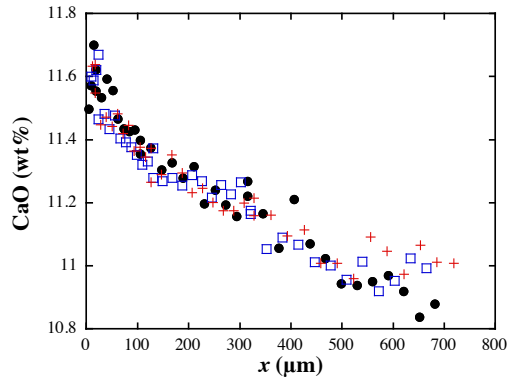
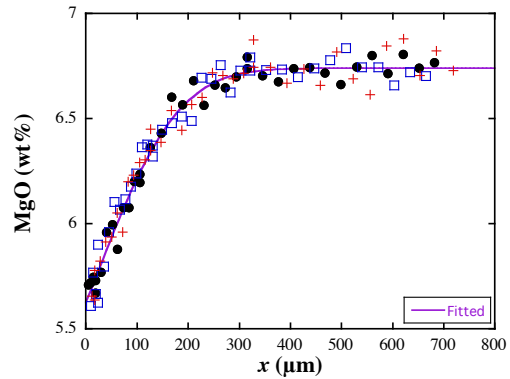
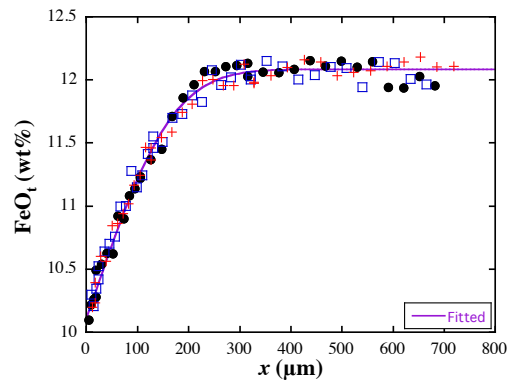
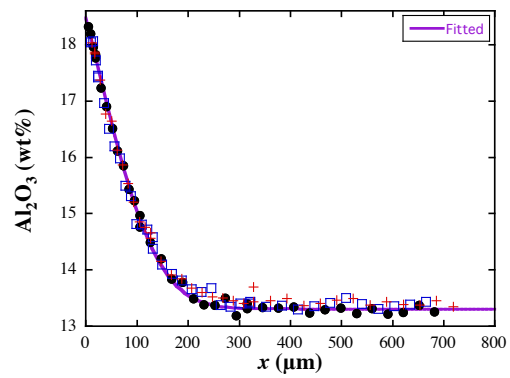
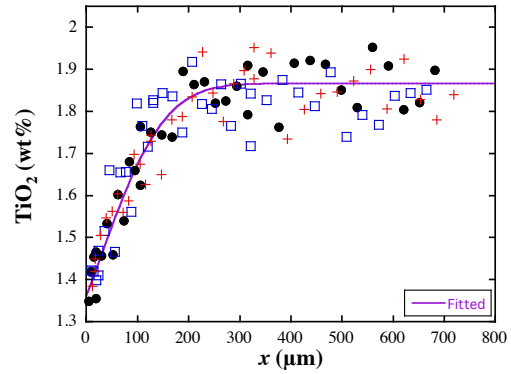
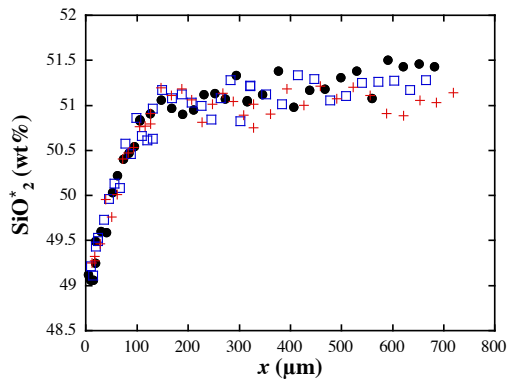
Exp 203 (1280 °C, 0.5 GPa, 338s)



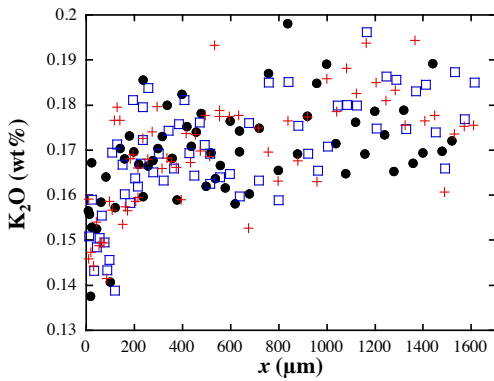
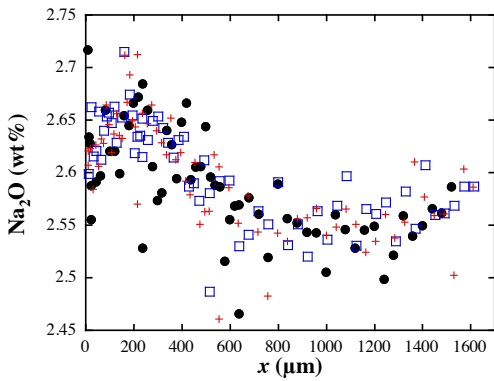
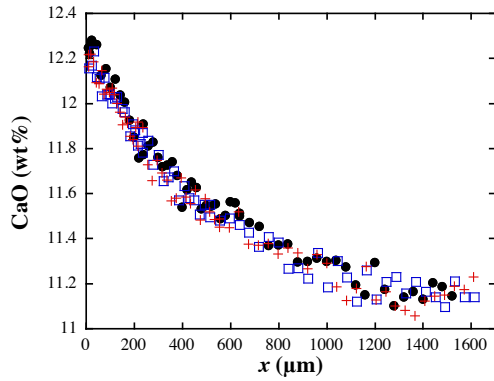
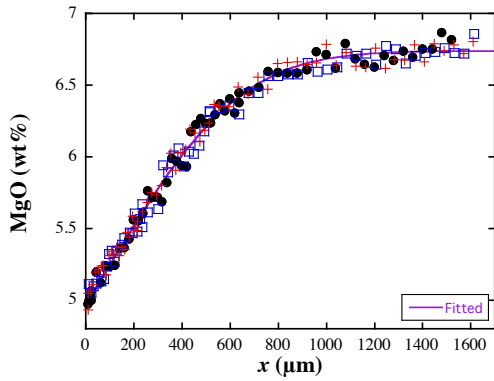
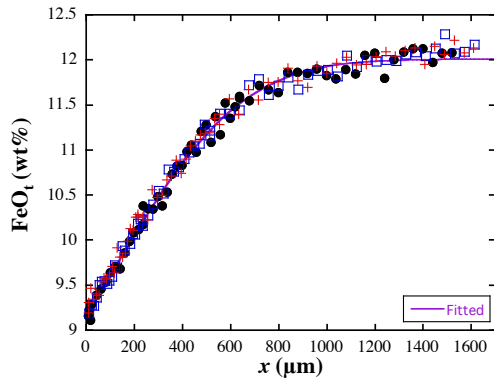
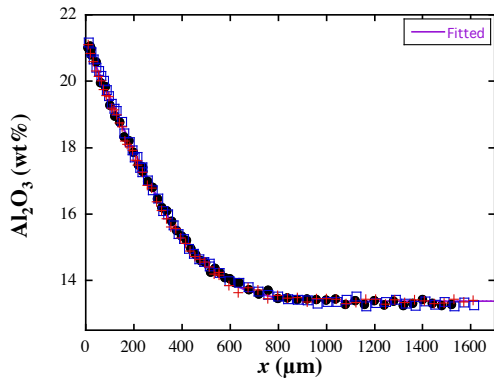
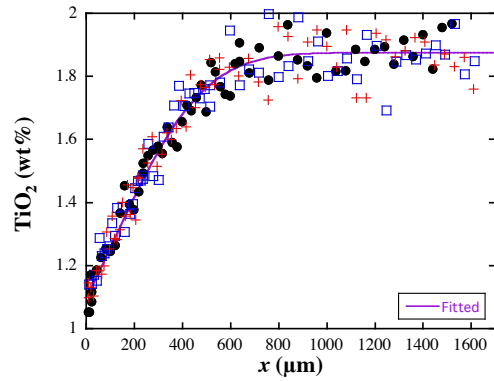
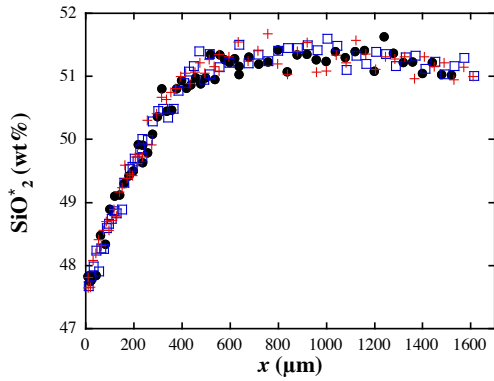
Exp 205 (1286 °C, 0.5 GPa, 201s)



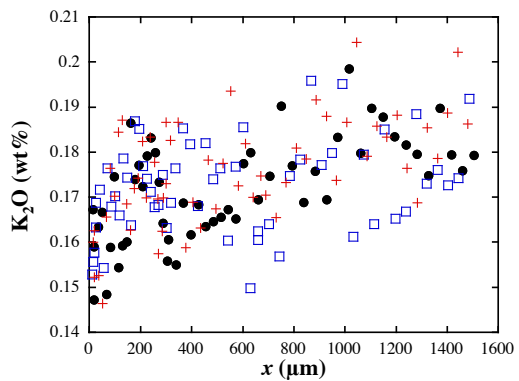
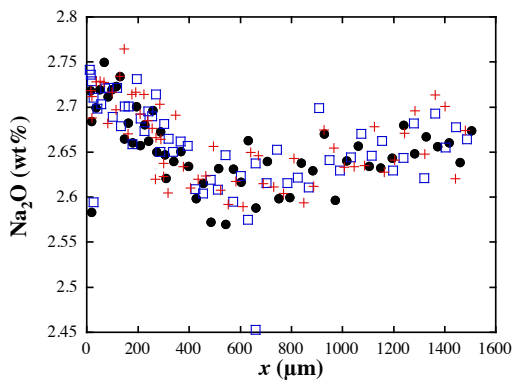
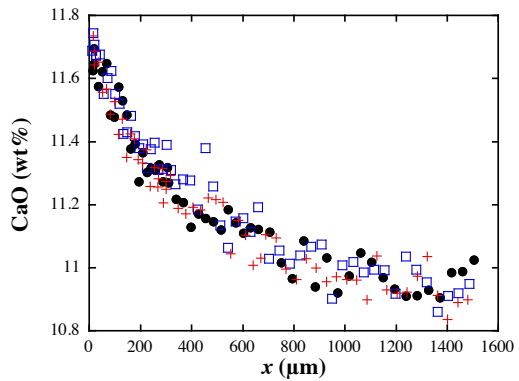
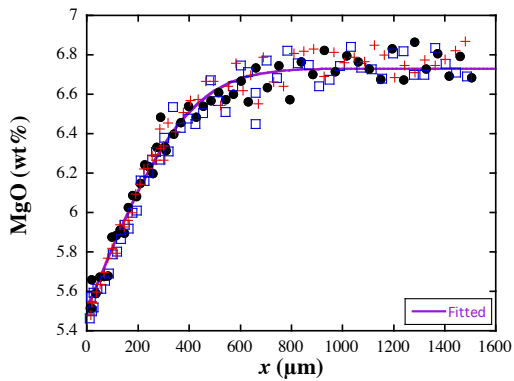
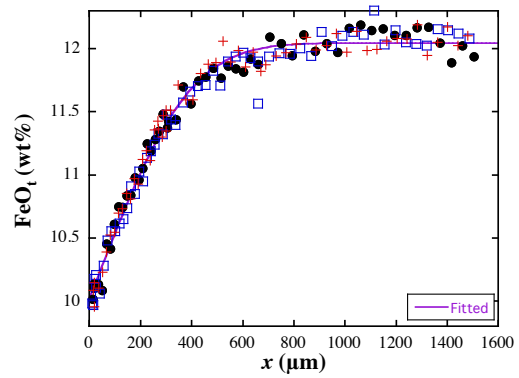
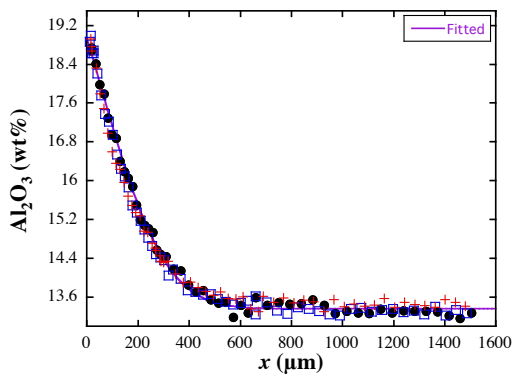
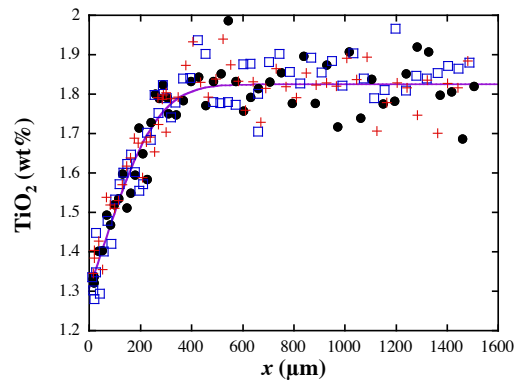
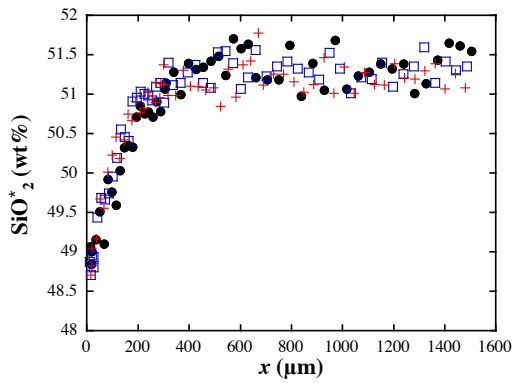
Exp 207 (1278 °C, 0.5 GPa, 1223s)



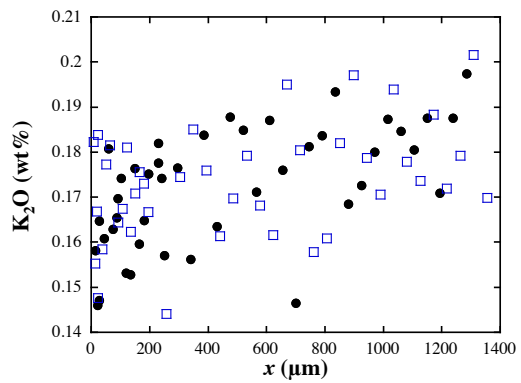
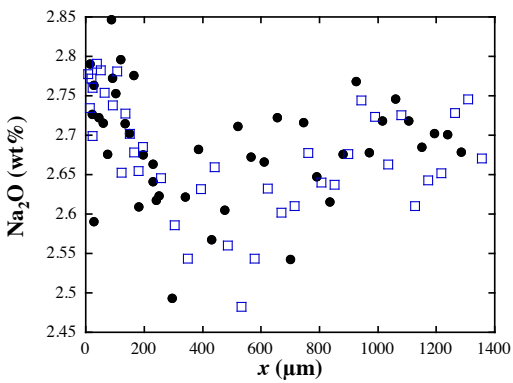
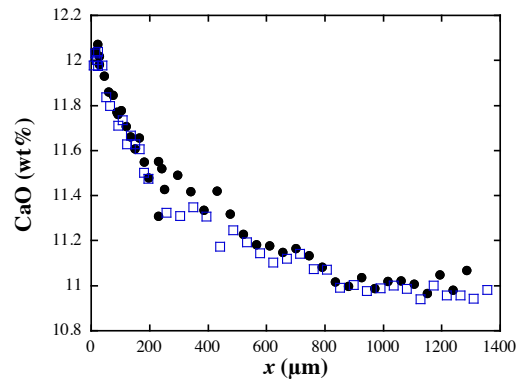
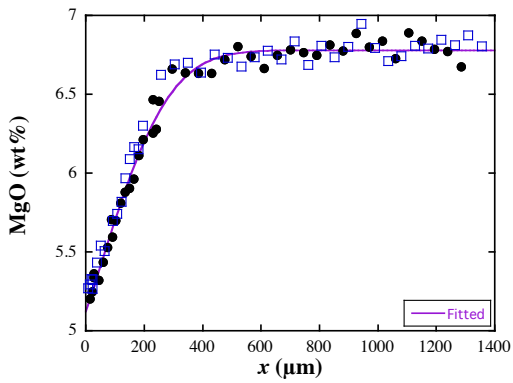
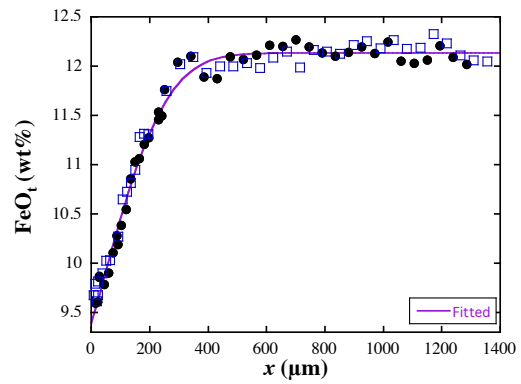
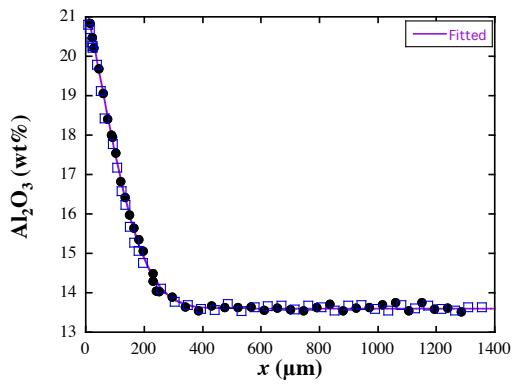
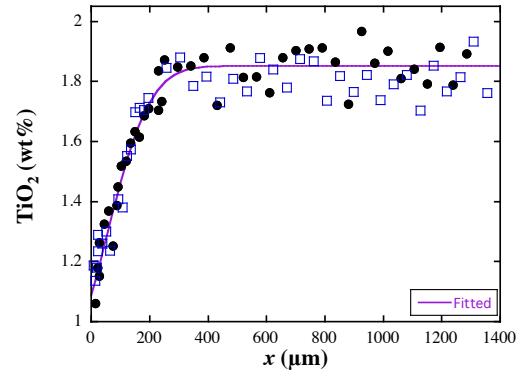
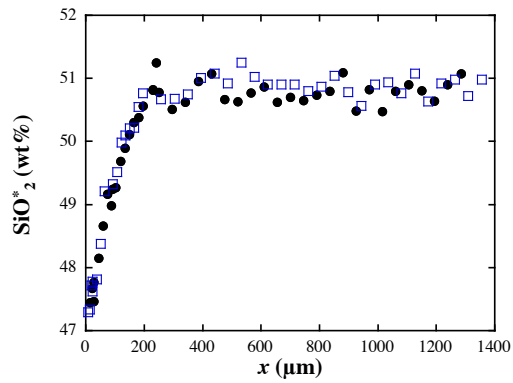
Exp 208 (1278 °C, 0.5 GPa, 6015s)



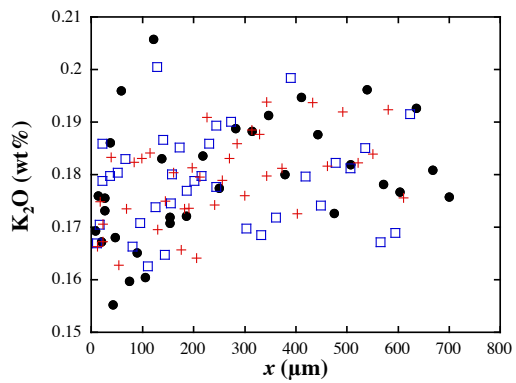
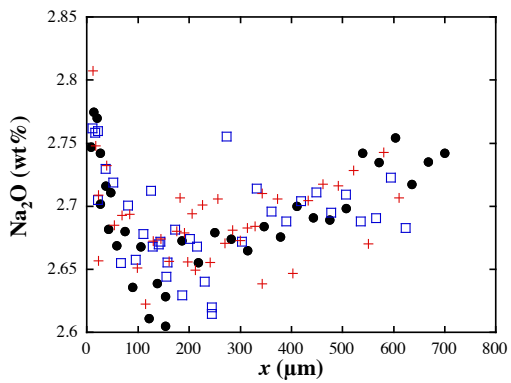
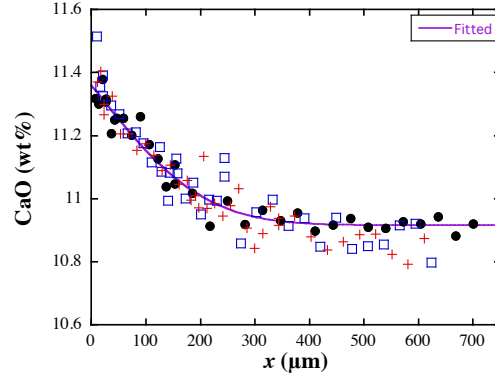
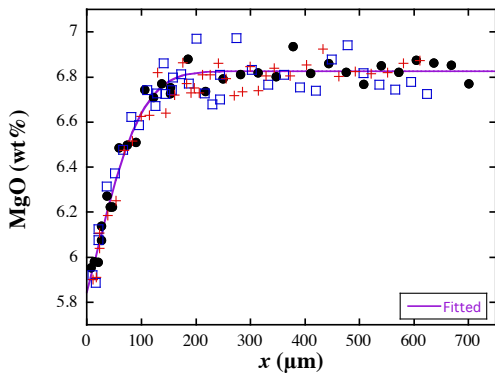
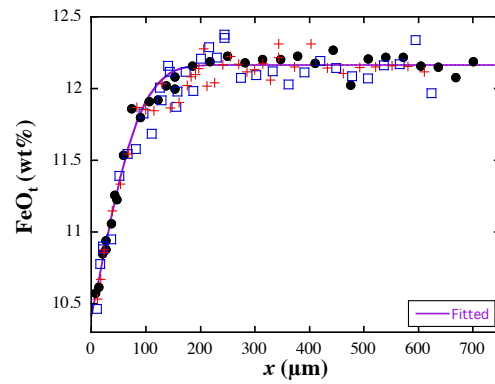
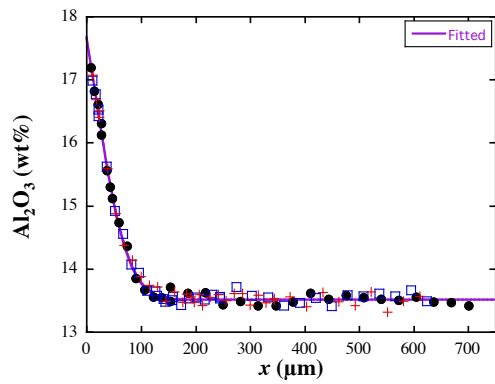
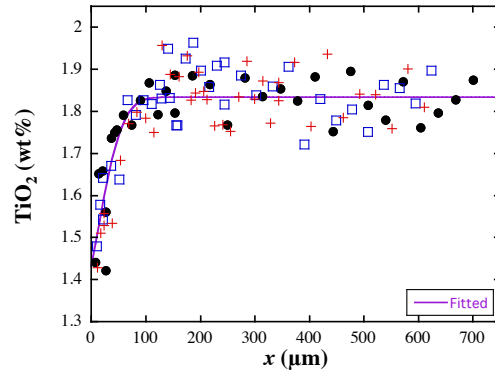
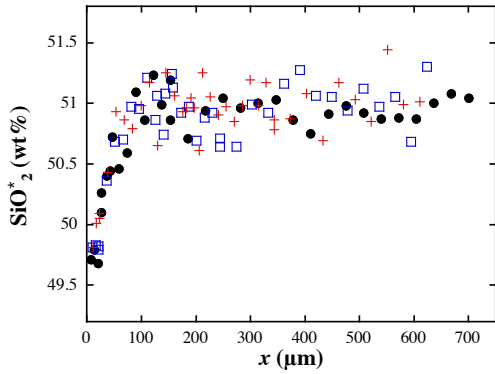
Exp 209 (1280 °C, 0.5 GPa, 3615s)



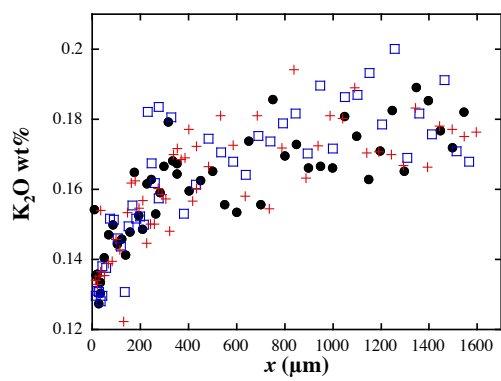
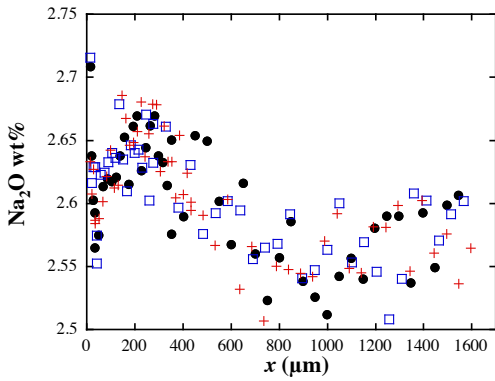
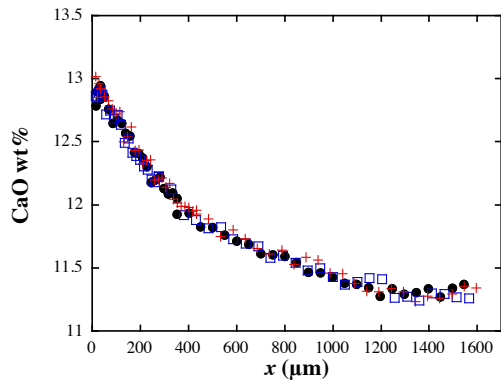
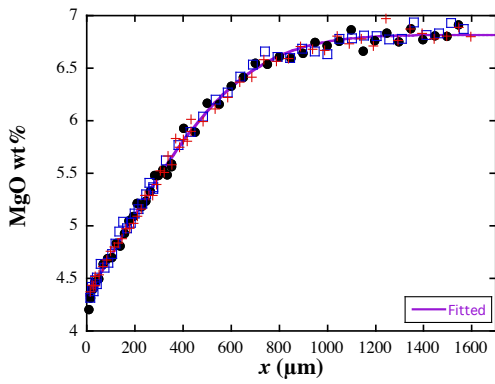
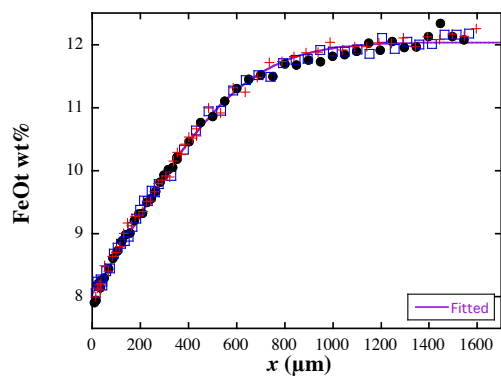
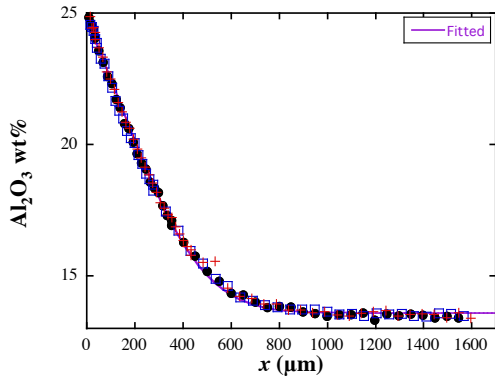
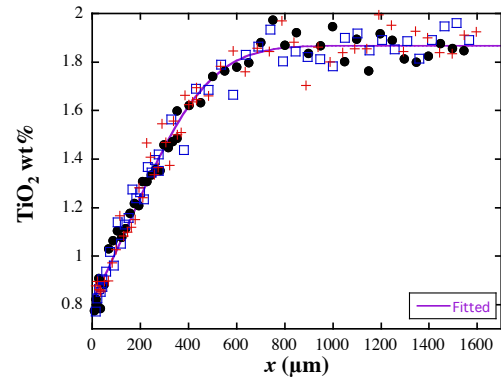
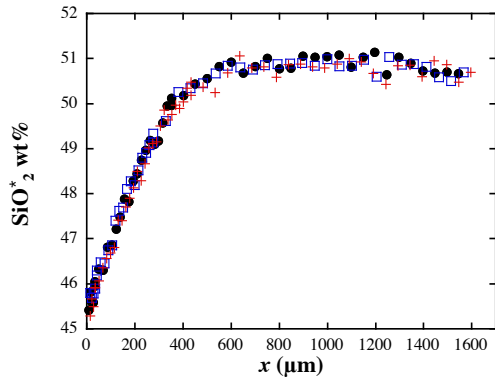
Exp 221 (1284 °C, 0.5 GPa, 1827s)



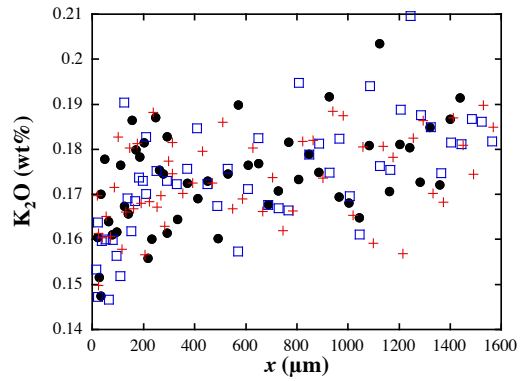
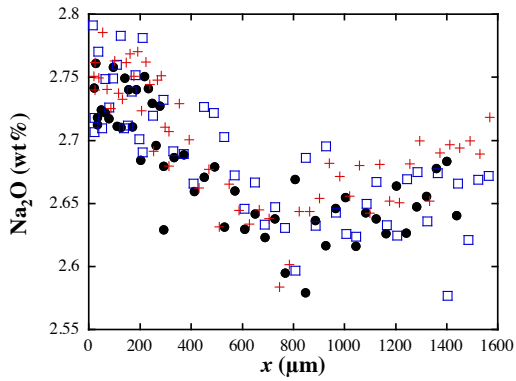
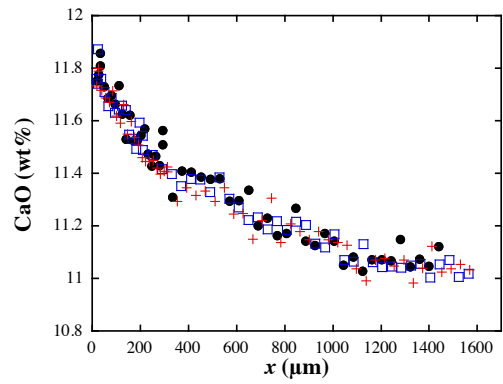
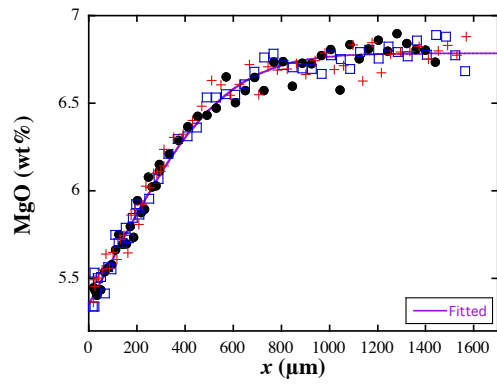
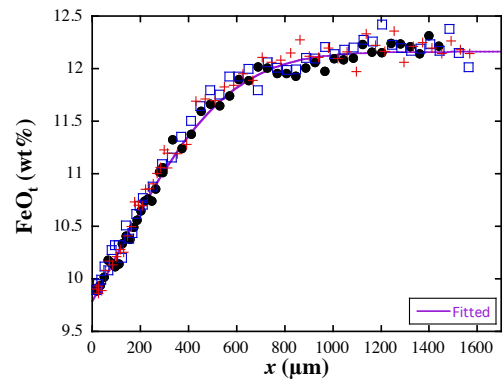
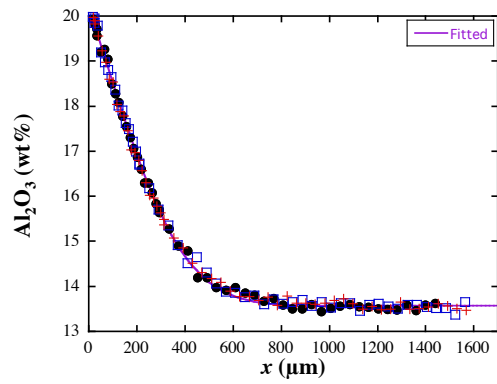
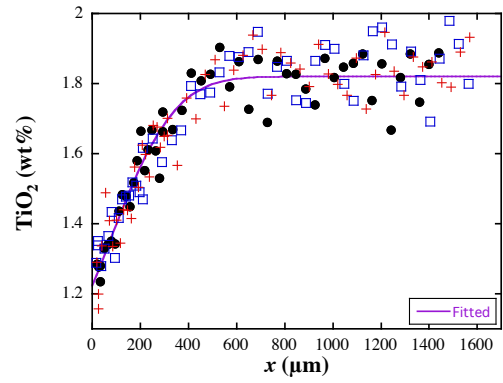
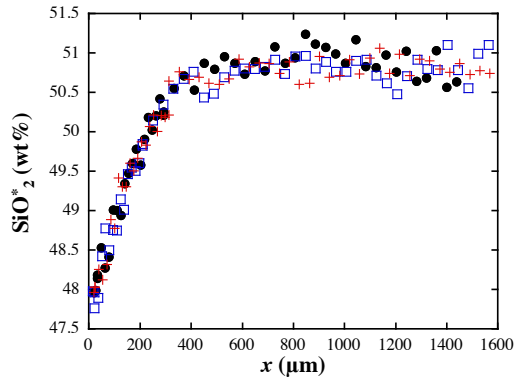
Exp 222 (1279 °C, 0.5 GPa, 329s)



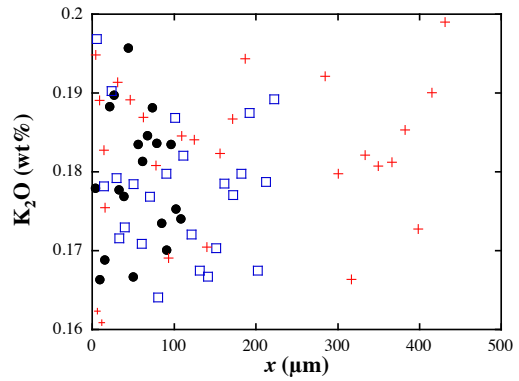
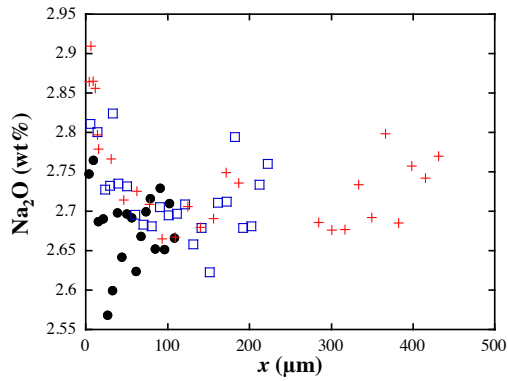
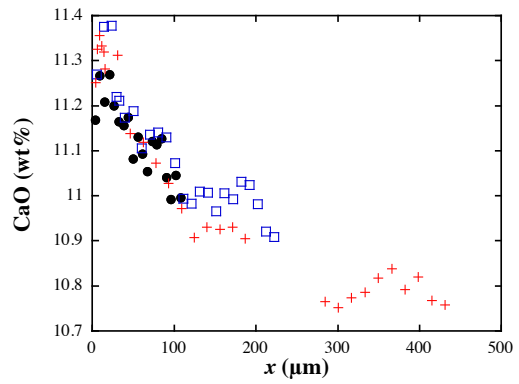
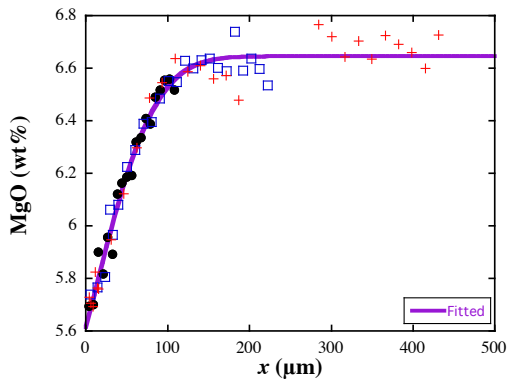
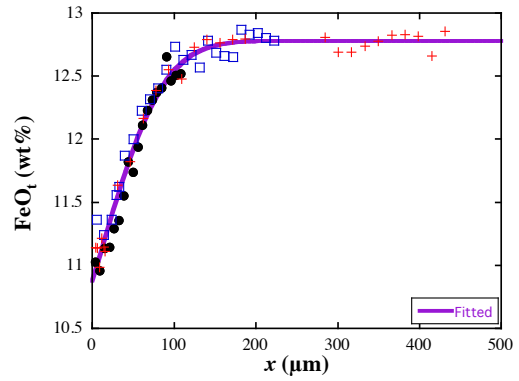
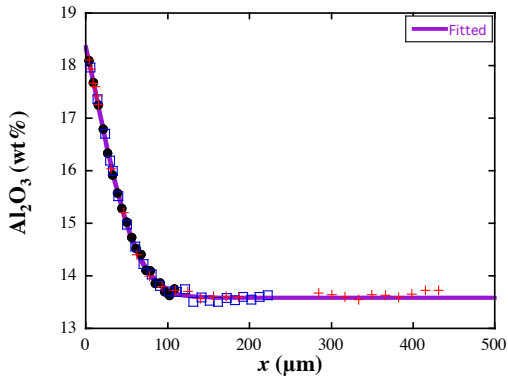
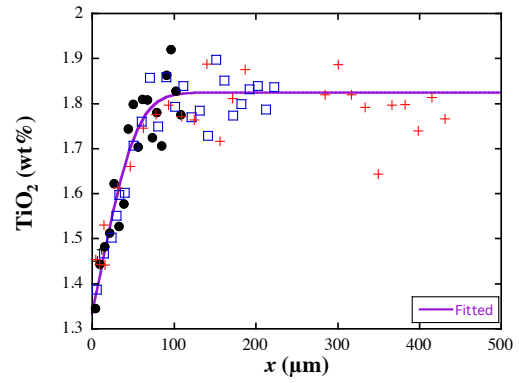
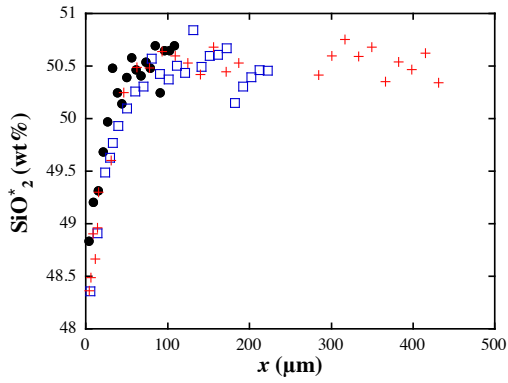
Exp 223 (1280 °C, 0.5 GPa, 6005s)



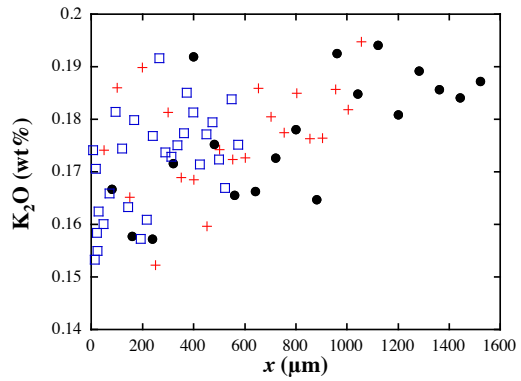
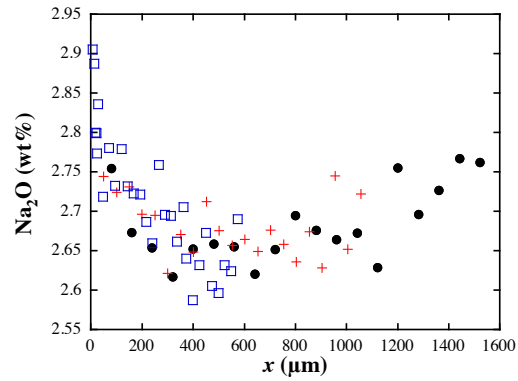
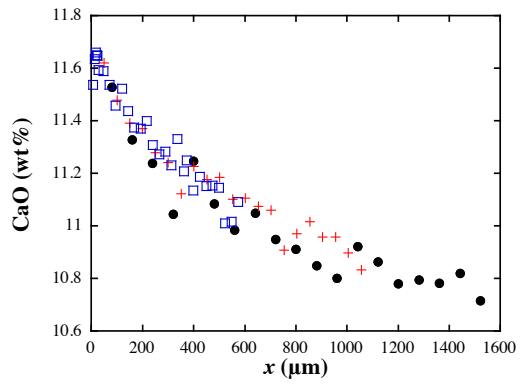
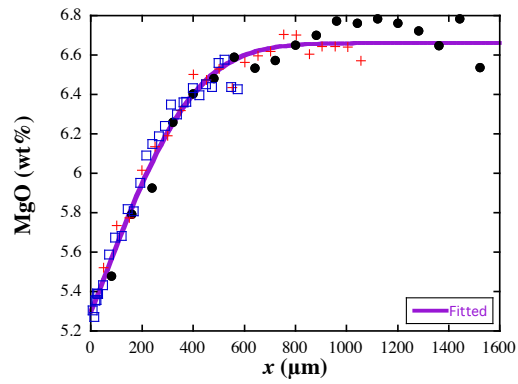
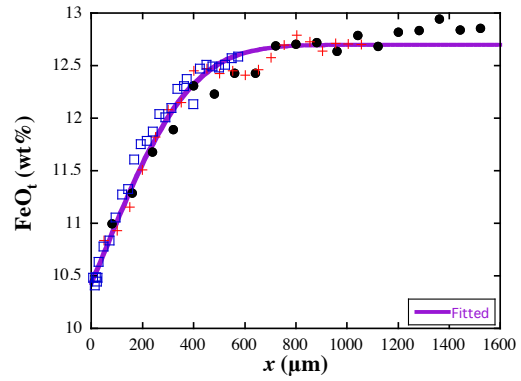
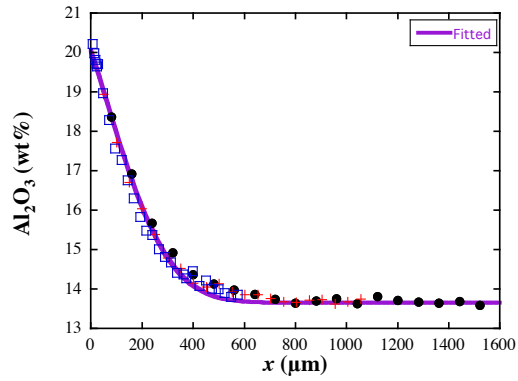
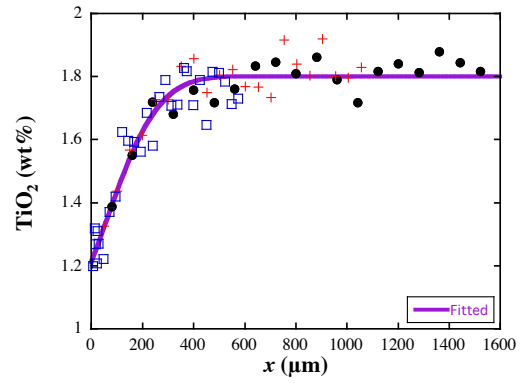
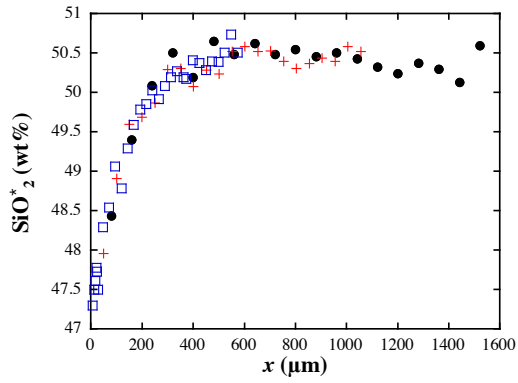
Exp 227 (1283 °C, 0.5 GPa, 6009s)



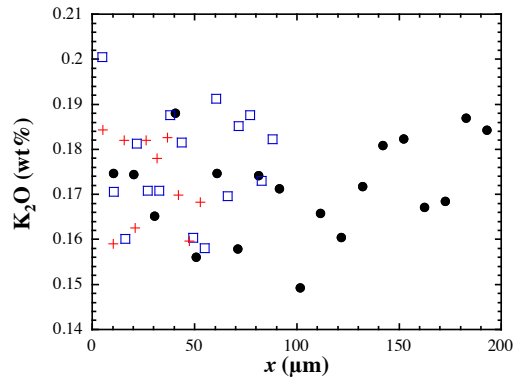
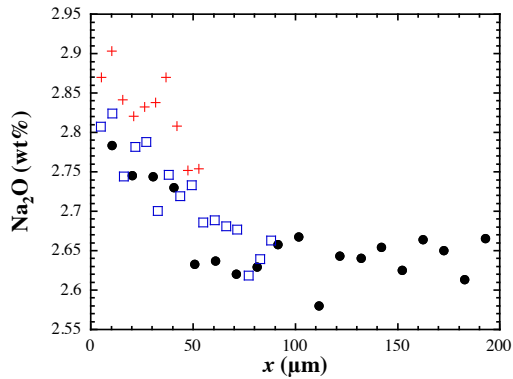
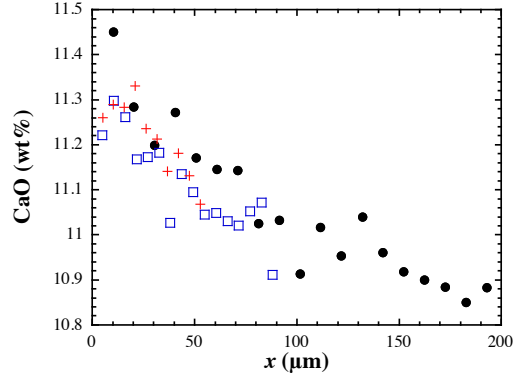
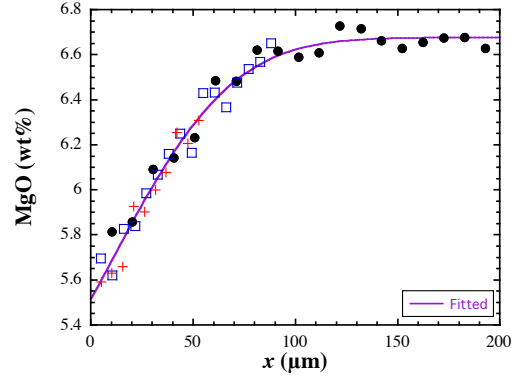
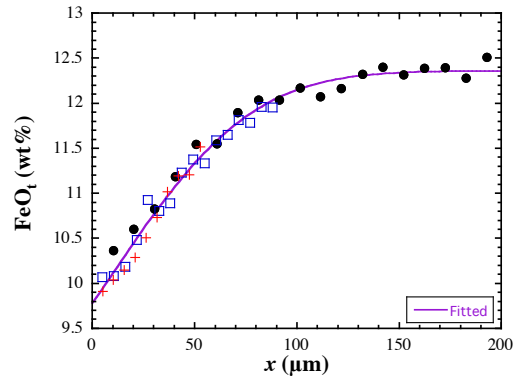
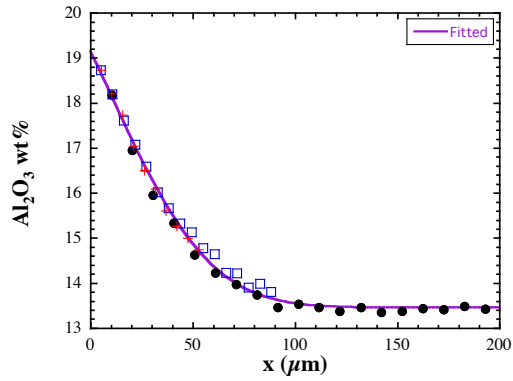
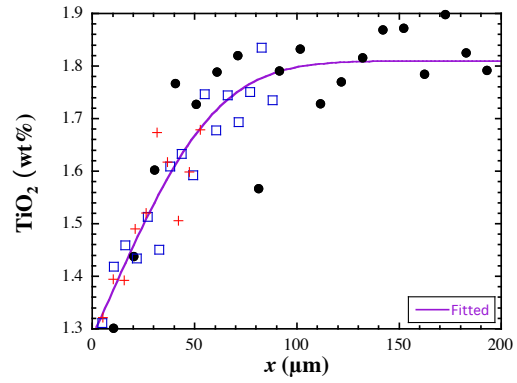
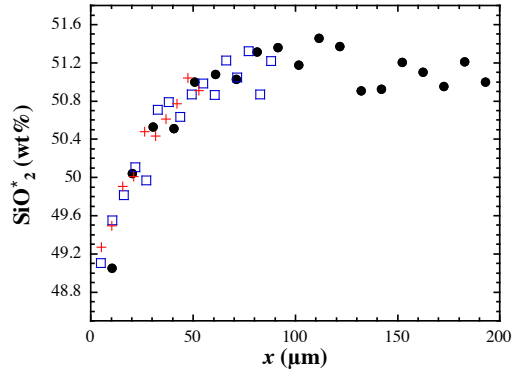
Exp 301 (1284 °C, 0.5 GPa, 319s)



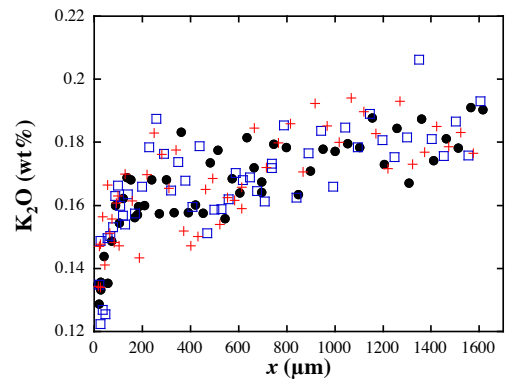
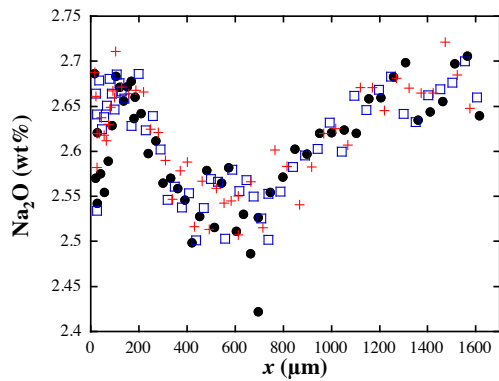
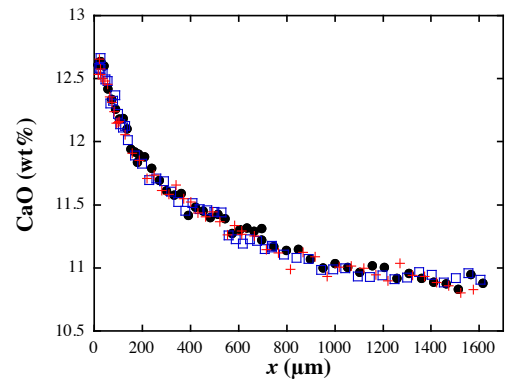
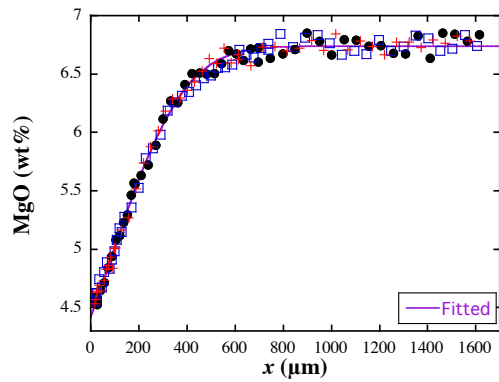
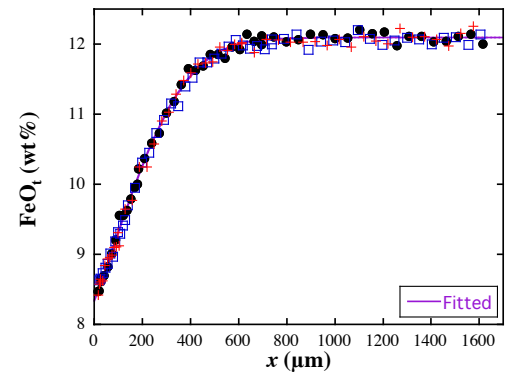
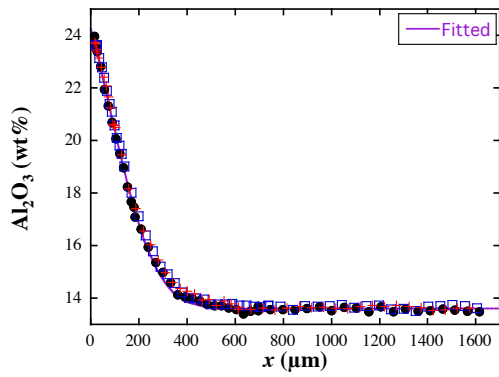
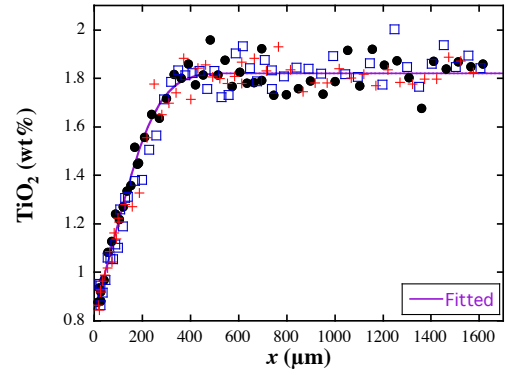
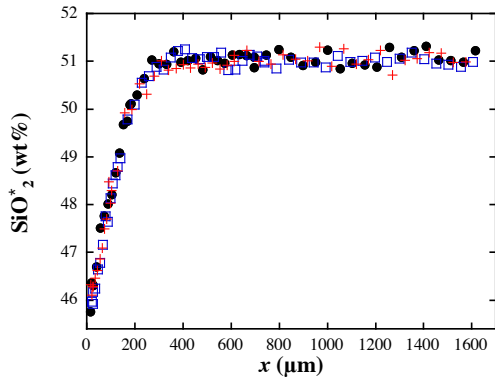
Exp 302 (1284 °C, 0.5 GPa, 3615s)



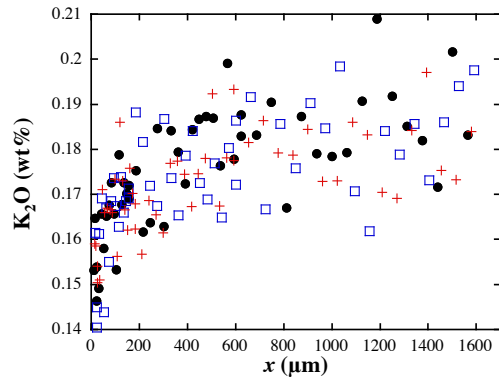
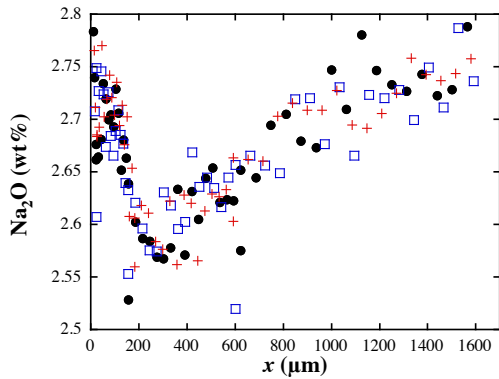
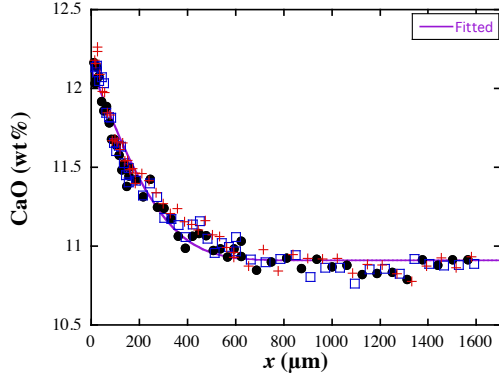
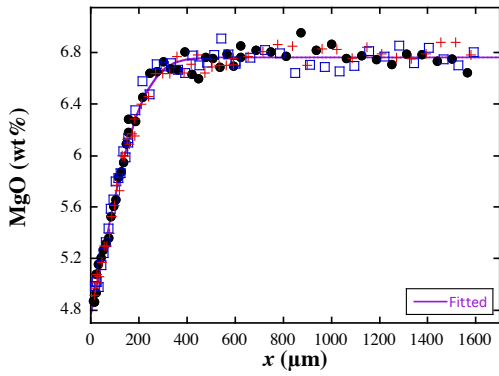
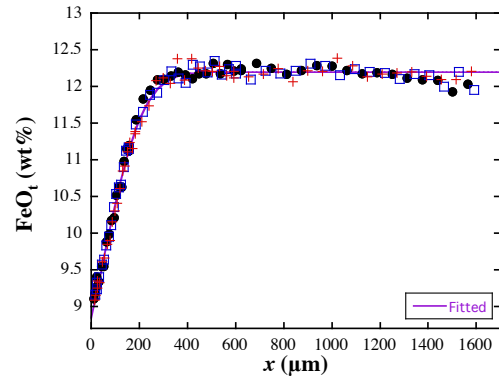
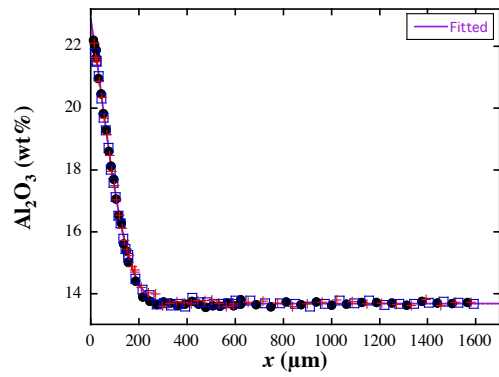
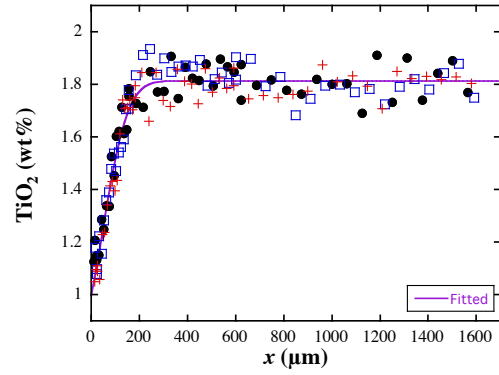
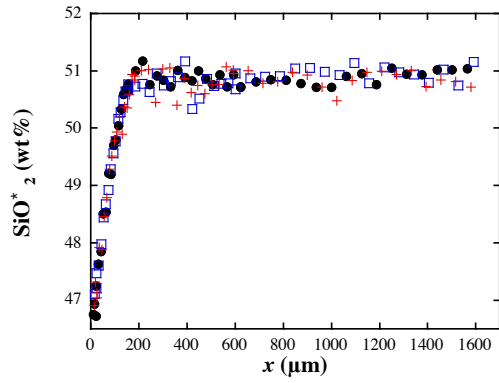
Exp 304 (1281 °C, 0.5 GPa, 149s)



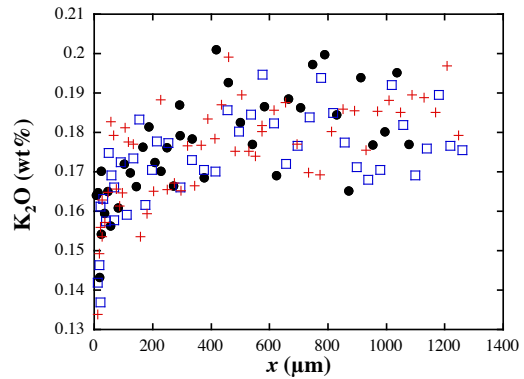
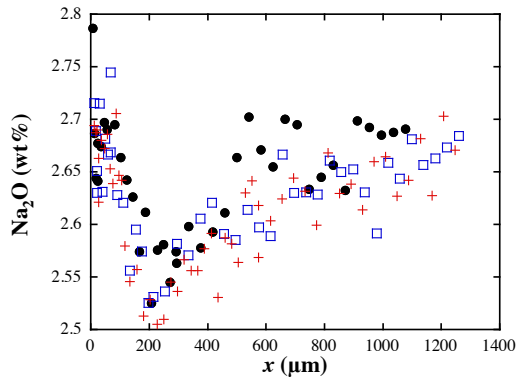
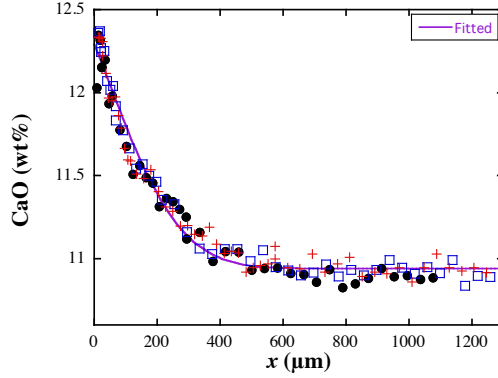
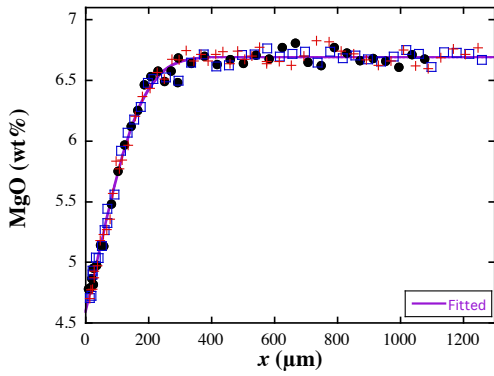
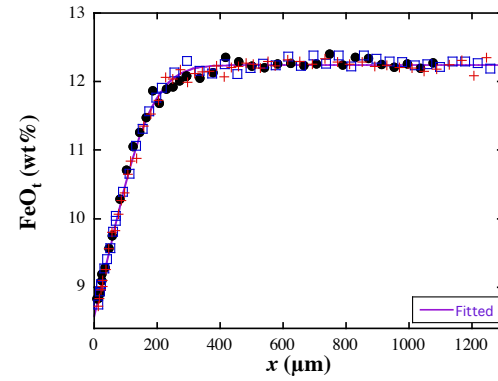
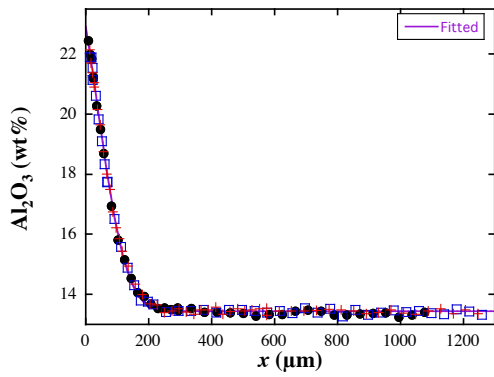
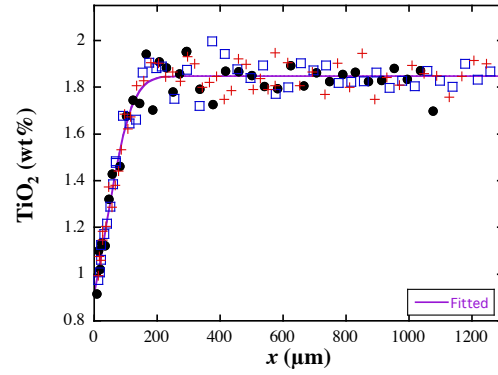
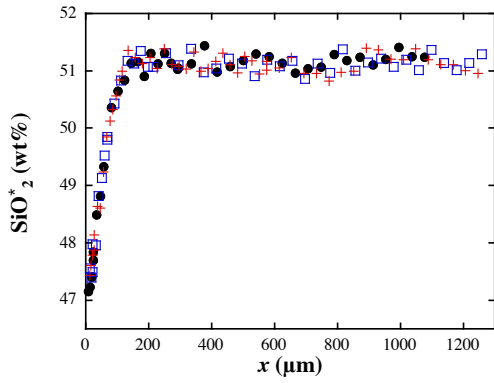
Exp 210 (1333 °C, 0.5 GPa, 1819s)



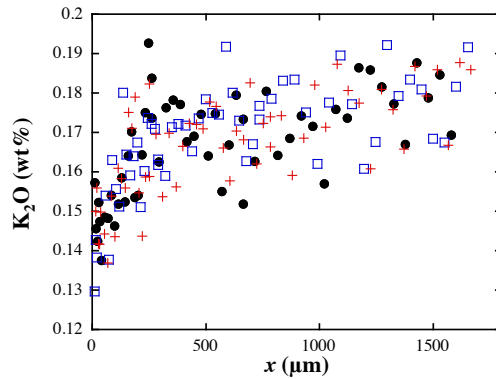
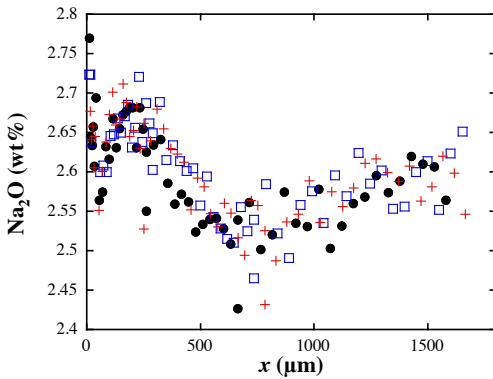
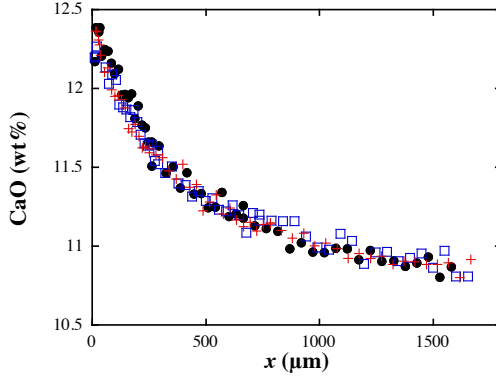
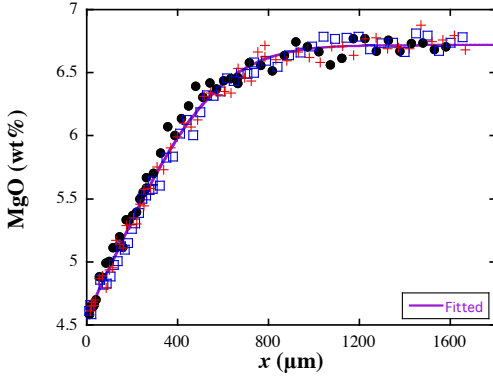
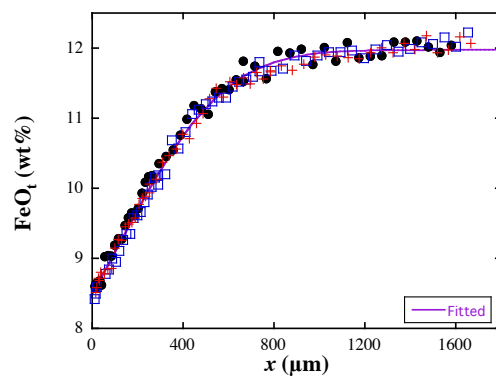
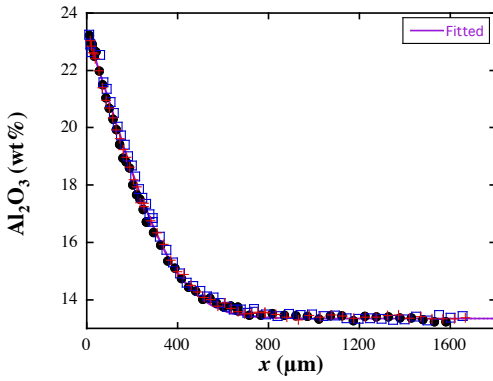
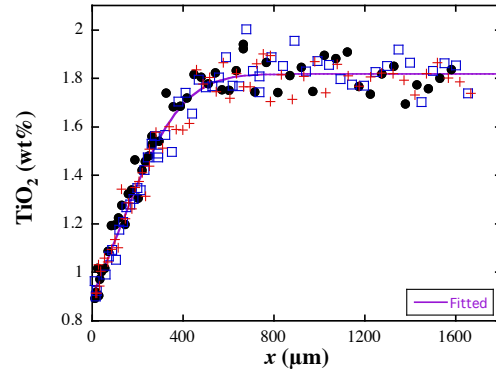
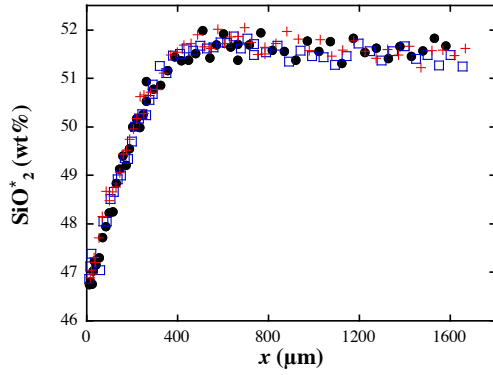
Exp 211 (1333 °C, 0.5 GPa, 919s)



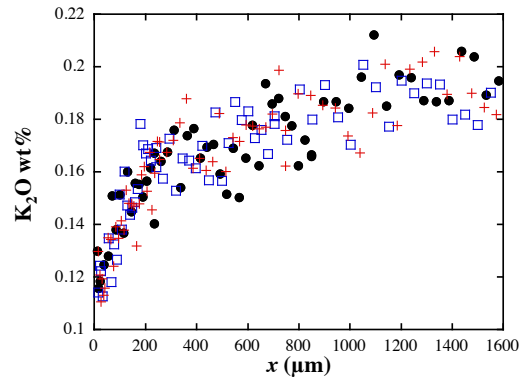
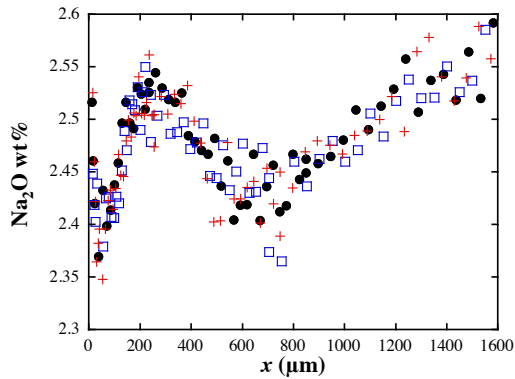
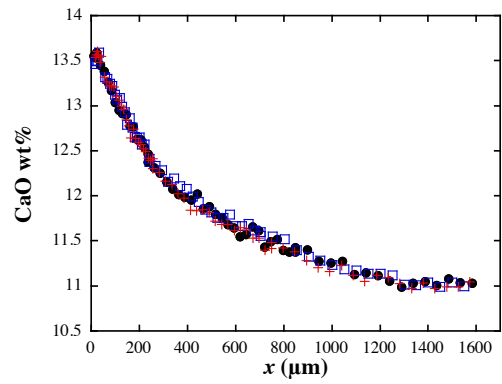
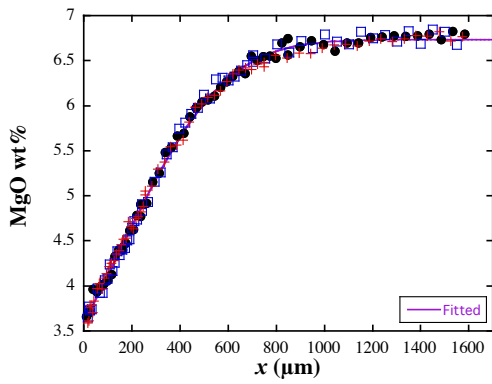
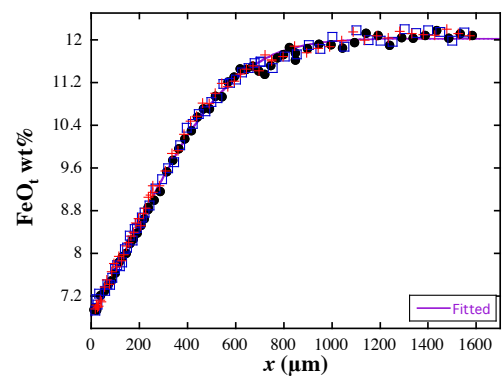
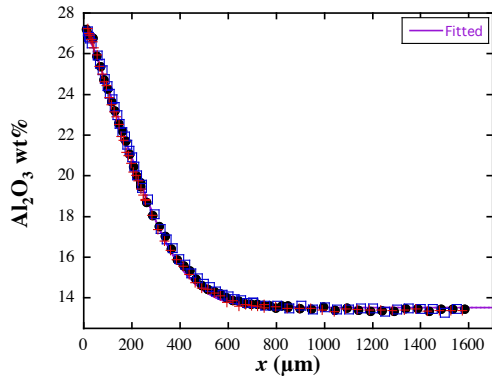
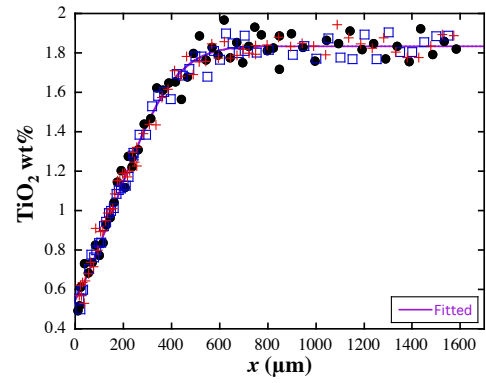
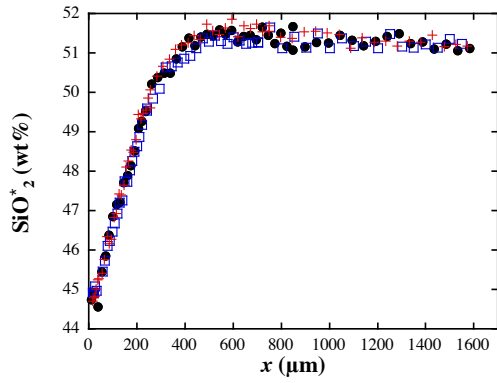
Exp 212 (1334 °C, 0.5 GPa, 443s)



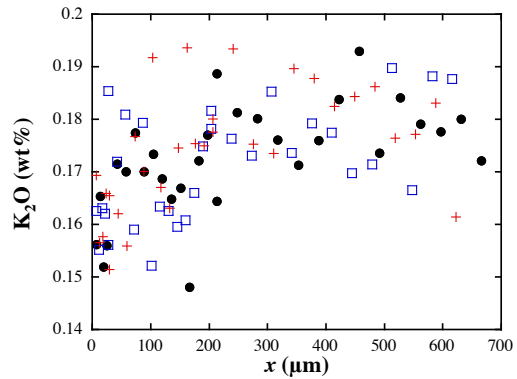
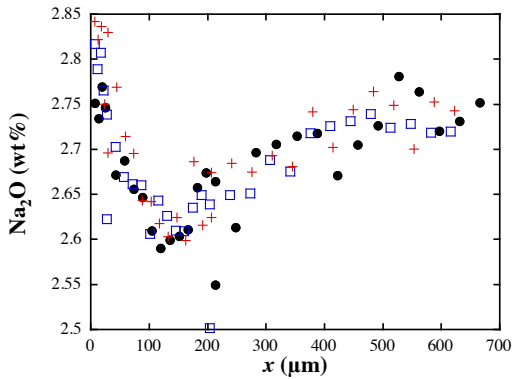
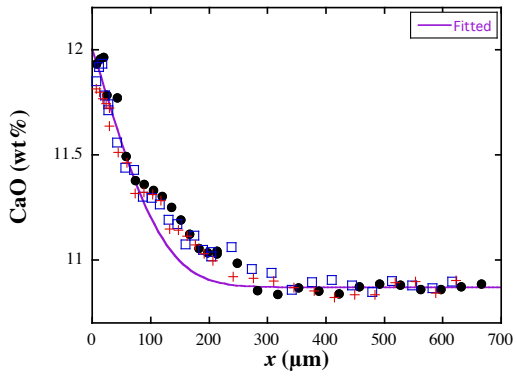
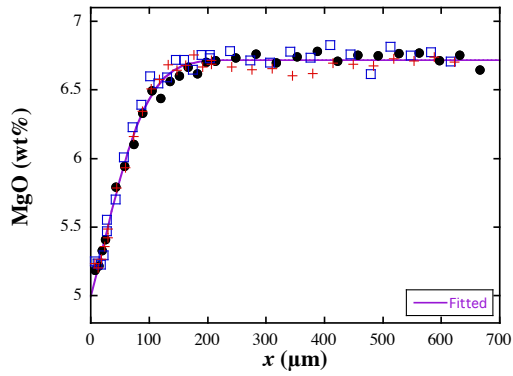
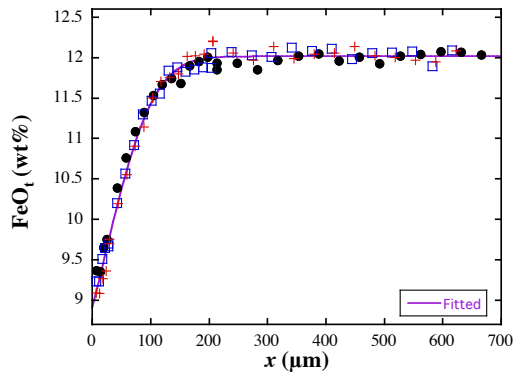
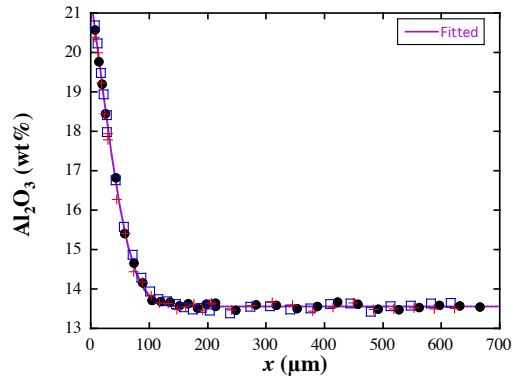
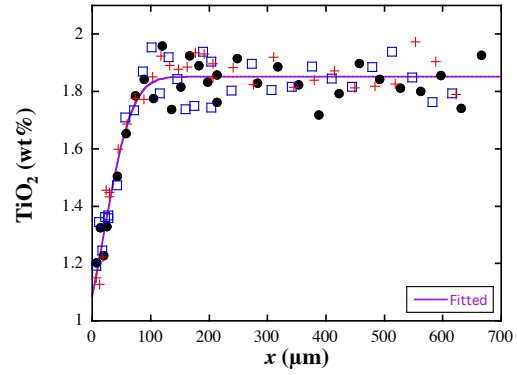
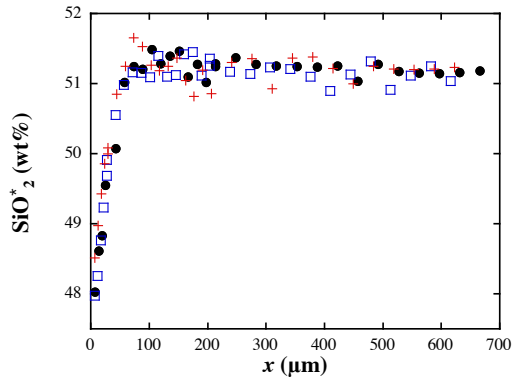
Exp 213 (1328 °C, 0.5 GPa, 3615s)



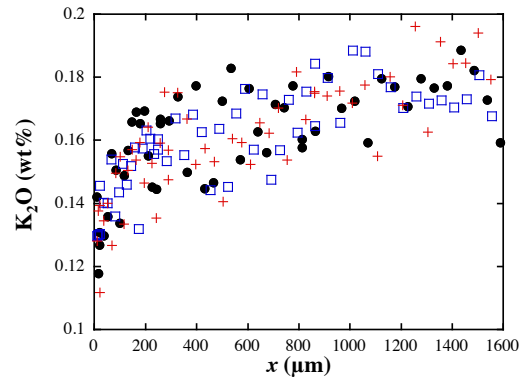
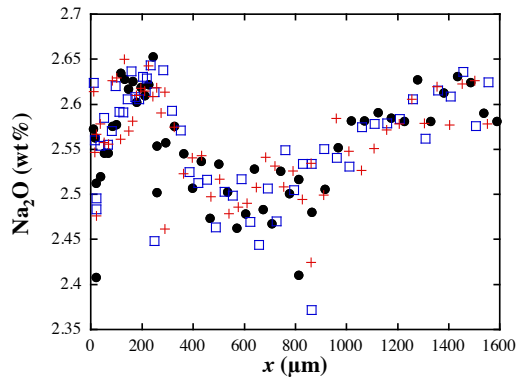
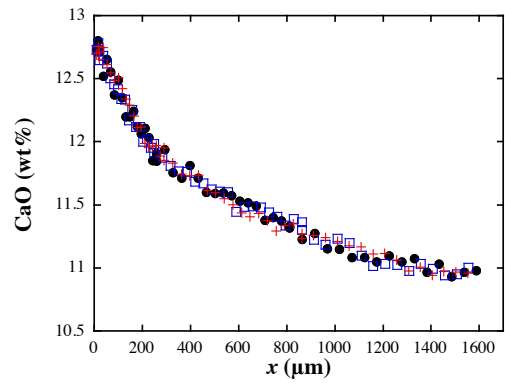
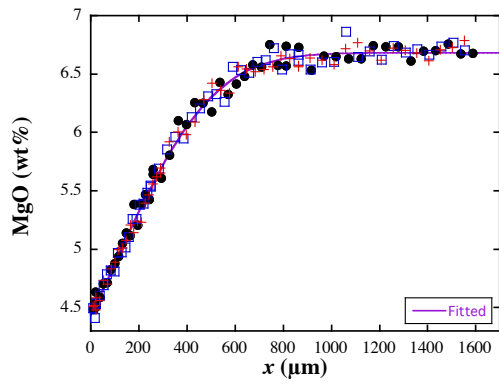
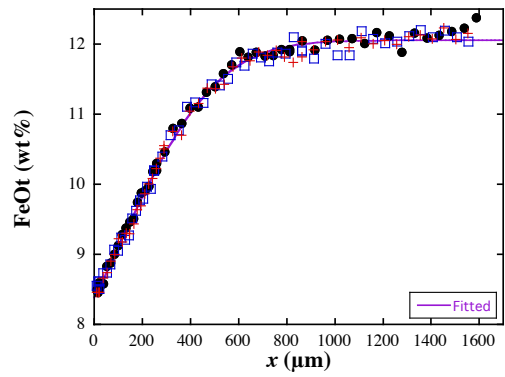
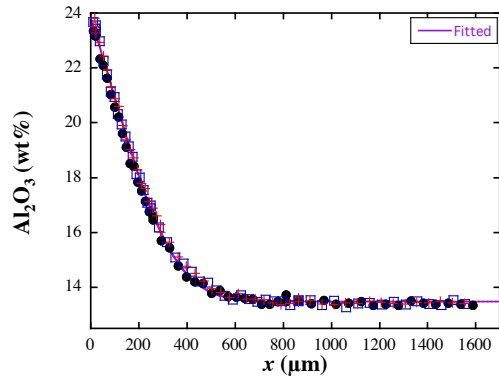
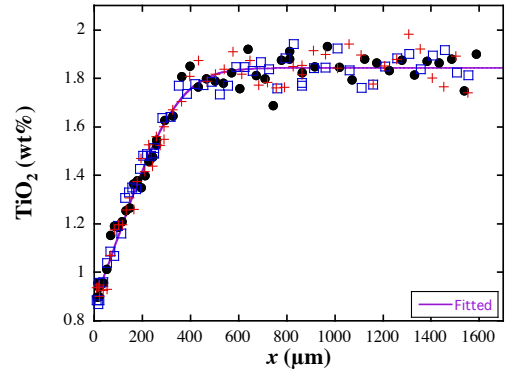
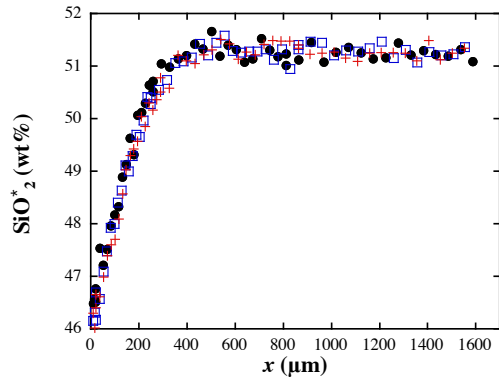
Exp 214 (1327 °C, 0.5 GPa, 2538s)



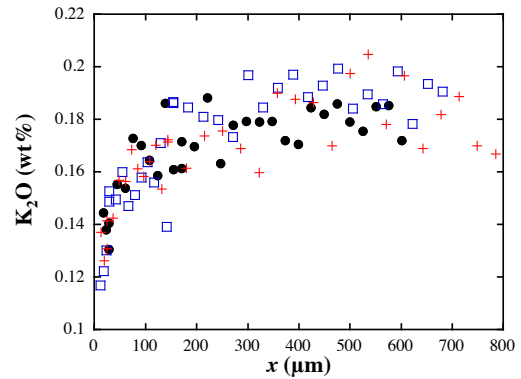
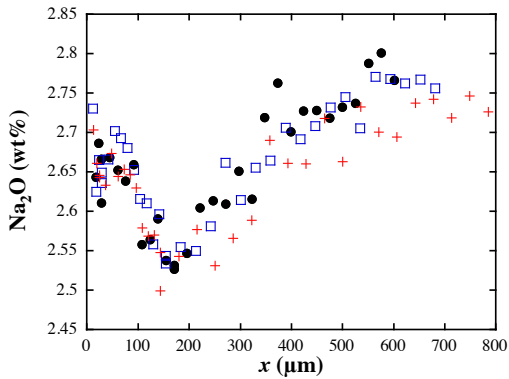
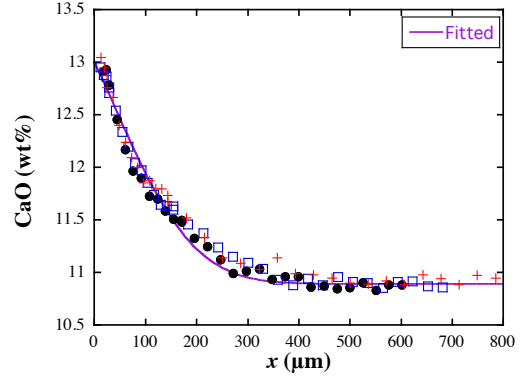
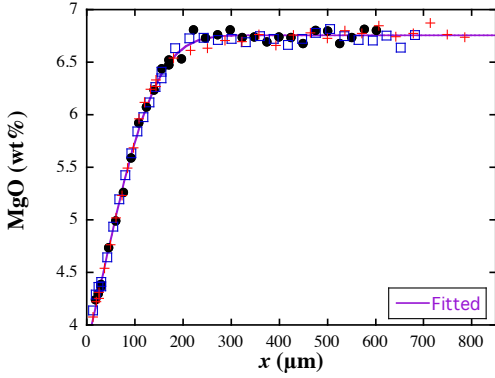
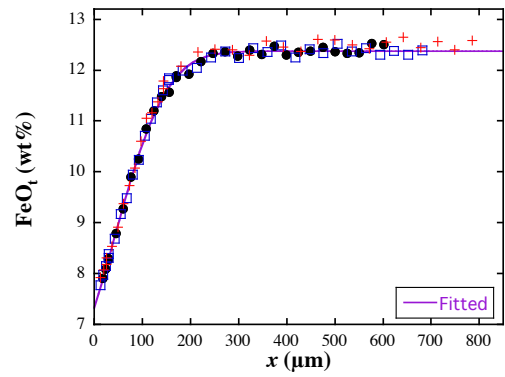
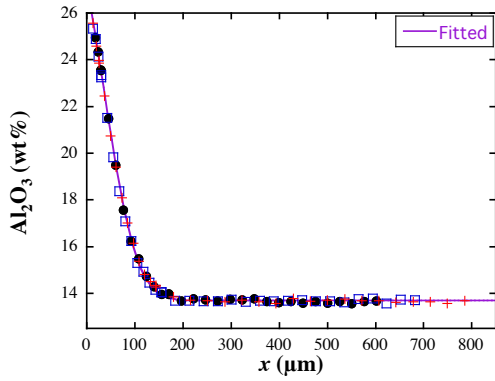
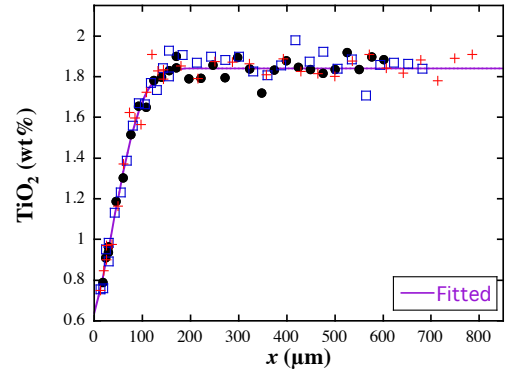
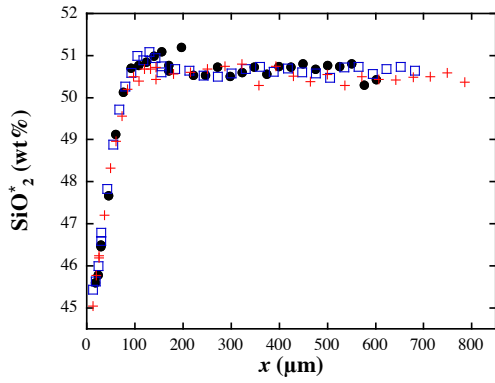
Exp 215 (1327 °C, 0.5 GPa, 143s)



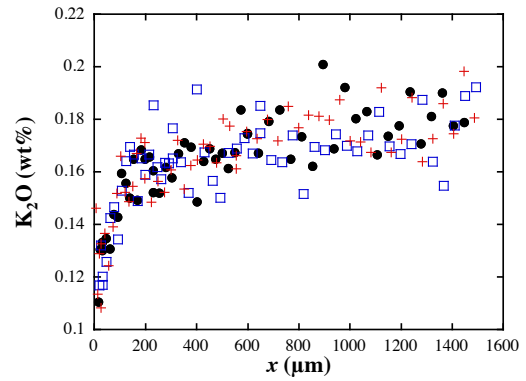
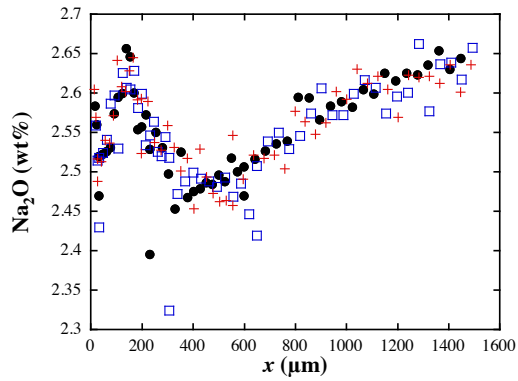
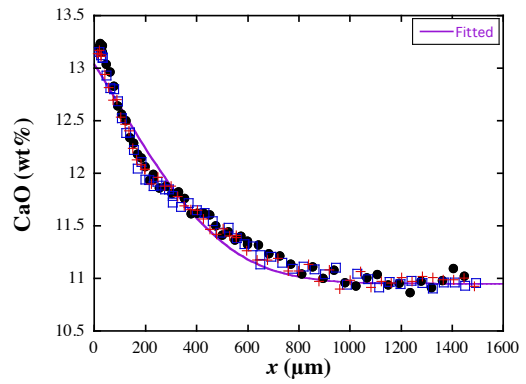
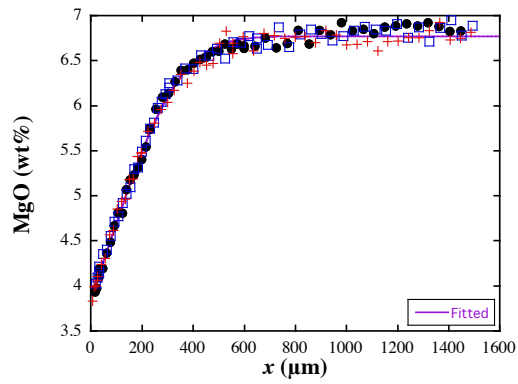
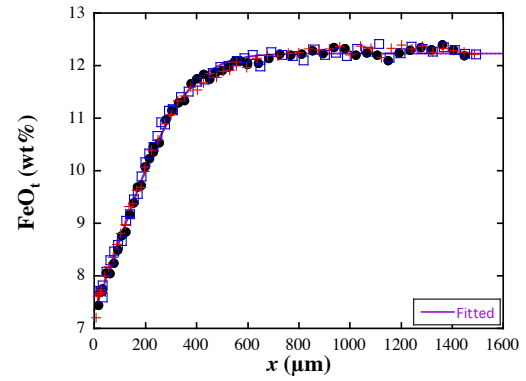
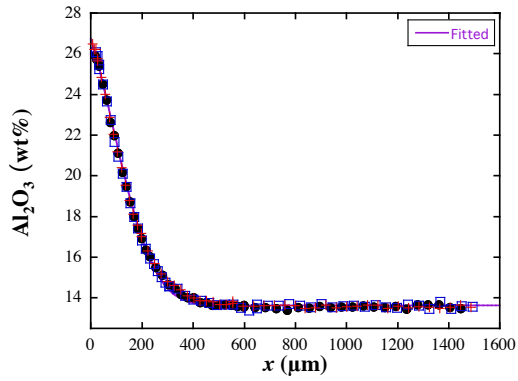
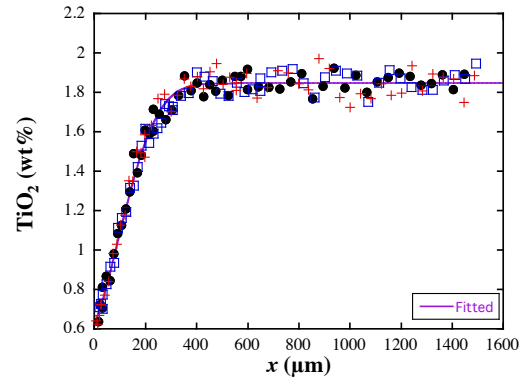
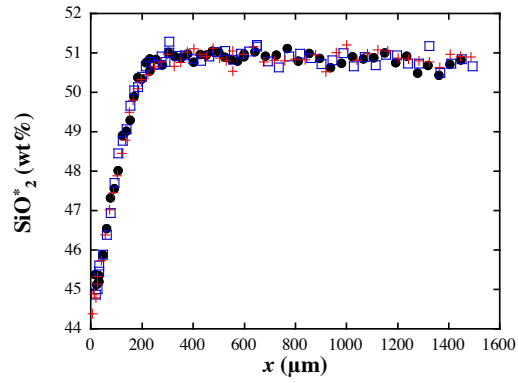
Exp 216 (1326 °C, 0.5 GPa, 2540s)



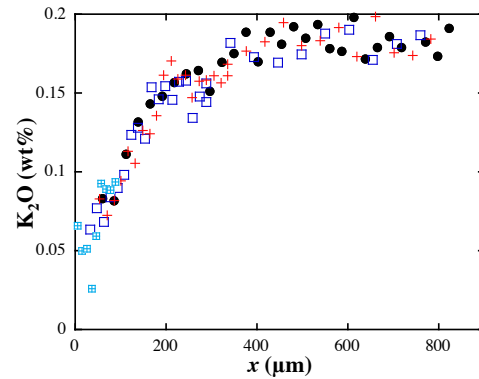
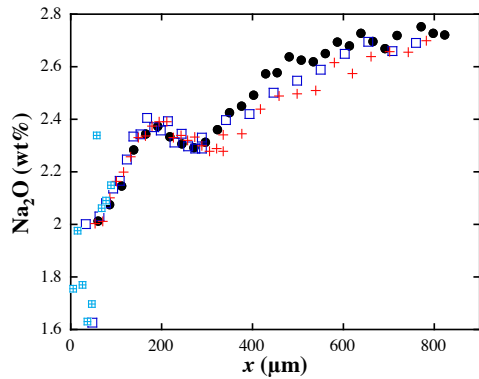
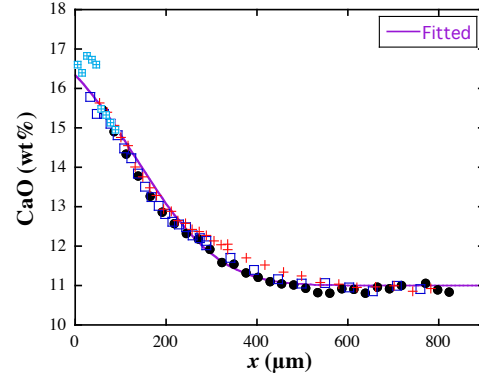
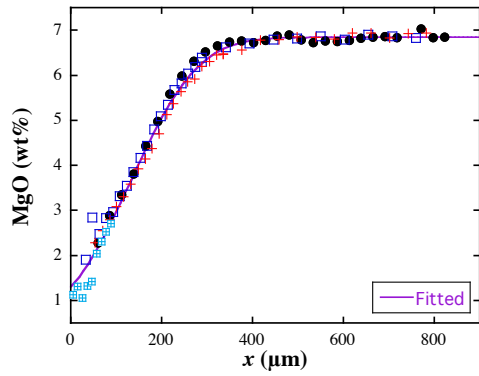
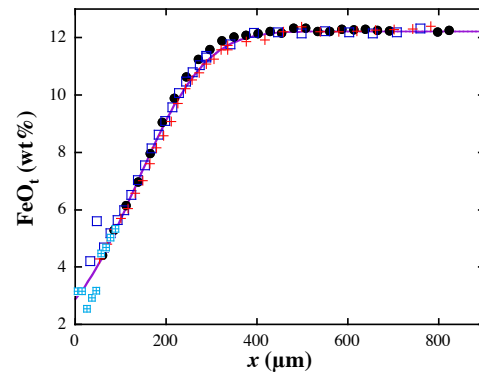
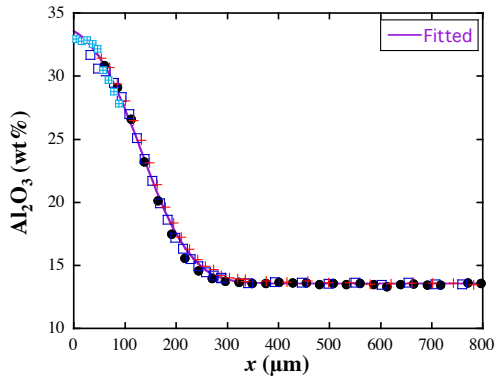
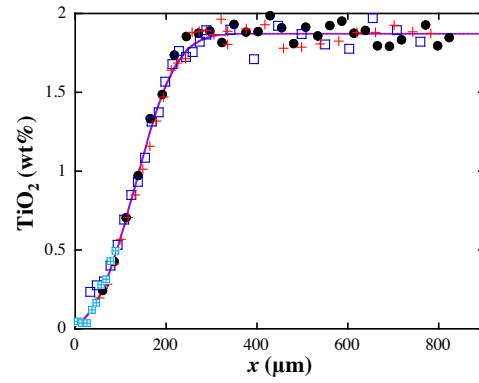
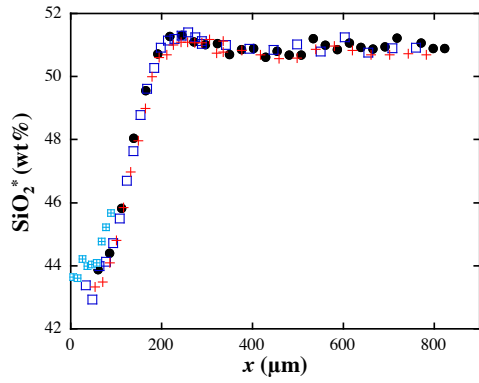
Exp 228 (1408 °C, 0.5 GPa, 143s)



Exp 233 (1405 °C, 0.5 GPa, 620s)



Exp 230 (1506 °C, 0.5 GPa, 134s)



Appendix C

Literature Data on Al₂O₃ Diffusivity During Mineral Dissolution Experiments

Table Part 1

Source	Sample#	Dissolving mineral	Tc (°C)	P (kbar)	D _{Al₂O₃} (m ² /s)	Interface melt (wt%)							
						SiO ₂	TiO ₂	Al ₂ O ₃	FeO _t	MnO	MgO	CaO	Na ₂ O
This study	201	An	1293	5	4.69E-12	47.47	1.17	20.14	9.51	0.18	5.18	11.86	2.70
This study	202	An	1284	5	6.53E-12	47.33	1.16	20.61	9.52	0.20	5.07	11.96	2.65
This study	203	An	1280	5	4.54E-12	48.72	1.36	18.59	10.17	0.20	5.56	11.61	2.80
This study	205	An	1286	5	3.04E-12	49.17	1.46	17.12	10.44	0.23	5.83	11.27	2.85
This study	207	An	1278	5	3.55E-12	48.82	1.36	18.42	10.14	0.20	5.60	11.57	2.80
This study	208	An	1278	5	7.21E-12	47.23	1.11	21.12	9.19	0.17	4.99	12.19	2.65
This study	209	An	1280	5	5.11E-12	47.85	1.31	18.98	10.01	0.18	5.49	11.65	2.75
This study	221	An	1284	5	4.13E-12	48.16	1.10	21.22	9.44	0.20	5.15	11.98	2.80
This study	222	An	1279	5	3.98E-12	48.87	1.44	17.66	10.43	0.20	5.83	11.37	2.80
This study	227	An	1283	5	5.47E-12	48.06	1.24	20.20	9.80	0.19	5.35	11.74	2.75
This study	301	An	1284	5	2.86E-12	47.84	1.36	18.27	10.88	0.20	5.61	11.30	2.90
This study	302	An	1284	5	5.49E-12	47.00	1.21	19.68	9.83	0.21	5.30	11.60	2.92
This study	304	An	1281	5	5.07E-12	48.99	1.29	19.14	9.78	0.19	5.51	11.33	2.90
This study	210	An	1333	5	6.79E-12	45.80	0.84	24.33	8.37	0.15	4.50	12.52	2.60
This study	211	An	1333	5	4.95E-12	46.66	0.98	22.83	8.92	0.16	4.79	12.08	2.75
This study	212	An	1334	5	6.44E-12	46.71	0.92	22.91	8.52	0.18	4.60	12.30	2.70
This study	213	An	1328	5	7.50E-12	47.38	0.90	23.36	8.49	0.16	4.57	12.27	2.50

This study	215	An	1327	5	6.46E-12	48.48	1.09	21.35	8.91	0.15	4.99	12.00	2.80
This study	216	An	1326	5	8.05E-12	46.85	0.89	23.76	8.39	0.15	4.44	12.63	2.55
This study	228	An	1408	5	1.01E-11	45.70	0.62	26.92	7.39	0.11	3.87	13.00	2.60
This study	233	An	1405	5	1.33E-11	45.90	0.61	26.87	7.27	0.14	3.85	13.08	2.60
This study	230	An	1506	5	2.23E-11	44.48	0.02	34.00	2.66	0.05	1.26	16.65	2.00
Chen08	315	Ol	1271	4.7	4.45E-12	47.56	1.72	12.35	13.00	0.20	10.41	10.75	2.20
Chen08	316	Ol	1270	4.7	5.38E-12	47.50	1.62	11.74	13.10	0.20	10.85	10.35	2.00
Chen08	318	Ol	1270	4.7	7.30E-12	48.12	1.72	11.97	13.10	0.20	10.75	10.58	2.10
Chen08	320	Ol	1270	4.7	3.86E-12	47.69	1.71	11.88	13.20	0.20	10.31	10.50	2.20
Chen08	321	Ol	1270	4.7	6.61E-12	47.75	1.69	11.58	13.60	0.20	11.44	10.14	1.90
Chen08	323	Ol	1373	4.7	1.80E-11	46.69	1.51	9.93	13.80	0.20	15.44	9.85	1.60
Chen08	325	Ol	1376	4.7	1.59E-11	46.77	1.46	9.37	14.00	0.20	16.20	9.63	1.60
Chen08	326	Ol	1370	4.7	1.99E-11	46.51	1.48	9.88	14.00	0.20	15.40	9.75	1.60
Chen08	329	Ol	1372	4.7	2.00E-11	46.11	1.44	9.10	13.50	0.20	17.23	9.50	1.60
Chen08	333	Ol	1368	4.7	1.99E-11	46.87	1.50	9.76	14.00	0.20	15.46	9.96	1.70
Chen08	334	Ol	1473	4.7	6.08E-11	45.17	1.20	6.84	13.80	0.20	22.71	8.14	1.30
Chen08	337	Ol	1476	4.7	5.84E-11	44.06	1.17	7.22	14.00	0.20	22.39	8.12	1.20
Chen08	338	Ol	1477	4.7	7.00E-11	43.96	1.20	6.98	14.00	0.20	22.10	8.34	1.20
Chen08	339	Ol	1374	9.4	1.35E-11	47.51	1.58	10.51	13.50	0.20	13.55	10.08	1.90
Chen08	340	Ol	1376	9.4	1.45E-11	47.36	1.53	10.54	13.50	0.20	14.01	9.98	1.90
Chen08	341	Ol	1379	9.4	1.77E-11	47.52	1.54	10.99	13.50	0.20	13.27	10.05	1.90
Chen08	343	Ol	1480	9.4	6.34E-11	45.81	1.25	8.02	13.60	0.20	20.96	8.39	1.40
Chen08	344	Ol	1374	14.2	1.33E-11	49.00	1.66	12.24	13.50	0.20	10.62	10.41	2.20
Chen08	345	Ol	1422	14.2	3.25E-11	47.23	1.46	10.17	13.20	0.20	15.94	9.46	1.80
Chen08	346	Ol	1425	14.2	3.34E-11	47.08	1.39	10.32	13.20	0.20	15.26	9.44	1.80
Chen09	401	Cpx	1271	4.7	3.80E-12	51.21	1.37	9.57	11.60	0.20	9.40	13.12	2.14
Chen09	405	Cpx	1362	9.4	1.00E-11	52.73	1.07	7.10	10.50	0.20	10.92	14.64	1.85
Chen09	406	Cpx	1446	14.2	4.51E-11	52.81	0.69	5.08	8.50	0.20	13.13	17.40	1.40

Chen09	407	Cpx	1321	4.7	1.04E-11	53.05	0.62	3.71	8.70	0.20	13.84	17.58	1.39
Chen09	408	Cpx	1394	9.4	1.93E-11	53.78	0.52	3.40	8.50	0.20	13.98	17.66	1.25
Chen09	411	Cpx	1422	19	3.55E-11	51.54	1.42	10.10	10.70	0.20	9.31	13.68	2.06
Chen09	412	Cpx	1368	14.2	1.61E-11	50.95	1.36	10.86	11.20	0.20	8.78	12.84	2.23
Chen09	414	Cpx	1236	4.7	4.30E-12	50.50	1.66	12.50	12.00	0.20	7.64	11.71	2.54
Chen09	415	Cpx	1517	19	7.16E-11	53.51	0.68	5.31	8.50	0.20	12.87	17.77	1.28
Zhang89	Y212	Ol	1285	5.5	3.30E-12	51.84	1.19	14.50	8.97	0.16	10.87	8.24	2.56
Zhang89	Y216	Ol	1250	5.5	1.40E-12	54.14	1.15	15.76	8.06	0.13	8.65	7.85	2.84
Zhang89	Y219	Ol	1250	5.5	1.60E-12	53.20	1.12	14.94	8.38	0.18	9.98	8.28	2.54
Zhang89	Y222	Ol	1300	5	4.20E-12	51.96	1.13	13.54	10.07	0.18	11.54	8.20	2.30
Zhang89	Y223	Di	1305	10.5	2.50E-12	57.64	1.08	12.60	7.76	0.15	7.26	10.52	2.30
Zhang89	Y225	Di	1305	10.5	3.80E-12	56.11	1.06	12.81	7.00	0.13	7.54	10.84	2.40
Zhang89	Y226	Fo	1285	5.5	2.60E-12	53.48	1.30	15.29	7.71	0.16	9.49	8.45	2.49
Zhang89	Y227	Fo	1300	5.5	3.00E-12	53.64	1.31	15.31	7.45	0.17	9.75	8.47	2.58
Zhang89	Y228	Ol	1300	5	4.00E-12	52.62	1.16	13.96	8.97	0.19	11.36	8.27	2.54
Zhang89	Y228*	Fo	1300	5	4.70E-12	52.88	1.16	14.30	7.58	0.17	11.65	8.05	2.55
Zhang89	Y229	Ol	1185	5	1.10E-12	54.20	1.23	15.89	8.45	0.18	6.80	8.35	2.91
Zhang89	Y231	Ol	1365	13	8.50E-12	52.28	1.16	13.58	9.41	0.17	11.53	7.84	2.24
Zhang89	Y231*	Sp	1385	13	3.80E-12	48.80	1.27	24.73	7.13	0.15	5.85	8.43	3.28
Zhang89	Y231**	Di	1365	13	7.30E-12	58.37	0.85	9.10	7.21	0.13	9.62	13.25	2.13
Zhang89	Y234	Qz	1300	5.5	4.20E-13	73.33	0.72	12.34	3.56	0.06	1.93	3.42	2.62
Zhang89	Y235	Ol	1350	5	7.00E-12	51.96	1.12	13.43	9.28	0.18	13.16	7.73	1.84
Zhang89	Y236	Ol	1375	15	1.60E-11	52.04	1.20	14.28	8.75	0.18	12.24	7.71	2.29
Zhang89	Y239	Ol	1420	5.5	1.20E-11	52.37	1.13	12.99	8.99	0.18	14.13	7.99	2.51
Zhang89	Y242	Di	1375	22	1.00E-11	56.58	1.00	12.59	6.99	0.13	7.85	11.75	2.07
Morgan05	AnDis4	An	1400	6	4.10E-11	41.96	0.00	32.15	6.10	0.00	0.00	15.65	0
Morgan06	AnDis5	An	1400	6	5.30E-11	41.96	0.02	32.62	5.56	0.00	0.00	16.04	0
Finnila94	1340	An	1340	0.001	1.00E-12	44.00	5.50	23.00	0.00	0.00	12.20	15.80	0

Finnila94	1390	An	1390	0.001	1.00E-11	43.12	3.90	26.88	0.00	0.00	10.78	15.71	0
-----------	------	----	------	-------	----------	-------	------	-------	------	------	-------	-------	---

Table Part 2

Source	Sample#	Interface melt (wt%)		farfield melt (wt%)									
		K2O	H2O	SiO2	TiO2	Al2O3	FeOt	MnO	MgO	CaO	Na2O	K2O	H2O
This study	201	0.17	0.32	50.62	1.85	13.38	11.87	0.21	6.70	11.02	2.59	0.18	0.32
This study	202	0.16	0.32	50.72	1.80	13.35	11.95	0.18	6.78	11.04	2.59	0.18	0.32
This study	203	0.16	0.32	51.49	1.85	13.40	12.23	0.21	6.74	11.00	2.73	0.18	0.32
This study	205	0.17	0.32	51.04	1.79	13.41	11.95	0.25	6.67	10.89	2.68	0.18	0.32
This study	207	0.17	0.32	51.49	1.82	13.34	12.00	0.21	6.77	10.97	2.73	0.18	0.32
This study	208	0.16	0.32	50.89	1.88	13.32	12.11	0.22	6.76	11.16	2.56	0.17	0.32
This study	209	0.17	0.32	50.04	1.83	13.33	12.06	0.21	6.76	10.93	2.66	0.18	0.32
This study	221	0.17	0.32	51.65	1.84	13.61	12.14	0.22	6.82	10.99	2.70	0.18	0.32
This study	222	0.17	0.32	50.46	1.82	13.52	12.16	0.19	6.82	10.88	2.71	0.18	0.32
This study	227	0.16	0.32	50.71	1.84	13.52	12.22	0.22	6.82	11.06	2.66	0.18	0.32
This study	301	0.18	0.32	49.97	1.79	13.62	12.78	0.20	6.66	10.79	2.72	0.18	0.32
This study	302	0.17	0.32	49.98	1.82	13.68	12.76	0.21	6.68	10.87	2.69	0.18	0.32
This study	304	0.18	0.32	50.78	1.83	13.43	12.38	0.21	6.65	10.89	2.64	0.18	0.32
This study	210	0.14	0.32	50.65	1.86	13.60	12.06	0.21	6.77	10.89	2.68	0.18	0.32
This study	211	0.16	0.32	50.97	1.83	13.68	12.10	0.21	6.78	10.87	2.74	0.18	0.32
This study	212	0.14	0.32	51.03	1.84	13.38	12.24	0.22	6.70	10.91	2.68	0.18	0.32
This study	213	0.15	0.32	51.92	1.80	13.33	12.06	0.22	6.73	10.87	2.60	0.18	0.32
This study	215	0.16	0.32	51.89	1.85	13.55	12.02	0.21	6.73	10.88	2.73	0.18	0.32
This study	216	0.13	0.32	51.88	1.85	13.42	12.14	0.20	6.70	10.97	2.61	0.18	0.32
This study	228	0.12	0.32	51.19	1.87	13.64	12.42	0.22	6.75	10.90	2.76	0.18	0.32

This study	233	0.12	0.32	51.50	1.86	13.57	12.28	0.23	6.84	10.98	2.63	0.18	0.32
This study	230	0.04	0.32	50.97	1.87	13.52	12.15	0.20	6.88	10.93	2.69	0.18	0.32
Chen08	315	0.10	0.32	48.61	1.88	13.92	12.00	0.20	6.96	11.20	2.7	0.2	0.32
Chen08	316	0.10	0.32	48.80	1.87	13.94	12.00	0.20	6.88	11.12	2.7	0.2	0.32
Chen08	318	0.10	0.32	49.85	1.88	14.10	11.70	0.20	6.89	11.21	2.8	0.2	0.32
Chen08	320	0.10	0.32	49.09	1.87	13.95	12.20	0.20	6.86	11.16	2.7	0.2	0.32
Chen08	321	0.10	0.32	49.38	1.88	14.04	12.30	0.20	6.96	11.12	2.7	0.2	0.32
Chen08	323	0.10	0.32	49.63	1.88	14.17	12.10	0.20	6.87	11.14	2.7	0.2	0.32
Chen08	325	0.10	0.32	49.53	1.89	13.99	12.40	0.20	6.76	11.17	2.7	0.2	0.32
Chen08	326	0.10	0.32	49.74	1.89	14.15	12.10	0.20	6.75	11.22	2.8	0.2	0.32
Chen08	329	0.10	0.32	49.63	1.87	14.03	12.00	0.20	6.87	11.13	2.7	0.2	0.32
Chen08	333	0.10	0.32	50.51	1.90	14.17	11.80	0.20	6.86	11.41	2.8	0.2	0.32
Chen08	334	0.10	0.32	50.14	1.87	14.13	12.00	0.20	6.81	11.08	2.7	0.2	0.32
Chen08	337	0.10	0.32	49.04	1.86	14.18	11.80	0.20	6.77	11.06	2.8	0.2	0.32
Chen08	338	0.10	0.32	48.76	1.88	14.16	12.40	0.20	6.78	11.07	2.7	0.2	0.32
Chen08	339	0.10	0.32	49.79	1.80	13.96	12.00	0.20	7.00	11.13	2.7	0.2	0.32
Chen08	340	0.10	0.32	49.91	1.82	14.01	12.00	0.20	7.03	11.12	2.7	0.2	0.32
Chen08	341	0.10	0.32	49.76	1.84	14.08	12.20	0.20	6.84	11.20	2.7	0.2	0.32
Chen08	343	0.10	0.32	49.62	1.78	14.06	12.00	0.20	7.00	11.17	2.7	0.2	0.32
Chen08	344	0.10	0.32	49.75	1.88	13.96	12.20	0.20	7.03	11.25	2.7	0.2	0.32
Chen08	345	0.10	0.32	49.76	1.80	13.94	12.20	0.20	7.04	11.13	2.7	0.2	0.32
Chen08	346	0.10	0.32	49.35	1.84	14.00	12.00	0.20	7.08	11.16	2.7	0.2	0.32
Chen09	401	0.10	0.32	50.23	1.94	13.61	12.06	0.22	7.05	10.75	2.7	0.2	0.32
Chen09	405	0.10	0.32	50.23	1.94	13.61	12.06	0.22	7.05	10.75	2.7	0.2	0.32
Chen09	406	0.10	0.32	50.23	1.94	13.61	12.06	0.22	7.05	10.75	2.7	0.2	0.32
Chen09	407	0.10	0.32	50.23	1.94	13.61	12.06	0.22	7.05	10.75	2.7	0.2	0.32
Chen09	408	0.10	0.32	50.23	1.94	13.61	12.06	0.22	7.05	10.75	2.7	0.2	0.32
Chen09	411	0.10	0.32	50.23	1.94	13.61	12.06	0.22	7.05	10.75	2.7	0.2	0.32

Chen09	412	0.10	0.32	50.23	1.94	13.61	12.06	0.22	7.05	10.75	2.7	0.2	0.32
Chen09	414	0.10	0.32	50.23	1.94	13.61	12.06	0.22	7.05	10.75	2.7	0.2	0.32
Chen09	415	0.10	0.32	50.23	1.94	13.61	12.06	0.22	7.05	10.75	2.7	0.2	0.32
Zhang89	Y212	0.87	0	56.54	1.28	18.42	6.41	0.11	4.00	7.49	3.8	1.6	0
Zhang89	Y216	1.07	0	56.81	1.29	18.19	6.76	0.13	4.07	7.38	3.2	1.6	0
Zhang89	Y219	1.00	0	55.49	1.25	18.44	5.83	0.12	4.04	7.53	3.7	1.7	0
Zhang89	Y222	0.76	0	56.16	1.24	18.08	6.69	0.12	3.92	7.37	3.7	1.5	0
Zhang89	Y223	0.91	0	57.62	1.29	18.29	6.67	0.13	3.86	7.58	2.6	1.6	0
Zhang89	Y225	0.89	0	56.31	1.30	18.45	6.61	0.14	3.92	7.76	3.3	1.4	0
Zhang89	Y226	0.93	0	56.84	1.29	17.90	6.88	0.12	3.84	7.59	2.6	1.6	0
Zhang89	Y227	0.90	0	56.93	1.30	17.88	6.78	0.13	3.87	7.45	2.6	1.6	0
Zhang89	Y228	0.72	0	57.44	1.28	18.25	6.27	0.11	4.56	7.06	3.1	1.3	0
Zhang89	Y228*	0.66	0	56.85	1.29	18.07	6.52	0.13	4.02	7.48	3.2	1.0	0
Zhang89	Y229	1.16	0	57.27	1.23	18.08	6.70	0.12	3.78	7.45	3.2	1.7	0
Zhang89	Y231	0.70	0	58.61	1.28	18.25	6.68	0.11	4.16	7.27	3.7	1.6	0
Zhang89	Y231*	1.08	0	57.36	1.29	18.56	6.43	0.13	4.20	7.22	3.7	1.7	0
Zhang89	Y231**	0.63	0	57.66	1.29	18.26	6.38	0.12	3.92	7.78	3.7	1.8	0
Zhang89	Y234	2.40	0	57.38	1.28	18.10	6.86	0.11	3.98	7.60	3.6	1.5	0
Zhang89	Y235	0.66	0	56.82	1.25	17.98	6.85	0.13	4.31	7.37	2.7	1.7	0
Zhang89	Y236	0.72	0	57.07	1.27	18.29	6.95	0.11	3.94	7.50	3.7	1.6	0
Zhang89	Y239	0.60	0	57.25	1.27	18.06	6.71	0.12	4.08	7.37	4.0	1.7	0
Zhang89	Y242	1.07	0	55.91	1.26	18.65	6.66	0.12	4.03	7.50	3.7	1.6	0
Morgan05	AnDis4	0	0	44.26	3.63	9.08	21.65	0.57	10.97	8.76	0.4	0	0
Morgan06	AnDis5	0	0	36.76	13.89	7.51	22.95	0.05	10.16	8.57	0.6	0	0
Finnila94	1340	0	0	44.40	11.70	11.10	0.00	0.00	20.00	12.80	0	0	0
Finnila94	1390	0	0	44.40	11.70	11.10	0.00	0.00	20.00	12.80	0	0	0

* and ** mean different samples in the same experiment capsule and setting

Appendix D

Derivation of Boltzmann Analysis for Diffusion During Crystal Dissolution

Diffusion equation of mineral dissolution in the melt:

$$\frac{\partial C}{\partial t} = \frac{\partial}{\partial x} \left(D \frac{\partial C}{\partial x} \right) - V \frac{\partial C}{\partial x}, \quad (\text{D-1})$$

Boundary condition at interface:

$$\left(D \frac{\partial C}{\partial x} \right) \Big|_{x=0} + V(C_c - C_{x=0}) = 0, \quad (\text{D-2})$$

Set:

$$\eta = \frac{x}{\sqrt{t}}; \frac{\partial \eta}{\partial x} = \frac{1}{\sqrt{t}}; \frac{\partial \eta}{\partial t} = -\frac{\eta}{2t}, \quad (\text{D-3})$$

Transform the diffusion equation using η :

$$-\frac{\eta}{2t} \frac{\partial C}{\partial \eta} = \frac{1}{t} \left(\frac{\partial}{\partial \eta} \left(D \frac{\partial C}{\partial \eta} \right) \right) - \frac{V}{\sqrt{t}} \frac{\partial C}{\partial \eta}, \quad (\text{D-4})$$

$$V(C_c - C_{x=0}) + \frac{1}{\sqrt{t}} \left(D \frac{\partial C}{\partial \eta} \right) \Big|_{\eta=0} = 0, \quad (\text{D-5})$$

Substitute V from Eq. (D-5) into the diffusion equation (D-4):

$$-\frac{\eta}{2} \frac{\partial C}{\partial \eta} = \left(\frac{\partial}{\partial \eta} \left(D \frac{\partial C}{\partial \eta} \right) \right) + \frac{\left(D \frac{\partial C}{\partial \eta} \right) \Big|_{\eta=0}}{C_c - C_{\eta=0}} \frac{\partial C}{\partial \eta}, \quad (\text{D-6})$$

Rearrange the equation (note that $D_{\eta=0}$ is a constant):

$$\left(\frac{D \frac{\partial C}{\partial \eta}}{C_c - C_{\eta=0}} + \frac{\eta}{2} \right) \frac{\partial C}{\partial \eta} + \left(\frac{\partial}{\partial \eta} \left(D \frac{\partial C}{\partial \eta} \right) \right) = 0, \quad (\text{D-7})$$

Integrate the above differential equation along η from η_0 to ∞ and recognizing $(\partial C / \partial \eta)_{\eta=\infty} = 0$:

$$\frac{\left(D \frac{\partial C}{\partial \eta} \right) \Big|_{\eta=0}}{C_c - C_{\eta=0}} (C_\infty - C_{\eta_x}) + \frac{1}{2} \int_{C_{\eta_x}}^{C_\infty} \eta dC - D \frac{\partial C}{\partial \eta} \Big|_{\eta_x} = 0, \quad (\text{D-8})$$

Express D as the function of the rest parameters:

$$D = \frac{\left. \left(D \frac{\partial C}{\partial \eta} \right) \right|_{\eta=0} (C_\infty - C_{\eta_x}) + \frac{1}{2} \int_{C_{\eta_x}}^{C_\infty} \eta dC}{\left. \frac{\partial C}{\partial \eta} \right|_{\eta_x}} = \frac{\left. \left(D \frac{\partial C}{\partial x} \right) \right|_{x=0} \frac{(C_\infty - C_x)}{C_c - C_{x=0}} + \frac{1}{2t} \int_{C_x}^{C_\infty} x dC}{\left. \frac{\partial C}{\partial x} \right|_x}, \quad (\text{D-9})$$

When $x = 0$; $D = D_{x=0}$

$$D_{x=0} = \frac{C_c - C_0}{C_c - C_\infty} \frac{\int_{C_0}^{C_\infty} x dC}{2t \left. \frac{\partial C}{\partial x} \right|_{x=0}}, \quad (\text{D-10})$$

Substitute $D_{x=0}$ into Eq. (D-9):

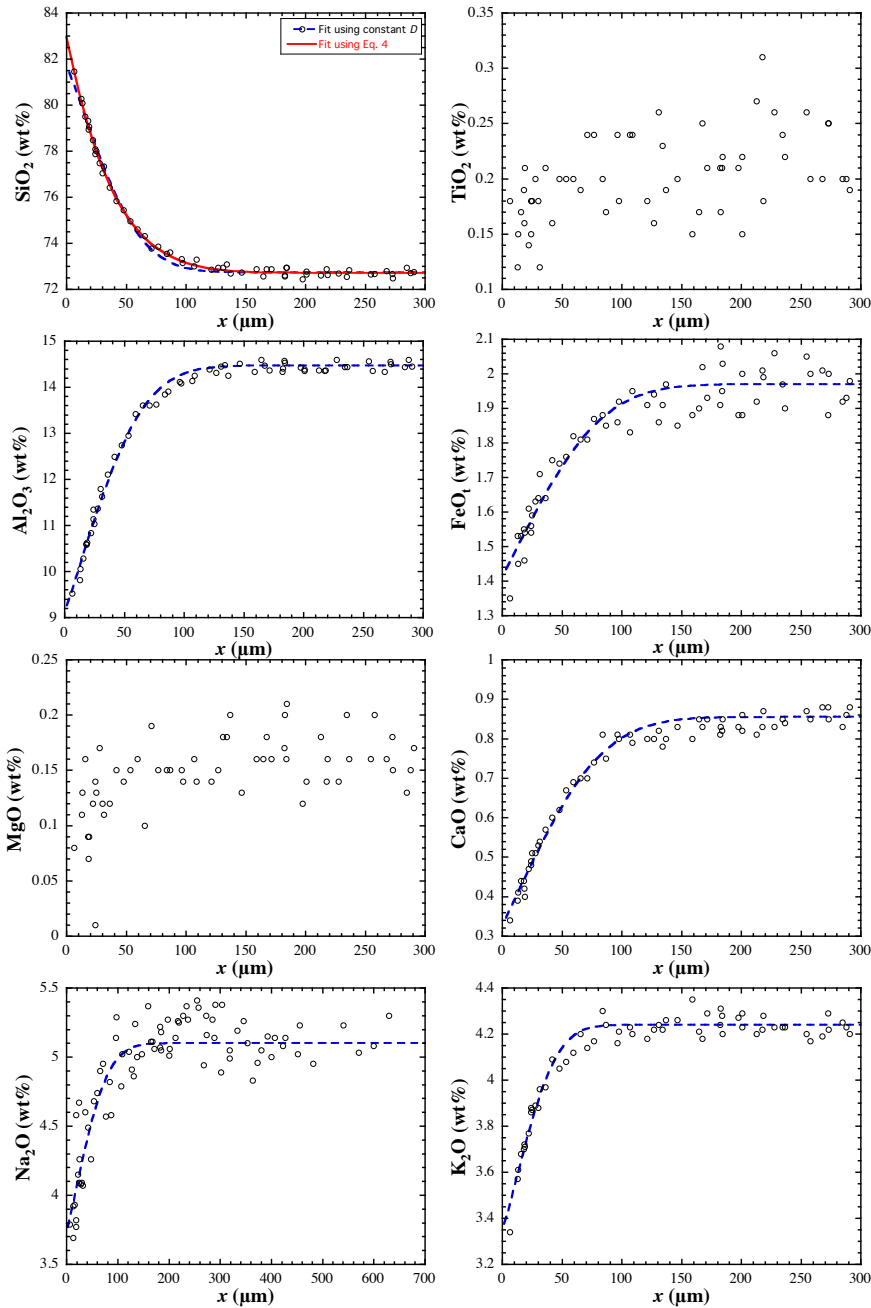
$$D = \frac{\frac{C_\infty - C_x}{C_c - C_\infty} \int_{C_0}^{C_\infty} x dC + \int_{C_x}^{C_\infty} x dC}{2t \left. \frac{\partial C}{\partial x} \right|_x}, \quad (\text{D-11})$$

Hence, to calculate D at a given point x , we need C_x , $(\partial C/\partial x)_x$, $\int x dC$ from C_x to C_∞ . Other parameters in the above equation are constants for a given experiment and a given profile.

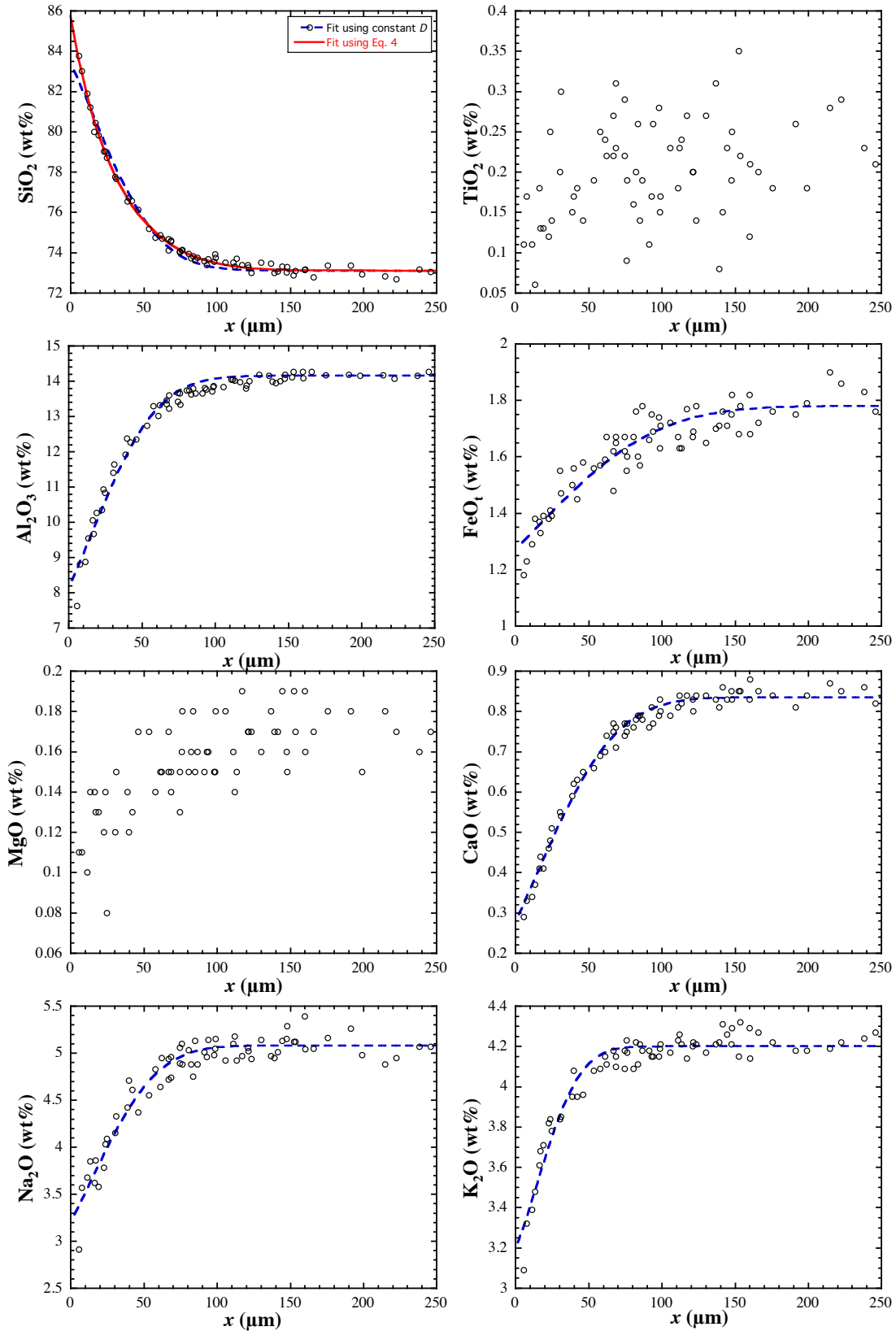
Appendix E

Composition Profiles of Quartz Dissolution in Rhyolitic and Basaltic Melts

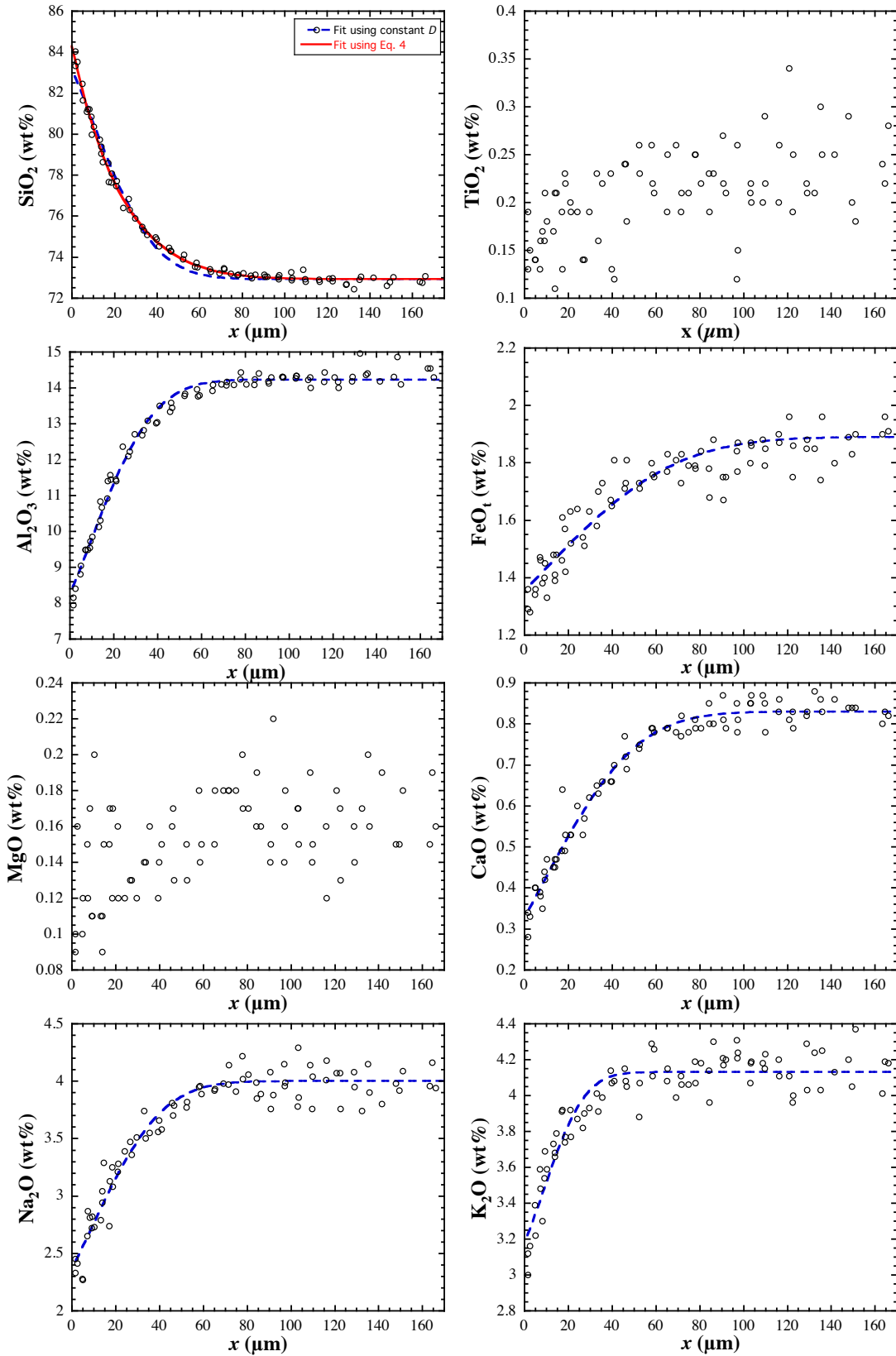
QzDisRh103



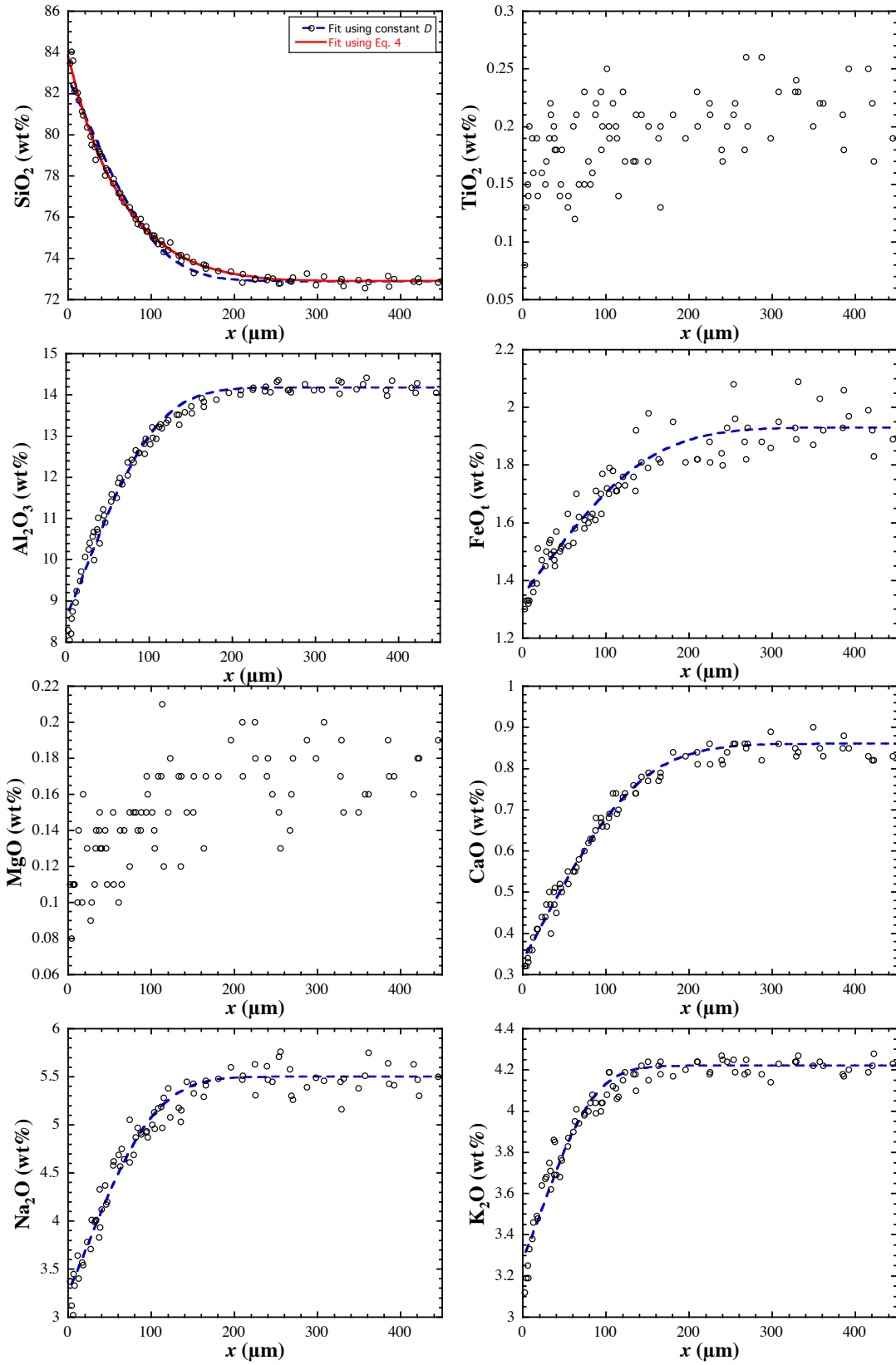
QzDisRh111



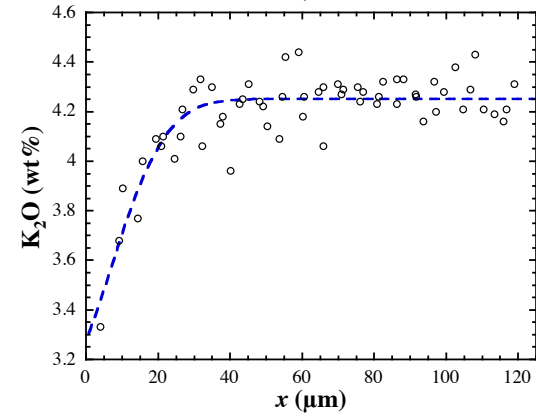
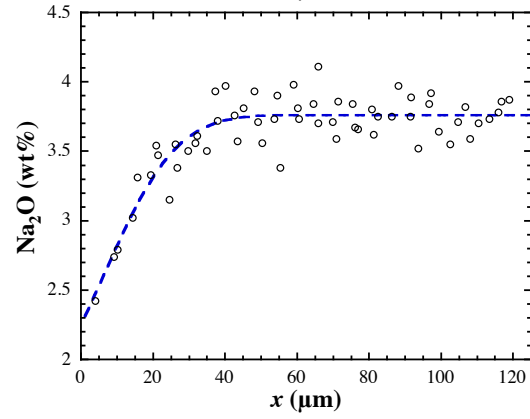
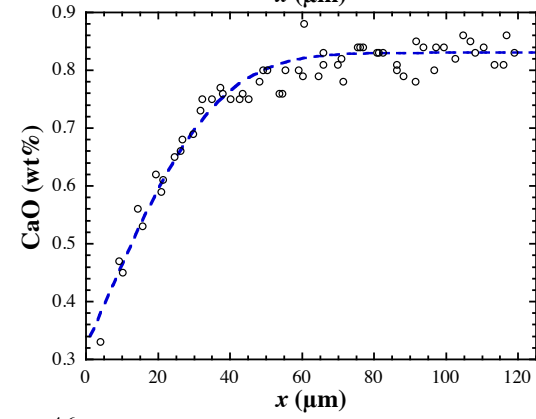
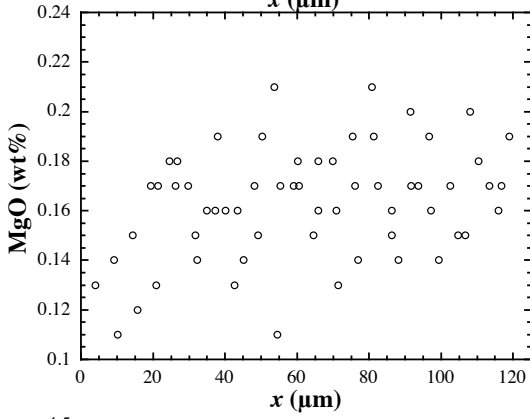
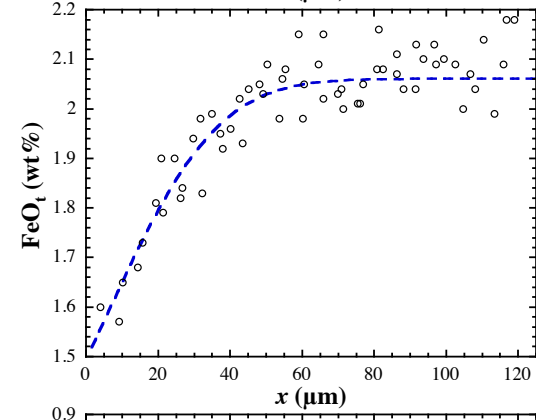
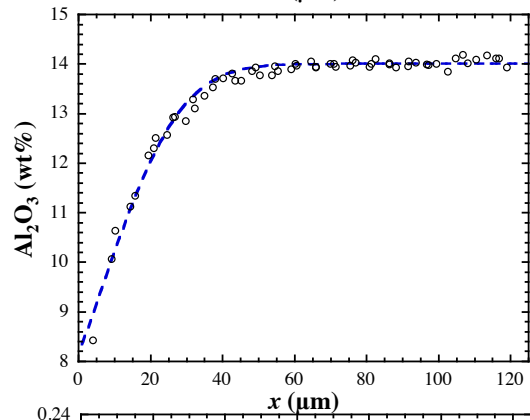
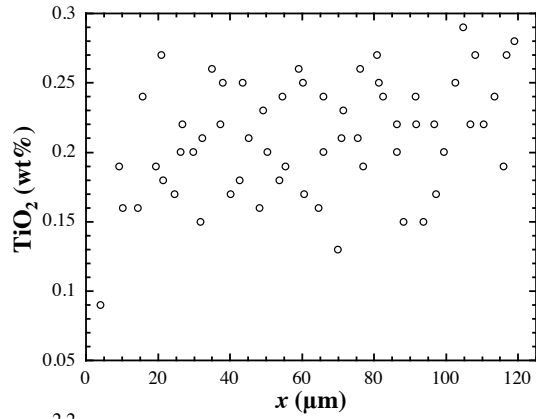
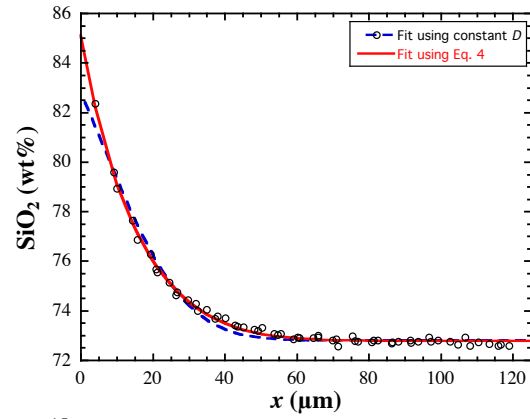
QzDisRh112



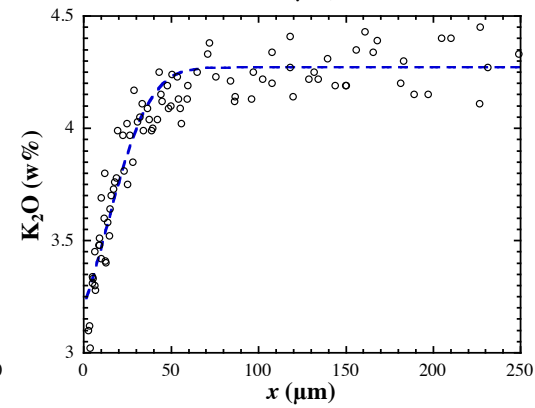
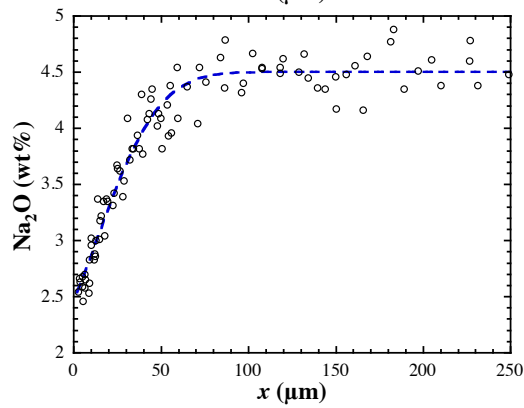
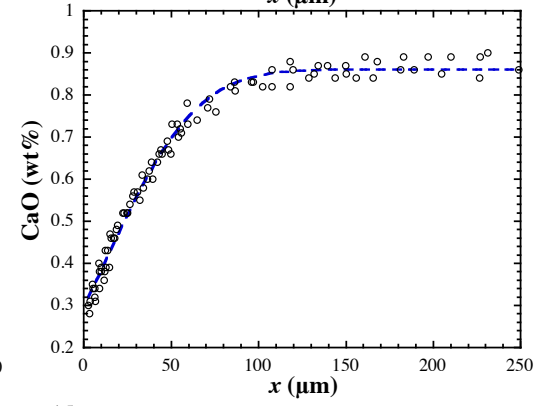
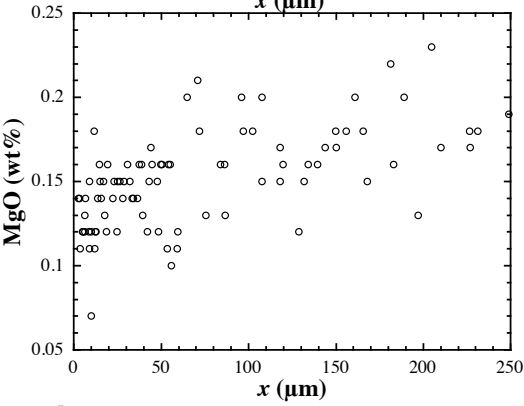
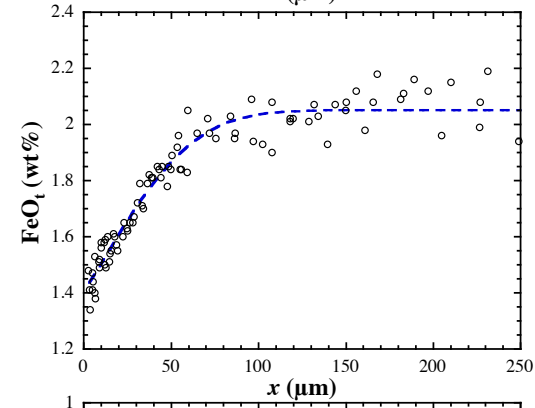
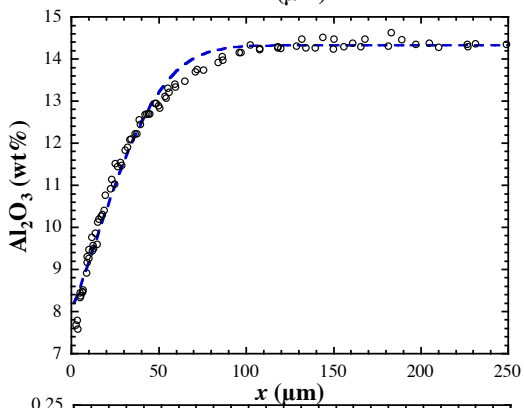
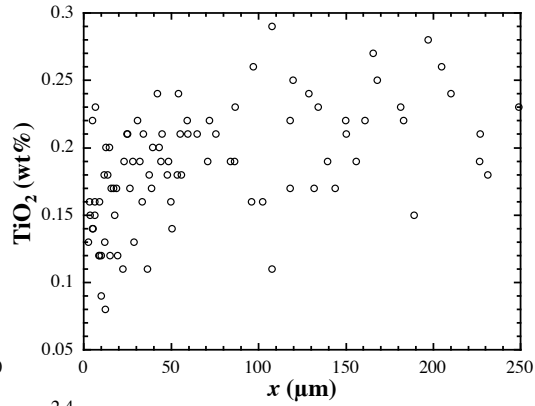
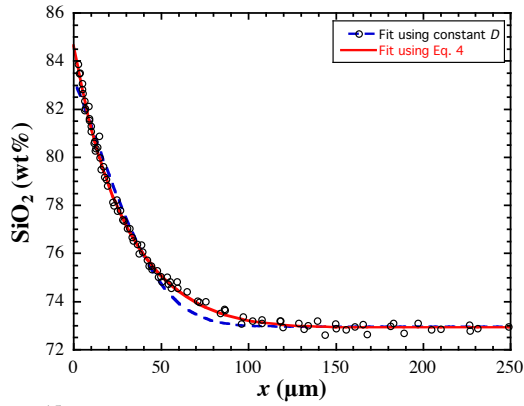
QzDisRh115



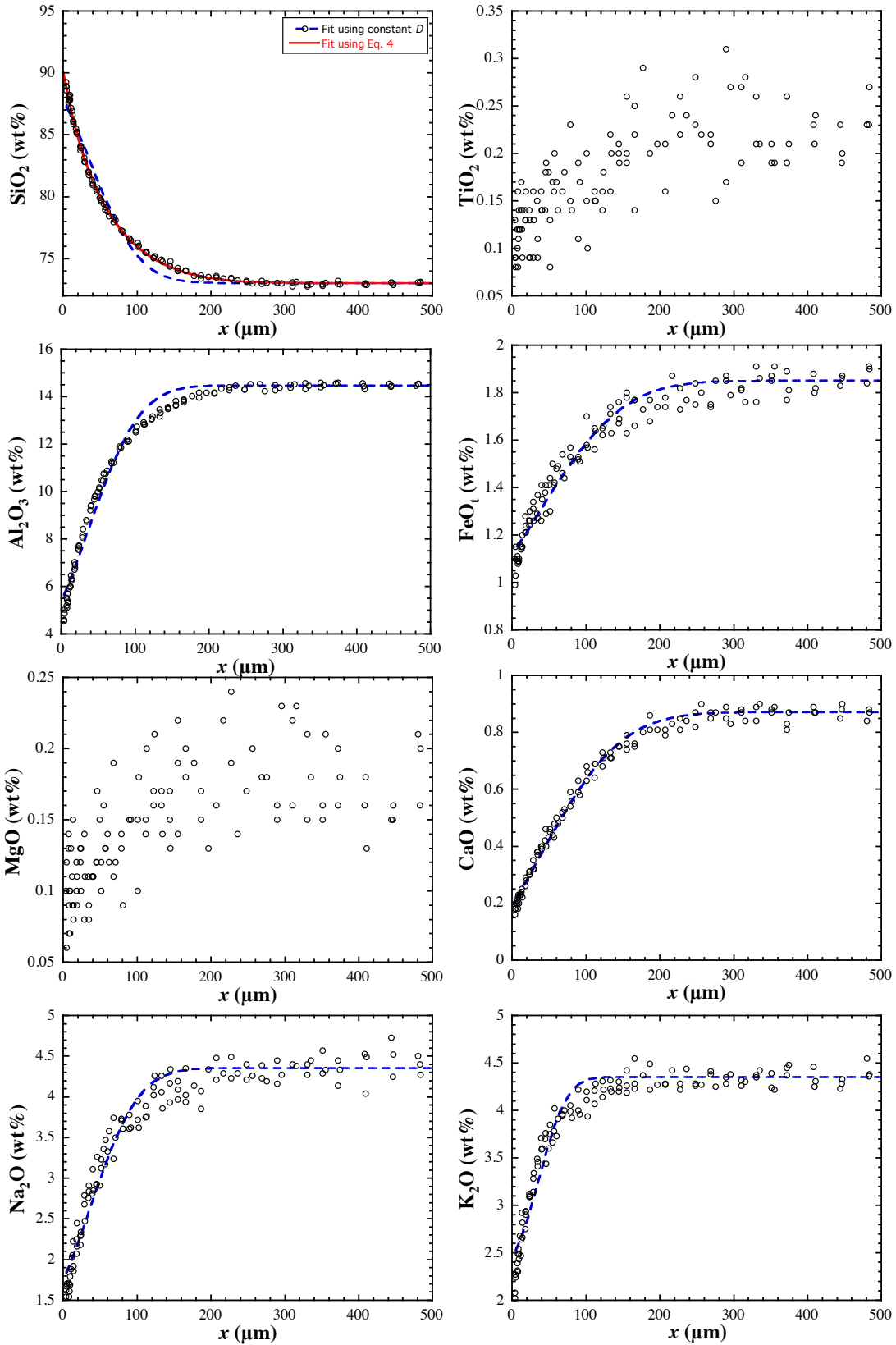
QzDisRh201



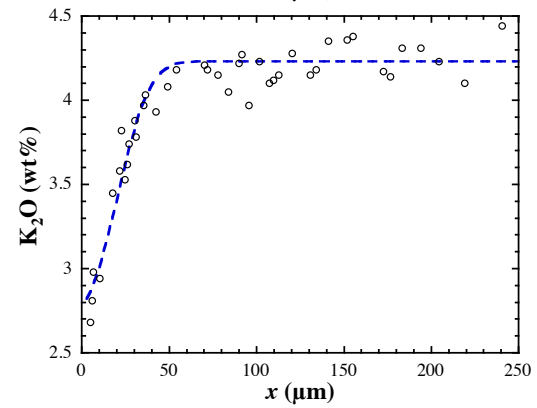
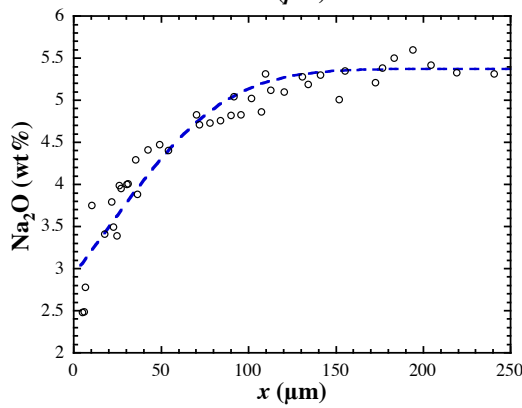
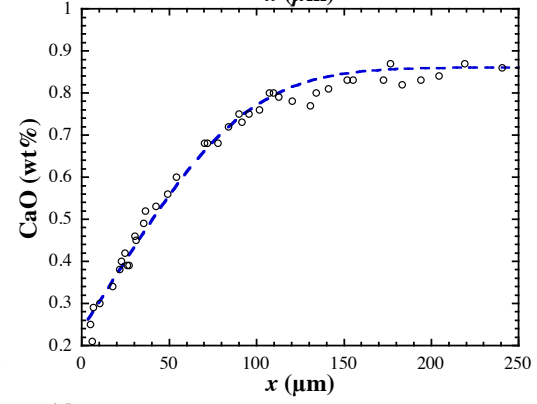
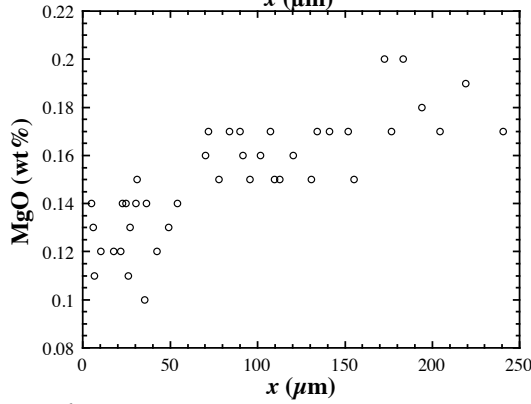
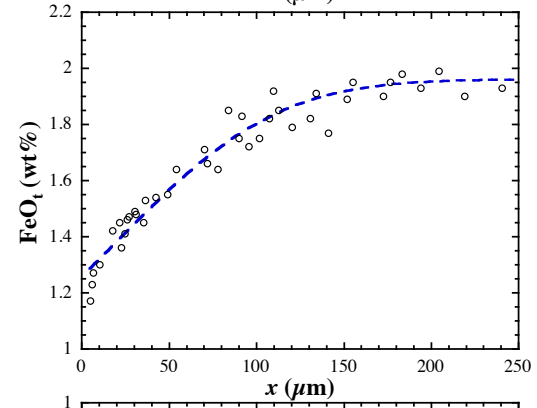
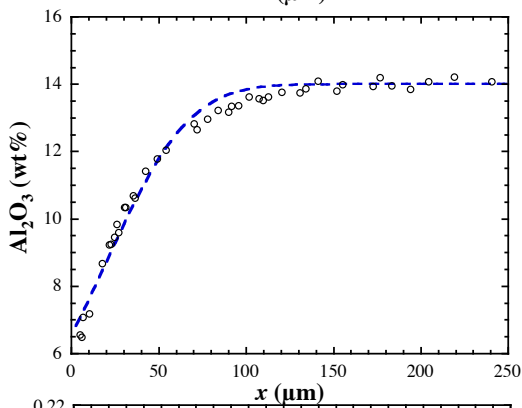
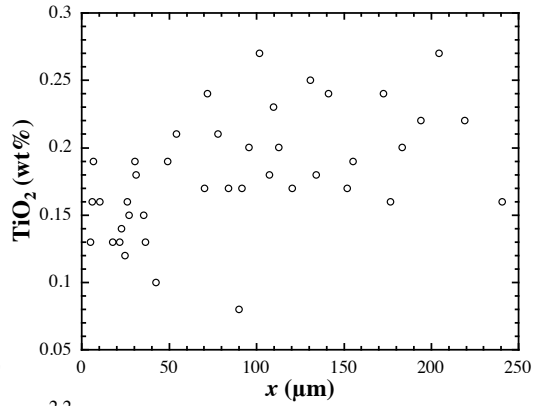
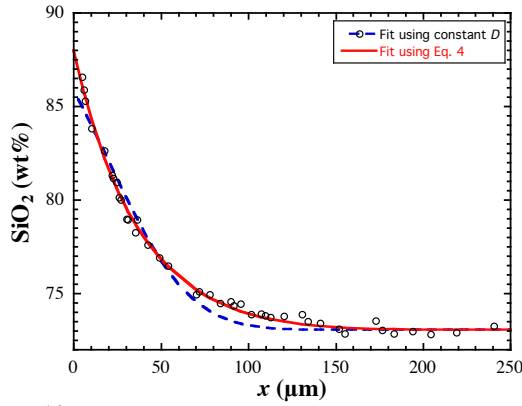
QzDisRh203



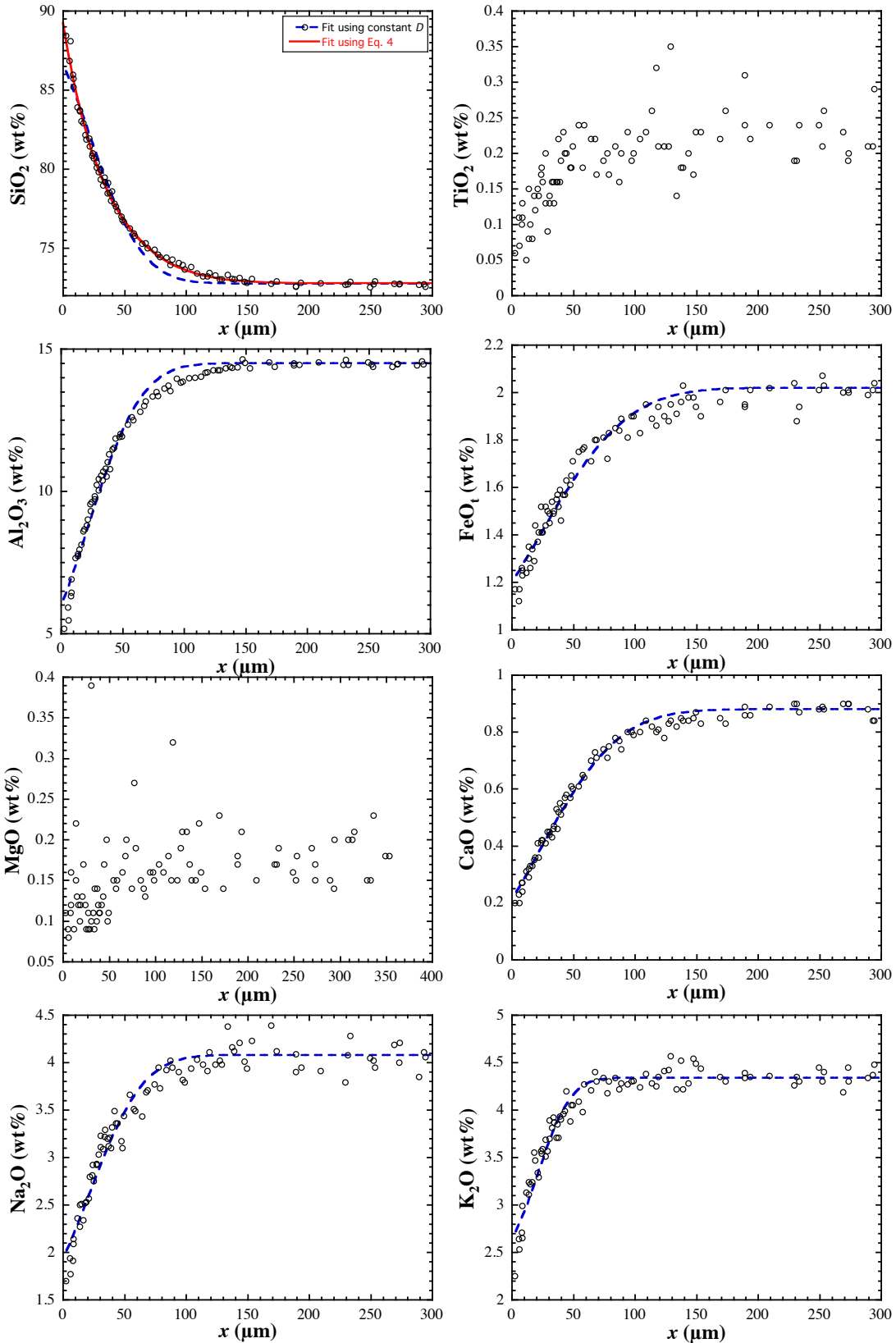
QzDisRh105



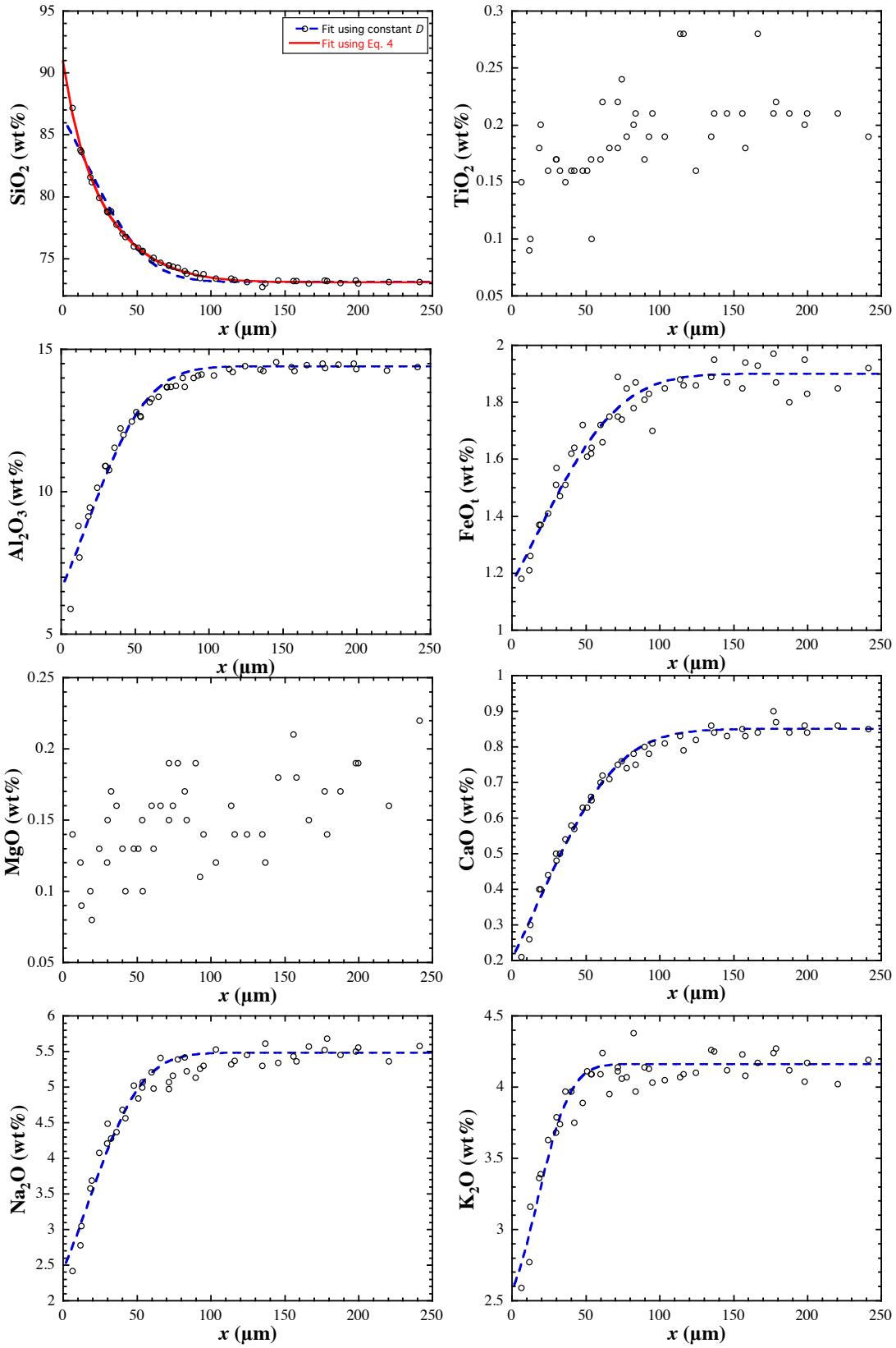
QzDisRh113



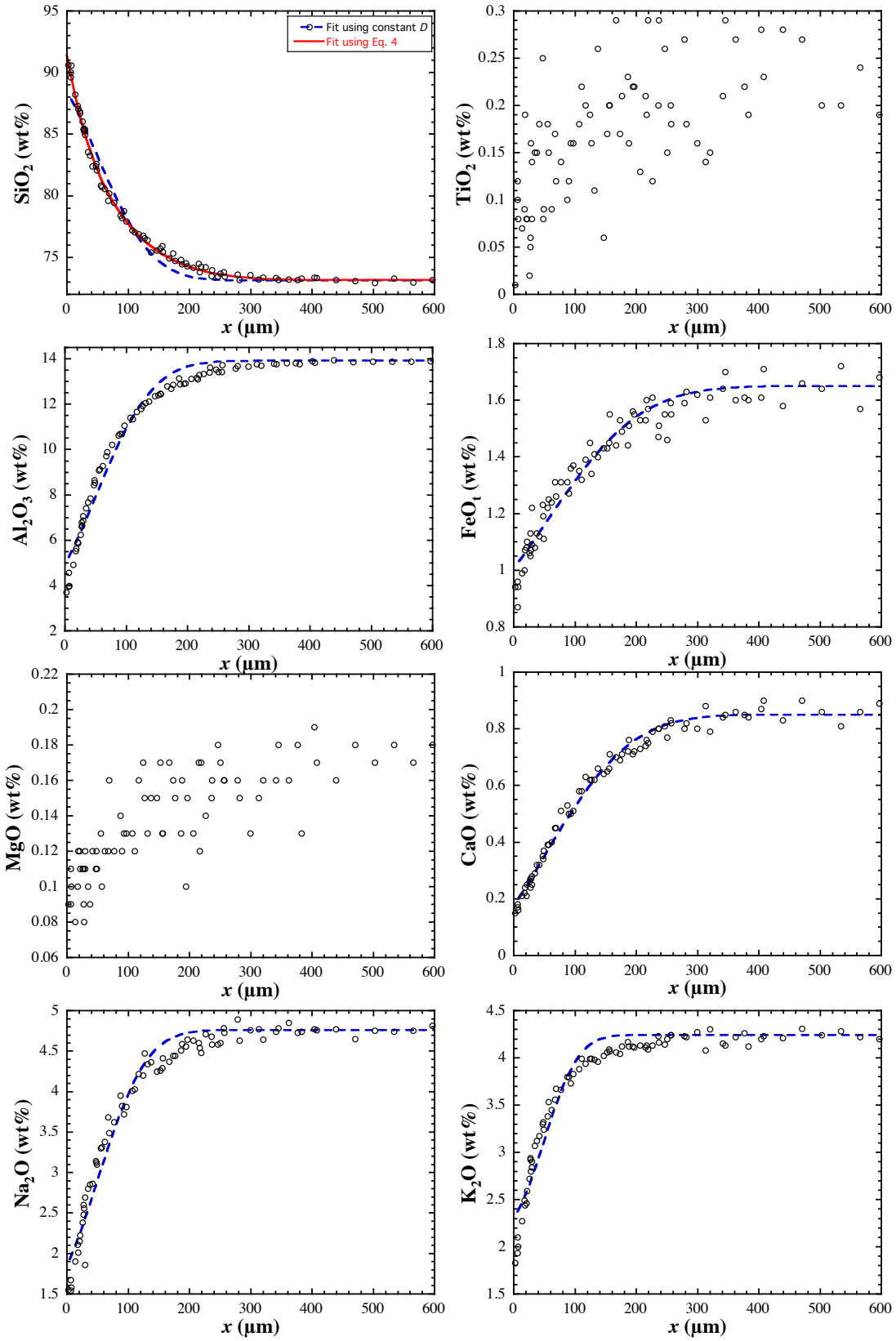
QzDisRh114



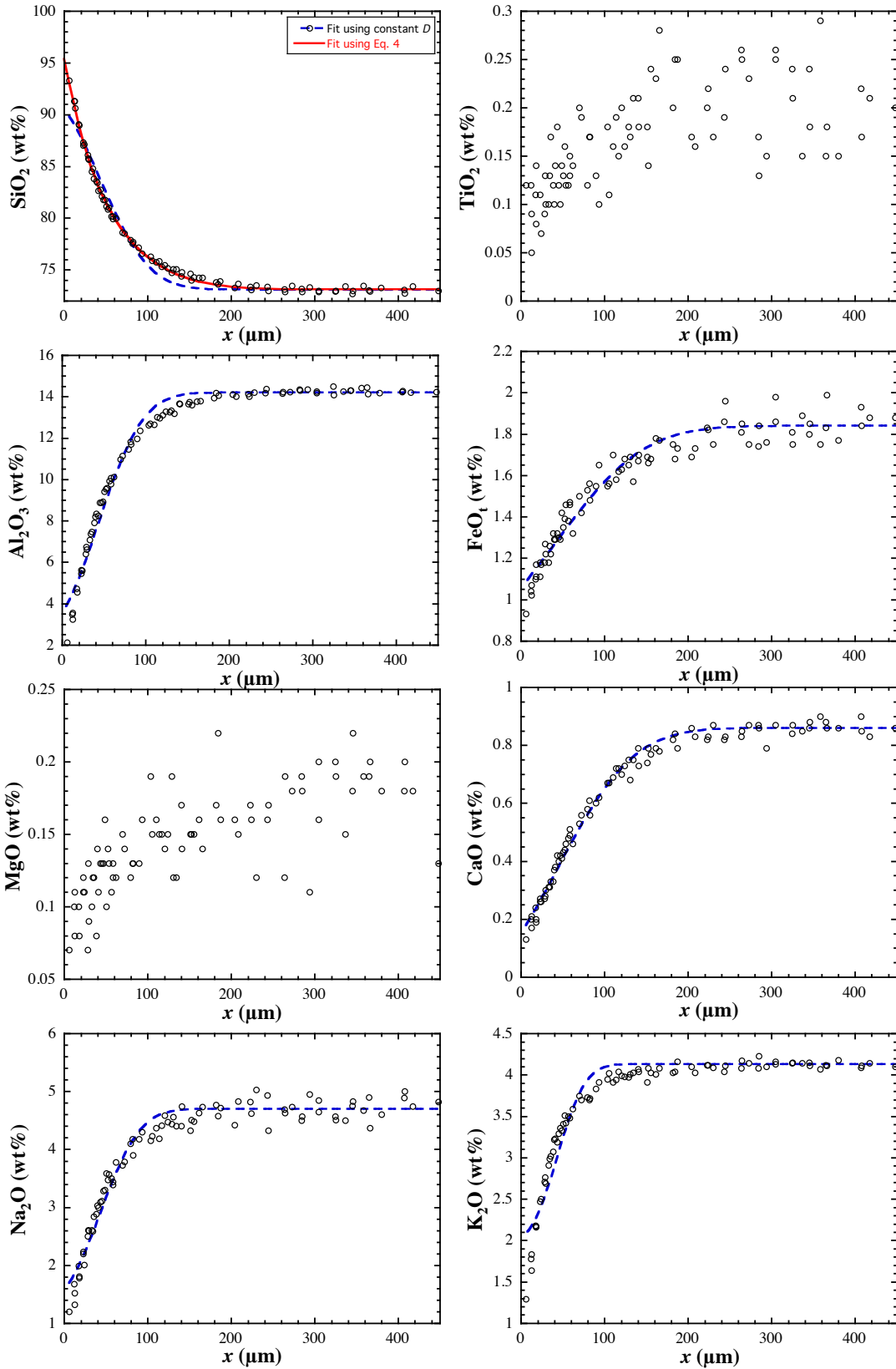
QzDisRh102



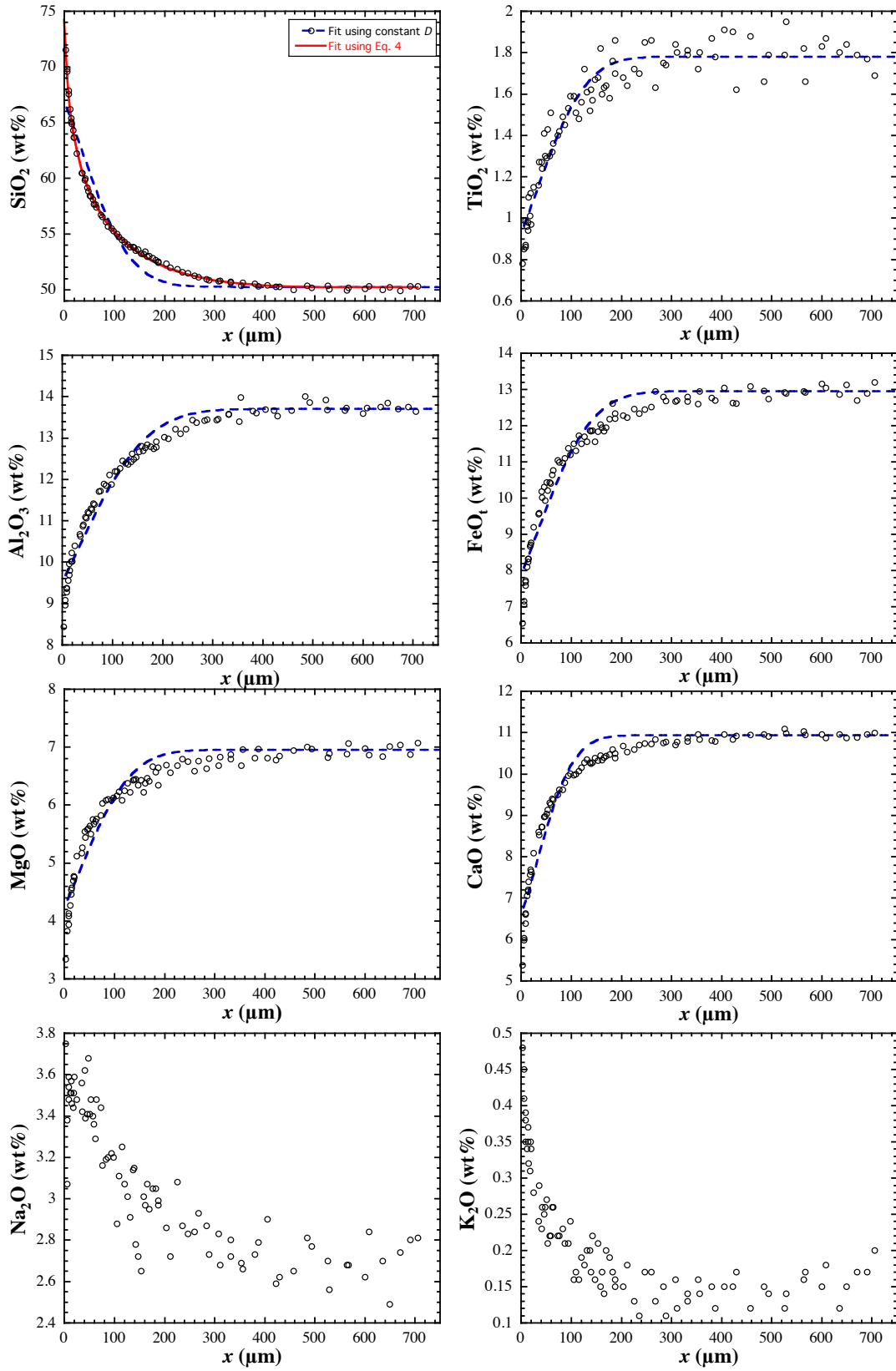
QzDisRh104



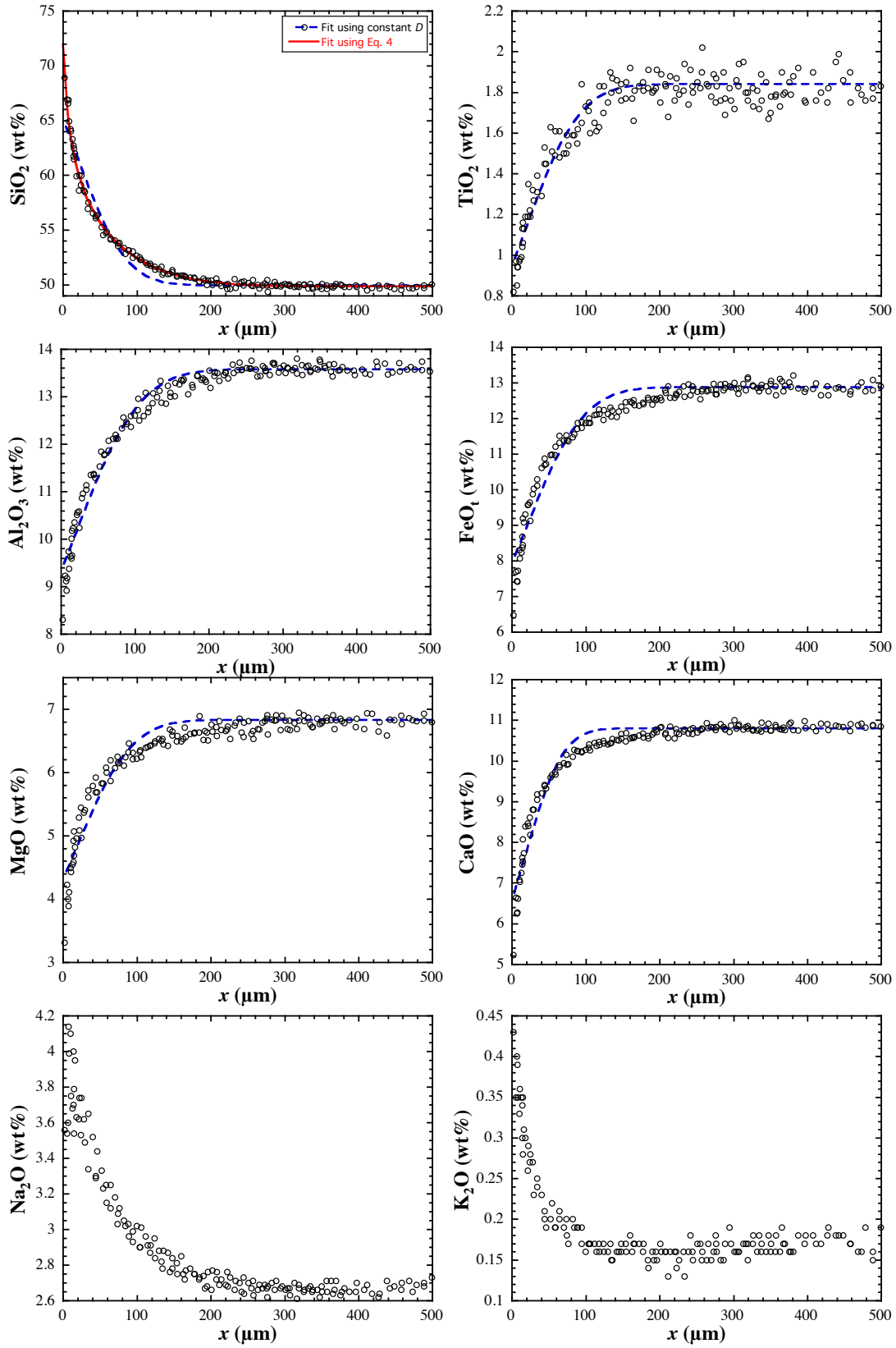
QzDisRh106

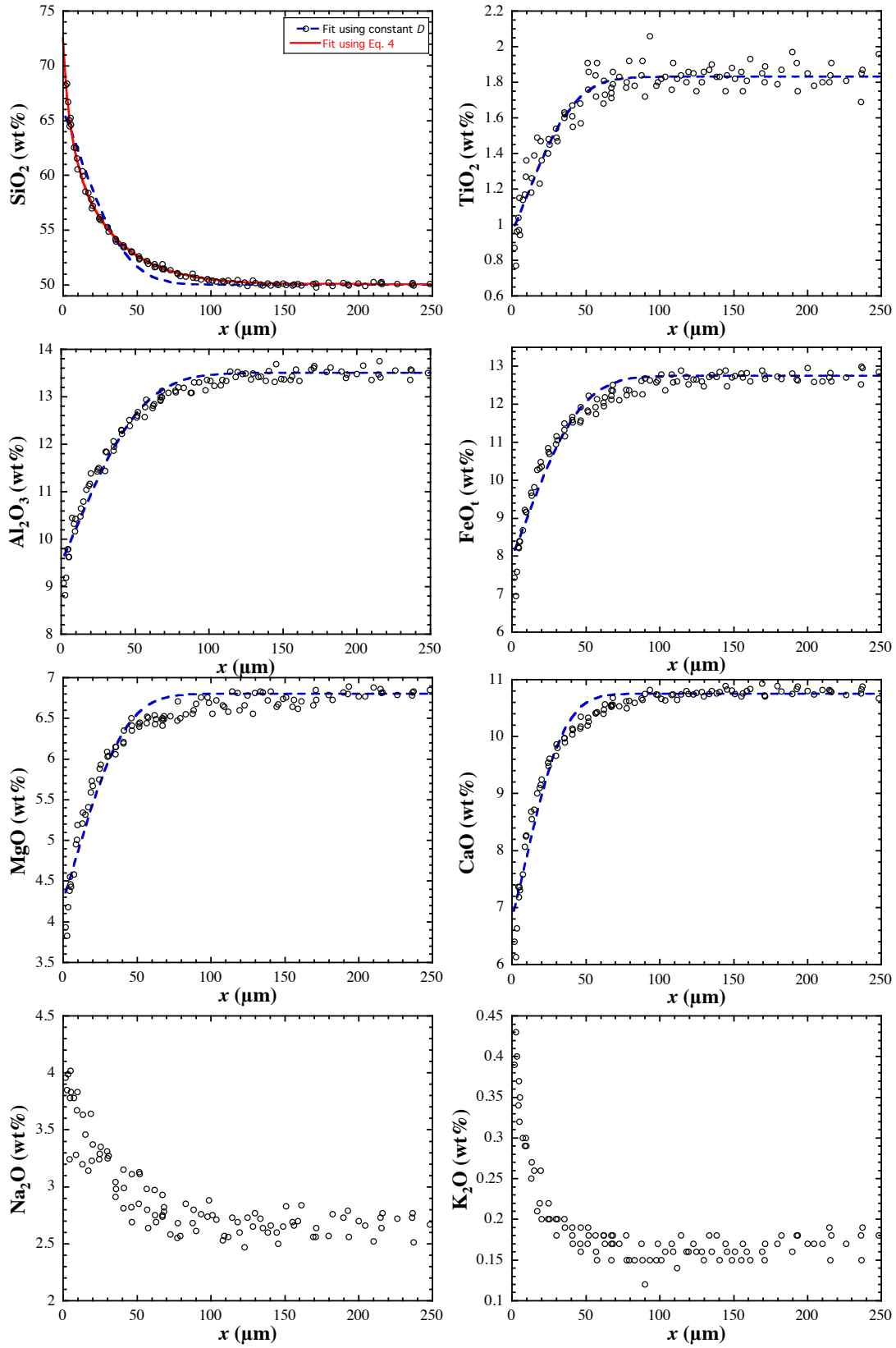


QzDisBa101

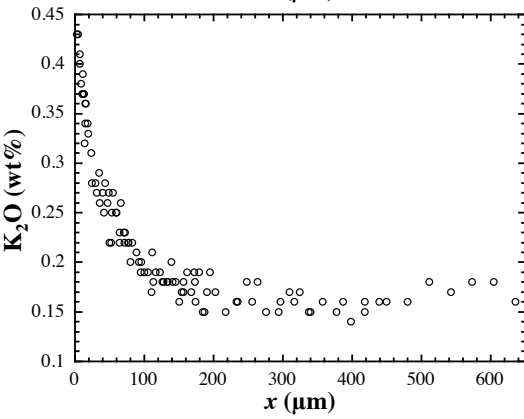
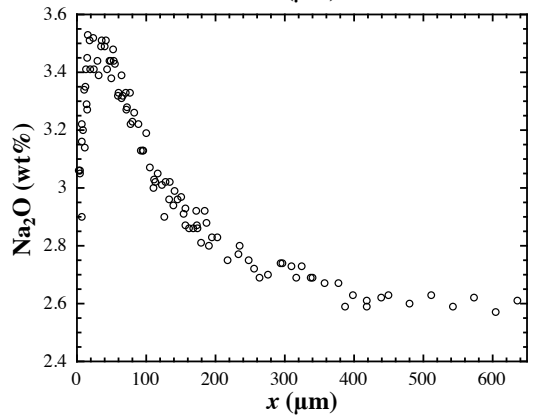
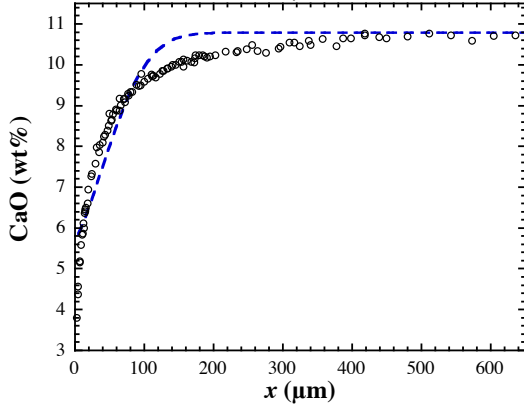
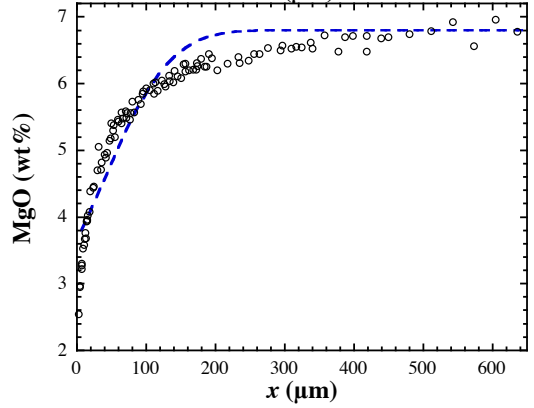
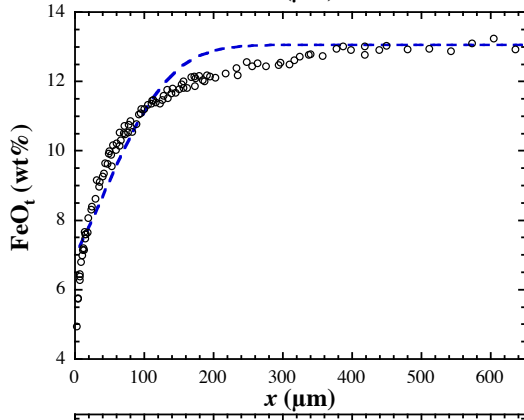
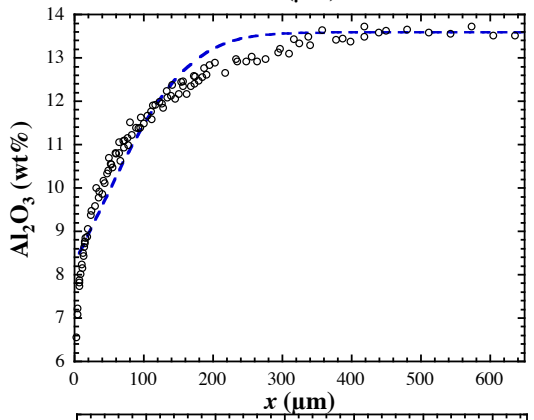
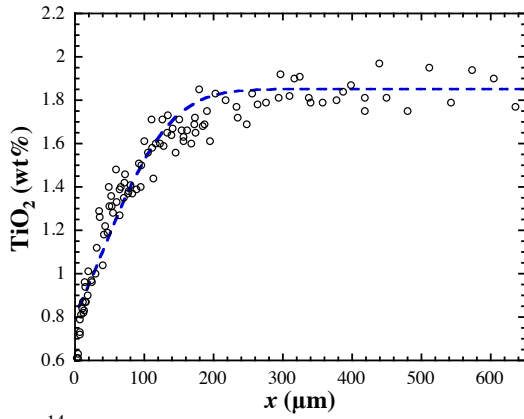
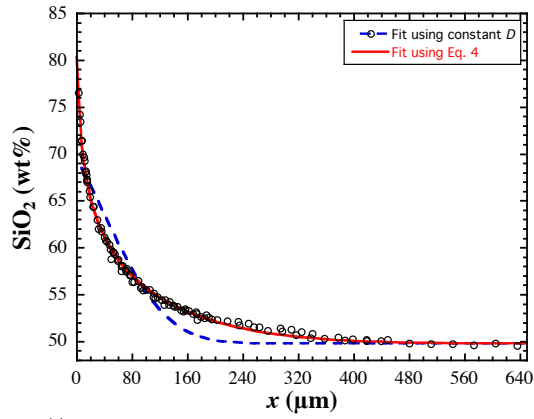


QzDisBa102

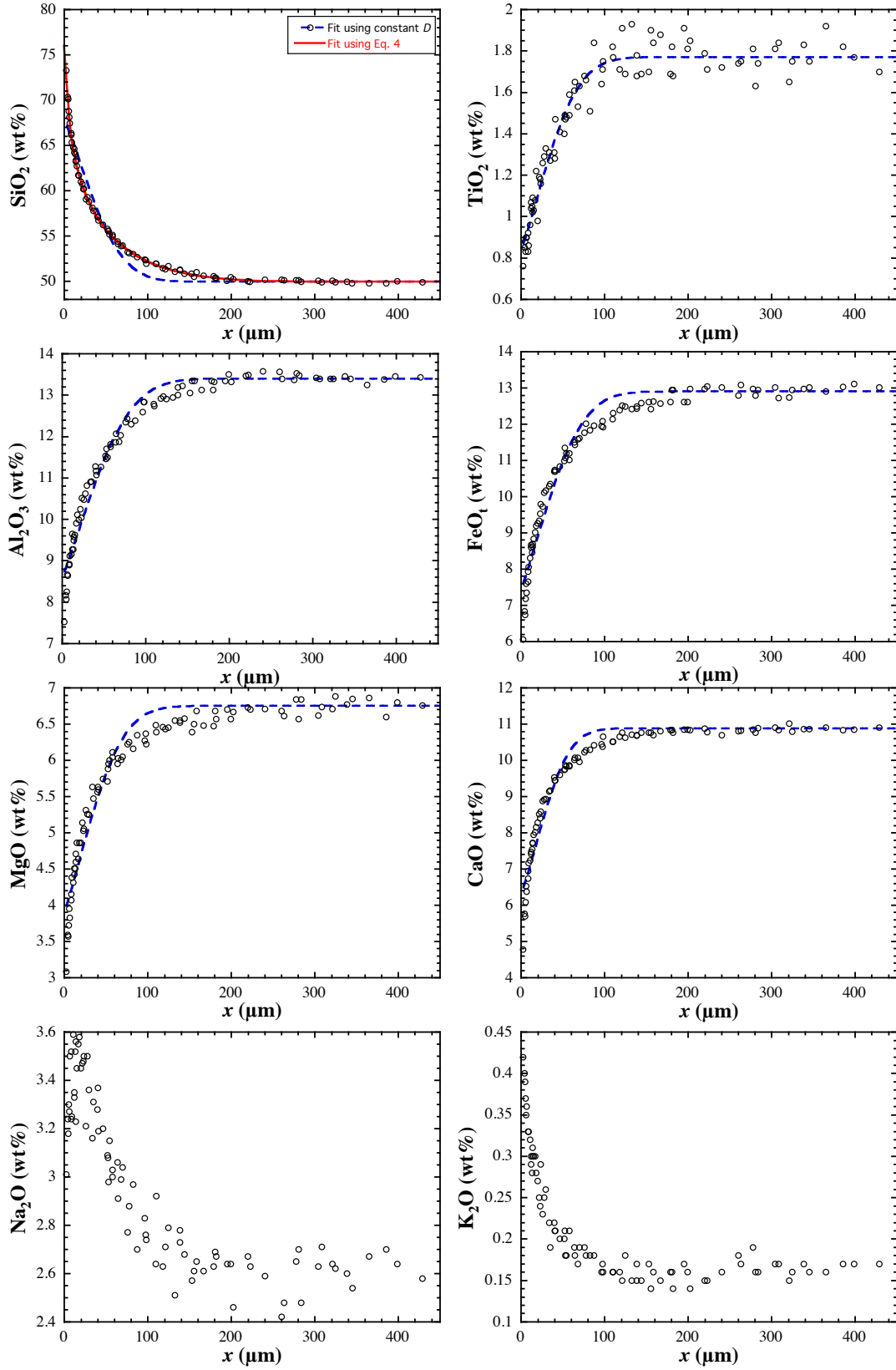




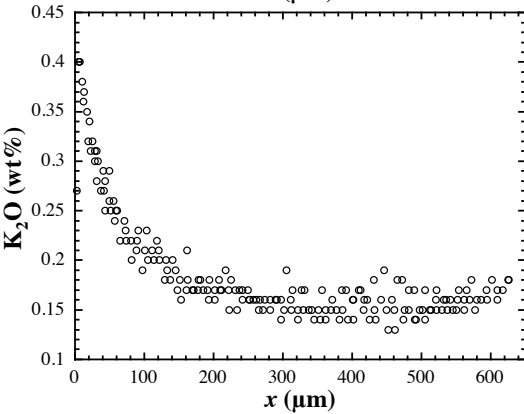
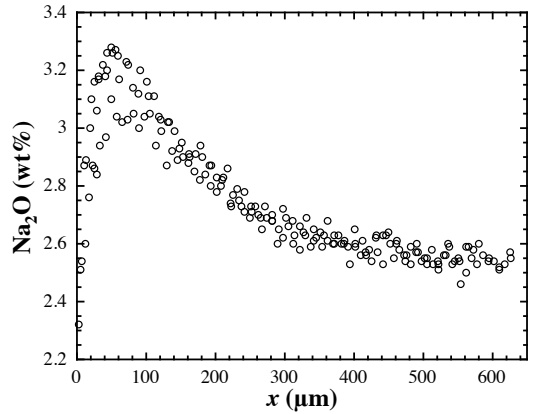
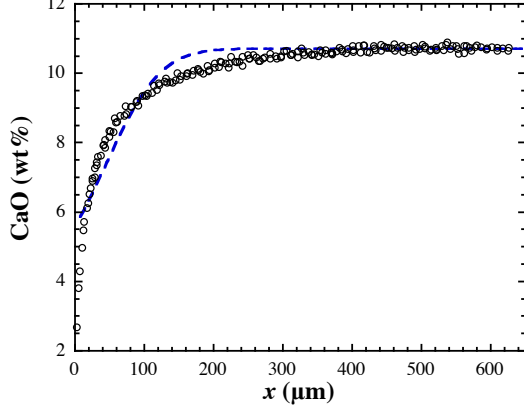
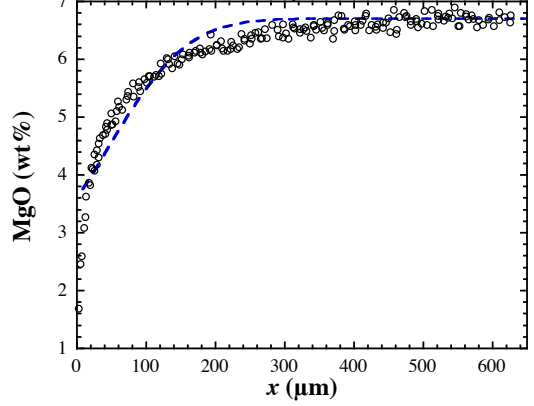
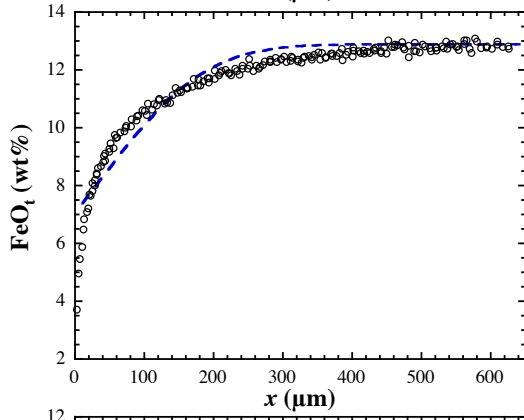
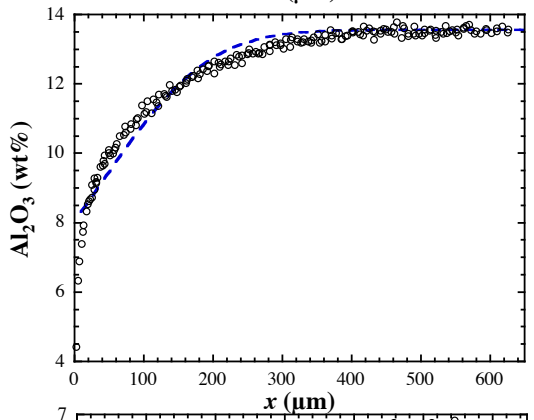
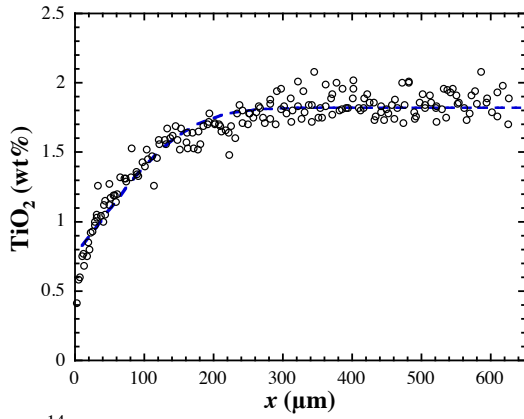
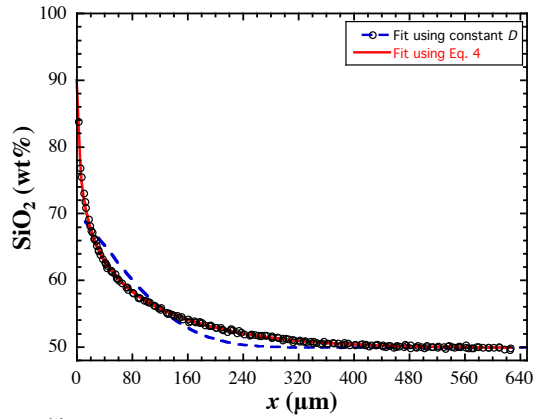
QzDisBa110

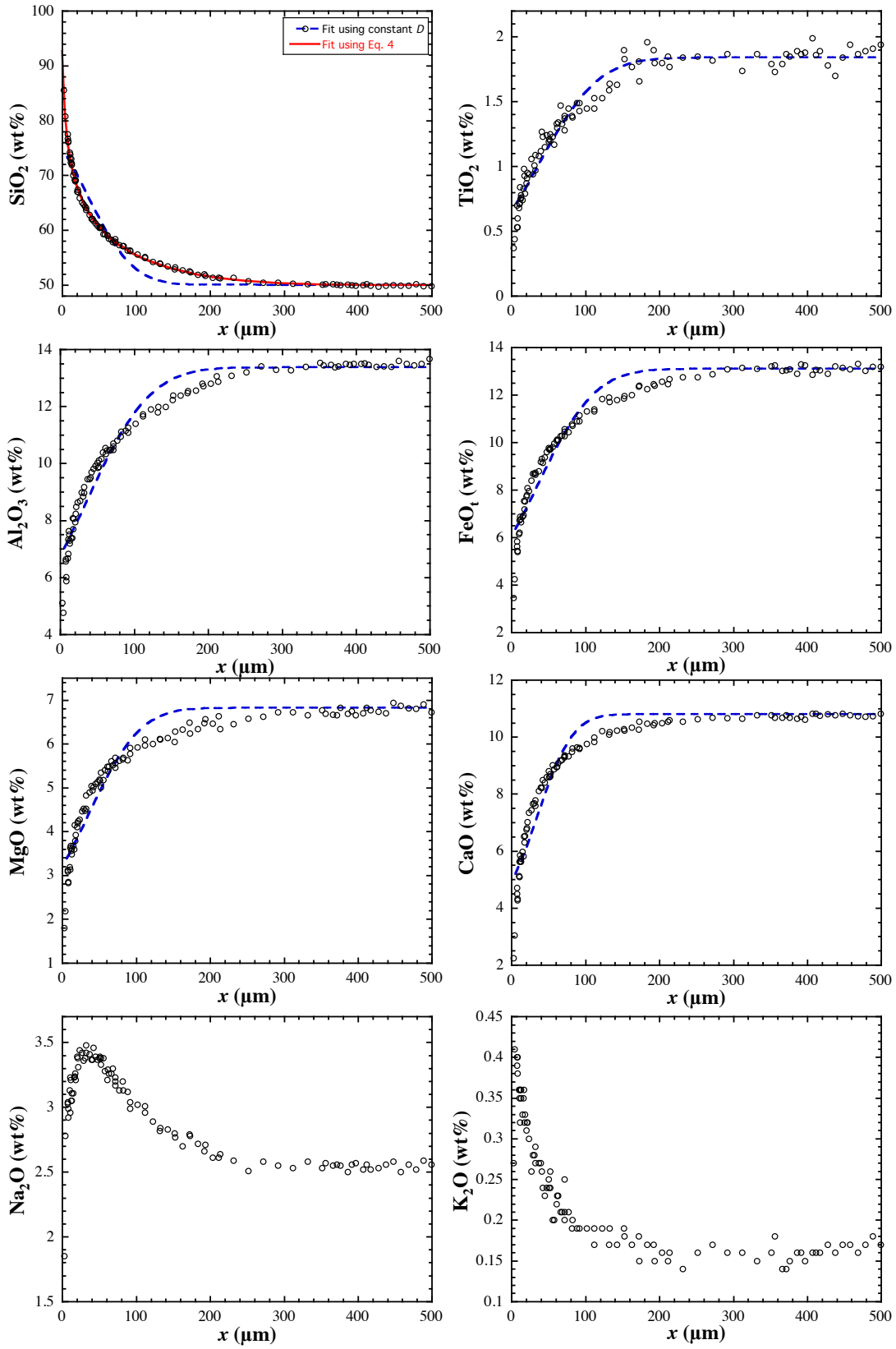


QzDisBa111



QzDisBa104





Appendix F

Fittings to SiO₂ Concentration Profiles of Quartz Dissolution in Rhyolitic and Basaltic

Melts

QzDisRh103, starting rhyolite: NCO; T=1303 °C, P=0.5GPa, t=172811s, H₂O=0.1wt%

x / sqrt(t)	x (μm)	SiO ₂ ⁺	TiO ₂	Al ₂ O ₃	FeO	MnO	MgO	CaO	Na ₂ O	K ₂ O	lnD_SiO ₂ (m ² /s)
0.02	6.3	81.46	0.18	9.52	1.35	0.01	0.08	0.34	3.79	3.34	-33.44
0.03	12.5	80.28	0.12	9.81	1.53	0.04	0.11	0.39	3.69	3.57	-33.32
0.03	13.1	80.09	0.15	10.05	1.45	0.03	0.13	0.41	3.92	3.61	-33.30
0.04	15.6	79.50	0.17	10.28	1.53	0.08	0.16	0.44	3.93	3.68	-33.23
0.04	18.1	79.32	0.19	10.59	1.55	0.00	0.09	0.44	3.77	3.70	-33.21
0.04	18.3	78.94	0.16	10.58	1.46	-0.04	0.07	0.42	4.58	3.72	-33.17
0.04	18.7	79.06	0.21	10.62	1.54	0.12	0.09	0.40	3.82	3.71	-33.18
0.05	21.8	78.48	0.14	10.83	1.61	0.08	0.12	0.47	4.15	3.77	-33.12
0.06	23.9	77.87	0.18	11.34	1.54	0.02	0.14	0.48	4.67	3.86	-33.05
0.06	24.0	78.08	0.15	11.13	1.56	0.06	0.01	0.49	4.09	3.88	-33.08
0.06	24.9	78.01	0.18	11.03	1.59	0.04	0.13	0.51	4.26	3.87	-33.07
0.07	27.4	77.49	0.20	11.37	1.63	0.10	0.17	0.51	4.08	3.89	-33.01
0.07	29.9	77.05	0.18	11.79	1.64	0.04	0.12	0.53	4.09	3.88	-32.96
0.07	31.1	77.33	0.12	11.62	1.71	0.06	0.11	0.54	4.07	3.96	-32.99
0.09	35.8	76.42	0.21	12.10	1.64	0.05	0.12	0.57	4.60	3.97	-32.89
0.10	41.7	75.84	0.16	12.49	1.75	0.09	0.15	0.60	4.49	4.09	-32.82
0.11	47.5	75.44	0.20	12.74	1.74	0.06	0.14	0.62	4.26	4.05	-32.77
0.13	53.4	74.96	0.20	12.95	1.76	0.12	0.15	0.67	4.68	4.08	-32.71
0.14	59.3	74.61	0.20	13.42	1.82	0.07	0.16	0.69	4.74	4.12	-32.67
0.16	65.2	74.31	0.19	13.60	1.81	0.10	0.10	0.70	4.90	4.20	-32.63
0.17	71.1	73.77	0.24	13.61	1.81	0.08	0.19	0.70	4.95	4.14	-32.56
0.18	76.4	73.85	0.24	13.63	1.87	0.06	0.15	0.74	4.57	4.17	-32.57
0.20	83.7	73.54	0.20	13.84	1.88	0.02	0.15	0.81	4.82	4.30	-32.53
0.21	86.5	73.61	0.17	13.91	1.85	0.08	0.15	0.75	4.58	4.24	-32.54
0.23	96.2	73.30	0.24	14.11	1.86	0.06	0.15	0.81	5.14	4.16	-32.50
0.23	97.3	73.15	0.18	14.09	1.92	0.04	0.14	0.80	5.29	4.21	-32.48
0.26	106.7	73.00	0.24	14.14	1.83	0.12	0.16	0.81	4.79	4.23	-32.46
0.26	108.8	73.28	0.24	14.25	1.95	0.07	0.14	0.79	5.02	4.20	-32.49
0.29	121.3	72.85	0.18	14.39	1.91	0.12	0.14	0.80	5.04	4.18	-32.43
0.31	126.9	72.94	0.16	14.31	1.94	0.02	0.15	0.80	4.91	4.22	-32.45
0.31	130.9	72.93	0.26	14.45	1.86	0.07	0.18	0.82	4.86	4.24	-32.45
0.32	133.9	73.08	0.23	14.48	1.91	0.02	0.18	0.78	5.24	4.22	-32.47
0.33	137.0	72.68	0.19	14.25	1.97	0.06	0.20	0.80	5.00	4.26	-32.41
0.35	146.4	72.73	0.20	14.51	1.85	0.04	0.13	0.83	5.02	4.26	-32.42
0.38	159.0	72.88	0.15	14.34	1.88	0.09	0.16	0.80	5.37	4.35	-32.44
0.40	164.6	72.56	0.17	14.59	1.90	0.06	0.16	0.85	5.11	4.21	-32.39
0.40	167.2	72.88	0.25	14.47	2.02	0.09	0.18	0.83	5.11	4.18	-32.44
0.41	171.5	72.88	0.21	14.37	1.93	0.06	0.16	0.85	5.06	4.29	-32.44

0.44	182.4	72.60	0.21	14.33	1.91	0.09	0.17	0.81	5.07	4.24	-32.40
0.44	182.6	72.57	0.17	14.41	2.08	-0.02	0.20	0.83	5.22	4.31	-32.39
0.44	184.0	72.94	0.21	14.57	1.95	0.02	0.16	0.82	5.18	4.28	-32.45
0.44	184.1	72.93	0.22	14.53	2.03	0.08	0.21	0.85	5.05	4.20	-32.45
0.48	197.5	72.43	0.21	14.43	1.88	-0.01	0.12	0.83	5.27	4.27	-32.38
0.48	200.6	72.64	0.15	14.39	2.00	0.04	0.14	0.86	5.01	4.23	-32.41
0.48	200.8	72.77	0.22	14.36	1.88	0.08	0.14	0.82	5.06	4.29	-32.42
0.51	212.6	72.60	0.27	14.37	1.92	0.05	0.18	0.81	5.14	4.20	-32.40
0.52	217.5	72.89	0.31	14.35	2.01	0.06	0.14	0.83	5.26	4.22	-32.44
0.53	218.6	72.62	0.18	14.37	1.99	0.11	0.16	0.87	5.25	4.28	-32.40
0.55	227.7	72.68	0.26	14.59	2.06	0.07	0.14	0.83	5.30	4.23	-32.41
0.56	234.3	72.55	0.24	14.44	1.97	0.02	0.20	0.85	5.37	4.23	-32.39
0.57	236.6	72.83	0.22	14.44	1.90	0.08	0.16	0.84	5.27	4.23	-32.43
0.61	254.6	72.64	0.26	14.56	2.05	0.00	0.16	0.87	5.41	4.20	-32.41
0.62	257.8	72.67	0.20	14.35	2.00	0.09	0.20	0.85	5.36	4.17	-32.41
0.64	267.9	72.80	0.20	14.34	2.01	0.07	0.16	0.88	4.94	4.19	-32.43
0.66	272.6	72.66	0.25	14.55	1.88	0.00	0.18	0.88	5.30	4.29	-32.41
0.66	272.9	72.49	0.25	14.50	2.00	0.00	0.15	0.85	5.16	4.22	-32.38
0.68	284.6	72.94	0.20	14.44	1.92	-0.01	0.13	0.83	5.27	4.25	-32.45
0.69	288.0	72.71	0.20	14.59	1.93	0.06	0.15	0.86	5.14	4.23	-32.41
0.70	290.6	72.75	0.19	14.45	1.98	0.11	0.17	0.88	5.38	4.20	-32.42
0.72	301.4	72.85	0.20	14.49	1.94	0.09	0.17	0.84	4.89	4.19	-32.43
0.73	303.1	72.60	0.24	14.43	1.95	0.13	0.14	0.86	5.38	4.17	-32.40
0.77	318.2	72.87	0.20	14.35	1.98	0.09	0.12	0.83	4.99	4.23	-32.44
0.77	318.2	72.74	0.25	14.41	1.91	0.06	0.13	0.84	5.05	4.22	-32.42
0.80	333.3	72.51	0.27	14.34	2.02	0.07	0.17	0.87	5.19	4.30	-32.39
0.83	345.5	72.85	0.19	14.42	2.00	0.09	0.20	0.85	5.26	4.24	-32.43
0.85	353.3	72.67	0.25	14.41	1.94	0.04	0.19	0.90	5.10	4.22	-32.41
0.87	362.9	72.69	0.22	14.56	2.04	0.04	0.18	0.87	4.83	4.24	-32.41
0.90	372.9	72.64	0.22	14.34	1.91	0.06	0.18	0.86	4.96	4.24	-32.40
0.91	380.1	72.79	0.23	14.44	1.92	0.10	0.16	0.87	5.05	4.29	-32.43
0.94	392.5	72.62	0.24	14.46	2.02	0.13	0.17	0.86	5.15	4.23	-32.40
0.96	400.2	72.72	0.17	14.45	2.02	0.02	0.13	0.83	5.00	4.22	-32.42
0.98	406.8	72.77	0.27	14.46	2.06	0.07	0.19	0.83	5.14	4.23	-32.42
1.02	422.1	72.70	0.25	14.43	2.04	0.04	0.19	0.87	5.08	4.25	-32.41
1.03	427.5	72.72	0.20	14.43	1.93	0.00	0.16	0.84	5.14	4.25	-32.42
1.09	451.7	72.67	0.21	14.40	2.02	0.11	0.15	0.87	5.02	4.27	-32.41
1.09	454.9	72.84	0.25	14.46	1.94	0.05	0.21	0.85	5.23	4.27	-32.43
1.16	481.3	72.39	0.22	14.55	1.93	0.08	0.19	0.87	4.95	4.19	-32.37
1.30	540.5	72.70	0.19	14.45	2.00	0.08	0.17	0.89	5.23	4.22	-32.41
1.37	570.1	72.46	0.26	14.42	2.02	0.04	0.19	0.81	5.03	4.28	-32.38
1.44	599.7	72.48	0.23	14.48	1.91	0.07	0.17	0.84	5.08	4.24	-32.38
1.51	629.3	72.59	0.17	14.31	2.01	0.04	0.14	0.89	5.30	4.30	-32.40

$\text{SiO}_2^+ = \text{SiO}_2 * (\text{Dry Total}/100)$; assuming that quartz has 100 wt% SiO_2 .

QzDisRh111, starting rhyolite: NCO; T=1304 °C, P=0.5GPa, t=87060s, H2O=0.1wt%

x / sqrt(t)	x (μm)	SiO2+	TiO2	Al2O3	FeO	MnO	MgO	CaO	Na2O	K2O	lnD_SiO2 (m^2/s)
0.02	5.7	83.76	0.11	7.63	1.18	-0.01	0.11	0.29	2.91	3.09	-33.26
0.03	7.5	83.02	0.17	8.81	1.23	0.05	0.11	0.33	3.57	3.32	-33.16
0.04	11.3	81.90	0.11	8.88	1.29	0.03	0.10	0.34	3.68	3.39	-33.00
0.04	13.2	81.21	0.06	9.54	1.38	0.07	0.14	0.37	3.85	3.48	-32.91
0.05	16.1	80.00	0.18	10.05	1.37	0.06	0.14	0.41	3.62	3.61	-32.75
0.06	17.0	80.43	0.13	9.66	1.33	0.04	0.13	0.44	3.86	3.68	-32.80
0.06	19.0	79.83	0.13	10.27	1.39	0.04	0.13	0.41	3.58	3.71	-32.72
0.08	22.5	79.03	0.12	10.35	1.38	0.05	0.12	0.46	3.78	3.82	-32.62
0.08	23.5	79.02	0.25	10.93	1.41	0.08	0.14	0.48	4.03	3.84	-32.62
0.08	24.6	78.71	0.14	10.84	1.39	0.00	0.08	0.51	4.09	3.78	-32.58
0.10	30.4	77.76	0.20	11.40	1.55	0.02	0.12	0.55	4.15	3.84	-32.45
0.11	31.1	77.66	0.30	11.64	1.47	0.11	0.15	0.54	4.33	3.85	-32.44
0.13	38.6	76.55	0.15	11.92	1.50	0.10	0.14	0.59	4.42	3.95	-32.30
0.13	39.7	76.71	0.17	12.38	1.56	0.06	0.12	0.62	4.71	4.08	-32.32
0.14	41.9	76.57	0.18	12.26	1.45	0.03	0.13	0.63	4.61	3.95	-32.30
0.16	46.1	76.12	0.14	12.35	1.58	0.04	0.17	0.65	4.37	3.96	-32.25
0.18	53.3	75.19	0.19	12.74	1.56	0.06	0.17	0.66	4.55	4.08	-32.13
0.20	57.8	74.75	0.25	13.29	1.57	0.05	0.14	0.69	4.83	4.09	-32.07
0.21	61.1	74.86	0.24	13.02	1.59	0.06	0.15	0.70	4.64	4.15	-32.09
0.21	62.3	74.70	0.22	13.32	1.67	0.09	0.15	0.74	4.95	4.11	-32.07
0.23	66.7	74.68	0.22	13.35	1.62	0.06	0.15	0.77	4.72	4.18	-32.07
0.23	66.8	74.11	0.27	13.46	1.48	0.09	0.17	0.75	4.94	4.18	-32.00
0.23	68.4	74.60	0.23	13.60	1.67	0.12	0.14	0.76	4.96	4.15	-32.06
0.23	68.6	74.54	0.31	13.23	1.65	0.12	0.15	0.71	4.74	4.10	-32.05
0.25	74.5	74.02	0.22	13.67	1.67	0.00	0.15	0.74	5.06	4.18	-31.99
0.25	74.5	74.07	0.29	13.42	1.62	0.02	0.13	0.77	4.89	4.09	-31.99
0.26	75.8	74.12	0.09	13.66	1.55	0.03	0.16	0.75	5.10	4.23	-32.00
0.26	76.2	74.15	0.19	13.33	1.60	0.09	0.18	0.77	4.88	4.17	-32.00
0.27	80.6	73.95	0.16	13.74	1.67	0.07	0.15	0.76	5.03	4.09	-31.98
0.28	82.3	73.72	0.20	13.74	1.76	-0.04	0.16	0.78	4.88	4.22	-31.95
0.28	83.6	73.82	0.26	13.62	1.60	0.02	0.18	0.79	4.75	4.11	-31.96
0.29	84.8	73.62	0.14	13.79	1.57	0.08	0.15	0.79	5.13	4.21	-31.93
0.29	86.7	73.76	0.19	13.66	1.78	0.07	0.16	0.78	4.88	4.18	-31.95
0.31	91.2	73.59	0.11	13.66	1.66	0.05	0.15	0.76	5.01	4.18	-31.93
0.31	92.8	73.39	0.17	13.81	1.75	0.00	0.16	0.81	4.96	4.15	-31.91
0.32	93.9	73.69	0.26	13.76	1.69	0.05	0.16	0.77	5.14	4.15	-31.94
0.33	97.9	73.56	0.28	13.71	1.74	0.01	0.15	0.79	4.98	4.15	-31.93
0.33	98.7	73.93	0.15	13.83	1.63	0.11	0.15	0.83	5.05	4.19	-31.97
0.34	98.9	73.76	0.17	13.87	1.71	0.03	0.18	0.80	5.15	4.21	-31.95
0.36	105.7	73.51	0.23	13.83	1.72	0.07	0.18	0.79	4.92	4.17	-31.92
0.38	111.1	73.51	0.18	14.05	1.67	0.05	0.16	0.81	5.10	4.23	-31.92
0.38	111.9	73.31	0.23	14.05	1.63	0.13	0.14	0.84	5.18	4.26	-31.90
0.38	113.5	73.69	0.24	14.01	1.63	0.11	0.15	0.82	4.92	4.21	-31.94
0.40	117.1	73.38	0.27	13.97	1.77	0.12	0.19	0.84	4.97	4.14	-31.91
0.41	121.0	73.38	0.20	13.80	1.67	0.07	0.17	0.83	5.06	4.20	-31.90
0.41	121.3	73.27	0.20	13.88	1.69	0.04	0.17	0.80	5.02	4.22	-31.89
0.42	123.3	73.00	0.14	14.00	1.78	0.06	0.17	0.84	4.94	4.21	-31.86
0.44	130.0	73.51	0.27	14.18	1.65	0.01	0.16	0.84	5.14	4.17	-31.92
0.46	136.8	73.45	0.31	14.16	1.70	0.09	0.18	0.83	4.97	4.21	-31.91
0.47	139.0	72.99	0.08	13.99	1.71	0.08	0.17	0.81	4.95	4.22	-31.86

0.48	141.5	73.06	0.15	13.95	1.76	0.01	0.17	0.86	5.01	4.31	-31.87
0.49	144.6	73.31	0.23	14.00	1.71	0.02	0.19	0.83	5.13	4.26	-31.90
0.50	147.6	73.01	0.19	14.07	1.75	0.06	0.16	0.85	5.15	4.21	-31.86
0.50	148.0	73.30	0.25	14.18	1.82	0.11	0.15	0.83	5.29	4.29	-31.90
0.52	152.4	72.88	0.35	14.12	1.68	0.08	0.19	0.85	5.12	4.15	-31.84
0.52	153.6	73.10	0.22	14.26	1.78	0.07	0.17	0.85	5.12	4.32	-31.87
0.54	159.8	73.15	0.12	14.26	1.82	0.04	0.19	0.83	5.39	4.29	-31.88
0.54	160.2	73.17	0.21	14.09	1.68	0.04	0.16	0.88	5.04	4.14	-31.88
0.56	165.8	72.78	0.20	14.27	1.72	0.03	0.17	0.85	5.05	4.27	-31.83
0.60	175.7	73.35	0.18	14.17	1.76	0.13	0.18	0.84	5.16	4.22	-31.90
0.65	191.3	73.36	0.26	14.18	1.75	0.02	0.18	0.81	5.26	4.18	-31.90
0.67	199.1	72.93	0.18	14.16	1.79	0.07	0.15	0.84	4.98	4.18	-31.85
0.73	214.7	72.83	0.28	14.17	1.90	0.09	0.18	0.87	4.88	4.19	-31.84
0.75	222.5	72.68	0.29	14.07	1.86	0.05	0.17	0.85	4.95	4.22	-31.82
0.81	238.1	73.17	0.23	14.16	1.83	0.05	0.16	0.86	5.07	4.24	-31.88
0.83	245.9	73.05	0.21	14.26	1.76	0.03	0.17	0.82	5.07	4.27	-31.87
0.89	261.5	72.98	0.25	14.19	1.70	0.05	0.18	0.84	5.14	4.18	-31.86
0.91	269.2	73.08	0.16	14.01	1.68	0.04	0.18	0.81	5.05	4.13	-31.87
0.97	284.8	72.83	0.27	13.97	1.75	0.01	0.19	0.84	4.97	4.24	-31.84
1.02	300.4	73.12	0.20	14.13	1.77	0.06	0.18	0.86	5.22	4.23	-31.87
1.04	308.2	73.24	0.14	14.04	1.81	0.10	0.15	0.83	5.21	4.16	-31.89
1.10	323.8	72.94	0.19	14.08	1.86	0.01	0.18	0.82	5.13	4.22	-31.85

QzDisRh12, starting rhyolite: NCO; T=1305 °C, P=0.5GPa, t=43219s, H2O=0.1wt%

x / sqrt(t)	x (μm)	SiO2+	TiO2	Al2O3	FeO	MnO	MgO	CaO	Na2O	K2O	lnD_SiO2 (m^2/s)
0.01	1.4	84.03	0.19	7.95	1.36	0.02	0.09	0.28	2.45	3.00	-33.25
0.01	1.4	83.32	0.13	8.16	1.29	0.11	0.10	0.34	2.33	3.12	-33.17
0.01	2.4	83.52	0.15	8.40	1.28	-0.02	0.16	0.33	2.41	3.16	-33.19
0.02	4.8	82.45	0.14	8.81	1.34	0.09	0.10	0.40	2.28	3.39	-33.06
0.02	5.0	81.66	0.14	9.04	1.36	-0.03	0.12	0.40	2.27	3.22	-32.97
0.03	7.0	81.09	0.13	9.48	1.47	0.11	0.15	0.39	2.65	3.59	-32.90
0.04	7.3	81.22	0.16	9.48	1.46	0.05	0.12	0.38	2.87	3.48	-32.91
0.04	8.1	81.21	0.17	9.48	1.38	0.05	0.17	0.35	2.81	3.30	-32.91
0.04	9.0	80.85	0.16	9.54	1.40	0.02	0.11	0.44	2.72	3.54	-32.87
0.04	9.2	79.98	0.21	9.72	1.45	0.04	0.11	0.42	2.82	3.69	-32.77
0.05	10.2	80.37	0.18	9.84	1.33	0.07	0.20	0.47	2.73	3.59	-32.81
0.06	13.0	79.73	0.17	10.12	1.48	0.14	0.11	0.45	2.79	3.73	-32.74
0.07	13.7	79.05	0.21	10.84	1.41	-0.01	0.09	0.47	2.94	3.66	-32.66
0.07	13.7	79.39	0.11	10.30	1.39	0.08	0.11	0.45	3.04	3.68	-32.70
0.07	14.5	78.65	0.21	10.67	1.48	0.04	0.15	0.47	3.29	3.79	-32.61
0.08	17.0	78.58	0.19	10.92	1.46	0.08	0.15	0.49	2.74	3.91	-32.60
0.08	17.3	77.67	0.13	11.41	1.61	0.11	0.17	0.64	3.13	3.92	-32.49
0.09	18.3	77.64	0.23	11.57	1.57	0.00	0.12	0.49	3.25	3.74	-32.49
0.09	18.6	78.08	0.22	11.45	1.42	-0.02	0.17	0.53	3.08	3.77	-32.54
0.10	20.8	77.47	0.20	11.44	1.63	0.11	0.16	0.53	3.21	3.92	-32.47
0.10	21.1	77.71	0.19	11.41	1.52	0.03	0.12	0.53	3.28	3.77	-32.50
0.12	24.0	76.40	0.19	12.36	1.64	0.06	0.12	0.60	3.39	3.87	-32.34
0.13	26.5	76.84	0.14	12.10	1.54	0.03	0.13	0.53	3.47	3.82	-32.39
0.13	27.2	76.29	0.14	12.23	1.51	0.00	0.13	0.57	3.36	3.90	-32.33
0.14	29.6	75.90	0.19	12.71	1.63	0.11	0.12	0.62	3.51	3.93	-32.28
0.16	32.9	75.49	0.23	12.68	1.58	0.13	0.14	0.65	3.74	4.01	-32.23
0.16	33.5	75.31	0.16	12.82	1.70	0.02	0.14	0.63	3.50	3.91	-32.21
0.17	35.3	75.09	0.22	13.09	1.73	-0.04	0.16	0.66	3.55	3.99	-32.18
0.19	39.3	74.96	0.23	13.01	1.67	0.06	0.12	0.66	3.56	4.14	-32.16
0.19	39.8	74.87	0.13	13.04	1.65	0.09	0.14	0.66	3.66	4.07	-32.15
0.20	40.9	74.52	0.12	13.50	1.81	0.06	0.15	0.70	3.58	4.08	-32.11
0.22	45.7	74.45	0.24	13.34	1.71	0.06	0.16	0.77	3.81	4.15	-32.10
0.22	46.2	74.32	0.24	13.59	1.73	0.03	0.17	0.72	3.70	4.08	-32.08
0.22	46.6	74.28	0.18	13.44	1.81	0.05	0.13	0.69	3.79	4.05	-32.08
0.25	52.2	73.89	0.26	13.78	1.73	0.10	0.15	0.74	3.77	3.88	-32.03
0.25	52.6	74.11	0.23	13.84	1.71	0.10	0.13	0.75	3.82	4.07	-32.06
0.28	57.9	73.54	0.26	13.96	1.80	0.06	0.18	0.79	3.95	4.29	-31.98
0.28	58.5	73.73	0.22	13.77	1.76	0.04	0.14	0.79	3.96	4.11	-32.01
0.28	59.0	73.51	0.21	13.79	1.75	0.03	0.15	0.78	3.89	4.26	-31.98
0.31	64.9	73.41	0.19	13.92	1.77	0.09	0.15	0.79	3.92	4.08	-31.97
0.31	65.3	73.28	0.25	14.09	1.83	0.03	0.18	0.79	3.93	4.15	-31.95
0.33	69.2	73.23	0.26	14.10	1.81	0.05	0.18	0.78	3.98	3.99	-31.94
0.34	71.3	73.45	0.19	14.07	1.73	0.05	0.18	0.77	3.97	4.11	-31.97
0.34	71.7	73.42	0.21	14.17	1.83	0.03	0.18	0.82	4.14	4.06	-31.97
0.36	74.8	73.19	0.21	14.08	1.79	0.08	0.18	0.78	3.91	4.06	-31.94
0.37	77.7	73.13	0.25	14.24	1.79	0.02	0.20	0.81	4.22	4.19	-31.93
0.38	78.1	73.13	0.25	14.43	1.78	0.01	0.17	0.79	4.02	4.07	-31.93
0.39	80.5	73.21	0.22	14.10	1.84	0.03	0.17	0.79	4.06	4.18	-31.94
0.40	84.1	73.09	0.23	14.09	1.78	0.01	0.16	0.85	3.99	4.14	-31.92
0.41	84.4	72.97	0.19	14.24	1.68	0.03	0.19	0.80	3.85	3.96	-31.91

0.41	86.1	73.15	0.23	14.40	1.88	-0.04	0.16	0.80	3.89	4.30	-31.93
0.44	90.5	73.13	0.27	14.18	1.75	0.12	0.14	0.87	4.08	4.21	-31.93
0.44	90.8	73.05	0.22	14.13	1.67	0.06	0.15	0.81	3.76	4.17	-31.92
0.44	91.8	73.04	0.21	14.30	1.75	0.07	0.22	0.79	3.88	4.20	-31.92
0.47	96.9	73.01	0.12	14.31	1.84	0.13	0.14	0.85	4.15	4.31	-31.91
0.47	97.2	72.92	0.26	14.31	1.77	0.05	0.16	0.78	3.96	4.21	-31.90
0.47	97.4	73.11	0.15	14.30	1.87	0.07	0.18	0.81	3.99	4.24	-31.93
0.50	103.1	73.26	0.21	14.26	1.80	0.05	0.17	0.85	3.78	4.07	-31.95
0.50	103.2	72.88	0.22	14.33	1.87	0.11	0.17	0.85	4.29	4.18	-31.90
0.50	103.5	72.96	0.20	14.33	1.86	0.09	0.15	0.87	3.86	4.19	-31.91
0.52	108.7	73.39	0.20	14.23	1.88	0.00	0.19	0.87	4.14	4.18	-31.96
0.53	109.6	72.91	0.29	14.29	1.79	0.07	0.14	0.85	3.76	4.15	-31.90
0.53	109.9	72.80	0.22	14.00	1.85	0.07	0.15	0.78	4.04	4.23	-31.89
0.56	116.0	72.90	0.20	14.17	1.90	0.08	0.16	0.83	4.01	4.20	-31.90
0.56	116.3	72.79	0.26	14.43	1.87	0.03	0.12	0.86	4.18	4.11	-31.89
0.58	120.8	72.95	0.34	14.30	1.96	0.02	0.18	0.81	4.07	4.11	-31.91
0.59	122.4	72.82	0.19	14.17	1.75	-0.02	0.17	0.83	4.07	3.96	-31.89
0.59	122.6	72.97	0.25	14.00	1.86	0.05	0.13	0.79	3.76	4.00	-31.91
0.62	128.8	72.66	0.22	14.19	1.85	0.03	0.16	0.82	4.08	4.29	-31.87
0.62	129.0	72.68	0.21	14.31	1.88	0.04	0.14	0.83	3.95	4.03	-31.87
0.64	132.5	72.44	0.21	14.96	1.85	0.11	0.17	0.88	3.74	4.24	-31.84
0.65	135.2	72.90	0.30	14.36	1.74	0.07	0.20	0.86	4.15	4.03	-31.90
0.65	135.9	73.05	0.25	14.41	1.96	0.05	0.16	0.83	3.90	4.25	-31.92
0.68	141.6	73.00	0.25	14.19	1.80	0.05	0.19	0.86	3.80	4.13	-31.91
0.71	148.0	72.61	0.29	14.31	1.89	0.05	0.15	0.84	3.98	4.20	-31.86
0.72	149.5	72.79	0.20	14.87	1.83	0.08	0.15	0.84	3.92	4.05	-31.89
0.73	151.0	73.03	0.18	14.10	1.90	0.11	0.18	0.84	4.09	4.37	-31.92
0.79	163.4	72.80	0.24	14.54	1.90	0.00	0.15	0.80	3.96	4.01	-31.89
0.79	164.6	72.74	0.22	14.54	1.96	0.07	0.19	0.83	4.16	4.19	-31.88
0.80	166.0	73.08	0.28	14.30	1.91	0.12	0.16	0.82	3.94	4.18	-31.92
0.86	178.9	72.71	0.19	14.56	1.91	0.09	0.16	0.86	3.91	3.86	-31.87
0.86	179.6	72.89	0.19	14.36	1.85	0.08	0.19	0.84	3.97	4.21	-31.90
0.87	181.1	73.05	0.23	14.32	1.89	0.05	0.22	0.77	4.33	4.16	-31.92
0.93	194.4	72.68	0.27	14.49	1.90	0.07	0.19	0.83	4.00	4.11	-31.87
0.94	194.6	72.91	0.27	14.36	1.88	0.01	0.13	0.83	3.85	4.19	-31.90
0.94	196.1	72.99	0.31	14.16	1.98	0.06	0.16	0.80	4.07	4.00	-31.91
1.01	209.8	72.97	0.24	14.44	1.89	0.11	0.13	0.85	4.08	4.10	-31.91
1.02	211.2	72.73	0.27	14.23	1.88	0.06	0.18	0.81	3.97	4.35	-31.88
1.08	224.8	73.02	0.22	14.31	1.87	-0.06	0.14	0.84	4.24	4.16	-31.92
1.08	225.2	72.69	0.21	14.43	1.93	0.10	0.16	0.84	4.20	4.30	-31.87
1.09	226.2	73.17	0.23	14.24	1.84	0.04	0.20	0.78	3.89	4.20	-31.94
1.15	239.8	72.96	0.28	14.22	2.03	0.13	0.15	0.84	3.96	3.95	-31.91
1.16	240.6	72.82	0.24	14.31	1.92	0.06	0.18	0.80	4.13	4.36	-31.89
1.16	241.3	73.08	0.27	14.33	1.99	0.08	0.21	0.80	3.86	4.28	-31.92
1.23	254.9	72.97	0.23	14.56	1.92	0.06	0.16	0.81	4.26	4.23	-31.91
1.23	256.1	72.88	0.25	14.29	1.90	0.02	0.17	0.84	3.88	4.22	-31.90
1.23	256.4	73.03	0.35	14.32	1.92	0.12	0.18	0.88	4.06	4.16	-31.92
1.30	270.0	72.49	0.25	14.59	2.08	0.12	0.17	0.82	4.08	4.01	-31.85
1.31	271.5	73.13	0.22	14.33	1.95	0.03	0.19	0.83	4.16	4.23	-31.93
1.31	271.6	72.83	0.28	14.31	1.94	0.00	0.13	0.82	3.95	4.02	-31.89
1.37	285.0	73.22	0.18	14.48	1.85	0.07	0.14	0.83	3.95	4.26	-31.94
1.38	286.6	72.85	0.24	14.15	1.96	0.07	0.19	0.82	4.08	4.21	-31.89
1.38	287.0	72.88	0.25	14.29	1.85	0.06	0.19	0.84	4.08	4.23	-31.90
1.44	300.1	72.69	0.23	14.27	1.92	0.12	0.18	0.83	4.05	4.00	-31.87

1.45	301.6	73.06	0.24	14.15	1.94	0.04	0.13	0.81	3.89	4.04	-31.92
1.46	302.5	73.19	0.24	14.78	1.94	0.00	0.16	0.81	4.42	4.02	-31.94
1.52	315.2	72.96	0.20	14.15	1.95	0.07	0.17	0.86	3.89	4.03	-31.91
1.52	316.6	72.93	0.19	14.16	1.88	0.01	0.16	0.85	4.11	4.03	-31.90
1.59	330.2	73.10	0.25	14.08	1.91	0.08	0.13	0.83	4.19	3.89	-31.93
1.66	345.2	72.82	0.29	14.45	1.86	0.08	0.13	0.87	3.80	4.14	-31.89

QzDisRh115, starting rhyolite: NCO; T=1293 °C, P=0.5GPa, t=346258s, H2O=0.1wt%

x / sqrt(t)	x (μm)	SiO2+	TiO2	Al2O3	FeO	MnO	MgO	CaO	Na2O	K2O	lnD_SiO2 (m^2/s)
0.00	2.3	83.47	0.08	8.29	1.30	0.01	0.11	0.32	3.37	3.12	-33.26
0.01	3.7	84.04	0.13	8.05	1.33	0.03	0.08	0.32	3.12	3.19	-33.34
0.01	5.6	83.59	0.15	8.21	1.33	0.02	0.11	0.34	3.02	3.25	-33.28
0.01	6.1	82.39	0.14	8.57	1.32	0.01	0.11	0.33	3.45	3.19	-33.11
0.01	7.4	82.12	0.20	8.74	1.33	0.07	0.11	0.36	3.33	3.33	-33.07
0.02	11.3	82.04	0.19	8.96	1.39	0.02	0.10	0.36	3.64	3.38	-33.06
0.02	12.6	81.67	0.16	9.24	1.36	0.07	0.14	0.39	3.40	3.46	-33.01
0.03	16.4	81.14	0.19	9.48	1.39	0.00	0.10	0.41	3.57	3.49	-32.94
0.03	17.7	80.95	0.14	9.71	1.51	0.07	0.16	0.41	3.54	3.48	-32.91
0.04	22.9	80.35	0.16	10.07	1.47	0.06	0.13	0.44	3.78	3.64	-32.83
0.05	26.8	79.93	0.15	10.25	1.45	0.06	0.09	0.44	3.71	3.67	-32.77
0.05	28.0	79.51	0.17	10.41	1.50	0.02	0.10	0.47	4.01	3.68	-32.72
0.05	31.9	79.42	0.19	10.56	1.53	0.08	0.11	0.50	3.99	3.75	-32.70
0.06	33.2	78.78	0.22	10.67	1.54	0.01	0.13	0.47	4.00	3.71	-32.62
0.06	33.5	79.61	0.21	9.99	1.49	0.04	0.14	0.40	4.01	3.62	-32.73
0.06	37.1	79.21	0.20	10.74	1.50	0.07	0.14	0.50	3.83	3.86	-32.68
0.06	37.4	79.13	0.19	10.68	1.47	0.12	0.15	0.47	4.33	3.69	-32.67
0.07	38.3	79.06	0.18	11.01	1.45	0.07	0.13	0.51	3.93	3.85	-32.66
0.07	40.3	78.95	0.18	10.39	1.57	0.11	0.13	0.45	4.12	3.69	-32.64
0.08	44.5	78.04	0.14	11.22	1.50	0.04	0.14	0.52	4.37	3.68	-32.52
0.08	45.7	78.38	0.15	11.07	1.51	0.03	0.13	0.51	4.17	3.77	-32.56
0.08	47.0	78.28	0.18	10.91	1.52	0.08	0.11	0.50	4.20	3.76	-32.55
0.09	54.0	77.64	0.13	11.42	1.63	0.06	0.15	0.55	4.58	3.83	-32.47
0.09	54.3	77.86	0.14	11.58	1.52	0.09	0.11	0.52	4.62	3.87	-32.49
0.10	60.6	77.16	0.20	11.50	1.53	0.06	0.10	0.55	4.69	3.90	-32.40
0.11	62.3	77.17	0.12	11.86	1.58	0.09	0.14	0.55	4.57	3.95	-32.40
0.11	64.1	76.95	0.21	11.99	1.70	0.07	0.11	0.56	4.75	4.01	-32.37
0.11	67.3	76.71	0.15	11.83	1.62	0.04	0.14	0.58	4.64	3.94	-32.34
0.13	73.9	76.48	0.15	12.37	1.61	0.02	0.12	0.60	5.05	3.98	-32.31
0.13	74.1	76.46	0.23	12.05	1.58	0.00	0.15	0.60	4.61	3.99	-32.31
0.13	78.9	76.12	0.17	12.43	1.60	0.06	0.15	0.62	4.69	4.00	-32.26
0.14	80.9	75.91	0.15	12.37	1.62	0.03	0.15	0.63	4.87	4.04	-32.24
0.14	83.7	75.67	0.16	12.65	1.63	0.09	0.14	0.63	4.97	4.08	-32.20
0.15	87.2	75.91	0.21	12.60	1.61	0.04	0.14	0.65	4.92	4.04	-32.24
0.15	87.6	75.60	0.22	12.59	1.71	0.05	0.15	0.68	4.90	3.99	-32.19
0.16	93.5	75.54	0.23	12.82	1.70	0.12	0.15	0.68	4.92	4.00	-32.19
0.16	94.4	75.30	0.18	12.57	1.63	0.04	0.17	0.67	4.93	4.04	-32.15
0.16	95.5	75.29	0.20	12.94	1.77	0.03	0.16	0.66	4.87	4.04	-32.15
0.17	101.2	75.11	0.25	12.80	1.72	0.07	0.15	0.66	5.00	4.08	-32.13
0.18	103.3	75.12	0.20	13.22	1.70	0.07	0.14	0.68	5.13	4.19	-32.13
0.18	103.8	74.97	0.19	12.96	1.79	0.05	0.13	0.69	4.96	4.19	-32.11
0.18	108.0	74.70	0.22	12.94	1.78	0.05	0.17	0.74	5.17	4.12	-32.07
0.19	112.1	74.87	0.20	13.23	1.71	0.06	0.17	0.74	5.19	4.11	-32.10
0.19	113.1	74.68	0.19	13.29	1.71	0.01	0.21	0.69	4.97	4.06	-32.07
0.19	114.7	74.31	0.14	13.19	1.73	0.09	0.12	0.70	5.28	4.07	-32.02
0.20	120.4	74.41	0.23	13.32	1.76	0.11	0.15	0.73	5.38	4.15	-32.04
0.21	122.9	74.77	0.17	13.38	1.73	0.06	0.18	0.74	5.08	4.19	-32.08
0.23	132.7	74.13	0.17	13.52	1.76	0.11	0.17	0.76	5.18	4.18	-32.00
0.23	135.4	74.17	0.17	13.52	1.71	0.06	0.12	0.74	5.03	4.18	-32.00
0.23	136.2	73.86	0.21	13.27	1.92	0.04	0.17	0.74	5.15	4.10	-31.96

0.24	142.5	74.06	0.21	13.58	1.81	0.07	0.15	0.78	5.45	4.22	-31.99
0.26	150.4	73.83	0.17	13.72	1.79	0.06	0.15	0.77	5.43	4.24	-31.96
0.26	150.9	73.28	0.20	13.55	1.98	0.07	0.17	0.79	5.33	4.15	-31.89
0.28	163.2	73.72	0.19	13.92	1.82	0.09	0.13	0.77	5.29	4.22	-31.94
0.28	165.4	73.65	0.13	13.83	1.81	0.13	0.17	0.78	5.41	4.18	-31.94
0.28	165.6	73.51	0.20	13.71	1.81	0.11	0.17	0.79	5.46	4.24	-31.92
0.31	180.4	73.39	0.21	13.88	1.95	0.06	0.17	0.84	5.48	4.17	-31.90
0.33	195.4	73.36	0.19	14.05	1.81	0.07	0.19	0.83	5.60	4.20	-31.90
0.36	209.6	72.83	0.23	14.00	1.82	0.04	0.20	0.84	5.47	4.24	-31.83
0.36	210.3	73.23	0.20	14.12	1.82	0.03	0.17	0.81	5.51	4.24	-31.88
0.38	224.3	72.96	0.22	14.13	1.88	0.08	0.20	0.86	5.63	4.18	-31.84
0.38	225.3	73.01	0.21	14.17	1.81	0.05	0.18	0.81	5.31	4.19	-31.85
0.41	239.0	72.94	0.18	14.09	1.84	0.03	0.17	0.82	5.61	4.27	-31.84
0.41	240.3	73.11	0.17	14.20	1.80	0.01	0.18	0.81	5.47	4.25	-31.86
0.42	245.9	73.02	0.20	14.07	1.93	0.02	0.16	0.84	5.45	4.24	-31.85
0.43	253.7	72.77	0.21	14.32	2.08	0.02	0.15	0.86	5.71	4.25	-31.82
0.43	255.3	72.81	0.22	14.36	1.96	0.05	0.13	0.86	5.76	4.19	-31.82
0.45	266.6	72.91	0.18	14.11	1.88	0.11	0.14	0.86	5.58	4.18	-31.84
0.46	268.4	72.88	0.26	14.13	1.82	0.07	0.16	0.85	5.30	4.25	-31.83
0.46	270.3	73.06	0.20	14.07	1.93	0.00	0.18	0.86	5.26	4.19	-31.86
0.49	287.3	73.25	0.26	14.26	1.88	0.04	0.19	0.82	5.39	4.18	-31.88
0.51	297.9	72.70	0.19	14.11	1.86	0.05	0.18	0.89	5.49	4.14	-31.81
0.52	308.0	73.11	0.23	14.13	1.95	0.07	0.20	0.86	5.46	4.23	-31.86
0.56	327.4	72.88	0.23	14.34	1.93	0.08	0.17	0.85	5.45	4.24	-31.83
0.56	328.7	72.99	0.24	14.03	1.89	0.03	0.19	0.83	5.16	4.24	-31.85
0.56	331.1	72.66	0.23	14.31	2.09	0.08	0.15	0.84	5.48	4.27	-31.80
0.59	349.4	72.96	0.20	14.14	1.87	0.05	0.15	0.90	5.38	4.22	-31.84
0.61	356.9	72.57	0.22	14.26	2.03	0.09	0.16	0.85	5.51	4.24	-31.79
0.61	361.5	72.85	0.22	14.42	1.92	0.05	0.16	0.83	5.75	4.22	-31.83
0.65	385.1	73.15	0.21	14.11	1.93	0.04	0.19	0.85	5.64	4.18	-31.87
0.66	386.3	72.63	0.18	13.98	2.06	0.04	0.17	0.88	5.43	4.17	-31.80
0.67	391.8	73.00	0.25	14.34	1.97	0.08	0.17	0.85	5.41	4.20	-31.85
0.71	415.8	72.87	0.25	14.18	1.99	0.03	0.16	0.83	5.63	4.19	-31.83
0.72	420.7	73.02	0.22	14.06	1.92	0.03	0.18	0.82	5.47	4.22	-31.85
0.72	422.2	72.86	0.17	14.28	1.83	0.07	0.18	0.82	5.30	4.28	-31.83
0.76	445.3	72.83	0.19	14.06	1.89	0.04	0.19	0.83	5.50	4.23	-31.83
0.77	452.6	72.76	0.18	14.20	1.89	0.00	0.14	0.88	5.70	4.24	-31.82
0.78	456.4	73.06	0.17	14.35	2.01	0.11	0.18	0.84	5.24	4.16	-31.86
0.81	474.8	72.74	0.24	14.12	1.89	0.07	0.18	0.86	5.57	4.21	-31.81
0.82	483.0	72.70	0.18	14.22	2.03	0.14	0.15	0.86	5.46	4.19	-31.81
0.84	492.1	73.03	0.25	14.26	1.88	0.14	0.17	0.83	5.47	4.20	-31.85
0.86	504.3	72.82	0.24	14.25	1.94	0.05	0.21	0.86	5.76	4.23	-31.82
0.87	513.4	73.08	0.26	14.26	1.92	0.02	0.18	0.86	5.56	4.26	-31.86
0.90	527.8	72.97	0.22	14.17	1.89	0.05	0.18	0.84	5.39	4.15	-31.85
0.91	533.8	72.89	0.18	14.17	1.97	0.05	0.16	0.89	5.44	4.23	-31.83
0.92	543.8	72.87	0.18	14.18	1.89	0.11	0.16	0.90	5.72	4.23	-31.83
0.96	563.3	72.97	0.22	14.20	1.91	0.02	0.17	0.86	5.31	4.23	-31.84
0.98	574.2	72.84	0.25	14.12	1.90	0.08	0.20	0.86	5.51	4.23	-31.83
1.02	599.1	72.90	0.28	14.09	2.04	0.09	0.17	0.83	5.57	4.16	-31.83
1.04	612.9	72.99	0.19	14.25	1.94	0.08	0.19	0.85	5.57	4.23	-31.85
1.07	630.9	73.05	0.20	14.15	1.88	0.02	0.18	0.85	5.11	4.19	-31.86
1.08	634.8	73.04	0.22	13.97	1.94	0.02	0.18	0.85	5.50	4.26	-31.85
1.13	662.6	72.54	0.26	13.97	1.97	0.06	0.18	0.88	5.58	4.28	-31.79
1.14	670.5	72.95	0.26	14.19	1.85	0.08	0.18	0.85	5.50	4.25	-31.84

1.17	687.8	72.99	0.24	14.11	1.86	0.08	0.18	0.88	5.56	4.07	-31.85
1.20	706.2	72.94	0.17	13.99	1.94	0.10	0.19	0.87	5.52	4.20	-31.84
1.21	712.3	72.76	0.21	14.12	1.86	0.06	0.19	0.87	5.31	4.15	-31.82
1.29	757.9	73.05	0.10	14.22	1.87	-0.01	0.14	0.85	5.50	4.29	-31.86
1.30	762.0	73.01	0.29	14.28	1.99	0.02	0.19	0.86	5.53	4.17	-31.85
1.36	801.3	73.15	0.24	14.21	1.94	0.04	0.18	0.85	5.31	4.23	-31.87
1.38	811.7	72.74	0.25	14.09	2.12	0.07	0.18	0.86	5.37	4.18	-31.81
1.46	858.2	72.88	0.20	14.17	1.99	0.06	0.20	0.89	5.81	4.24	-31.83
1.46	861.3	72.93	0.23	14.18	1.94	0.14	0.17	0.86	5.49	4.24	-31.84
1.46	861.4	72.91	0.16	14.26	2.01	0.06	0.20	0.89	5.64	4.23	-31.84
1.55	911.1	72.79	0.23	14.08	2.06	0.01	0.16	0.91	5.43	4.27	-31.82
1.55	913.1	73.04	0.20	14.13	2.05	0.07	0.17	0.90	5.51	4.18	-31.85
1.55	915.0	72.76	0.19	14.18	2.02	0.04	0.17	0.91	5.39	4.14	-31.82

QzDisRh201, starting rhyolite: NCO; T=1294 °C, P=0.5GPa, t=21583s, H2O=0.1wt%

x / sqrt(t)	x (μm)	SiO2+	TiO2	Al2O3	FeO	MnO	MgO	CaO	Na2O	K2O	lnD_SiO2 (m^2/s)
0.03	4.0	82.35	0.09	8.43	1.60	0.04	0.13	0.33	2.42	3.33	-33.15
0.06	9.1	79.59	0.19	10.07	1.57	0.10	0.14	0.47	2.74	3.68	-32.80
0.07	10.1	78.93	0.16	10.64	1.65	0.08	0.11	0.45	2.79	3.89	-32.72
0.10	14.3	77.64	0.16	11.13	1.68	0.08	0.15	0.56	3.02	3.77	-32.56
0.11	15.7	76.86	0.24	11.34	1.73	0.03	0.12	0.53	3.31	4.00	-32.47
0.13	19.4	76.27	0.19	12.16	1.81	0.06	0.17	0.62	3.33	4.09	-32.40
0.14	20.9	75.67	0.27	12.30	1.90	0.11	0.13	0.59	3.54	4.06	-32.33
0.14	21.3	75.55	0.18	12.51	1.79	0.02	0.17	0.61	3.47	4.10	-32.31
0.17	24.6	75.13	0.17	12.57	1.90	0.09	0.18	0.65	3.15	4.01	-32.26
0.18	26.3	74.64	0.20	12.92	1.82	0.02	0.17	0.66	3.55	4.10	-32.21
0.18	26.7	74.74	0.22	12.94	1.84	0.00	0.18	0.68	3.38	4.21	-32.22
0.20	29.7	74.44	0.20	12.85	1.94	0.10	0.17	0.69	3.50	4.29	-32.19
0.22	31.8	74.28	0.15	13.29	1.98	0.05	0.15	0.73	3.56	4.33	-32.17
0.22	32.3	74.00	0.21	13.11	1.83	0.09	0.14	0.75	3.61	4.06	-32.14
0.24	34.9	74.04	0.26	13.36	1.99	0.07	0.16	0.75	3.50	4.30	-32.14
0.25	37.2	73.67	0.22	13.53	1.95	0.03	0.16	0.77	3.93	4.15	-32.10
0.26	37.9	73.76	0.25	13.70	1.92	0.11	0.19	0.76	3.72	4.18	-32.11
0.27	40.1	73.70	0.17	13.71	1.96	0.10	0.16	0.75	3.97	3.96	-32.10
0.29	42.7	73.40	0.18	13.81	2.02	0.07	0.13	0.75	3.76	4.23	-32.07
0.30	43.5	73.37	0.25	13.66	1.93	0.08	0.16	0.76	3.57	4.25	-32.06
0.31	45.2	73.34	0.21	13.67	2.04	0.10	0.14	0.75	3.81	4.31	-32.06
0.33	48.1	73.23	0.16	13.86	2.05	0.05	0.17	0.78	3.93	4.24	-32.05
0.33	49.1	73.19	0.23	13.93	2.03	0.06	0.15	0.80	3.71	4.22	-32.04
0.34	50.4	73.31	0.20	13.78	2.09	0.08	0.19	0.80	3.56	4.14	-32.06
0.36	53.6	73.07	0.18	13.78	1.98	0.02	0.21	0.76	3.73	4.09	-32.03
0.37	54.6	73.02	0.24	13.96	2.06	0.00	0.11	0.76	3.90	4.26	-32.02
0.38	55.4	73.06	0.19	13.86	2.08	0.10	0.17	0.80	3.38	4.42	-32.03
0.40	59.0	72.84	0.26	13.90	2.15	0.00	0.17	0.80	3.98	4.44	-32.00
0.41	60.2	72.94	0.25	14.00	1.98	0.06	0.18	0.79	3.81	4.18	-32.02
0.41	60.6	72.89	0.17	13.97	2.05	0.14	0.17	0.88	3.73	4.26	-32.01
0.44	64.5	72.90	0.16	14.06	2.09	0.01	0.15	0.79	3.84	4.28	-32.01
0.45	65.8	72.93	0.24	13.93	2.02	0.07	0.18	0.81	3.70	4.06	-32.02
0.45	65.8	72.98	0.20	13.95	2.15	0.04	0.16	0.83	4.11	4.30	-32.02
0.48	69.9	72.80	0.13	14.00	2.03	0.07	0.18	0.81	3.71	4.31	-32.00
0.48	70.9	72.84	0.21	14.00	2.04	0.03	0.16	0.82	3.59	4.27	-32.00
0.49	71.4	72.55	0.23	13.95	2.00	-0.03	0.13	0.78	3.86	4.29	-31.97
0.51	75.4	72.97	0.21	13.97	2.01	0.07	0.19	0.84	3.84	4.30	-32.02
0.52	76.1	72.78	0.26	14.08	2.01	0.07	0.17	0.84	3.67	4.24	-32.00
0.52	76.9	72.74	0.19	14.03	2.05	0.00	0.14	0.84	3.66	4.28	-31.99
0.55	80.8	72.72	0.27	13.95	2.08	0.10	0.21	0.83	3.80	4.23	-31.99
0.55	81.2	72.79	0.25	14.00	2.16	0.11	0.19	0.83	3.62	4.26	-32.00
0.56	82.5	72.81	0.24	14.10	2.08	0.05	0.17	0.83	3.75	4.32	-32.00
0.59	86.3	72.68	0.22	14.02	2.11	0.04	0.16	0.81	3.75	4.33	-31.99
0.59	86.4	72.74	0.20	13.99	2.07	0.07	0.15	0.80	3.75	4.23	-31.99
0.60	88.1	72.74	0.15	13.93	2.04	0.04	0.14	0.79	3.97	4.33	-31.99
0.62	91.5	72.80	0.24	13.96	2.04	0.10	0.20	0.78	3.75	4.27	-32.00
0.62	91.7	72.69	0.22	14.05	2.13	0.04	0.17	0.85	3.89	4.26	-31.99
0.64	93.7	72.75	0.15	14.03	2.10	0.05	0.17	0.84	3.52	4.16	-31.99
0.66	96.7	72.92	0.22	13.99	2.13	0.04	0.19	0.80	3.84	4.32	-32.01
0.66	97.2	72.74	0.17	13.98	2.09	0.07	0.16	0.84	3.92	4.20	-31.99

0.68	99.3	72.81	0.20	14.00	2.10	0.01	0.14	0.84	3.64	4.28	-32.00
0.70	102.5	72.74	0.25	13.85	2.09	0.00	0.17	0.82	3.55	4.38	-31.99
0.71	104.8	72.64	0.29	14.11	2.00	0.02	0.15	0.86	3.71	4.21	-31.98
0.73	106.7	72.93	0.22	14.19	2.07	0.08	0.15	0.85	3.82	4.29	-32.01
0.74	108.0	72.58	0.27	14.02	2.04	0.03	0.20	0.83	3.59	4.43	-31.98
0.75	110.4	72.71	0.22	14.09	2.14	0.05	0.18	0.84	3.70	4.21	-31.99
0.77	113.4	72.66	0.24	14.17	1.99	0.05	0.17	0.81	3.73	4.19	-31.98
0.79	115.9	72.59	0.19	14.11	2.09	0.12	0.16	0.81	3.78	4.16	-31.98
0.79	116.7	72.64	0.27	14.11	2.18	0.01	0.17	0.86	3.86	4.21	-31.98
0.81	118.9	72.58	0.28	13.93	2.18	0.06	0.19	0.83	3.87	4.31	-31.98
0.86	126.7	72.90	0.20	14.00	2.06	0.06	0.17	0.83	3.63	4.44	-32.01
0.88	129.8	72.65	0.21	14.16	2.08	0.01	0.18	0.81	3.81	4.36	-31.98
0.89	130.1	72.60	0.27	14.21	2.05	0.11	0.19	0.86	3.75	4.21	-31.98
0.93	136.7	72.89	0.23	14.10	2.13	0.05	0.20	0.86	3.94	4.33	-32.01
0.96	140.7	72.80	0.25	13.81	2.04	-0.01	0.20	0.85	3.66	4.30	-32.00
0.98	144.3	72.54	0.23	14.12	2.01	0.08	0.19	0.82	3.51	4.27	-31.97
1.00	146.6	73.01	0.28	13.93	2.01	0.07	0.15	0.82	3.80	4.20	-32.02
1.03	151.6	72.79	0.25	13.89	2.10	0.07	0.19	0.85	3.81	4.16	-32.00
1.07	156.6	72.91	0.20	14.14	2.13	0.08	0.18	0.82	3.96	4.26	-32.01
1.08	158.6	72.57	0.23	14.07	2.04	0.05	0.14	0.81	3.60	4.27	-31.97
1.11	162.5	72.78	0.29	14.09	2.08	0.14	0.17	0.81	3.79	4.17	-32.00
1.13	166.6	72.86	0.26	14.08	2.03	0.07	0.20	0.80	3.86	4.26	-32.01
1.18	172.8	72.78	0.29	14.20	2.13	0.07	0.18	0.84	3.81	4.14	-32.00
1.18	173.4	72.74	0.27	13.92	2.15	0.10	0.18	0.85	4.01	4.15	-31.99
1.20	176.6	72.92	0.18	13.99	2.12	0.06	0.16	0.84	4.04	4.40	-32.01
1.25	184.3	72.91	0.28	14.11	2.09	0.06	0.17	0.85	3.78	4.31	-32.01
1.27	186.6	72.72	0.17	14.21	2.07	0.09	0.18	0.82	3.75	4.24	-31.99
1.27	187.0	72.84	0.20	13.84	1.96	0.12	0.17	0.82	3.81	4.18	-32.00
1.33	195.1	72.71	0.22	14.04	2.07	0.05	0.18	0.82	3.99	4.41	-31.99
1.34	196.6	72.75	0.25	14.01	2.03	0.07	0.16	0.84	3.75	4.47	-31.99
1.37	201.2	72.78	0.24	14.10	2.08	0.01	0.19	0.84	4.03	4.25	-32.00
1.40	206.0	72.76	0.26	14.04	2.11	0.12	0.19	0.84	3.79	4.25	-32.00
1.47	215.4	72.71	0.24	13.90	2.04	0.00	0.13	0.81	3.87	4.44	-31.99
1.48	216.9	72.64	0.22	13.91	2.10	0.03	0.19	0.83	3.63	4.31	-31.98
1.55	227.8	72.80	0.21	13.94	2.17	0.06	0.17	0.82	3.73	4.34	-32.00
1.56	229.6	72.94	0.25	14.13	2.06	0.05	0.23	0.83	3.86	4.18	-32.02
1.66	243.8	72.79	0.27	13.91	1.95	0.08	0.16	0.78	3.52	4.33	-32.00

QzDisRh203, starting rhyolite: NCO; T=1292 °C, P=0.5GPa, t=86397s, H2O=0.1wt%

x / sqrt(t)	x (μm)	SiO2+	TiO2	Al2O3	FeO	MnO	MgO	CaO	Na2O	K2O	lnD_SiO2 (m^2/s)
0.01	2.4	83.86	0.13	7.68	1.48	0.05	0.14	0.30	2.54	3.10	-33.45
0.01	3.2	83.48	0.16	7.79	1.41	0.04	0.14	0.28	2.66	3.12	-33.39
0.01	3.5	83.51	0.15	7.58	1.34	0.05	0.11	0.31	2.63	3.02	-33.40
0.02	4.8	83.06	0.14	8.44	1.47	0.01	0.12	0.35	2.59	3.31	-33.33
0.02	5.0	82.81	0.22	8.33	1.41	0.06	0.12	0.35	2.68	3.34	-33.29
0.02	5.1	82.64	0.14	8.38	1.44	0.01	0.12	0.34	2.46	3.33	-33.27
0.02	6.1	82.33	0.15	8.47	1.53	0.07	0.12	0.34	2.70	3.45	-33.22
0.02	6.1	81.93	0.16	8.46	1.40	0.05	0.13	0.32	2.58	3.30	-33.16
0.02	6.5	82.02	0.23	8.52	1.38	0.05	0.14	0.31	2.65	3.28	-33.17
0.03	8.6	82.12	0.12	8.91	1.51	0.08	0.12	0.40	2.53	3.48	-33.19
0.03	9.0	81.54	0.16	9.16	1.52	0.09	0.11	0.38	2.83	3.51	-33.10
0.03	9.0	81.60	0.12	9.31	1.49	0.03	0.15	0.34	2.62	3.48	-33.11
0.03	9.8	81.07	0.12	9.47	1.56	0.02	0.07	0.39	3.02	3.69	-33.03
0.03	10.0	81.29	0.09	9.27	1.58	0.03	0.12	0.38	2.96	3.42	-33.07
0.04	11.5	80.59	0.18	9.77	1.58	0.00	0.18	0.36	2.83	3.60	-32.96
0.04	12.0	80.67	0.13	9.45	1.50	0.05	0.11	0.38	2.88	3.80	-32.98
0.04	12.1	80.28	0.08	9.57	1.59	0.03	0.12	0.43	2.86	3.41	-32.92
0.04	12.5	80.35	0.20	9.50	1.49	0.06	0.12	0.39	3.00	3.40	-32.93
0.05	13.6	80.41	0.18	9.86	1.60	0.04	0.14	0.43	3.37	3.58	-32.94
0.05	14.7	80.89	0.20	9.60	1.51	0.04	0.16	0.39	3.01	3.52	-33.01
0.05	14.8	79.97	0.12	10.12	1.54	0.03	0.15	0.47	3.18	3.64	-32.88
0.05	15.5	79.48	0.17	10.20	1.55	0.05	0.14	0.46	3.22	3.70	-32.81
0.06	17.0	79.60	0.17	10.26	1.61	-0.03	0.15	0.46	3.35	3.73	-32.82
0.06	17.6	79.17	0.15	10.31	1.60	0.11	0.13	0.46	3.04	3.76	-32.76
0.06	18.5	79.09	0.17	10.41	1.57	0.07	0.12	0.48	3.37	3.78	-32.75
0.07	19.3	78.80	0.12	10.77	1.55	0.02	0.16	0.49	3.35	3.99	-32.71
0.08	22.4	78.12	0.11	10.92	1.60	0.05	0.14	0.52	3.31	3.97	-32.61
0.08	23.0	77.97	0.19	11.14	1.65	0.01	0.15	0.52	3.42	3.81	-32.59
0.08	24.5	78.21	0.21	11.03	1.63	0.05	0.12	0.52	3.67	4.02	-32.63
0.08	25.0	77.77	0.21	11.51	1.62	0.06	0.15	0.52	3.64	3.75	-32.57
0.09	26.5	77.78	0.17	11.45	1.65	0.04	0.15	0.54	3.62	3.97	-32.57
0.10	27.9	77.41	0.19	11.54	1.65	0.00	0.14	0.56	3.39	3.85	-32.51
0.10	28.5	77.35	0.13	11.48	1.67	0.01	0.15	0.57	3.53	4.17	-32.51
0.10	30.7	77.02	0.22	11.84	1.72	0.10	0.16	0.57	4.09	4.03	-32.46
0.11	32.0	77.03	0.19	11.91	1.79	0.03	0.15	0.55	3.72	4.05	-32.46
0.11	33.3	76.67	0.16	12.09	1.71	0.07	0.14	0.61	3.82	4.11	-32.41
0.12	33.9	76.52	0.21	12.10	1.70	0.05	0.14	0.58	3.82	3.99	-32.39
0.12	36.4	76.37	0.11	12.22	1.79	0.06	0.14	0.60	3.94	4.09	-32.37
0.13	37.5	75.98	0.18	12.22	1.82	0.09	0.16	0.62	3.82	4.04	-32.32
0.13	38.8	76.34	0.17	12.56	1.81	0.05	0.16	0.64	4.30	3.99	-32.37

0.13	39.4	76.07	0.20	12.44	1.81	0.06	0.13	0.60	3.77	4.00	-32.33
0.14	42.1	75.72	0.24	12.68	1.85	0.06	0.12	0.64	4.08	4.04	-32.29
0.15	43.0	75.49	0.20	12.69	1.84	0.04	0.15	0.66	4.13	4.25	-32.26
0.15	44.2	75.48	0.19	12.69	1.81	0.05	0.17	0.67	4.26	4.15	-32.25
0.15	44.8	75.34	0.21	12.69	1.85	-0.01	0.16	0.66	4.35	4.12	-32.24
0.16	47.8	75.28	0.18	12.95	1.78	0.03	0.15	0.69	4.02	4.19	-32.23
0.17	48.5	75.02	0.19	12.95	1.85	0.07	0.12	0.67	4.13	4.09	-32.19
0.17	49.7	75.05	0.16	12.89	1.84	0.06	0.16	0.66	4.09	4.10	-32.20
0.17	50.3	74.82	0.14	12.83	1.89	0.03	0.16	0.73	3.82	4.24	-32.17
0.18	53.5	75.01	0.18	13.11	1.92	0.10	0.11	0.73	4.21	4.23	-32.19
0.18	54.0	74.73	0.24	13.07	1.96	0.00	0.16	0.70	3.93	4.13	-32.15
0.19	55.1	74.82	0.21	13.30	1.84	0.03	0.16	0.72	4.38	4.09	-32.17
0.19	55.7	74.56	0.18	13.21	1.84	0.08	0.10	0.71	3.96	4.02	-32.13
0.20	59.2	74.83	0.22	13.40	1.83	0.07	0.11	0.78	4.54	4.13	-32.17
0.20	59.5	74.54	0.21	13.33	2.05	0.03	0.12	0.73	4.09	4.19	-32.13
0.22	64.9	74.41	0.21	13.47	1.97	0.05	0.20	0.74	4.37	4.25	-32.11
0.24	70.9	74.01	0.19	13.69	2.02	0.05	0.21	0.77	4.04	4.33	-32.06
0.24	71.8	73.96	0.22	13.75	1.97	0.04	0.18	0.79	4.54	4.38	-32.05
0.26	75.6	73.99	0.21	13.74	1.95	0.03	0.13	0.76	4.41	4.23	-32.06
0.29	83.8	73.51	0.19	13.92	2.03	0.05	0.16	0.82	4.63	4.21	-32.00
0.29	86.2	73.67	0.19	14.06	1.95	0.04	0.16	0.83	4.36	4.12	-32.02
0.30	86.7	73.63	0.23	13.97	1.97	0.11	0.13	0.81	4.79	4.14	-32.01
0.33	95.8	73.08	0.16	14.15	2.09	0.05	0.20	0.83	4.32	4.13	-31.94
0.33	96.9	73.37	0.26	14.16	1.94	0.05	0.18	0.83	4.40	4.25	-31.98
0.35	102.4	73.19	0.16	14.34	1.93	0.10	0.18	0.82	4.67	4.22	-31.96
0.37	107.6	73.25	0.11	14.22	1.90	0.10	0.15	0.86	4.53	4.34	-31.96
0.37	107.8	73.10	0.29	14.25	2.08	0.08	0.20	0.82	4.54	4.20	-31.94
0.40	118.2	73.20	0.17	14.30	2.01	0.06	0.17	0.88	4.49	4.41	-31.96
0.40	118.2	73.20	0.22	14.27	2.02	0.02	0.15	0.82	4.54	4.27	-31.96
0.41	119.8	72.91	0.25	14.25	2.02	0.06	0.16	0.86	4.62	4.14	-31.92
0.44	128.9	73.09	0.24	14.31	2.01	0.04	0.12	0.84	4.50	4.22	-31.94
0.45	131.8	72.85	0.17	14.47	2.07	0.11	0.15	0.85	4.66	4.25	-31.91
0.46	134.0	73.00	0.23	14.27	2.03	0.01	0.16	0.87	4.45	4.22	-31.93
0.47	139.6	73.19	0.19	14.27	1.93	0.02	0.16	0.87	4.36	4.31	-31.96
0.49	143.8	72.60	0.17	14.51	2.07	0.07	0.17	0.84	4.35	4.19	-31.88
0.51	149.8	73.07	0.22	14.24	2.05	0.02	0.18	0.87	4.46	4.19	-31.94
0.51	150.2	72.88	0.21	14.48	2.08	0.13	0.17	0.85	4.17	4.19	-31.92
0.53	155.8	72.82	0.19	14.30	2.12	0.06	0.18	0.84	4.48	4.35	-31.91
0.55	160.9	72.94	0.22	14.38	1.98	0.08	0.20	0.89	4.56	4.43	-31.92
0.56	165.5	73.04	0.27	14.29	2.08	0.11	0.18	0.84	4.16	4.34	-31.94
0.57	167.8	72.62	0.25	14.47	2.18	0.05	0.15	0.88	4.64	4.39	-31.88
0.62	181.3	72.98	0.23	14.31	2.09	0.08	0.22	0.86	4.77	4.20	-31.93
0.62	182.9	73.10	0.22	14.63	2.11	0.10	0.16	0.89	4.88	4.30	-31.94

0.64	188.9	72.69	0.15	14.46	2.16	0.14	0.20	0.86	4.35	4.15	-31.89
0.67	197.1	73.10	0.28	14.35	2.12	0.05	0.13	0.89	4.51	4.15	-31.94
0.70	204.9	72.82	0.26	14.38	1.96	0.10	0.23	0.85	4.61	4.40	-31.91
0.71	210.0	72.84	0.24	14.28	2.15	0.06	0.17	0.89	4.38	4.40	-31.91
0.77	226.5	73.01	0.19	14.35	1.99	0.09	0.18	0.84	4.60	4.11	-31.93
0.77	226.9	72.77	0.21	14.30	2.08	0.06	0.17	0.89	4.78	4.45	-31.90
0.79	231.1	72.87	0.18	14.37	2.19	0.14	0.18	0.90	4.38	4.27	-31.92
0.85	248.9	72.95	0.23	14.35	1.94	0.06	0.19	0.86	4.48	4.33	-31.93
0.86	252.2	72.71	0.26	14.37	2.16	0.02	0.19	0.87	4.39	4.18	-31.90
0.87	255.9	73.00	0.22	14.22	2.10	0.04	0.14	0.90	4.47	4.36	-31.93
0.92	270.9	72.85	0.21	14.16	1.98	0.06	0.15	0.88	4.48	4.34	-31.91
0.93	273.4	72.79	0.21	14.54	2.20	0.05	0.18	0.84	4.41	4.28	-31.91
0.97	285.2	72.90	0.20	14.23	2.07	0.02	0.19	0.88	4.01	4.46	-31.92
1.00	292.8	72.99	0.21	14.29	2.10	0.09	0.18	0.86	4.51	4.30	-31.93
1.00	294.5	72.92	0.21	14.10	2.08	0.08	0.19	0.83	4.45	4.26	-31.92
1.07	314.6	73.20	0.20	14.29	1.99	0.04	0.18	0.87	4.30	4.40	-31.96
1.07	314.8	72.90	0.25	14.28	2.09	0.01	0.18	0.89	4.57	4.39	-31.92
1.07	315.6	72.83	0.25	14.35	2.20	0.09	0.21	0.87	4.40	4.10	-31.91
1.15	336.7	72.87	0.19	14.30	2.19	0.07	0.16	0.87	4.57	4.36	-31.91
1.15	336.8	73.04	0.26	14.31	2.09	0.06	0.16	0.89	4.71	4.12	-31.94
1.17	344.0	73.06	0.18	14.30	2.07	0.02	0.15	0.88	4.53	4.22	-31.94
1.22	357.8	72.95	0.25	14.31	2.11	0.05	0.21	0.87	4.46	4.24	-31.93
1.22	358.8	72.87	0.20	14.37	2.10	0.08	0.18	0.85	4.26	4.45	-31.91
1.27	373.4	73.09	0.18	14.31	2.12	0.10	0.16	0.89	4.38	4.25	-31.94
1.34	392.4	73.08	0.25	14.31	2.03	0.01	0.17	0.91	4.41	4.16	-31.94
1.34	392.7	72.96	0.25	14.23	2.15	0.11	0.18	0.86	4.38	4.31	-31.93
1.37	402.7	73.13	0.24	14.26	2.11	0.06	0.15	0.85	4.40	4.30	-31.95
1.45	425.9	72.65	0.26	14.32	2.01	0.06	0.19	0.89	4.00	4.27	-31.89
1.45	427.6	72.74	0.19	14.22	2.08	0.11	0.13	0.88	4.49	4.22	-31.90
1.47	432.1	73.01	0.18	14.15	2.03	0.07	0.15	0.86	4.38	4.20	-31.93
1.56	459.5	72.55	0.20	14.42	2.11	0.10	0.17	0.88	4.57	4.32	-31.88
1.57	462.4	72.99	0.23	14.27	2.22	0.05	0.20	0.88	4.30	4.24	-31.93
1.63	478.1	73.03	0.29	14.42	2.12	0.09	0.18	0.91	4.45	4.33	-31.94
1.68	493.1	72.97	0.14	14.53	2.16	0.05	0.18	0.90	4.55	4.11	-31.93
1.69	497.3	73.00	0.20	14.20	2.20	0.08	0.20	0.90	4.73	4.34	-31.93
1.78	524.1	73.08	0.25	14.41	2.21	0.08	0.14	0.90	4.41	4.30	-31.94
1.79	526.7	72.64	0.23	14.54	2.08	0.08	0.12	0.91	4.62	4.28	-31.89
1.81	532.2	72.76	0.23	14.03	2.18	0.09	0.20	0.91	4.50	4.26	-31.90
1.91	560.2	72.73	0.20	14.32	2.02	0.07	0.22	0.86	4.11	4.37	-31.90
1.93	567.1	72.89	0.19	14.26	2.12	0.02	0.18	0.93	4.23	4.38	-31.92
1.94	570.1	73.00	0.24	14.25	2.14	0.19	0.18	0.87	4.64	4.35	-31.93
2.02	593.8	72.85	0.26	14.25	2.01	0.07	0.21	0.88	4.42	4.37	-31.91
2.05	601.9	72.83	0.22	14.18	2.27	0.07	0.19	0.88	4.60	4.32	-31.91

2.10	616.1	72.71	0.21	14.16	2.07	0.09	0.17	0.86	4.43	4.26	-31.90
2.17	636.7	72.86	0.26	14.02	2.27	0.06	0.19	0.90	4.30	4.42	-31.91

QzDisRh105, starting rhyolite: NCO; T=1408 °C, P=0.5GPa, t=86433s, H2O=0.1wt%

x / sqrt(t)	x (μm)	SiO2+	TiO2	Al2O3	FeO	MnO	MgO	CaO	Na2O	K2O	lnD_SiO2 (m^2/s)
0.01	3.5	88.94	0.09	4.58	1.10	0.01	0.10	0.18	1.62	2.08	-32.54
0.01	4.0	89.26	0.13	4.54	0.99	0.05	0.10	0.16	1.54	2.02	-32.59
0.01	4.2	88.88	0.08	4.85	1.15	0.04	0.12	0.18	1.70	2.27	-32.53
0.02	4.4	88.59	0.09	5.01	1.03	-0.01	0.06	0.20	1.67	2.24	-32.49
0.02	7.0	87.60	0.10	5.19	1.10	0.04	0.14	0.20	1.85	2.31	-32.35
0.03	7.4	88.07	0.12	5.51	1.11	0.01	0.13	0.21	1.71	2.39	-32.42
0.03	7.8	87.87	0.16	5.43	1.08	0.06	0.09	0.22	1.54	2.49	-32.39
0.03	7.9	88.14	0.08	5.10	1.09	-0.01	0.07	0.18	1.70	2.30	-32.43
0.03	8.4	87.73	0.11	5.68	1.09	-0.04	0.10	0.23	1.61	2.54	-32.37
0.03	8.8	88.20	0.14	5.31	1.10	0.02	0.10	0.20	1.69	2.43	-32.44
0.03	8.8	87.84	0.12	5.35	1.09	0.02	0.07	0.20	1.79	2.49	-32.39
0.03	10.2	87.19	0.12	5.91	1.16	-0.03	0.13	0.23	1.88	2.68	-32.30
0.04	11.9	86.92	0.14	5.97	1.15	0.10	0.11	0.23	2.02	2.47	-32.26
0.04	12.6	86.62	0.17	5.99	1.14	0.00	0.09	0.24	2.05	2.64	-32.22
0.04	13.1	86.11	0.12	6.45	1.15	0.00	0.15	0.25	2.22	2.92	-32.15
0.05	13.6	86.05	0.09	6.25	1.15	0.02	0.09	0.22	1.86	2.66	-32.14
0.05	14.1	85.86	0.14	6.31	1.20	-0.01	0.08	0.22	1.92	2.82	-32.12
0.06	17.5	85.50	0.13	6.72	1.21	0.10	0.10	0.26	2.07	2.75	-32.07
0.06	18.1	85.22	0.14	7.02	1.28	0.01	0.12	0.26	2.25	2.93	-32.03
0.06	18.3	85.25	0.13	6.80	1.21	0.05	0.11	0.29	2.16	2.94	-32.04
0.06	18.4	85.11	0.16	6.92	1.24	-0.02	0.09	0.28	2.45	2.90	-32.02
0.08	23.1	83.75	0.14	7.60	1.24	0.03	0.12	0.30	2.18	3.09	-31.84
0.08	23.1	84.05	0.09	7.54	1.26	0.02	0.13	0.31	2.29	3.12	-31.88
0.08	23.5	84.09	0.13	7.68	1.26	0.08	0.13	0.30	2.34	3.10	-31.88
0.08	23.7	83.94	0.09	7.74	1.30	0.01	0.10	0.31	2.30	3.09	-31.87
0.10	28.7	82.83	0.09	8.14	1.34	0.11	0.08	0.32	2.79	3.14	-31.72
0.10	28.7	83.13	0.16	8.07	1.31	0.03	0.14	0.35	2.68	3.28	-31.76
0.10	29.2	82.80	0.13	8.41	1.26	0.10	0.11	0.32	2.47	3.34	-31.72
0.12	33.9	82.04	0.15	8.79	1.29	0.04	0.11	0.38	2.76	3.49	-31.62
0.12	34.3	81.73	0.11	8.74	1.37	0.01	0.08	0.38	2.84	3.41	-31.58
0.12	34.8	81.99	0.09	8.74	1.27	0.09	0.09	0.37	2.91	3.46	-31.62
0.13	39.1	81.35	0.16	9.21	1.26	0.08	0.11	0.40	2.81	3.71	-31.54
0.14	39.9	80.96	0.14	9.39	1.41	0.01	0.11	0.39	3.11	3.59	-31.49
0.14	40.3	81.09	0.14	9.42	1.35	0.02	0.11	0.40	2.85	3.60	-31.51
0.15	44.3	80.58	0.14	9.66	1.38	0.09	0.12	0.42	2.92	3.70	-31.44
0.15	45.5	80.43	0.18	9.80	1.41	-0.02	0.12	0.46	2.93	3.76	-31.43
0.16	45.9	80.75	0.19	9.81	1.29	0.05	0.17	0.40	3.26	3.44	-31.46
0.17	49.5	79.89	0.18	9.98	1.41	0.03	0.15	0.43	2.91	3.60	-31.36
0.17	51.1	79.64	0.08	10.13	1.44	0.03	0.12	0.46	3.23	3.85	-31.33
0.18	51.5	79.74	0.13	10.17	1.30	0.05	0.10	0.45	3.12	3.75	-31.34

0.19	54.7	79.44	0.17	10.47	1.50	0.02	0.16	0.44	3.36	3.66	-31.30
0.19	56.7	78.95	0.16	10.46	1.41	0.02	0.13	0.43	3.17	3.78	-31.25
0.19	57.0	79.16	0.20	10.76	1.42	0.02	0.13	0.48	3.47	4.02	-31.27
0.20	59.9	78.81	0.17	10.75	1.48	0.11	0.14	0.50	3.33	3.73	-31.23
0.21	62.3	78.43	0.14	10.88	1.49	0.11	0.12	0.48	3.58	3.91	-31.18
0.23	67.9	78.35	0.16	11.18	1.54	0.08	0.11	0.50	3.24	3.95	-31.17
0.23	67.9	77.94	0.16	11.27	1.46	0.09	0.19	0.52	3.74	3.96	-31.13
0.24	70.5	78.10	0.18	11.22	1.44	0.03	0.12	0.53	3.50	4.00	-31.14
0.27	78.8	77.28	0.15	11.89	1.57	0.03	0.14	0.59	3.71	3.99	-31.05
0.27	78.8	77.27	0.23	11.81	1.53	0.05	0.13	0.54	3.73	4.05	-31.05
0.28	81.1	77.21	0.14	11.85	1.51	0.01	0.09	0.56	3.61	3.92	-31.04
0.30	89.7	76.63	0.11	12.19	1.52	0.09	0.15	0.59	3.61	4.00	-30.97
0.30	89.7	76.58	0.19	12.10	1.53	0.06	0.15	0.63	3.78	4.22	-30.97
0.31	91.7	76.47	0.17	12.13	1.51	0.10	0.15	0.58	3.62	3.96	-30.95
0.34	100.6	76.28	0.15	12.51	1.70	0.05	0.10	0.68	3.95	4.20	-30.93
0.34	100.6	75.96	0.20	12.57	1.58	0.11	0.15	0.63	3.72	4.11	-30.90
0.35	102.3	76.04	0.10	12.74	1.57	0.11	0.18	0.66	3.62	3.94	-30.90
0.38	111.5	75.53	0.15	12.92	1.65	0.00	0.14	0.64	3.75	4.21	-30.85
0.38	111.5	75.46	0.16	12.84	1.56	0.07	0.15	0.69	3.89	4.07	-30.84
0.38	112.9	75.51	0.15	12.83	1.64	0.02	0.20	0.69	3.76	4.28	-30.84
0.42	122.4	75.06	0.14	13.05	1.62	0.09	0.17	0.73	4.02	4.14	-30.79
0.42	122.4	75.02	0.16	13.07	1.65	0.09	0.16	0.68	4.12	4.31	-30.79
0.42	123.5	75.20	0.18	13.16	1.66	0.02	0.21	0.71	4.26	4.22	-30.81
0.45	133.3	74.91	0.16	13.47	1.71	0.04	0.17	0.73	4.06	4.23	-30.78
0.45	133.3	74.93	0.22	13.17	1.74	0.09	0.16	0.71	4.26	4.32	-30.78
0.46	134.1	74.75	0.20	13.31	1.63	0.08	0.14	0.71	3.86	4.20	-30.76
0.49	144.2	74.44	0.20	13.49	1.67	0.09	0.15	0.75	3.93	4.30	-30.72
0.49	144.2	74.35	0.21	13.56	1.76	0.10	0.17	0.75	4.17	4.20	-30.71
0.49	144.7	74.81	0.19	13.51	1.69	0.06	0.13	0.75	4.34	4.24	-30.76
0.53	155.1	74.23	0.20	13.81	1.63	0.07	0.22	0.79	4.09	4.26	-30.70
0.53	155.1	74.04	0.26	13.62	1.80	0.11	0.14	0.74	3.97	4.42	-30.68
0.53	155.3	74.00	0.19	13.65	1.78	0.06	0.19	0.76	4.19	4.19	-30.67
0.56	165.9	74.05	0.22	13.87	1.77	0.08	0.20	0.76	4.02	4.23	-30.68
0.56	166.0	74.00	0.25	13.83	1.66	0.08	0.18	0.76	3.94	4.55	-30.67
0.56	166.0	74.03	0.14	13.78	1.77	0.13	0.18	0.75	4.35	4.28	-30.68
0.60	176.9	73.59	0.29	14.02	1.73	0.05	0.19	0.80	4.14	4.37	-30.63
0.63	186.5	73.63	0.20	13.96	1.68	0.02	0.17	0.86	3.85	4.49	-30.63
0.63	186.5	73.41	0.20	14.16	1.77	0.00	0.15	0.81	4.07	4.22	-30.61
0.67	196.7	73.52	0.21	14.16	1.74	0.07	0.13	0.81	4.34	4.27	-30.62
0.70	207.1	73.60	0.21	14.13	1.78	0.08	0.32	0.79	4.48	4.27	-30.63
0.70	207.1	73.46	0.16	14.17	1.74	0.03	0.16	0.81	4.21	4.28	-30.61
0.74	216.5	73.41	0.24	14.33	1.87	-0.01	0.22	0.83	4.29	4.42	-30.61
0.77	227.7	73.34	0.22	14.40	1.73	0.09	0.19	0.81	4.23	4.28	-30.60

0.77	227.7	73.44	0.26	14.28	1.82	0.07	0.24	0.85	4.49	4.22	-30.61
0.80	236.3	73.22	0.24	14.46	1.77	0.00	0.14	0.84	4.29	4.44	-30.59
0.84	248.3	73.21	0.28	14.32	1.84	0.08	0.49	0.82	4.21	4.26	-30.59
0.84	248.3	73.12	0.23	14.29	1.75	0.07	0.17	0.87	4.40	4.28	-30.58
0.87	256.1	72.98	0.22	14.52	1.80	0.02	0.20	0.90	4.26	4.27	-30.56
0.91	268.9	73.21	0.21	14.52	1.75	0.07	0.18	0.87	4.23	4.41	-30.59
0.91	268.9	72.94	0.22	14.53	1.74	0.11	0.18	0.85	4.39	4.38	-30.56
0.94	275.9	73.04	0.15	14.23	1.85	0.11	0.18	0.87	4.19	4.25	-30.57
0.98	289.5	73.02	0.31	14.48	1.87	0.06	0.16	0.85	4.16	4.28	-30.56
0.98	289.5	73.02	0.17	14.27	1.85	0.07	0.15	0.89	4.45	4.35	-30.56
1.01	295.7	73.00	0.27	14.38	1.79	-0.05	0.23	0.83	4.27	4.38	-30.56
1.05	310.1	72.77	0.27	14.37	1.82	0.12	0.22	0.87	4.40	4.32	-30.54
1.05	310.1	73.06	0.19	14.51	1.81	0.04	0.16	0.88	4.40	4.26	-30.57
1.07	315.5	73.13	0.28	14.53	1.76	0.05	0.23	0.84	4.38	4.30	-30.58
1.12	330.7	72.76	0.26	14.31	1.91	-0.01	0.15	0.84	4.40	4.37	-30.54
1.13	330.7	72.89	0.21	14.57	1.76	0.02	0.21	0.89	4.27	4.35	-30.55
1.14	335.3	72.91	0.21	14.46	1.86	0.00	0.18	0.90	4.45	4.42	-30.55
1.19	351.3	72.92	0.19	14.59	1.85	0.11	0.15	0.88	4.57	4.24	-30.55
1.20	351.3	72.81	0.21	14.39	1.87	0.06	0.16	0.87	4.29	4.39	-30.54
1.21	355.1	73.05	0.19	14.48	1.91	0.12	0.21	0.89	4.33	4.22	-30.57
1.27	371.9	72.96	0.19	14.56	1.77	0.03	0.16	0.81	4.14	4.45	-30.56
1.27	371.9	73.18	0.26	14.54	1.89	0.09	0.20	0.83	4.45	4.37	-30.58
1.28	374.9	72.91	0.21	14.59	1.81	0.05	0.18	0.87	4.33	4.48	-30.55
1.39	408.1	72.90	0.23	14.56	1.88	0.05	0.16	0.89	4.53	4.46	-30.55
1.39	409.2	72.99	0.21	14.45	1.80	0.05	0.18	0.87	4.04	4.25	-30.56
1.40	411.0	72.89	0.24	14.31	1.82	0.03	0.13	0.87	4.49	4.31	-30.55
1.51	444.4	73.06	0.23	14.54	1.83	0.05	0.15	0.85	4.73	4.23	-30.57
1.52	446.5	72.98	0.19	14.42	1.86	0.07	0.15	0.88	4.25	4.28	-30.56
1.52	447.1	72.86	0.20	14.47	1.87	0.04	0.16	0.90	4.52	4.33	-30.55
1.63	480.6	73.09	0.23	14.47	1.84	0.12	0.21	0.84	4.50	4.55	-30.57
1.64	483.2	73.07	0.23	14.52	1.91	0.10	0.16	0.88	4.40	4.36	-30.57
1.65	483.8	73.13	0.27	14.54	1.90	0.09	0.20	0.87	4.27	4.38	-30.58
1.76	516.8	73.18	0.23	14.57	1.91	0.11	0.23	0.85	4.37	4.25	-30.58
1.77	519.4	72.87	0.17	14.33	1.89	0.08	0.21	0.87	4.19	4.36	-30.55
1.77	521.0	72.98	0.26	14.53	1.90	0.13	0.18	0.87	4.32	4.35	-30.56
1.88	553.0	72.97	0.18	14.42	1.87	0.07	0.18	0.88	4.04	4.28	-30.56
1.89	555.5	72.98	0.13	14.42	1.87	0.11	0.19	0.86	4.39	4.41	-30.56
1.90	558.3	73.03	0.24	14.44	1.76	0.09	0.18	0.89	4.36	4.24	-30.57
2.00	589.2	73.04	0.20	14.50	1.88	0.04	0.16	0.86	4.38	4.33	-30.57
2.01	591.6	72.70	0.22	14.40	1.79	0.05	0.18	0.88	4.42	4.45	-30.53
2.03	595.6	72.86	0.21	14.40	1.86	0.04	0.19	0.87	4.38	4.51	-30.55
2.13	625.5	73.08	0.21	14.31	1.79	0.02	0.16	0.88	4.14	4.36	-30.57
2.13	627.7	72.84	0.17	14.61	1.77	0.03	0.18	0.88	4.26	4.23	-30.54

2.15	632.9	72.71	0.24	14.24	1.87	0.04	0.18	0.86	4.33	4.63	-30.53
2.25	661.7	72.97	0.17	14.55	1.92	0.05	0.15	0.85	4.50	4.26	-30.56
2.26	663.8	72.97	0.20	14.45	1.90	0.08	0.16	0.88	4.16	4.38	-30.56
2.37	697.9	73.06	0.20	14.37	1.84	0.05	0.17	0.86	4.53	4.39	-30.57
2.38	699.9	72.82	0.29	14.58	1.87	0.07	0.11	0.88	4.17	4.21	-30.54

QzDisRh113, starting rhyolite: NCO; T=1414 °C, P=0.5GPa, t=44970s, H2O=0.1wt%

x / sqrt(t)	x (μm)	SiO2+	TiO2	Al2O3	FeO	MnO	MgO	CaO	Na2O	K2O	lnD_SiO2 (m^2/s)
0.02	5.0	86.55	0.13	6.55	1.17	0.03	0.14	0.25	2.48	2.68	-32.50
0.03	6.0	85.89	0.16	6.48	1.23	0.07	0.13	0.21	2.49	2.81	-32.41
0.03	6.5	85.28	0.19	7.08	1.27	0.04	0.11	0.29	2.78	2.98	-32.33
0.05	10.2	83.81	0.16	7.18	1.30	0.07	0.12	0.30	3.75	2.94	-32.15
0.08	17.7	82.62	0.13	8.68	1.42	0.08	0.12	0.34	3.41	3.45	-32.00
0.10	21.8	81.30	0.13	9.23	1.45	0.08	0.12	0.38	3.79	3.58	-31.84
0.11	22.7	81.16	0.14	9.25	1.36	0.07	0.14	0.40	3.49	3.82	-31.82
0.12	24.6	80.95	0.12	9.46	1.41	0.06	0.14	0.42	3.39	3.53	-31.80
0.12	26.1	80.12	0.16	9.83	1.46	0.08	0.11	0.39	3.99	3.62	-31.70
0.13	26.9	80.02	0.15	9.59	1.47	0.03	0.13	0.39	3.95	3.74	-31.68
0.14	30.3	78.97	0.19	10.34	1.49	0.04	0.14	0.46	4.00	3.88	-31.56
0.15	31.1	78.93	0.18	10.34	1.48	0.03	0.15	0.45	4.01	3.78	-31.55
0.17	35.2	78.25	0.15	10.68	1.45	0.03	0.10	0.49	4.29	3.97	-31.47
0.17	36.5	78.94	0.13	10.61	1.53	0.07	0.14	0.52	3.88	4.03	-31.55
0.20	42.3	77.59	0.10	11.41	1.54	0.04	0.12	0.53	4.41	3.93	-31.39
0.23	49.0	76.91	0.19	11.79	1.55	0.04	0.13	0.56	4.47	4.08	-31.31
0.26	54.2	76.47	0.21	12.05	1.64	0.04	0.14	0.60	4.40	4.18	-31.25
0.33	70.3	74.94	0.17	12.82	1.71	0.04	0.16	0.68	4.83	4.21	-31.06
0.34	71.9	75.09	0.24	12.66	1.66	0.12	0.17	0.68	4.71	4.18	-31.08
0.37	77.9	74.93	0.21	12.96	1.64	0.05	0.15	0.68	4.73	4.15	-31.06
0.40	83.8	74.46	0.17	13.22	1.85	0.01	0.17	0.72	4.76	4.05	-31.00
0.42	89.8	74.57	0.08	13.17	1.75	0.05	0.17	0.75	4.82	4.22	-31.01
0.43	91.6	74.35	0.17	13.35	1.83	0.03	0.16	0.73	5.04	4.27	-30.98
0.45	95.7	74.43	0.20	13.37	1.72	0.05	0.15	0.75	4.83	3.97	-31.00
0.48	101.6	73.88	0.27	13.62	1.75	0.05	0.16	0.76	5.02	4.23	-30.92
0.51	107.5	73.89	0.18	13.57	1.82	0.11	0.17	0.80	4.86	4.10	-30.93
0.52	109.7	73.81	0.23	13.52	1.92	0.09	0.15	0.80	5.31	4.12	-30.91
0.53	112.8	73.72	0.20	13.63	1.85	0.08	0.15	0.79	5.12	4.15	-30.90
0.57	120.2	73.78	0.17	13.77	1.79	0.04	0.16	0.78	5.10	4.28	-30.91
0.62	130.7	73.88	0.25	13.75	1.82	0.06	0.15	0.77	5.28	4.15	-30.92
0.63	134.1	73.51	0.18	13.87	1.91	0.07	0.17	0.80	5.19	4.18	-30.87
0.67	141.2	73.42	0.24	14.09	1.77	0.04	0.17	0.81	5.30	4.35	-30.86
0.72	151.8	73.08	0.17	13.79	1.89	0.07	0.17	0.83	5.01	4.36	-30.82
0.73	155.3	72.83	0.19	13.99	1.95	0.10	0.15	0.83	5.35	4.38	-30.78
0.82	172.8	73.54	0.24	13.93	1.90	0.12	0.20	0.83	5.21	4.17	-30.88
0.83	176.6	73.05	0.16	14.19	1.95	0.06	0.17	0.87	5.38	4.14	-30.81
0.86	183.4	72.84	0.20	13.96	1.98	0.13	0.20	0.82	5.50	4.31	-30.79
0.91	193.9	72.95	0.22	13.85	1.93	0.06	0.18	0.83	5.60	4.31	-30.80
0.96	204.4	72.82	0.27	14.07	1.99	0.10	0.17	0.84	5.42	4.23	-30.78
1.03	219.1	72.89	0.22	14.22	1.90	0.07	0.19	0.87	5.33	4.10	-30.79
1.13	240.4	73.26	0.16	14.08	1.93	0.05	0.17	0.86	5.31	4.44	-30.84
1.23	261.7	72.73	0.18	14.19	1.99	0.08	0.17	0.89	5.10	4.48	-30.77
1.33	282.9	72.95	0.22	14.05	2.04	0.05	0.20	0.82	5.23	4.17	-30.80
1.53	325.5	72.80	0.21	13.97	2.01	0.05	0.17	0.91	5.05	4.43	-30.78
1.63	346.7	72.83	0.22	14.05	1.98	0.11	0.20	0.88	5.62	4.29	-30.78
1.74	368.0	72.99	0.26	13.87	1.94	0.06	0.19	0.85	5.28	4.42	-30.81
1.84	389.2	73.02	0.17	14.02	2.00	0.05	0.17	0.82	5.36	4.27	-30.81

QzDisRh14, starting rhyolite: NCO; T=1403 °C, P=0.5GPa, t=21627s, H2O=0.1wt%

x / sqrt(t)	x (μm)	SiO2+	TiO2	Al2O3	FeO	MnO	MgO	CaO	Na2O	K2O	lnD_SiO2 (m^2/s)
0.02	2.4	88.45	0.06	5.17	1.17	0.05	0.11	0.20	1.70	2.25	-32.07
0.04	5.3	86.85	0.11	5.92	1.12	0.02	0.09	0.23	1.94	2.64	-31.85
0.04	5.8	88.09	0.07	5.47	1.17	-0.02	0.08	0.20	1.77	2.53	-32.02
0.05	8.0	85.97	0.10	6.32	1.26	0.05	0.11	0.27	1.91	2.71	-31.74
0.06	8.4	85.72	0.13	6.45	1.23	0.06	0.16	0.24	2.09	2.65	-31.71
0.06	8.4	85.19	0.11	6.91	1.25	0.02	0.12	0.27	2.14	2.99	-31.64
0.08	11.5	83.91	0.05	7.66	1.24	0.06	0.09	0.31	2.36	3.13	-31.49
0.09	13.5	83.66	0.15	7.73	1.35	0.14	0.15	0.29	2.50	3.24	-31.46
0.09	13.6	83.72	0.08	7.80	1.30	0.08	0.22	0.32	2.27	3.11	-31.46
0.10	14.7	83.02	0.10	7.95	1.26	0.06	0.13	0.33	2.51	3.22	-31.38
0.11	16.4	82.90	0.08	8.13	1.34	0.07	0.12	0.33	2.34	3.24	-31.37
0.12	17.8	82.14	0.14	8.60	1.29	0.08	0.10	0.35	2.52	3.55	-31.28
0.13	18.6	81.88	0.12	8.67	1.44	0.06	0.12	0.36	2.53	3.47	-31.24
0.14	20.9	81.94	0.15	8.80	1.37	0.08	0.13	0.41	2.57	3.34	-31.25
0.15	21.7	81.43	0.14	9.01	1.41	0.05	0.17	0.36	2.80	3.29	-31.19
0.16	23.7	80.84	0.17	9.55	1.52	0.05	0.12	0.41	2.81	3.57	-31.12
0.16	24.1	81.01	0.18	9.31	1.41	0.04	0.12	0.42	2.92	3.54	-31.14
0.17	24.8	80.68	0.16	9.61	1.41	0.03	0.09	0.42	2.75	3.59	-31.11
0.18	27.0	80.11	0.13	9.83	1.52	0.01	0.09	0.41	2.92	3.51	-31.04
0.18	27.2	80.40	0.20	9.72	1.44	0.01	0.11	0.41	2.93	3.69	-31.07
0.20	28.8	79.82	0.09	10.22	1.50	0.05	0.09	0.45	3.03	3.57	-31.01
0.21	30.3	79.98	0.13	10.03	1.45	0.00	0.10	0.45	3.11	3.70	-31.02
0.21	30.4	79.35	0.14	10.44	1.49	0.11	0.39	0.44	3.23	3.89	-30.95
0.22	32.3	78.96	0.16	10.56	1.54	0.01	0.11	0.43	3.09	3.81	-30.91
0.23	33.5	79.46	0.16	10.39	1.49	0.03	0.09	0.46	3.22	3.92	-30.97
0.23	33.9	79.19	0.13	10.70	1.50	0.10	0.14	0.47	3.29	3.87	-30.93
0.24	36.0	78.46	0.16	10.80	1.55	0.01	0.10	0.53	3.20	3.71	-30.85
0.25	36.6	79.14	0.16	10.53	1.57	0.08	0.14	0.46	3.12	3.85	-30.93
0.26	37.6	78.51	0.22	11.03	1.52	0.09	0.12	0.52	3.21	3.71	-30.86
0.26	39.0	78.02	0.16	11.31	1.59	0.10	0.11	0.55	3.10	3.93	-30.80
0.27	39.7	78.59	0.19	10.79	1.46	0.06	0.11	0.51	3.32	3.90	-30.87
0.28	41.6	77.80	0.23	11.48	1.57	0.07	0.12	0.54	3.49	3.96	-30.78
0.29	42.9	77.62	0.20	11.52	1.57	0.05	0.13	0.57	3.36	3.99	-30.76
0.30	44.1	77.34	0.20	11.85	1.63	0.06	0.17	0.58	3.36	4.20	-30.73
0.32	47.2	77.01	0.18	11.91	1.61	0.04	0.20	0.57	3.17	3.88	-30.69
0.33	48.2	76.78	0.18	12.02	1.65	0.05	0.10	0.61	3.10	4.05	-30.66
0.33	49.2	76.67	0.21	11.92	1.71	0.04	0.11	0.60	3.44	4.05	-30.65
0.37	54.3	76.25	0.24	12.35	1.75	0.02	0.15	0.61	3.66	4.09	-30.61
0.39	57.2	75.95	0.18	12.61	1.76	0.03	0.14	0.65	3.51	3.98	-30.57
0.40	58.3	75.77	0.24	12.51	1.77	0.08	0.15	0.64	3.49	4.27	-30.55
0.44	64.2	75.27	0.22	12.79	1.71	0.05	0.16	0.70	3.43	4.21	-30.50
0.46	67.2	75.30	0.22	13.01	1.80	0.06	0.18	0.73	3.69	4.40	-30.50
0.46	68.4	75.01	0.17	13.17	1.80	0.07	0.20	0.71	3.71	4.30	-30.47
0.50	74.1	74.90	0.19	13.33	1.81	0.05	0.14	0.74	3.77	4.34	-30.46
0.52	77.2	74.59	0.20	13.50	1.72	0.00	0.27	0.71	3.95	4.18	-30.42
0.53	78.5	74.45	0.17	13.36	1.83	0.01	0.19	0.75	3.73	4.30	-30.41
0.57	84.0	74.39	0.21	13.61	1.85	0.05	0.15	0.78	3.92	4.34	-30.40
0.59	87.2	73.94	0.16	13.71	1.84	0.12	0.14	0.77	4.02	4.22	-30.35
0.60	88.6	74.28	0.20	13.53	1.89	0.01	0.13	0.74	3.95	4.28	-30.39
0.64	93.9	74.05	0.23	13.96	1.81	0.05	0.16	0.80	3.90	4.27	-30.36

0.66	97.2	73.95	0.19	13.83	1.90	0.02	0.16	0.80	3.82	4.30	-30.35
0.67	98.6	73.66	0.20	13.86	1.90	0.11	0.15	0.79	3.79	4.31	-30.32
0.71	103.8	73.82	0.22	13.98	1.83	0.08	0.17	0.80	3.94	4.24	-30.34
0.74	108.7	73.42	0.23	14.00	1.95	0.09	0.16	0.84	4.03	4.38	-30.29
0.77	113.7	73.23	0.26	14.03	1.89	0.01	0.18	0.82	3.98	4.28	-30.27
0.80	117.1	73.23	0.32	14.16	1.86	0.02	0.15	0.80	3.91	4.25	-30.27
0.81	118.8	73.43	0.21	14.19	1.94	0.12	0.32	0.81	4.11	4.35	-30.29
0.84	123.6	73.27	0.21	14.26	1.90	0.05	0.15	0.78	3.98	4.41	-30.28
0.86	127.1	73.02	0.21	14.26	1.88	0.07	0.19	0.83	4.02	4.42	-30.25
0.88	128.9	73.04	0.35	14.26	1.95	0.08	0.21	0.84	3.98	4.57	-30.25
0.91	133.5	73.31	0.14	14.32	1.91	0.05	0.21	0.82	4.38	4.22	-30.28
0.93	137.1	73.07	0.18	14.37	1.96	0.01	0.17	0.85	4.16	4.52	-30.25
0.95	139.0	73.02	0.18	14.34	2.03	0.03	0.15	0.84	4.12	4.22	-30.25
0.97	143.4	73.14	0.20	14.36	1.98	0.08	0.15	0.84	4.21	4.28	-30.26
1.00	147.1	72.89	0.17	14.64	1.98	0.08	0.22	0.85	4.01	4.54	-30.24
1.01	149.1	72.82	0.23	14.52	1.94	0.07	0.16	0.87	3.94	4.49	-30.23
1.04	153.3	73.08	0.23	14.32	1.90	0.04	0.14	0.83	4.23	4.44	-30.26
1.15	169.1	72.74	0.22	14.53	1.96	0.07	0.23	0.85	4.39	4.35	-30.22
1.18	173.3	72.90	0.26	14.38	2.01	0.03	0.14	0.83	4.12	4.30	-30.24
1.29	189.1	72.60	0.24	14.49	1.94	0.04	0.18	0.86	4.09	4.39	-30.20
1.29	189.1	72.55	0.31	14.43	1.95	0.02	0.17	0.89	3.90	4.34	-30.20
1.31	193.3	72.80	0.22	14.44	2.01	0.05	0.21	0.86	3.95	4.35	-30.23
1.42	209.1	72.78	0.24	14.54	2.02	0.03	0.15	0.89	3.91	4.36	-30.22
1.56	229.1	72.67	0.19	14.44	2.04	0.03	0.17	0.90	3.79	4.26	-30.21
1.57	231.1	72.70	0.19	14.62	1.88	0.07	0.17	0.90	4.08	4.35	-30.21
1.59	233.2	72.87	0.24	14.45	1.94	0.00	0.19	0.87	4.28	4.30	-30.23
1.69	249.1	72.54	0.24	14.53	2.01	0.09	0.16	0.88	4.05	4.45	-30.20
1.71	252.1	72.71	0.21	14.46	2.07	0.01	0.15	0.89	4.02	4.30	-30.21
1.72	253.2	72.89	0.26	14.38	2.03	0.03	0.18	0.88	3.95	4.40	-30.24
1.83	269.1	72.75	0.23	14.37	2.00	0.04	0.19	0.90	4.19	4.19	-30.22
1.86	273.1	72.71	0.19	14.47	2.01	0.07	0.17	0.90	4.00	4.45	-30.22
1.86	273.2	72.76	0.20	14.48	2.00	0.02	0.15	0.90	4.21	4.30	-30.22
1.97	289.1	72.67	0.21	14.43	1.99	0.11	0.15	0.88	3.85	4.34	-30.21
1.99	293.2	72.71	0.21	14.56	2.01	0.08	0.14	0.84	4.11	4.37	-30.22
2.00	294.1	72.57	0.29	14.46	2.04	0.13	0.20	0.84	4.06	4.48	-30.20
2.10	309.1	72.61	0.26	14.30	2.02	0.09	0.20	0.85	3.88	4.44	-30.20
2.13	313.2	72.79	0.21	14.52	1.97	0.09	0.20	0.86	3.89	4.40	-30.22
2.14	315.1	72.71	0.19	14.34	1.96	0.05	0.21	0.88	3.97	4.22	-30.21
2.24	329.1	72.72	0.18	14.45	2.11	0.08	0.15	0.87	4.06	4.46	-30.22
2.27	333.2	72.65	0.16	14.54	2.11	0.04	0.15	0.85	4.35	4.47	-30.21
2.29	336.1	72.70	0.23	14.53	2.01	0.08	0.23	0.87	4.18	4.47	-30.21
2.37	349.1	72.78	0.19	14.43	2.08	0.04	0.18	0.88	3.90	4.32	-30.22
2.40	353.2	72.58	0.18	14.34	2.11	0.06	0.18	0.85	4.06	4.54	-30.20

QzDisRh102, starting rhyolite: NCO; T=1505 °C, P=0.5GPa, t=14386s, H2O=0.1wt%

x / sqrt(t)	x (μm)	SiO2+	TiO2	Al2O3	FeO	MnO	MgO	CaO	Na2O	K2O	lnD_SiO2 (m^2/s)
0.05	6.3	87.17	0.15	5.88	1.18	0.02	0.14	0.21	2.42	2.59	-32.02
0.10	11.5	83.76	0.09	8.81	1.21	0.09	0.12	0.26	2.78	2.77	-31.53
0.10	12.3	83.64	0.10	7.69	1.26	0.04	0.09	0.30	3.05	3.16	-31.51
0.15	18.2	81.59	0.18	9.13	1.37	0.05	0.10	0.40	3.58	3.36	-31.23
0.16	19.1	81.20	0.20	9.45	1.37	-0.03	0.08	0.40	3.69	3.39	-31.17
0.20	24.2	79.90	0.16	10.14	1.41	0.07	0.13	0.44	4.08	3.63	-31.00
0.25	29.6	78.84	0.17	10.91	1.51	0.05	0.12	0.50	4.21	3.68	-30.86
0.25	30.1	78.76	0.17	10.90	1.57	0.08	0.15	0.48	4.49	3.79	-30.85
0.27	32.4	78.85	0.16	10.76	1.47	0.05	0.17	0.50	4.28	3.74	-30.86
0.30	36.0	77.74	0.15	11.54	1.51	0.09	0.16	0.54	4.37	3.97	-30.72
0.33	40.1	77.03	0.16	12.22	1.62	0.09	0.13	0.58	4.68	3.97	-30.64
0.35	42.0	76.77	0.16	12.00	1.64	0.00	0.10	0.57	4.56	3.75	-30.60
0.40	47.9	76.01	0.16	12.47	1.72	0.02	0.13	0.63	5.02	3.89	-30.51
0.42	50.6	75.87	0.16	12.80	1.61	0.08	0.13	0.63	4.84	4.11	-30.50
0.44	53.3	75.56	0.17	12.65	1.62	0.06	0.15	0.66	4.99	4.09	-30.46
0.45	53.9	75.61	0.10	12.62	1.64	0.06	0.10	0.65	5.07	4.09	-30.47
0.50	59.8	74.89	0.17	13.14	1.72	0.04	0.16	0.70	5.21	4.09	-30.38
0.51	61.2	75.06	0.22	13.26	1.66	0.05	0.13	0.72	4.98	4.24	-30.40
0.55	65.7	74.67	0.18	13.34	1.75	0.06	0.16	0.71	5.41	3.95	-30.36
0.60	71.7	74.48	0.22	13.66	1.75	0.05	0.19	0.75	4.97	4.11	-30.33
0.60	71.7	74.44	0.18	13.68	1.89	0.06	0.15	0.75	5.07	4.14	-30.33
0.62	74.2	74.33	0.24	13.68	1.74	0.03	0.16	0.76	5.16	4.06	-30.32
0.65	77.6	74.27	0.19	13.72	1.85	0.07	0.19	0.74	5.39	4.07	-30.31
0.69	82.2	74.01	0.20	13.99	1.78	0.10	0.17	0.78	5.42	4.38	-30.28
0.70	83.6	73.80	0.21	13.68	1.87	0.04	0.15	0.75	5.22	3.97	-30.26
0.75	89.5	73.83	0.17	14.00	1.81	0.00	0.19	0.80	5.13	4.14	-30.26
0.77	92.7	73.45	0.19	14.08	1.83	0.08	0.11	0.78	5.26	4.13	-30.22
0.79	95.1	73.75	0.21	14.12	1.70	0.09	0.14	0.81	5.30	4.03	-30.25
0.86	103.3	73.38	0.19	14.09	1.85	0.07	0.12	0.81	5.53	4.05	-30.21
0.95	113.8	73.39	0.28	14.31	1.88	0.01	0.16	0.83	5.32	4.07	-30.21
0.97	116.0	73.28	0.28	14.21	1.86	0.09	0.14	0.79	5.37	4.09	-30.20
1.04	124.3	73.12	0.16	14.42	1.86	0.11	0.14	0.82	5.45	4.10	-30.18
1.12	134.8	72.72	0.19	14.30	1.89	0.09	0.14	0.86	5.30	4.26	-30.14
1.14	136.9	73.00	0.21	14.24	1.95	0.01	0.12	0.84	5.61	4.25	-30.17
1.21	145.4	73.25	0.21	14.55	1.87	0.12	0.18	0.83	5.34	4.12	-30.20
1.30	155.9	73.20	0.21	14.37	1.85	0.03	0.21	0.85	5.43	4.23	-30.19
1.32	157.8	73.21	0.18	14.24	1.94	0.08	0.18	0.83	5.36	4.08	-30.19
1.39	166.4	73.01	0.28	14.45	1.93	0.03	0.15	0.84	5.57	4.17	-30.17
1.48	177.0	73.23	0.21	14.49	1.97	0.10	0.17	0.90	5.52	4.24	-30.19
1.49	178.7	73.20	0.22	14.35	1.87	0.04	0.14	0.87	5.68	4.27	-30.19
1.56	187.5	73.04	0.21	14.46	1.80	0.05	0.17	0.84	5.45	4.12	-30.17
1.65	198.0	73.23	0.20	14.49	1.95	0.06	0.19	0.86	5.50	4.04	-30.19
1.66	199.6	73.00	0.21	14.31	1.83	0.04	0.19	0.84	5.56	4.17	-30.17
1.84	220.5	73.12	0.21	14.26	1.85	0.09	0.16	0.86	5.36	4.02	-30.18
2.01	241.3	73.12	0.19	14.37	1.92	0.06	0.22	0.85	5.58	4.19	-30.18
2.19	262.2	72.99	0.19	14.13	1.89	0.04	0.16	0.84	5.50	3.99	-30.17
2.36	283.1	73.16	0.21	14.37	1.82	0.06	0.16	0.85	5.33	4.14	-30.19
2.53	304.0	72.90	0.26	14.36	1.93	0.08	0.18	0.85	5.64	4.25	-30.16
2.71	324.9	73.07	0.24	14.26	1.86	0.05	0.15	0.87	5.45	4.33	-30.18
2.88	345.8	72.88	0.26	14.44	1.90	0.05	0.16	0.86	5.70	4.08	-30.16

3.06	366.7	73.04	0.23	14.23	1.84	0.04	0.17	0.85	5.50	4.08	-30.17
3.23	387.6	73.02	0.21	14.46	1.81	0.09	0.19	0.86	5.63	4.28	-30.17
3.41	408.5	73.13	0.19	14.29	1.96	0.06	0.14	0.81	5.51	4.24	-30.18

QzDisRh104, starting rhyolite: NCO; T=1501 °C, P=0.5GPa, t=86432s, H2O=0.1wt%

x / sqrt(t)	x (µm)	SiO2+	TiO2	Al2O3	FeO	MgO	CaO	Na2O	K2O	lnD_SiO2 (m ² /s)
0.01	2.0	90.62	0.01	3.70	0.94	0.09	0.15	1.55	1.83	-32.23
0.02	6.1	89.60	0.10	4.57	0.96	0.09	0.18	1.67	2.10	-32.09
0.02	6.4	90.02	0.12	3.95	0.87	0.11	0.17	1.54	1.93	-32.15
0.02	6.8	90.59	0.08	3.97	0.94	0.10	0.16	1.58	2.00	-32.23
0.05	13.4	88.24	0.07	4.90	0.99	0.08	0.21	1.90	2.27	-31.90
0.06	17.3	87.32	0.09	5.52	1.00	0.10	0.22	2.11	2.49	-31.78
0.06	17.9	87.06	0.19	5.62	1.07	0.12	0.24	2.01	2.44	-31.74
0.07	20.4	86.87	0.08	5.90	1.08	0.12	0.21	2.15	2.46	-31.72
0.07	21.7	86.68	0.08	5.86	1.10	0.11	0.25	2.22	2.59	-31.69
0.09	25.4	86.02	0.02	6.23	1.06	0.11	0.26	2.38	2.72	-31.61
0.09	27.0	85.43	0.06	6.77	1.13	0.11	0.24	2.60	2.94	-31.53
0.09	27.2	85.37	0.05	6.61	1.05	0.09	0.27	2.48	2.92	-31.52
0.09	27.4	85.22	0.16	6.65	1.07	0.08	0.27	2.56	2.80	-31.50
0.10	29.1	85.39	0.08	6.87	1.09	0.12	0.25	1.86	2.84	-31.52
0.10	29.8	84.96	0.14	7.06	1.22	0.11	0.28	2.69	2.90	-31.47
0.12	34.4	83.56	0.15	7.40	1.08	0.10	0.29	2.80	3.07	-31.29
0.13	37.2	83.28	0.15	7.66	1.13	0.09	0.32	2.85	3.12	-31.26
0.14	41.4	82.39	0.18	7.83	1.12	0.12	0.32	2.86	3.17	-31.15
0.16	47.0	82.37	0.25	8.42	1.23	0.11	0.35	3.14	3.30	-31.14
0.16	47.9	82.56	0.08	8.64	1.19	0.12	0.34	3.12	3.32	-31.17
0.16	48.4	82.07	0.09	8.54	1.11	0.11	0.37	3.10	3.24	-31.11
0.19	55.4	80.84	0.18	9.07	1.22	0.13	0.39	3.30	3.38	-30.96
0.19	57.0	80.72	0.15	9.13	1.25	0.10	0.39	3.31	3.53	-30.95
0.21	61.4	80.56	0.09	9.26	1.24	0.12	0.40	3.38	3.45	-30.93
0.23	67.0	79.58	0.17	9.71	1.31	0.12	0.45	3.68	3.56	-30.81
0.23	68.8	80.17	0.12	9.87	1.26	0.16	0.45	3.49	3.67	-30.88
0.26	76.9	79.44	0.14	10.21	1.31	0.12	0.51	3.62	3.66	-30.79
0.30	86.9	78.37	0.10	10.61	1.31	0.14	0.53	3.95	3.80	-30.67
0.31	89.8	78.19	0.12	10.69	1.27	0.12	0.50	3.82	3.80	-30.65
0.32	92.9	78.75	0.16	10.69	1.36	0.13	0.50	3.72	3.73	-30.72
0.33	96.8	77.92	0.16	11.05	1.37	0.13	0.51	3.81	3.83	-30.62
0.36	106.8	77.19	0.18	11.39	1.35	0.13	0.58	4.01	3.88	-30.54
0.38	110.7	77.03	0.22	11.34	1.32	0.12	0.58	4.03	3.99	-30.52
0.40	116.8	76.88	0.20	11.66	1.39	0.16	0.63	4.22	3.94	-30.50
0.42	124.3	76.75	0.19	11.79	1.45	0.17	0.62	4.20	3.99	-30.49
0.43	126.7	76.54	0.16	11.91	1.34	0.15	0.62	4.47	3.99	-30.47
0.45	131.7	76.39	0.11	12.06	1.41	0.13	0.62	4.34	3.98	-30.45
0.46	136.7	75.38	0.26	12.12	1.40	0.15	0.66	4.36	3.96	-30.34
0.50	146.6	75.55	0.06	12.35	1.43	0.15	0.64	4.25	4.02	-30.36
0.52	152.5	75.72	0.17	12.39	1.43	0.17	0.65	4.26	4.06	-30.38
0.53	155.8	75.91	0.20	12.47	1.45	0.13	0.66	4.29	4.09	-30.40
0.53	156.6	75.43	0.20	12.45	1.55	0.13	0.71	4.41	4.07	-30.34
0.57	166.5	74.91	0.29	12.78	1.44	0.17	0.70	4.37	4.06	-30.29
0.59	173.5	75.31	0.17	12.69	1.53	0.16	0.69	4.44	4.04	-30.33
0.60	176.4	74.70	0.21	12.85	1.49	0.15	0.71	4.44	4.12	-30.27
0.63	186.4	74.81	0.23	13.13	1.44	0.13	0.72	4.51	4.17	-30.28
0.64	187.4	74.42	0.16	12.88	1.51	0.16	0.76	4.59	4.12	-30.23
0.66	194.4	74.51	0.22	12.89	1.56	0.10	0.71	4.56	4.12	-30.24
0.67	196.3	74.28	0.22	12.92	1.55	0.15	0.72	4.64	4.11	-30.22
0.70	206.3	74.18	0.13	13.11	1.53	0.13	0.73	4.63	4.13	-30.21

0.73	215.4	74.47	0.21	13.15	1.53	0.17	0.74	4.60	4.11	-30.24
0.74	216.3	73.78	0.19	13.09	1.60	0.12	0.76	4.54	4.13	-30.17
0.74	218.9	74.22	0.29	13.29	1.57	0.17	0.75	4.48	4.09	-30.21
0.77	226.2	74.20	0.12	13.33	1.61	0.14	0.79	4.71	4.13	-30.21
0.80	236.2	73.47	0.20	13.40	1.47	0.15	0.80	4.68	4.23	-30.13
0.80	236.3	73.96	0.29	13.61	1.51	0.16	0.80	4.58	4.16	-30.19
0.84	246.1	73.45	0.26	13.53	1.55	0.18	0.81	4.58	4.14	-30.13
0.85	250.3	73.70	0.15	13.42	1.46	0.17	0.77	4.60	4.20	-30.16
0.87	256.1	73.78	0.20	13.43	1.59	0.16	0.83	4.78	4.24	-30.17
0.87	257.2	73.45	0.18	13.72	1.55	0.16	0.82	4.73	4.24	-30.13
0.95	278.1	73.62	0.27	13.57	1.59	0.16	0.80	4.89	4.23	-30.15
0.96	281.8	73.14	0.18	13.68	1.63	0.15	0.82	4.63	4.22	-30.10
1.02	299.1	73.55	0.16	13.65	1.62	0.13	0.80	4.76	4.27	-30.14
1.07	313.4	73.19	0.14	13.76	1.53	0.15	0.88	4.77	4.08	-30.10
1.09	320.0	73.36	0.15	13.70	1.61	0.16	0.79	4.64	4.30	-30.12
1.16	341.0	73.31	0.21	13.78	1.64	0.16	0.84	4.74	4.15	-30.12
1.17	344.8	73.15	0.29	13.77	1.70	0.18	0.85	4.78	4.13	-30.10
1.23	361.9	73.18	0.27	13.81	1.60	0.16	0.86	4.85	4.22	-30.10
1.28	376.3	73.16	0.22	13.80	1.61	0.18	0.85	4.73	4.26	-30.10
1.30	382.8	73.29	0.19	13.77	1.60	0.13	0.84	4.74	4.12	-30.12
1.37	403.7	73.36	0.28	13.90	1.61	0.19	0.87	4.77	4.20	-30.12
1.39	407.8	73.34	0.23	13.83	1.71	0.17	0.90	4.76	4.23	-30.12
1.49	439.4	73.14	0.28	13.93	1.58	0.16	0.83	4.77	4.21	-30.10
1.60	470.8	73.08	0.27	13.85	1.66	0.18	0.90	4.65	4.31	-30.09
1.71	502.3	72.90	0.20	13.88	1.64	0.17	0.86	4.75	4.24	-30.07
1.82	533.9	73.27	0.20	13.88	1.72	0.18	0.81	4.74	4.28	-30.11
1.92	565.4	72.94	0.24	13.87	1.57	0.17	0.86	4.75	4.22	-30.08
2.03	596.8	73.15	0.19	13.89	1.68	0.18	0.89	4.81	4.20	-30.10
2.34	687.1	72.96	0.15	13.93	1.74	0.19	0.86	4.78	4.23	-30.08
2.64	777.4	72.87	0.27	13.92	1.67	0.17	0.88	4.81	4.26	-30.07
2.95	867.6	72.89	0.17	13.93	1.65	0.16	0.85	4.70	4.27	-30.07
3.26	957.8	72.71	0.26	13.68	1.69	0.15	0.88	4.71	4.21	-30.05
3.57	1048.1	73.09	0.24	13.99	1.66	0.20	0.90	4.67	4.31	-30.09
3.87	1138.4	72.99	0.17	13.85	1.66	0.16	0.85	4.72	4.27	-30.08
4.18	1228.6	73.19	0.28	13.79	1.62	0.20	0.89	4.82	4.11	-30.10
4.49	1318.9	72.75	0.17	13.87	1.64	0.19	0.87	4.63	4.14	-30.06
4.79	1409.1	72.75	0.23	13.89	1.70	0.19	0.92	4.80	4.13	-30.06

QzDisRh106, starting rhyolite: NCO; T=1600 °C, P=0.5GPa, t=14435s, H2O=0.1wt%

x / sqrt(t)	x (μm)	SiO2+	TiO2	Al2O3	FeO	MnO	MgO	CaO	Na2O	K2O	lnD_SiO2 (m^2/s)
0.05	6.0	93.28	0.12	2.13	0.93	0.00	0.07	0.13	1.20	1.29	-31.34
0.10	11.6	91.30	0.12	3.48	1.04	0.01	0.10	0.20	1.68	1.78	-31.07
0.10	12.1	91.29	0.05	3.25	1.07	0.00	0.11	0.17	1.32	1.64	-31.07
0.11	12.7	90.64	0.09	3.56	1.02	0.00	0.08	0.21	1.52	1.83	-30.98
0.14	17.2	89.08	0.11	4.72	1.10	0.02	0.10	0.24	1.99	2.18	-30.78
0.15	17.8	88.99	0.14	4.55	1.11	0.07	0.08	0.19	1.78	2.17	-30.77
0.15	17.9	88.96	0.08	4.54	1.17	0.04	0.08	0.20	1.81	2.16	-30.77
0.19	22.8	87.02	0.11	5.62	1.11	0.03	0.12	0.26	2.20	2.47	-30.53
0.19	22.9	87.34	0.11	5.46	1.18	-0.01	0.11	0.27	2.23	2.47	-30.57
0.20	23.6	87.12	0.07	5.60	1.17	0.02	0.11	0.26	2.01	2.50	-30.54
0.23	28.0	86.08	0.09	6.41	1.18	0.04	0.07	0.27	2.50	2.71	-30.42
0.24	28.4	85.77	0.13	6.75	1.27	0.01	0.13	0.28	2.61	2.76	-30.39
0.24	29.3	85.67	0.10	6.61	1.22	0.10	0.09	0.30	2.60	2.69	-30.37
0.28	33.1	84.50	0.10	7.08	1.18	0.06	0.10	0.31	2.61	2.91	-30.24
0.28	33.9	84.81	0.13	7.38	1.26	0.03	0.12	0.31	2.59	2.99	-30.28
0.29	35.1	83.82	0.17	7.46	1.22	0.06	0.12	0.33	2.84	3.02	-30.17
0.32	38.1	83.59	0.12	7.90	1.32	0.10	0.08	0.33	2.88	3.07	-30.14
0.33	39.5	83.43	0.10	8.19	1.29	-0.01	0.14	0.37	3.03	3.22	-30.13
0.34	40.9	82.62	0.14	8.35	1.29	-0.01	0.11	0.38	3.00	3.23	-30.04
0.36	43.2	82.73	0.18	8.25	1.32	0.02	0.13	0.42	3.09	3.19	-30.05
0.38	45.1	82.13	0.12	8.87	1.30	-0.01	0.13	0.40	3.11	3.29	-29.99
0.39	46.6	81.77	0.10	8.87	1.29	0.01	0.13	0.42	3.28	3.36	-29.95
0.40	48.3	81.78	0.14	8.93	1.42	0.06	0.16	0.41	3.30	3.33	-29.95
0.42	50.7	81.16	0.13	9.41	1.35	0.04	0.10	0.43	3.59	3.41	-29.89
0.44	52.4	80.83	0.16	9.54	1.39	0.07	0.14	0.44	3.47	3.51	-29.85
0.44	53.4	81.01	0.12	9.59	1.46	-0.02	0.13	0.46	3.57	3.42	-29.87
0.47	56.2	80.16	0.12	9.92	1.38	0.02	0.11	0.48	3.50	3.50	-29.79
0.48	58.1	79.94	0.15	10.08	1.47	0.04	0.13	0.51	3.39	3.48	-29.76
0.49	58.5	80.15	0.13	9.77	1.46	0.03	0.12	0.49	3.44	3.48	-29.78
0.51	61.8	79.98	0.14	10.13	1.32	0.01	0.12	0.46	3.78	3.59	-29.77
0.58	69.9	78.63	0.20	10.97	1.50	0.03	0.15	0.53	3.73	3.75	-29.63
0.60	72.2	78.51	0.19	11.15	1.42	0.00	0.14	0.56	3.79	3.70	-29.62
0.66	79.0	77.90	0.12	11.45	1.53	0.12	0.12	0.58	4.10	3.73	-29.56
0.68	81.7	77.55	0.17	11.83	1.56	0.05	0.13	0.61	4.18	3.70	-29.53
0.69	82.6	77.68	0.17	11.70	1.48	0.11	0.13	0.56	3.90	3.72	-29.54
0.74	89.3	77.14	0.13	11.98	1.55	0.10	0.13	0.60	4.18	3.83	-29.49
0.78	93.3	76.57	0.10	12.35	1.65	0.05	0.16	0.62	4.30	3.91	-29.44
0.86	103.3	76.28	0.18	12.63	1.55	0.09	0.19	0.67	4.15	3.95	-29.41
0.87	105.1	75.87	0.11	12.69	1.56	0.04	0.15	0.67	4.23	4.02	-29.38
0.91	109.8	75.72	0.16	12.66	1.70	0.07	0.16	0.69	4.37	3.91	-29.36

0.95	113.6	75.82	0.19	13.01	1.58	0.02	0.15	0.72	4.19	3.94	-29.37
0.97	116.8	75.32	0.15	12.96	1.62	0.08	0.15	0.72	4.41	4.04	-29.33
1.00	120.0	75.45	0.20	13.10	1.63	0.03	0.14	0.70	4.59	3.99	-29.34
1.03	124.0	75.14	0.16	13.27	1.68	0.10	0.15	0.73	4.47	3.98	-29.31
1.07	128.6	74.71	0.18	13.26	1.65	0.01	0.19	0.75	4.44	3.97	-29.27
1.08	130.3	75.07	0.17	13.32	1.69	0.08	0.12	0.68	4.56	4.01	-29.30
1.12	134.4	75.04	0.21	13.19	1.57	0.07	0.12	0.75	4.40	4.03	-29.30
1.17	140.2	74.36	0.21	13.66	1.67	0.06	0.17	0.79	4.40	4.07	-29.24
1.17	140.6	74.78	0.18	13.65	1.70	0.04	0.14	0.73	4.74	4.04	-29.28
1.26	150.8	74.64	0.18	13.64	1.69	0.02	0.15	0.74	4.33	3.91	-29.27
1.27	152.0	73.99	0.14	13.74	1.66	0.00	0.15	0.79	4.51	4.08	-29.21
1.29	155.1	74.29	0.24	13.59	1.68	0.03	0.15	0.77	4.48	4.03	-29.24
1.34	161.1	74.22	0.23	13.78	1.78	0.06	0.16	0.79	4.63	4.01	-29.23
1.38	165.4	74.24	0.28	13.79	1.77	0.01	0.14	0.78	4.73	4.08	-29.23
1.51	181.6	73.78	0.20	13.94	1.75	0.02	0.17	0.82	4.77	4.03	-29.19
1.53	183.9	73.63	0.25	14.17	1.68	0.06	0.22	0.84	4.58	4.04	-29.18
1.56	186.9	73.89	0.25	14.05	1.73	0.08	0.16	0.79	4.72	4.16	-29.20
1.70	204.0	73.25	0.17	14.10	1.69	0.10	0.16	0.86	4.42	4.10	-29.14
1.73	208.3	73.66	0.16	14.00	1.73	0.11	0.15	0.83	4.83	4.03	-29.18
1.85	222.7	73.34	0.20	14.14	1.83	0.05	0.17	0.82	4.82	4.12	-29.15
1.87	224.1	73.08	0.22	14.02	1.82	0.11	0.16	0.83	4.62	4.12	-29.13
1.91	229.7	73.51	0.17	14.21	1.75	0.04	0.12	0.87	5.03	4.09	-29.17
2.02	243.2	73.34	0.19	14.19	1.86	0.09	0.16	0.82	4.93	4.04	-29.15
2.03	244.3	72.99	0.24	14.38	1.96	-0.01	0.17	0.83	4.33	4.11	-29.12
2.19	263.7	73.12	0.26	14.16	1.81	0.03	0.12	0.83	4.69	4.08	-29.13
2.20	264.4	72.87	0.25	14.23	1.85	0.10	0.19	0.85	4.63	4.17	-29.11
2.27	272.6	73.45	0.23	14.24	1.75	0.03	0.18	0.87	4.73	4.14	-29.16
2.37	284.2	73.16	0.17	14.35	1.74	0.06	0.19	0.87	4.50	4.08	-29.14
2.37	284.5	72.90	0.13	14.31	1.84	0.09	0.18	0.86	4.57	4.23	-29.11
2.45	294.0	73.33	0.15	14.34	1.76	0.07	0.11	0.79	4.95	4.10	-29.15
2.54	304.6	72.90	0.25	14.19	1.86	0.02	0.20	0.87	4.85	4.16	-29.11
2.54	304.8	72.96	0.26	14.26	1.98	0.10	0.16	0.87	4.65	4.13	-29.12
2.70	324.8	72.91	0.24	14.50	1.81	0.08	0.20	0.84	4.57	4.14	-29.11
2.71	325.3	72.98	0.21	14.09	1.75	0.06	0.19	0.87	4.51	4.15	-29.12
2.80	336.8	73.41	0.15	14.25	1.89	0.05	0.15	0.85	4.50	4.14	-29.16
2.87	344.9	72.67	0.24	14.30	1.80	0.06	0.18	0.86	4.75	4.15	-29.09
2.88	345.8	72.99	0.18	14.31	1.85	0.13	0.22	0.88	4.83	4.11	-29.12
2.98	358.2	73.43	0.29	14.42	1.75	0.01	0.19	0.90	4.67	4.07	-29.16
3.04	365.0	73.00	0.15	14.44	1.83	0.08	0.19	0.88	4.90	4.12	-29.12
3.05	366.3	72.95	0.18	14.14	1.99	0.05	0.20	0.86	4.37	4.11	-29.12
3.16	379.7	73.28	0.15	14.19	1.77	0.07	0.18	0.86	4.60	4.18	-29.15
3.39	407.3	73.08	0.22	14.23	1.93	0.04	0.18	0.90	4.89	4.09	-29.13
3.39	407.6	72.75	0.17	14.28	1.84	0.05	0.20	0.85	5.00	4.11	-29.10

3.47	417.4	73.41	0.21	14.21	1.88	0.07	0.18	0.83	4.74	4.14	-29.16
3.73	448.2	72.96	0.20	14.22	1.88	0.05	0.13	0.86	4.82	4.10	-29.12
3.79	455.2	73.20	0.19	14.21	1.82	0.11	0.15	0.84	4.56	4.15	-29.14
4.07	489.2	72.86	0.29	14.07	1.83	0.06	0.17	0.84	4.52	4.15	-29.11
4.10	492.6	72.78	0.23	14.45	1.79	0.10	0.18	0.91	4.72	4.21	-29.10
4.10	493.0	73.07	0.23	14.47	2.01	-0.01	0.18	0.88	4.58	4.17	-29.13
4.41	530.1	72.83	0.27	14.26	1.95	0.01	0.19	0.83	4.49	4.04	-29.11
4.42	530.7	73.24	0.28	14.38	1.82	0.07	0.21	0.88	4.65	4.10	-29.14
4.45	535.1	72.99	0.21	14.28	1.92	0.07	0.17	0.89	4.51	4.20	-29.12
4.73	568.4	73.26	0.29	14.25	1.93	0.10	0.18	0.87	4.87	4.08	-29.14
4.75	571.2	72.96	0.18	13.99	1.95	0.06	0.21	0.90	4.81	4.08	-29.12
4.81	577.5	72.83	0.24	14.22	1.88	0.05	0.17	0.91	4.59	4.11	-29.11
5.05	606.1	73.17	0.22	14.31	1.86	0.08	0.16	0.87	4.98	4.17	-29.14
5.09	612.1	72.93	0.18	14.25	1.98	0.08	0.19	0.85	4.54	4.12	-29.12
5.16	620.1	72.89	0.11	14.22	1.87	0.06	0.17	0.85	4.71	4.07	-29.11
5.36	643.9	73.19	0.21	14.30	1.87	0.08	0.12	0.91	5.03	4.20	-29.14
5.44	653.1	72.91	0.16	14.24	2.02	0.04	0.16	0.87	4.62	4.17	-29.11
5.52	662.6	72.85	0.25	14.11	1.88	0.12	0.20	0.86	4.60	4.17	-29.11
5.67	681.7	73.02	0.22	14.35	1.86	0.10	0.18	0.90	4.47	4.17	-29.12
5.78	694.0	73.02	0.20	14.35	1.85	0.05	0.18	0.85	4.59	4.13	-29.12
5.87	705.1	73.07	0.20	14.19	1.98	0.06	0.16	0.84	4.80	4.08	-29.13
5.99	719.4	73.16	0.21	14.28	1.77	0.01	0.18	0.89	4.82	4.15	-29.14
6.12	735.0	72.59	0.21	14.29	1.81	0.07	0.22	0.92	4.48	4.14	-29.09
6.22	747.6	72.81	0.18	14.28	1.81	0.05	0.17	0.85	4.77	4.09	-29.11

QzDisBa101, starting basalt: JDF; T=1293 °C, P=0.5 GPa, t =3667s, H2O=0.32wt%

x / sqrt(t)	x (μm)	SiO2	TiO2	Al2O3	FeO	MnO	MgO	CaO	Na2O	K2O	lnD_SiO2 (m^2/s)
0.03	2.1	71.53	0.78	8.44	6.54	0.10	3.34	5.37	3.75	0.48	-29.77
0.09	5.3	69.58	0.99	8.96	7.16	0.12	3.82	5.99	3.38	0.41	-29.37
0.09	5.4	69.82	0.85	9.08	7.05	0.16	3.82	6.03	3.07	0.45	-29.42
0.14	8.2	67.85	0.86	9.36	7.58	0.14	3.94	6.39	3.59	0.39	-29.02
0.14	8.4	67.56	0.99	9.37	7.72	0.07	4.09	6.60	3.54	0.35	-28.97
0.14	8.5	67.54	0.87	9.28	7.68	0.10	4.13	6.63	3.48	0.38	-28.96
0.19	11.4	66.22	0.96	9.56	8.10	0.18	4.27	7.06	3.51	0.34	-28.71
0.22	13.4	65.07	0.98	9.96	8.32	0.08	4.54	7.20	3.51	0.35	-28.49
0.23	13.8	65.39	0.94	9.69	8.23	0.14	4.46	7.16	3.57	0.37	-28.55
0.24	14.4	64.87	1.10	9.80	8.32	0.16	4.57	7.39	3.46	0.32	-28.45
0.29	17.4	64.31	1.01	10.02	8.66	0.18	4.69	7.57	3.44	0.31	-28.35
0.31	18.8	63.68	1.12	10.22	8.71	0.11	4.77	7.69	3.51	0.35	-28.23
0.32	19.4	63.65	0.97	10.02	8.77	0.13	4.75	7.64	3.59	0.34	-28.22
0.40	24.2	62.22	1.15	10.39	9.20	0.30	5.12	8.09	3.48	0.28	-27.97
0.58	35.0	60.45	1.16	10.68	9.56	0.17	5.17	8.60	3.56	0.24	-27.66
0.60	36.2	60.47	1.27	10.63	9.58	0.22	5.27	8.52	3.42	0.29	-27.66
0.67	40.4	59.86	1.27	10.87	10.18	0.18	5.54	8.72	3.62	0.23	-27.56
0.69	41.8	59.98	1.24	10.91	10.02	0.19	5.44	8.72	3.39	0.26	-27.58
0.76	45.8	59.14	1.41	11.09	10.31	0.16	5.58	8.96	3.41	0.25	-27.44
0.78	47.4	58.84	1.30	11.06	9.93	0.19	5.60	8.97	3.68	0.26	-27.39
0.85	51.2	58.42	1.29	11.21	10.43	0.20	5.64	9.03	3.41	0.27	-27.32
0.88	53.0	58.38	1.43	11.19	10.21	0.16	5.50	9.13	3.48	0.21	-27.31
0.93	56.6	58.13	1.30	11.30	10.43	0.15	5.75	9.30	3.40	0.22	-27.27
0.97	58.6	57.66	1.51	11.27	10.41	0.26	5.67	9.27	3.36	0.22	-27.19
1.02	62.0	57.65	1.32	11.42	10.64	0.23	5.72	9.40	3.29	0.26	-27.19
1.06	64.2	57.39	1.36	11.39	10.77	0.21	5.76	9.38	3.48	0.26	-27.15
1.20	72.7	56.74	1.40	11.71	11.04	0.20	5.82	9.50	3.44	0.22	-27.05
1.25	75.4	56.55	1.42	11.72	10.99	0.21	6.03	9.62	3.16	0.22	-27.02
1.38	83.4	56.07	1.49	11.89	10.97	0.20	6.08	9.62	3.19	0.23	-26.95
1.43	86.6	55.68	1.45	11.85	11.10	0.23	6.10	9.79	3.20	0.21	-26.89
1.55	94.1	55.52	1.53	12.11	11.38	0.24	6.08	9.96	3.22	0.21	-26.86
1.61	97.7	55.28	1.59	11.88	11.20	0.14	6.13	10.01	3.20	0.24	-26.83
1.73	104.8	54.99	1.59	12.19	11.50	0.15	6.16	9.97	2.88	0.16	-26.79
1.80	108.9	54.72	1.51	12.19	11.30	0.20	6.23	10.00	3.11	0.17	-26.75
1.91	115.5	54.44	1.48	12.27	11.72	0.18	6.08	10.07	3.25	0.16	-26.71
1.98	120.1	54.26	1.56	12.45	11.50	0.25	6.25	10.16	3.07	0.19	-26.68
2.08	126.2	54.04	1.72	12.39	11.69	0.16	6.38	10.27	3.01	0.18	-26.65
2.17	131.3	53.85	1.61	12.37	11.55	0.18	6.22	10.35	2.91	0.20	-26.62
2.26	136.9	53.84	1.52	12.42	11.86	0.21	6.43	10.27	3.14	0.20	-26.62
2.30	139.5	53.77	1.62	12.62	11.85	0.18	6.44	10.25	3.15	0.17	-26.61

2.35	142.5	53.54	1.57	12.49	11.86	0.11	6.45	10.28	2.78	0.22	-26.58
2.44	147.6	53.60	1.67	12.53	11.56	0.23	6.34	10.39	2.72	0.16	-26.59
2.54	153.7	53.23	1.68	12.67	11.84	0.21	6.43	10.33	2.65	0.21	-26.54
2.61	158.3	53.22	1.82	12.80	12.03	0.28	6.22	10.45	3.01	0.15	-26.53
2.66	160.9	53.42	1.60	12.69	11.95	0.22	6.38	10.34	2.97	0.17	-26.56
2.72	164.8	52.96	1.63	12.77	11.85	0.19	6.46	10.40	3.07	0.14	-26.50
2.79	169.0	53.04	1.64	12.84	11.94	0.19	6.41	10.44	2.95	0.20	-26.51
2.91	176.0	52.85	1.58	12.79	12.18	0.15	6.66	10.47	3.05	0.19	-26.48
3.01	182.3	52.65	1.76	12.74	12.61	0.21	6.57	10.59	3.05	0.17	-26.46
3.09	187.1	52.52	1.86	12.91	12.20	0.18	6.65	10.50	2.97	0.15	-26.44
3.09	187.2	52.43	1.70	12.78	12.34	0.18	6.34	10.39	2.99	0.16	-26.43
3.36	203.7	52.35	1.68	13.02	12.28	0.27	6.69	10.68	2.86	0.15	-26.42
3.49	211.3	51.97	1.64	12.99	12.23	0.25	6.56	10.53	2.72	0.18	-26.37
3.72	225.1	51.82	1.72	13.22	12.46	0.26	6.68	10.59	3.08	0.13	-26.35
3.89	235.5	51.59	1.70	13.10	12.33	0.16	6.79	10.70	2.87	0.11	-26.32
4.07	246.5	51.47	1.85	13.22	12.44	0.18	6.75	10.74	2.83	0.17	-26.30
4.29	259.7	51.23	1.86	13.43	12.52	0.18	6.59	10.73	2.84	0.17	-26.27
4.42	267.9	51.12	1.63	13.37	12.95	0.22	6.76	10.83	2.93	0.13	-26.26
4.69	283.9	50.93	1.75	13.42	12.79	0.22	6.63	10.75	2.87	0.15	-26.23
4.78	289.3	50.85	1.74	13.45	12.68	0.19	6.80	10.77	2.73	0.11	-26.22
5.09	308.1	50.77	1.84	13.43	12.67	0.23	6.68	10.70	2.83	0.16	-26.21
5.13	310.7	50.78	1.80	13.46	12.69	0.12	6.83	10.78	2.68	0.12	-26.22
5.48	332.1	50.61	1.79	13.57	12.80	0.25	6.87	10.87	2.72	0.14	-26.19
5.49	332.3	50.70	1.81	13.58	12.67	0.22	6.79	10.79	2.80	0.13	-26.20
5.84	353.5	50.35	1.72	13.40	12.60	0.29	6.68	10.96	2.69	0.16	-26.16
5.89	356.5	50.62	1.80	13.98	12.94	0.18	6.96	10.83	2.66	0.14	-26.19
6.29	380.7	50.52	1.87	13.65	12.76	0.22	6.81	10.81	2.73	0.15	-26.18
6.40	387.3	50.31	1.78	13.60	12.70	0.20	6.97	10.79	2.79	0.12	-26.16
6.69	404.9	50.38	1.91	13.69	13.04	0.26	6.81	10.96	2.90	0.15	-26.17
6.98	422.7	50.29	1.90	13.66	12.62	0.17	6.78	10.84	2.59	0.15	-26.15
7.09	429.1	50.27	1.62	13.53	12.61	0.21	6.85	10.92	2.62	0.17	-26.15
7.57	458.1	50.01	1.88	13.67	13.08	0.12	6.94	10.95	2.65	0.12	-26.12
8.01	485.1	50.36	1.66	14.01	12.96	0.15	7.00	10.96	2.81	0.15	-26.16
8.15	493.5	50.17	1.79	13.86	12.74	0.34	6.97	10.91	2.77	0.14	-26.14
8.69	526.2	50.33	1.79	13.92	12.92	0.22	6.82	11.09	2.70	0.12	-26.16
8.73	528.9	50.03	1.95	13.68	12.89	0.17	6.89	10.98	2.56	0.14	-26.12
9.32	564.3	49.96	1.82	13.66	12.94	0.33	6.88	11.03	2.68	0.16	-26.11
9.37	567.3	50.15	1.66	13.73	12.92	0.17	7.06	10.94	2.68	0.17	-26.14
9.90	599.7	50.07	1.83	13.59	13.16	0.26	6.98	10.96	2.62	0.15	-26.13
10.05	608.4	50.33	1.87	13.72	13.05	0.21	6.86	10.87	2.84	0.18	-26.16
10.49	635.1	49.99	1.80	13.75	12.86	0.23	6.84	10.96	2.70	0.12	-26.12
10.73	649.5	50.21	1.84	13.85	13.13	0.20	7.01	10.87	2.49	0.15	-26.14
11.07	670.5	49.92	1.79	13.70	12.70	0.16	7.04	10.88	2.74	0.17	-26.11

11.40	690.6	50.31	1.77	13.75	12.89	0.19	6.87	10.96	2.80	0.17	-26.16
11.66	705.9	50.32	1.69	13.64	13.20	0.19	7.07	10.99	2.81	0.20	-26.16

QzDisBa102, starting basalt: JDF; T=1306 °C, P=0.5 GPa, t =918s, H2O=0.32wt%

x / sqrt(t)	x (μm)	SiO2	TiO2	Al2O3	FeO	MnO	MgO	CaO	Na2O	K2O	lnD_SiO2 (m^2/s)
0.05	1.5	68.91	0.82	8.30	6.47	0.10	3.31	5.23	3.56	0.43	-28.97
0.16	4.8	66.92	0.97	9.23	7.69	0.11	4.23	6.64	3.54	0.35	-28.57
0.21	6.3	66.58	0.85	9.12	7.43	0.12	4.00	6.25	3.60	0.40	-28.51
0.23	7.0	66.86	0.94	8.92	7.42	0.17	3.89	6.27	4.14	0.39	-28.56
0.25	7.7	64.96	0.94	9.18	7.72	0.11	4.11	6.62	3.99	0.35	-28.19
0.32	9.8	64.20	0.97	9.74	8.30	0.12	4.49	7.08	4.10	0.33	-28.05
0.35	10.6	64.02	0.98	9.38	8.07	0.17	4.43	7.03	3.75	0.36	-28.01
0.41	12.3	63.30	0.99	9.64	8.24	0.15	4.55	7.25	3.68	0.35	-27.88
0.44	13.5	62.72	1.13	10.01	8.68	0.18	4.92	7.63	3.70	0.30	-27.77
0.46	14.0	61.74	1.04	9.59	8.38	0.22	4.59	7.45	4.00	0.34	-27.59
0.47	14.2	62.47	1.06	9.66	8.45	0.17	4.69	7.53	3.79	0.35	-27.72
0.48	14.6	61.46	1.16	10.18	9.19	0.14	5.07	8.07	3.54	0.28	-27.54
0.52	15.8	61.98	1.13	10.23	9.08	0.13	4.82	7.74	3.95	0.31	-27.64
0.59	17.8	59.92	1.19	10.35	9.31	0.18	4.96	8.39	3.63	0.30	-27.27
0.71	21.5	58.63	1.19	10.51	9.57	0.22	5.29	8.46	3.62	0.26	-27.05
0.72	21.8	60.01	1.35	10.56	9.58	0.14	5.09	8.40	3.74	0.29	-27.29
0.78	23.6	59.13	1.22	10.58	9.64	0.13	5.45	8.61	3.53	0.27	-27.13
0.80	24.2	59.96	1.19	10.24	9.12	0.25	4.97	8.19	3.74	0.28	-27.28
0.92	27.8	58.61	1.32	10.86	9.87	0.16	5.37	8.80	3.62	0.27	-27.05
0.97	29.4	58.47	1.27	10.96	10.03	0.14	5.41	8.80	3.49	0.23	-27.02
1.11	33.6	56.97	1.39	11.14	10.30	0.35	5.72	9.18	3.34	0.24	-26.78
1.12	33.8	57.55	1.31	11.04	10.12	0.13	5.61	9.05	3.65	0.25	-26.87
1.31	39.8	56.53	1.29	11.35	10.61	0.21	5.79	9.21	3.52	0.23	-26.70
1.44	43.7	56.09	1.53	11.35	10.88	0.21	5.92	9.39	3.29	0.20	-26.64
1.46	44.2	56.25	1.45	11.38	10.70	0.16	5.69	9.41	3.30	0.21	-26.66
1.51	45.8	56.36	1.45	11.29	10.72	0.16	5.69	9.33	3.44	0.19	-26.68
1.71	51.8	55.29	1.63	11.53	10.97	0.14	5.83	9.60	3.33	0.20	-26.51
1.77	53.7	54.56	1.51	11.84	10.99	0.21	5.83	9.65	3.23	0.22	-26.40
1.91	57.8	54.75	1.49	11.77	10.98	0.23	6.08	9.73	3.25	0.19	-26.43
1.95	59.0	54.88	1.61	11.79	11.21	0.19	6.00	9.67	3.15	0.19	-26.45
2.10	63.8	54.16	1.48	12.07	11.51	0.25	6.20	9.85	3.12	0.21	-26.34
2.11	63.8	54.25	1.61	11.87	11.32	0.08	5.87	9.90	3.25	0.20	-26.36
2.30	69.8	54.05	1.50	12.12	11.38	0.17	6.07	9.95	3.18	0.19	-26.33
2.43	73.7	53.55	1.50	12.20	11.53	0.27	6.25	10.15	3.03	0.20	-26.25
2.43	73.8	53.79	1.59	12.13	11.39	0.15	6.16	9.91	3.09	0.18	-26.29
2.50	75.8	53.82	1.54	12.12	11.36	0.24	6.15	9.92	3.12	0.17	-26.29
2.70	81.8	53.37	1.59	12.33	11.47	0.23	6.11	10.11	3.05	0.20	-26.23
2.77	83.8	52.82	1.59	12.56	11.55	0.22	6.24	10.28	3.02	0.19	-26.15
2.90	87.8	53.13	1.55	12.47	11.71	0.20	6.32	10.25	3.03	0.19	-26.19
2.92	88.6	53.17	1.62	12.43	11.87	0.28	6.46	10.24	2.96	0.19	-26.20

3.10	93.8	53.07	1.84	12.37	11.74	0.17	6.21	10.22	2.99	0.17	-26.19
3.10	93.8	52.50	1.65	12.59	11.90	0.21	6.31	10.24	2.93	0.19	-26.10
3.29	99.8	52.66	1.73	12.60	11.87	0.13	6.22	10.27	3.02	0.16	-26.13
3.41	103.4	52.51	1.71	12.72	11.88	0.19	6.33	10.32	2.90	0.17	-26.11
3.43	103.9	52.28	1.75	12.96	12.00	0.24	6.35	10.41	2.90	0.17	-26.08
3.49	105.8	52.29	1.60	12.50	11.88	0.26	6.24	10.26	3.01	0.17	-26.08
3.69	111.8	52.01	1.65	12.59	12.10	0.16	6.39	10.45	2.96	0.17	-26.04
3.76	114.0	51.83	1.61	13.09	12.11	0.16	6.41	10.37	2.91	0.16	-26.01
3.89	117.8	51.94	1.63	12.68	12.25	0.23	6.42	10.47	2.87	0.17	-26.03
3.90	118.2	51.75	1.83	12.76	12.13	0.25	6.43	10.40	2.91	0.16	-26.00
4.09	123.8	51.66	1.70	12.87	11.96	0.16	6.46	10.50	2.95	0.17	-25.99
4.09	124.0	51.40	1.83	13.07	12.24	0.22	6.49	10.44	2.84	0.16	-25.96
4.28	129.8	51.43	1.75	12.99	12.13	0.24	6.53	10.41	2.88	0.16	-25.96
4.39	133.0	51.67	1.90	13.13	12.30	0.26	6.50	10.44	2.82	0.17	-25.99
4.43	134.1	50.93	1.80	13.33	12.05	0.23	6.53	10.45	2.78	0.15	-25.90
4.48	135.8	51.11	1.87	12.88	12.23	0.23	6.45	10.54	2.88	0.15	-25.92
4.68	141.8	50.99	1.86	12.86	12.04	0.13	6.42	10.52	2.87	0.16	-25.90
4.76	144.1	51.04	1.81	13.23	12.20	0.24	6.68	10.51	2.76	0.16	-25.91
4.88	147.8	51.35	1.84	13.00	12.34	0.17	6.65	10.67	2.78	0.16	-25.95
4.88	147.8	51.18	1.76	13.09	12.33	0.17	6.59	10.56	2.84	0.17	-25.93
5.08	153.8	50.78	1.77	13.01	12.46	0.19	6.49	10.48	2.81	0.17	-25.88
5.09	154.2	50.87	1.85	13.29	12.23	0.11	6.58	10.69	2.75	0.16	-25.89
5.27	159.8	50.83	1.92	13.26	12.48	0.22	6.49	10.56	2.85	0.18	-25.88
5.37	162.6	50.86	1.77	13.35	12.45	0.16	6.53	10.58	2.75	0.16	-25.89
5.42	164.2	50.79	1.66	13.33	12.51	0.15	6.71	10.57	2.72	0.17	-25.88
5.47	165.8	50.71	1.81	13.37	12.38	0.21	6.56	10.59	2.77	0.17	-25.87
5.67	171.8	50.66	1.83	13.05	12.36	0.24	6.61	10.63	2.78	0.17	-25.86
5.85	177.4	50.67	1.85	13.25	12.45	0.17	6.62	10.68	2.75	0.16	-25.86
5.87	177.8	50.56	1.81	13.20	12.41	0.26	6.63	10.58	2.75	0.17	-25.85
6.07	183.8	50.32	1.82	13.44	12.59	0.25	6.63	10.62	2.72	0.15	-25.82
6.08	184.3	50.32	1.91	13.45	12.53	0.16	6.89	10.55	2.73	0.14	-25.82
6.26	189.8	50.56	1.80	13.36	12.39	0.32	6.52	10.65	2.74	0.16	-25.85
6.34	192.2	50.42	1.81	13.39	12.56	0.17	6.66	10.70	2.67	0.15	-25.83
6.42	194.4	50.00	1.82	13.36	12.51	0.14	6.63	10.77	2.68	0.16	-25.78
6.46	195.8	50.40	1.91	13.31	12.56	0.24	6.51	10.71	2.76	0.15	-25.83
6.62	200.7	50.38	1.75	13.55	12.58	0.26	6.76	10.82	2.66	0.17	-25.82
6.66	201.8	49.99	1.89	13.19	12.51	0.19	6.65	10.83	2.77	0.16	-25.78
6.83	207.0	50.57	1.84	13.44	12.79	0.26	6.72	10.65	2.72	0.16	-25.85
6.86	207.8	50.16	1.83	13.51	12.72	0.20	6.58	10.69	2.76	0.16	-25.80
6.98	211.6	50.13	1.68	13.50	12.91	0.17	6.81	10.57	2.69	0.13	-25.79
7.06	213.8	49.90	1.88	13.33	12.59	0.24	6.67	10.85	2.72	0.16	-25.76
7.25	219.8	49.98	1.76	13.46	12.59	0.22	6.66	10.56	2.69	0.16	-25.77
7.32	221.8	49.63	1.82	13.51	12.70	0.22	6.68	10.79	2.76	0.16	-25.73

7.34	222.4	50.11	1.87	13.51	12.65	0.18	6.73	10.70	2.68	0.14	-25.79
7.45	225.8	49.64	1.79	13.39	12.75	0.21	6.53	10.67	2.73	0.15	-25.73
7.67	232.3	50.53	1.81	13.68	12.90	0.20	6.74	10.72	2.66	0.16	-25.84
7.70	233.3	49.74	1.94	13.50	12.61	0.25	6.79	10.78	2.71	0.13	-25.74
7.87	238.5	50.11	1.74	13.56	12.96	0.22	6.85	10.68	2.70	0.16	-25.79
7.98	241.7	50.27	1.91	13.72	12.66	0.14	6.63	10.78	2.65	0.18	-25.81
8.06	244.1	49.96	1.83	13.56	12.91	0.23	6.56	10.66	2.73	0.16	-25.77
8.08	244.7	50.31	1.80	13.58	12.79	0.21	6.79	10.81	2.64	0.15	-25.82
8.28	251.0	50.18	1.85	13.61	12.75	0.23	6.81	10.70	2.70	0.17	-25.80
8.42	255.0	49.95	1.82	13.59	12.54	0.20	6.61	10.76	2.67	0.17	-25.77
8.49	257.1	50.44	1.90	13.59	12.77	0.35	6.66	10.80	2.71	0.15	-25.83
8.49	257.2	49.89	2.02	13.76	12.82	0.23	6.53	10.79	2.63	0.16	-25.76
8.69	263.4	50.00	1.84	13.57	12.77	0.20	6.69	10.93	2.66	0.15	-25.78
8.77	265.8	49.66	1.83	13.43	12.79	0.26	6.68	10.81	2.69	0.17	-25.73
8.90	269.6	49.92	1.78	13.44	12.81	0.23	6.79	10.83	2.67	0.15	-25.77
9.00	272.6	50.11	1.89	13.65	12.98	0.17	6.81	10.82	2.69	0.16	-25.79
9.10	275.8	49.96	1.75	13.60	12.68	0.14	6.85	10.76	2.67	0.18	-25.77
9.11	276.1	50.44	1.87	13.54	12.81	0.21	6.91	10.83	2.62	0.17	-25.83
9.13	276.7	49.35	1.83	13.55	12.68	0.29	6.60	10.84	2.68	0.16	-25.70
9.31	282.0	49.92	1.76	13.46	12.96	0.22	6.84	10.91	2.70	0.15	-25.77
9.45	286.2	50.27	1.90	13.71	12.80	0.23	6.82	10.83	2.66	0.15	-25.81
9.51	288.0	50.01	1.77	13.68	12.97	0.19	6.91	10.79	2.71	0.17	-25.78
9.51	288.3	49.89	1.69	13.71	12.86	0.22	6.83	10.78	2.71	0.17	-25.76
9.72	294.5	49.85	1.82	13.51	12.90	0.21	6.67	10.71	2.67	0.19	-25.76
9.78	296.4	50.01	1.76	13.61	12.88	0.20	6.90	10.87	2.68	0.17	-25.78
9.92	300.7	50.07	1.72	13.66	13.00	0.26	6.82	11.00	2.66	0.16	-25.79
10.02	303.5	50.00	1.86	13.50	12.84	0.16	6.69	10.80	2.67	0.16	-25.78
10.12	306.5	50.06	1.83	13.62	12.69	0.25	6.82	10.86	2.67	0.16	-25.78
10.13	306.9	49.89	1.94	13.59	12.85	0.16	6.67	10.90	2.63	0.16	-25.76
10.33	313.1	49.83	1.95	13.56	12.98	0.25	6.78	10.77	2.70	0.17	-25.76
10.45	316.6	49.87	1.80	13.60	12.80	0.20	6.69	10.84	2.61	0.17	-25.76
10.53	318.9	50.03	1.80	13.80	13.15	0.18	6.95	10.86	2.69	0.15	-25.78
10.54	319.3	49.82	1.76	13.49	13.11	0.29	6.82	10.80	2.67	0.17	-25.75
10.75	325.6	50.00	1.82	13.67	12.93	0.17	6.91	10.75	2.65	0.17	-25.78
10.78	326.7	50.02	1.73	13.46	12.91	0.15	6.81	10.78	2.66	0.18	-25.78
10.95	331.8	49.66	1.81	13.64	12.87	0.24	6.87	10.75	2.67	0.16	-25.73
11.04	334.4	50.07	1.72	13.66	12.76	0.22	6.76	10.78	2.68	0.18	-25.78
11.12	336.9	49.77	1.89	13.52	12.87	0.29	6.72	10.73	2.65	0.16	-25.75
11.15	338.0	49.65	1.76	13.55	12.94	0.17	6.72	10.94	2.66	0.17	-25.73
11.36	344.2	49.80	1.85	13.59	12.91	0.18	6.85	10.79	2.66	0.16	-25.75
11.45	347.0	49.85	1.67	13.57	12.76	0.16	6.77	10.92	2.62	0.18	-25.76
11.55	349.8	49.62	1.70	13.78	12.98	0.17	6.78	10.75	2.68	0.16	-25.73
11.56	350.4	50.06	1.78	13.74	13.06	0.17	6.81	10.75	2.65	0.17	-25.78

11.77	356.6	49.95	1.78	13.65	12.90	0.26	6.87	10.89	2.71	0.16	-25.77
11.79	357.1	49.62	1.79	13.61	12.66	0.31	6.82	10.84	2.65	0.18	-25.73
11.98	362.9	49.85	1.73	13.68	13.12	0.21	6.83	10.79	2.71	0.16	-25.76
12.06	365.3	49.75	1.90	13.53	13.05	0.25	6.91	10.77	2.64	0.19	-25.75
12.12	367.3	49.89	1.79	13.43	12.77	0.17	6.69	10.82	2.66	0.17	-25.76
12.18	369.1	50.08	1.80	13.69	12.92	0.25	6.83	10.76	2.71	0.17	-25.79
12.39	375.3	50.02	1.85	13.55	13.01	0.21	6.85	10.91	2.63	0.16	-25.78
12.46	377.4	49.95	1.79	13.56	12.89	0.13	6.81	10.95	2.65	0.16	-25.77
12.57	380.7	49.83	1.88	13.63	13.21	0.20	6.78	10.76	2.67	0.16	-25.76
12.79	387.5	49.82	1.92	13.55	12.85	0.27	6.83	10.75	2.65	0.18	-25.75
13.07	396.1	49.92	1.76	13.55	12.75	0.22	6.72	10.98	2.65	0.17	-25.77
13.12	397.6	49.83	1.75	13.46	12.83	0.18	6.85	10.81	2.70	0.18	-25.76
13.46	407.8	49.89	1.90	13.58	12.83	0.21	6.69	10.84	2.66	0.18	-25.76
13.59	411.6	49.48	1.76	13.49	12.99	0.23	6.94	10.74	2.69	0.17	-25.71
13.79	417.9	49.73	1.80	13.47	12.65	0.15	6.93	10.92	2.64	0.17	-25.74
14.09	427.0	49.94	1.75	13.74	12.91	0.19	6.65	10.91	2.62	0.18	-25.77
14.13	428.0	49.66	1.82	13.64	12.65	0.12	6.80	10.76	2.64	0.19	-25.73
14.46	438.2	49.91	1.95	13.70	12.85	0.20	6.59	10.87	2.71	0.18	-25.77
14.61	442.5	49.81	1.99	13.47	12.88	0.17	6.84	10.85	2.67	0.18	-25.75
14.80	448.3	49.63	1.86	13.51	12.82	0.27	6.83	10.83	2.68	0.18	-25.73
15.11	457.9	49.54	1.90	13.71	12.68	0.22	6.90	10.74	2.66	0.17	-25.72
15.13	458.4	49.97	1.75	13.53	12.77	0.22	6.77	10.91	2.70	0.17	-25.77
15.46	468.5	49.74	1.82	13.57	12.90	0.20	6.86	10.89	2.71	0.16	-25.74
15.63	473.4	49.67	1.79	13.63	13.01	0.16	6.83	10.92	2.65	0.16	-25.74
15.80	478.7	49.81	1.76	13.57	12.76	0.21	6.81	10.82	2.69	0.19	-25.75
16.13	488.8	49.93	1.77	13.56	12.79	0.15	6.93	10.87	2.70	0.16	-25.77
16.13	488.8	49.70	1.82	13.74	13.08	0.21	6.82	10.88	2.68	0.15	-25.74
16.47	498.9	50.02	1.83	13.53	12.90	0.22	6.80	10.85	2.73	0.19	-25.78
16.65	504.3	49.83	1.60	13.53	13.03	0.26	6.74	10.78	2.69	0.15	-25.76
16.80	509.0	49.99	1.98	13.62	12.65	0.26	6.98	10.81	2.67	0.19	-25.78
17.14	519.2	49.65	1.89	13.54	12.68	0.20	6.87	10.77	2.66	0.15	-25.73
17.15	519.7	49.88	1.77	13.57	12.98	0.23	6.87	10.84	2.70	0.17	-25.76
17.47	529.3	49.81	1.81	13.48	12.96	0.19	6.64	10.77	2.68	0.18	-25.75
17.66	535.1	49.98	1.81	13.63	12.96	0.19	6.97	10.78	2.65	0.19	-25.77
17.80	539.4	49.71	1.85	13.50	12.55	0.13	6.73	10.90	2.69	0.18	-25.74
18.14	549.6	49.77	1.94	13.64	12.95	0.23	6.84	10.77	2.68	0.17	-25.75
18.17	550.6	49.84	1.74	13.55	13.07	0.23	6.86	10.90	2.68	0.18	-25.76
18.47	559.7	50.00	1.77	13.67	12.84	0.19	6.96	10.89	2.68	0.18	-25.78
18.68	566.0	49.86	1.78	13.56	12.92	0.19	6.83	10.77	2.67	0.17	-25.76
18.81	569.8	49.90	1.69	13.54	12.88	0.23	6.79	10.87	2.76	0.18	-25.76
19.14	579.9	49.79	1.83	13.54	12.86	0.25	6.76	10.83	2.72	0.18	-25.75
19.19	581.5	49.73	1.98	13.54	12.77	0.24	6.86	10.80	2.72	0.18	-25.74
19.48	590.1	50.02	1.76	13.49	12.73	0.18	6.86	10.76	2.71	0.16	-25.78

19.70	596.9	49.74	1.96	13.55	13.22	0.21	7.08	10.81	2.71	0.19	-25.74
19.81	600.2	49.77	1.74	13.68	12.89	0.16	6.66	10.87	2.70	0.20	-25.75
20.14	610.3	49.81	1.72	13.69	12.77	0.19	6.88	10.75	2.73	0.16	-25.75
20.21	612.4	49.72	1.87	13.54	12.96	0.22	6.67	10.87	2.70	0.18	-25.74
20.48	620.5	49.91	1.87	13.59	12.94	0.19	6.84	10.93	2.63	0.18	-25.77
20.72	627.8	49.81	1.72	13.38	13.07	0.27	6.87	10.87	2.71	0.17	-25.75
20.81	630.6	49.76	1.83	13.75	12.65	0.20	6.97	10.79	2.66	0.17	-25.75
21.15	640.7	49.89	1.73	13.44	12.72	0.20	6.96	10.77	2.68	0.16	-25.76
21.23	643.3	49.79	1.77	13.42	13.00	0.26	6.99	10.82	2.63	0.18	-25.75
21.48	650.8	49.69	1.82	13.71	12.74	0.26	6.92	10.75	2.69	0.19	-25.74
21.74	658.7	49.66	1.91	13.56	12.83	0.14	6.75	10.86	2.67	0.18	-25.73
21.82	661.0	49.70	1.73	13.55	12.71	0.19	6.94	10.82	2.71	0.19	-25.74
22.15	671.1	49.78	1.88	13.61	12.70	0.22	6.76	10.73	2.72	0.19	-25.75

QzDisBa103, starting basalt: JDF; T=1304 °C, P=0.5 GPa, t =257s, H2O=0.32wt%

x / sqrt(t)	x (μm)	SiO2	TiO2	Al2O3	FeO	MnO	MgO	CaO	Na2O	K2O	lnD_SiO2 (m^2/s)
0.10	1.5	68.22	0.87	9.07	7.43	0.10	3.93	6.40	3.96	0.39	-28.75
0.16	2.6	68.36	0.77	8.82	6.95	0.08	3.83	6.13	3.85	0.43	-28.77
0.19	3.1	66.72	0.96	9.19	7.59	0.14	4.18	6.63	3.99	0.40	-28.48
0.26	4.2	65.05	1.04	9.78	8.24	0.16	4.38	7.36	3.24	0.34	-28.19
0.27	4.4	64.51	0.97	9.79	8.22	0.19	4.55	7.18	3.78	0.37	-28.09
0.30	4.8	65.25	1.15	9.63	8.40	0.14	4.46	7.35	4.02	0.32	-28.22
0.32	5.2	64.64	0.94	9.62	8.38	0.16	4.43	7.30	3.83	0.35	-28.12
0.45	7.2	62.55	1.14	10.45	8.68	0.07	4.58	7.58	3.78	0.30	-27.76
0.53	8.5	62.48	1.17	10.32	9.22	0.15	4.95	8.07	3.28	0.29	-27.75
0.58	9.3	61.56	1.27	10.17	9.17	0.23	5.01	8.25	3.67	0.30	-27.60
0.60	9.6	60.55	1.36	10.43	9.17	0.12	5.19	8.27	3.83	0.29	-27.43
0.80	12.8	60.35	1.18	10.48	9.67	0.06	5.21	8.68	3.20	0.25	-27.40
0.83	13.3	59.92	1.26	10.65	9.59	0.13	5.34	8.55	3.63	0.27	-27.33
0.93	14.9	58.52	1.39	10.79	9.81	0.17	5.32	8.72	3.46	0.26	-27.11
1.06	17.1	58.38	1.49	11.04	10.27	0.21	5.41	9.00	3.14	0.21	-27.09
1.17	18.8	57.78	1.23	11.13	10.31	0.28	5.59	9.10	3.64	0.22	-27.00
1.21	19.4	56.98	1.47	11.17	10.48	0.17	5.73	9.15	3.23	0.26	-26.87
1.25	20.1	57.22	1.36	11.39	10.36	0.12	5.67	9.25	3.37	0.20	-26.91
1.52	24.3	56.06	1.40	11.43	10.85	0.09	5.75	9.54	3.24	0.20	-26.74
1.54	24.7	56.19	1.48	11.47	10.74	0.15	5.88	9.48	3.29	0.22	-26.76
1.58	25.3	55.90	1.45	11.50	10.69	0.16	5.93	9.61	3.35	0.20	-26.71
1.86	29.8	55.27	1.54	11.44	10.95	0.19	6.09	9.66	3.31	0.20	-26.62
1.87	30.0	55.26	1.49	11.84	11.16	0.14	6.03	9.86	3.25	0.18	-26.62
1.91	30.6	54.88	1.47	11.83	11.05	0.15	6.04	9.80	3.27	0.20	-26.56
2.20	35.3	54.16	1.63	11.86	11.32	0.23	6.15	9.98	2.91	0.20	-26.46
2.20	35.3	54.18	1.60	12.06	11.50	0.10	6.06	9.97	3.04	0.20	-26.46
2.23	35.8	53.98	1.62	11.95	11.16	0.28	6.15	9.90	2.98	0.19	-26.43
2.53	40.6	53.47	1.61	12.29	11.67	0.27	6.21	10.04	2.81	0.19	-26.36
2.55	40.8	53.61	1.67	12.30	11.59	0.18	6.19	10.14	3.15	0.18	-26.38
2.56	41.0	53.42	1.55	12.22	11.52	0.21	6.35	10.12	2.99	0.17	-26.35
2.86	45.9	53.08	1.68	12.51	11.52	0.18	6.50	10.14	2.82	0.17	-26.30
2.89	46.3	52.95	1.57	12.39	11.57	0.18	6.35	10.35	3.11	0.16	-26.29
2.89	46.3	53.00	1.57	12.39	11.92	0.34	6.41	10.18	2.69	0.19	-26.29
3.19	51.2	52.61	1.91	12.56	11.83	0.16	6.43	10.19	2.85	0.17	-26.24
3.21	51.5	52.36	1.76	12.61	11.79	0.13	6.40	10.33	3.13	0.19	-26.20
3.23	51.8	52.44	1.86	12.68	12.23	0.18	6.45	10.26	3.11	0.18	-26.21
3.52	56.5	52.14	1.84	12.57	11.93	0.33	6.44	10.41	2.98	0.18	-26.17
3.53	56.7	52.16	1.72	12.78	11.74	0.17	6.52	10.41	2.80	0.16	-26.17
3.58	57.3	51.92	1.91	12.94	12.13	0.21	6.51	10.43	2.64	0.15	-26.14
3.86	61.8	51.88	1.68	12.76	12.04	0.18	6.54	10.40	2.97	0.18	-26.14

3.86	62.0	51.61	1.81	12.81	11.95	0.15	6.43	10.47	2.75	0.18	-26.10
3.92	62.8	51.64	1.73	12.84	12.19	0.21	6.49	10.57	2.69	0.17	-26.10
4.19	67.1	51.49	1.77	12.92	12.23	0.22	6.41	10.54	2.93	0.17	-26.08
4.19	67.1	51.91	1.71	12.99	12.37	0.25	6.50	10.56	2.74	0.15	-26.14
4.19	67.2	51.42	1.74	12.94	12.12	0.17	6.48	10.52	2.75	0.18	-26.07
4.26	68.3	51.45	1.79	12.99	12.36	0.26	6.53	10.56	2.78	0.18	-26.08
4.26	68.3	51.48	1.86	13.13	12.51	0.23	6.49	10.68	2.82	0.17	-26.08
4.51	72.4	51.33	1.83	13.08	12.11	0.19	6.53	10.53	2.58	0.17	-26.06
4.82	77.3	51.10	1.77	13.13	12.38	0.18	6.47	10.62	2.55	0.18	-26.03
4.84	77.7	50.97	1.80	13.10	12.24	0.20	6.71	10.50	2.68	0.15	-26.01
4.94	79.2	50.81	1.92	13.20	12.37	0.24	6.50	10.63	2.57	0.15	-25.99
5.17	82.9	50.76	1.78	13.19	12.28	0.23	6.55	10.59	2.85	0.15	-25.98
5.46	87.5	51.02	1.84	13.09	12.62	0.20	6.56	10.67	2.68	0.17	-26.02
5.49	88.1	50.65	1.92	13.09	12.27	0.26	6.60	10.65	2.80	0.15	-25.97
5.62	90.1	50.64	1.72	13.30	12.68	0.19	6.68	10.75	2.61	0.12	-25.97
5.82	93.4	50.50	2.06	13.30	12.63	0.28	6.76	10.82	2.76	0.15	-25.95
6.09	97.7	50.55	1.78	13.14	12.57	0.18	6.76	10.74	2.74	0.15	-25.95
6.15	98.6	50.40	1.80	13.35	12.63	0.14	6.69	10.73	2.88	0.17	-25.93
6.29	100.9	50.41	1.82	13.33	12.78	0.19	6.56	10.66	2.75	0.15	-25.94
6.47	103.8	50.31	1.83	13.23	12.37	0.20	6.72	10.64	2.71	0.16	-25.92
6.74	108.0	50.35	1.76	13.24	12.79	0.26	6.66	10.73	2.53	0.17	-25.93
6.80	109.1	50.26	1.91	13.36	12.58	0.18	6.64	10.74	2.57	0.16	-25.92
6.97	111.8	50.38	1.82	13.34	12.60	0.24	6.58	10.65	2.56	0.14	-25.93
7.13	114.3	50.17	1.84	13.53	12.89	0.20	6.83	10.74	2.73	0.18	-25.90
7.37	118.2	50.45	1.80	13.42	12.72	0.26	6.81	10.80	2.69	0.16	-25.94
7.45	119.5	50.10	1.86	13.52	12.52	0.19	6.60	10.75	2.60	0.16	-25.90
7.65	122.7	50.24	1.85	13.48	12.65	0.20	6.66	10.74	2.47	0.17	-25.91
7.78	124.8	49.90	1.75	13.49	12.65	0.27	6.78	10.77	2.73	0.16	-25.87
8.01	128.4	50.38	1.80	13.37	12.60	0.22	6.56	10.78	2.65	0.16	-25.93
8.11	129.9	50.19	1.86	13.49	12.47	0.20	6.81	10.71	2.77	0.15	-25.91
8.33	133.6	50.05	1.87	13.42	12.72	0.24	6.83	10.75	2.72	0.18	-25.89
8.43	135.1	49.93	1.90	13.43	12.77	0.22	6.82	10.80	2.64	0.16	-25.87
8.65	138.6	50.12	1.83	13.34	12.72	0.16	6.72	10.76	2.60	0.18	-25.90
8.76	140.4	49.94	1.83	13.54	12.85	0.27	6.83	10.78	2.66	0.15	-25.87
9.01	144.4	50.08	1.75	13.31	12.89	0.22	6.64	10.89	2.60	0.17	-25.89
9.09	145.6	50.01	1.84	13.69	12.47	0.22	6.67	10.83	2.50	0.16	-25.88
9.28	148.8	50.14	1.88	13.38	12.71	0.21	6.74	10.81	2.65	0.15	-25.90
9.41	150.8	50.01	1.82	13.37	12.75	0.23	6.76	10.75	2.83	0.16	-25.88
9.69	155.3	49.96	1.86	13.35	12.81	0.16	6.64	10.71	2.69	0.15	-25.88
9.74	156.1	50.05	1.75	13.43	12.71	0.22	6.73	10.76	2.66	0.17	-25.89
9.92	159.0	50.09	1.81	13.57	12.82	0.23	6.62	10.80	2.70	0.16	-25.89
10.06	161.3	49.94	1.93	13.33	12.60	0.29	6.71	10.84	2.84	0.15	-25.87
10.55	169.2	50.08	1.85	13.58	12.89	0.27	6.66	10.93	2.56	0.16	-25.89

10.66	170.9	50.13	1.80	13.60	12.76	0.28	6.85	10.72	2.56	0.15	-25.90
10.69	171.3	49.77	1.89	13.65	12.67	0.21	6.73	10.71	2.64	0.17	-25.85
11.20	179.5	50.20	1.79	13.52	12.73	0.22	6.79	10.89	2.57	0.17	-25.91
11.37	182.3	49.90	1.87	13.62	12.67	0.32	6.73	10.79	2.76	0.18	-25.87
11.83	189.7	50.15	1.97	13.53	12.81	0.19	6.82	10.75	2.73	0.16	-25.90
12.03	192.8	50.02	1.91	13.40	12.66	0.17	6.80	10.84	2.79	0.18	-25.88
12.06	193.3	49.94	1.75	13.47	12.63	0.26	6.89	10.88	2.56	0.18	-25.87
12.47	199.9	50.12	1.85	13.48	12.96	0.28	6.77	10.80	2.70	0.17	-25.90
12.75	204.3	49.91	1.78	13.66	12.59	0.22	6.77	10.74	2.66	0.17	-25.87
13.10	210.1	50.25	1.80	13.35	12.60	0.19	6.88	10.82	2.52	0.17	-25.91
13.40	214.7	50.18	1.80	13.47	12.71	0.26	6.86	10.82	2.73	0.19	-25.91
13.43	215.3	50.25	1.84	13.75	12.83	0.18	6.81	10.80	2.64	0.15	-25.91
13.47	216.0	50.10	1.91	13.41	12.61	0.16	6.82	10.78	2.77	0.18	-25.89
14.12	226.3	50.10	1.81	13.55	12.71	0.33	6.79	10.73	2.72	0.17	-25.89
14.72	236.1	50.04	1.69	13.35	12.52	0.17	6.78	10.76	2.73	0.18	-25.89
14.75	236.5	50.16	1.85	13.57	12.99	0.20	6.82	10.83	2.77	0.15	-25.90
14.80	237.3	49.96	1.87	13.55	12.96	0.20	6.83	10.88	2.51	0.19	-25.88
15.49	248.3	50.10	1.96	13.50	12.85	0.19	6.85	10.67	2.67	0.18	-25.90
15.98	256.2	50.18	1.73	13.55	12.87	0.19	6.79	10.88	2.75	0.16	-25.91
16.12	258.4	50.21	1.90	13.52	12.65	0.21	6.77	10.70	2.81	0.19	-25.91
16.18	259.3	50.25	1.79	13.43	12.71	0.21	6.87	10.68	2.66	0.14	-25.91
16.86	270.3	50.04	1.73	13.45	12.50	0.25	6.78	10.67	2.66	0.17	-25.89
17.23	276.3	50.00	1.79	13.51	12.96	0.28	6.74	10.76	2.59	0.19	-25.88
17.49	280.3	50.09	1.84	13.56	12.69	0.19	6.71	10.68	2.74	0.19	-25.89
17.55	281.3	50.06	1.93	13.46	12.77	0.24	6.68	10.63	2.41	0.18	-25.89
18.23	292.3	50.22	1.98	13.59	12.77	0.20	6.90	10.71	2.69	0.18	-25.91
18.49	296.3	49.94	1.82	13.42	12.87	0.28	6.78	10.73	2.77	0.21	-25.87
18.85	302.2	50.07	1.84	13.46	12.81	0.18	6.92	10.93	2.59	0.18	-25.89
18.92	303.3	50.11	1.78	13.49	12.85	0.27	6.83	10.68	2.63	0.18	-25.90
19.61	314.3	49.94	1.81	13.46	12.68	0.28	6.74	10.67	2.83	0.18	-25.87
19.74	316.4	50.14	1.75	13.50	12.83	0.25	6.88	10.75	2.63	0.17	-25.90
20.21	324.0	50.19	1.86	13.38	12.83	0.19	6.74	10.76	2.76	0.20	-25.91
20.29	325.3	50.26	1.79	13.41	12.81	0.27	6.80	10.80	2.87	0.18	-25.92
20.98	336.3	50.17	1.93	13.60	12.96	0.23	6.79	10.75	2.55	0.17	-25.90
20.99	336.5	49.99	1.88	13.60	12.78	0.22	6.69	10.81	2.88	0.19	-25.88
21.58	345.9	50.12	1.70	13.54	12.71	0.25	6.94	10.81	3.01	0.16	-25.90
21.66	347.3	50.09	1.83	13.32	12.63	0.23	6.84	10.80	2.69	0.20	-25.89
22.25	356.6	49.95	1.93	13.43	12.76	0.12	6.72	10.82	2.79	0.18	-25.88
22.35	358.3	50.28	1.82	13.62	12.48	0.21	6.90	10.71	3.03	0.17	-25.92
23.04	369.3	50.25	1.90	13.60	12.71	0.20	6.85	10.71	2.52	0.16	-25.91
23.50	376.7	50.04	1.69	13.38	12.78	0.24	6.77	10.79	2.57	0.17	-25.89
23.72	380.3	50.17	1.74	13.48	12.60	0.28	6.82	10.77	2.64	0.21	-25.90
23.72	380.3	50.30	1.78	13.58	12.49	0.16	6.68	10.78	2.76	0.17	-25.92

24.75	396.8	50.15	1.82	13.40	12.82	0.25	6.74	10.73	2.90	0.16	-25.90
25.65	411.2	50.06	1.92	13.60	12.40	0.20	6.86	10.73	2.53	0.19	-25.89
26.01	416.9	50.16	1.95	13.59	12.93	0.23	6.74	10.75	2.73	0.19	-25.90

QzDisBa104, starting basalt: JDF; T=1508 °C, P=0.5 GPa, t =928s, H2O=0.32wt%

x / sqrt(t)	x (μm)	SiO2	TiO2	Al2O3	FeO	MnO	MgO	CaO	Na2O	K2O	lnD_SiO2 (m^2/s)
0.06	1.9	83.76	0.41	4.41	3.71	0.03	1.69	2.68	2.32	0.27	-29.78
0.15	4.7	76.81	0.58	6.33	4.96	0.06	2.46	3.80	2.51	0.40	-28.52
0.22	6.7	75.42	0.60	6.89	5.45	0.10	2.59	4.30	2.54	0.40	-28.27
0.34	10.4	73.00	0.75	7.39	5.87	0.03	3.08	4.97	2.87	0.38	-27.85
0.38	11.5	71.76	0.77	7.74	6.47	0.09	3.27	5.48	2.60	0.36	-27.63
0.42	12.8	70.83	0.68	7.92	6.83	0.13	3.62	5.72	2.89	0.37	-27.47
0.56	17.0	69.08	0.75	8.33	7.08	0.07	3.86	6.12	2.76	0.35	-27.18
0.62	18.9	68.17	0.85	8.53	7.21	0.07	3.82	6.26	3.00	0.32	-27.03
0.67	20.5	67.43	0.80	8.61	7.69	0.07	4.13	6.52	3.10	0.34	-26.91
0.74	22.5	67.14	0.92	8.67	7.64	0.14	4.10	6.69	2.87	0.31	-26.86
0.82	25.1	66.28	0.93	8.73	7.81	0.14	4.07	6.90	3.16	0.32	-26.72
0.83	25.1	66.18	0.93	9.09	8.08	0.09	4.35	6.96	2.86	0.32	-26.70
0.92	28.0	65.84	0.97	8.94	8.00	0.17	4.18	7.00	2.84	0.31	-26.65
0.94	28.6	65.13	1.00	9.28	8.19	0.13	4.43	7.27	3.06	0.30	-26.54
1.00	30.6	64.56	1.05	9.14	8.42	0.12	4.54	7.43	3.18	0.28	-26.45
1.02	31.2	64.32	1.03	9.17	8.37	0.15	4.30	7.35	3.17	0.31	-26.41
1.09	33.1	63.80	1.26	9.30	8.61	0.16	4.64	7.59	2.94	0.30	-26.33
1.22	37.3	63.18	1.04	9.61	8.66	0.08	4.69	7.63	3.22	0.27	-26.23
1.33	40.6	62.64	1.00	9.64	8.82	0.16	4.71	7.93	3.18	0.29	-26.15
1.35	41.2	62.44	1.12	9.78	9.02	0.16	4.83	7.94	2.97	0.27	-26.12
1.42	43.3	62.17	1.05	9.69	8.86	0.11	4.78	7.86	3.20	0.25	-26.08
1.43	43.4	61.78	1.15	9.94	9.10	0.08	4.90	8.07	3.26	0.28	-26.02
1.61	49.2	61.46	1.27	10.10	9.28	0.11	5.06	8.34	3.10	0.26	-25.97
1.63	49.5	61.33	1.12	10.01	9.17	0.16	4.86	8.16	3.28	0.29	-25.95
1.66	50.7	61.16	1.17	9.94	9.45	0.11	4.88	8.32	3.26	0.25	-25.92
1.83	55.6	60.90	1.19	9.99	9.30	0.17	4.93	8.30	3.27	0.26	-25.89
1.88	57.2	60.31	1.19	10.10	9.75	0.18	5.10	8.70	3.04	0.24	-25.80
1.92	58.4	60.15	1.14	10.16	9.65	0.19	5.27	8.59	3.25	0.25	-25.78
1.99	60.6	59.94	1.20	10.27	9.67	0.11	5.18	8.60	3.17	0.25	-25.75
2.14	65.2	59.58	1.32	10.49	9.84	0.23	5.13	8.77	3.02	0.22	-25.69
2.32	70.7	58.94	1.31	10.52	9.87	0.14	5.30	8.78	3.23	0.24	-25.60
2.40	73.2	58.96	1.31	10.77	10.00	0.15	5.37	9.06	3.03	0.23	-25.60
2.41	73.3	58.60	1.29	10.60	10.06	0.16	5.44	8.83	3.22	0.22	-25.55
2.65	80.7	58.11	1.32	10.70	10.05	0.15	5.58	9.04	3.14	0.22	-25.48
2.67	81.2	57.98	1.53	10.84	10.29	0.13	5.35	9.03	3.05	0.20	-25.47
2.90	88.3	57.34	1.36	10.80	10.25	0.11	5.52	9.18	3.12	0.21	-25.38
2.93	89.2	57.31	1.34	10.99	10.40	0.25	5.61	9.21	3.00	0.22	-25.37
2.98	90.8	57.27	1.33	11.01	10.41	0.19	5.45	9.07	3.20	0.23	-25.37
3.19	97.2	56.95	1.43	11.38	10.61	0.24	5.66	9.35	3.04	0.19	-25.32
3.31	100.8	56.81	1.40	11.14	10.59	0.20	5.59	9.37	3.16	0.21	-25.30

3.39	103.1	56.69	1.52	11.19	10.45	0.21	5.71	9.35	3.11	0.23	-25.29
3.46	105.3	56.69	1.45	11.50	10.84	0.20	5.71	9.42	3.05	0.20	-25.29
3.64	110.8	56.25	1.47	11.16	10.63	0.18	5.70	9.44	3.11	0.21	-25.23
3.72	113.3	56.15	1.26	11.55	10.81	0.19	5.73	9.64	2.94	0.20	-25.22
3.88	118.1	55.72	1.46	11.47	10.77	0.12	5.71	9.52	3.04	0.22	-25.16
3.97	120.8	55.62	1.59	11.37	10.96	0.16	5.93	9.71	3.03	0.21	-25.15
3.98	121.3	55.85	1.56	11.69	11.01	0.18	5.75	9.65	2.99	0.20	-25.18
4.24	129.2	55.10	1.59	11.71	10.83	0.12	6.02	9.77	2.87	0.18	-25.08
4.30	130.9	54.99	1.56	11.65	10.96	0.23	6.00	9.85	3.02	0.20	-25.06
4.36	133.0	55.07	1.67	11.63	10.87	0.06	5.92	9.73	3.02	0.19	-25.07
4.51	137.3	54.87	1.60	11.97	10.85	0.19	5.85	9.74	2.92	0.18	-25.05
4.63	141.0	54.70	1.62	11.80	11.13	0.21	6.05	9.73	2.99	0.20	-25.03
4.77	145.3	54.70	1.69	11.83	11.38	0.21	5.93	9.79	2.89	0.19	-25.02
4.85	147.8	54.44	1.59	11.76	11.22	0.15	5.91	10.00	2.93	0.17	-24.99
4.96	151.0	54.46	1.52	11.92	11.30	0.16	6.00	9.81	2.95	0.18	-24.99
5.03	153.3	54.15	1.67	11.96	11.24	0.29	6.09	9.91	2.90	0.16	-24.95
5.29	161.0	54.10	1.57	12.03	11.37	0.18	6.06	9.92	2.88	0.17	-24.95
5.30	161.4	53.67	1.64	12.10	11.35	0.09	6.03	9.99	2.91	0.21	-24.89
5.34	162.8	53.89	1.53	12.14	11.38	0.18	6.11	10.01	2.90	0.18	-24.92
5.56	169.4	53.91	1.64	12.20	11.42	0.14	6.12	9.96	2.85	0.17	-24.92
5.61	171.0	53.70	1.53	12.23	11.69	0.15	6.15	10.07	2.91	0.17	-24.90
5.82	177.3	53.63	1.52	12.38	11.46	0.20	6.19	10.12	2.82	0.17	-24.89
5.83	177.7	53.73	1.65	12.16	11.66	0.14	6.11	10.09	2.94	0.18	-24.90
5.95	181.1	53.61	1.56	12.28	11.46	0.26	6.08	10.04	2.90	0.18	-24.89
6.08	185.3	53.23	1.69	12.43	11.60	0.22	6.14	9.99	2.84	0.17	-24.84
6.27	191.1	53.18	1.70	12.37	11.71	0.22	6.18	10.21	2.87	0.17	-24.83
6.32	192.6	53.25	1.72	12.51	11.57	0.26	6.43	10.05	2.80	0.16	-24.84
6.35	193.4	53.18	1.78	12.52	11.72	0.16	6.15	10.10	2.87	0.18	-24.83
6.60	201.2	52.89	1.70	12.30	11.69	0.26	6.24	10.16	2.83	0.16	-24.80
6.61	201.4	52.87	1.71	12.65	11.99	0.13	6.25	10.28	2.78	0.17	-24.80
6.81	207.5	52.83	1.70	12.61	11.82	0.20	6.31	10.18	2.80	0.18	-24.79
6.87	209.4	52.57	1.69	12.50	11.90	0.25	6.19	10.34	2.82	0.17	-24.76
6.93	211.1	52.54	1.65	12.56	11.96	0.17	6.15	10.32	2.83	0.17	-24.76
7.14	217.4	52.26	1.66	12.65	12.00	0.19	6.15	10.29	2.86	0.19	-24.72
7.26	221.2	52.56	1.64	12.55	11.89	0.22	6.18	10.17	2.74	0.17	-24.76
7.30	222.5	52.69	1.48	12.64	11.87	0.28	6.30	10.28	2.73	0.15	-24.77
7.40	225.5	52.54	1.69	12.74	11.81	0.19	6.24	10.47	2.77	0.18	-24.76
7.59	231.2	52.09	1.60	12.55	12.05	0.18	6.18	10.34	2.79	0.17	-24.70
7.66	233.4	52.38	1.78	12.84	11.95	0.23	6.21	10.31	2.75	0.15	-24.74
7.79	237.4	52.17	1.84	12.78	11.83	0.18	6.44	10.33	2.73	0.17	-24.71
7.92	241.3	51.90	1.71	12.60	12.14	0.10	6.36	10.22	2.78	0.17	-24.68
7.93	241.4	51.89	1.80	12.83	12.04	0.20	6.32	10.48	2.71	0.16	-24.68
8.19	249.4	51.68	1.70	12.86	12.05	0.13	6.27	10.52	2.69	0.17	-24.65

8.25	251.4	51.80	1.78	12.90	12.37	0.14	6.42	10.43	2.73	0.16	-24.67
8.28	252.3	51.88	1.78	12.99	12.14	0.26	6.35	10.42	2.71	0.16	-24.68
8.45	257.5	51.83	1.75	12.87	11.95	0.12	6.46	10.52	2.73	0.16	-24.67
8.58	261.3	51.71	1.79	12.93	12.14	0.25	6.47	10.46	2.70	0.16	-24.65
8.71	265.5	51.64	1.83	12.87	12.05	0.21	6.35	10.36	2.69	0.15	-24.65
8.77	267.2	51.69	1.82	12.90	12.11	0.26	6.37	10.36	2.65	0.16	-24.65
8.91	271.4	51.72	1.75	12.85	12.17	0.17	6.52	10.42	2.73	0.15	-24.66
8.98	273.5	51.67	1.71	13.06	12.30	0.29	6.37	10.46	2.69	0.16	-24.65
9.24	281.4	51.42	1.74	13.13	12.27	0.24	6.60	10.42	2.68	0.15	-24.62
9.24	281.5	51.62	1.85	13.12	12.36	0.14	6.60	10.56	2.70	0.16	-24.64
9.26	282.1	51.33	1.88	12.94	12.29	0.22	6.59	10.56	2.68	0.16	-24.61
9.50	289.5	51.46	1.70	13.21	12.42	0.16	6.51	10.50	2.60	0.16	-24.63
9.57	291.5	51.33	1.94	13.11	12.28	0.14	6.40	10.42	2.65	0.16	-24.61
9.75	297.0	51.02	1.81	13.12	12.37	0.20	6.38	10.46	2.72	0.16	-24.58
9.77	297.5	51.25	1.96	13.17	12.36	0.25	6.61	10.50	2.62	0.14	-24.60
9.90	301.5	51.23	1.83	13.02	12.46	0.19	6.45	10.63	2.69	0.15	-24.60
10.03	305.5	51.14	1.78	13.30	12.28	0.22	6.36	10.65	2.66	0.19	-24.59
10.23	311.6	51.06	1.89	13.07	12.31	0.20	6.61	10.52	2.68	0.16	-24.58
10.24	311.9	50.67	1.72	13.27	12.47	0.18	6.55	10.53	2.60	0.15	-24.53
10.29	313.6	50.95	1.80	13.35	12.41	0.20	6.53	10.56	2.63	0.17	-24.57
10.55	321.5	51.00	2.01	13.29	12.35	0.21	6.52	10.46	2.66	0.15	-24.57
10.56	321.6	50.82	1.83	13.23	12.29	0.21	6.46	10.63	2.58	0.14	-24.55
10.73	326.9	50.84	1.74	13.18	12.26	0.22	6.52	10.72	2.64	0.17	-24.55
10.82	329.6	50.85	1.94	13.21	12.42	0.12	6.55	10.60	2.63	0.15	-24.55
10.89	331.6	50.74	1.79	13.30	12.47	0.22	6.49	10.52	2.69	0.17	-24.54
11.08	337.5	50.78	1.84	13.22	12.48	0.25	6.38	10.62	2.59	0.15	-24.55
11.21	341.6	50.83	1.72	13.19	12.43	0.21	6.60	10.53	2.61	0.15	-24.55
11.22	341.8	50.53	1.84	13.26	12.35	0.20	6.58	10.54	2.65	0.15	-24.52
11.35	345.6	50.61	2.08	13.34	12.52	0.26	6.51	10.55	2.62	0.14	-24.53
11.54	351.7	50.39	1.75	13.43	12.60	0.20	6.65	10.50	2.64	0.15	-24.50
11.61	353.6	50.57	1.82	13.19	12.35	0.33	6.54	10.67	2.59	0.14	-24.52
11.71	356.7	50.77	1.75	13.24	12.58	0.13	6.50	10.60	2.63	0.17	-24.55
11.87	361.6	50.43	1.99	13.41	12.41	0.24	6.63	10.57	2.61	0.15	-24.51
11.88	361.8	50.54	1.83	13.22	12.43	0.22	6.59	10.67	2.68	0.14	-24.52
12.13	369.6	50.64	1.89	13.55	12.57	0.14	6.35	10.60	2.60	0.15	-24.53
12.20	371.6	50.55	1.77	13.31	12.48	0.15	6.49	10.58	2.60	0.16	-24.52
12.20	371.7	50.54	1.92	13.39	12.57	0.20	6.68	10.54	2.63	0.16	-24.52
12.40	377.7	50.58	2.00	13.47	12.48	0.27	6.76	10.63	2.63	0.15	-24.52
12.53	381.8	50.29	1.80	13.46	12.58	0.26	6.75	10.74	2.60	0.14	-24.49
12.66	385.6	50.61	1.81	13.29	12.73	0.17	6.53	10.68	2.60	0.17	-24.53
12.69	386.5	50.34	1.96	13.29	12.34	0.15	6.51	10.63	2.61	0.15	-24.50
12.86	391.8	50.56	1.82	13.37	12.52	0.19	6.60	10.58	2.59	0.17	-24.52
12.92	393.6	50.24	1.82	13.39	12.63	0.19	6.58	10.70	2.53	0.14	-24.49

13.18	401.4	50.33	1.89	13.52	12.46	0.10	6.66	10.78	2.65	0.16	-24.50
13.19	401.7	50.35	2.02	13.52	12.66	0.23	6.50	10.62	2.60	0.14	-24.50
13.19	401.9	50.28	1.96	13.48	12.78	0.22	6.60	10.67	2.59	0.16	-24.49
13.45	409.7	50.33	1.82	13.49	12.64	0.23	6.60	10.79	2.56	0.17	-24.50
13.52	411.9	50.40	1.80	13.43	12.59	0.27	6.67	10.59	2.61	0.17	-24.50
13.67	416.3	50.25	1.82	13.40	12.67	0.23	6.75	10.80	2.57	0.15	-24.49
13.71	417.7	50.39	1.89	13.65	12.56	0.24	6.79	10.80	2.56	0.16	-24.50
13.85	421.9	50.09	1.92	13.53	12.63	0.26	6.50	10.61	2.58	0.16	-24.47
13.97	425.7	50.29	1.86	13.60	12.59	0.21	6.59	10.60	2.54	0.14	-24.49
14.16	431.3	50.28	1.86	13.52	12.74	0.22	6.56	10.78	2.62	0.18	-24.49
14.18	431.9	50.22	1.73	13.28	12.67	0.22	6.51	10.72	2.63	0.15	-24.48
14.24	433.8	50.33	1.76	13.50	12.78	0.23	6.61	10.67	2.57	0.14	-24.50
14.50	441.7	50.11	1.79	13.53	12.59	0.22	6.54	10.82	2.53	0.16	-24.47
14.51	442.0	50.25	1.83	13.44	12.65	0.18	6.64	10.65	2.63	0.16	-24.49
14.65	446.2	50.01	1.73	13.59	12.78	0.26	6.64	10.76	2.63	0.19	-24.46
14.76	449.7	50.20	1.81	13.56	12.56	0.24	6.71	10.74	2.64	0.15	-24.48
14.84	452.0	50.18	1.78	13.49	13.02	0.15	6.47	10.73	2.60	0.13	-24.48
15.03	457.7	49.84	1.84	13.50	12.79	0.17	6.86	10.72	2.55	0.16	-24.44
15.14	461.1	50.00	1.74	13.64	12.79	0.22	6.44	10.84	2.60	0.15	-24.46
15.17	462.1	50.18	1.88	13.45	12.88	0.18	6.51	10.64	2.61	0.13	-24.48
15.29	465.8	50.12	1.82	13.78	12.86	0.21	6.73	10.74	2.58	0.18	-24.47
15.50	472.1	50.00	2.00	13.32	12.96	0.14	6.80	10.79	2.56	0.18	-24.46
15.55	473.8	50.36	1.71	13.68	12.77	0.25	6.73	10.62	2.54	0.14	-24.50
15.63	476.0	50.17	1.84	13.61	12.70	0.21	6.75	10.74	2.56	0.15	-24.48
15.81	481.8	50.27	2.01	13.44	12.83	0.23	6.66	10.67	2.59	0.15	-24.49
15.83	482.1	49.79	2.00	13.37	12.45	0.25	6.60	10.74	2.53	0.17	-24.43
16.08	489.7	49.99	1.79	13.45	12.64	0.17	6.70	10.79	2.57	0.17	-24.46
16.11	490.9	49.94	1.74	13.66	12.95	0.16	6.66	10.61	2.60	0.14	-24.45
16.16	492.2	50.16	1.76	13.40	12.65	0.16	6.55	10.68	2.57	0.14	-24.48
16.34	497.8	50.01	1.86	13.44	12.60	0.16	6.62	10.70	2.54	0.15	-24.46
16.49	502.2	49.78	1.92	13.40	12.87	0.17	6.83	10.82	2.55	0.15	-24.43
16.60	505.8	50.13	1.82	13.46	12.81	0.21	6.60	10.77	2.53	0.14	-24.47
16.61	505.8	49.98	1.84	13.57	12.81	0.16	6.59	10.71	2.55	0.17	-24.46
16.82	512.3	49.97	1.91	13.54	12.76	0.31	6.86	10.65	2.58	0.15	-24.46
16.87	513.8	49.98	1.86	13.56	12.64	0.16	6.58	10.69	2.53	0.15	-24.46
17.09	520.7	49.92	1.82	13.42	12.77	0.20	6.75	10.74	2.54	0.16	-24.45
17.13	521.9	50.12	1.72	13.32	12.77	0.21	6.69	10.68	2.53	0.15	-24.47
17.14	522.2	50.06	1.83	13.53	12.66	0.20	6.79	10.67	2.51	0.17	-24.47
17.39	529.9	50.03	1.81	13.50	12.81	0.19	6.67	10.78	2.56	0.15	-24.46
17.47	532.3	49.68	1.96	13.44	12.75	0.20	6.74	10.66	2.56	0.16	-24.42
17.58	535.7	50.04	1.75	13.67	12.99	0.28	6.72	10.83	2.60	0.16	-24.46
17.66	537.9	50.19	1.95	13.46	12.73	0.19	6.79	10.89	2.59	0.15	-24.48
17.80	542.3	49.97	1.93	13.52	12.87	0.21	6.71	10.70	2.53	0.16	-24.46

17.92	545.8	49.85	1.96	13.55	12.90	0.22	6.90	10.79	2.54	0.15	-24.44
18.07	550.6	50.02	1.91	13.48	12.80	0.25	6.58	10.79	2.55	0.15	-24.46
18.13	552.4	50.06	1.85	13.56	12.81	0.23	6.58	10.70	2.54	0.16	-24.47
18.18	553.9	49.94	1.86	13.39	12.69	0.17	6.80	10.57	2.46	0.17	-24.45
18.45	561.9	50.26	1.82	13.63	12.89	0.18	6.74	10.78	2.50	0.15	-24.49
18.46	562.4	49.91	1.82	13.58	13.03	0.23	6.78	10.58	2.59	0.16	-24.45
18.56	565.5	49.82	1.73	13.68	13.03	0.22	6.69	10.78	2.59	0.17	-24.44
18.71	569.9	49.84	1.78	13.71	12.73	0.20	6.76	10.74	2.55	0.16	-24.44
18.79	572.5	49.79	1.91	13.55	12.58	0.23	6.70	10.64	2.58	0.18	-24.44
18.97	577.9	49.97	1.94	13.45	13.08	0.22	6.55	10.75	2.53	0.15	-24.46
19.05	580.4	50.02	1.85	13.51	12.98	0.20	6.68	10.80	2.60	0.16	-24.46
19.24	586.0	49.86	2.08	13.45	12.76	0.17	6.59	10.75	2.56	0.16	-24.44
19.50	593.9	49.92	1.86	13.58	12.78	0.20	6.69	10.68	2.54	0.17	-24.45
19.54	595.3	49.85	1.89	13.55	12.81	0.28	6.72	10.72	2.55	0.16	-24.44
19.76	601.9	49.93	1.79	13.46	12.73	0.30	6.58	10.75	2.54	0.18	-24.45
20.02	609.9	49.94	1.93	13.60	12.87	0.21	6.68	10.74	2.52	0.16	-24.45
20.03	610.2	49.93	1.76	13.51	12.98	0.21	6.81	10.65	2.51	0.17	-24.45
20.29	618.0	49.62	1.98	13.66	12.79	0.21	6.73	10.72	2.53	0.17	-24.42
20.52	625.1	49.49	1.70	13.48	12.82	0.17	6.64	10.65	2.57	0.18	-24.40
20.55	626.0	49.81	1.89	13.57	12.74	0.18	6.76	10.74	2.55	0.18	-24.44

QzDisBa107, starting basalt: JDF; T=1576 °C, P=0.5 GPa, t=322s, H2O=0.32wt%

x / sqrt(t)	x (μ m)	SiO2	TiO2	Al2O3	FeO	MnO	MgO	CaO	Na2O	K2O	lnD_SiO2 (m ² /s)
0.11	2.1	85.53	0.37	5.12	3.45	-0.01	1.80	2.24	1.85	0.27	-29.04
0.21	3.9	80.80	0.44	4.76	4.25	0.02	2.19	3.04	2.78	0.41	-28.25
0.39	7.0	76.69	0.70	6.57	5.84	0.04	3.09	4.70	3.03	0.39	-27.60
0.40	7.2	77.55	0.53	6.64	5.62	0.11	3.12	4.51	3.04	0.40	-27.73
0.42	7.6	76.07	0.60	6.02	5.39	0.11	2.85	4.28	2.99	0.38	-27.50
0.43	7.8	76.22	0.53	5.87	5.44	0.13	2.83	4.33	2.92	0.40	-27.53
0.54	9.7	74.14	0.68	6.67	6.15	0.04	3.19	5.13	3.13	0.36	-27.21
0.56	10.1	73.16	0.71	7.34	6.74	0.12	3.63	5.63	3.23	0.35	-27.07
0.57	10.2	73.85	0.72	6.83	6.21	0.10	3.13	5.09	2.96	0.36	-27.17
0.61	11.0	72.39	0.84	7.63	6.87	0.09	3.68	5.86	3.21	0.32	-26.95
0.65	11.7	73.02	0.75	7.50	6.77	0.06	3.56	5.65	3.05	0.36	-27.05
0.68	12.3	72.18	0.76	7.19	6.64	0.09	3.48	5.63	3.05	0.36	-26.92
0.69	12.4	71.94	0.78	7.30	6.65	0.17	3.61	5.73	3.11	0.35	-26.89
0.82	14.7	70.02	0.74	7.38	6.88	0.08	3.68	5.98	3.11	0.33	-26.61
0.87	15.6	70.57	0.83	7.39	6.93	0.09	3.60	5.82	3.23	0.35	-26.69
0.90	16.2	69.23	0.98	8.08	7.55	0.10	4.15	6.51	3.24	0.36	-26.50
0.96	17.3	68.94	0.93	7.70	7.18	0.14	3.79	6.30	3.26	0.32	-26.46
0.99	17.8	69.09	0.79	8.06	7.51	0.24	3.92	6.54	3.21	0.33	-26.48
1.11	19.8	67.02	0.87	7.95	7.74	0.06	4.10	6.76	3.39	0.31	-26.20
1.13	20.3	67.43	0.91	8.23	7.79	0.19	4.19	6.81	3.38	0.32	-26.25
1.19	21.3	66.98	0.95	8.48	8.08	0.15	4.24	7.02	3.31	0.32	-26.19
1.29	23.2	65.90	0.94	8.64	7.96	0.10	4.27	7.35	3.44	0.30	-26.05
1.47	26.4	65.03	1.06	8.68	8.39	0.15	4.47	7.44	3.42	0.26	-25.93
1.59	28.6	64.74	0.94	8.99	8.68	0.10	4.52	7.66	3.36	0.28	-25.89
1.70	30.5	64.31	1.01	8.85	8.69	0.09	4.48	7.68	3.38	0.28	-25.84
1.76	31.6	63.69	1.09	9.18	8.65	0.16	4.82	7.79	3.42	0.27	-25.76
1.77	31.8	64.07	0.97	8.97	8.73	0.14	4.52	7.59	3.48	0.29	-25.81
2.05	36.8	62.82	1.08	9.46	8.79	0.12	4.89	8.11	3.41	0.27	-25.64
2.19	39.3	62.12	1.12	9.45	9.19	0.17	5.04	8.24	3.37	0.27	-25.56
2.26	40.6	62.12	1.27	9.51	9.32	0.16	4.94	8.21	3.37	0.26	-25.55
2.34	42.0	61.69	1.23	9.70	9.14	0.14	5.02	8.49	3.46	0.24	-25.50
2.49	44.7	61.24	1.15	9.81	9.38	0.18	5.09	8.40	3.39	0.23	-25.44
2.63	47.2	60.85	1.24	9.93	9.60	0.14	5.13	8.60	3.37	0.24	-25.40
2.79	50.1	60.45	1.19	10.03	9.77	0.25	5.19	8.80	3.38	0.25	-25.35
2.83	50.8	60.44	1.21	9.85	9.71	0.09	5.17	8.60	3.39	0.24	-25.35
2.88	51.7	60.52	1.20	9.89	9.75	0.14	5.01	8.61	3.38	0.24	-25.36
2.92	52.3	60.42	1.25	10.11	9.71	0.16	5.35	8.71	3.33	0.26	-25.34
3.09	55.5	59.33	1.23	10.16	9.81	0.20	5.18	9.02	3.38	0.20	-25.21
3.20	57.4	59.33	1.17	10.39	9.95	0.18	5.40	8.87	3.28	0.20	-25.21
3.39	60.9	59.01	1.33	10.54	10.08	0.15	5.48	8.95	3.21	0.22	-25.17
3.40	61.0	59.15	1.30	10.34	10.12	0.19	5.38	8.96	3.29	0.23	-25.19
3.49	62.6	58.47	1.34	10.46	10.10	0.15	5.48	9.08	3.26	0.23	-25.11
3.69	66.3	58.29	1.47	10.47	10.27	0.18	5.60	9.18	3.26	0.21	-25.09
3.78	67.8	57.85	1.33	10.47	10.29	0.17	5.52	9.21	3.30	0.21	-25.03
3.96	71.1	57.73	1.39	10.47	10.47	0.23	5.56	9.37	3.17	0.20	-25.02
3.99	71.6	57.89	1.28	10.70	10.27	0.15	5.68	9.30	3.20	0.21	-25.04
4.00	71.7	58.35	1.37	10.60	10.56	0.15	5.46	9.32	3.23	0.25	-25.09
4.29	77.0	57.32	1.45	10.81	10.44	0.16	5.62	9.33	3.13	0.21	-24.97
4.53	81.3	57.14	1.39	10.95	10.78	0.21	5.65	9.48	3.20	0.19	-24.95
4.59	82.4	57.07	1.38	11.12	10.72	0.20	5.68	9.61	3.13	0.20	-24.94

4.89	87.8	56.28	1.49	11.16	10.89	0.19	5.63	9.64	3.12	0.19	-24.85
5.10	91.5	56.31	1.43	11.08	10.89	0.10	5.91	9.59	2.99	0.19	-24.86
5.11	91.7	56.20	1.49	11.25	11.15	0.14	5.78	9.63	3.04	0.19	-24.84
5.66	101.6	55.60	1.45	11.40	11.32	0.24	5.92	9.76	3.02	0.19	-24.77
6.23	111.7	55.11	1.45	11.66	11.31	0.19	5.97	9.84	3.01	0.17	-24.72
6.23	111.8	54.93	1.53	11.72	11.39	0.14	6.10	9.98	2.96	0.19	-24.70
6.80	122.0	54.26	1.53	11.90	11.84	0.17	6.00	10.22	2.89	0.19	-24.62
7.34	131.7	53.97	1.59	11.79	11.90	0.25	6.11	10.09	2.82	0.17	-24.59
7.37	132.2	53.86	1.64	11.98	11.72	0.16	6.10	10.18	2.84	0.19	-24.58
7.93	142.3	53.43	1.63	11.99	11.79	0.24	6.14	10.24	2.83	0.17	-24.53
8.45	151.7	52.85	1.90	12.24	11.85	0.21	6.05	10.28	2.80	0.19	-24.47
8.50	152.5	53.21	1.83	12.39	11.95	0.18	6.28	10.24	2.77	0.18	-24.51
9.07	162.7	52.69	1.77	12.38	12.01	0.22	6.33	10.34	2.70	0.17	-24.45
9.57	171.7	52.55	1.81	12.47	12.35	0.14	6.49	10.27	2.79	0.18	-24.44
9.63	172.8	52.37	1.66	12.54	12.39	0.11	6.24	10.55	2.78	0.15	-24.42
10.20	183.0	51.91	1.96	12.56	12.25	0.10	6.34	10.48	2.72	0.17	-24.37
10.68	191.7	51.98	1.90	12.80	12.47	0.27	6.48	10.42	2.66	0.17	-24.38
10.77	193.2	51.68	1.80	12.72	12.39	0.24	6.56	10.50	2.71	0.15	-24.35
11.33	203.4	51.39	1.80	12.81	12.56	0.22	6.46	10.49	2.61	0.16	-24.31
11.79	211.6	51.30	1.85	13.06	12.47	0.18	6.63	10.54	2.61	0.15	-24.31
11.90	213.5	51.29	1.77	12.87	12.66	0.26	6.34	10.59	2.64	0.16	-24.30
12.91	231.7	51.30	1.84	13.08	12.76	0.19	6.45	10.54	2.59	0.14	-24.31
14.02	251.6	50.66	1.85	13.21	12.76	0.19	6.58	10.63	2.51	0.16	-24.24
15.14	271.7	50.42	1.82	13.42	12.87	0.10	6.62	10.69	2.58	0.17	-24.21
16.25	291.6	50.46	1.87	13.29	13.08	0.27	6.72	10.66	2.55	0.16	-24.22
17.37	311.6	50.23	1.74	13.27	13.15	0.13	6.72	10.64	2.53	0.16	-24.19
18.48	331.6	50.17	1.87	13.39	13.11	0.25	6.65	10.77	2.58	0.15	-24.19
19.60	351.6	50.09	1.79	13.53	13.21	0.26	6.77	10.77	2.53	0.16	-24.18
19.82	355.7	50.19	1.73	13.44	13.26	0.20	6.69	10.69	2.57	0.18	-24.19
20.39	366.0	50.14	1.79	13.46	13.02	0.20	6.67	10.68	2.55	0.14	-24.19
20.71	371.6	50.04	1.87	13.38	13.04	0.16	6.66	10.76	2.56	0.14	-24.18
20.96	376.1	49.97	1.85	13.41	13.08	0.28	6.82	10.69	2.55	0.15	-24.17
21.53	386.4	50.11	1.89	13.49	12.89	0.25	6.69	10.65	2.50	0.16	-24.18
21.82	391.6	50.02	1.87	13.47	13.30	0.21	6.75	10.72	2.56	0.16	-24.17
22.10	396.6	49.92	1.88	13.50	13.25	0.28	6.65	10.62	2.57	0.15	-24.16
22.67	406.8	50.01	1.99	13.50	12.85	0.19	6.70	10.82	2.52	0.16	-24.17
22.94	411.6	50.16	1.86	13.52	13.06	0.23	6.83	10.83	2.56	0.16	-24.19
23.24	417.1	49.90	1.89	13.46	13.05	0.28	6.77	10.75	2.52	0.16	-24.16
23.81	427.3	49.72	1.78	13.40	12.89	0.21	6.73	10.80	2.53	0.17	-24.14
24.38	437.6	49.85	1.70	13.41	13.21	0.20	6.70	10.77	2.56	0.16	-24.16
24.95	447.7	50.03	1.84	13.39	13.15	0.21	6.94	10.83	2.58	0.17	-24.17
25.52	458.0	49.92	1.94	13.60	13.08	0.27	6.87	10.76	2.50	0.17	-24.16
26.09	468.2	49.93	1.87	13.50	13.32	0.19	6.81	10.74	2.56	0.16	-24.16
26.66	478.4	50.21	1.89	13.45	13.02	0.21	6.80	10.71	2.52	0.17	-24.19
27.23	488.7	49.83	1.91	13.50	13.19	0.20	6.90	10.74	2.59	0.18	-24.15
27.80	498.9	49.82	1.94	13.68	13.20	0.26	6.72	10.82	2.56	0.17	-24.15
28.37	509.1	50.08	1.68	13.51	13.40	0.13	6.86	10.71	2.59	0.17	-24.18
28.94	519.3	49.93	1.66	13.41	13.52	0.21	6.76	10.83	2.53	0.18	-24.16
29.51	529.6	49.87	1.93	13.26	13.17	0.21	6.74	10.81	2.60	0.17	-24.16
30.08	539.9	50.09	1.89	13.47	13.36	0.20	6.78	10.76	2.55	0.17	-24.18
30.65	550.0	50.09	1.82	13.26	13.32	0.20	6.78	10.86	2.51	0.19	-24.18
31.22	560.3	50.00	1.80	13.54	13.34	0.24	6.66	10.76	2.54	0.19	-24.17
31.79	570.5	49.84	2.01	13.29	13.12	0.21	6.87	10.69	2.65	0.16	-24.16
32.36	580.7	49.57	1.80	13.38	13.17	0.21	6.79	10.86	2.57	0.17	-24.13

32.93	590.9	49.90	1.94	13.33	13.17	0.21	6.79	10.88	2.60	0.18	-24.16
33.50	601.2	50.05	1.85	13.41	13.27	0.22	6.84	10.78	2.61	0.16	-24.18
34.07	611.4	49.90	1.73	13.55	13.19	0.22	6.89	10.77	2.56	0.18	-24.16
34.64	621.6	50.23	1.73	13.43	13.17	0.27	6.84	10.77	2.56	0.19	-24.19
35.21	631.9	50.03	1.71	13.33	13.13	0.22	6.84	10.80	2.60	0.15	-24.17
35.78	642.1	49.86	1.72	13.50	12.89	0.26	6.82	10.67	2.52	0.17	-24.16
36.35	652.3	50.12	1.83	13.40	13.14	0.21	6.78	10.82	2.56	0.17	-24.18
36.93	662.6	49.85	1.79	13.28	13.11	0.23	6.77	10.92	2.55	0.16	-24.16
37.49	672.8	49.78	1.89	13.32	13.20	0.23	6.98	10.86	2.52	0.17	-24.15
38.06	683.0	49.76	1.93	13.25	13.20	0.17	6.56	10.79	2.49	0.17	-24.15
38.63	693.2	49.72	1.89	13.40	13.08	0.19	6.86	10.90	2.52	0.18	-24.14
39.20	703.5	49.77	1.82	13.53	13.10	0.17	6.79	10.76	2.58	0.18	-24.15
39.77	713.6	50.01	1.82	13.42	13.16	0.17	6.79	10.87	2.58	0.17	-24.17
40.34	723.9	50.07	1.90	13.46	13.15	0.25	6.72	10.88	2.52	0.17	-24.18
40.91	734.2	49.84	1.87	13.52	12.94	0.21	6.91	10.76	2.60	0.17	-24.16
41.48	744.4	49.70	1.94	13.26	12.97	0.26	6.76	10.70	2.62	0.18	-24.14
42.05	754.6	50.03	1.92	13.61	13.14	0.17	6.88	10.63	2.59	0.17	-24.17
42.62	764.8	49.90	1.82	13.13	13.05	0.29	6.88	10.78	2.58	0.17	-24.16
43.19	775.1	49.96	1.81	13.22	13.08	0.22	6.66	10.84	2.64	0.18	-24.17
43.77	785.3	50.17	1.91	13.25	13.03	0.20	6.79	10.87	2.54	0.18	-24.19
44.33	795.5	50.34	1.86	13.38	13.24	0.24	6.76	10.87	2.63	0.18	-24.21

QzDisBa110, starting basalt: JDF; T=1394 °C, P=0.5 GPa, t=1232s, H2O=0.32wt%

x / sqrt(t)	x (μm)	SiO2	TiO2	Al2O3	FeO	MnO	MgO	CaO	Na2O	K2O	lnD_SiO2 (m^2/s)
0.07	2.5	76.56	0.61	6.56	4.93	0.01	2.54	3.79	3.06	0.43	-29.28
0.11	4.0	74.22	0.61	7.09	5.75	0.00	2.97	4.37	3.05	0.43	-28.83
0.13	4.5	73.45	0.63	7.22	5.74	0.08	2.95	4.57	3.06	0.43	-28.68
0.18	6.5	71.37	0.79	7.87	6.28	0.14	3.27	5.16	3.16	0.40	-28.29
0.19	6.8	71.41	0.72	7.82	6.37	0.09	3.22	5.15	3.22	0.40	-28.29
0.20	6.9	71.43	0.73	7.74	6.44	0.11	3.30	5.19	2.90	0.41	-28.30
0.24	8.5	70.00	0.81	8.01	6.80	0.13	3.53	5.58	3.20	0.38	-28.03
0.30	10.5	69.66	0.84	8.23	6.99	0.06	3.58	5.84	3.34	0.37	-27.97
0.31	10.7	69.28	0.87	8.15	7.15	0.07	3.67	5.86	3.14	0.39	-27.90
0.35	12.2	68.04	0.82	8.50	7.20	0.12	3.76	6.11	3.35	0.37	-27.67
0.36	12.5	68.17	0.83	8.43	7.15	0.04	3.68	5.99	3.41	0.37	-27.70
0.40	13.9	67.79	0.96	8.64	7.66	0.11	3.93	6.37	3.29	0.32	-27.63
0.41	14.5	67.05	0.87	8.76	7.60	0.11	3.96	6.46	3.45	0.34	-27.50
0.42	14.6	67.25	0.94	8.72	7.48	0.07	3.94	6.41	3.27	0.36	-27.53
0.42	14.9	67.21	0.87	8.84	7.59	0.12	4.02	6.50	3.53	0.36	-27.52
0.50	17.6	66.08	0.90	8.88	7.65	0.18	4.08	6.60	3.51	0.34	-27.32
0.54	19.1	65.39	1.01	9.06	8.06	0.15	4.38	6.94	3.41	0.33	-27.20
0.67	23.5	64.39	0.97	9.38	8.30	0.10	4.44	7.27	3.52	0.31	-27.03
0.69	24.1	64.38	0.96	9.48	8.39	0.04	4.46	7.33	3.41	0.28	-27.03
0.83	29.2	63.00	1.00	9.59	8.62	0.16	4.70	7.58	3.44	0.28	-26.80
0.89	31.2	61.98	1.12	10.00	9.16	0.12	5.05	7.97	3.39	0.27	-26.63
0.98	34.3	62.17	1.29	9.78	8.96	0.07	4.71	7.86	3.49	0.29	-26.66
1.00	35.2	61.77	1.26	9.92	9.10	0.12	4.82	8.04	3.51	0.26	-26.60
1.12	39.4	61.09	1.04	9.86	9.27	0.22	4.93	8.09	3.49	0.27	-26.49
1.17	41.1	60.80	1.18	10.17	9.34	0.12	4.89	8.24	3.51	0.25	-26.44
1.23	43.1	60.69	1.22	10.11	9.64	0.17	4.96	8.28	3.41	0.28	-26.42
1.34	46.9	60.32	1.19	10.34	9.62	0.11	5.14	8.39	3.44	0.26	-26.36
1.39	48.7	59.84	1.40	10.41	9.92	0.17	5.18	8.51	3.44	0.27	-26.29
1.40	49.2	58.81	1.31	10.69	9.99	0.10	5.40	8.80	3.38	0.22	-26.13
1.47	51.5	59.57	1.36	10.56	9.88	0.20	5.30	8.62	3.48	0.22	-26.25
1.50	52.8	59.49	1.31	10.54	9.56	0.17	5.38	8.65	3.44	0.25	-26.24
1.55	54.4	59.28	1.28	10.47	10.16	0.17	5.20	8.79	3.43	0.27	-26.20
1.67	58.6	58.60	1.48	10.80	10.02	0.18	5.46	8.91	3.32	0.25	-26.10
1.71	60.1	58.73	1.33	10.79	10.22	0.14	5.43	8.87	3.33	0.25	-26.12
1.84	64.5	58.02	1.27	10.81	10.14	0.20	5.40	8.87	3.39	0.22	-26.01
1.84	64.5	57.49	1.39	11.05	10.52	0.17	5.57	9.17	3.31	0.23	-25.94
1.87	65.7	58.12	1.40	10.63	10.30	0.13	5.48	9.01	3.32	0.26	-26.03
2.00	70.3	57.66	1.35	11.09	10.51	0.20	5.59	9.16	3.33	0.23	-25.96
2.03	71.4	57.43	1.42	10.93	10.72	0.18	5.49	9.17	3.27	0.22	-25.93
2.05	71.9	57.79	1.46	11.10	10.47	0.18	5.56	9.08	3.28	0.23	-25.98
2.17	76.2	57.03	1.37	11.15	10.53	0.16	5.46	9.29	3.33	0.22	-25.87
2.19	77.1	57.15	1.38	10.99	10.76	0.12	5.56	9.24	3.22	0.22	-25.89
2.27	79.8	56.35	1.41	11.52	10.86	0.15	5.73	9.34	3.23	0.20	-25.77
2.34	82.0	56.37	1.37	11.23	10.55	0.15	5.57	9.34	3.26	0.22	-25.78
2.52	88.4	56.50	1.39	11.39	10.78	0.18	5.76	9.51	3.22	0.21	-25.79
2.63	92.3	55.69	1.51	11.38	11.05	0.19	5.69	9.48	3.13	0.20	-25.68
2.68	94.1	55.87	1.40	11.39	11.09	0.16	5.85	9.49	3.13	0.19	-25.71
2.71	95.1	55.42	1.50	11.63	11.21	0.20	5.88	9.77	3.13	0.20	-25.65
2.84	99.7	55.52	1.61	11.48	11.20	0.17	5.93	9.59	3.19	0.19	-25.66
3.00	105.3	55.50	1.56	11.67	11.32	0.16	5.90	9.66	3.07	0.19	-25.66

3.14	110.4	54.76	1.71	11.77	11.37	0.14	6.00	9.76	3.00	0.17	-25.56
3.16	111.0	55.15	1.58	11.58	11.45	0.26	5.85	9.71	3.03	0.21	-25.61
3.21	112.7	54.64	1.44	11.91	11.46	0.16	6.02	9.73	3.02	0.18	-25.54
3.32	116.6	54.75	1.60	11.92	11.40	0.16	5.89	9.69	3.05	0.19	-25.55
3.48	122.3	54.40	1.60	11.98	11.37	0.21	6.05	9.78	3.01	0.19	-25.51
3.58	125.7	53.88	1.71	11.94	11.47	0.20	5.99	9.85	2.90	0.18	-25.44
3.65	128.0	54.44	1.59	11.85	11.59	0.13	5.96	9.85	3.02	0.18	-25.51
3.79	133.1	53.91	1.65	12.24	11.77	0.14	6.12	9.91	2.96	0.18	-25.44
3.81	133.6	54.23	1.73	12.09	11.52	0.17	6.04	9.90	3.02	0.18	-25.49
3.97	139.3	53.87	1.64	12.12	11.65	0.26	6.02	9.96	2.94	0.20	-25.44
4.02	141.0	53.70	1.67	12.38	11.80	0.21	6.19	10.00	2.99	0.18	-25.42
4.13	145.0	53.74	1.56	12.05	11.67	0.30	6.11	9.99	2.96	0.18	-25.42
4.29	150.6	53.31	1.71	12.17	11.78	0.17	6.08	10.07	2.97	0.16	-25.37
4.37	153.5	53.19	1.66	12.45	11.92	0.25	6.29	10.07	2.91	0.17	-25.35
4.45	156.3	53.31	1.61	12.46	12.01	0.17	6.18	9.95	2.87	0.17	-25.37
4.45	156.3	53.47	1.63	12.35	11.82	0.27	6.30	10.13	2.93	0.18	-25.39
4.62	162.0	53.29	1.66	12.17	11.81	0.16	6.20	10.10	2.86	0.19	-25.36
4.77	167.6	52.94	1.60	12.35	12.12	0.16	6.21	10.07	2.86	0.17	-25.32
4.89	171.6	53.15	1.69	12.59	12.15	0.18	6.21	10.06	2.92	0.19	-25.35
4.94	173.3	52.91	1.72	12.40	11.86	0.27	6.31	10.16	2.87	0.18	-25.32
4.95	173.9	52.32	1.65	12.57	12.09	0.21	6.26	10.23	2.86	0.16	-25.24
5.10	179.0	52.65	1.85	12.48	12.17	0.16	6.37	10.23	2.81	0.19	-25.28
5.26	184.6	52.52	1.68	12.56	12.04	0.17	6.25	10.23	2.92	0.15	-25.27
5.32	186.9	52.81	1.69	12.76	12.01	0.17	6.25	10.21	2.88	0.15	-25.30
5.42	190.3	52.59	1.75	12.61	12.18	0.22	6.44	10.17	2.80	0.17	-25.28
5.53	194.3	52.38	1.61	12.83	12.14	0.19	6.38	10.21	2.83	0.19	-25.25
5.76	202.2	52.31	1.83	12.89	12.11	0.17	6.20	10.23	2.83	0.17	-25.24
6.19	217.5	52.17	1.80	12.65	12.23	0.16	6.30	10.32	2.75	0.15	-25.23
6.63	232.8	52.14	1.77	12.98	12.39	0.19	6.40	10.31	2.77	0.16	-25.22
6.70	235.1	51.73	1.72	12.92	12.18	0.24	6.31	10.34	2.80	0.16	-25.17
7.07	248.0	51.90	1.69	12.92	12.56	0.18	6.34	10.38	2.75	0.18	-25.19
7.28	255.5	51.51	1.83	13.03	12.44	0.32	6.44	10.49	2.72	0.16	-25.15
7.50	263.3	51.55	1.78	12.92	12.53	0.18	6.44	10.34	2.69	0.18	-25.15
7.86	275.9	51.14	1.79	12.97	12.44	0.23	6.53	10.29	2.70	0.15	-25.10
8.37	293.9	51.38	1.81	13.13	12.47	0.20	6.50	10.40	2.74	0.15	-25.13
8.44	296.3	51.08	1.92	13.21	12.54	0.23	6.57	10.44	2.74	0.16	-25.10
8.81	309.2	51.28	1.82	13.10	12.49	0.24	6.52	10.54	2.73	0.17	-25.12
9.02	316.7	50.70	1.90	13.44	12.61	0.20	6.55	10.55	2.69	0.16	-25.05
9.24	324.5	51.01	1.91	13.34	12.72	0.25	6.54	10.45	2.73	0.17	-25.09
9.60	337.0	50.39	1.81	13.49	12.76	0.17	6.61	10.59	2.69	0.15	-25.02
9.68	339.8	50.81	1.79	13.30	12.79	0.10	6.52	10.49	2.69	0.15	-25.07
10.18	357.4	50.33	1.79	13.64	12.73	0.21	6.72	10.63	2.67	0.16	-25.01
10.76	377.8	50.44	1.80	13.42	12.95	0.26	6.48	10.46	2.67	0.15	-25.02
11.03	387.1	50.14	1.84	13.45	13.01	0.27	6.70	10.65	2.59	0.16	-24.99
11.34	398.2	50.26	1.87	13.38	12.91	0.18	6.71	10.65	2.63	0.14	-25.00
11.91	418.2	50.03	1.81	13.49	13.01	0.23	6.71	10.72	2.59	0.15	-24.98
11.92	418.6	50.20	1.75	13.72	12.77	0.32	6.48	10.76	2.61	0.16	-25.00
12.51	439.0	50.08	1.97	13.59	12.91	0.23	6.68	10.68	2.62	0.16	-24.98
12.80	449.3	50.18	1.81	13.63	13.03	0.26	6.70	10.65	2.63	0.16	-24.99
13.68	480.4	49.81	1.75	13.65	12.93	0.13	6.74	10.69	2.60	0.16	-24.95
14.57	511.5	49.73	1.95	13.58	12.94	0.15	6.79	10.77	2.63	0.18	-24.95
15.45	542.6	49.70	1.79	13.56	12.87	0.23	6.92	10.72	2.59	0.17	-24.94
16.34	573.5	49.59	1.94	13.73	13.10	0.25	6.56	10.59	2.62	0.18	-24.93
17.22	604.6	49.77	1.90	13.51	13.24	0.21	6.96	10.70	2.57	0.18	-24.95

18.11	635.7	49.53	1.77	13.52	12.93	0.28	6.78	10.72	2.61	0.16	-24.92
18.99	666.8	49.57	2.05	13.56	13.11	0.19	6.72	10.73	2.60	0.17	-24.93
19.88	697.9	49.53	1.89	13.68	13.12	0.19	6.80	10.76	2.62	0.17	-24.92
20.76	729.0	49.67	1.87	13.60	13.21	0.25	6.94	10.85	2.65	0.16	-24.94
22.17	778.5	49.71	1.94	13.52	13.21	0.16	6.85	10.79	2.62	0.15	-24.94
23.58	828.0	49.53	1.83	13.59	12.99	0.23	6.81	10.84	2.61	0.17	-24.92
24.99	877.4	49.41	1.86	13.59	13.13	0.24	6.79	10.70	2.56	0.16	-24.91
26.40	926.9	49.35	1.78	13.63	13.29	0.19	6.76	10.74	2.61	0.18	-24.91
27.81	976.4	49.45	1.83	13.69	13.04	0.26	6.69	10.89	2.60	0.18	-24.92
29.22	1025.9	49.28	1.83	13.62	13.11	0.25	6.67	10.72	2.63	0.16	-24.90
30.63	1075.4	49.54	1.83	13.50	12.98	0.24	6.84	10.82	2.65	0.16	-24.93
32.04	1124.9	49.80	1.97	13.56	12.91	0.25	6.79	10.78	2.59	0.17	-24.95
33.45	1174.3	49.50	1.79	13.47	12.90	0.19	6.83	10.76	2.64	0.19	-24.92
34.86	1223.8	49.35	1.99	13.63	12.85	0.24	6.91	10.68	2.68	0.19	-24.90

QzDisBa111, starting basalt: JDF; T=1400 °C, P=0.5 GPa, t =318s, H2O=0.32wt%

x / sqrt(t)	x (μm)	SiO2	TiO2	Al2O3	FeO	MnO	MgO	CaO	Na2O	K2O	lnD_SiO2 (m^2/s)
0.14	2.4	73.27	0.76	7.52	6.06	0.08	3.08	4.78	3.01	0.42	-28.64
0.23	4.1	70.31	0.85	8.17	6.84	0.14	3.59	5.77	3.24	0.40	-28.10
0.24	4.3	70.12	0.88	8.07	6.74	0.12	3.57	5.69	3.18	0.39	-28.06
0.29	5.2	68.77	0.83	8.25	7.18	0.08	3.72	6.08	3.30	0.37	-27.82
0.33	5.9	68.09	0.90	8.67	7.60	0.08	3.95	6.53	3.27	0.35	-27.70
0.35	6.2	67.47	0.90	8.64	7.35	0.14	3.83	6.37	3.50	0.36	-27.59
0.45	8.1	66.36	0.83	8.92	7.66	0.13	4.07	6.74	3.24	0.33	-27.40
0.47	8.4	66.17	0.92	8.89	7.93	0.13	4.15	6.95	3.52	0.33	-27.37
0.50	8.9	65.36	0.86	9.11	8.05	0.16	4.38	7.17	3.25	0.33	-27.23
0.61	10.9	64.75	0.96	9.15	8.31	0.20	4.31	7.24	3.59	0.32	-27.13
0.66	11.7	64.60	1.07	9.27	8.59	0.15	4.42	7.47	3.35	0.29	-27.10
0.66	11.7	64.20	1.04	9.65	8.66	0.13	4.51	7.42	3.33	0.30	-27.03
0.72	12.8	64.03	1.05	9.27	8.46	0.13	4.51	7.54	3.52	0.28	-27.01
0.76	13.6	63.32	1.09	9.49	8.63	0.11	4.60	7.71	3.23	0.31	-26.89
0.77	13.8	63.24	1.02	9.58	8.69	0.14	4.71	7.73	3.56	0.30	-26.88
0.83	14.9	62.73	1.03	9.62	8.83	0.14	4.86	7.94	3.45	0.30	-26.79
0.93	16.6	61.73	1.08	9.90	9.01	0.19	4.64	8.02	3.55	0.30	-26.63
0.98	17.5	61.66	1.22	10.11	9.20	0.12	4.86	8.15	3.58	0.28	-26.62
1.09	19.4	61.01	0.98	9.99	9.26	0.18	4.86	8.28	3.45	0.27	-26.52
1.21	21.6	60.70	1.19	10.25	9.34	0.09	5.14	8.51	3.47	0.25	-26.47
1.28	22.8	60.16	1.18	10.04	9.53	0.25	5.03	8.40	3.48	0.24	-26.38
1.30	23.2	60.23	1.16	10.51	9.80	0.16	5.06	8.59	3.50	0.29	-26.40
1.45	25.8	59.07	1.26	10.48	9.73	0.17	5.31	8.87	3.21	0.23	-26.22
1.55	27.6	59.26	1.29	10.62	10.11	0.24	5.26	8.92	3.50	0.25	-26.25
1.63	29.0	58.79	1.33	10.82	10.17	0.15	5.25	8.93	3.36	0.26	-26.18
1.88	33.6	58.12	1.31	10.90	10.29	0.14	5.63	9.14	3.16	0.22	-26.08
1.95	34.8	57.78	1.27	10.91	10.35	0.12	5.47	9.17	3.31	0.19	-26.03
2.22	39.6	57.11	1.31	11.28	10.70	0.08	5.56	9.53	3.28	0.22	-25.93
2.24	39.9	57.12	1.28	11.17	10.74	0.21	5.63	9.45	3.37	0.21	-25.93
2.28	40.6	56.75	1.47	11.07	10.70	0.12	5.60	9.44	3.19	0.21	-25.88
2.60	46.3	56.25	1.41	11.27	10.83	0.26	5.74	9.60	3.20	0.20	-25.81
2.89	51.6	55.78	1.40	11.54	10.99	0.19	5.71	9.74	3.09	0.20	-25.74
2.92	52.1	55.58	1.49	11.46	11.35	0.19	5.88	9.75	3.08	0.21	-25.71
2.97	52.9	55.53	1.47	11.71	11.07	0.10	5.95	9.86	2.98	0.18	-25.71
3.02	53.9	55.19	1.48	11.50	11.20	0.18	6.00	9.83	3.15	0.18	-25.66
3.23	57.6	54.98	1.59	11.81	11.02	0.24	6.04	9.86	3.03	0.21	-25.63
3.25	57.9	55.09	1.49	11.75	11.19	0.27	6.11	9.83	3.00	0.21	-25.65
3.56	63.6	54.39	1.61	11.86	11.50	0.17	5.95	10.02	3.06	0.19	-25.55
3.60	64.2	54.13	1.65	12.07	11.43	0.19	6.03	10.07	2.91	0.18	-25.52
3.81	68.0	53.86	1.53	11.87	11.58	0.18	6.01	10.07	2.99	0.17	-25.48
3.90	69.6	53.93	1.63	12.03	11.61	0.11	6.05	9.96	3.04	0.19	-25.49
4.24	75.6	53.22	1.68	12.35	11.77	0.22	6.22	10.23	2.77	0.19	-25.40
4.33	77.2	53.12	1.66	12.43	12.01	0.25	6.25	10.28	2.88	0.18	-25.38
4.60	82.1	53.02	1.51	12.30	11.84	0.08	6.16	10.29	2.97	0.18	-25.37
4.87	86.9	52.68	1.84	12.39	11.96	0.16	6.35	10.42	2.70	0.18	-25.33
5.39	96.2	52.39	1.64	12.59	11.95	0.25	6.27	10.44	2.83	0.16	-25.29
5.47	97.5	52.33	1.71	12.83	12.08	0.16	6.37	10.38	2.76	0.17	-25.28
5.51	98.2	51.96	1.75	12.83	11.92	0.22	6.22	10.66	2.74	0.16	-25.24
6.15	109.6	51.95	1.82	12.79	12.14	0.24	6.49	10.52	2.64	0.16	-25.23
6.18	110.2	51.94	1.77	12.74	12.30	0.13	6.39	10.52	2.92	0.16	-25.23

6.61	117.9	51.44	1.71	12.92	12.39	0.16	6.46	10.65	2.63	0.16	-25.17
6.78	120.9	51.36	1.91	12.97	12.52	0.16	6.43	10.77	2.71	0.15	-25.16
6.97	124.3	51.66	1.69	12.91	12.49	0.23	6.45	10.63	2.79	0.18	-25.20
7.41	132.2	51.06	1.93	12.95	12.42	0.18	6.55	10.71	2.51	0.15	-25.13
7.75	138.2	51.22	1.68	13.19	12.43	0.19	6.55	10.69	2.78	0.15	-25.15
7.76	138.4	51.25	1.78	13.01	12.49	0.20	6.52	10.68	2.73	0.17	-25.15
8.05	143.6	50.84	1.69	13.22	12.58	0.16	6.58	10.77	2.68	0.15	-25.10
8.55	152.5	50.82	1.70	13.06	12.61	0.23	6.39	10.77	2.57	0.17	-25.10
8.69	154.9	50.49	1.90	13.35	12.42	0.26	6.50	10.76	2.61	0.14	-25.06
8.89	158.5	51.02	1.84	13.35	12.62	0.15	6.68	10.70	2.65	0.16	-25.12
9.34	166.5	50.61	1.88	13.13	12.57	0.24	6.48	10.81	2.61	0.15	-25.07
10.03	178.9	50.58	1.69	13.34	12.61	0.16	6.47	10.84	2.63	0.16	-25.07
10.13	180.6	50.37	1.82	13.13	12.95	0.17	6.68	10.83	2.69	0.16	-25.04
10.18	181.6	50.31	1.68	13.32	12.94	0.16	6.57	10.77	2.67	0.14	-25.04
10.92	194.7	50.06	1.91	13.34	12.61	0.24	6.70	10.85	2.64	0.17	-25.01
11.17	199.2	50.46	1.81	13.51	12.61	0.25	6.57	10.85	2.64	0.16	-25.05
11.33	202.0	50.22	1.85	13.32	12.98	0.13	6.67	10.83	2.46	0.14	-25.03
12.31	219.5	50.03	1.79	13.47	12.97	0.18	6.73	10.88	2.67	0.15	-25.00
12.47	222.4	49.96	1.71	13.49	13.05	0.14	6.70	10.78	2.63	0.15	-25.00
13.45	239.9	50.17	1.72	13.58	13.01	0.20	6.71	10.69	2.59	0.16	-25.02
14.59	260.2	50.17	1.74	13.57	12.79	0.23	6.68	10.81	2.42	0.18	-25.02
14.76	263.2	50.13	1.75	13.40	13.09	0.17	6.61	10.82	2.48	0.17	-25.01
15.58	277.9	50.11	1.81	13.37	12.98	0.20	6.84	10.85	2.65	0.19	-25.01
15.73	280.5	50.12	1.63	13.53	12.80	0.21	6.57	10.76	2.70	0.16	-25.01
15.90	283.6	49.93	1.74	13.48	12.94	0.16	6.84	10.89	2.48	0.16	-24.99
17.05	304.0	50.05	1.81	13.42	13.01	0.10	6.62	10.90	2.63	0.17	-25.01
17.27	308.1	49.89	1.84	13.39	12.73	0.14	6.74	10.83	2.71	0.17	-24.99
18.01	321.2	50.08	1.65	13.40	12.74	0.26	6.71	11.02	2.64	0.15	-25.01
18.19	324.4	49.90	1.75	13.40	12.95	0.22	6.88	10.80	2.62	0.16	-24.99
18.97	338.3	49.94	1.83	13.46	12.97	0.19	6.77	10.86	2.60	0.17	-24.99
19.33	344.8	49.79	1.75	13.39	13.01	0.22	6.85	10.87	2.54	0.16	-24.98
20.48	365.2	49.77	1.92	13.25	12.90	0.23	6.86	10.91	2.67	0.16	-24.97
21.62	385.6	49.80	1.82	13.38	13.03	0.23	6.60	10.83	2.70	0.17	-24.98
22.36	398.7	50.02	1.77	13.46	13.12	0.22	6.80	10.85	2.64	0.17	-25.00
24.05	428.9	49.87	1.70	13.43	13.01	0.19	6.76	10.90	2.58	0.17	-24.99
25.74	459.1	49.95	1.69	13.34	13.03	0.32	6.67	10.89	2.65	0.18	-24.99
27.44	489.3	50.01	1.86	13.56	12.96	0.18	6.73	10.97	2.55	0.17	-25.00
29.13	519.5	49.83	1.76	13.35	13.01	0.19	6.75	10.90	2.61	0.19	-24.98
30.82	549.7	49.83	1.77	13.41	13.16	0.24	6.80	10.98	2.59	0.17	-24.98
32.52	579.9	49.86	1.84	13.32	12.99	0.22	6.79	11.05	2.73	0.18	-24.98
34.20	609.9	49.80	1.86	13.33	13.08	0.22	6.83	10.87	2.57	0.17	-24.98
37.01	660.0	49.96	1.70	13.21	13.05	0.27	6.79	10.90	2.68	0.20	-24.99
39.82	710.1	49.80	1.72	13.38	13.00	0.22	6.82	10.95	2.53	0.20	-24.98
42.63	760.2	49.75	1.79	13.46	13.10	0.28	6.66	10.95	2.65	0.18	-24.97
48.25	860.4	49.88	1.76	13.46	13.09	0.21	6.61	10.88	2.70	0.17	-24.99
51.06	910.5	50.26	1.87	13.40	12.97	0.22	6.82	10.95	2.68	0.17	-25.03
53.87	960.6	49.73	1.80	13.39	12.89	0.20	6.91	10.87	2.72	0.18	-24.97
56.67	1010.7	49.72	1.78	13.47	12.93	0.22	6.69	10.99	2.79	0.16	-24.97
59.48	1060.8	49.85	1.87	13.33	12.91	0.19	6.55	10.85	2.75	0.19	-24.98
62.29	1110.9	50.01	1.79	13.50	12.99	0.20	6.81	10.85	2.75	0.18	-25.00
65.56	1169.2	49.81	1.79	13.31	12.95	0.26	6.74	10.79	2.72	0.17	-24.98
68.84	1227.6	49.88	1.72	13.44	13.03	0.23	6.70	10.95	2.67	0.17	-24.99
72.11	1285.9	50.17	1.77	13.45	12.80	0.22	6.84	10.92	2.58	0.18	-25.02
75.38	1344.2	50.29	1.79	13.50	12.68	0.23	6.78	10.93	2.79	0.18	-25.03

78.65	1402.6	49.85	1.77	13.50	12.62	0.23	6.69	10.91	2.82	0.17	-24.98
-------	--------	-------	------	-------	-------	------	------	-------	------	------	--------